The Geology of Libya
Volume V

Third Symposium on the Geology of Libya, held at Tripoli,
September 27–30, 1987

Editors

M.J. Salem M.N. Belaid

Al-Fateh University, Tripoli, Great Socialist People's Libyan
Arab Jamahiriya

Digitized by the Internet Archive
in 2022 with funding from
Kahle/Austin Foundation

https://archive.org/details/geologyoflibyath0005symp

The Geology of Libya
Volume V

The Geology of Libya
Volume V

Third Symposium on the Geology of Libya, held at Tripoli, September 27–30, 1987

Editors

M.J. Salem   M.N. Belaid

Al-Fateh University, Tripoli, Great Socialist People's Libyan Arab Jamahiriya

1991

Elsevier

Amsterdam · London · New York · Tokyo

ELSEVIER SCIENCE PUBLISHERS B.V.
Sara Burgerhartstraat 25
P.O. Box 211, 1000 AE Amsterdam, The Netherlands

ISBN 0-444-88844-6

Copyright © 1991 by
Al-Fateh University, Tripoli

All Rights Reserved

No part of this book may be reproduced in any form by photostat, microfilm, or any other means, without written permission from the copyright holders

Contents of Volume V

Part 10. Sedimentation and Sedimentary Petrology

Palaeozoic Deltaic Sedimentation in the Southeastern Part of Al Kufrah Basin, Libya . . . 1713
Brian R. Turner

Sedimentology of the Silurian–Devonian Series in the Southeastern Part of the Ghadāmis Basin . . . 1727
V. Bracaccia, C. Carcano and K. Drera

Application of Neutron Activation Methods for Trace Element Analysis in the Nubian Sandstone of Southern Libya . . . 1745
A. El-Zouki and A. Alian

Tempestite Facies, Murzuq Basin, Great Socialist People's Libyan Arab Jamahiriya: Their Recognition and Stratigraphic Implications . . . 1757
Joel Carneiro de Castro, Jorge Carlos Della Favera and Muftah El-Jadi

Contribution to the Stratigraphy of the Murzuq Basin, SW Libya . . . 1767
E.S.T. Pierobon

Neogene to Pleistocene Continental Deposits in Northern Fazzān and the Central Sirt Basin . . . 1785
Luděk Domácí, Pavel Röhlich and Pavel Bosák

Advanced Palaeoclimate Weathering in Soils of the Fazzān Area of Libya . 1803
Gilani M. Abudelgawad and K. Ben Mahmoud

Cyclic Transgressive and Regressive Sequences and their Association with Hydrocarbons — Ghānī Field, Sirt Basin, Libya . . . 1827
Sulaiman A. Abushagur

Petrography and Lithofacies of the Satal Formation in Northwestern Sirt Basin, Libya . . . 1841
Ahmed J. Mouzughi

Sedimentology and Geochemistry of the Jir Formation in Jabal al Jīr and the Western Sirt Basin . . . 1855
Mokhtar I. Lashhab and Ian M. West

Depositional Facies and Diagenesis as a Guide to Correlating Porosity Zones — Al Fūrūd Formation, Ghānī Field, Sirt Basin, Libya . . . 1871
Sulaiman A. Abushagur and David V. LeMone

Sedimentary History of the Āṣiyah Formation — Upper Eocene of Al Ḥufrah Area, Western Sirt Basin, G.S.P.L.A.J. . . . 1883
J.M. Anketell and S.M. Kumati

Sedimentology, Petrography and Diagenesis of Metlaoui Group in the Offshore Northwest of Tripoli . . . 1907
A. Bernasconi, G. Poliani and A. Dakshe

Petrography and Facies of the Middle and Upper Eocene Rocks (Tellil Group), Offshore Western Libya . . . 1929
A.M. Sbeta

The Jifarah Formation — Aeolian and Fluvial Deposits of Quaternary Age, Jifārah Plain, G.S.P.L.A.J. A Redefinition in Terms of Composite Stratotype . 1967
J.M. Anketell and S.M. Ghellali

Quaternary Sediments of the Jifārah Plain 1987
J.M. Anketell and S.M. Ghellali

Part 11. *Hydrogeology and Hydrology*

Sedimentological Time Markers and Groundwater Dating: A Study of the Quaternary Evolution of Al Kufrah Area 2017
R.E. Becker and M. Fürst
Lakes in the Awbārī Sand Sea of Fazzān, Libya 2027
David J. Burdon and Roberto Gonfiantini
Isotope Hydrological Investigations in the Tāwarghā' Area, Libya . . 2043
M. Wolf, H. Moser and H. Zeino
A Review of Arid Zone Hydrogeological Mechanisms in Regional Sedimentary Basins 2051
J.W. Lloyd
A Stochastic Rainfall Model for the Wādī Zārat Watershed, Northwestern Libya 2059
Sanousi Salem Sanousi
Ground Water of Sabhā Area (in Arabic) 2096
Mehimed M. El-Chair

Contents of Volume I

Part 1. Stratigraphy

A Stratigraphic Contribution to the Palaeozoic of the Southern Basins of Libya 3
E. Bellini and D. Massa

Stratigraphic Nomenclature of the pre-Upper Cretaceous Mesozoic Rocks of Jabal Nafūsah. NW Libya 57
A.N. Fatmi, Bahlul A. Eliagoubi and Omar S. Hammuda

The Upper Cretaceous–Tertiary Formations of Northern Libya 67
Mohamed Megerisi and V.D. Mamgain

Al Khowaymat Formation — An Enigma in the Stratigraphy of Northeastern Libya 73
Mohamed Megerisi and V.D. Mamgain

The Trans-Saharan Seaway During the Cretaceous 91
Cornelius A. Kogbe

Middle Miocene Stratigraphy, Al Khums Area, Northwestern Libya . . . 97
M.J. Salem and Alfred C. Spreng

Stratigraphic and Micropalaeontologic Expression of the Mediterranean Late Miocene (Messinian) Regression and Early Pliocene (Zanclean) Transgression in Northeastern Tunisia 117
Stephen K. Wiman

A Preliminary Revision of the Sahabi Formation 127
Jean de Heinzelin, Ali El-Arnauti and Wahid Gaziry

Part 2. Biostratigraphy and Palaeontology

Biostratigraphy and Palaeoenvironment of Upper Cretaceous (Maastrichtian) Foraminifera of North-central and Northwestern Libya 137
Bahlul A. Eliagoubi and J. Dan Powell

Planktonic Foraminifera of the Palaeocene Al Uwayliah Formation at its Type Locality — Northeastern Libya 155
Bahlul A. Eliagoubi

Lower Tertiary Biostratigraphy and Tectonics of Northeastern Libya . . 163
F.T. Barr and W.A. Berggren

Planktonic Foraminifera from the Middle Eocene of the Northern Escarpment of Al Jabal al Akhḍar, NE Libya 193
Riyad Hassan El Khoudary

Micropalaeontologic Record of the Messinian Event at Esso Libya Inc. Well B1-NC35A on the Pelagian Platform 205
J.E. van Hinte, J.P. Colin and R. Lehmann

The Palaeocene Trans-Saharan Transgression and its Ostracod Fauna . 245
R.A. Reyment and E.R. Reyment

Ostracoda and Planktonic Foraminifera from the Late Eocene of Al Jabal al Akhḍdar, Northeastern Libya 255
F. Helmdach and Riyad Hassan El Khoudary

Early Cenozoic Calcareous Nannoplankton Biostratigraphy and Palaeobiogeography of North Africa and the Middle East and Trans-Tethyan Correlations 271
Bilal U. Haq and Marie-Pierre Aubry
A New Large Nuculoid Bivalve in the Devonian Binem Formation of Al Kufrah (SE Libya) 305
Henri Termier and Genevieve Termier
Palaeogene Vertebrate Fauna and Regressive Sediments of Dūr at Ṭalḥah, Southern Sirt Basin, Libya 309
A.W.R. Wight
The Discovery of a New Species of Pipid Frog (Anura, Pipidae) in the Oligocene of Central Libya 327
Zdeněk V. Špinar

Contents of Volume II

Part 3. Sedimentation and Petroleum Geology

Palaeozoic Sedimentology of the Southeastern Part of Al Kufrah Basin, Libya: A Model for Oil Exploration 351
Brian R. Turner

The Sedimentology and Facies Development of the Hasáwnah Formation in Libya 375
Petr Čepek

Late Jurassic–Early Cretaceous Sedimentation and Tectonics of the Murzuq Basin, Southwestern Libya 383
John Lorenz

Stratigraphy and Lithofacies of the Continental Clastics (Upper Jurassic and Lower Cretaceous) of Jabal Nafūsah, NW Libya 393
Ashour Y. El-Zouki

Depositional Environments of the Chicla, Cabao and Chameau Mort Formations as Revealed by Scanning Electron Microscopy 419
Ashour Y El-Zouki

Carbonate–Terrigenous Cyclic Sedimentation and Palaeogeography of the Marada Formation (Middle Miocene), Sirt Basin 427
Ahmed S. El-Hawat

Intertidal and Storm Sedimentation from Wadi al Qattarah Member, Ar Rajmah Formation (Middle Miocene), Al Jabal al Akhḍar 449
Ahmed S. El-Hawat

Post-Eocene Sedimentation in the Eastern Sirt Basin, Libya 463
A.C. Benfield and E.P. Wright

Geologic Factors Controlling Fluid Trapping and Anomalous Freshwater Occurrence in the Tadrart Sandstone, Al Ḥamādah al Ḥamrā' Area, Ghadāmis Basin 501
Omar S. Hammuda

Sediments and Palaeogeography of the Lower Campanian Sand Bodies Along the Southern Tip of Ad Daffah-Al Wāḥah Ridge, Sirt Basin . . . 509
Omar S. Hammuda

Geology of a Stratigraphic Giant — The Messlah Oil Field 521
Exploration Staff of the Arabian Gulf Oil Company

Part 4. Hydrogeology

Water Resources of the Socialist People's Libyan Arab Jamahiriya . . 539
P. Pallas

Infiltration Conditions of a Major Sandstone Aquifer around Ghāt, Libya . 595
David J. Burdon

Ground Water in Wādī ash Shāṭi', Fazzān — A Case History of Resource Development 611
Laszlo Dubay

Hydrogeological Studies in a Part of Murzuq Basin using Geophysical Logs . 629
S.C. Sinha and S.M. Pandey
Hydrogeology of Mesozoic Aquifers in the Western Part of Wādī al Ajāl . 635
Marek Zaluski and Kamal E. Sadek
On the Application of Geophysical Logging in the Assessment of Groundwater Potential in Al Ḥamādah al Ḥamrā' Basin 643
S.C. Sinha
Al Kufrah Pleistocene Lake — Its Evolution and Role in Present-day Land Reclamation 659
Ismail Mahmoud ElRamly
Hydrology and Water Balance of the Binghāzī Plain 671
T.S. Raju
Hydrogeological Study of the Coastal Karstic Spring of 'Ayn az Zayānah, Eastern Libya 685
A. Guerre
The Hydrogeochemical Characterization of Ground Waters in the Sirt Basin, using Strontium and other Elements 703
W.M. Edmunds
Groundwater Evaluation in Wādī Zamzam, NW Libya 715
Omar A. Jarroud
Groundwater Cooling in Wādī Zamzam 731
Omar A. Jarroud
Structural Control of Groundwater Flow in the Mesozoic Sandstone Aquifers of the Eastern Part of Jabal Nafūsah, Libya 753
G.D.S. Singh
Hydrogeology of the Jifārah, NW Libya 763
G.P. Kruseman and H. Floegel

Contents of Volume III

Part 5. Geomorphology and Quaternary Geology

Climatic History in the Late Quaternary in Southern Libya and the Western Libyan Desert . . . 781
Hans-Joachim Pachur

An Investigation of Current Geologic Processes and an Interpretation of Saharan Palaeoenvironments . . . 789
Erhard Schulz

Preliminary Data on Quaternary Palaeolacustrine Deposits in the Wādī ash Shāṭi' Area, Libya . . . 797
N. Petit-Maire, L. Casta, G. Delibrias, Ch. Gaven with an appendix by A.-M. Testud

Comparative Study of Quaternary and Present-day Lagoon Populations of *Cardium glaucum* (syn. *Cerastoderma glaucum* (Bruguière)), Mollusca, Bivalvia . . . 809
Jean M. Gaillard and A.-M. Testud

Comparison between the Late Quaternary Terraces around Atakor and Tībistī . . . 815
Pierre Rognon

Geological and Geomorphological Observations on the Northern Slope of the Tībistī Mountains, Central Sahara . . . 823
Horst Hagedorn

On the Origin of the Msāk Mallat and Ḥamādat Mānghīnī Escarpment . . . 837
Detlef Busche

Large-scale Fossil Landslides at the Msāk Mallat and Ḥamādat Mānghīnī Escarpment . . . 849
Jörg Grunert and Detlef Busche

Current Weathering and Fluvio-Geomorphological Processes in the Area of Jabal as Sawdā' . . . 861
Dieter Jäkel

Part 6. Tectonics and Geophysics

Structure — Libya . . . 879
Gus H. Goudarzi

Meteorite Impact Structures, Southeast Libya . . . 893
James R. Underwood, Jr. and Edward P. Fisk

Age and Metamorphic Evolution of the Basement Complex around Jabal al' Awaynāt . . . 901
J. Klerkx

In Situ Stresses and Palaeostresses in Libya . . . 907
K. Schäfer, K.-H. Kraft, H. Häusler and J. Erdmann

Tectonic Development of Al Jabal al Akhḍar . . . 923
P. Röhlich

Utilization of Orbital Imagery and Conventional Aerial Photography in the Delineation of the Regional Lineation Pattern of the Central Western Desert of Egypt with Particular Emphasis on the Bahariya Region 933
Hassan A. El-Etr and Adel R. Moustafa
Seismicity and Seismotectonics of Libya 955
Rashad M. Kebeasy
The Geological Interpretation of a Gravity Map of the Northern Part of Marādah Graben (Sirt Basin, Libya) 965
Salah I. El-Batroukh and Ahmed S. Zentani
Gravity-tectonic Trend Analysis in Siwa-Al Jaghbūb Region, NE Africa . 979
Samir Riad, Hassan A. El-Etr and Magdy A. Mohammed

Part 7. Geochemistry, Mineralogy and Ore Deposits

Studies of Some Clays in Libya 993
J. Šindelář and P. Jadrníček
The Kaolin Deposit of Al 'Awaynāt, Fazzān 1001
Werner Smykatz-Kloss, Khaled R. Mahmoud and Gilani Abdelgawad
Mineralogical Properties of the Clay Fraction of the Saharan Sarir Soils and Sediments — A Preliminary Study 1007
Gilani Abdelgawad, Ezzeddin Rahoma and W.M. Bausch
A Contribution to the Study of the Gargaresh Calcarenite, NW Libya . 1013
Miloje Ilich and Werner Smykatz-Kloss
A Review of the Recent Investigation on the Wādī ash Shāṭi' Iron Ore Deposits, Northern Fazzān, Libya 1019
Tarek M. Turk, Abdolrahman K. Doughri and Syamadas Banerjee
Uranium in Pan-African Belts 1045
John J.W. Rogers
Pan-African Age Granites of Northeastern Africa: New of Reworked Sialic Materials? 1051
Paul D. Fullagar
Pan-African Evolution in Jamahiriya and North Africa 1059
Mohammed A. Ghuma and John J.W. Rogers
High-pressure Megacrysts in Basaltic Lavas from Djanet Oasis, Eastern Hoggar, Algerian Sahara 1065
L. Morten, P.L. Rossi, M. Bondi and A.O. Brunfelt
Preliminary Chemical Data on the Volcanic Rocks of Al Harūj Area, Central Libya 1077
M.T. Busrewil and W.J. Wadsworth
Volcanic Rocks of Jabal as Sawdā' 1081
František Woller and Ferry Fediuk
The Basanitic Volcanoes of the Gharyān Area, NW Libya 1095
M.T. Busrewil and W.J. Wadsworth
Mineralogical Composition of Jabal Nafūsah Phonolites 1107
W.M. Bausch

Contents of Volume IV

Part 8. Palaeontology and Biostratigraphy

Palaeozoic and Mesozoic Subsurface Palynostratigraphy in the Al Kufrah Basin, Libya 1159
D. Grignani, E. Lanzoni and H. Elatrash
Palynological Studies in the Mesák Formation (Central Libya) . . . 1229
Magda Konzalová
Silurian Spores, Acritarchs and Chitinozoans from the Banī Walīd Borehole of the Ghadāmis Basin, Northwest Libya 1243
Ali O. Tekbali and Gordon D. Wood
Late Palaeozoic Floras of the Wādī ash Shāṭi' Area, Libya 1275
Antonín Hluštík
Latest Devonian Miospores and Acritarchs from the Surface Samples of the Ashkídah Formation 1285
Milada Vavrdová
Contribution of Conodonts to the Devonian Biostratigraphy of Western Libya 1297
Marcel Weyant and Dominique Massa
Stratigraphic and Biogeographic Significance of Upper Ordovician Conodonts from Northwestern Libya 1323
Stig M. Bergström and Dominique Massa
The Importance of Libyan Devono-Carboniferous Palaeofloras: A Comparison with Egyptian and New Nigerian Ones 1343
Annie Lejal-Nicol
Preliminary Palynological Study of the Upper Cretaceous Al Hilal Formation, Ra's Al Hilāl Area, NE Libya 1351
Ali Daw El-Mehdawi
Campanian–Maastrichtian Inoceramid (Bivalvia) Assemblages from NW Libya 1357
Karl-Armin Tröger and Pavel Röhlich
A New Species of *Nostoceras* (Ammonites: Nostoceratidae) in Northern Libya and its Affinities with Other Global Finds 1383
Jerzy Lefeld and Janusz Uberna
The Libyan Tertiary Molluscs in the Tethyan Faunas 1389
Giuliano Piccoli
Oligocene Carbonate Buildups of the Sirt Basin, Libya 1401
Jindřich Hladil, Jiří Otava and Arnošt Galle
Biostratigraphy of the Miocene in Al Khums Area, Northwestern Libya . 1421
Khaled A.T. Sherif
Miocene Ostracoda from Al Khums Formation, Northwestern Libya . . 1457
Ahmed Ammar El-Waer

Biostratigraphic Correlation of the Middle Miocene Mammal Locality of Jabal Zalṭan, Libya 1483
Martin Pickford
Revision of the Neogene Anthracotheriidae of Africa 1491
Martin Pickford

Part 9. Stratigraphy

Stratigraphy of Western Fazzān (SW Libya) 1529
A. Grubić, M. Dimitrijević, M. Galečić, Ž. Jakovljević, S. Komarnicki, D. Protić, P. Radulović and G. Rončević
An Updated *Cruziana* Stratigraphy of Gondwanan Palaeozoic Sandstones . 1565
Adolf Seilacher
The Age of Mesozoic Continental Formations on the Western Margin of the Murzuq Basin 1583
Ž. Jakovljević, A. Grubić and N. Pantić
Stratigraphy of the Offshore Cyrenaica (Libya) 1589
P. Duronio, A. Dakshe and E. Bellini
Al Gharbıyah Formation, Upper Campanian–Upper Maastrichtian (Northwest Libya) 1621
A.E.M. Nairn and J. Salaj
A Modified Farwah Group Type Section and its Application to Understanding Stratigraphy and Sedimentation along an E–W Section through NC35A, Ṣabrātah Basin 1637
Arebi El-Ghoul
Geohistory Analysis Mapping in Central and Southern Ṭarābulus Basin, Northwestern Offshore of Libya 1657
O.S. Hammuda, J.E. van Hinte and S. Nederbragt
The Jurassic of Tunisia: an Attempt at Reconstruction of the South Neotethyan Margin during and after the Rifting Phase 1681
B. Peybernès

Contents of Volume VI

Part 12. General Geology

Palaeoenvironmental Evidence from the Palaeozoic "Nubian Sandstones" of the Sahara 2099
D.D. Clark-Lowes and J. Ward
Geology of Al Kufrah Basin, Libya 2155
E. Bellini, I. Giori, O. Ashuri and F. Benelli
Geology of the Aouinet Ouenine and Tahara Formations, al Ḥamādah al Ḥamrā' Area, Ghadāmis Basin 2185
Wanis S. El-Rweimi
Depositional and Structural Evolution of the Middle and Late Devonian on the Northwestern Margin of the Sahara Craton (Morocco, Algeria, Libya) . 2195
Jobst Wendt
Latest Jurassic–Early Cretaceous Deposits in the Subsurface of the Eastern Sirt Basin (Libya): Facies and Relationships with Tectonics and Sea-Level Changes 2211
Massimo E. Rossi, Mauro Tonna and M. Larbash
The Significance of the Occurrence of Abu Ghaylan and Kiklah Formations East of Wādī Ghān, Eastern Jabal Nafūsah 2227
Ali N. Fatmi and A.M. Sbeta
Sand Desert Forms in Libya — Remote Sensing Analysis 2235
A. Linsenbarth

Part 13. Structure and Tectonics

The Precambrian Tectonic Structure of North Africa 2259
J.R. Vail
Identification in the Middle Nile Valley of Compressive Structures Induced in the Sedimentary Cover by Reactivated Sliding of a Large Shear Zone in the African Plate During the Neogene 2269
Patrick Gigot, Mohammed Habib, Alia El Houssaini, Marcel Lanteaume, Shamir Riad and Mustapha Youssef
Folding Structure in the Basement Rocks of the Jabal Nuqay Area, Southern Libya 2287
H.S. Assaf
A Preliminary Photogeologic Investigation of the Basement Rocks and Structures of the Jabal Eghī Area, Libya 2295
Malcolm R. Gent
Disruption of the African Plate Margin in the Eastern Mediterranean . 2319
J.M. Woodside
The Medina and Sirt Wrenches: A Quantitative Estimate of Strike-Slip Deformation within the Sirt Rise over the Past 5 Ma 2331
Derk Jongsma
Structure of Al Ḥufrah Region — Western Sirt Basin, G.S.P.L.A.J. . . . 2353
J.M. Anketell and S.M. Kumati

The Ghadāmis Fault — A Disputed Structure in NW Libya 2371
Pavel Röhlich and Bashir M. Youshah
A Palaeogeologic Map of the Pre-Tertiary Surface in the Region of the Jifārah Plain and its Implication to the Structural History of Northern Libya . 2381
J.M. Anketell and S.M. Ghellali
Is There Plate Tectonics in the Mediterranean Area? 2407
Erwin Geiss

Part 14. Geophysics

Geophysical Study of the Sirt Rise 2417
A. Del Ben and I. Finetti
First Results of the Palaeomagnetic Study of Libyan Mesozoic Limestones: The Carnian Azizia Limestone Formation —Preliminary Data 2433
D.L. Martin, H.D. Munroe and A.E.M. Nairn
Seismicity and Related Phenomena in the Hellenic Arc: Their Influence on the Eastern Mediterranean Region 2441
G.A. Papadopoulos
Correlation of Satellite Geoid Features and Hot-Spot Activity with the Tectonic Framework of Libya 2451
Kadry M. Fouad
Gravity Study of the Sirt Basin, Libya 2461
I.S. Suleiman, G.R. Keller and A.S. Suleiman
Refraction Seismograph Soundings of Near-Surface Geology in the Vicinity of Tripoli, Libya 2469
M. Rida Bakbak and M.S.V. Raghava
Reconnaissance Survey of 'Ayn Zārah Upper Aquifer Using Resistivity Sounding 2479
M. Rida Bakbak and R. Hassaballa

Contents of Volume VII

Part 15. Geochemistry, Mineralogy and Ore Deposits

Anorogenic Magmatism in Northeast Africa 2495
David C. Almond

Geochemical and Rb–Sr Isotopic Data on Felsic Rocks from the Jabal al ‘Awaynāt Alkaline Intrusive Complex (SE Libya) 2511
L. Andre, J. Klerkx and M.T. Busrewil

The Geology and Geochemistry of the South Al ‘Awaynāt Ultrabasic Body, Southeast Libya 2529
S. Lagha

The Rock-forming Minerals of the Jabal Arknū and Jabal al ‘Awaynāt Alkaline Ring Complexes of SE Libya 2539
Derek Flinn, Salem Lagha, Michael P. Atherton and R.A. Cliff

The Geochemistry and Petrology of the Jabal Arknū and Jabal al ‘Awaynāt Alkaline Ring Complexes of SE Libya 2559
Michael P. Atherton, Salem Lagha and Derek Flinn

CO_2 Emanations, Alkaline Magmatism and the Relationship between Rift Structures and Mineralizations in the African Plate 2577
Jacques Maisonneuve

Geochemistry of the Tertiary Alkaline Rocks of Jabal Al Ḥasāwinah, West Central Libya 2587
Mabrouk T. Busrewil and Khaled M. Oun

Chronology and Composition of the Igneous Rocks of Jabal as Sawdā’ . 2599
M.T. Busrewil and J. Esson

Alum Deposits of Fazzān and the Sahara: Their Origin, Distribution and Importance 2605
Jean Philippe Lefranc

Al ‘Awaynāt Surface Uranium Mineralization — A New Approach to Its Origin 2619
M.B. Baegi, H.S. Assaf and K.M. Hangari

Uranium Potential in and around the Tībistī and Hoggar Massifs . . 2627
Philip C. Goodell

Gold Deposits in the Northern Nubian Desert, Sudan 2637
A. Fuganti, G. Morteani and G. Grundmann

Radioactive Elements in Sedimentary Rocks of the Western Part of Murzuq Basin, Libya 2645
B. Almehdi, S. Gojkovic, M. Megerisi, M. Obrenovic, D. Puric and J. Zelenka

Opal-CT as the Main Constituent in Insoluble Residues of Limestones (Apollonia Limestone), NE Libya 2659
Hans Schellhorn

Rhythmically Alternating Limestones of Differing Stages of Diagenetic Development (Eocene, Al Jabal Al Akhḍar) 2671
W.M. Bausch and H. Schellhorn

Geochemical Position of the Jabal Nafūsah Phonolites 2681
W.M. Bausch and J.U. Meduna
Some Geochemical Aspects of Al Aziziyah Formation, Jabal Nafūsah . 2689
A.M. Ben Ashour, A. Zaied and M. Bakush
Kaolinic Clay and Quartzose Sandstone — The Chief Mineral Raw Material in the Central Sahara 2697
A. Antonović, M. Stojković, P. Radulović and D. Pešić
The Palaeozoic Oolitic Ironstone Belt of North Africa: From the Zemmour to Libya 2703
Salah Guerrak

Part 16. Petroleum Geology

The Origin and Migration Fairways of Petroleum in the Murzuq Basin, Libya: An Alternative Exploration Model 2725
Egon M. Meister, Elson F. Ortiz, Elder S.T. Pierobon, Abilio A. Arruda and Marco A.M. Oliveira
Petroleum Geochemical Aspects of Cyrenaica, NE Libya 2743
K. Ameed R. Ghori
Petroleum Geology of the Sirt Group Sandstones, Eastern Sirt Basin . . 2757
M.W. Ibrahim

Glossary

abū	father of
abyār	wells
‘aqīrah, ‘aqīrat	depression, mudflat
‘awaynat	spring
‘awaynāt	springs
awlād	sons, family
‘ayn	spring
bāb	gate, pass
baḥr	sea, lake
balṭat	depression, mudflat
balṭāt	depressions, mudflats
banī	children or descendants of
bin	son or descendant of
bi’r	well
birkah, birkat	lake, intermittent lake
buḥayrat	small cultivated area, lake
buwayrāt	wells
dalu	special type of bucket used in traditional wells
ḍarārī	children
dūr	hills, mountainous or hilly area surrounding a plain
ehi	peak, rocky hill
emi	mountain, massif
ennedi	wadi
enneri	wadi
fesh-fesh	soft, fine, very loose soil material consisting of gypsum, clay minerals and other very fine detritus
funduq	mart, yard, animal pen
gilf	escarpment
ḥalaq	small wadi
ḥamādah, ḥamādat	hamada, rocky desert plateau
ḥasy	well
ḥaṭīyah, ḥaṭīyat	depression, oasis, valley
hawā	cave, depression, sinkhole
ibn	son of
‘ilat	family of
‘ilwah, ‘ilwat	cairn, hill
‘irq	dunes, sand sea
jabal	mountain
kabīr	big, large, great
kāf	cliff, mountain, peak, ridge, spur
karkūr	wadi, valley
kharrūbah kharrūbat	carob tree
khurmah, khurmat, khuraymah, khuraymat	pass
khuraymāt	passes
maghreb	west; also used for Morocco and northwest Africa in general
marsa	port, bay, bight, cove
minqār	mesa, point, ridge, spur
naqqāzah, naqqāzat	terrace
oued	wadi
qabīlat	tribal area
qabr	tomb
qārah, qārat	low, generally flat-topped hill(s)
qarārah, qarārat, qarār	depression, valley, wadi
qarārāt	depressions, valleys, wadis
qaryah, qaryat	village
qaṣr	fort, abandoned fort
quray‘ah, quray‘at	low hill
quray‘āt	low hills
ramlah, ramlat	dunes
ra’s	hill, peak, point, promontory, ridge, spur
sabkhah, sabkhat	sabkha
sahel	shore, coastal area
sāniyah, sāniyat	well, small traditional farm
sarīr	sarir, gravel plain
sawānī	wells, small traditional farms
shāṭi’	beach, shore
shaṭīb	wadi, valley
shaṭṭ	beach, shore
sūq	market
tādrārt	mountain, massif
tarso	high plateau, gently sloping mountainside
tassili	great barren plateau
ṭawīl, ṭawīlah, ṭawīlat	long
tmad	shallow waterhole
wādī	wadi
washkah, washkat	palm tree
wāw	crater
ẓahr	escarpment, plateau
ẓahrah, ẓahrat	hill
zāwiyah, zāwiyat	mosque, religious centre

Part 10

Sedimentation and Sedimentary Petrology

Palaeozoic Deltaic Sedimentation in the Southeastern Part of Al Kufrah Basin, Libya

BRIAN R. TURNER[1]

ترسيب دلتات دهر الحياة القديمة في الجزء الجنوبي الشرقي من حوض الكفرة بليبيا

ب. ر. تيرنر

الخلاصـــة

تتميز تتابعات دهر الحياة القديمة (السيلوري — الديفوني) المتكشفة في جبل العسبة بالجنوب الشرقي لحوض الكفرة بمراحل متعالية وتجاوزية من الترسيب البحري ربما نشأت كجزء من مركّب شاطئ دلتي. وقد سجل تعالي الترسيب في شكل تتابع سحنى متخشن إلى أعلى مؤلف من غضار وحجر غريني مترسب على الرف البحري ومتغير إلى أعلى إلى حجر رملي شاطئ. ويعلو كل هذه الرواسب المجدولة لسهول الدلتا فوق سطح تعرية. ويكون سطح التعرية هذا جزءاً من سطح عدم توافق إقليمي. وبذلك تكون سحنات الشاطئ وسحنات سهل الدلتا غير متزامنة مع بعضها، وليس من المؤكد أن يكون سطح الشاطئ مرتبطاً بالدلتا، أو أن يكون سهل تزامن مدى، أو أن يمثل الجانب البحري لعقبة شاطئية.

ودليل التأثير البحري على الترسيب في الجزء الأعلى من سحنات سهل الدلتا متوافق تماماً مع بداية تجاوز البحار. وقد تم ذلك بترسيب سحنات مسطحات المد والجزر التي تعلوها عندما سادت الرواسب البحرية على إمتداد سهل الدلتا من جهة الشمال الغربي. ولكن لم يكن تقدم البحار متكاملاً نتيجة لزيادة الرواسب النهرية إلى خط الشاطئ قبل مرحلة الإنحسار التالية.

Abstract. The Palaeozoic (Silurian–Devonian) succession at Jabal Asba in the southeastern part of Al Kufrah basin, Libya, is characterized by progradational and transgressive phases of deposition that may have originated as part of a deltaic shoreline complex. Progradation is recorded by a coarsening-upward facies sequence comprising marine shelf shale and siltstone that grades up into shoreface sandstone. These are erosionally overlain by a braided delta plain deposit. The erosion surface forms part of a regionally extensive unconformity. Thus, the shoreface and delta plain facies were not contemporaneous with one another, and it is uncertain whether the shoreface was attached to a delta, a strand plain or the seaward side of a barrier beach.

Evidence of a marine influence on sedimentation in the upper part of the delta plain facies is consistent with the beginnings of abandonment and transgression. This was completed with deposition of the overlying channelled tidal flat facies, when marine conditions spread across the delta plain from the northwest. However, transgression was incomplete due to increased fluvial sediment supply to the shoreline, prior to another regressive phase of deposition.

INTRODUCTION

The Palaeozoic (Late Ordovician to Early Carboniferous) succession at Jabal Asba in the southeastern part of Al Kufrah basin, Libya (Fig. 1) consists of a 250 m-thick sequence of clastic sediments discontinuously exposed along the faulted southern limb of a low amplitude synclinal structure dipping at between 5 and 10° to the south. The base of the succession is only seen at Jabal Arknū, some 60 km south of Jabal Asba, where it rests unconformably on Precambrian basement. The top of the succession is truncated by flat-lying Mesozoic strata.

A marginal marine depositional setting for the succession was documented by Turner (1980) who interpreted lithofacies patterns in terms of coastline interaction with a braided alluvial plain. A more

---

[1] Department of Geological Sciences, Science Laboratories, South Road, Durham DH1 3LE, U.K.

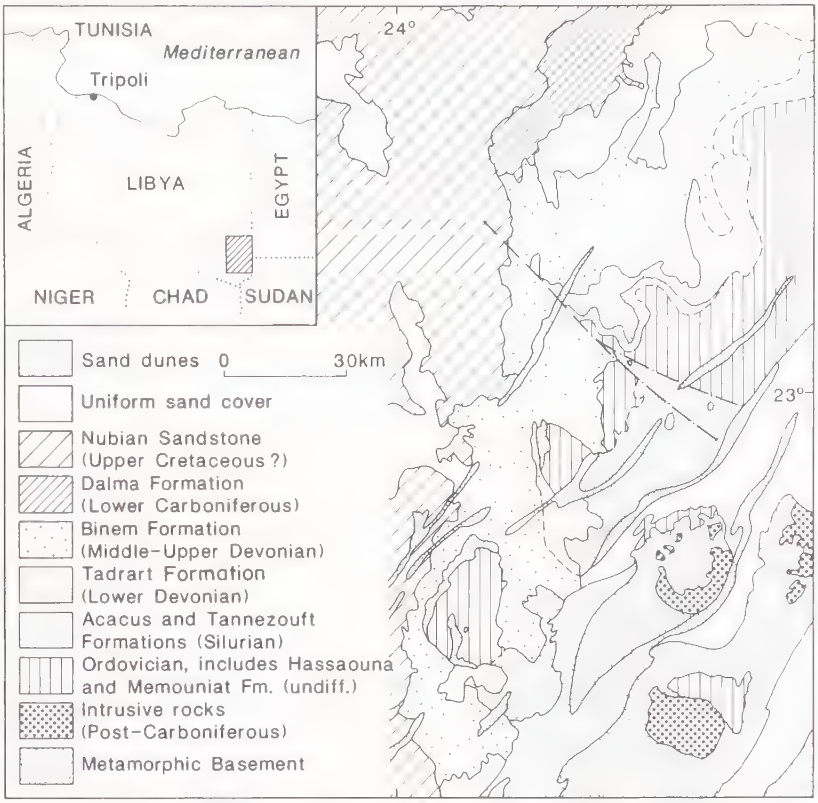
TUNISIA
Mediterranean
Tripoli
ALGERIA
LIBYA
EGYPT
NIGER
CHAD
SUDAN
24°
23°
Sand dunes
0 30km
Uniform sand cover
Nubian Sandstone (Upper Cretaceous ?)
Dalma Formation (Lower Carboniferous)
Binem Formation (Middle–Upper Devonian)
Tadrart Formation (Lower Devonian)
Acacus and Tannezouft Formations (Silurian)
Ordovician, includes Hassaouna and Memouniat Fm. (undiff.)
Intrusive rocks (Post-Carboniferous)
Metamorphic Basement

Fig. 1. Geological map of the Jabal Asba area and location of Al Kufrah basin.

detailed analysis of the lithofacies present within a 165 m-thick conformable sequence in the middle of the Palaeozoic succession of Jabal Asba (Fig. 2) allows for a more refined interpretation of the depositional model and documents the presence of progradational and transgressive deposits within a major Palaeozoic (Silurian–Devonian) deltaic complex.

Lithofacies data, based on lateral and vertical associations of lithologies, sedimentary structures and biogenic features were obtained from good exposures in central and northern Jabal Asba (Fig. 1). Comparison of these associations with Holocene depositional processes and models enables the facies to be assigned to specific depositional environments related to constructive (progradation) and destructive (transgression) phases of delta building.

SEDIMENTARY FACIES

The progradational deltaic deposits exposed at Jabal Asba form a coarsening-upward sequence about 110 m thick assigned to the Silurian Tannezouft and Acacus Formations and the Lower Devonian Tadrart Formation (Turner, 1980) (Fig. 2). The sequence can be subdivided into marine shelf, shoreface and delta plain facies. Transgressive tidal flats and tidal channel deposits overlie the progradational sequence and are assigned to the Middle–Upper Devonian Binem Formation which is exposed only at the northern end of Jabal Asba.

Marine shelf

This facies is well exposed in central and northern Jabal Asba where it consists of up to 38 m of interbedded shale, silty-shale, siltstone and sandstone showing a coarsening-upward trend (Fig. 3). A thickness of up to 54 m has been recorded in the AGIP KW2 well north of Jabal Asba, suggesting a basinward thickening of the facies. The shales are confined to the lower part of the facies. They are laminated and white to pale grey and violet in colour, with individual beds ranging from 0.5 to 10 cm in thickness. They show an upward decrease in thickness towards the top of the lower, more shaley part of the succession, where they become more

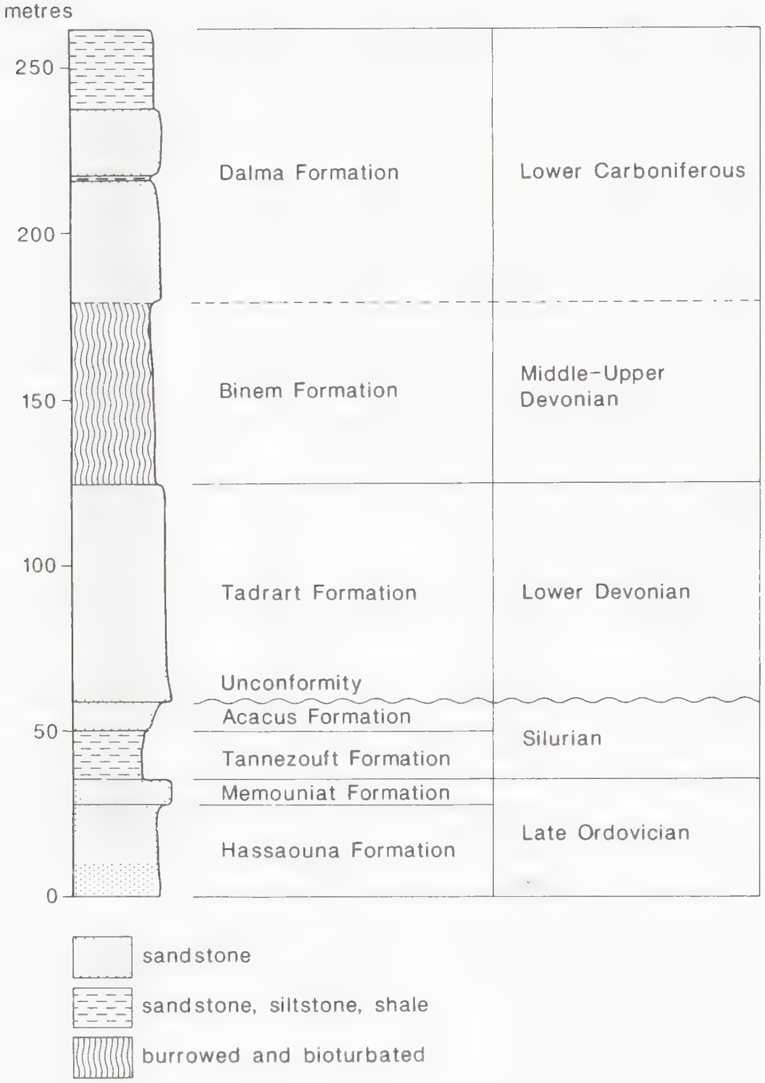
metres
250
200
150
100
50
0
Dalma Formation
Lower Carboniferous
Binem Formation
Middle-Upper Devonian
Tadrart Formation
Lower Devonian
Unconformity
Acacus Formation
Tannezouft Formation
Silurian
Memouniat Formation
Hassaouna Formation
Late Ordovician
sandstone
sandstone, siltstone, shale
burrowed and bioturbated

Fig. 2. Stratigraphic section of the Palaeozoic succession in the southeastern part of Al Kufrah basin.

lenticular in character. When traced southwards the facies thickens from about 15 m to over 38 m and the proportion of shale in the lower part increases.

The siltstone and silty-shale are micaceous, purplish-grey to fawn-yellow in colour, and structured by horizontal lamination and locally developed ripple cross-lamination. Individual beds range from a few millimetres up to 1 m in thickness. The sandstones are micaceous, fawn to pale grey in colour, and fine to very fine-grained. Bed thickness varies from 1 to 70 cm. They have sharp bases and sharp or gradational tops, overlain by siltstone and silty-shale. Shale occurs above the siltstone and silty-shale in the lower part of the facies. Individual sequences in the succession show fining, and to a lesser extent coarsening-upward trends. The sandstones increase in grain size and bed thickness upward through the facies, and they occur mainly as tabular lenses that can be traced laterally for up to 40 m.

Ripple cross-lamination is the predominant sedimentary structure in the sandstones, although some of the thicker beds towards the top of the facies contain horizontal lamination and cross-lamination. The ripple cross-lamination generally occurs at the top of the beds, and it may be locally deformed into convolute lamination. Sandstone beds near the top of the facies occasionally show the following sequence of sedimentary structures overlying a sharp

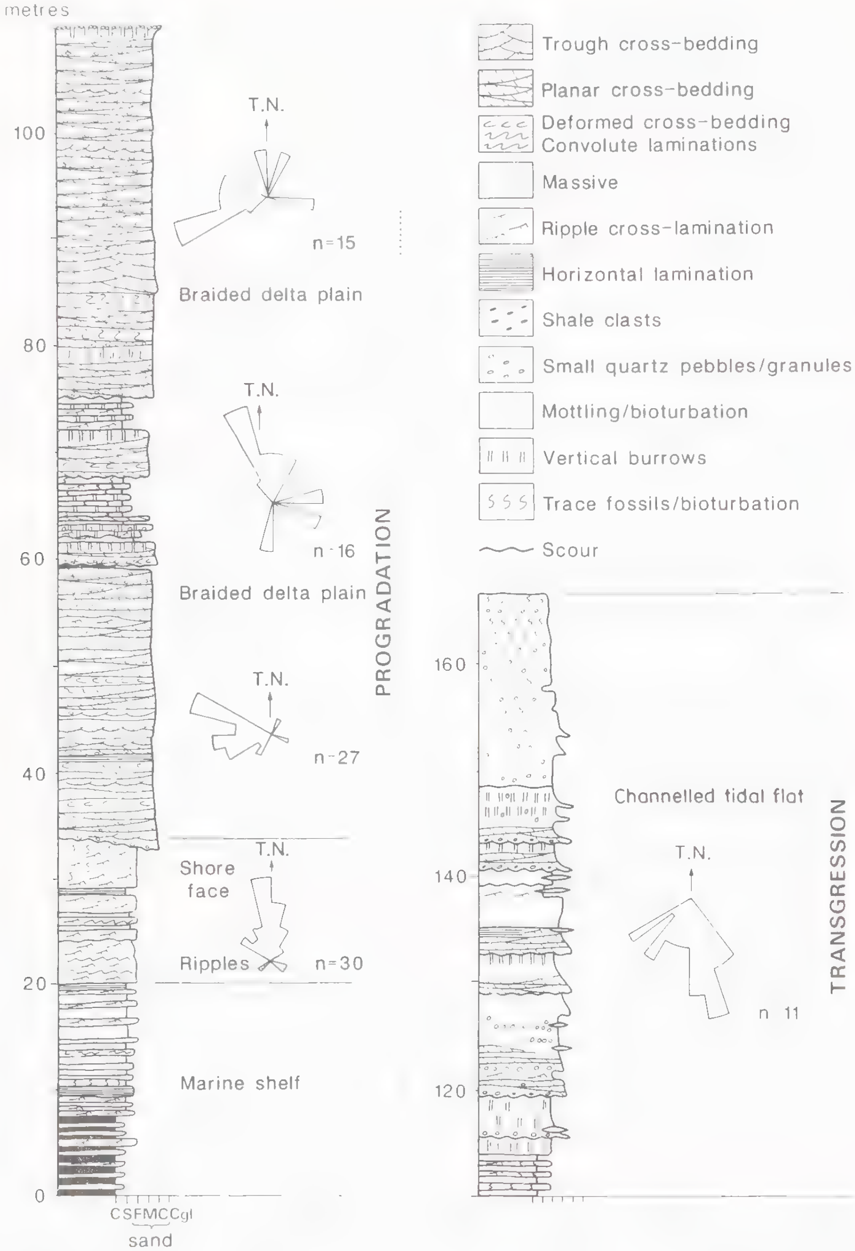
metres
100
80
60
40
20
0
CSFMCCgl
sand
T.N.
n=15
Braided delta plain
T.N.
n-16
Braided delta plain
PROGRADATION
T.N.
n-27
Shore face
T.N.
Ripples
n=30
Marine shelf
Trough cross-bedding
Planar cross-bedding
Deformed cross-bedding
Convolute laminations
Massive
Ripple cross-lamination
Horizontal lamination
Shale clasts
Small quartz pebbles/granules
Mottling/bioturbation
Vertical burrows
Trace fossils/bioturbation
Scour
160
140
120
Channelled tidal flat
T.N.
n 11
TRANSGRESSION

Fig. 3. Measured section in central Jabal Asba showing coarsening-upward progradational shoreline sequence overlain by transgressive channelled tidal flats. Other transgressions occur at the base of the marine shelf facies and in the middle of the braided delta plain facies. The erosional surface at the base of the delta plain facies defines part of a regionally extensive Lower Devonian unconformity (see text for details).

scoured planar base: horizontal laminations, wave ripple cross-lamination (wavelength 40 cm, height 5 cm) with locally developed convolutions and poorly defined irregular laminations at the top. Trace fossils occur mainly as walking and surface crawling traces (*Diplichnites* and *Planolites*, Turner and Benton, 1983) on sandstone bedding planes, and they increase in abundance upward through the facies, most of them being concentrated in the uppermost 6 m. A few vertical burrows are also present. Body fossils have not been found, but graptolites, chitinozoa and pelecypods have been recorded from a borehole penetrating the lower part of the facies in central Jabal Asba (AGIP, 1976).

The sedimentological characteristics of the facies, its position beneath shoreface sands and the marine fauna indicate a marine shelf environment receiving fine-grained sediment from suspension alternating with longer periods of high energy bedload processes. These became increasingly important towards the top of the facies as the shelf shallowed resulting in higher energy conditions and the deposition of laterally more persistent and thicker, horizontally laminated and rippled sandstones. The alternation of contrasting energy states on marine shelves is generally attributed to storm processes (Swift *et al.*, 1971; Sternberg and McManus, 1972). The sharp, scoured base to the sandstones is consistent with the erosive ability and sudden onset of storm surge flood (Hayes, 1967). Turbulence generated during the initial surge and return ebb underflow scours the shelf and entrains sand in the flow. As the storm surge wanes sand is deposited as horizontally laminated units followed by rippled units, due to rapid attenuation of the storm.

The presence of horizontal lamination closely associated with and overlain by wave ripple cross-lamination reflects high-energy plane bed depositional conditions, subsequently modified by oscillatory storm wave currents. The thinner, locally rippled and laminated sandstone beds are lower energy deposits, which may owe their origin to episodic flows of tidal or oceanic origin rather than storms. A return to fair weather conditions is seen in the trace fossils on the upper bedding surfaces of sandstones, which represent the establishment of a shallow benthic fauna occupying a fine, mainly silty substrate. Despite this, there is no evidence of a shell lag commonly associated with storm deposits (Hayes, 1967; Vos, 1977), possibly because conditions were not conducive to the preservation of hard parts (pore water chemistry). The lack of hummocky and swaley cross-stratification suggests that, unlike other Palaeozoic shelves, it was not subjected to severe storms (cf. Castro *et al.*, 1985). This may reflect the shelf width, since wide shelves inhibit storm conditions and favour tidal action. Some evidence of tidal activity is seen in the sediments at the top of the overlying shoreface sands in central Jabal Asba.

Shoreface

Gradationally overlying the marine shelf deposits is a laterally persistent coarsening-upward sequence up to 15 m thick, comprising sandstone with occasional interbeds of siltstone and silty-shale (Fig. 3). The siltstone and silty-shale beds are mainly confined to the lower part of the facies and range from 1 to 10 cm in thickness. They are fawn yellow, micaceous, and contain horizontal laminations and ripple cross-lamination, but on a scale smaller than in the interbedded sandstones.

The sandstones are micaceous, fawn-yellow to white in colour, but with paler, more quartzose sandstones concentrated towards the top of the facies. The sandstones coarsen upwards from very fine to fine and medium-grained varieties, accompanied by an increase in bed thickness (0.5 to 35 cm), sorting and maturity. Ripple cross-lamination is the dominant sedimentary structure in the sandstones, with bedding surfaces covered with a variety of ripple types, including straight, sinuous, linguoid, interference, double crested and flat-topped ripples. The ripples show form discordant symmetrical and asymmetrical profiles. Ripple indices (ratio of wavelength to amplitude) range from 4 to about 8.7 indicating wave- and current-produced structures (Reineck and Singh, 1973). Orientation of ripple crests is variable but with a north-northwest to south-southeast trend predominating. Horizontal lamination is present in some of the sandstone beds lower in the facies, and is occasionally overlain by ripples as in the shelf deposits. However, the sandstones are thicker, coarser grained and contain a much more diverse trace fossil assemblage than in the deeper water, lower energy shelf deposits. The abundance of traces increases towards the top of the facies. Dominant types include *Planolites*, *Arthrophycus*, *Cruziana* and *Rusophycus* (Turner and Benton, 1983), characteristic of Seilacher's (1967) *Cruziana* ichnofossil assemblage (littoral zone to wave base). Although *Arthrophycus* and *Cruziana* are the most abundant trace fossils they are not found together. The facies shows no evidence of subaerial exposure.

Convolute laminations occur in two closely spaced, black to dark-brown weathered, Fe-rich sandstones near the top of the facies. Flaser and lenticular bedded, rippled fine-grained sandstone and clay-rich siltstone form a locally developed wedge, 3 m thick at the top of the facies in central Jabal Asba. Immediately beneath and laterally adjacent to this wedge is a sequence of small, stacked channels (Turner, 1980, fig. 13). The lateral extent of these features is uncertain because of limited exposure, but they range from 1.5 to 2.5 m thick. They consist of a scoured base of low relief overlain by a fining-upward sandstone sequence with a basal shale intraclast lag. The lower part of the sequence comprises a 1–1.4 m-thick, coarse to medium-grained poorly sorted micaceous sandstone containing occasional mudclasts. The sandstone is structured by medium to small-scale planar cross-bedding which shows an upward decrease in set thickness. One set near the base of the succession shows local flexuring of the foresets. Burrowing is present, but not common, in the upper part of the sandstone. Planar foreset azimuths are directed predominantly northwards, but with a secondary mode towards the east-southeast.

Gradationally overlying the coarser grained sandstone is a 0.5–1.4 m-thick unit of fine, white sandstone with occasional thin silty-shale interbeds. The sandstones are very rich in white mica, which concentrates on bedding surfaces imparting a platy character to the rock. Ripple cross-lamination occurs throughout the sandstones. Ripple marks on bedding surfaces are commonly of the asymmetric linguoid type with azimuths directed north-northwest, consistent with the palaeocurrent trend shown by the underlying planar cross-beds. The sandstones are locally burrowed, and contain trace fossils typical of the rest of the facies.

The vertical position of this facies between marine shelf and delta plain deposits, and its coarsening-upward trend suggest that it accumulated along the front of a prograding shoreline system. The upward increase in bed thickness and the scale and variety of ripple cross-lamination supports this view, and indicates increasing proximity to detrital clastic influx and a gradual shallowing of the water. This is likewise reflected in the increased maturity of the sands and evidence of reworking by waves and currents. The presence of flaser and lenticular bedding may have resulted from tidal current activity or possibly interaction between fluvial and marine processes. The close association of ripple cross-lamination and convolute lamination towards the top of the facies suggests relatively rapid rates of sedimentation within the more proximal (steeper) parts of the shoreface (Coleman, 1976). In the more distal parts conditions were less conducive to deformation probably as a result of lower depositional slopes and a general lack of mud to facilitate instability.

The interbedded sandstone and siltstone and silty-shale with smaller scale ripple cross-lamination point to fluctuating energy levels. Periods of higher than normal discharge (floods) in the fluvial system are indicated by the channel-like features cut into the shoreface. These resemble the channel deposits of the overlying delta plain and are interpreted as distal subaqueous distributary channels on the evidence of the channel-fill marine fossils (*Cruziana* attributed to Trilobites; Turner and Benton, 1983), burrowing and the sharp boundary between individual beds (Coleman and Prior, 1982). The occurrence of a weak bimodal, bipolar foreset azimuth trend, indicates a predominantly offshore flow (northwest), with minor reworking by tidal processes (southeast). Trace fossils of the *Cruziana* ichnofacies reflect the activities of a benthic fauna of epifaunal and shallow burrowing infaunal detrital feeders. The behavioural response of animals to different energy levels and rates of sedimentation (Crimes, 1970) is thought to be responsible for the close association but mutual exclusiveness of *Arthrophycus* and *Cruziana*. The facies distribution of *Cruziana* and *Diplichnites* supports Crimes (1970) contention that *Cruziana* is mainly found in sediments deposited in a higher energy environment than those containing *Diplichnites*.

Delta Plain

This facies is well exposed in northern and central Jabal Asba where it forms prominent cliffs. Access to the cliff face is often difficult with the result that lateral relationships have to be reconstructed from photomosaics. The facies can be divided into two subfacies each of which is described separately.

Subfacies 1:

This subfacies forms a 30 m-thick sheet sand body, erosively overlying the shoreface deposits (Fig. 3). Immediately above the erosion surface, which has a local scour relief up to 50 cm, is a lag composed of shale intraclasts and scattered quartz granules and small pebbles (<2 cm long). The shelf sandstones are generally feldspathic or lithic arenites. They are predominantly coarse to medium-grained, poorly sorted and micaceous, with scattered shale clasts and angular to subrounded quartz granules and small pebbles, locally concentrated into conglomerate lenses up to 30 cm long. Internally the sandstones are structured by large to small-scale planar cross-bedding, with occasional small to medium-scale troughs, ripple cross-lamination and horizontal lamination. Planar foresets are graded from coarse to fine with foreset azimuths directed mainly towards the west-northwest (Fig. 3). The base of individual sets is characteristically scoured and overlain by a thin, basal lag of coarser granular and pebbly sand. Foresets are typically straight and angular or tangentially based. Most planar sets are overlain by the scoured base of the set above, although in places they grade upwards into fine sandstone and siltstone up to 25 cm thick, containing small trough or planar cross-beds, ripple cross-lamination and horizontal lamination. These structures may occur individually, together, or in various combinations above the planar sets. Deformed foresets are very common, especially in the lower and middle parts of the facies, and include oversteepening, local flexuring, overturning, recumbent folding and more complex convolute patterns. Deformation occurs in individual planar sets or in successively superimposed sets. Reactivation surfaces are present in a few sets, but the majority have a relatively simple internal geometry. A characteristic feature of the facies is the presence of planar and trough cosets arranged in erosively bounded thinning and upward fining sequences from 0.75 to 2.8 m thick, and rare thickening and upward-coarsening sequences. Bounding surfaces between individual sets and sedimentation units (sequences) are generally planar to undulatory in both dip and strike sections. These correspond to the first- and second-order bounding surfaces of Allen (1983). These sequences are superimposed on much larger megasequences tens of metres thick, which show an overall upward decrease in cross-bed set thickness and grain size.

In central Jabal Asba a large planar set up to 1.8 m thick and 18–25 m in lateral extent is bounded above and below by sharply defined planar to undulatory scour surfaces. Individual foresets are straight and tabular, and inclined at about 15°. When traced in the downdip direction the set gradually increases in thickness from about 1 to 1.8 m. Directly beneath the lower bounding surface is a small, erosively based, lenticular channel sand body up to 1.2 m thick and 15–18 m long. The sandstone fill shows low-angle bedding surfaces dipping at about 2–3° that gradually become horizontal when traced downdip. The base of this channel feature marks a laterally more persistent erosional feature near the top of the cliffs at Jabal Asba, beneath which the vertically stacked planar cosets show a gradual overall upward decrease in set thickness. Overlying the large planar set near the top of the cliff are low-angle bedding surfaces dipping at about 5° in the downcurrent direction. Internally these bedding surfaces show cross-bedding and resemble the more complex bar foresets described by Allen (1983) and Haszeldine (1983) and the macroform elements of Miall (1983).

In northern Jabal Asba the facies contains a higher proportion of finer grained sandstone, which increases towards the top of the succession. Two fundamental types of fining-upward sequence from 0.86 to 2.35 m thick have been recognized in the lower 12 m of the facies. The first type consists of a scoured surface of low relief strewn with shale intraclasts and gradationally overlain by coarse trough cross-bedded sandstone and fine ripple cross-laminated sandstone. The second type is 1.1 m thick. It has a similar scoured base but is overlain by two stacked planar sets with rippled foresets, capped by a finer grained and horizontally laminated sandstone, 40 cm thick. Occasional thin silty-shale beds, 10–52 cm thick, occur in the upper part of this facies in northern Jabal Asba.

The internal scouring, scattered quartz granules and pebbles and vertical stacking of sedimentation units suggest deposition under conditions of fluctuating discharge typical of fluvial systems. The lack of overbank fines, abandoned channel-fills, preserved backswamp and lateral accretion deposits, as well as the essentially unidirectional palaeocurrent trend are consistent with deposition on a sandy braid plain.

Individual cross-beds are interpreted as transverse to linguoid bars (Smith, 1970). Most bars have a simple internal structure and correspond to the cross-bedded simple bars of Allen (1983). Downstream migration of the bars across granular and pebbly channel sands led to the development of the scoured and conglomeratic bounding surfaces. The larger scale interbedded and superimposed sequences into which the bars are sometimes organized lack the macroform architecture indicative of complex-compound bar features (Miall, 1983). Thus, the sequences are interpreted to be a result of short-term fluctuations in river stage, superimposed on longer term stage changes. Deposition occurred mainly under decelerating and shallowing flow conditions, as evidenced by the bar top bedforms (short-term stage changes) and the thinning and fining-upward sedimentation units (longer-term changes). The rare thickening and coarsening-upward sequences indicate deposition under conditions of increased flow depth and discharge, increasing the local competency of the flow. The best example of this situation occurs at the base of the succession in central Jabal Asba, where it comprises a sequence of stacked troughs.

The sequence in central Jabal Asba provides a good example of the local internal complexity of the facies. The small shallow channel, superimposed on the sheet-like (non-channelized) geometry of the facies forms part of a laterally more persistent phase of scouring (third order bounding surface) cut into the top of a thinning and fining-upwards megasequence of cross-beds. This is attributed to gradual abandonment of the braid plain due to channel switching. Following this, the abandoned part of the braid plain was reoccupied through gradient advantages and channelling and bar formation re-established themselves as before. The scale of the channel and the associated bars point to a channel system of shallow to moderate flow depths. The large-scale, erosively bounded, cross-bedded simple bar above the channelized sands is indicative of a non-repetitive transverse to linguoid bar bedform. The steep, tabular foresets and downstream thickening are hydrodynamically compatible with the development of a strong separation eddy system on the downstream face of the bar as it built into deeper water. The internally cross-bedded convex-up, low-angle foresets correspond to the second order bounding surfaces of Allen (1983) and the foreset macroforms of Miall (1983). They are thought to have originated from small bed forms advancing down the slope (defined by the second order surfaces) of a low relief bar (no separation eddy system). This local complexity may reflect variations in channel depth or stage (Miall, 1983).

Subfacies 2:
This is similar to subfacies 1 except that:

(1) The sandstones are finer, being predominantly medium-grained, and there is a much higher proportion of fine sandstone and siltstone, especially towards the top of the succession.
(2) The coarse-grained sandstones with scoured bases contain a higher proportion of trough cross-bedding than subfacies 1, and individual sets, both planar and trough varieties, are smaller in scale (from 0.05 to 1 m thick, average 20 cm). Palaeocurrents based on foreset azimuths are more variable and also show a weak bimodal trend dominated by a west-northwesterly mode (Fig. 3).
(3) The coarser sandstones are commonly overlain by up to 1.5 m of fine sandstone and siltstone containing ripple cross-lamination and horizontal lamination. Rippled bedding surfaces show mainly symmetric linguoid ripple types. The boundary between coarse and fine sandstone is often marked by a zone of vertical burrows. Evidence of vertical burrowing occurs throughout the subfacies, but is mainly concentrated in the lower 18 m. Individual burrows range from 0.5 to 3 cm in diameter and attain lengths of up to 20 cm. Most burrowed beds retain little or no internal structure, and may be mottled. Horizontal burrows are also present.

The lower part of the subfacies is only completely exposed at the northern end of Jabal Asba. It overlies subfacies 1 with a sharp erosional surface and consists of two fining-upward sequences, making a total thickness of some 18 m (Fig. 3). The scoured surface at the base of the lowermost sequence is of low relief and overlain by shale intraclasts and a coarse to very coarse-grained poorly sorted sandstone containing scattered granule and pebble conglomerate lenses. Internally the sandstone is structured by planar cross-beds, each set being characterized by a basal gravel lag. The cross-beds show an overall increase in scale upwards (from 5–10 cm to 20 cm) through the sandstone, with the uppermost set penetrated by numerous, closely spaced vertical burrow tubes, lined with $CaCO_3$. Foreset azimuths have a bimodal–bipolar trend to the northwest–southeast.

Above the burrowed zone the sequence can be divided into two parts. The lower part, 1.7 m thick, consists of fine-grained sandstone interbedded with medium to coarse-grained sandstone containing scattered shale clasts and quartz granules locally concentrated into conglomerate lenses. The fine sandstones are rippled, or less commonly contain horizontal laminations, and may grade up into silty-shale. The coarse sandstones are thicker as a rule, and structured by a few small planar cross-beds. The top of these sandstones is burrowed and structureless to a depth of between 2 and 15 cm, whilst the base of one such sandstone is covered with *Arthrophycus* traces. The upper part of the sequence is thicker (3.3 m) and comprises burrowed and structureless fine-grained sandstone interbedded with poorly laminated burrowed siltstones. *Arthrophycus* traces occur in the sandstone interbeds.

The second fining-upward sequence is similar except that the sandstones and interbedded siltstones at the top are less intensely burrowed, and *Arthrophycus* traces are absent. Small planar cross-beds occur in the sandstones and ripple cross-lamination in the siltstones, mainly as rippled lenses. The sequence is erosively overlain by the upper part of the subfacies.

The sedimentological characteristics of the subfacies indicate a distributary channel origin. The channels occupied a more distal position than those of the underlying subfacies, as shown by the occasional bimodal–bipolar cross-bedding (indicating tidal current activity), the variable ripple directions (waves and currents) and the extensive vertical burrowing. The position of the channels relative to the marine influence appears to have changed, with the more extensive burrowing, and evidence of tidal current activity within fining-upward sequences at the base of the subfacies pointing to a closer proximity to the sea. Although the marine influence is still present right through the subfacies, it did not have as strong an influence on sedimentation.

The finer grained sandstones and interbedded siltstones between the distributary channel sandstones are interpreted as interdistributary channel deposits. These show evidence of rapidly fluctuating discharge in the fine rippled sandstone and coarser cross-bedded sandstone, but with abundant burrowing at the top of the beds. Foreset azimuths of the cross-beds indicate a north-northeasterly trend, as opposed to the more northerly trend of the cross-bedded channel sandstones. These features are consistent with flooding of the interdistributary area by distal distributary channels.

Tidal Channel/Tidal Flat

This facies attains a thickness of 52 m and consists of quartz arenites with subordinate interbeds of siltstone, silty shale and shale (<25 cm thick) arranged in vertically stacked fining-upward sequences. Individual sequences range from 1 to 5 m in thickness and are poorly defined as a rule, due to extensive burrowing and bioturbation of the sediments. The only exception occurs in the middle of the facies where biogenic reworking has been less effective. Here the fining-upward sequences (Fig. 3) comprise an erosively based coarse-grained quartz arenite from 0.3 to 1.8 m thick, internally structured by small to large-scale planar cosets (15–75 cm thick). Shale intraclasts and quartz granules are concentrated along the scoured surface at the base of the sequence. Planar foreset azimuths are directed consistently southwards (Fig. 3) and show little deviation about the mean. Vertical burrows occur locally in the lower and upper part of the sandstones, which also contain shale intraclasts along planar foresets and occasional coarser sandstone lenses.

The top of the fining-upward sequence consists of fine-grained, white, purplish-grey mottled sandstone showing traces of ripple cross-lamination and horizontal lamination. These are overlain in turn by fine-grained extensively burrowed sandstones with trace fossils on bedding surfaces. Coarser pods and lenses occur within these finer grained sandstones which attain a maximum thickness of about 75 cm.

The biogenically reworked sandstones and siltstones contain few preserved primary sedimentary structures other than some ripple cross-lamination and poorly defined horizontal bedding surfaces. The effects of biogenic reworking can be seen in the white to pale grey and maroon mottling of the sandstones and the presence of coarser quartz grains and granules scattered throughout the sediment or concentrated into small pods and lenses. Despite the extensive burrowing and bioturbation no body fossils have been found. However, trace fossils are common in the sandstones which are crowded with long vertical *Skolithos*-type burrows up to 30 cm deep and 1–1.5 cm wide, extending down from bedding planes. The burrows have a simple internal structure and are filled by sand and silt of a slightly coarser texture and darker colour than the surrounding sediment. The *Skolithos* burrows are confined to the lower part of the facies; the upper 10 cm of the facies is dominated by horizontal *Zoophycos* spreite.

The presence of fining-upward sequences analogous to modern tidalite deposits, and their association with trace fossils of shallow-water marine affinities suggests deposition in a tidal flat environment. However, there is no direct evidence of periodic emergence and alternating traction and suspension load sedimentation typical of tidal flats, possibly due to the extensive biogenic reworking of the sediments. *Skolithos* burrows are produced mainly by hemisessile suspension feeders within current influenced estuarine and shallow marine environments (Frey and Pemberton, 1984). The depth of the *Skolithos* burrows falls within the range for intertidal and subtidal burrowers (Rhoads, 1967). *Skolithos* burrows are typical of many modern tidal flat deposits but tend to be most extensively developed where they are afforded some protection from the full force of the sea (Jansa, 1975). This suggests the possible development of an embayed coastline or barrier protected tidally influenced lagoon. The presence of mud and intense bioturbation together with fining-upward sequences ascribed to tidal channels favours a tidal flat environment. This view is consistent with the presence of the facies above distal braided river sediments, but below *Zoophycos* bearing sediments. Although *Skolithos* and *Zoophycos* have been recorded together from tidal flat deposits (Tankard and Barwis, 1983), their mutual exclusiveness in this facies may indicate a change in environmental conditions towards the top of the succession. The similar pattern of sedimentation at the top of the facies and biogenic reworking suggests that bathymetry may not have been important in promoting *Zoophycos*. Modern studies show that *Zoophycos* was adapted to a variety of ecological conditions and may occur in a wide range of bathymetric zones. The most important control is thought to be an organic-rich oxygen depleted stressed quiet water setting (Frey and Seilacher, 1980).

Preservation of delicate trace fossil structures such as *Zoophycos* spreiten and the presence of reworked mudclasts associated with the less burrowed and bioturbated, more rapidly deposited tidal channel sands show that mud was originally present on the tidal flat. Its absence in this facies is attributed to erosion and intense bioturbation and thorough mixing of the mud with the sand. Most of the bioturbated sands are mud-rich, and may have been deposited as part of a mixed tidal flat sequence. Modern mixed flats are often highly bioturbated by deposit feeding invertebrates (Weimer *et al.*, 1982).

Palaeocurrent data shows that the preserved channel-fills are dominated by flood (onshore) oriented bed forms. The dominance of ebb or flood tidal bed forms is a characteristic feature of many of the present-day North Sea tidal channels (Weimer *et al.*, 1982). The shallow depths of the channels (<2 m) indicates a microtidal environment (Hayes and Kana, 1977).

SUMMARY AND DEPOSITIONAL MODEL

The Palaeozoic succession in the southeastern part of Al Kufrah basin is punctuated by a series of transgressive and regressive events. The transgressive events are not always easy to identify in the rock record because of the proximal setting of the basin, but at least two major transgressions (Late Ordovician and Middle to Upper Devonian) and two regressions (Silurian and Lower Devonian) have been recognized. Smaller scale transgressions and regressions occur within the Middle and Middle to Upper Devonian, within an overall transgressive sequence. Facies interpretations suggest that the succession may have originated as part of a deltaic shoreline complex, showing both progradational and transgressive phases of deposition (Fig. 4).

Progradation

The coarsening-upward progradational phase of delta building is dominated by a braided delta plain facies which overlies shoreface and marine shelf deposits. This suggests that deposition was fluvially dominated, and that as the braided delta plain prograded basinwards its seaward margin may have been reworked by marine processes as depicted in Fig. 4A. Finer grained sediments were flushed out onto the shelf during progradation. Despite the basinward thickening of the marine shelf facies recorded in the subsurface (Grignani *et al.*, Vol. IV, this Symposium) the shelf shales lack organic material compared to other Palaeozoic basins in Libya. This may reflect the more proximal setting of the basin and the influx of coarse clastics preventing the build-up and concentration of organic material in the bottom sediments.

The erosion surface between the shoreface and braided delta plain facies has been recognized in other parts of Libya where it forms part of a regionally extensive unconformity (Pierobon, this volume; M. Rossi, pers. comm., 1986). Castro *et al.* (1985) report partial to complete truncation of the Silurian by this early to middle Devonian unconformity in the Dūr al Quṣṣah and west Al Qarqaf areas of the Murzuq basin. The presence of Lower Silurian species of *Cruziana* at the top of the shoreface sands (A. Seilacher, pers. comm., 1986) and the absence of the lowermost Devonian in the overlying delta plain facies (Grignani *et al.*, Vol. IV, this Symposium) confirms a major stratigraphic break at this level. Thus, the shoreface sands and overlying delta plain facies were not contemporaneous with one another, and it is uncertain as to whether the shorefacies was attached to a delta, a strand plain or the seaward side of a barrier beach. Although there is evidence of storms in the upper part of the marine shelf facies, these were not severe and do not appear to have affected the shoreface. The channels cut into the top of the shoreface have been interpreted as distributary channels, although they could equally well be supplying sand to the strand plain, or to the shoreface and nearshore shelf via tidal channels. Until the three dimensional geometry of the sand body is determined the problem remains unresolved.

Although the geometry of the delta plain facies is difficult to determine from available outcrop data it probably forms part of a northwesterly thinning clastic wedge that interfingers basinward with more

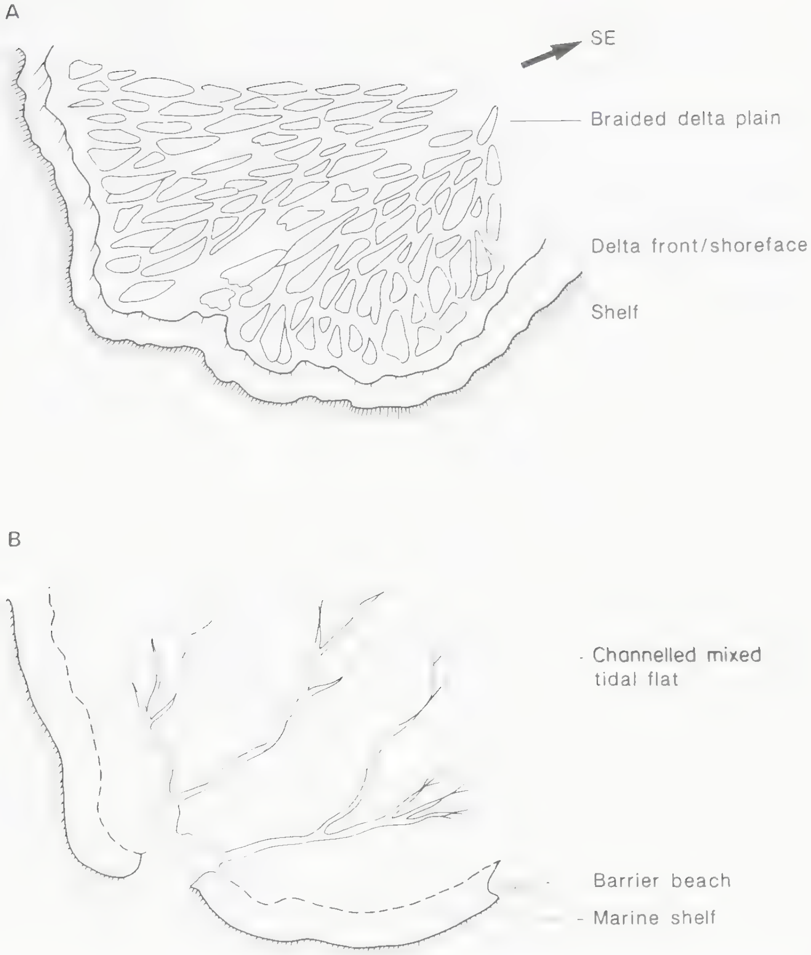

Fig. 4. Generalized depositional model for the Silurian–Devonian succession in northern and central Jabal Asba. A. Delta progradation and contemporaneous reworking of delta plain margin by marine processes. B. Delta abandonment and transgression with reworking of delta plain into a channelled tidal flat.

marine facies. In the AGIP A1 and B1 wells west and south of Al Kufrah oasis up to 80% of the succession is considered to be of continental origin (Grignani *et al.*, Vol. IV, this Symposium) with an overall southward thinning of the Palaeozoic sequence (Bellini *et al.*, Vol. VI, this Symposium). The abundance of continental clastics and lack of marine shales confirms the proximal setting of the depositional system (Turner, 1980).

The erosional surface at the base of the delta plain facies signifies a sudden progradation of the depositional system. The delta plain advanced basinwards across its own distal base as gradients and sediment supply increased. This may be due to delta shifting, tectonism or possibly a fall in sea level. The amount of erosion that has taken place is unknown, but in the Mississippi delta plain channels are capable of eroding more than 30 m below the contemporaneous delta front deposits (McBride *et al.*, 1975). Without adequate subsidence the channels would cut down through the entire delta front/shoreline facies.

Evidence of a marine influence on deposition in the upper part of the braided delta plain facies and the presence of vertical *Skolithos*-type burrows (periods of waning fluvial discharge?) is consistent with the early stages of abandonment and transgression of the delta plain. The marine influence is particularly well marked at the base of the upper delta plain facies where it defines a minor transgressive event. A similar transgression at about this stratigraphic level has been recorded by Castro *et al.* (1985) in the Murzuq basin where the marine facies (estuarine-tidal bar) becomes more abundant basinwards. Another minor transgression lying above a deflation surface was noted by M. Rossi (pers. comm. 1986) at this same stratigraphic level elsewhere in Libya.

The basal transgressive part of the upper part of the delta plain facies is sharply overlain by a major erosion surface. The lateral extent of this surface is unknown but a regional erosional event (unconformity) of late Middle Devonian age has been documented by Pierobon (this volume) in the Murzuq basin. The channelled tidal flat facies above the delta plain records a major transgressive event, as marine conditions spread across the delta plain from the north-northwest. Evidence of this is seen in the burrows and pebble conglomerate along the contact between the two facies. The pebble conglomerate is attributed to transgressive reworking and the formation of a transgressive lag. Thus, part of the succession between the delta plain and channelled tidal flat facies may be missing through erosion, and it is unclear from the evidence whether the tidal flat was barrier protected or not. The presence of well-developed *Skolithos* burrows implies that the tidal flat may have been protected from the full force of the sea. However, such protection could be provided by a coastal embayment and not a barrier beach sand body. As a result of the transgression and diminished fluvial input the delta plain became transformed into a tidal flat (Fig. 4B) fed by nearby active fluvial systems creating tidal creeks and channels draining the flat. The absence of any overlying deeper water marine facies suggests that the transgression was unable to sustain itself, possibly due to a subsequent increase in the rate of fluvial sediment supply to the shoreline. Support for this interpretation is seen in the northern part of Jabal Asba where the tidal flats are succeeded by regressive braided stream deposits at the base of the Carboniferous (Tournaisian to Visean) Dalma Formation (Turner, 1980).

The fining-upward channelled tidal flat sequences are attributed to seaward progradation of the flat. Vertical stacking of these sequences is indicative of a series of transgressive–regressive events, possibly controlled by variations in the rate of subsidence or sediment supply. Preservation of facies depends largely on the rate of sea level rise accompanying transgression (Kraft, 1971). A rapid rise in sea level, for example, may lead to partial or complete retention of the sequences in the rock record (Reinson, 1984). Under these conditions tidal channel deposits have the highest preservation potential, and because of their relatively rapid rate of deposition burrowing and bioturbation is less intense.

It is unclear whether the coastline was barred or non-barred (Fig. 4B). However, an incompletely exposed sequence of shoreface sands occurs stratigraphically below the marine shelf deposits in central and northern Jabal Asba (Fig. 5) (Turner, 1980). The characteristics of these shoreface sands suggest that they may form part of a beach sequence deposited along a coastline of moderate wave energy. The shoreface sands form a coarsening-upward sequence typical of prograding shoreline models, which are normally overlain by other elements of the beach environment (foreshore, backshore, dunes).

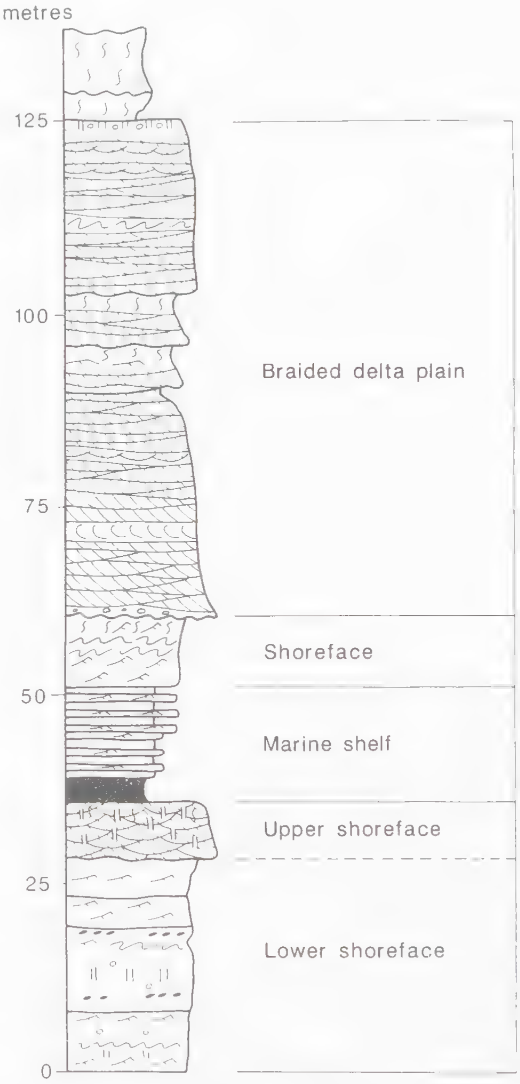

Fig. 5. Measured section through the Palaeozoic succession in central Jabal Asba showing the Silurian marine shelf deposits and the underlying Ordovician shoreface sands. The boundary between them may define a transgressive event.

The incompleteness of the sequence here may reflect its position relative to the shoreline (seaward) or shoreface erosion during a transgressive event. If transgression did occur, the only evidence of it in the rock record is a sharp contact between the shoreface sands and overlying marine shelf facies (Fig. 5). Pierobon (this volume) and Castro *et al.* (1985) consider the lower, more shaley part of the Tannezouft Formation to represent a broad marine transgressive phase of deposition over the North African craton, followed by a regressive phase in the overlying Acacus Formation. In Al Kufrah basin it is difficult to separate transgressive and regressive phases as both the Tannezouft and Acacus appear to form part of a major coarsening-upward progradational sequence. However, the possible presence of a transgression from the north-northwest along the contact of the Memouniat (upper shoreface) and overlying Tannezouft (marine shelf) Formations is consistent with the results of Pierobon (this volume) in the Murzuq basin in southwest Libya where transgressive–regressive events have been correlated with the sea level curves of Vail *et al.* (1977).

REFERENCES

AGIP (1976). Kufra Basin Study. Technical Rep. Tripoli.

ALLEN, J.R.L. (1983). Studies in Fluviatile sedimentation: bars, bar complexes and sandstone sheets (low sinuosity braided streams) in the Brownstones (L. Devonian), Welsh Borders. *Sediment. Geol.*, **33**, 237–293.

BELLINI, E., GIORI, E., ASHURI, O. and BENELLI, F. (1991). Geology of Al Kufrah basin. (Vol. VI, this Symposium).

CASTRO, J.C., DELLA FAVERA, J.C. and EL-JADI, M. (1985). Palaeozoic sedimentary facies, Murzuq Basin, Socialist People's Libyan Arab Jamahiriya. Internal Report, Braspetro-Petrobras, Rio de Janeiro, 117 p.

COLEMAN, J.M. (1976). *Deltas: Processes of Deposition and Models for Exploration*. Continuing Educ. Publ. Co., Champaign, Ill., 102 p.

COLEMAN, J.M. and PRIOR, D.B. (1982). Deltaic Environments. *In*: Sandstone Depositional Environments (*eds* P.S. Scholle and Darwin Spearing). *Mem. Am. Assoc. Petrol. Geol.*, **31**, 139–178.

CRIMES, T.P. (1970). The significance of trace fossils in sedimentology, stratigraphy, and palaeoecology with examples from Lower Palaeozoic strata. *In*: Trace Fossils (*eds* T.P. Crimes and J.C. Harper). *Geol. J. Spec. Issue*, **3**, 101–126.

FREY, R.W. and PEMBERTON, S.G. (1984). Trace fossil facies models. *In: Facies Models* (*ed.* R.G. Walker). Geoscience Canada, Reprint Series, **1**, 189–208.

FREY, R.W. and SEILACHER, A. (1980). Uniformity in marine invertebrate ichnology. *Lethaia*, **13**, 183–207.

GRIGNANI, D., LANZONI, E. and ELATRASH, H. (1991). Mesozoic and Palaeozoic subsurface palynostratigraphy in Al Kufrah Basin. (Vol. IV, this Symposium).

HASZELDINE, R.S. (1983). Fluvial bars reconstructed from a deep, straight channel, Upper Carboniferous coalfield of northeast England. *J. Sediment. Petrology*, **53**, 1233–1248.

HAYES, M.O. (1967). Hurricanes as geological agents: case studies of hurricanes Carla, 1961, and Cindy, 1963. *Bur. Econ. Geol.*, Rep. Invest. No. 61, Univ. Texas, Austin, 54 p.

HAYES, M.D. and KANA, T.W. (1977). Terrigenous Clastic Depositional Environments some modern examples. *Univ. South Carolina, Tech. Rep.*, 11-CRD, 131 p.

JANSA, L.F. (1975). Tidal deposits in the Zabriskie Quartzite (Cambrian), eastern California and Western Nevada. *In: Tidal Deposits* (*ed.* R.N. Ginsburg). Springer-Verlag, Berlin, 153–162.

KRAFT, J.C. (1971). Sedimentary facies patterns and geological history of a Holocene marine transgression. *Bull. Geol. Soc. Am.*, **82**, 2131–2158.

MCBRIDE, E.F., WEIDIE, A.E. and WOLLENBEN, J.A. (1975). Deltaic and associated deposits of Difunta Group (Late Cretaceous to Paleocene), Parras and La Popa Basins, Northeast Mexico. *In: Deltas* (*ed.* M.L. Broussard). Houston Geol. Soc., 485–522.

MIALL, A.D. (1977). A review of the braided river depositional environment. *Earth Sci. Rev.*, **13**,1–62.

MIALL, A.D. (1983). Architectural-element analysis: a new method of facies analysis applied to fluvial deposits. *Earth Sci. Rev.*, **22**, 261–308.

PIEROBON, E.S.T. (1991). Contribution to the stratigraphy of Murzuq Basin, Great Socialist People's Libyan Arab Jamahiriya. (This volume).

REINECK, H.E. and SINGH, I.B. (1973). *Depositional Sedimentary Environments*. Springer-Verlag, Berlin, 439 p.

REINSON, G.E. (1984). Barrier island and associated strandplain systems. *In: Facies Models* (*ed.* R.G. Walker). Geoscience Canada, Reprint Series, **1**, 119–140.

RHOADS, D.C. (1967). Biogenic reworking of intertidal and subtidal sediments in Barnstable Harbour and Buzzards Bay, Massachusetts. *J. Geol.*, **75**, 461–476.

SEILACHER, A. (1967). Bathymetry of trace fossils. *Mar. Geol.*, **5**, 413–428.

SMITH, N.D. (1970). The braided river depositional environment: comparison of the Platte River with some Silurian clastic rocks, north-central Appalachians. *Bull. Geol. Soc. Am.*, **81**, 2993–3014.

STERNBERG, R.W. and MCMANUS, D.A. (1972). Implications of sediment dispersal from long-term bottom current measurements on the continental shelf of Washington. *In: Shelf Sediment Transport, Processes and Patterns* (*eds* D.J.P. Swift, D.P. Duane and O.H. Pilkey). Dowden, Hutchinson and Ross, Stroudsberg, Pa., 303–372.

SWIFT, D.J.P., STANLEY, D.J. and CURRAY, J.R. (1971). Relic sediments on continental shelves: a construction. *J. Geol.*, **79**, 322–346.

TANKARD, A.J. and BARWIS, J.H. (1983). Wave dominated deltaic sedimentation in the Devonian Bokkeveld Basin of South Africa. *J. Sediment. Petrology*, **52**, 959–974.

TURNER, B.R. (1980). Palaeozoic sedimentology of the southeastern part of Al Kufrah Basin, Libya: a model for oil exploration. *In: The Geology of Libya* (*eds* M.J. Salem and M.T. Busrewil). Academic Press, London, **II**, 351–374.

TURNER, B.R. and BENTON, M.J. (1983). Palaeozoic trace fossils from the Kufra Basin, Libya. *J. Paleontol.*, **57**, 447–460.

VAIL, P.R., MITCHUM, R.M. and THOMPSON, S. (1977). Seismic stratigraphy and global changes of sea level from coastal onlap. *In*: Seismic Stratigraphy — Applications to hydrocarbon exploration. (*ed.* C.E. Payton). *Mem. Am. Assoc. Petrol. Geol.*, **26**, 83–98.

VOS, R.G. (1977). Sedimentology of an upper Palaeozoic river, wave and tide influenced delta system in southern Morocco. *J. Sediment. Petrology*, **47**, 1242–1260.

WEIMER, R.J., HOWARD, J.D. and LINDSAY, D.R. (1982). Tidal Flats. *In*: Sandstone Depositional Environments (*eds* P.A. Scholle and Darwin Spearing). *Mem. Am. Assoc. Petrol. Geol.*, **31**, 191–246.

Sedimentology of the Silurian–Devonian Series in the Southeastern Part of the Ghadāmis Basin

V. Bracaccia[1], C. Carcano[1] and K. Drera[1]

الجيولوجيا الترسيبية للمجموعة السيلورية الديڤونية بجنوب شرقي حوض الحمادة الحمراء الترسيبي

ف. براكاشيا وس. كاركانو وك. دريرة

الخلاصـــة

لقد تمت دراسة التطور الترسيبي للسلسلة الفتاتية التي ترجع إلى الحينين السيلوري والديڤوني بالجانب الجنوبي الشرقي لحوض الحمادة الحمراء، وذلك بواسطة تحليل معلومات السرود ومضاهاة الآبار وتحليل البيئات الترسيبية.

وبالرغم من أن هذه الدراسة تخص منطقة محددة من حوض الحمادة فإنها توفر الدليل على بعض التغيرات الرئيسة للسحنات في بعض الوحدات الفتاتية، كما أنها تعطي الدليل على العلاقة بين زمن ومكان ترسيب الوحدات الصخرية.

وحيث أن مرتفعات طرابلس — تيبستي وقرقاف قد كانت موجودة منذ بداية الحين السيلوري الباكر، فان ذلك ساعد على تضخيم الإختلافات بين السحنات أفقياً. ويبدو أن بيئات الترسيب قد بقيت على نفس الوتيرة طوال الحينين السيلوري والديڤونى ما عدا زمن الديڤونى الأوسط. وقد تم تمييز عدة دورات ترسيبية في التتابع الطبقي العام. ويمكن أن يعزى ذلك إلى زمن ومكان إنتقال الحاجز البيئي مع مسطح مد وجزر متكامل.

وعموماً فإن كل الدورات الترسيبية مبتورة القاعدة. ويمكن إرجاع هذه الفجوة الطبقية إلى سرعة إندفاع مياه البحر المتقدمة فوق أرضية منبسطة. وهكذا فإن الترسيب قد تحكمت فيه تغيرات مستوى مياه سطح البحر و(أو) الحركات التكتونية الخفيفة.

وربما يفسر وجود تتابع انحساري سميك تدفق المياه العذبة شمالاً الذي قد أثر بالمنطقة.

ومن المحتمل أن تكون هذه العملية الهيدروديناميكية قد أثرت في هجرة النفط شمالاً، خصوصاً وإن المصائد التركيبية غير مزودة بموانع تكتونية في الجنوب. وعملياً فإن الذي يؤمن تجمعات النفط ضد تدفق المياه العذبة هي الأجسام الرملية العدسية ضمن دورات تقدم مياه البحر. وفي الحقيقة تحت هذه الظروف فقط، يمكن أن تتكون مكامن رملية (جزر الحواجز الرملية) مغطاة بطفل بحري عديم النفاذية لتعمل كمانع جيد للتسرب. وعلى العكس من ذلك، فإن الإستمرارية الجانبية الجديدة يمكن أن تنبيء بوجود جزر حواجز من الصخور الرملية، وهذه من المرجح أن تتغير إلى أعلى إلى سحنات بحيرات شاطئية (قنوات حد) ونهرية ذات نفاذية.

Abstract. The sedimentary evolution of the Silurian–Devonian clastic series in the subcrop of the SE flank of the Ghadāmis basin has been studied through log analysis, well correlations and sedimentological environmental interpretation.

This study, although relevant to only a restricted area of the basin, includes evidence of some major lateral facies variations within some of the clastic units. Lateral facies variations are magnified in this area where the "Tripoli–Tībistī" and "Al Qarqaf" uplifts have been acting as structural highs, at least from Lower Silurian time.

The sedimentary environment seems to have been stable for almost all the Silurian and Devonian, except for the middle Devonian period, but several sedimentary cycles have been recognized in the overall sequence. They can be related to the time–space migration of an"arcuate delta–delta-estuary(?)" complex with a well-developed tidal flat.

Almost all of the sedimentary cycles are "base truncated"; this basal stratigraphic "gap" is normally due to fast transgressive pulses over the very flat palaeolandscape. The presence of thick regressive sequences could explain the heavy northward freshwater flushing that affects the area.

---

[1] AGIP NAME, P.O. Box 346, Tripoli, Libya, G.S.P.L.A.J.

This hydrodynamic process probably led to the generalized northward migration of the generated oil, especially if the structural traps are not provided with a tectonic sealing to the south.

In practice, only lenticular sand bodies within transgressive and well-developed cycles could secure oil accumulations from the freshwater flushing. In fact under these conditions possible "tide ridges" and "barrier island" sandstone reservoirs are overlain by impervious marine shales, thus providing a good seal.

On the contrary, within regressive cycles, a good lateral continuity could be forecast for the same sandstone bodies. These are very likely to pass updip (southwards) into permeable tidal (tidal channels), and fluvial facies.

GEOLOGICAL OUTLINE

The area is located in the Ghadāmis basin, NW Libya (Fig. 1). The Ghadāmis basin is one of the major depositional basins of North Africa extending into large areas of the eastern Algerian desert and southern Tunisia. It has a NE–SW axis, and is delimited in the north by the Nafūsah uplift and to the east and south by the Hūn graben and by the Al Qarqaf uplift, respectively. The basin is mostly filled by Palaeozoic rocks overlain by a relatively thin Mesozoic–Tertiary sequence.

METHOD OF STUDY

This study is mainly based on the well data relevant to NC40A + B Contract sub-areas, granted to AGIP NAME, together with traded data of the surrounding areas.

Lithological descriptions, cores, wireline logs and test results were taken into consideration in attempting the reconstruction of the sedimentary evolution of this part of the Ghadāmis basin.

In particular, the thickness and lithological variations of each unit, integrated with the sedimentological and depositional interpretation of the cores and the presence of electrical "markers", themselves assuming an environmental meaning, have been arranged so as to define different sedimentary cycles.

GEOLOGY AND HYDROCARBON OCCURRENCES

The stratigraphic series is mainly made up of clastic sediments except for the uppermost carbonatic units.

The northern portion of the study area lies near the synclinal axis which has a NE–SW strike. Southward, the sedimentary sequence outcrops on Al Qarqaf uplift. This regional high is probably due to the Caledonian orogenesis. In fact the Lower Devonian unconformity, related to this Lower Palaeozoic phase, reaches its maximum erosional extent on Al Qarqaf uplift.

Another major unconformity marks the end of the Palaeozoic Era and it is certainly related to the Hercynian orogenesis.

Westward, the Permo-Triassic sequence lies on gently folded Hercynian structures, while southwards the stratigraphic gap gets wide and the Cretaceous sediments rest unconformably on the Palaeozoic series.

Other erosional surfaces are present in the overall Palaeozoic–Tertiary sequence, but most of them are simply due to the sedimentary evolution of the basin related to the latero-vertical migration of transitional environments. The above-mentioned tectonic phases affect the Ghadāmis basin, with folds and faults having different trends. The Ordovician–Silurian units are gently folded by the Caledonian phase.

Most Ordovician structures dip NNW. Hercynian structures develop with E–W (northern part of Ghadāmis basin) and NE–SW trends.

The major targets, as far as hydrocarbon exploration is concerned, are the sandstone intervals of Palaeozoic age, out of Ras Hamia Formation which are, however, missing in the SE area.

From the top to the bottom, the main targets of the area can be referred to as sandstone bodies within:

- Tahara Formation (Devonian–Carboniferous?)
- Aouinet–Ouenine Group (Devonian)
- Tadrart Formation (Devonian)
- Acacus Formation (Silurian)
- Memouniat Formation (Ordovician)

These stratigraphic units, almost all deposited in a transitional environment, provide both seal and reservoir rocks for the possible generation of hydrocarbons. The Tanezzuft Formation (Silurian) is reputed to be a good source rock as far as oil generation is concerned and, furthermore, the shales interbedded within the reservoirs could contribute, at least partially, to hydrocarbon generation.

An unfavourable element for hydrocarbon accumulation in this area together with the lack of large structural closures, is represented by a generalized south to north freshwater flushing. This, starting from the Palaeozoic outcrops on Al Qarqaf uplift, affects, to different degrees, almost all the possible reservoirs.

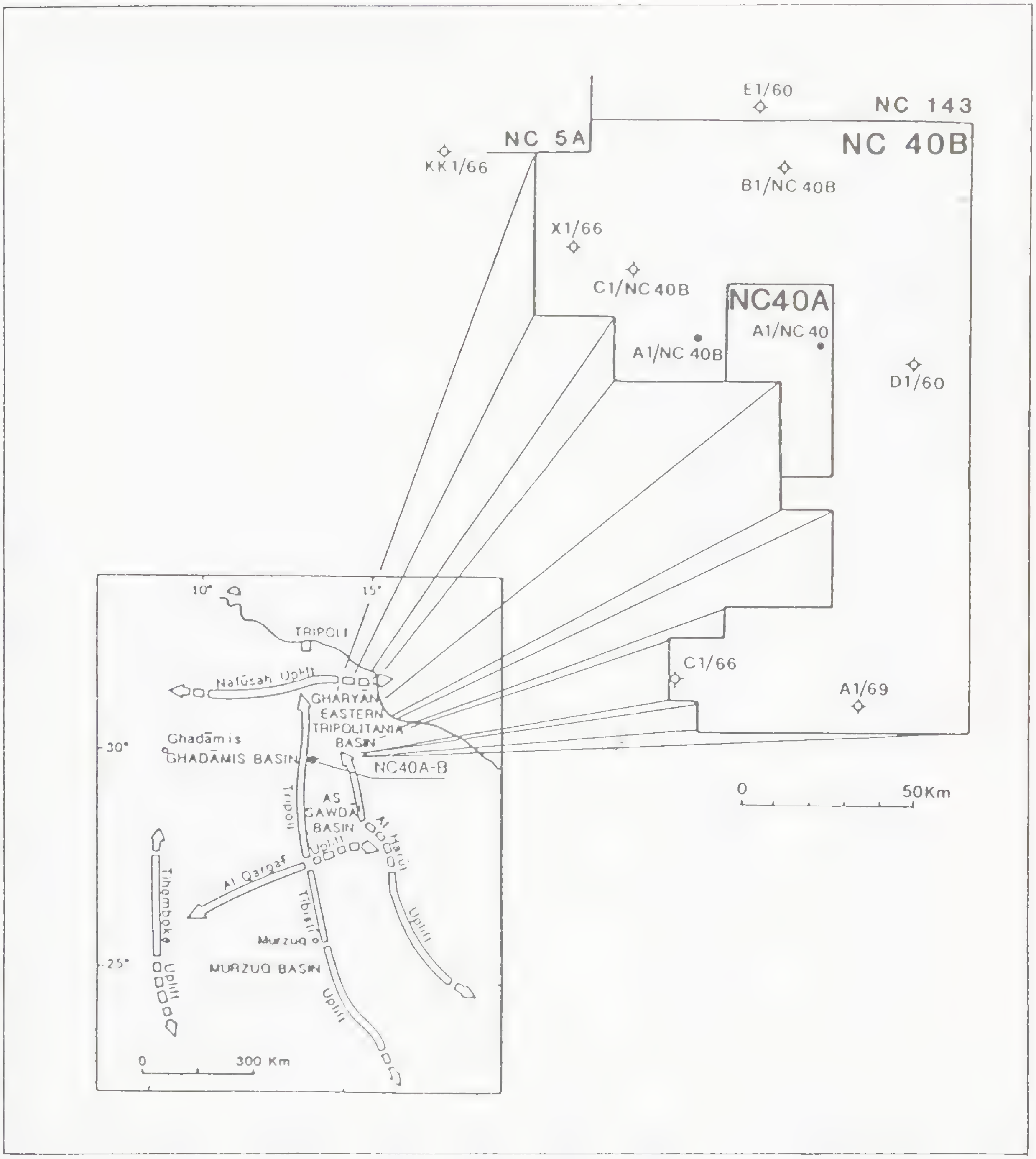
E1/60
NC 143
NC 5A
NC 40B
KK1/66
B1/NC 40B
X1/66
C1/NC 40B
NC40A
A1/NC 40
A1/NC 40B
D1/60
C1/66
A1/69
0
50Km
10°
15°
TRIPOLI
Nafūsah Uplift
GHARYAN
EASTERN
TRIPOLITANIA
BASIN
30°
Ghadāmis
GHADĀMIS BASIN
NC40A-B
AS
SAWDA
BASIN
Tripoli
Al Haruj
Uplift
Al Qarqaf
Tihombokа
Tibisti
Uplift
Murzuq
25°
MURZUQ BASIN
Uplift
Uplift
0
300 Km

Fig. 1. Location of the area studied.

THE SILURIAN–DEVONIAN SEQUENCE

The Silurian–Devonian (plus Upper Ordovician) series will be considered both from an environmental and depositional point of view in an attempt to form a tentative reconstruction of the sedimentary evolution of the basin.

As core interpretation shows, sedimentation seems to have been quite uniform within the transitional environment, in spite of two major phases of orogenesis.

Fortunately, the interpretation and the careful analysis of the electrical logs reveal some "electrical markers" whose correlation can be considered as following isochronal lines in the evolution of this wide sedimentary basin.

SEDIMENTOLOGY

The sedimentology and the related environments of the core units investigated so far by AGIP NAME will be discussed.

Except for the Aouinet–Ouenine Group and the Ouan Kasa Formation, each formation has at least one core cut. The cores (Figs 2–4) give quite a good picture of the environment dominating the area during the Silurian–Devonian (plus Upper Ordovician) period and of the large-scale environmental changes.

FACIES AND FACIES ASSOCIATIONS

The analysis and the interpretation of the core sequence (with the detection of diagnostic sedimentary structures) allow ten different facies to be singled out.

Each one of these facies can be related to a peculiar sedimentary process within a particular environment and/or subenvironment.

Different facies were then grouped according to their lateral–vertical relationships, in facies associations.

The facies associations reflect the diagnostic characters of an environment and/or subenvironment within a depositional complex.

Facies Description

The different sedimentary facies, as far as lithological and sedimentological characters are concerned, can be summarized as follows:

"Facies a". Black silty shales and black pyritic shales with thin (max. 2 cm) interbeds of fine-grained sandstone and/or sandstone lenses. Sand/shale ratio $\ll 1$. The sandstone intervals show lenticular and wavy beddings.

Ripple lamination is often present as a single set. Bioturbation is very light or completely lacking. In this particular case, oligotypical benthonic shell casts are abundant. This fact reflects a very restricted environment with peculiar bottom conditions.

"Facies b". Black silty shales with frequent interbeds of fine-grained sandstones. (max. 5 cm). Sand/shale ratio from <1 to >1. Sedimentary structures are present as lenticular to wavy to flaser beddings. The sediment is sometimes heavily bioturbated and deformed by load.

"Facies c". Sandstone, fine to medium grained, in layers up to 10–15 cm thick. The base is always erosional. Ripple cross- and "hummocky" beddings are the most typical sedimentary structures. The facies is always associated with facies a and b but, especially in the latter case, it does not appear so much involved in processes of load deformation and bioturbation.

"Facies d". Sandstone, fine- to medium-grained, in layers up to 50 cm thick, the base is sharp and only lightly erosional. Sedimentary structures are: lack of appreciable grading, wedge — "low angle" — trough cross-beddings, sometimes associated with planar bedding. Flaser and "herringbone" beddings are sometimes present. This facies seems to be related to migration–progradation processes (due to avalanching megaripples) of tidally influenced sand bars.

"Facies e". Sandstone, sometimes glauconitic, coarse- to medium-grained in layers up to 150 cm thick, with erosional base.

The sedimentary structures are sometimes not very clear save for the graded bedding. The structures, when clear, are the inclined bedding and cross-trough (sometimes bipolar) to planar cross-beddings. Shell fragments are occasionally present as "lag deposit" and/or aligned along cripto-laminae.

"Facies f". Sandstone, coarse- to medium-grained with erosional base in layers 5–25 cm thick. It shows structures such as grading, cross-trough and "herringbone" to flaser bedding. Burrowing is present. This facies is associated with "facies e".

"Facies g". Sandstone quartzose, well sorted and clean, coarse- to medium-grained, with erosional base in layers up to 40 cm thick. It shows graded bedding and inclined to planar cross bedding. Shell fragments are present at the base associated with some clay pebbles. This facies is connected with "facies h".

"Facies h". Sandstone, fine- to medium-grained, in layers up to 100 cm thick. The base is sharp but not erosional. Grading is not appreciable; trough-

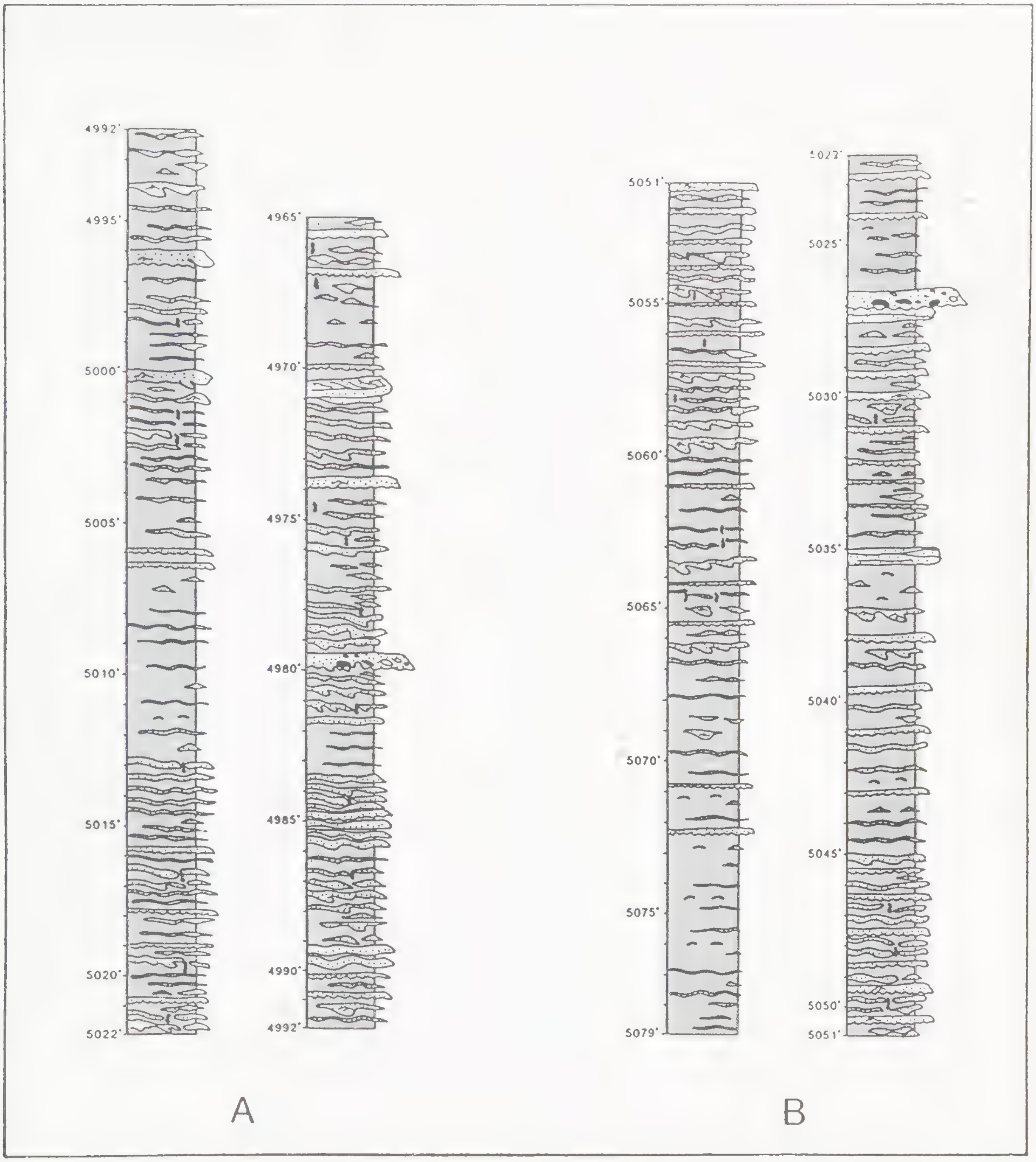
4992'
4995'
5000'
5005'
5010'
5015'
5020'
5022'
4965'
4970'
4975'
4980'
4985'
4990'
4992'
A
5051'
5055'
5060'
5065'
5070'
5075'
5079'
5023'
5025'
5030'
5035'
5040'
5045'
5050'
5051'
B

Fig. 2. A. A1 NC-40B, Core 1, Tahara Formation. B. A1 NC-40B, Core 2, Tahara Formation.

cross to wedge and planar beddings are present. Sediments are sometimes deformed by load.

"Facies i". Sandstone, fine and well sorted, with wedge lamination and "low angle" cross bedding. Shell fragments are present along the laminae. Base lightly erosional on facies "h".

"Facies j". Extra formational breccias, up to 15 cm thick, with shale pebbles and sand-silty matrix. The sediment is weathered and oxidized. The base is erosional.

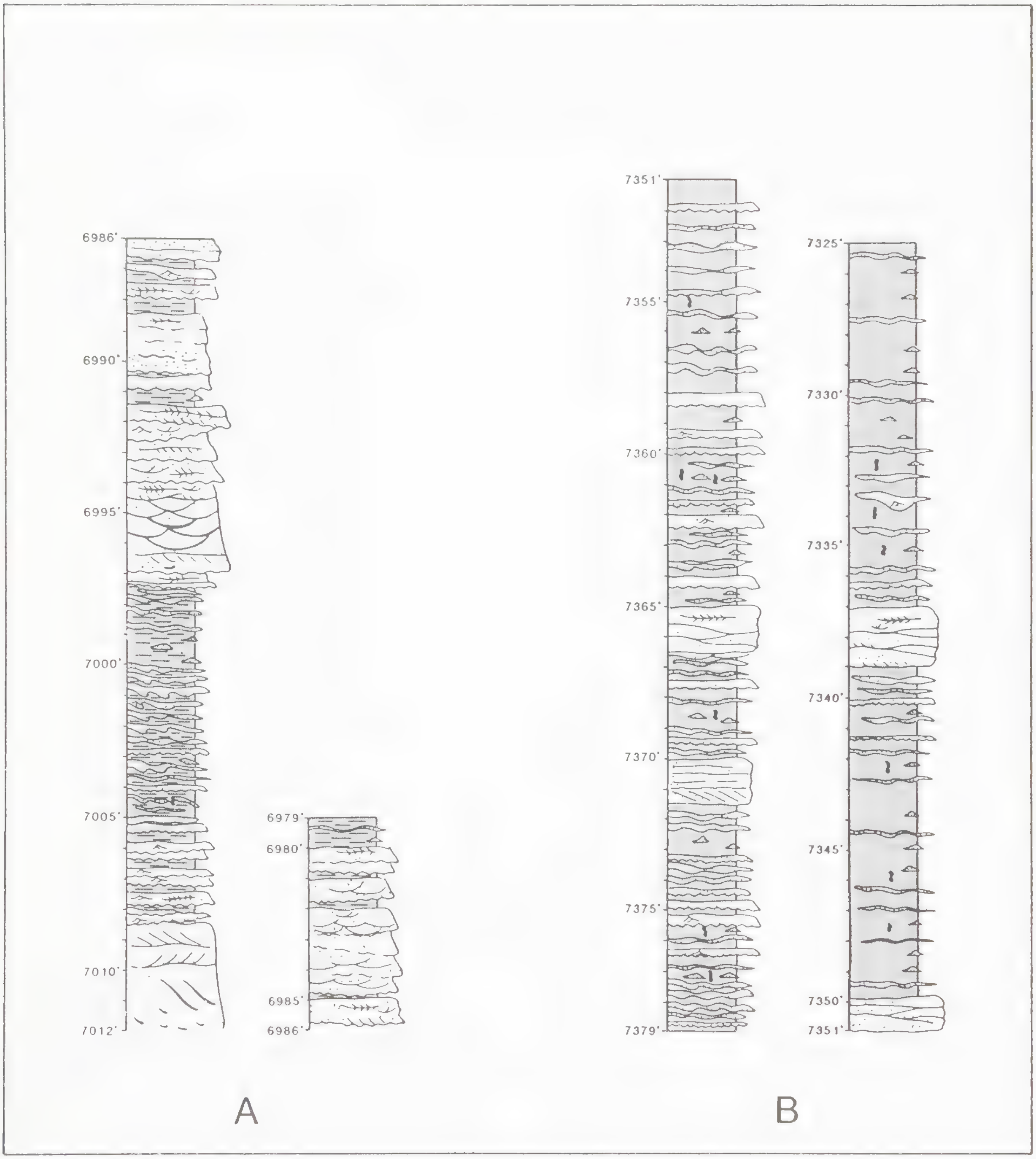
6986'
6990'
6995'
7000'
7005'
7010'
7012'
6979'
6980'
6985'
6986'
A
7351'
7355'
7360'
7365'
7370'
7375'
7379'
7325'
7330'
7335'
7340'
7345'
7350'
7351'
B

Fig. 3. A. A1 NC-40B, Core 3, Acacus Formation. B. A1 NC-40B, Core 4, Acacus Formation.

Facies Interpretation

"Facies a" could be referred to as a protected lagoonal environment, probably with reducing bottom conditions as is suggested by pyrite and an oligotypical fauna.

Thin interbeds of sandstone, with lenticular bedding and sand lenses are related to tidal action within the protected lagoon, where the deposition was mainly due to clay flocculation.

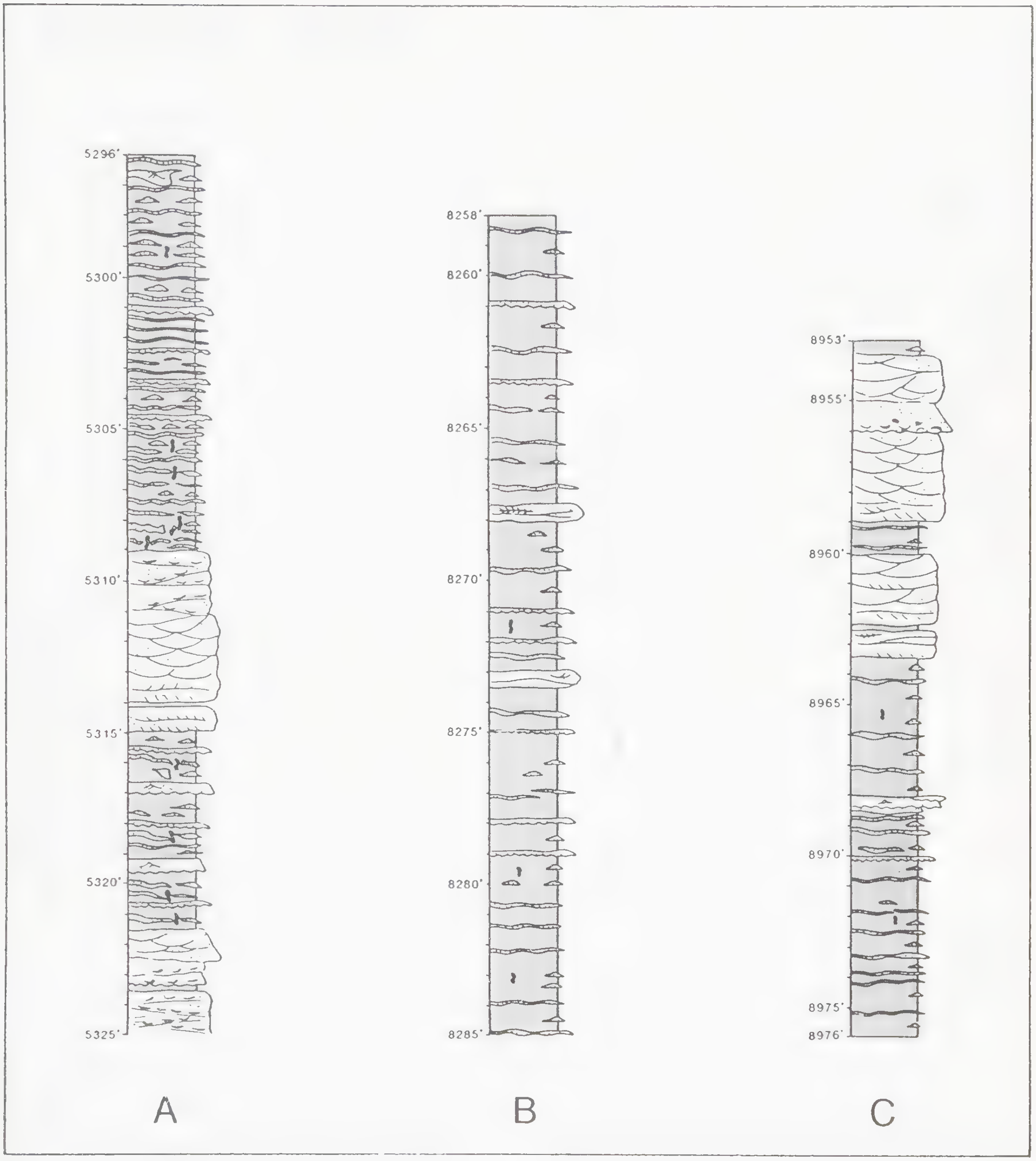
5296'
5300'
5305'
5310'
5315'
5320'
5325'
8258'
8260'
8265'
8270'
8275'
8280'
8285'
8953'
8955'
8960'
8965'
8970'
8975'
8976'
A
B
C

Fig. 4.. A. C1 NC-40B, Core 1, Tahara Formation. B. C1 NC-40B, Core 2, Tanezzuft Formation. C. C1 NC-40B, Core 3, Memouniat Formation.

"Facies b" is connected to a higher energy subenvironment like the intertidal flat (mixed flat), that is normally dominated by tidal action. In any case, sequences with sand/shale ratio <1 could be relevant to supratidal (mud flat) deposition (Ricci-Lucchi, 1970; Reineck and Singh, 1973). A better marine organic supply and/or more oxygenated bottom conditions allow a heavy bioturbation.

Load deformations are due to the thixotropic behaviour of the mud deposited during lower energy periods.

"Facies c" is related to high energy streams (storms?) that could erode the tidal flat sediments and then deposit sand layers with ripple-cross and "hummocky" bedding.

"Facies d" reflects the migration (progradation) within the tidal flats of the sand bars. As indicated by the sedimentary structures this facies could be related to "tide ridges" within an open tidal inlet.

"Facies e" represents the tidal and/or distributary channel deposit. The channel movement could be either fluvial or tidal, depending on which of these two processes was prevalent.

The presence of inclined bedding could suggest the meandering geometry of some of these channels, with "point bars" prograding within the erosional surface.

"Facies f" reflects "scour and fill' sedimentation processes. These cut the top of the channel bar and the tidal flat deposits close to the channel during the highest energy tides and/or floods.

The textural characters and sedimentary structures of "Facies g" show that we are dealing with a marine-nearshore sediment deposited within a barrier beach (subtidal shoreface). The presence of grey clay pebbles and shell fragments at the base, lead to the conclusion that this facies could be related to a "washover" fan.

"Facies h" can be referred to littoral deposits (Ingle, 1975). The stratigraphic position of this facies within the cores and its association with tidal flat deposits could suggest its relation to the "subtidal shoreface" of a beach ridge.

"Facies i" presents peculiar structures such as "wedge" or low-angle cross-bedding, and textural characters such as sorting, that matches the "fore shore facies" within the beach-ridge environment.

"Facies j" is related to high-energy continental derived streams, unusual within facies "a and b" deposits. The textural character of this facies with chaotic sediments, could be referred to unconfined flood streams.

Facies Associations

The "mixed" tidal flat (facies "b") is the lithotype most represented in the overall core sequence.

This fact would suggest persistent or transitional conditions of deposition over the area from the Upper Ordovician up to the end of the Devonian.

The association of the tidal flat with other sedimentary facies, most of them diagnostic of peculiar physiographic elements, reflects the development of different subenvironments within a transitional complex, either under depositional regression or relative transgressive pulses.

The following facies associations are proposed:

Facies association "A"

This is made up of facies "a–b–c–j"; it represents the depositional results of a protected tidal flat. Here, in fact, lagoonal-type sediments could be deposited in very restricted areas, behind a physiographic barrier (beach ridge and/or barrier island) together with continental flood sediments.

This environment could be referred to as a lagoonal tidal flat complex, lateral to an arcuate type delta. (Allen, 1965, 1970; Le Blanc, 1972; Ricci-Lucchi, 1980).

Facies association "B"

This is represented by three facies: "b–c–d". The presence of tide ridges associated with tidal flat sediments could suggest the disappearance of possible barriers to the open shelf, and the deposition of large tidal inlets within an estuary fringe zone. (Coleman *et al.*, 1970; Coleman and Wright, 1975).

Facies association "C"

Facies association "C" is characterized by "facies e and f". These two facies are related to the subtidal channel deposits of a tidally influenced delta plain. They cut laterally and are overlain by interchannel sediments of the tidal flat.

Facies association "D"

Facies association "D" is characterized by facies "g–h–i". It represents on the whole, the beach ridge "shoreface–foreshore" sediments, with possible "washover fan" episodes. These sediments are genetically related to the progradation of an arcuate-type delta and provide the physiographic barrier to the lagoonal tidal flats.

LOG ANALYSIS AND CORRELATIONS

An arcuate log analysis and interpretation has revealed peculiar lithofacies whose position within sedimentary sequences has given a better understanding of lateral facies variations. In practice it is possible to correlate some diagnostic electrofacies to bottom hole cores and/or sidewall cores. These results are then extrapolated, in terms of electrofacies, over the whole area.

Some electrofacies were detected as being relevant to particular lithofacies.

The position of these lithofacies within different sedimentary cycles (*i.e.* haematitic sandstone layers over tidal flat sediments recognized in the cores) allows a better understanding of the sedimentary evolution of the basin.

MARKER LAYERS

Layers with "abnormal" log responses, related to particular lithologies and defined marker layers, have been recognized in the different units.

Aouinet–Ouenine Group. A limestone layer (Fig. 5), 10–25 ft thick, is present in all the wells of the area, at about 30–70 m below the top of the unit.

Due to its reduced thickness it is hardly spotted from the cuttings but it is easily recognizable from the logs. High resistivity and moreover, high gamma ray values, due to an unusually high uranium content, characterize the "*Tornoceras*" limestone layer. This layer also presents a marker on the seismic sections.

Ouan Kasa Formation and Acacus Formation. Both units are characterized by the presence of sandstone layers rich in iron oxides (Fig. 6) at the top and near the bottom of the Ouan Kasa Formation and in the uppermost part of the Acacus Formation. These sandstone layers rich in iron oxides are widespread all over the investigated area and acquire great importance for correlations. They are not present in a few wells (A1-NC40 and D1/60): in these cases it becomes difficult, if not impossible, to discriminate between the Acacus Formation and the Tadrart Formation.

The iron oxide-rich layers are easily detected from cuttings and from log interpretations. These layers are easily recognized through the logs because they give very peculiar electrical and density responses if the layer is thick and the heavy mineral content is sufficiently high to be properly detected. Abrupt drops of resistivity values compared to the nearby clean, water-bearing sandstone layers and an increase in density up to 2.85 g/cc, are among the characteristics of the layers.

Tanezzuft Formation. Inside this unit black shale layers are present (Fig. 7), a first one (30–60 m thick) occurs at the very bottom and a second one (15–60 m thick) is located roughly in the middle part of the formation. These layers are described from the cuttings as black shale, very rich in carbonaceous matter. On the logs they are distinguished by high GR values, 200° API to more than 350° API.

In the wells where the GR was not recorded it is still possible to define them through their resistivity. In fact these layers normally show high resistivity values (200–2000 ohm/m). In more recently drilled wells, where the NGS have been run, through the comparison of SGR and CGR curves, the high radioactivity is associated with an abnormally high uranium content.

SEDIMENTARY EVOLUTION

It is possible to postulate a picture of the sedimentary evolution of this part of the Ghadāmis basin by integrating the sedimentological data with the presence of "marker layers" (and their environmental meaning) and by taking into consideration the thickness variations of each unit.

This approach would allow some sedimentary cycles to be defined within the Silurian–Devonian series.

Most of the sequences that were singled out would represent major sedimentary cycles (II order) and were therefore strongly regulated by external factors such as sea level changes and tectonics.

In any case, minor cycles could also be accounted for and possibly detected.

These could be controlled by those inner dynamic processes that do not seem to be very important as far as the development of the major cycles is concerned.

Figures 8 and 9 summarize the stratigraphic relationships existing among the different units for the Ordovician–Silurian and Devonian periods.

Ordovician Deposition

Memouniat Formation (the deepest target of the area) is the only Ordovician unit known, at least in its upper part, from an environmental and sedimentological point of view. The depositional environment is characterized by beach deposits (within a barrier island) and tidal flat sediments.

Silurian Deposition

The Tanezzuft Formation sediments, deposited over the regional unconformity that marks the top of the

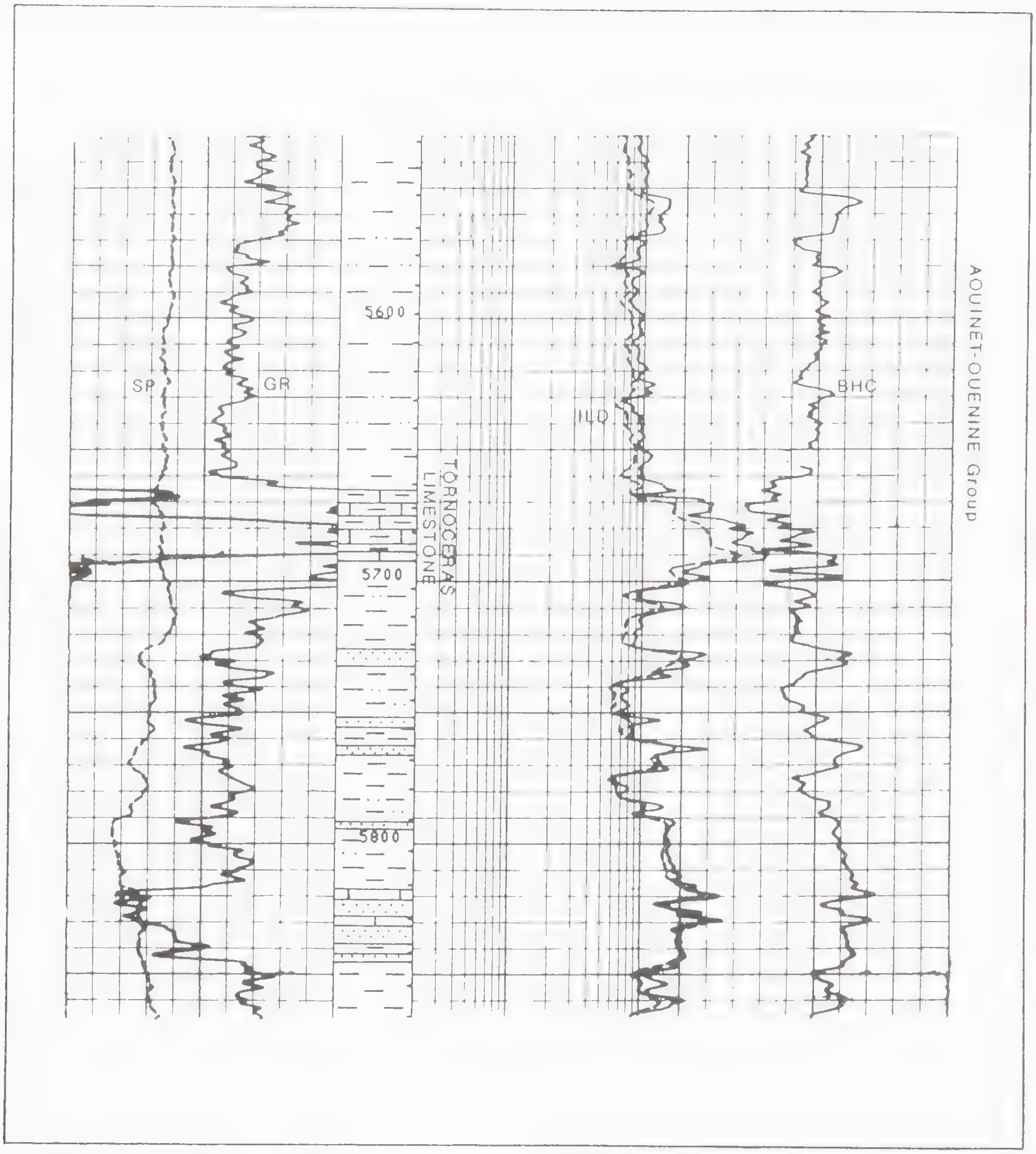

Fig. 5. Wireline logs relevant to the "*Tornoceras*" limestone layer, Aouinet–Ouenine Formation.

Memouniat Formation, are represented by two peculiar lithofacies:

- very radioactive shales rich in organic carbonaceous matter and probably corresponding to a marsh;
- tidal flat, muddy, deposits (as shown by the cores).

The marsh seems to have dominated the southern part of the Ghadāmis basin during the early Silurian, suggesting Al Qarqaf area was already acting as a structural high.

The interfingering between marsh deposits and tidal and/or transitional marine sediments to the north stands for transgressive–regressive pulses, whose extent seems to be regional.

The Acacus Formation is normally divided into three members. Each one of these from both geometrical and sedimentological characters, can be accounted for by giving particular stratigraphic and environmental meanings.

The sandy portion of the Acacus 3rd member thickens towards the basin axis and pinches

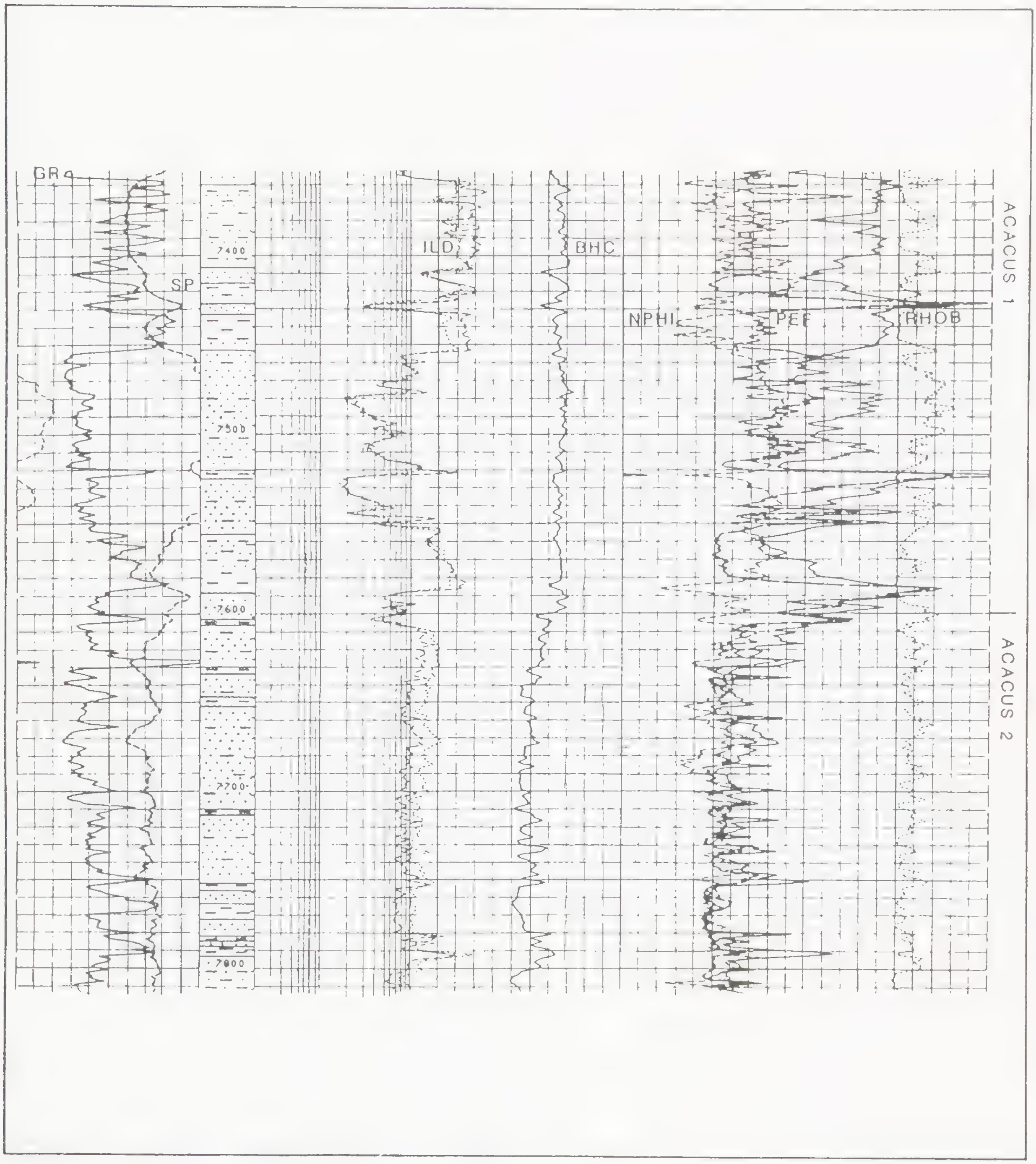

Fig. 6. Wireline logs relevant to the "iron oxide-rich" layers, Acacus Formation, unit 1.

out on the the Al Qarqaf emerging area, and to the NE, passing to shaley deposits. For these geometrical and lithological characters this sand body could be related to a depositional regression (deltaic?).

According to the sedimentological evidence, the heteropic shaley unit is made up of estuarine "tidal flat" sediments.

The Acacus 2nd member deposition is still connected to a wide tidal flat (with subtidal channellized

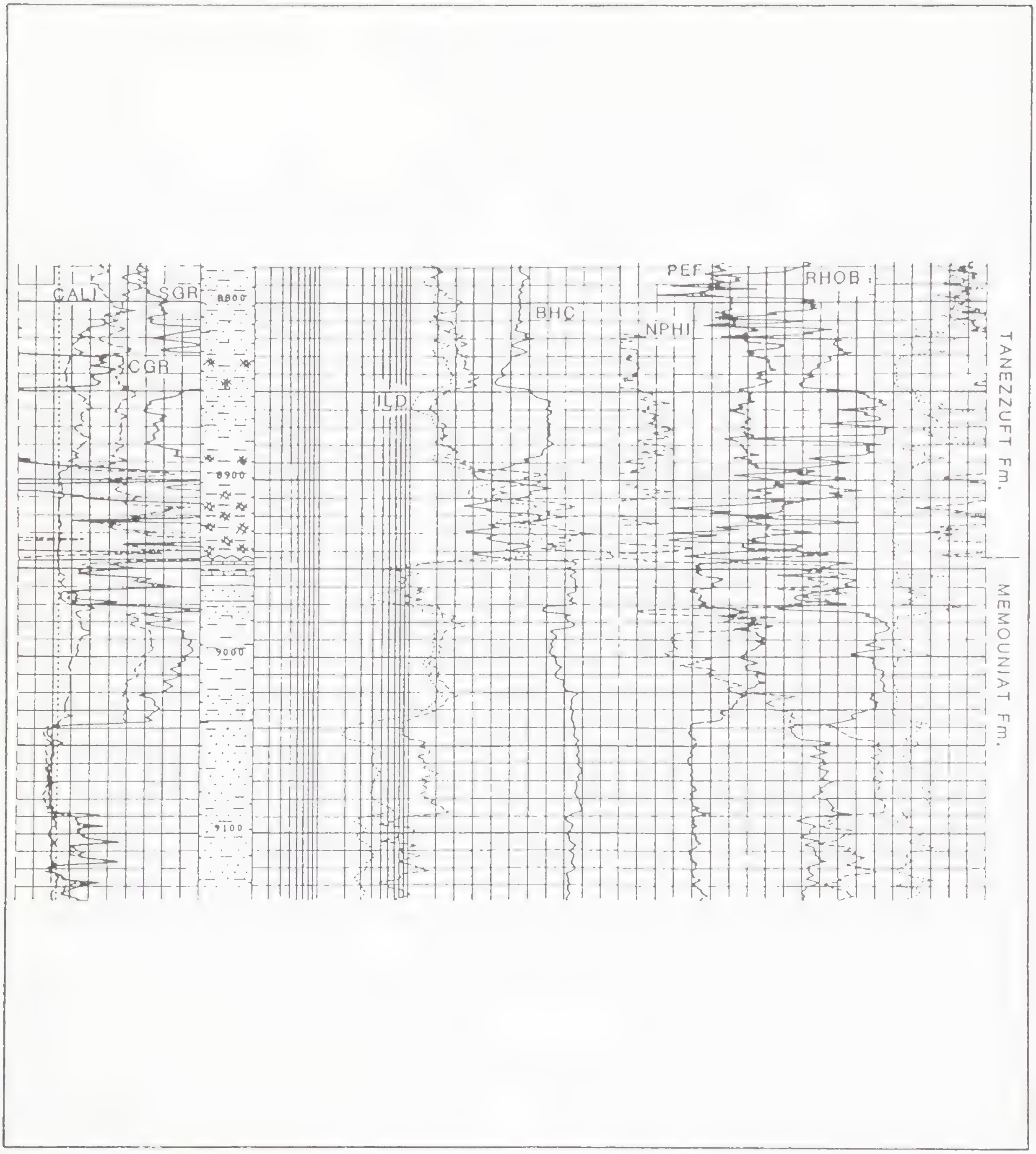

Fig. 7. Wireline logs relevant to "carbonaceous" shale layers, Tanezzuft Formation.

facies as shown by the cores) that covered the entire area.

These sediments are overlain by the first "iron oxide"-rich layer of the Acacus 1st member.

A depositional regression took place shortly after a very fast transgression over the Middle Silurian unconformity (top Tanezzuft Formation) leading a deltaic complex to be overlain by probable alluvial deposits.

Unfortunately, the interpretation of the transgres-

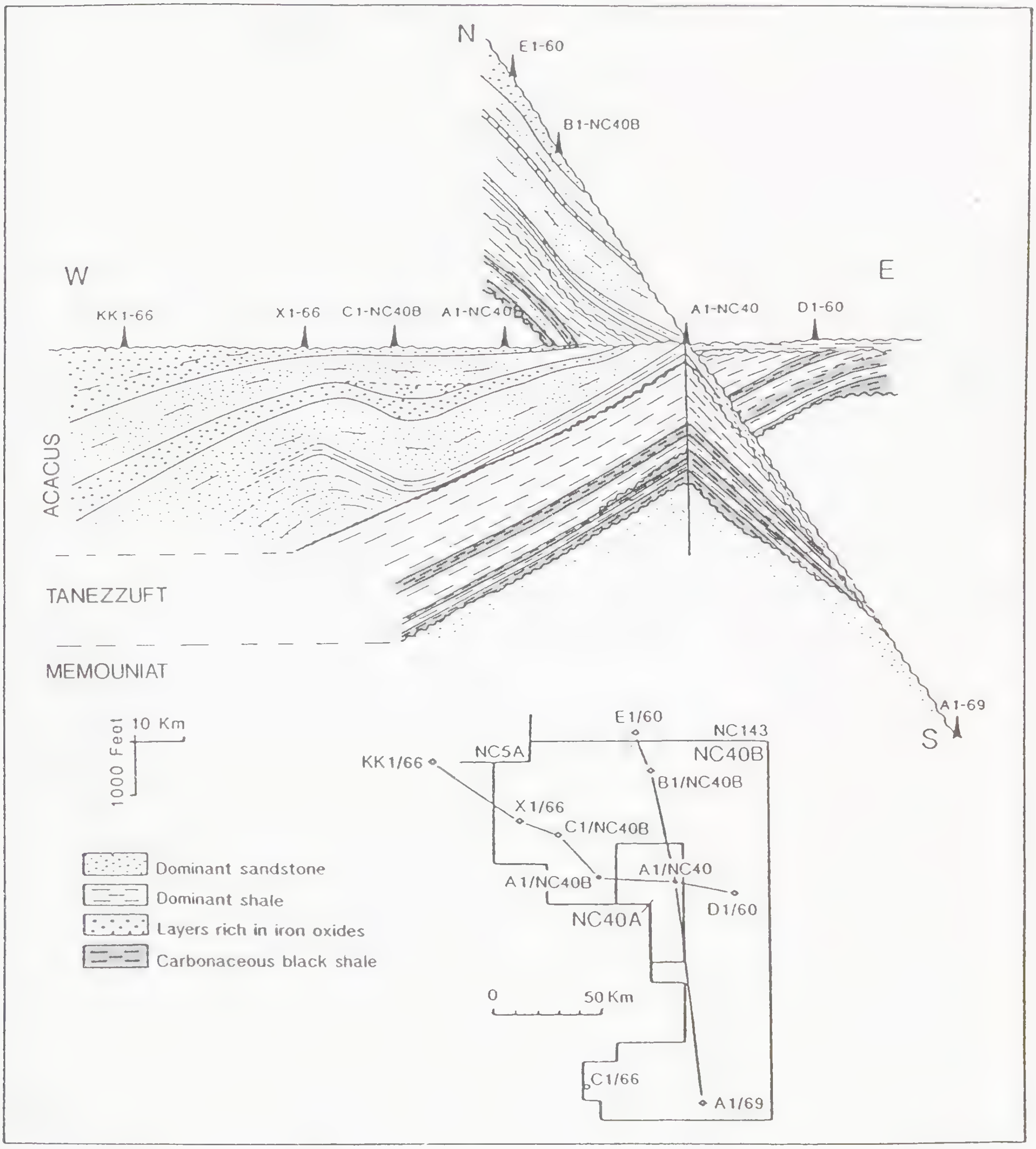
N
E1-60
B1-NC40B
W
E
KK1-66
X1-66
C1-NC40B
A1-NC40B
A1-NC40
D1-60
ACACUS
TANEZZUFT
MEMOUNIAT
A1-69
S
10 Km
1000 Feet
Dominant sandstone
Dominant shale
Layers rich in iron oxides
Carbonaceous black shale
E1/60
NC143
NC5A
NC40B
KK1/66
B1/NC40B
X1/66
C1/NC40B
A1/NC40
A1/NC40B
D1/60
NC40A
0
50 Km
C1/66
A1/69

Fig. 8. Stratigraphic sketch for Silurian time. (Datum plain top Acacus Formation).

sive pulse present in the middle of this section is, at this moment, problematic as far as understanding what regulating factors are concerned. If this fast transgressive pulse is related to either the avulsion of the distributary apparatus of a deltaic complex or to changes in sea level and/or the ratio between rate of sedimentation and rate of subsidence then the entire sequence could be either considered as a single II order cycle or as a couple of II order cycles.

The middle-upper part of the Acacus 1st member

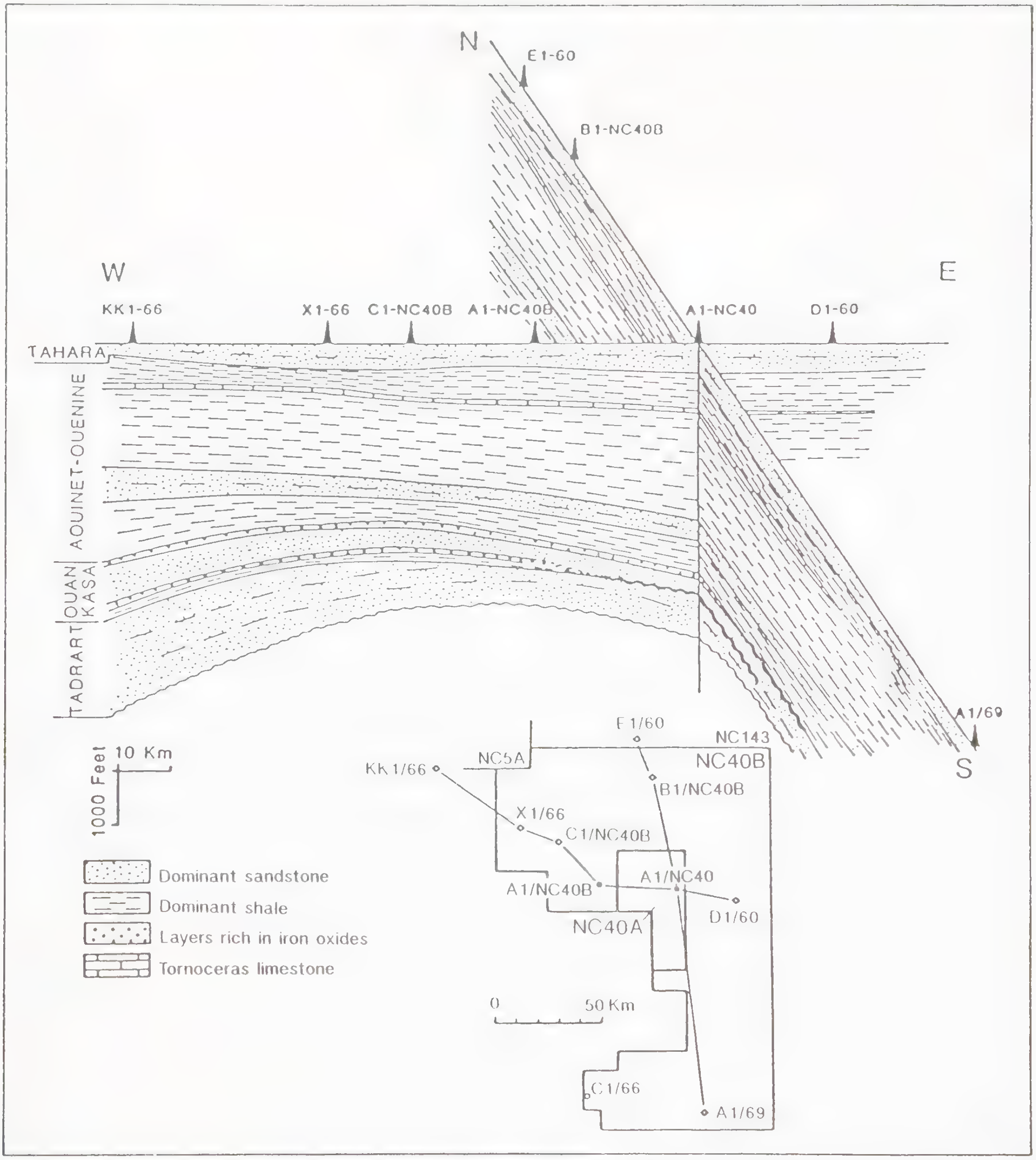
N
E1-60
B1-NC40B
W
E
KK1-66
X1-66
C1-NC40B
A1-NC40B
A1-NC40
D1-60
TAHARA
AOUINET-OUENINE
OUAN KASA
TADRART
A1/69
S
10 Km
1000 Feet
E1/60
NC143
NC5A
NC40B
Kk1/66
B1/NC40B
X1/66
C1/NC40B
A1/NC40
A1/NC40B
D1/60
NC40A
0
50 Km
C1/66
A1/69
Dominant sandstone
Dominant shale
Layers rich in iron oxides
Tornoceras limestone

Fig. 9. Stratigraphic sketch for Devonian time. (Datum plain top Tahara Formation).

represents another sedimentary cycle similar to the previous one.

It is worth stressing that the "iron oxide"-rich layers probably mark subaerial conditions at the end of each sedimentary cycle.

Red (iron oxide-rich) sandstone facies are well known in north central Europe in both Precambrian (Torridonian sequence) and Devonian ("Old red" sandstones) series.

Their sedimentary environment (Selley, 1970), is described as the "braided" channels portion of an alluvial plain, overlying "grey" shaley facies, related to a "tidal flat" environment.

These "grey" facies are quite similar to the Acacus 2nd member and to the middle part of Acacus 1st member.

Devonian Deposition

The first Devonian sediments are represented by the Tadrart Formation sandstones deposited over the Upper Silurian–Lower Devonian unconformity that marks the end of the Caledonian orogenesis. Unfortunately, only scant information is available on the sedimentary environment of the Tadrart Formation. Interpretation of the cores demonstrates that its upper part is made up of transitional-tidal flat sediments.

Basinward, where the formation achieves its maximum thickness, the sand/shale ratio tends to increase and an "iron oxide"-rich layer develops.

These facts represent a "depositional regression" in a "base truncated" sedimentary cycle.

The Ouan Kasa Formation represents a sedimentary cycle itself. In fact, the bottom is marked by the emersion at the end of the Tadrart depositional regression; the top is characterized by tight weathered horizons ("iron oxide"-rich layers).

The Aouinet–Ouenine Group is related to a widespread transgressive pulse that also reached the Al Qarqaf area.

Since no cores were cut within this unit the data to infer the relevant sedimentary environment are lacking. Anyway, it can be postulated that during the Aouinet–Ouenine Group deposition, a new, secondary, depocentre developed in this portion of the Ghadāmis basin. In fact, the thickness of the lower part of this unit increases in the NE part of the area. The "*Tornoceras*" limestone deposition proves that the physiography of the basin, at least in this part became quite flat once again.

Despite the lack of sedimentological and palaeontological data this "marker layer" (*Tornoceras*) could represent an instantaneous depositional phase within the Devonian.

The Tahara Formation marks the end of the Devonian.

The sedimentological interpretation suggests that "tidal flat" conditions were widespread over the whole area.

It is possible to consider the Aouinet–Ouenine Group plus the Tahara Formation as a single sedimentary cycle, although minor cycles could be accounted for at least within the Aouinet–Ouenine Group (*Tornoceras* layer ?).

Depositional Model

The following depositional model, relevant to the Silurian–Devonian period, is proposed for the area.

Taking into consideration the sedimentological interpretation of the cores together with the depositional significance of peculiar electrofacies, such as the carbonaceous shale and the "iron-oxide"-rich layers, it is possible to envisage an environment that seems to have remained quite uniform (except for the Aouinet–Ouenine Group) within the transitional complex. This environment was strongly tide and wave dominated and, therefore, both arcuate and estuary delta sequences could develop (Figs 10 and 11) depending on either sea level changes or variations in the inner dynamic processes.

The proposed model matches the sedimentological interpretation given by Whitbread and Kelling (1982) for the Carboniferous Mrar Formation in the same area.

CONCLUSIONS

The tentative reconstruction of the Silurian–Devonian sedimentary evolution of this part of the Ghadāmis basin, should allow a better understanding of the lateral variations of the lithostratigraphic units and their space–time relationship within transgressive–regressive sequences.

This study could also help in solving some of the exploration problems so far met in this area, such as:

- flushing of freshwater
- which unit of the Palaeozoic series could, reasonably, be flushed at a lesser extent (for its stratigraphic meaning) especially where antithetic faults do not exist and/or they do not provide sufficient sealing.

The main results of the present study emphasize the following points:

- During the middle–upper Palaeozoic the sedimentary environment seems to have remained quite uniform in this part of Ghadāmis basin.
- Except for the Middle Devonian (Aouinet–

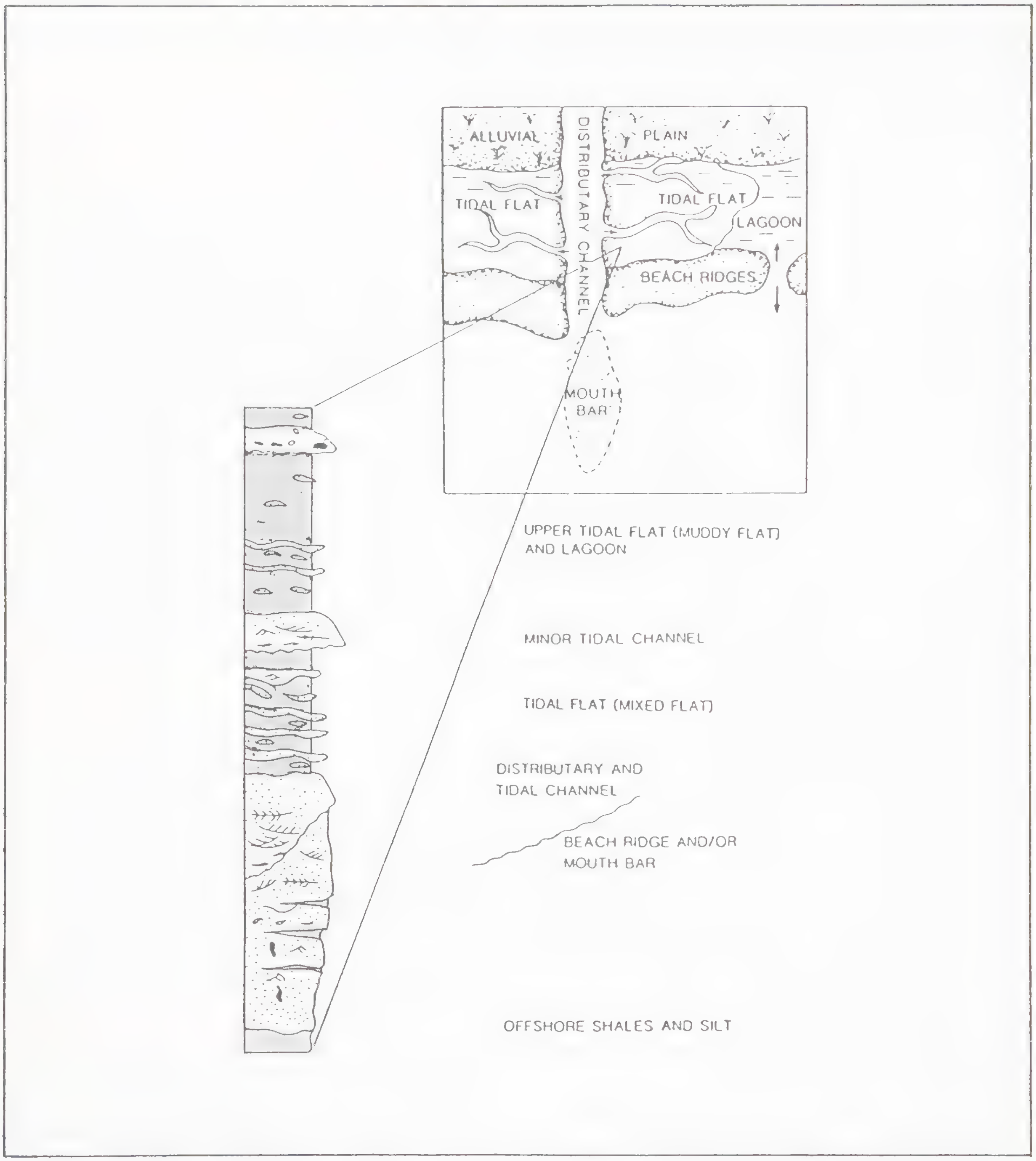
ALLUVIAL
PLAIN
DISTRIBUTARY CHANNEL
TIDAL FLAT
TIDAL FLAT
LAGOON
BEACH RIDGES
MOUTH BAR
UPPER TIDAL FLAT (MUDDY FLAT) AND LAGOON
MINOR TIDAL CHANNEL
TIDAL FLAT (MIXED FLAT)
DISTRIBUTARY AND TIDAL CHANNEL
BEACH RIDGE AND/OR MOUTH BAR
OFFSHORE SHALES AND SILT

Fig. 10. Depositional example of a regressive sequence referred to as an "arcuate" delta complex (from cores).

Ouenine Group deposition) the sediments can be related to a tide-dominated transitional environment where arcuate delta and delta-estuary complexes could develop, depending on both sea level variations and/or the inner dynamic processes (as the avulsion of the distributary apparatus).

- Almost all the sedimentary cycles are "base truncated". This fact is related to very fast transgressive pulses over a quite flat landscape.
- The freshwater flushing of the Silurian–Devonian

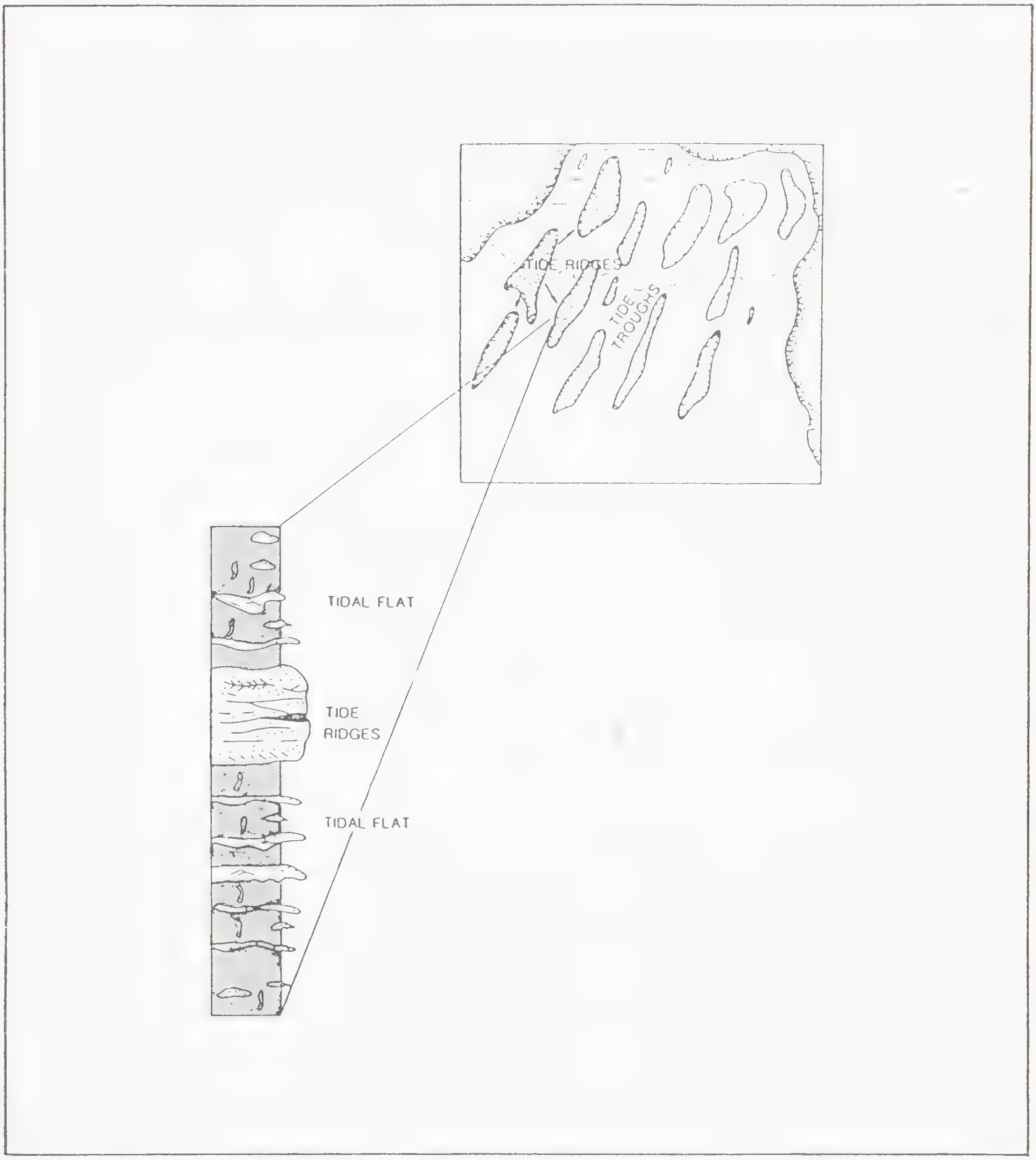
TIDE RIDGES
TIDE TROUGHS
TIDAL FLAT
TIDE RIDGES
TIDAL FLAT

Fig. 11. Depositional example of a tidal inlet referred to as an estuarine delta fringe (from cores).

units can be related to the presence of thick regressive sequences.

- The proposed depositional model shows a good lateral continuity of the sand bodies, especially within regressive sequences. Under these conditions beach and tide ridge sandstones are likely to pass updip into permeable tidal (tidal channel?) and fluvial facies.

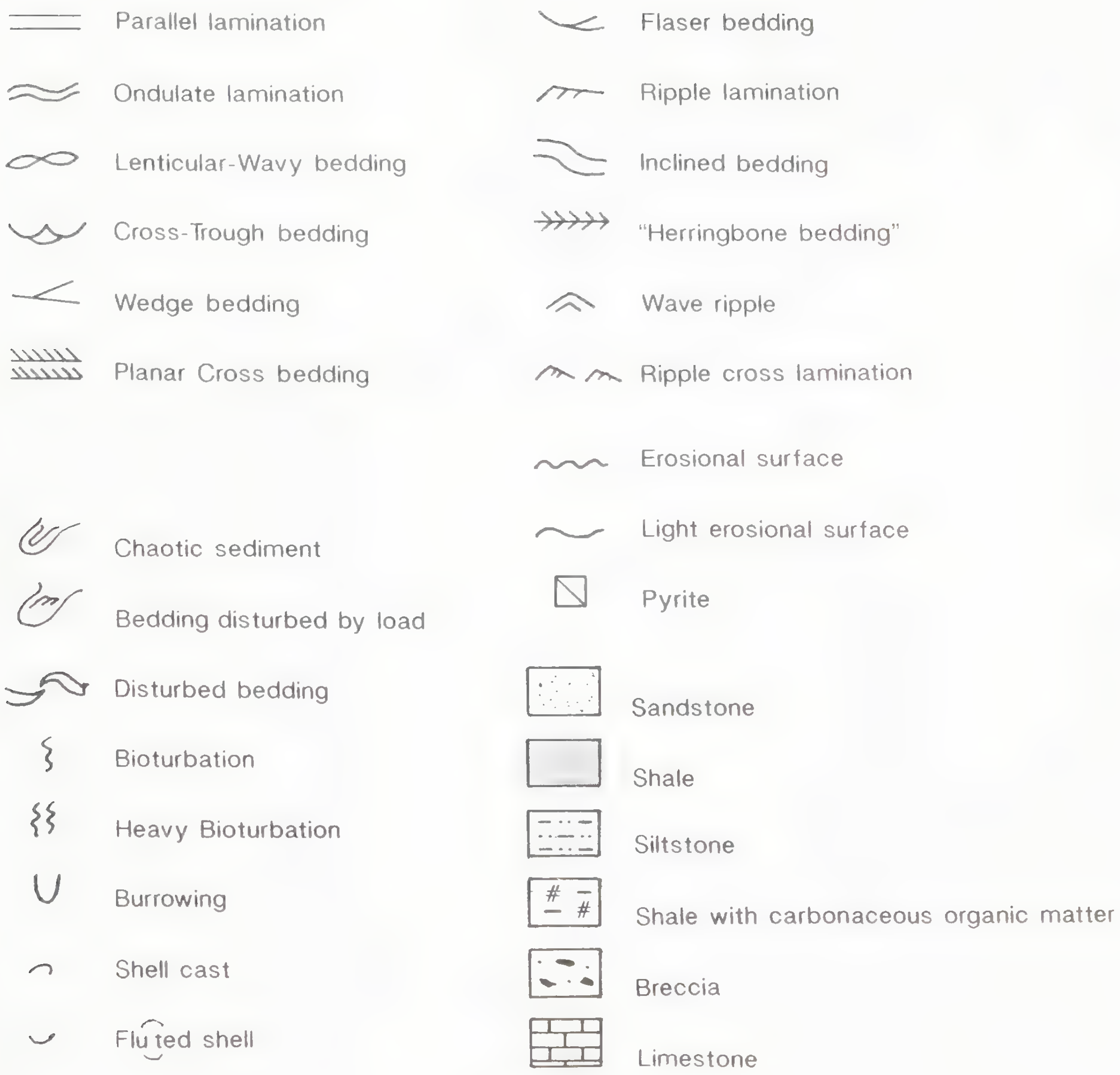
Parallel lamination
Ondulate lamination
Lenticular-Wavy bedding
Cross-Trough bedding
Wedge bedding
Planar Cross bedding
Chaotic sediment
Bedding disturbed by load
Disturbed bedding
Bioturbation
Heavy Bioturbation
Burrowing
Shell cast
Fluted shell
Flaser bedding
Ripple lamination
Inclined bedding
"Herringbone bedding"
Wave ripple
Ripple cross lamination
Erosional surface
Light erosional surface
Pyrite
Sandstone
Shale
Siltstone
Shale with carbonaceous organic matter
Breccia
Limestone

Fig. 12. Legend to Figs. 10 and 11.

REFERENCES

ALLEN, J.R.L. (1965). Late Quaternary Niger Delta and adjacent areas: sedimentary environments and lithofacies. *Bull. Am. Assoc. Petrol. Geol.*, **49**, 547–600.

ALLEN, J.R.L. (1970). Sediments of the modern Niger delta. *In*: Deltaic Sedimentation, Modern and Ancient (*ed.* J.P. Morgan). *S.E.P.M. Spec. Issue*, **15**, 138–151.

COLEMAN, J.M., GAGLIANO, S.M. and SMITH, W.G. (1970). Sedimentation in a Malasian high tide tropical delta. *In*: Deltaic Sedimentation, Modern and Ancient (*ed.* J.P. Morgan). *S.E.P.M. Spec. Issue*, **15**, 185–197.

COLEMAN, J.M. and WRIGHT, L.D. (1975). Modern river deltas, variability of processes and sand bodies. *In*: Deltas, Models for Exploration (*ed.* M.L. Broussard). *Houston Geol. Soc.*, 99–150.

INGLE, J.C. (1975). Nearshore processes and beach deposits. *In*: Current Concepts of Depositional Systems with Application for Petroleum Geology. *S. Joaquin Geol. Soc.*, 2–11.

LE BLANC, J.R. (1972). Geometry of sandstone reservoir bodies. *Mem. Am. Assoc. Petrol. Geol.*, **18**, 133–189.

REINECK, H.E. and SINGH, I.B. (1973). *Depositional Sedimentary Environments*. Springer-Verlag, Berlin, 440 p.

RICCI-LUCCHI, F. (1970). *Sedimentografia*. Zanichelli, Italy, 288 p.

RICCI-LUCCHI, F. (1980). *Sedimentologia*, parte III. *C.L.U.E.B.*, Bologna, 545 p.

SELLEY, R. (1970). *Ancient Sedimentary Environments*. Chapman and Hall, London, 237 p.

WHITBREAD, T. and KELLING, G. (1982). Mrar Formation of Western Libya – Evolution of an early Carboniferous delta system. *Bull. Am. Assoc. Petrol. Geol.*, **66**, 1091–1107.

Application of Neutron Activation Methods for Trace Element Analysis in the Nubian Sandstone of Southern Libya

A. EL-ZOUKI[1] AND A. ALIAN[1]

تطبيق طريقة تنشيط النيوترونات لتحليل العناصر الضئيلة بالرمال النوبية جنوب ليبيا

ع. الزوكي وأ. عليان

الخلاصـــة

لقد تم تحليل أربعين عينة من الرمال النوبية مجمعة من مواقع ومقاطع مختلفة (عند مستويات مختلفة) لحوضي مرزق والكفرة الترسيبيين، وذلك لعناصر عدة باستعمال طرق تنشيط النيوترونات. ولقد تم إختبار طريقة المعيار الواحد لتنشيط النيوترونات بتحليل عينات بهذه الطريقة وطريقة نسبية باستعمال ي ج – 1 للمقارنة. والعناصر التي تم تحليلها بالطريقتين هي كا، ح (محتوى عيني)، سر، كو، كر، سز، أو، هف، لن، لت، بيد، سك، سم، ست، تا، تر، ثو، يتر. (عناصر ضئيلة) بينما لم يكن بالإمكان تحليل ذ، ز، بر، أو، بو. لت، ص، نيو، يب، إلاّ بطريقة أحادي المعيار. وقد كان التناسق بين الطريقتين جيداً.

ولقد وجد شبه كبير في وفرة العناصر بين الحوضين الترسيبيين فيما عدا (ثو) الذي يوجد بكمية كبيرة في معظم عينات حوض مرزق الترسيبي والحديد الذي هو أغنى بحوض الكفرة الترسيبي. ولقد قارنا نتائجنا بتلك الواردة في ماكسينوفيش والأسكنجي. ونجد هنا أن مدى العديد من العناصر الضئيلة بالصخور الرملية ينشر لأول مرة. ولقد أوردنا أيضاً القيم المنشورة حول الصخور الرملية لمقارنتها بنتائجنا.

Abstract. Forty Nubian Sandstone samples from various localities in the Murzuq and Al Kufrah basins, southern Libya, were analyzed for major and trace elements by neutron activation analysis methods using both the relative (RNAA) and monostandard (MNAA) techniques. For the relative method a standard reference (SR) material, namely Andesite KA-3 and the Japanese granite JG-1 were used. For the monostandard method iron or cobalt was used as a single comparator (standard) for all elements giving rise to photopeaks in the measured gamma spectra of reactor-irradiated samples. Using Andesite KA-3 as an SR material, the elements analyzed in 30 samples from Murzuq basin were Ca, Fe (macroconstituents), Ce, Co, Cr, Cs, Eu, Hf, La, Lu, Rb, Sc, Sm, Sr, Ta, Tb, Th, and Yb, while U could only be analyzed by MNAA. On the other hand, using JG-1, only Ba, Ca, Ce, Co, Cr, Cs, Hf, Fe, La, Rb, Sc, Sm, Ta, Th, and U could be analyzed by RNAA in 10 samples from Al Kufrah basin. The peaks appearing in the gamma spectra of 5 of these samples were utilized for the determination of the corresponding elements by MNAA, so that in addition to the above 14 elements, As, Au, Br, Eu, K, Lu, Na, Nd, and Yb could be analyzed by MNAA.

The abundance of elements was very similar in the two basins, except for Th, which is noticeably high in the Murzuq basin and Fe which is more enriched in some samples from Al Kufrah basin. The range of many trace elements in sandstones is reported for the first time in this work.

INTRODUCTION

Perhaps due to their economic potential (petroleum and water) the Nubian Sandstones have recently been the subject of detailed investigations by scientists. The determination of the levels of major and trace elements in these rocks is a prerequisite for their regional stratigraphic and sedimentological investigation. A detailed review of the literature has indicated that published work on the chemical analysis of Nubian Sandstones is quite scarce (El-

---

[1] Faculty of Science, University of Garyounis, P.O. Box 9480, Binghāzī, Libya, G.S.P.L.A.J.

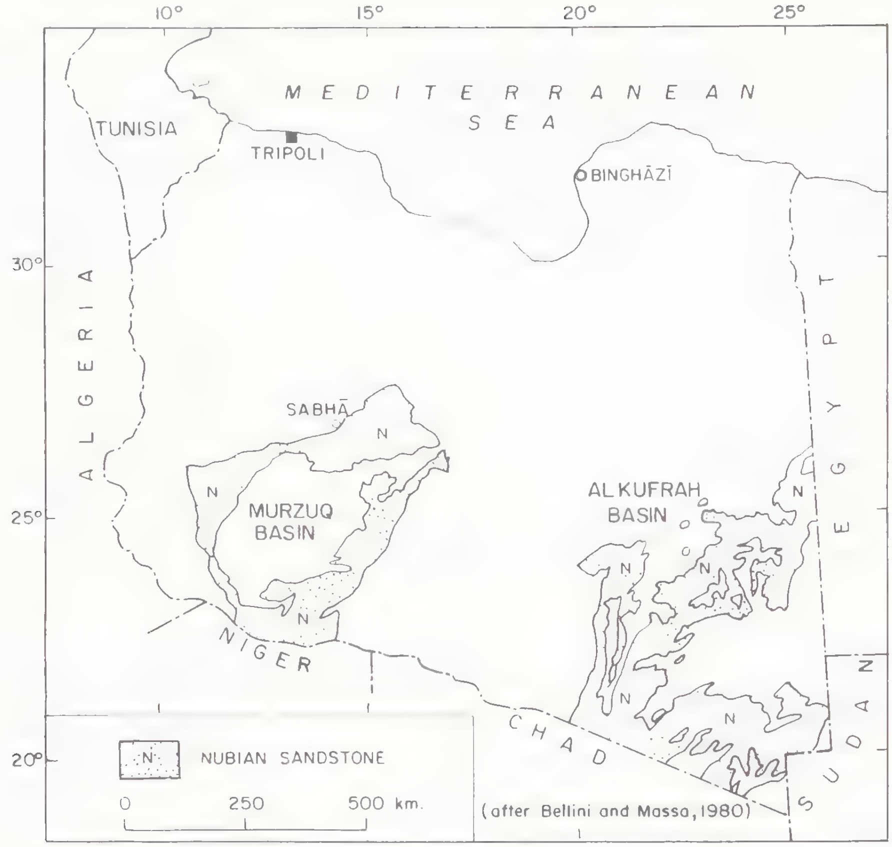

Fig. 1. Location map showing the aerial distribution of the Nubian Sandstone in Southern Libya.

Zouki, 1981). The work of El-Hinnawy *et al.* (1973) dealt with the analysis of major elements in only two Nubian Sandstones samples from the central Eastern Desert of Egypt. It has been claimed (Turekian, 1982) that the scarcity of work on these rocks is due to the fact that their analysis was carried out only in those cases where they seemed to be of direct economic interest. Accordingly the average levels of the components of sandstones are based on the few data so far available. The present paper summarizes an extensive analysis of more than 20 elements in 40 Nubian Sandstone samples taken from various localities and levels in the Murzuq and Al Kufrah basins, southern Libya. The methods used were the relative and monostandard neutron activation analysis methods (RNAA and MNAA), respectively.

This work is interesting not only for the geology of Libya but also provides new data for many trace elements in Nubian Sandstones in general.

The MNAA technique has recently been elaborated (Alian and Sansoni, 1980; Alian *et al.*, 1983), and a comparison of the use of various NAA techniques for geological samples has also been presented (Alian and Sansoni, 1980). The MNAA method of calculation developed was tested on standard reference (SR) materials (Alian *et al.*, 1983) and found to be reliable. The same method was therefore used in the present work. It is simple, since only one equation (equation (1) below) is used twice, firstly for evaluation of the neutron reaction cross sections and secondly for evaluation of the contents of the elements.

EXPERIMENTAL METHOD

The analyzed samples were mostly with grain sizes ranging from very fine sandstone (0.125–0.06 mm), siltstone (0.06–0.004 mm) and claystone (<0.004 mm) to coarser particles in few samples (0.25–2.00 mm). These coarse-grained samples contained higher mineral concentrations as could be seen. The depositional environment of the analyzed samples can

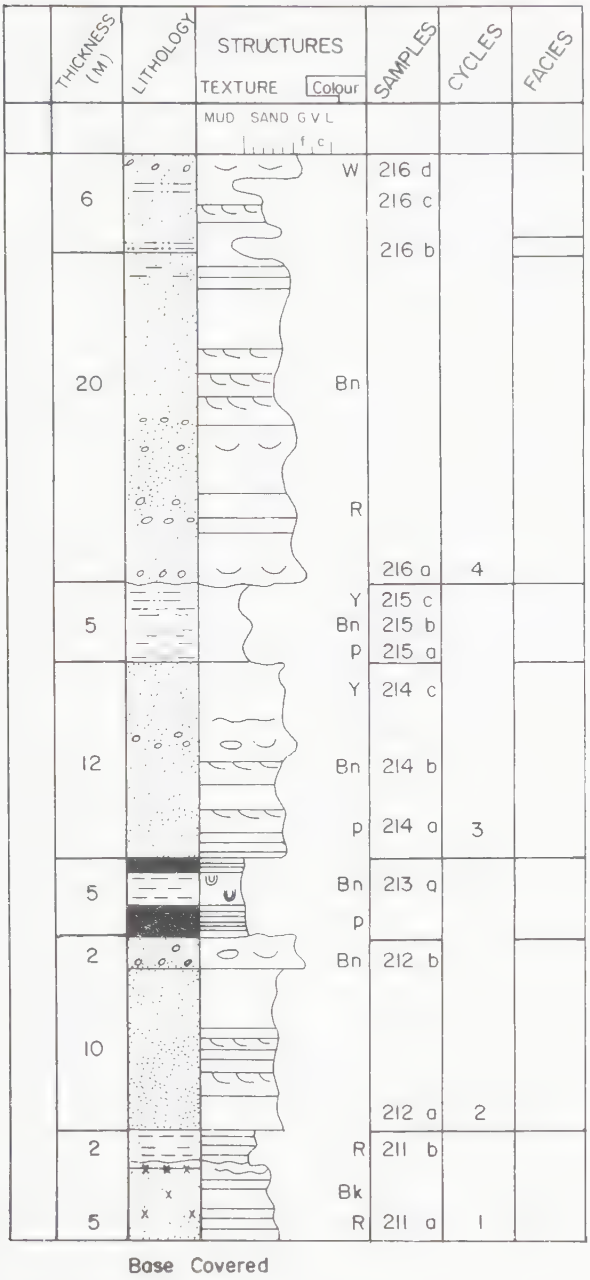

Fig. 2. Type stratigraphic section of the Nubian Sandstone, Murzuq basin; Section 21 about 65 km SW of Sabhā along the main road to Awbārī.

be regarded as a nonmarine, continental (fluvial) one. They mostly represent flood-plain, overbank and lake deposits.

For Murzuq basin, the sample numbers indicate the section, the lithologic unit and the subunit from which the sample was taken. Sampling was done from 6 different stratigraphic sections, given the numbers 21, 22, 23, 24, 25, and 26, *i.e.*, the first two figures on the left of each sample number. The third figure (1, 2, 3, *etc.*) represents units numbered from the base upwards for the respective stratigraphic sections while subunits from the base upwards, are indicated by the letters A, B, and C (see Figs 1–3).

STANDARD REFERENCE MATERIALS

The standard reference (SR) materials used as comparators in the present work were Andesite KA-3 of the DFG (Deutsche Forschungsgemeinschaft) and the Japanese standard granite rock JG-1. The first SR material was selected from 5 DFG standards analyzed previously by RNAA (Alian and Sansoni, 1980) since preliminary investigation had shown that the measured gamma-spectrum of this standard was rather similar to that of the samples under investigation. On the other hand, JG-1 which had been studied more showed only some of the photopeaks which appeared in our samples and was therefore used only for checking the results. Its iron or cobalt content was used for calculations in analysis by MNAA.

SAMPLES AND STANDARD IRRADIATIONS

Samples and standards, each about 100 mg, were placed in pure “Suprasil” quartz ampoules about 5 mm in diameter and 3–4 cm in length; the ampoules were then sealed and placed in aluminium irradiation cans. Irradiation was then carried out for 10 hours in the research Reactor DIDO in Juelich, Juelich Nuclear Research Establishment, West Germany, at a neutron flux of about 10^{13} n/cm^2/s. After irradiation the samples and standards were allowed to cool for about 5 days to permit the decay of undesirable short-lived isotopes.

MEASUREMENT OF GAMMA SPECTRA

The gamma spectra were measured for 2 hours each after the given cooling period, using two Ge(Li)-detectors, (a) Canberra 7249, 33 cm^3 and 8% efficiency, resolution 2.4 keV for the 1.332 MeV line; peak/compton ratio 18 : 1 for the same line, (b) GTCW-170-20, cylindrical coaxially drifted; 25 cm^3 and 16% efficiency, resolution 2.0 keV and peak/compton ratio 38 : 1 for the 1.332 MeV line of Co-60. The multichannel analyzer (Nuclear Data ND4420) had 8k, a magnetic tape drive (pertec), printer (Centronics 30b) and X-Y recorder Hewlett Packard 7004 B.

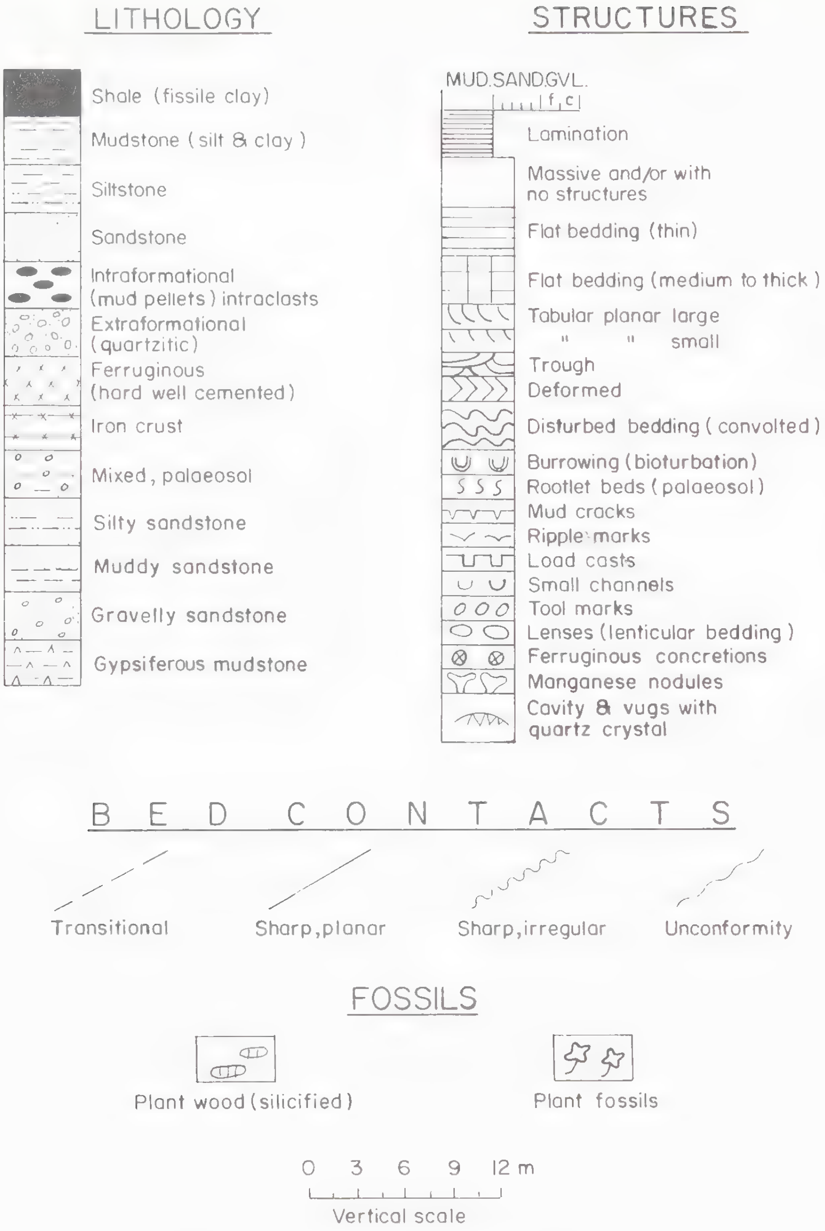
LITHOLOGY
Shale (fissile clay)
Mudstone (silt & clay)
Siltstone
Sandstone
Intraformational (mud pellets) intraclasts
Extraformational (quartzitic)
Ferruginous (hard well cemented)
Iron crust
Mixed, palaeosol
Silty sandstone
Muddy sandstone
Gravelly sandstone
Gypsiferous mudstone
STRUCTURES
MUD.SAND.GVL.
f c
Lamination
Massive and/or with no structures
Flat bedding (thin)
Flat bedding (medium to thick)
Tabular planar large
" " small
Trough
Deformed
Disturbed bedding (convolted)
Burrowing (bioturbation)
Rootlet beds (palaeosol)
Mud cracks
Ripple marks
Load casts
Small channels
Tool marks
Lenses (lenticular bedding)
Ferruginous concretions
Manganese nodules
Cavity & vugs with quartz crystal
BED CONTACTS
Transitional
Sharp, planar
Sharp, irregular
Unconformity
FOSSILS
Plant wood (silicified)
Plant fossils
0 3 6 9 12 m
Vertical scale

Fig. 3. Key to the stratigraphic section of Fig. 2.

QUANTITATIVE ASSESSMENTS

NAA is based on the measurement of intensities of gamma rays with characteristic energies. These gamma rays are emitted from radioisotopes produced due to nuclear reactions from inactive isotopes of the elements to be determined in the samples due to irradiation. The intensity measured as the peak area in counts per unit time (from the gamma spectra), is only a relative signal and is linearly proportional to the radionuclide content produced during neutron activation and therefore to the inactive element to be determined. In RNAA, the measured peak area for a given element in the analyzed sample is compared with the corresponding peak area in the SR material. Accordingly, it is possible to analyze only those elements for which certified element contents in the SR material are available. For

MNAA the determination of a photopeak counting ratio A/A^* for a nuclide of interest in the sample and a monostandard nuclide (indicated by *) irradiated simultaneously with that sample, leads to the determination of the elements concentration from equation (1) (Alian *et al.*, 1983).

$$m = \frac{A}{A^*} \cdot \frac{m^* \sigma_0^* f^* b^* E^*}{\sigma_0 f\, bE} \cdot \frac{S^* D^* M}{SDM^*} \qquad (1)$$

where σ_0 = thermal neutron cross section; f = fractional abundance of the activated isotope; b = absolute intensity of the measured γ-line; E = detector efficiency for that γ-line; S = saturation factor $(1 - e^{-\lambda t_1})$, where λ is the decay constant and t_1 is the irradiation time; D = decay factor $(e^{-\lambda t_2})$, where t_2 is the decay time; and M = atomic weight of the element to be determined.

Equation (1) is obtained from the division of two similar equations, one for the element to be determined and another for the monostandard. These two equations represent the relation between the activity obtained from the irradiation of a given stable nuclide and the number of its atoms (expressed in weight m, atomic weight M, Avogadro's number N which disappears after dividing the two equations by each other and fractional abundance f; the other parameters in the equations are related to the counting process (absolute intensity of the measured γ-line (b) detector efficiency (E) saturation and decay factors (S and D, respectively)). The cross section σ represents the proportionality constant of the activation process and is a characteristic parameter for each nuclide. The above nuclear and measuring parameters for the monostandard and for the elements analyzed can be taken from nuclear data compilations (f, b, λ and M) or determined experimentally (σ, E, S and D), as shown by Alian *et al.* (1983). It is to be noted that the thermal cross section σ_0 was used as the effective cross section since we selected an irradiation position in the DIDO Reactor in which the epithermal neutron flux was very small compared to the total neutron flux. Thus the thermal neutron flux was 9×10^{12} n/cm^2 s, while the epithermal flux was only 3×10^9 n/cm^2 s (0.033%). Quantitative assessment by RNAA was carried out either manually or using the computer program ZCH-PAPI, version 1981, developed by Erdtmann, Freiburg and Kaysser (Alian *et al.*, 1983). Quantitative assessment by MNAA was performed manually using a small calculator.

RESULTS AND DISCUSSION

Tables 1–6 show the results of NAA of Ca, Fe as macroconstituents and Ce, Co, Cr, Cs, Eu, Hf, La, Lu, Rb, Sc, Sm, Sr, Ta, Tb, Th, U, and Yb as trace elements in 30 samples of Nubian Sandstones from Murzuq basin. Here RNAA was used with Andesite of DFG as an SR material, except U, which was determined in the same samples by MNAA, when the photopeak of ^{239}NP at 277.6 keV induced from U

Table 1. Neutron Activation Analysis of Nubian Sandstone samples from section 21 of Murzuq basin. (Results from RNAA except for U which is by MNAA). Contents in ppm, except Ca and Fe, in %

Element	Sample					
	211A	211B	213B	215A	216B	216C
Ca %	–	1.0 ± 0.01	1.1 ± 0.01	0.9 ± 0.01	1.26 ± 0.01	1.1 ± 0.08
Ce	36 ± 1	0.6 ± 0.05	63 ± 6.7	64 ± 7	122 ± 3	95 ± 13
Co	2 ± 0.1	62 ± 2	7 ± 0.8	3.5 ± 0.4	1.4 ± 0.1	2.4 ± 0.2
Cr	8 ± 1	2 ± 0.1	31 ± 5	186 ± 28	34 ± 4	74 ± 1
Cs	–	23 ± 3	–	–	–	–
Fu	0.3 ± 0.05	1 ± 0.1	1 ± 0.1	–	1.7 ± 0.3	1 ± 0.04
Fe %	1 ± 0.1	1.4 ± 0.2	2.83 ± 0.5	3 ± 0.6	2 ± 0.2	0.8 ± 0.1
Hf	6 ± 3	7 ± 0.5	–	–	19 ± 10	6.5 ± 0.7
La	18 ± 3	27 ± 5	33 ± 0.5	35 ± 4	43 ± 8	53 ± 6
Lu	0.2 ± 0.01	0.4 ± 0.01	0.4 ± 0.1	0.5 ± 0.1	0.7 ± 0.02	0.5 ± 0.2
Sc	3 ± 0.3	5 ± 0.5	10 ± 1	10 ± 1	27 ± 0.6	8.5 ± 0.7
Sm	2 ± 0.05	4 ± 0.07	5.7 ± 0.5	–	–	5 ± 0.5
Ta	0.4 ± 0.3	1.3 ± 1	0.2 ± 0.2	0.2 ± 0.1	1.3 ± 1	0.5 ± 0.8
Tb	0.2 ± 0.03	0.3 ± 0.05	0.2 ± 0.02	0.2 ± 0.03	0.3 ± 0.04	–
U	–	2.0 ± 0.1	–	–	–	34 ± 12
Yb	0.5 ± 0.03	1 ± 0.6	0.9 ± 0.001	1 ± 0.002	1.1 ± 0.06	0.8 ± 0.03

Table 2. Neutron Activation Analysis of Nubian Sandstone samples from section 22 of Murzuq basin. (Results are from RNAA except for U which is by MNAA). Contents in ppm, except Ca and Fe, in %

Element	Sample			
	221 A	221 B	222 B	222 C
Ca %	1 ± 0.1	–	1.4 ± 0.1	0.8 ± 0.06
Ce	50 ± 1.3	38 ± 4	36 ± 5	90 ± 13
CO	1.5 ± 0.1	1.3 ± 0.15	1.8 ± 0.2	0.3 ± 0.02
Cr	63 ± 8	24 ± 4	9 ± 0.5	18 ± 1
Eu	0.7 ± 0.1	0.5 ± 0.1	1.4 ± 0.1	1.3 ± 0.6
Fe %	1.5 ± 0.2	0.42 ± 0.5	0.1 ± 0.01	0.2 ± 0.2
Hf	4 ± 0.3	–	18 ± 2	3 ± 0.3
La	–	20 ± 2	26 ± 4	54 ± 9
Lu	0.3 ± 0.001	–	1 ± 0.2	0.5 ± 0.1
Se	11 ± 1	10 ± 1	6.5 ± 0.5	7 ± 0.6
Sm	3 ± 1	3 ± 0.4	2.6 ± 0.04	–
Ta	1 ± 0.7	0.2 ± 0.2	0.6 ± 1.3	0.6 ± 1
Tb	0.1 ± 0.02	0.2 ± 0.03	0.1 ± 0.04	0.1 ± 0.04
Th	144 ± 10	110 ± 30	81 ± 13	108 ± 17
U	2 ± 0.1	–	1.6 ± 0.6	–
Yb	0.6 ± 0.04	0.9 ± 0.002	1.2 ± 0.7	0.5 ± 0.04

Table 3. Neutron Activation Analysis of Nubian Sandstone samples from section 23 of Murzuq basin. (Results are from RNAA except for U which is by MNAA). Contents in ppm, except Ca and Fe, in %

Element	Sample			
	232 A	233 B	234 B	238 A
Ca %	2.0 ± 0.15	1.3 ± 0.1	1.6 ± 0.1	0.9 ± 0.1
Ce	121 ± 12	171 ± 25	50 ± 7	33 ± 1
CO	3.7 ± 0.2	8 ± 0.3	3 ± 0.2	21 ± 1.5
Cr	66 ± 1	41 ± 1	–	20 ± 2
Cs	1 ± 0.1	–	–	–
Eu	1.09 ± 0.1	2.8 ± 0.1	0.5 ± 0.02	0.3 ± 0.05
Fe %	2 ± 0.2	1.9 ± 0.2	0.4 ± 0.04	3 ± 0.4
Hf	7 ± 0.7	9 ± 1	41 ± 0.3	24 ± 12
La	91 ± 16	108 ± 19	29 ± 5	28 ± 5
Lu	0.5 ± 0.2	1 ± 0.3	1 ± 3	0.3 ± 0.01
Rb	18 ± 0.3	–	–	–
Sc	13 ± 1.1	9 ± 0.8	7 ± 0.7	5 ± 0.5
Ta	1 ± 2	0.5 ± 1	0.6 ± 1	0.3 ± 0.2
Tb	0.3 ± 0.1	0.4 ± 0.2	0.2 ± 0.1	0.1 ± 0.02
Th	97 ± 16	235 ± 38	232 ± 54	69 ± 5.0
U	–	1.7 ± 0.6	–	0.3 ± 0.01
Yb	1 ± 0.07	1.6 ± 0.1	1.5 ± 0.1	0.5 ± 0.4

appeared in the corresponding gamma spectra. The data in each table correspond to a certain stratigraphic section of the basin. In Table 7 the results of 5 Nubian Sandstone samples from Al Kufrah basin are represented for RNAA and MNAA using JG-1 as an SR material. The latter results show that the 9 elements As, Au, Br, Eu, K, Lu, Na, Nd and Yb can be determined by MNAA only, since the photopeaks of the corresponding radioisotopes appeared only in the spectra of the irradiated samples and did not appear in the spectra of the SR JG-1, or their concentration in the latter were not known (Alian and Sansoni, 1980). For the rest of the elements which were determined by both RNAA and MNAA methods correspondence is seen to be good. The results in Table 8, on the other hand, were obtained

Table 4. Neutron Activation Analysis of Nubian Sandstone samples from section 24 of Murzuq basin. (Results are from RNAA except for U which is by MNAA). Contents in ppm, except Ca and Fe, in %

Element	Sample						
	241 A	241 C	242 A	245 A	245 B	246 A	246 C
Ba	–	–	–	–	347 ± 21	–	–
Ca %	1.6 ± 0.2	1.9 ± 0.2	0.5 ± 0.4	–	–	1.1 ± 0.1	0.55 ± 0.06
Ce	109 ± 16	140 ± 20	–	25 ± 1	160 ± 4	47 ± 7	136 ± 15
Co	5 ± 0.4	4 ± 0.4	8 ± 0.7	1.3 ± 0.1	27 ± 2	8 ± 0.7	2 ± 0.2
Cr	63 ± 1	86 ± 1	36 ± 1	10 ± 1	72 ± 9	18 ± 0.7	28 ± 4
Cs	–	1.1 ± 0.1	–	–	–	0.5 ± 0.04	–
Eu	1.6 ± 0.1	2.6 ± 0.1	2.6 ± 0.1	0.3 ± 0.05	4 ± 0.5	1.2 ± 0.05	0.7 ± 0.07
Fe %	1.1 ± 0.1	2.3 ± 0.3	–	0.4 ± 0.3	6.6 ± 0.8	0.86 ± 0.1	1.8 ± 0.3
Hf	9 ± 1	7 ± 0.8	21 ± 0.4	7 ± 0.3	4 ± 0.3	12 ± 2.4	–
La	68 ± 12	74 ± 12	18 ± 3	10 ± 1.7	65 ± 11	28 ± 5.0	20 ± 2.0
Lu	1.1 ± 0.3	1 ± 0.3	1 ± 0.2	–	1 ± 0.3	0.7 ± 0.2	0.3 ± 0.06
Rb	–	54 ± 1	–	–	–	25 ± 0.5	–
Sc	12 ± 1	17 ± 2	17 ± 1	2 ± 0.2	13 ± 1	5 ± 0.5	6 ± 0.7
Sm	–	2.5 ± 0.15	0.7 ± 0.1	2 ± 0.13	18 ± 0.3	4 ± 0.1	5 ± 0.4
Ta	1 ± 2	0.9 ± 2	0.3 ± 0.6	0.2 ± 0.1	0.8 ± 0.5	0.4 ± 0.8	0.1 ± 0.1
Tb	0.3 ± 0.1	–	0.2 ± 0.1	–	0.6 ± 0.1	0.2 ± 0.1	0.2 ± 0.03
Th	63 ± 1	205 ± 32	56 ± 9	34 ± 2	168 ± 11	50 ± 8	50 ± 11
U	2.6 ± 0.1	69 ± 43	0.5 ± 0.3	–	83 ± 5	–	–
Yb	2 ± 0.7	1.7 ± 0.1	1.7 ± 0.6	0.3 ± 0.03	2.4 ± 0.01	0.9 ± 0.06	0.7 ± 0.01

Table 5. Neutron Activation Analysis of Nubian Sandstone samples from section 25 of Murzuq basin. (Results are from RNAA except for U which is by MNAA). Contents in ppm, except Ca and Fe, in %

Element	Sample					
	251 A	251 B	253 A	254 A	254 B	254 C
Ba	–	248 ± 15	–	–	–	143 ± 9
Ca %	17 ± 1.4	0.6 ± 0.05	0.5 ± 0.01	0.23 ± 0.02	0.7 ± 0.1	0.3 ± 0.02
Ce	42 ± 0.4	25 ± 0.08	106 ± 15	19 ± 3	36 ± 1	12 ± 0.5
Co	0.3 ± 0.02	3 ± 0.2	5 ± 0.4	1.2 ± 0.1	3.1 ± 0.2	1.7 ± 0.2
Cr	2 ± 0.2	22 ± 3.5	36 ± 0.8	9 ± 0.4	52 ± 6	12 ± 1.5
Cs	0.2 ± 0.001	–	0.4 ± 0.04	0.4 ± 0.04	1.3 ± 1.4	–
Eu	0.1 ± 0.01	1 ± 0.1	1.2 ± 0.05	1.2 ± 0.01	0.5 ± 0.01	0.2 ± 0.04
Fe %	1.8 ± 0.3	3.4 ± 0.4	4.8 ± 0.53	1 ± 0.1	6.4 ± 0.05	3.6 ± 0.4
Hf	–	4 ± 0.3	4.3 ± 0.5	1.6 ± 0.2	19 ± 10	4 ± 0.3
La	2 ± 0.3	17 ± 3	49 ± 8	14 ± 2.3	26 ± 5	10 ± 2
Lu	–	0.2 ± 0.01	0.4 ± 0.09	0.1 ± 0.04	0.6 ± 0.002	0.15 ± 0.01
Rb	–	–	–	27 ± 0.5	–	–
Sc	0.3 ± 0.02	7 ± 0.6	10 ± 0.9	2.8 ± 0.24	8 ± 0.7	5 ± 0.4
Sm	0.23 ± 0.04	2.4 ± 0.03	–	–	3 ± 0.2	1.2 ± 0.03
Sr	–	–	208 ± 120	–	–	–
Ta	–	0.5 ± 0.3	0.4 ± 0.8	0.2 ± 0.4	1 ± 0.7	0.3 ± 0.2
Tb	–	–	–	0.03 ± 0.01	0.3 ± 0.04	0.1 ± 0.01
Th	6 ± 0.4	81 ± 5	82 ± 13	41 ± 7	70 ± 5	58 ± 4
U	–	2 ± 0.1	1.6 ± 0.7	2.4 ± 0.1	2.4 ± 0.1	1 ± 0.05
Yb	–	0.6 ± 0.03	0.5 ± 0.02	0.2 ± 0.01	0.6 ± 0.03	0.5 ± 0.03

by RNAA of 5 other samples from Al Kufrah basin, also using JG-1 as a comparator.

The range of contents of the elements in the various sections studied in the Murzuq basin (Tables 1–6) is given in Table 9. The Ba, Rb and Sr levels were beyond detection in most samples, being relatively high in only one sample of the last section. The high Ca content in one sample of section 25 (17%) was

Table 6. Neutron Activation Analysis of Nubian Sandstone samples from section 26 of Murzuq basin. (Results are from RNAA except for U which is by MNAA). Contents in ppm, except Ca and Fe, in %

Element	Sample		
	260	262 A	266 B
Ba	–	9940 ± 610	–
Ca %	3.9 ± 0.3	–	1.17 ± 0.09
Ce	42 ± 1	88 ± 2	55 ± 8.5
CO	0.5 ± 0.04	1.6 ± 0.1	1.9 ± 0.05
Cr	23 ± 3	28 ± 3	–
Eu	0.6 ± 0.1	1 ± 0.1	0.57 ± 0.2
Fe %	1.1 ± 0.1	1.3 ± 0.2	0.31 ± 0.1
Hf	7 ± 0.5	–	17 ± 4.7
La	26 ± 5	–	36 ± 1.3
Lu	0.2 ± 0.01	0.2 ± 0.01	0.23 ± 0.02
Sc	2.6 ± 0.1	12 ± 3	6.7 ± 0.3
Sm	3 ± 0.3	5 ± 0.4	–
Ta	0.4 ± 0.2	0.5 ± 0.4	–
Tb	0.2 ± 0.03	0.1	–
Th	83 ± 6	102 ± 7	390 ± 90
U	–	1.2 ± 0.06	1.3 ± 0.6
Yb	0.04 ± 0.02	0.7 ± 0.04	1.5 ± 0.05

due to the presence of gypsum, which was confirmed by conventional chemical analysis.

Table 10 gives the maximum and minimum concentrations of the various elements in samples obtained from the Murzuq basin compared with values obtained from Al Kufrah basin. Also given in the same table are the average values determined by Maksimovic and Eskangi (1978) for Al Kufrah basin and the values given by Turekian (1982) (international available values for sandstones and clay-rich sediments for shale). There is a strong similarity in the abundance of elements in the Murzuq and Al Kufrah basins except for Th which has a noticeably high content in most samples taken from the Murzuq basin and in Fe which is enriched in Al Kufrah basin. The Th concentration in Murzuq basin could be of economic interest, but further investigations are needed to estimate the potential of the region with respect to this element. The Th content in almost all samples taken from this basin is also much higher than in the SR material taken for quantitative assessments using RNAA (Andesite KA-3, from Santorin, Greece, which contains only about 7 ppm Th). However, the contents of lanthanides in this SR material (Alian and Sansoni, 1980) are rather similar to their range in the Nubian Sandstones studied from both basins (the Andesite KA-3 contents of lanthanides in ppm are Ce 41, Eu 1.1, La 18, Lu 0.5, Sm 4.8, Tb 0.43 and Yb 1.35). Although it is rather difficult to establish definite profiles for the contents of all elements in the various sections taken from the Murzuq area, the data obtained in the present study might be useful as regards the geochemistry of this type of sandstone. Thus, trace elements in sandstones are expected to be bound mainly to accessory minerals. Our results in general show a somewhat uniform level for many trace elements, indicting that these elements are bound mainly to accessory minerals. Some other elements, however, exhibit varying levels, being enriched in certain samples. This might indicate the presence of corresponding minerals.

The accuracy of our results which would evaluate the systematic error in the two methods can best be shown by comparing results for an SR material with certified values. The two methods were tested on JG-1 (Alian *et al.*, 1983). Agreement with the certified values was good except for Fe (1.85 instead of 1.54%). The precision of the element content in terms of standard deviation is also seen from our results to be good or satisfactory except for Ta. The reason for the poor precision of Ta might be due to the presence of some foreign activity of an energy similar to that of Ta (at 1221.2 keV).

The results obtained in this work will be helpful for mineralogical investigations of the sequence involved as well as for a regional stratigraphic and sedimentological study. All available literature on Nubian Sandstones has recently been compiled in a comprehensive biography of 346 references (El-Zouki, 1981). In Egypt, the mother country of these rocks, Nubian Sandstones have a long stratigraphic range extending from the Lower Palaeozoic to the Upper Cretaceous. In other countries, the term is mostly restricted to Upper Jurassic and Lower Cretaceous rocks. In Libya, however, it refers to the Upper Carboniferous and Lower Cretaceous range (El-Zouki, 1981).

ACKNOWLEDGEMENTS

The authors are grateful to the University of Garyounis Research Centre for initiating this project, the Soil and Water Authority of the General Secretariat of Agriculture of Libya for financial support of the project. One of us (A.A.) is grateful to Professor Dr. B. Sansoni and the other staff of Juelich Nuclear Research Centre, FRG, for their help and for permission to perform the analysis.

Table 7. Analysis of 5 Nubian Sandstone samples from A1 Kufrah basin by Monostandard (M) and Relative (R) Neutron Activation Analysis (NAA). Content in ppm, except Fe and K, in %

Element	Sample									
	S22d		154a		S11d		S15i		S22e	
	MNAA	RNAA	MNAA	RNAA	MNAA	RNAA	MNAA	RNAA	MNAA	RNAA
Ba	172.7 ± 10.1	–	199.6 ± 15.2	–	454.2 ± 30.1	424.1 ± 28.1	497.8 ± 32.3	–	112.3 ± 5.6	108.6 ± 43.0
Ca	132.5 ± 12	–	–	–	–	–	–	409.1 ± 303.2	131.1 ± 10.1	–
Ce	58.6 ± 10.1	41.3 ± 11.4	81.3 ± 9.3	67.0 ± 7.4	79.4 ± 8.9	–	11.4 ± 21	10.1 ± 1.0	22.2 ± 4.2	24.12 ± 3.6
Co	8.7 ± 0.9	18.0 ± 0.2	1.8 ± 0.2	1.6 ± 0.2	10.2 ± 0.8	10.32 ± 0.08	0.9 ± 0.1	1.3 ± 0.9	3.4 ± 0.6	2.7 ± 0.3
Cr	48.9 ± 1.5	–	20.7 ± 1.2	19.8 ± 0.5	81.4 ± 5.7	74.91 ± 2.0	6.2 ± 0.9	6.8 ± 2.1	8.4 ± 11	7.0 ± 0.5
Cs	2.7 ± 0.3	3.5 ± 0.4	–	–	5.1 ± 0.6	4.1 ± 0.5	0.61 ± 0.05	0.65 ± 0.02	–	–
Fe %	–	1.85 ± 0.5	–	7.91 ± 0.6	–	2.58 ± 0.16	–	0.54 ± 0.07	–	0.26 ± 0.05
Hf	–	–	98.2 ± 15.1	79.1 ± 19.2	50.5 ± 6.7	59.6 ± 15.3	18.1 ± 4.2	17.5 ± 4.3	17.9 ± 4.5	24.2 ± 5.0
La	28.5 ± 1.3	23.4 ± 1.0	36.7 ± 3.1	39.5 ± 1.7	44.4 ± 1.2	45.5 ± 2.0	8.2 ± 0.9	7.3 ± 0.3	16.2 ± 0.3	16.8 ± 0.7
Rb	88.6 ± 15.2	83.2 ± 67.0	–	–	128.1 ± 14.3	81.5 ± 11.2	13.4 ± 2.2	14.8 ± 2.1	–	–
Sc	5.1 ± 0.4	5.6 ± 0.3	7.8 ± 0.3	8.1 ± 0.4	16.5 ± 0.2	16.6 ± 0.1	1.7 ± 0.2	1.7 ± 0.7	4.4 ± 0.2	4.3 ± 0.1
Sm	5.5 ± 0.14	–	10.8 ± 0.4	–	6.6 ± 0.5	5.6 ± 0.2	1.2 ± 0.1	0.98 ± 0.03	0.96 ± 0.08	1.3 ± 0.4
Ta	–	–	4.1 ± 1.6	1.0 ± 0.4	2.5 ± 0.5	3.2 ± 0.1	0.23 ± 0.07	0.92 ± 0.91	0.35 ± 0.03	0.38 ± 0.0
Th	6.7 ± 0.3	7.5 ± 1.3	5.5 ± 0.7	4.1 ± 2.1	13.2 ± 1.1	13.82 ± 5.6	1.9 ± 0.3	1.9 ± 0.4	4.2 ± 1.1	2.4 ± 1.5
U	5.62 ± 1.11	–	–	–	56.4 ± 10.8	120.4 ± 50.5	–	–	7.04 ± 1.30	–
As	2.34 ± 0.9	–			2.2 ± 0.9		0.97 ± 0.09		1.4 ± 0.4	
Au	0.016 ± 0.003		0.017 ± 0.001		0.011 ± 0.002		0.015 ± 0.02		–	
Br	4.92 ± 0.5				7.3 ± 0.8		1.3 ± 0.2		–	
Eu	1.3 ± 0.1		1.9 ± 0.3		1.2 ± 0.1		0.91 ± 0.05		1.5 ± 0.1	
K %	3.16 ± 0.1				3.34 ± 0.12		3.4 ± 0.3		4.0 ± 0.2	
Lu	0.85 ± 0.07		0.69 ± 0.05		1.19 ± 0.1		0.21 ± 0.07		0.96 ± 0.08	
Na	760 ± 70		167 ± 14		359 ± 36		112 ± 12		550 ± 52	
Nd	111 ± 16		48 ± 9		76 ± 10		8 ± 3		16 ± 1.4	
Yb	3.8 ± 0.6		3.3 ± 0.4		6.1 ± 0.9		1.8 ± 0.2		8.7 ± 0.6	

Table 8. Neutron Activation Analysis of Trace Elements (ppm), Ca and Fe (%) in Nubian Sandstone from Al Kufrah basin using the Relative Method (RNAA)

Element	Sample				
	54b	64c	65a	43b	84b
Ba	116.3 ± 67	–	–	–	
Ca %	–	–	–	–	4.48 ± 1.35
Ce	207.2 ± 1	28.2 ± 0.14	16.1 ± 0.08	42.5 ± 0.2	24.63 ± 0.12
Co	9.5 ± 0.04	3.7 ± 0.015	0.567 ± 0.002	21.4 ± 0.09	4.66 ± 0.02
Cr	25.7 ± 2.4	15.3 ± 1.9	21.4 ± 1.3	47.7 ± 2.8	11.96 ± 1.48
Eu	1.05 ± 0.2	0.5 ± 0.09	–	0.7 ± 0.1	–
Fe %	6.4 ± 0.02	2.21 ± 0.01	0.366 ± 0.001	4.24 ± 0.01	1.64 ± 0.00
Hf	7.1 ± 1.4	–	3.7 ± 0.75	–	–
La	36.7 ± 0.26	34.95 ± 0.25	18.3 ± 0.13	39.2 ± 0.28	29.5 ± 0.21
Lu	0.19 ± 0.06	0.09 ± 0.03	0.051 ± 0.015	0.17 ± 0.05	0.086 ± 0.026
Sc	5.2 ± 1.1	4.52 ± 0.98	0.94 ± 0.2	3.8 ± 0.8	2.4 ± 0.5
Sm	3.6 ± 0.3	1.58 ± 0.02	0.72 ± 0.01	–	1.03 ± 0.02
Th	7.2 ± 3.3	4.6 ± 2.1	3.5 ± 1.6	7.4 ± 3.3	4.9 ± 2.2
U	–	–	–	1.7 ± 0.88	–
Yb	0.74 ± 0.19	0.38 ± 0.18	0.27 ± 0.07	1.1 ± 0.24	0.72 ± 0.1

Table 9. Range of elements (in ppm except Ca and Fe, in %) in various sections of sandstones from Murzuq basin

Element	Sample					
	21	22	23	24	25	26
Ba	–	–	–	347	143 –248	9940
Ca %	0.9– 1.26	0.8– 1.4	0.9– 2.0	0.55– 1.9	0.23– 17	1.17– 3.9
Ce	0.6–122	36 – 90	33 –771	25 –160	0.4 –106	42 – 88
Co	14 – 62	0.3– 1.8	3 – 21	2 – 27	0.3 – 5	0.5 – 1.9
Cr	2 –186	9 – 63	20 – 66	18 – 86	2 – 52	23 – 28
Cs	23	–	1.0	0.5 – 1.0	0.2 – 1.3	–
Eu	0.3– 1.7	0.5– 1.4	0.3– 2.8	0.3 – 4.0	0.1 – 1.2	0.57– 1.0
Fe %	0.8– 3	0.1– 1.5	0.4– 3	0.4 – 6.6	1 – 6.4	0.31– 1.3
Hf	6 – 19	3 – 18	7 – 41	4 – 21	1.6 – 19	7 – 17
La	18 – 53	20 – 54	27 –108	10 – 74	2 – 49	26 – 36
Lu	0.2– 0.7	0.3– 1	0.3– 1	0.3 – 1.1	0.1 – 0.6	0.2 – 0.23
Rb	–	–	18	25 – 54	27	–
Sc	2 – 27	6.5– 11	5 – 13	2 – 17	0.3 – 10	2.6 – 12
Sm	2 – 5.7	2.6– 3.0	–	2 – 18	0.23– 3	3 – 5
Sr	–	–	–	–	208	–
Ta	0.2– 1.3	0.2– 1.0	0.3– 1.0	0.1 – 1.0	0.2 – 1	0.4 – 0.5
Tb	0.2– 0.3	0.1– 0.2	0.1– 0.4	0.2 – 0.6	0.03– 0.3	0.1 – 0.2
Th	48 –170	81 –144	69 –235	34 –205	6 – 82	83 –390
U	2 – 34	1.6– 2	0.3– 1.7	0.5 – 83	1.24	1.2 – 1.3
Yb	0.5– 1.1	0.5– 1.2	0.5– 1.6	0.3 – 2.4	0.2 – 0.6	0.4 – 0.7

Table 10. Content of Ca, Fe and K (%) and trace elements (ppm) in sandstones from Murzuq and Al Kufrah basins

Element	Murzuq basin	Al Kufrah basin		International values (Turekian, 1982)	
	This work	This work	Maksinovic and Eskangi (1978)	Sandstone	Shales
As	–	0.97 – 2.34	1	1	13
Au	–	0.011– 0.017	–	–	–
Ba	143 –9940	108 –497	113	X0 *	580
Br	–	1.3 – 7.3	–	–	–
Ca %	0.23– 17	0.01 – 4.5	–	0.0X	0.3
Ce	0.3 – 171	10 –207	–	–	–
Co	0.3 – 62	0.57 – 21.4	1.3	0.3	19
Cr	2 – 186	6 – 81	15	35	90
Cs	0.1 – 23	0.6 – 5.1	–	–	–
Eu	0.1 – 4	0.5 – 1.9	–	–	–
Fe %	0.1 – 6.6	–	–	–	–
Hf	1.6 – 41	7 – 98	–	–	–
K %	–	3.16 – 4.0	–	–	–
La	2 – 108	7.3 – 45.5	35	7.2	39
Lu	0.1 – 1.1	0.05 – 1.2	–	–	–
Nd	–	7.8 –111	–	–	–
Rb	18 – 54	13 –128	–	–	–
Sc	0.3 – 17	1.7 – 16	4	1	13
Sm	0.23– 18	0.72 – 10.8	–	–	–
Sr	208 (one value)	–	13	20	300
Ta	0.1 – 1.3	0.23 – 4.1	–	–	–
Tb	0.03– 0.6	–	–	–	–
Th	6 – 390	1.9 – 13.8	–	–	–
U	0.3 – 83	1.3 –120.4	–	–	–
Yb	0.2 – 2.4	0.27 (one value)	–	–	–

* X0 = 10 → 90.

REFERENCES

ALIAN, A. and SANSONI, B. (1980). Comparison of different methods for activation analysis of geological and pedological samples: reactor and epithermal neutron activation, relative and monostandard methods. Report Juel-Spez-75, KFA Juelich Gmbh. ISSN 0366-0885, 46 p.

ALIAN, A., DJINGOUA, R.G., KROEMER, B. and SANSONI, B. (1983). The monostandard method in thermal neutron activation analysis, Juel-1982 Report, KFA, Juelich Gmbh, ISSN 0366-0885, 24 p.

EL-HINNAWY, E., KABESH, M.L. and ZAHRAN, I. (1973). Mineralogy and chemistry of Nubian Sandstones from the central eastern of Egypt. *Neues Jahrb. Mineral.*, **118**, 211–234.

EL-ZOUKI, A. (1981). Bibliography of Nubian Sandstones in North Africa and the Middle East with special reference to Libya. Res. Cent., Garyounis Univ., Binghazi, 63 p.

MAKSIMOVIC, Z. and ESKANGI, A.M. (1978). (Extract). *Bull. Acad. Serbe Sci. Arts Cl. Sci. Math. Nat.*, **LXI**, (17).

TUREKIAN, K.K. (1982). Chemistry of the earth hold. Rindart and Winston Inc., 84–85.

Tempestite Facies, Murzuq Basin, Great Socialist People's Libyan Arab Jamahiriya: Their Recognition and Stratigraphic Implications

JOEL CARNEIRO DE CASTRO [1], JORGE CARLOS DELLA FAVERA [1] AND MUFTAH EL-JADI [2]

سحنات العواصف بحوض مرزق ، ليبيا ، التعرف عليها ومضمونها الطبقي

ج . س . كاسترو وج . س . دلافافيرا وم . الجدي

الخلاصـــة

لقد دلت الدراسات الحقلية بحوض مرزق ، وهو حوض اقليمي راسخ بوسط جنوب ليبيا ، على وجود سحنات لرسوبيات العواصف لأول مرة وذلك بمعظم الرسوبيات البحرية التي ترجع إلى دهر الحياة القديمة .

وكان من أهم هذه الرسوبيات تلك التي بتكوينى تان الزفت وأكاكوس السيلوريين وتكوينى عوينات عوينين وطهارة الديفونيين وتكوين مرار الكربوني .

وتوجد رسوبيات العواصف في دورات ترسيبية واضحة يزداد حجم حبيباتها مع الزيادة في السمك إلى أعلى . ويصل سمك هذه الدورات الترسيبية إلى 50 متراً أو أكثر . وتتميز الصخور الرملية عند القمة وسمك يصل إلى 10 أمتار بطباقية متقاطعة تليلية . وتتكون الدورة الترسيبية الكاملة من طبقات منفردة يقل حجم الحبيبات بها تدريجياً إلى أعلى . وهي تّشبه في ذلك تتابع بوما المعروف . وغالباً ما تتبادل رسوبيات العواصف هذه مع فواصل رسوبية رقيقة محفورة . وتوجد علامات السقف عند القاعدة وعلامات التموج عند القمة . وذلك بمعظم رسوبيات العواصف .

وتنتمي هذه السحنات إلى رسوبيات ألسنة الرمال بالمنطقة المغمورة التي جاءت نتاجاً لموجات العواصف برف بحري مفتوح . وتشترك رسوبيات العواصف مع رسوبيات العكر في بعض المميزات ، غير أنها تختلف عنها في ظاهرة إنسيابها المتذبذب . ويرتبط أصل رسوبيات العواصف برسوبيات العكر بتكوين تان الزفت ، حيث أن الثانية ترسبت تحت عمق أمواج العواصف إلى جانب أن رسوبيات العواصف تدل على ظروف قاعية جيدة التأكسد .

ويبدو أن رسوبيات العواصف لا توجد في المقاطع البحرية الكمبروأردوفيشية والديفونية السفلى . وقد يكون غيابها هنا ذو علاقة بعرض الرف ، حيث أن الأرفف العريضة تحد من تأثير العواصف وتساعد على عمل المد والجزر ، الذي يدل عليه وجود التراكيب الترسيبية ذات العلاقة .

Abstract. Recent field work carried out in the Murzuq basin, an intracratonic basin in central southern Libya, revealed for the first time an abundance of tempestite facies in most of the marine deposits of Palaeozoic age.

The most impressive tempestite deposits are in the Silurian Tanezzuft and Acacus Formations, in the Devonian Aouinet Ouenine and Tahara Formations, and in the Carboniferous Mrar Formation.

Tempestites occur in very conspicuous coarsening-thickening upward sequences up to 50 m thick or even, exceptionally, thicker. At the base of each cycle, shales with lenticular and wavy bedding (oscillatory flow type) are the main subfacies. At the top, massive sandstones (up to 10 m thick) are characterized by the ever-present hummocky cross-stratification. The whole cycle is made up of individual beds which are fining upwards, similar to the Bouma Sequence. Interlayered with these "classical" tempestites very thin, strongly burrowed intervals ("hardgrounds") frequently occur. Sole marks at the base and ripple marks at the top are abundant in most tempestite beds.

These facies belong to offshore bar or lobe deposits produced by storm waves in open shelf. Tempestites bear some common characteristics to turbidites but differ from them in their oscillatory flow features. In the Tanezzuft

---

[1] PETROBRAS/CENPES, Cidade Universitaria, Quadra 7, Ilha do Fundao, 21910, Rio de Janeiro, Brazil.
[2] Formerly at BRASPETRO, Tripoli, Libya.

Formation, tempestites and turbidites are genetically related, the latter being deposited below the palaeostorm wave base.

On the other hand, tempestites apparently are absent in the Cambro-Ordovician and in the Lower Devonian marine sections. Such an absence could be related to shelf width since wide shelves preclude storm action and favour tidal action. The latter is indicated on those sections by the presence of tidal-related sedimentary structures.

INTRODUCTION

The Murzuq basin region includes the area between the Tībistī mountains and the Hoggar massif (Touareq and Tabū shields) on the south, and Al Ḥamadah al Ḥamrā' and the Jabal as Sawdā'-Al Qarqaf high on the north. Most of the basin is presently drowned by the Murzuq sand-sea.

The Murzuq basin is a classical Palaeozoic intracratonic basin. A thick blanket of continental Late Palaeozoic and Mesozoic strata covers the central part of the Murzuq basin. Only at the rims are the Lower Palaeozoic rocks spectacularly exposed especially in Al Qarqaf high on the north, the Ghāt area on the south, and the Dūr al Quṣṣah area on the east.

Field work was undertaken during the Autumn of 1984 in order to supplement with facies analyses the geological study of the Murzuq basin being carried out by Braspetro staff in Tripoli. The studied sections are situated on the margins of Al Qarqaf high (Brāk, Idrī, 'Awaynāt Wanīn, Mesa al Mrār), in the Ghāt area (Al 'Awaynāt, Tanezzuft valley, Wādī Iyadhar, Takharkhouri pass, Wādī Wān Kāsā), and in the Dūr al Quṣṣah area (Fig. 1).

As the Murzuq basin is a classical locality for world geology, a large number of papers have been written on several geological aspects, mainly sedimentary facies. However, the tempestites were not interpreted even though they are some of the most important facies occurring in marine deposits. The reason is that this kind of facies only became popular in geological literature at the end of the Seventies, although it had been described and interpreted with the present meaning by the end of the last century.

In this paper, we follow the stratigraphic column and nomenclature proposed by Bellini and Massa (1980) (Fig. 2).

THE TEMPESTITE MODEL

Tempestites, or storm deposits according to Seilacher (1982), are now some of the most studied sedimentary facies due to their abundance in the geological record and to some puzzling features related to their genesis. On the other hand, there are no modern analogues to this kind of facies and there is a high degree of speculation involved in assessing their genesis.

According to our experience from Libya and Brazil (Della Favera, 1984), tempestites occur in very conspicuous coarsening-thickening upwards cycles (up to 50 m thick or even, exceptionally, thicker) (Figs 3A, 7g). At the base of each cycle, shale and siltstone with lenticular and wavy bedding (oscillatory flow type) are the main subfacies. At the top, massive sandstones (up to 10 m thick) with the ever-present hummocky cross-stratification are the main feature. The whole cycle is made up of individual beds which are fining upwards (similar to the Bouma Sequence). Proximal tempestites are sandier and more massive than distal ones (Fig. 7e, f). Interlayered with these "classical" tempestites very thin, strongly burrowed intervals ("hardgrounds") frequently occur. Sole marks at the base and ripple marks (some wave interference ripples) are abundant in most tempestite beds.

Recognition of hummocky cross-stratification is very important since it is the key to environmental interpretation. It is better developed within coarse siltstones and very fine to fine sandstones which have been deposited in shallow marine environments. Due to difficulties in observation it has not been recognized with complete certainty from recent marine sediments. According to Duke (1982), its main elements (Figs 3B, 7a, b) are:

(1) Low-angle (generally less than 15°) undulatory cross-lamination which is the primary diagnostic feature.
(2) Within one bed, both concave and convex upward curvatures are present.
(3) Wavelengths range from one to several metres.
(4) Laminae may be erosively truncated by overlying laminae, or may be non-erosively terminated against underlying laminae.

This facies belongs to offshore bar or lobe deposits produced by storm waves in open shelf. Hummocky cross-stratification would occur only above depths of 200 m, according to modern indications. Tempestites are genetically similar to turbidites, except for their oscillatory flow features.

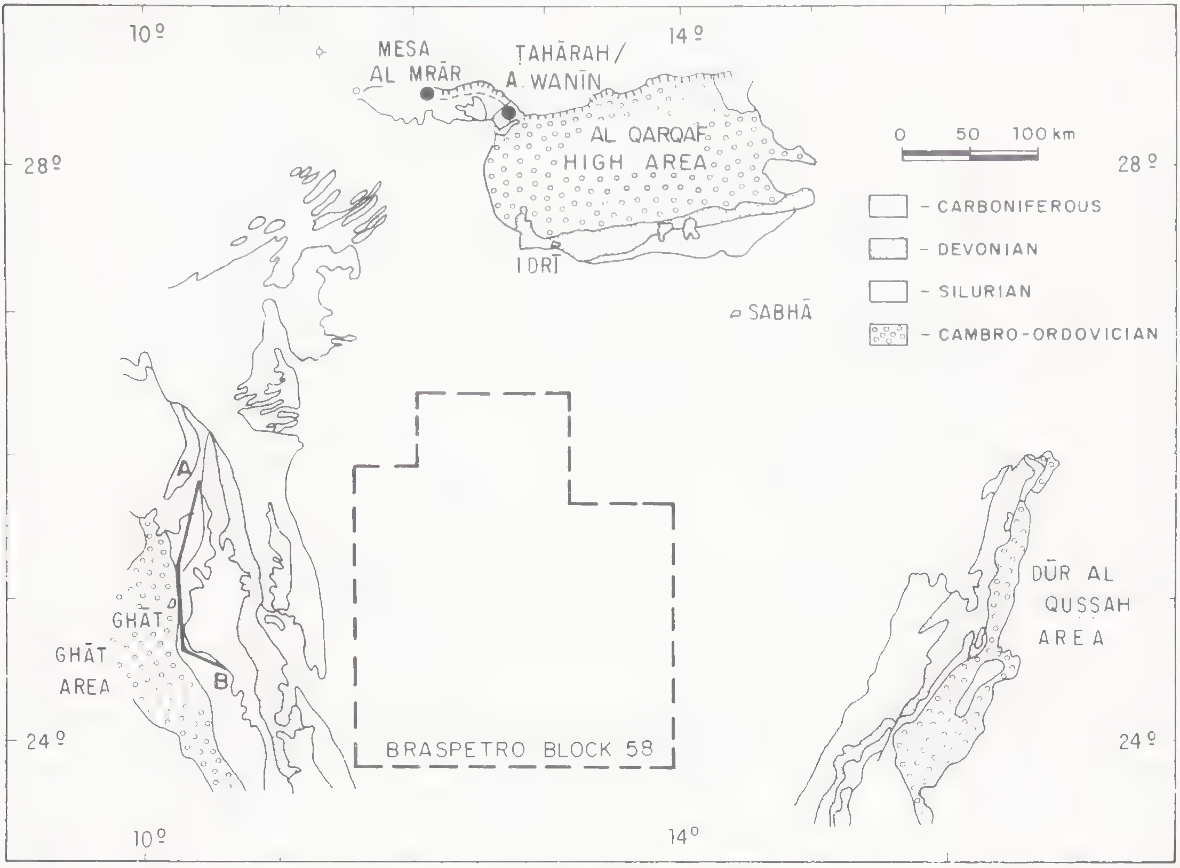

Fig. 1. Location map of the studied areas along the Murzuq basin margins. Line *A–B*, in the Ghāt area, indicates the stratigraphic section detailed in Fig. 4.

Tempestites are one of the strongest arguments in favour of the so-called "episodic sedimentation" (Dott, 1983). Each tempestite bed indicates instantaneous deposition from a turbulent suspension whereas burrowed hardgrounds would represent more normal "fairweather" conditions.

Tempestite facies were recognized in the Tanezzuft Formation, the lower part of the Acacus Formation, the Aouinet Ouenine Formation, the Tahara Formation, the Mrar Formation and the Assedjefar Formation.

GEOLOGICAL OCCURRENCE

Silurian

The Silurian System comprises two units: the graptolitic shales of the Tanezzuft Formation and the sandstones of the Acacus Formation. They are well exposed in SW Libya, in their type sections in the Takharkhouri pass 55 km SE of Ghāt.

The combined thickness of both formations is 600 m in the Wādī Iyadhar area where the contact is transitional and the units are diachronous, with progradation from south (SW Murzuq) to north (N Ghadāmis basin). Thus, to the Llandoverian age of these units which are recorded in the Ghāt area, younger ages are progressively added towards northern Ghadāmis–south Tunisia. Furthermore, in the same direction occurs an important facies change: the sandy fluvial–transitional Acacus Formation of Ghāt area is replaced by a sandy-shale marine unit in the northern Ghadāmis area (Bellini and Massa, 1980).

The Silurian sequence represents a perfect example of transgressive and regressive conditions present in the same cycle of relative rise of coastal onlap during the formation of a clastic wedge (Vail *et al.*, 1977, p. 67). The wedge base is made up of littoral facies which onlap the basal unconformity. After a sudden deepening of the basin, turbidites are deposited.

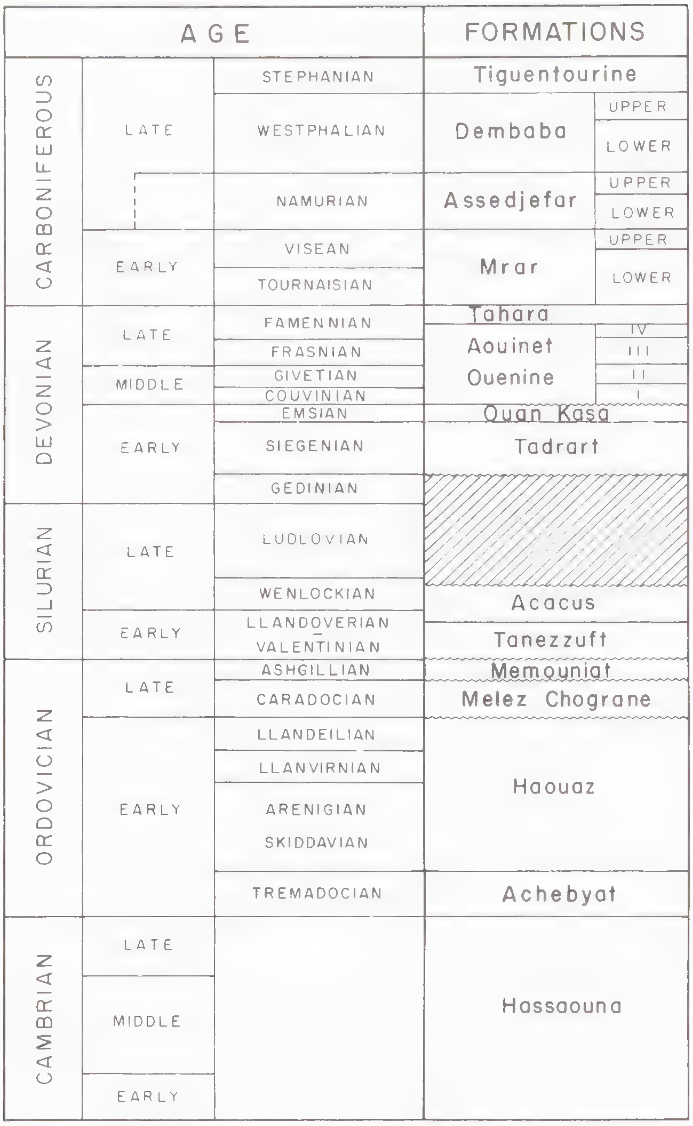

AGE			FORMATIONS	
CARBONIFEROUS	LATE	STEPHANIAN	Tiguentourine	
		WESTPHALIAN	Dembaba	UPPER
				LOWER
		NAMURIAN	Assedjefar	UPPER
				LOWER
	EARLY	VISEAN	Mrar	UPPER
		TOURNAISIAN		LOWER
DEVONIAN	LATE	FAMENNIAN	Tahara	
			Aouinet Ouenine	IV
		FRASNIAN		III
	MIDDLE	GIVETIAN		II
		COUVINIAN		I
	EARLY	EMSIAN	Ouan Kasa	
		SIEGENIAN	Tadrart	
		GEDINIAN	▨	
SILURIAN	LATE	LUDLOVIAN	▨	
		WENLOCKIAN	Acacus	
	EARLY	LLANDOVERIAN VALENTINIAN	Tanezzuft	
ORDOVICIAN	LATE	ASHGILLIAN	Memouniat	
		CARADOCIAN	Melez Chograne	
	EARLY	LLANDEILIAN	Haouaz	
		LLANVIRNIAN		
		ARENIGIAN SKIDDAVIAN		
		TREMADOCIAN	Achebyat	
CAMBRIAN	LATE		Hassaouna	
	MIDDLE			
	EARLY			

Fig. 2. Stratigraphic column of the Murzuq basin, according to Bellini and Massa (1980).

The coarse terrigenous influx vanishes as transgression reaches its acme (middle wedge). Regressive conditions start from this point upwards, beginning again with turbidites, then tempestites (sea bottom shallower than 200 m) and transitional facies, ending with continental facies (wedge top). The top of the Acacus Formation represents new transgressive conditions (Fig. 4).

Important facies and thickness changes in the Tanezzuft–Acacus sequence were observed in SW Murzuq basin: from south (Takharkhouri pass) to north — Al 'Awaynāt (Fig. 5). Southwards, the Silurian sequence is thicker and sandier. Northwards, there is a progressive facies change accompanied by a general thinning: the coarse-grained fluvial Acacus Formation, in the Jabal Ikbar area, passes to the fine-grained marine Acacus sandstones in the Ghāt area and finally to the thinnest northern section, in Al 'Awaynāt, with only the marine sand-shale "Tanezzuft facies".

Devonian

The Middle–Upper Devonian Aouinet Ouenine Group was described in the type section (W Al Qarqaf) where it attains a thickness of 225 m (Bellini

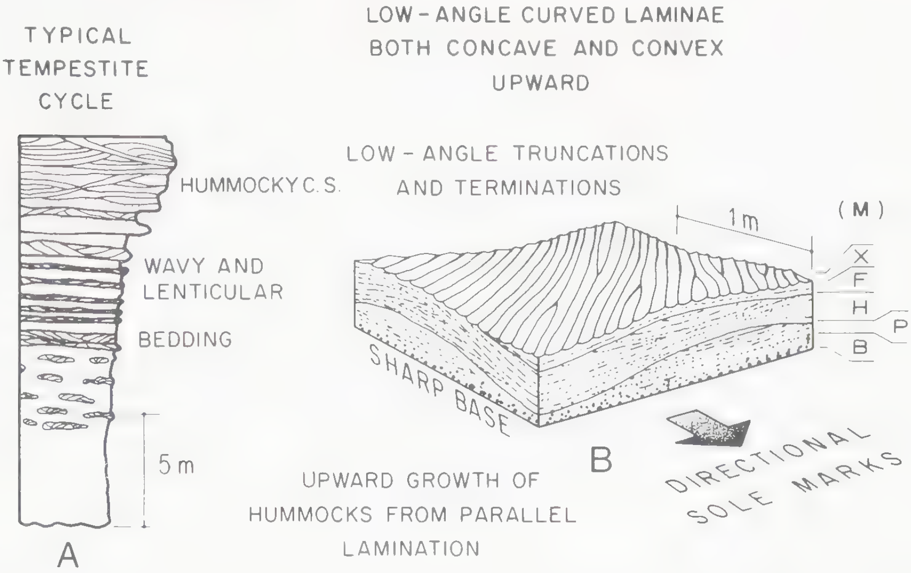
TYPICAL TEMPESTITE CYCLE
HUMMOCKY C.S.
WAVY AND LENTICULAR
BEDDING
5 m
A
LOW-ANGLE CURVED LAMINAE BOTH CONCAVE AND CONVEX UPWARD
LOW-ANGLE TRUNCATIONS AND TERMINATIONS
1 m
(M)
X
F
H
P
B
SHARP BASE
B
DIRECTIONAL SOLE MARKS
UPWARD GROWTH OF HUMMOCKS FROM PARALLEL LAMINATION

Fig. 3. The Tempestite Model: (A) Idealized cycle; (B) Main elements of hummocky cross-stratification, according to Duke (1982).

and Massa, 1980); these authors divided it into four formations (Aouinet Ouenine I to IV) with a chronostratigraphic character. More recently Vos (1981) studied the lower half of the group and recognized three cycles, which we use as a stratigraphic base in the present study (Fig. 6, left).

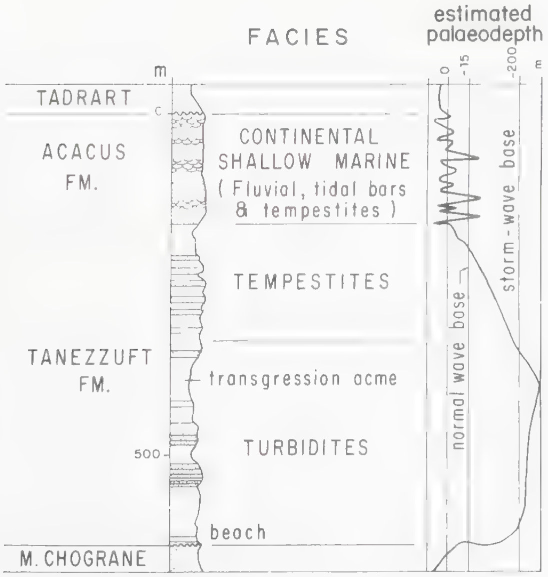
FACIES
estimated palaeodepth
m
0
-15
-200
m
TADRART
c
ACACUS FM.
CONTINENTAL SHALLOW MARINE (Fluvial, tidal bars & tempestites)
TEMPESTITES
TANEZZUFT FM.
transgression acme
TURBIDITES
500
beach
M. CHOGRANE
normal wave base
storm-wave base

Fig. 4. Silurian sequence in the Ghāt area. Notice the regressive–transgressive character of the section. Estimated palaeodepth is based on modern analogues of present continental shelves. Facies interpretation was set upon a formerly measured section by Collomb and Heller (1959) in the Wādī lyadhar area.

Marine sediments occur throughout the unit, except for the second cycle and the upper part of the first cycle, where fluvial-dominated deltaic deposits are present. Two key beds (tempestites) are conspicuous in the first cycle and in the top of the second cycle, and are associated with brachiopod coquinas.

Tempestites are mostly characteristic in the top of the third cycle, forming a coarsening upwards sequence capped by hummocky cross-bedded sandstones (Fig. 7b). *Tigillites* (*Skolithos* facies) is the main feature in the hardgrounds.

In the Dūr al Quṣṣah area, Devonian strata correlative with the Aouinet Ouenine cycles are dominated by tempestite deposits with monotonous and repetitive coarsening-upward cycles.

Tahara Formation

The Tahara Formation has been defined in well B1-49, which is located in Wādī Ṭahārah. Despite its age, which may be Strunian (Devonian–Carboniferous transition; Bellini and Massa, 1980) or early Tournaisian (Sanchez-Barreda, 1977), it has been placed with Devonian units because of similarities with the Aouinet Ouenine Group.

The Tahara Formation crops out in west Al Qarqaf along a belt 2 km long and 10 km NW of ‘Awaynāt Wanīn. Two coarsening upwards sequences of shales and sandstones, separated by a plane sur-

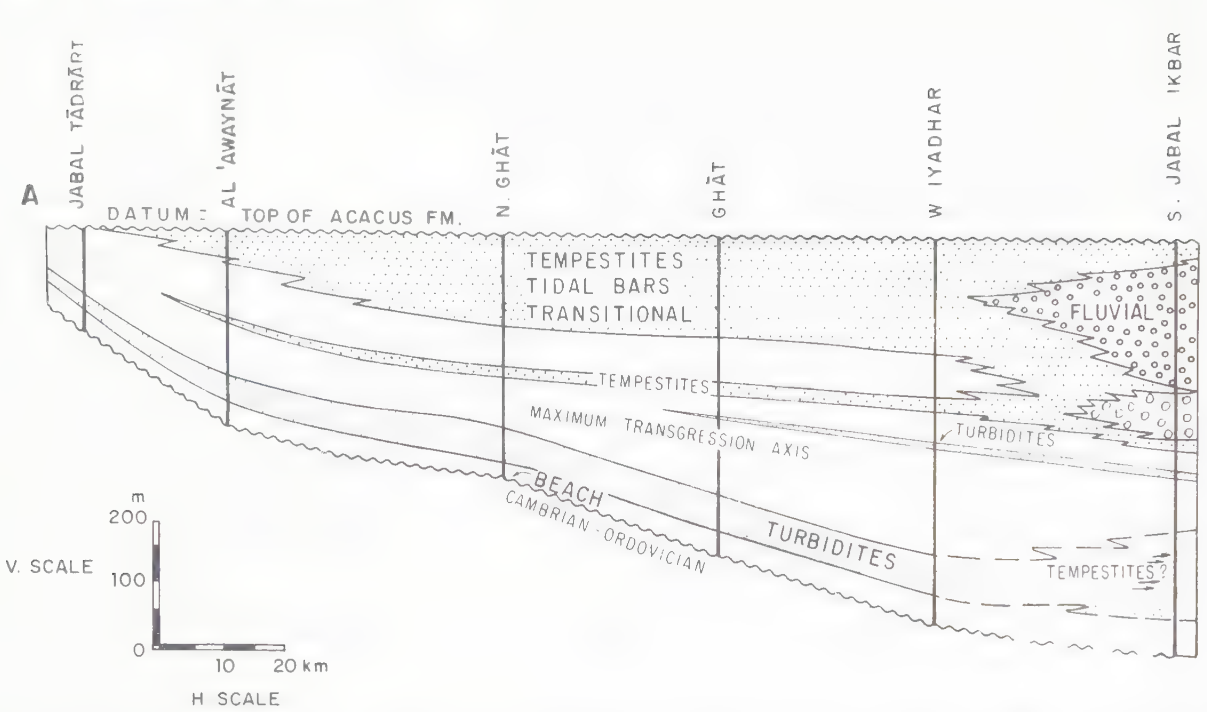

Fig. 5. Cross section showing facies distribution and stratigraphic relationships. Notice proximal (S)–distal (N) facies changes. Tempestites occur in the upper regressive section although they possibly may appear in the proximal part of the transgressive section. All units thin towards the Tanesfert high. Based upon measured sections by Collomb and Heller (1959) in the Ghāt area. Section location is shown in Fig. 1.

face (hardground) are spectacularly displayed in the outcrop (Fig. 7h).

The lower sequence is formed by tempestites in small coarsening upward sequences, from lenticular-wavy shales and sandstones to hummocky cross-stratified very fine sandstones. The top sandstones and shales are burrowed by *Skolithos* and form a plane surface or hardground.

On the other hand, the upper sequence tempestites are closely associated with tide-dominated facies (with herringbone cross-bedding) indicating alternations of very rapid open shelf conditions — during storms — with a tidal flat or nearshore scenario (Fig. 6, centre).

Carboniferous

The Carboniferous System represents the last Palaeozoic marine cycle in southern Libya; its thickness reaches 1000 m in the outcrops of the southern part of the Ghadāmis basin (west of Al Qarqaf high). It comprises four classical formations (Fig. 2).

The Mrar Formation comprises a thick, lower terrigenous unit, and an upper shale-carbonate unit (with *Collenia*) as shown in the Mesa al Mrār and Wādī al Mohr areas. Whitbread and Kelling (1982) recognized 15 depositional cycles, generally coarsening upwards, in the terrigenous unit. They correlated these cycles from west Al Qarqaf outcrops to wells as far away as 250 km in the Ghadāmis basin. They interpreted these cycles as fluvial-dominated deltas (cycles 1 to 4; 14 and 15) associated with lagoon/tidal flats, beach/marine, tidal ridges and troughs and marine bars (cycles 5 to 13) (Fig. 6, right).

From our observations, the upper cycles of the Mrar Formation (cycles 8 to 15) are formed by monotonous coarsening and shoaling upwards tempestite cycles, with the most dramatic tempestite features exposed at the Mesa al Mrār escarpments (Fig. 7g). The basinwide correlation and the lateral–vertical organization of the cycles as shown by the cross sections strongly suggest an epicontinental seaway with tempestite lobes or offshore bars migrating through time as being the main palaeogeographic features of the Mrar Formation in the Ghadāmis basin. The same type of cyclicity was observed in the Mrar and Assedjefar Formations in Al 'Awaynāt area.

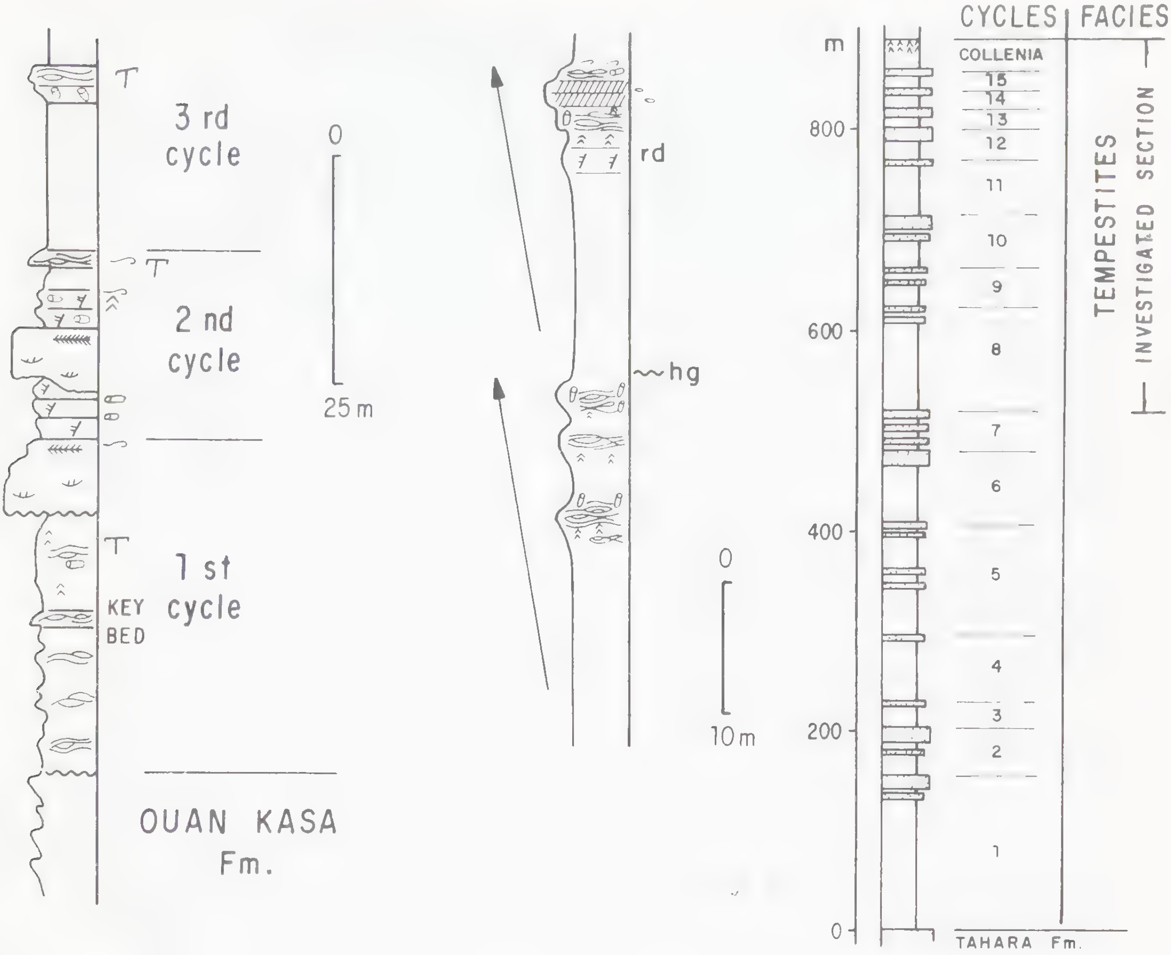

Fig. 6. Interpreted columnar sections. Left: Aouinet Ouenine Group, 'Awaynāt Wanīn area, Al Qarqaf high: tempestites occur in all cycles, although they present a typical vertical sequence only in the third cycle. Measured section based on Vos (1981). Centre: Tahara Formation in Ṭahārah area, Al Qarqaf high; Tempestites occur mainly in the lower sequence; notice hardground (hg) separating upper and lower sequences. Right: Mrar Formation at Mesa al Mrār and Wādī al Mohr areas; studied section begins at Cycle 8 and shows the absolute dominance of tempestites; Section was formerly defined by Whitbread and Kelling (1982).

CONCLUDING REMARKS

The overwhelming presence of tempestites (products of exceptional sedimentation events) in the marine sections of the Murzuq basin, supports the non-uniform modern view of the sedimentary record ("episodic sedimentation", Dott, 1983). In basins like Murzuq the large lateral extension of some facies is really impressive. These are facies measured in thousands of square kilometres, versus a very narrow vertical range. This fact was also observed by Burollet and Busson (1983) who explained it by catastrophic sedimentary processes acting during sedimentation with no modern analogue.

Although the abundance of tempestites in most of the marine sections is impressive, they are noticeably absent in the Cambro-Ordovician and Lower Devonian (Tadrart/Ouan Kasa Formations). Only a few observations in the Melez Chograne Formation point to features similar to the hummocky cross-stratification, although no classical tempestite facies could be defined. However, the marine character of its sedimentation is quite clear since marine fossils are present. Following Klein (1981) we think that this absence could be explained by shelf width. Modern oceanographic observations have shown that wide shelves preclude storm action, since storm energy is dissipated along an elongated path. On the

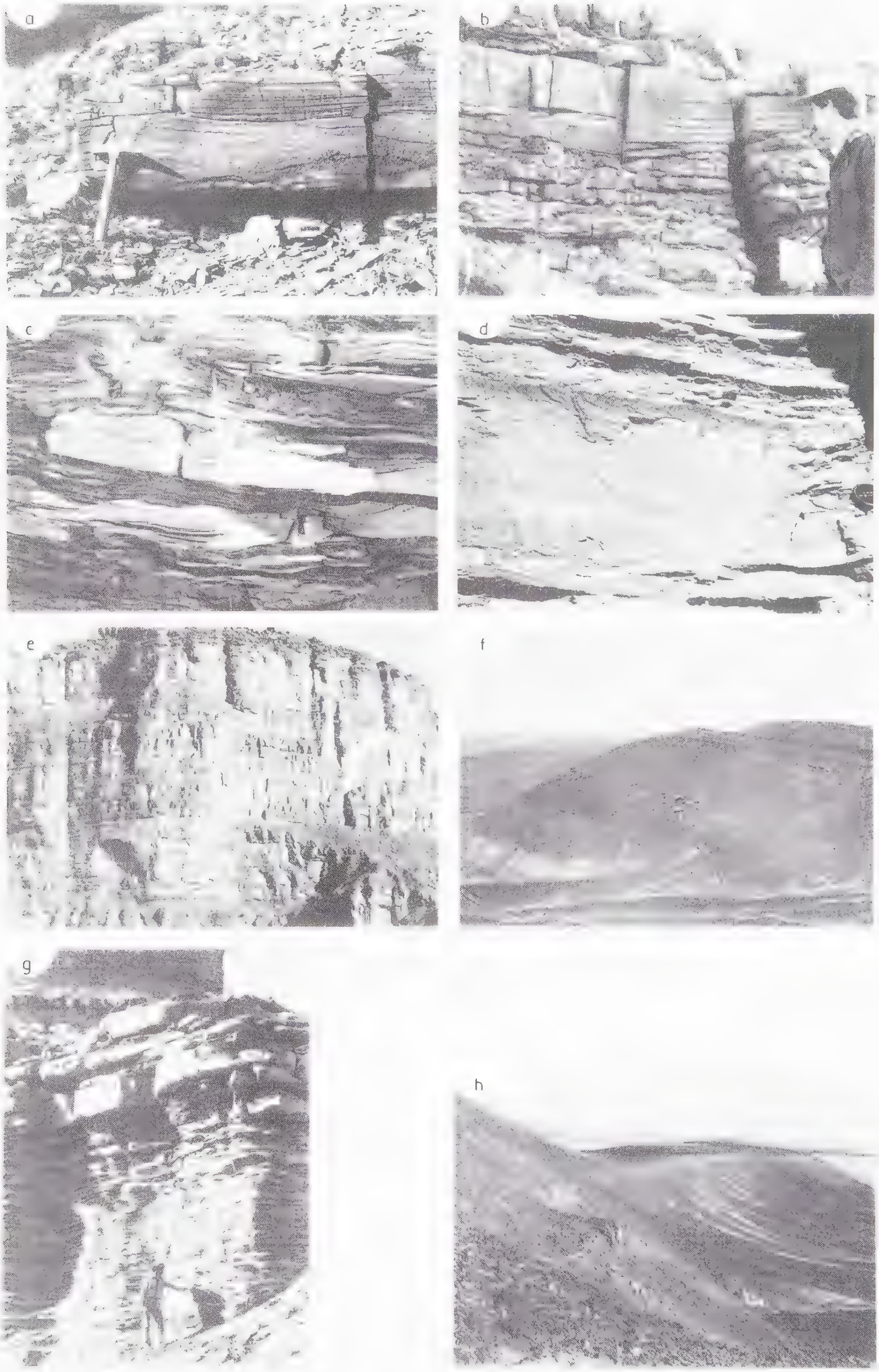

Fig. 7. (a) Part of a tempestite layer showing the typical hummocky cross-stratification. Notice the gradational sequence, low-angle curved laminae — both concave and convex upward — low-angle truncations and sharp base. Tanezzuft Formation. Northern escarpment; Dūr al Quṣṣah area.

other hand, wide shelves favour tide action and most of the present-day offshore tidal sands are being laid down on such shelves (Yellow Sea and northern Brazil, for example). Thus, it could be said that the Cambro-Ordovician and Lower Devonian formations represent deposition on shelves wider than those with tempestite facies.

ACKNOWLEDGEMENTS

The authors are indebted to Drs. R. Porto and M.A. de Oliveira, former Braspetro staff members in Tripoli for the realization of the field work. We express our gratitude to the National Oil Company of Libya and to Braspetro, Rio de Janeiro, for permission to publish this paper.

REFERENCES

BELLINI, E. and MASSA, D. (1980). A Stratigraphic contribution to the Palaeozoic of the Southern Basins of Libya. *In: The Geology of Libya* (*eds* M.J. Salem and M.T. Busrewil). Academic Press, London, **I**, 3–56.

BUROLLET, P.F. and BUSSON, G. (1983). Plate-formes et Bassins: Danger d'une Actualisme Exageré. *Notes Mém. Comp. Fr. Pétrole*, **18**, 9–16.

COLLOMB, G.R. and HELLER, CH. (1959). Rapport Géologique sur le Flanc Occidental du Bassin de Mourzouk. *C.P.T.*, Internal Report, 29 p.

DELLA FAVERA, J.C. (1982). Devonian storm- and tide-dominated shelf deposits, Parnaiba Basin, Brazil (Abstract). *Bull. Am. Assoc. Petrol. Geol.*, **66**(5), 562.

DELLA FAVERA, J.C. (1984). Eventos de Sedimentação Episódica nas Bacias Brasileiras. Uma contribuição para atestar o caráter pontuado do registro sedimentar. *Anais XXXIII° Congr. Brasil Geol.*, 489–501.

DOTT, R.H., JR. (1983). SEPM Presidential Address: Episodic Sedimentation — How normal is average? How rare is rare? Does it matter? *J. Sediment. Petrology*, **53**(1), 5–23.

DUKE, W.L. (1982). The "Type-locality" of Hummocky cross-stratification: the storm-dominated Silurian Medina Formation in the Niagara Gorge, New York and Ontario. *21st Annu. Ontario Petrol. Inst. Inc. Conf. Techn. Paper*, 2, 1–31.

KLEIN, G. DE V. (1981). Tidal processes. *In*: S.E.P.M. Research Conference on Modern Shelf and Ancient Cratonic Sedimentation: The Orthoquartzite-Carbonate suite revisited. *J. Sediment. Petrology*, **51**(1), 338.

SANCHEZ-BARREDA, M. (1977). Palaeoenvironmental reconstruction of the Tahara Formation of North-western Libya. *N.O.C.*, Tripoli, Int. Rept.

SEILACHER, A. (1982). Distinctive features of sandy tempestites. *In: Cyclic and Event Stratification* (*ed.* G. Einsele and A. Seilacher). Springer Verlag, Berlin, 333–349.

VAIL, P.R., MITCHUM, R.M. and THOMPSON, S. III (1977). Seismic-stratigraphy and global changes of sea level from coastal onlap. Part 4 — Global cycles of relative changes of sea level. *In*: Seismic Stratigraphy: Applications to hydrocarbon exploration (*ed.* C.E. Payton). *Mem. Am. Assoc. Petrol. Geol.*, **26**, 83–98.

VOS, R.G. (1981). Deltaic sedimentation in the Devonian of Western Libya. *Sediment. Geol.*, **29**, 67–88.

WHITBREAD, T. and KELLING, G. (1982). Mrar Formation of Western Libya: evolution of an early Carboniferous delta system. *Bull. Am. Assoc. Petrol. Geol.*, **66**(8), 1091–1107.

Fig. 7 (continued).

(b) Hummocky cross-stratification overlying wavy bedding with *Tigillites* (*Skolithos*) burrowing. Aouinet Ouenine Group, 3rd cycle — 'Awaynāt Wanīn, Al Qarqaf area

(c) Detail of oscillatory lenticular and wavy bedding — base of tempestite. Mrar Formation. Al 'Awaynāt Awbārī Highway, 9 km, Ghāt area.

(d) Burrowed hardground on top of a tempestite layer. Mrar Formation, limestone quarry, near Brāk, Al Qarqaf area.

(e) to (g) Tempestite cycles at three different situations: (e) Proximal tempestites. Notice high sand/shale ratio and massive character. Acacus Formation, Tanezzuft valley, 30 km north of Ghāt. (f) Distal tempestites. Observe low sandstone/shale ratio. Tanezzuft Formation, 100 km north of Ghāt. (g) Typical tempestite cycle. Bottom: lenticular and wavy bedding; top: hummocky cross-stratification. Mrar Formation, cycle 8, Mesa al Mrār, Al Qarqaf area.

(h) Top of the lower tempestite cycle. Tahara Formation, Ṭahārah, Al Qarqaf area.

Contribution to the Stratigraphy of the Murzuq Basin, SW Libya

E.S.T. Pierobon[1]

مراجعة للنواحي الطباقية والترسيبية لتتابعات الصخور الرئيسة لحوض مرزق جنوب غربي ليبيا

إ. س. ت. بيروبون

الخلاصـــة

يغطي حوض مرزق الترسيبي مساحة شاسعة من جنوب غربي ليبيا وهو يقع بين عنصرين تكتونيين بارزين وهما مرتفعي تيبستي/الهروج والهجار عند الحدود الشرقية والغربية على التوالي إلى جانب مرتفع قرقاف عند الشمال. ولقد قام العديد من الباحثين إلى جانب شركات النفط بدراسات مختلفة بحوض مرزق ومنطقة فزان على مدى السنتين غير أنه لم تكتمل الصورة الطباقية للمنطقة حتى الآن وذلك لعدم توفر الكثير من المعلومات التي أمكن الحصول عليها الآن.

وقد تم تفسير معظم المعلومات والبيانات المتحصل عليها عبر السنين بهدف المساهمة في تحسين الدراسات وأعمال الإستكشاف مستقبلاً بهذا الحوض. كما أنه بالإمكان إدخال بعض التعديلات الدقيقة على التاريخ الطبقي للحوض. وقد أدى تطبيق النماذج الترسيبية المستمدة من التكشفات السطحية إلى تعزيز التفسيرات الخاصة بجيولوجية ما تحت السطح تعزيزاً قوياً.

Abstract. The Murzuq basin, covering a vast area of SW Libya, is situated between three prominent tectonic elements, namely Al Qarqaf high in the north and Tībistī/Al Harūj and Hoggar uplifts, on its eastern and western borders, respectively. Several authors and companies have carried out geologic work of various types on the Murzuq and Fazzān areas over the years. A more comprehensive picture of regional stratigraphic aspects is now provided on the basis of surface and subsurface data acquired during the extensive exploratory campaign undertaken in the basin by Petrobrás Internacíonal S.A. – Braspetro. The bulk of the data gathered over the past decade has been interpreted with the aim of furnishing a contribution towards future studies and exploration work in the basin. Some refinements on the basin's stratigraphic history can be made. The application of depositional models generated from outcrop studies supports the interpretation of the subsurface geology on better grounds.

INTRODUCTION

The Murzuq basin covers a vast area of SW Libya and is situated between three prominent tectonic elements, namely, Al Qarqaf high in the north and the Tībistī/Al Harūj and Hoggar uplifts, on its western and eastern borders, respectively (Fig. 1.). Geologic work of various sorts has been performed by many authors in the Murzuq and Fazzān areas over many years. The results of extensive seismic surveys, eight wildcat wells and geological studies carried out by Petrobrás Internacíonal S.A. – Braspetro in the now relinquished NC58 block (Fig. 2a, b) have contributed significantly to improve the knowledge of the basin as a whole.

Most sedimentary units forming the stratigraphic column of the basin are widespread and have good correlation in the subsurface and outcrops. Many outstanding regional events of the past are preserved on the geological record.

The stratigraphic column presented shows the sequence of these events as well as lateral and vertical relationships of lithofacies (Fig. 3). Refinements in the area's stratigraphic history have been introduced by Castro *et al.* (1985, *int. rep.*) with the results of the surface geology work carried out in December

---

[1] Petrobrás Internacíonal S.A. – Braspetro. Current address: Rua Gal. Canabarro, 500-11° Andar, CEP 20271 – Rio de Janeiro, Brazil.

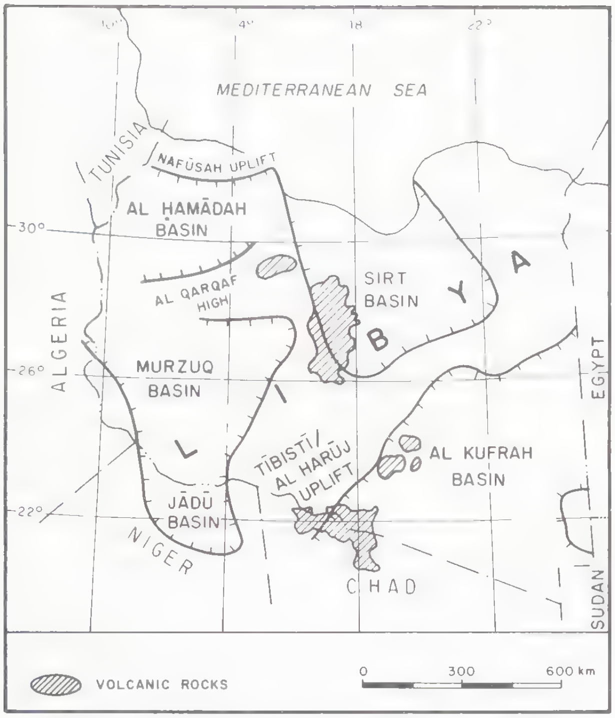
18
MEDITERRANEAN SEA
TUNISIA
NAFŪSAH UPLIFT
AL HAMĀDAH BASIN
30°
AL QARQAF HIGH
SIRT BASIN
L I B Y A
ALGERIA
26°
MURZUQ BASIN
EGYPT
TĪBISTĪ/ AL HARŪJ UPLIFT
AL KUFRAH BASIN
22°
JĀDŪ BASIN
NIGER
CHAD
SUDAN
VOLCANIC ROCKS
0
300
600 km

Fig. 1. Location map of Libyan sedimentary basins.

1984. This introduced some updated concepts on depositional processes of the various units studied. The main sources of stratigraphic data treated here are Banerjee (1980), Castro *et al.* (1985), and the results of Braspetro's seismic and drilling campaigns in the area.

LITHOFACIES AND DEPOSITIONAL ENVIRONMENT

Mourizidie and Precambrian Formations (Precambrian — Algonkian)

The basement substratum of the Murzuq basin is exposed in coring the Tībistī and Hoggar uplifts, and in some erosional windows in Jabal al Qarqaf. Basement rocks can be roughly divided into two main groups, a high-grade metamorphic series (Desio, 1942, 1943) and a semimetamorphic series (Desio, 1943) which includes the so-called Mourizidie Formation (Burollet *et al.*, 1963).

The Mourizidie is disconformably overlain by the basal conglomerate of the rather horizontal strata of the Cambrian Hassaouna Formation. In the Murzuq basin few wells have so far penetrated to this sequence; in well A1-NC115, extrusive acidic to intermediate rocks (rhyolite to rhyodacite) were penetrated in a section equivalent to the Mourizidie, for about 75 m.

Cambro-Ordovician System

The Cambro-Ordovician System of Libya was first defined in the area of Al Qarqaf arch. It is widespread over large portions of the North African craton. Five formations, four of them formally defined by Massa and Collomb (1960), represent this system in Libya; they were grouped into the Qarqaf Group by Burollet (1960).

These rocks show striking lithological similarities in areas widely apart. Their deposition started with

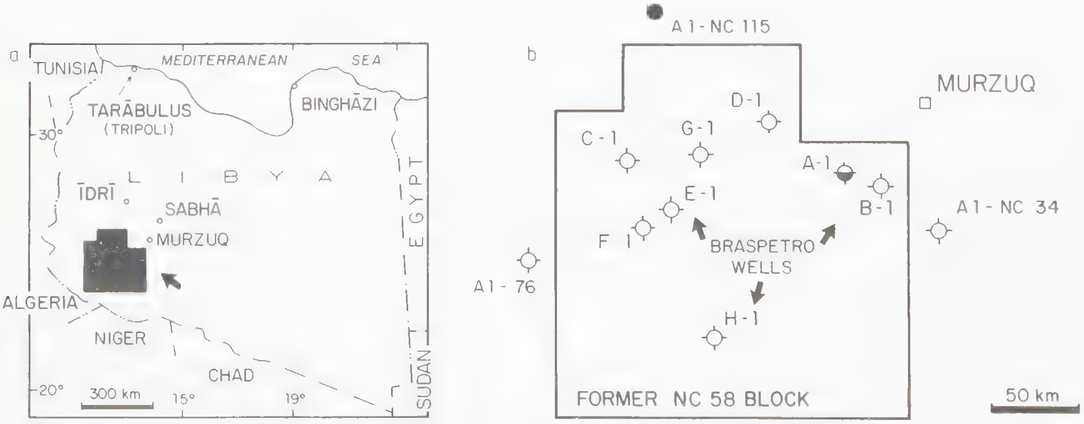
a
TUNISIA
MEDITERRANEAN SEA
TARĀBULUS (TRIPOLI)
BINGHĀZI
30°
L I B Y A
ĪDRĪ
SABHĀ
MURZUQ
EGYPT
ALGERIA
NIGER
CHAD
SUDAN
20°
300 km
15°
19°
b
A1-NC 115
MURZUQ
D-1
C-1
G-1
A-1
B-1
E-1
A1-NC 34
F 1
BRASPETRO WELLS
A1-76
H-1
FORMER NC 58 BLOCK
50 km

Fig. 2. (a) Location of former Braspetro NC58 block. (b) Braspetro's A1- to H1-NC58 wells.

a basal conglomerate marking the unconformable contact with the Precambrian basement. The whole sequence displays characteristic quartzitic and conglomeratic sandstones of fluvial, transitional and marine origin; glacial to periglacial conditions played an important role in deposition through Late Ordovician times. The entire section is barren of fossils, except for conspicuous *Tigillites* sp.

Hassaouna Formation (Cambrian)

The term "Hassaouna" was introduced by Massa and Collomb (1960) after Jabal al Hasāwinah. The formation represents extensive, blanket-type, sandstones medium- to coarse-grained, highly cross-bedded sandstones forming a 160–500 m thick uniform sandy complex spread over vast portions of the Sahara platform. Klitzsch (1963), though, assigned it a thickness of about 1700 m in the Dūr al Quṣṣah area. The formation is unconformably overlain by the fine-grained Ordovician clastics (Collomb, 1962); in the subsurface they are difficult to distinguish from each other.

Castro *et al.* (1985) described the Hassaouna sandstones in the W Al Qarqaf and in Dūr al Quṣṣah as a thick sequence of fluvio-continental deposits bearing conspicuous fining-upward cycles. Each cycle shows basal channel-scouring features, large-scale oblique and sigmoidal cross-beddings grading upward into tabular and festoon (trough) cross-beds; soft-sediment deformation ("de-watering" structures) is rather common. The depositional setting of the Hassaouna can be interpreted in its major part as braided-stream systems due to the high sandstone/shale ratio. The dipmeter log (Fig. 4) provides evidence that the lower 30 m of the Hassaouna could represent a fluvial plain with braided channels deposited during stages of high sediment discharge. The increasing upward marine influence can be correlated with a broad transgressive phase, as inferred from the global coastal onlap chart (Vail *et al.*, 1977; Fig. 3). Massa and Collomb (1960) separated the Haouaz from the Hassaouna Formation based upon *Tigillites*, having assigned a Cambrian age to it. More detailed stratigraphic work will eventually make age refinements possible.

Achebyat Formation (Lower Ordovician — Tremadocian)

The name Achebyat Formation was introduced by Havlicek and Massa (1973). According to Bellini and Massa (1980), the formation is represented by 65 m of medium- to coarse-grained, *Tigillites*-bioturbated sandstones, and common trace fossils like *Cruziana* and *Harlania*. This formation name has not been accepted by some authors, who prefer to include the corresponding interval in the lower part of Haouaz Formation.

Lithologically the Achebyat and the Hassaouna Formations are very similar. A conformable contact with the overlying Haouaz Formation was reported by Havlicek and Massa (1973). Castro *et al.* (1985) interpreted the Achebyat as a possible transition from a fluvial to a marine setting and stressed the predominantly lobate depositional geometry. It has been assigned an Early Ordovician (Tremadocian) age (Havlicek and Massa, 1973; Bellini and Massa, 1980).

Haouaz Formation (Middle Ordovician — Llandeilian to Llanvirnian)

The Haouaz Formation was introduced by Massa and Collomb (1960) after Jabal Ḥaouaz (W of Jabal al Qarqaf). It typically consists of cross-bedded, quartzitic sandstones, in part kaolinitic, with thin shaley intercalations. *Tigillites*-bioturbated levels and ripple marks are conspicuous. In Dūr al Quṣṣah, Klitzsch (1963) reported *Harlania* sp. and poorly preserved casts of brachiopods and bivalves, having also indicated a strong unconformity with the underlying Hassaouna. It is widely accepted today, though, that unconformities can progressively give way to conformable surfaces basinward, due to the relative uplifting of the source areas (or the basin's deepening) with regard to the sea level; other authors have provided field evidence suggesting a conformable contact in Jabal al Qarqaf area. The formation's thickness ranges from 50 m (Dūr al Quṣṣah) to 280 m (Al Qarqaf) in outcrops, and 30 m to 170 m in the subsurface.

Castro *et al.* (1985) described the Haouaz in the outcrops of W Al Qarqaf as a typical prograding alternation of thin non-resistant layers made up of very fine sandstones and siltstones with ripple-drift and micrograded laminae, and thick beds of fine- to medium-grained, tabular to sigmoidal cross-bedded sandstones (Della Favera, 1984; Fig. 6); the latter can be inferred from the dipmeter log (Fig. 4). The same authors suggested a probable transitional to shallow marine (foreshore to shoreface) depositional setting, indicating the "offshore tidal sands" (shoal massifs) of the continental shelves of northern Brazil, the North Sea and in China's Yellow Sea as a possible modern depositional analogue.

Based on brachiopods, Havlicek and Massa (1973)

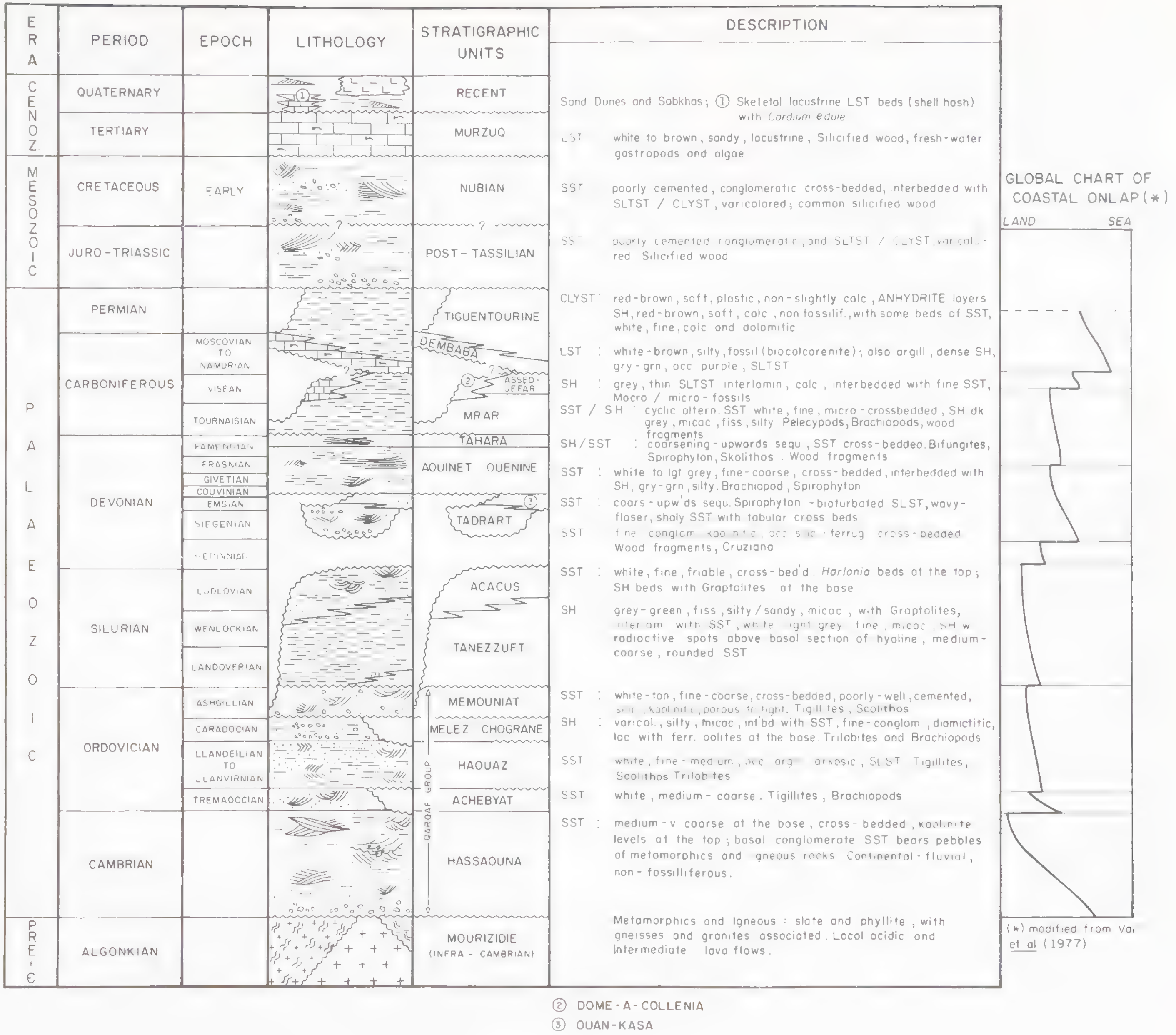
ERA
PERIOD
EPOCH
LITHOLOGY
STRATIGRAPHIC UNITS
DESCRIPTION
GLOBAL CHART OF COASTAL ONLAP (*)
LAND
SEA
CENOZ.
MESOZOIC
PALAEOZOIC
PRE-Є
QUATERNARY
TERTIARY
CRETACEOUS
JURO-TRIASSIC
PERMIAN
CARBONIFEROUS
DEVONIAN
SILURIAN
ORDOVICIAN
CAMBRIAN
ALGONKIAN
EARLY
MOSCOVIAN TO NAMURIAN
VISEAN
TOURNAISIAN
FAMENNIAN
FRASNIAN
GIVETIAN
COUVINIAN
EMSIAN
SIEGENIAN
GEDINNIAN
LUDLOVIAN
WENLOCKIAN
LANDOVERIAN
ASHGILLIAN
CARADOCIAN
LLANDEILIAN TO LLANVIRNIAN
TREMADOCIAN
①
②
③
?
RECENT
MURZUQ
NUBIAN
POST-TASSILIAN
TIGUENTOURINE
DEMBABA
ASSEDJEFAR
MRAR
TAHARA
AOUINET OUENINE
TADRART
ACACUS
TANEZZUFT
MEMOUNIAT
MELEZ CHOGRANE
HAOUAZ
ACHEBYAT
HASSAOUNA
GARGAF GROUP
MOURIZIDIE (INFRA - CAMBRIAN)
Sand Dunes and Sabkhas; ① Skeletal lacustrine LST beds (shell hash) with Cardium edule
LST white to brown, sandy, lacustrine, Silicified wood, fresh-water gastropods and algae
SST poorly cemented, conglomeratic cross-bedded, interbedded with SLTST / CLYST, varicolored; common silicified wood
SST poorly cemented conglomeratic, and SLTST / CLYST, varicol-red Silicified wood
CLYST red-brown, soft, plastic, non-slightly calc, ANHYDRITE layers SH, red-brown, soft, calc, non fossilif., with some beds of SST, white, fine, calc and dolomitic
LST : white-brown, silty, fossil (biocalcarenite); also argill, dense SH, gry-grn, occ purple, SLTST
SH : grey, thin SLTST interlamin, calc, interbedded with fine SST, Macro / micro-fossils
SST / SH : cyclic altern. SST white, fine, micro-crossbedded, SH dk grey, micac, fiss, silty Pelecypods, Brachiopods, wood fragments
SH / SST : coarsening-upwards sequ, SST cross-bedded. Bifungites, Spirophyton, Skolithos. Wood fragments
SST : white to lgt grey, fine-coarse, cross-bedded, interbedded with SH, gry-grn, silty. Brachiopod, Spirophyton
SST : coars-upw'ds sequ. Spirophyton - bioturbated SLST, wavy-flaser, shaly SST with tabular cross beds
SST fine conglom kaolinitic, occ silic / ferrug cross-bedded Wood fragments, Cruziana
SST : white, fine, friable, cross-bed'd. Harlania beds at the top; SH beds with Graptolites at the base
SH grey-green, fiss, silty / sandy, micac, with Graptolites, interlam with SST, white light grey fine, micac, SH w radioactive spots above basal section of hyaline, medium-coarse, rounded SST
SST : white-tan, fine-coarse, cross-bedded, poorly-well, cemented, silic, kaolinitic, porous to tight. Tigillites, Scolithos
SH : varicol., silty, micac, int'bd with SST, fine-conglom, diamictitic, loc with ferr. oolites at the base. Trilobites and Brachiopods
SST white, fine-medium, occ arg arkosic, SLST Tigillites, Scolithos Trilobites
SST white, medium-coarse. Tigillites, Brachiopods
SST : medium-v coarse at the base, cross-bedded, kaolinite levels at the top; basal conglomerate SST bears pebbles of metamorphics and igneous rocks. Continental-fluvial, non-fossiliferous.
Metamorphics and Igneous : slate and phyllite, with gneisses and granites associated. Local acidic and intermediate lava flows.
(*) modified from Va
et al (1977)
② DOME-A-COLLENIA
③ OUAN-KASA

Fig. 3. Stratigraphic column of Murzuq basin (ages according to Van Eysinga, 1975).

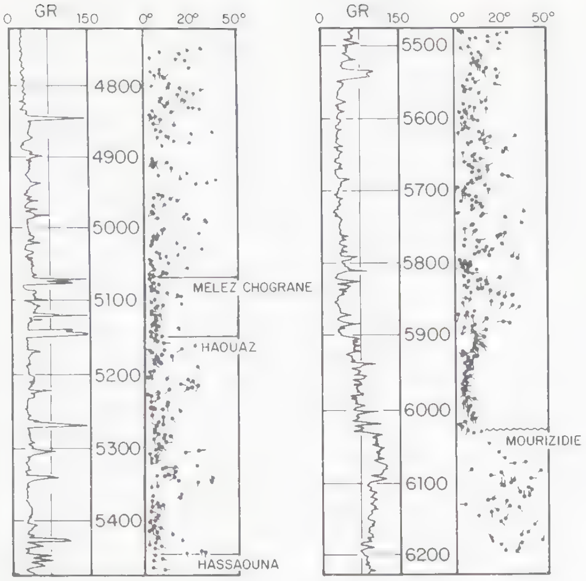

Fig. 4. Schlumberger's dipmeter log of well C1-NC58 (tadpoles show true dips; depths are in feet).

indicated an Early to Middle Ordovician (Llandeilian to Llanvirnian) age for the Haouaz; Millepied (1984) agrees on a probable Middle Ordovician age based on palynological analysis from well C1-NC58.

Melez Chograne Formation (Middle Ordovician — Caradocian)

The Melez Chograne Formation was introduced by Massa and Collomb (1960) after the Melez Chograne mountains in W Al Qarqaf. It is a pelitic to fine clastic sequence consisting of varicoloured, chloritic, thin-bedded shales and siltstones intercalated with angular to subangular, fine-grained sandstone exhibiting micro-hummocks, wave ripples and bioturbations which attest to a shallow marine facies. Abundant fossil tracks are encountered in these rocks. Blocks of granite, gneiss, quartzite and polished and striated clasts immersed in the pelitic matrix indicate a glacial derivation (Collomb, 1962; Bellini and Massa, 1980). The periglacial significance of the basal micro-conglomeratic shales (diamictites) was indicated by Burollet and Byramjee (1969) and corroborated by palaeo-ecological data (Havlicek and Massa, 1973). This same conspicuous shale fabric was reported in wells from Jādū basin, northern Niger.

In the type locality, the Melez Chograne's thickness is in the range of 10–45 m. In the subsurface significant facies changes seem to happen, for only thin, highly radioactive shales (on the gamma-ray logs) occur amid siltstones and fine sandstones; the formation's thickness ranges from 15 m to 75 m, and, exceptionally, reaches 120 m in well A1-NC34. In certain spots it is completely missing due to erosion.

The Melez Chograne Formation was deposited in a quiet marine setting, reflecting a widespread transgression. The contact with the Haouaz Formation is conformable (marked by the presence of ferruginous oolites), and in angular unconformity with the Hassaouna (Collomb, 1962; Castro *et al.*, 1985) where the Haouaz is missing. Marine fossils (brachiopods, bryozoans, crynoids, pelecypods, trilobites and graptolites) are commonly found. Collomb (1962) indicated a probable Middle Ordovician (Llanvirnian to Llandeilian) age based upon some of these; however, brachiopods (Havlicek and Massa, 1973) and palynological studies (Millepied, 1979, 1984; Uesugui, 1984) strongly indicate a Late Ordovician (Caradocian) as the most probable age.

Memouniat Formation (Upper Ordovician — Ashgillian)

The name Memouniat Formation was introduced by Massa and Collomb (1960) after Jabal al Memounīat (W Al Qarqaf). It is a regressive psammitic unit, composed of massive, cross-bedded, medium-grained to conglomeratic sandstones occasionally showing high percentages of kaolinitic matrix. The overall reservoir quality of the Memouniat sandstones ranges from very poor to good (Pierobon, 1984), but locally silicification in its upper part was very intense, seriously hindering the permo-porosities, as shown in Braspetro wells A1- and B1-NC58 (Fig. 2b).

The subsurface occurrence of the Memouniat Formation is widespread, with thicknesses in the range 20–170 m; a regional thickening towards Al Qarqaf high is noted. Its top part is normally in transitional contact with the transgressive Silurian shales, but an unconformable upper boundary (marked by a hematite-rich layer) was reported by Klitzsch (1966) in outcrops. Due to the regressive character of the sandstones, while the basin's borders and palaeohighs were being eroded, basinward the sedimentation occurred without significant interruptions (Fig. 5). Contact with the Melez Chograne Formation was reported as discordant by Bellini and Massa (1980) in outcrops, but the electric logs show no evidence of such a break in the subsurface.

The Memouniat Formation represents the second glacial-marine cycle of the Palaeozoic in Murzuq; a periglacial depositional setting is interpreted

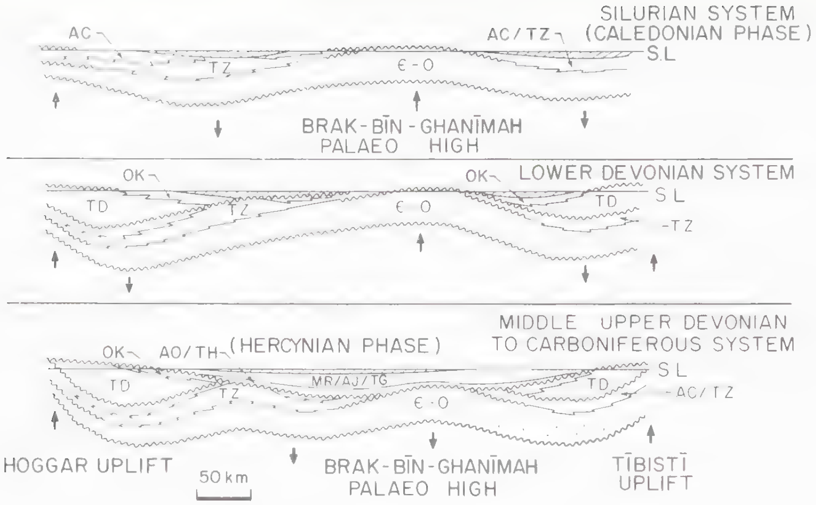
SILURIAN SYSTEM
(CALEDONIAN PHASE)
AC
AC/TZ
S.L
TZ
€-O
BRAK-BĪN-GHANĪMAH
PALAEO HIGH
OK
OK
LOWER DEVONIAN SYSTEM
TD
TZ
€ O
TD
S L
-TZ
MIDDLE UPPER DEVONIAN
TO CARBONIFEROUS SYSTEM
OK
AO/TH
(HERCYNIAN PHASE)
MR/AJ/TG
TD
TZ
€-O
TD
S L
-AC/TZ
HOGGAR UPLIFT
50 km
BRAK-BĪN-GHANĪMAH
PALAEO HIGH
TĪBISTĪ
UPLIFT

Fig. 5. Stratigraphic evolution of Murzuq basin from Silurian through Carboniferous. *C-O* = Cambro-Ordovician, *AC/TZ* = Acacus/Tanezzuft, *TD* = Tadrart, *OK* = Ouan Kasa, *AO/TH* = Aouinet Ouenine/Tahara, *MR/AJ/TG* = Mrar/Assedjefar/Tiguentourine.

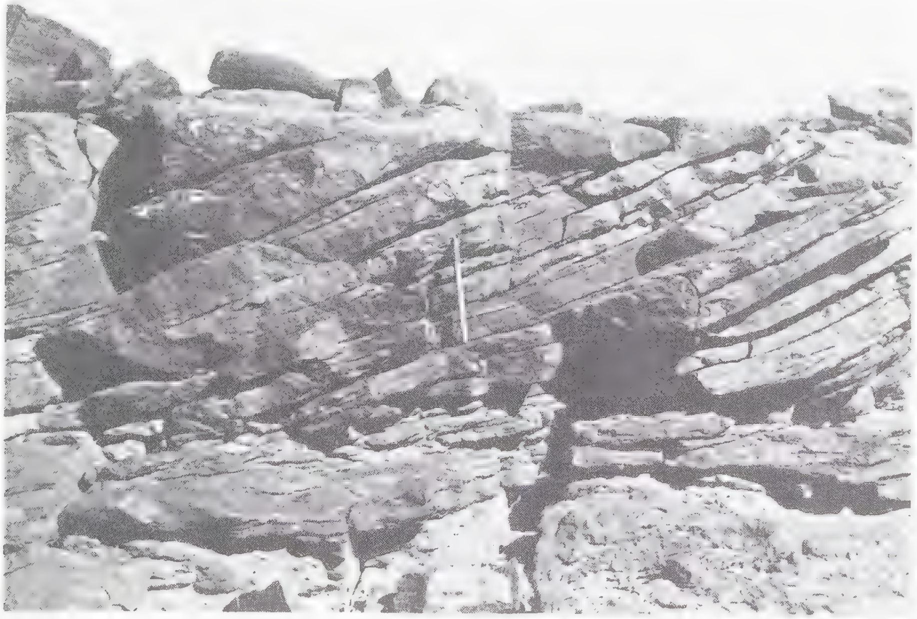

Fig. 6. Lateral view of sigmoidal lobe —Haouaz Formation (Al Qarqaf high, 110 km N of Idrī); notice "s"-shaped forms.

based on ecological grounds (Havlicek and Massa, 1973), sediment texture (diagenetic kaolinite) and structure (water-escape structures — indication of perma-frost?). Castro *et al.* (1985) described large-scale sigmoidal lobes forming a mound-shaped sedimentary geometry. Wave ripples and *Skolithos* tracks attest to a shallow-water marine deposition. The sandstone beds are usually unfossiliferous, with only local poorly preserved brachiopods and pelecypods. A Late Ordovician age (probably Caradocian) was established by Collomb (1962) on palynological grounds for the western basin; an Ashgillian age was suggested on the basis of brachiopods by Havlicek and Massa (1973), and corroborated by palynological studies of drill cuttings (Millepied, 1984; Uesugui, 1984).

Silurian System

Silurian rocks are widespread in Libya. In Murzuq basin they are formally grouped into the Tanezzuft and Acacus Formations. The Silurian sediments are generally conformable with the Ordovician Memouniat Formation. Fürst and Klitzsch (1963) reported the Silurian unconformably overlying older Cambro-Ordovician rocks. The transgressive Tanezzuft shales grade upward into the prograding Acacus sandstones and siltstones. A disconformity marks the contact of the predominantly marine Silurian with the continental Lower Devonian strata (Massa and Collomb, 1960; Collomb, 1962; Burollet *et al.*, 1963; Banerjee, 1980). Castro *et al.* (1985) reported the partial or total truncation of the Silurian by an early to middle Devonian unconformity in Dūr al Quṣṣah and W Al Qarqaf areas; this very pronounced, basin-wide unconformity represents a major change in the basin's sedimentary and tectonic history. Various authors have reported thicknesses reached by the Silurian in the order of 600–950 m.

Tanezzuft Formation (Silurian — early Llandoverian)

This formation was formally introduced by Desio (1936b) after Wādī Tanezzuft (about 65 km NE of Ghāt). Its type section was measured by Klitzsch (1963) at Takharkhouri pass (35 km S of Ghāt). The Tanezzuft Formation is a sequence of dark grey to black, graptolitic shales with intercalations of siltstones and fine-grained sandstones, often forming rhythmical alternations; it represents the broad marine transgression of the Silurian sea over the North African craton. Regional thickening occurs towards the outcrop belt in SW Murzuq, where it reaches 475 m; in the subsurface it ranges from 45 m to 320 m. Over the NE portion of the basin an erosional (and perhaps, in part, depositional) pinch-out resulted from the uplifting of the Brāk-Bin Ghanīmah palaeohigh (Fig. 6). In the subsurface the passage from the Tanezzuft to the Acacus Formation is gradational and conformable (Fig. 7).

The Silurian marine encroachment came from the NNW. In many wells and outcrops S of the 26° parallel, the basal Tanezzuft shows a gradational basal section of interbedded shales and medium- to coarse-grained sandstones (Figs 7, 8) which would have been derived from the reworking of the Cambro-Ordovician substratum under wave and tide action; this characterizes a nearshore littoral facies (Fig. 9a, b). The rhythmical alternation of shales, siltstones and very fine sandstones constitute strong evidence of turbiditic flows, with the intervals T_{b-e}, T_{c-e}, T_{d-e} of the classical Bouma Sequence. This could have precluded the formation of

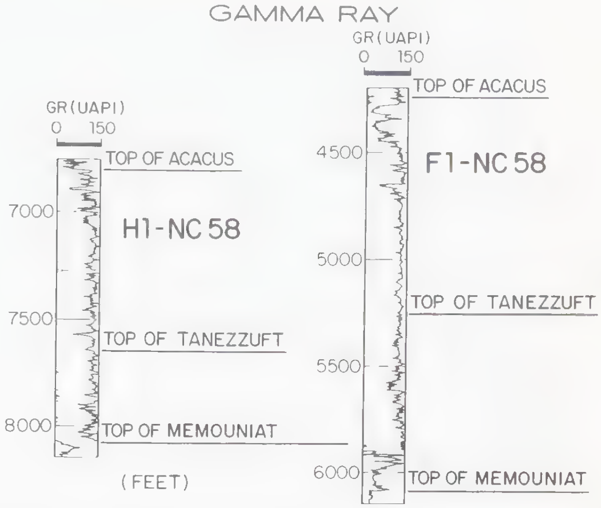

Fig. 7. Typical gamma-ray logs of Acacus and Tanezzuft Formations.

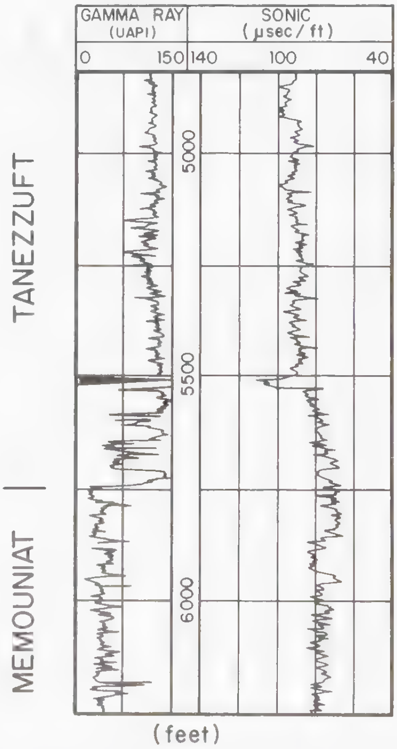

Fig. 8. Radioactive shale bed in the basal Tanezzuft Formation — well E1-NC58.

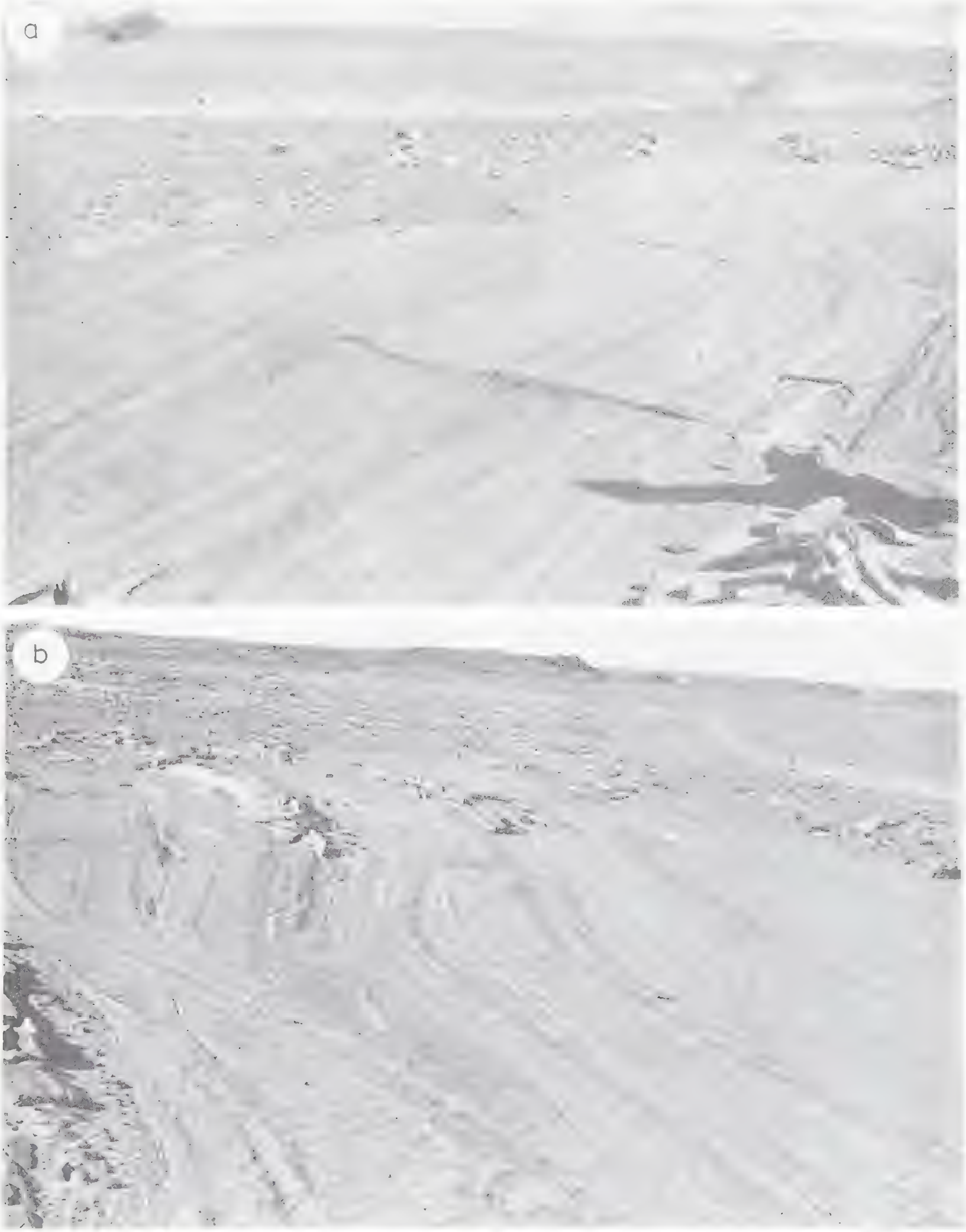

Fig. 9. (a) NE view of nearshore/littoral facies of basal Silurian transitional sandstones (some 5 km N of Ghāt, off the road to Al 'Awaynāt); notice low-angle internal truncations along strike. Silurian sediments form scarp on background. (b) SW view of same site in (a); low-angle dips of laminae appear in upper left corner.

good oil-source rocks since euxinic, organic-rich sediments (pelagic) might have been continuously “diluted” by terrigenous influxes. However, as gamma-ray log (Fig. 8) and geochemical data combined show, high amounts of hydrocarbon-prone organic matter were locally concentrated in the sediments; the radioactive shale marker of the basal Tanezzuft has a broad subsurface occurrence in Murzuq basin. Graptolites (Klitzsch, 1965, 1969) and palynology (Millepied, 1979; Uesugui, 1984) indicate an early Llandoverian age for the Tanezzuft Formation.

Acacus Formation (Silurian — Middle Llandoverian to Ludlovian)

The term "Acacus Sandstone" was introduced by Desio (1936a) after Jabal Akākūs in the Ghāt area. Klitzsch (1969) described a type section formed by 340 m of fine-grained sandstones containing frequent trace fossils (*Harlania harlani* Conrad; *Cruziana* sp.; *Tigillites* sp.), interbedded with dark-grey, graptolitic shales in the lower and middle parts. In Dūr al Quṣṣah the Acacus is a rhythmical alternation of shales, shaley siltstone and fine-grained sandstones which coarsen upward forming massive cross-beds of fluviatile/continental derivation.

The Acacus sandstones represent the regressive phase of the Early Silurian transgression. Castro *et al.* (1985) pointed out the continental to transitional (nearshore marine, Fig. 10a) character of the sedimentation in the outcrops from Takharkhouri to Al 'Awaynāt. They concluded that deposition of regressive clastics began after the transgression acme was reached in the Middle Silurian. A vertical stratigraphic profile of the Acacus "cycle" shows fan deltas and pulses of turbiditic flows (water depths down to 200 m), shallowing-upward into offshore sandbars and the prograding fluvial plain (Fig. 10b). This setting is exemplified by some coarsening-upward intervals of gamma-ray logs (Fig. 7). The lowermost Acacus shales were dated by Klitzsch (1965, 1969) as middle Llandoverian on the basis of graptolites (*Climacograptus* and *Monograptus*). Palynological data from Braspetro wells A1-NC58 (Millepied, 1979) and E1-NC58 (Uesugui, 1984) indicate a Ludlovian to Wenlockian age for the whole Acacus Formation.

Lower Devonian System

Lower Devonian rocks are widespread in the W and SW of Libya. In the Murzuq basin they are mainly represented by sandstones of the Tadrart Formation; the Ouan Kasa Formation has limited regional expression. The sequence is a typical seaward progradation and basinward-thinning of a clastic wedge showing a classical interfingering of facies patterns which change from fluvio-continental to estuarine and at the end of the cycle to shallow marine-neritic. The Tadrart reaches up to 700 m in some outcrops; the significant thickness variations reflect the strong tectonic control on the sedimentation.

Tadrart Formation (Early Devonian — Siegenian)

The Tadrart Formation was introduced by Burollet (1960). Its type section was described by Klitzsch (1965, 1969) at Takharkhouri pass along the eastern margin of Wādī Wān Kāsā. The formation crops out conspicuously in Al Qarqaf, Jabal Akākūs and Dūr al Quṣṣah, showing a marked wedge-out toward the N, into the basin between 25° and 26° latitude, and, toward the E, between 11° and 12° longitude. In Klitzsch's type section the Tadrart displays 310 m of continental to subcontinental, thick cross-bedded and conglomeratic sandstones with rare plant remains (*Lepidodendron*) in the lower half; the upper half displays thin-bedded marine sandstones with abundant *Tigillites*. Its basal part is marked by a ferruginous sandstone resting unconformably upon Silurian rocks. In the subsurface the same contact is clearly unconformable. Around Al Qarqaf high the Tadrart overlies unconformably the Memouniat Formation. The passage to the shales and sandstones of the Ouan Kasa Formation is gradational.

Generally speaking, the Tadrart deposits start with festoon cross-bedded, fluvial sandstones often reworked by tidal currents which cause tabular (herring-bone) crossbeds. Progressive thinning and fining-upward trends reflect an increasing tidal influence that continues into the Ouan Kasa in which coarsening-upward sequences can be attributed to offshore tidal bars. Palaeocurrent measurements in Tadrart megaripples are directed mainly NW, N and NE towards Al Ḥamādah basin. The Tadrart sandstones are usually poorly cemented; in well logs they show very good reservoir characteristics.

The depositional thinning can be attributed to a setting similar to an alpine molasse in which proximal continental facies predominate, and a thicker pile of sediments accumulates near the source areas. As the clastic wedge thins basinward, transitional to fully marine conditions prevail as a function of continuous peripheral reworking. This would explain the presence of both Tadrart (estuarine facies) and Ouan Kasa (tidal bar facies) with different thicknesses and in rapid facies changes either in proximal or in distal areas.

Klitzsch (1969) and Massa and Moreau-Benoit (1976) indicated Siegenian to Emsian as the age range for the Tadrart Formation. Burollet (1960), by analogy with a similar sequence found in Illīzī basin (Algeria), suggested Siegenian as its proba-

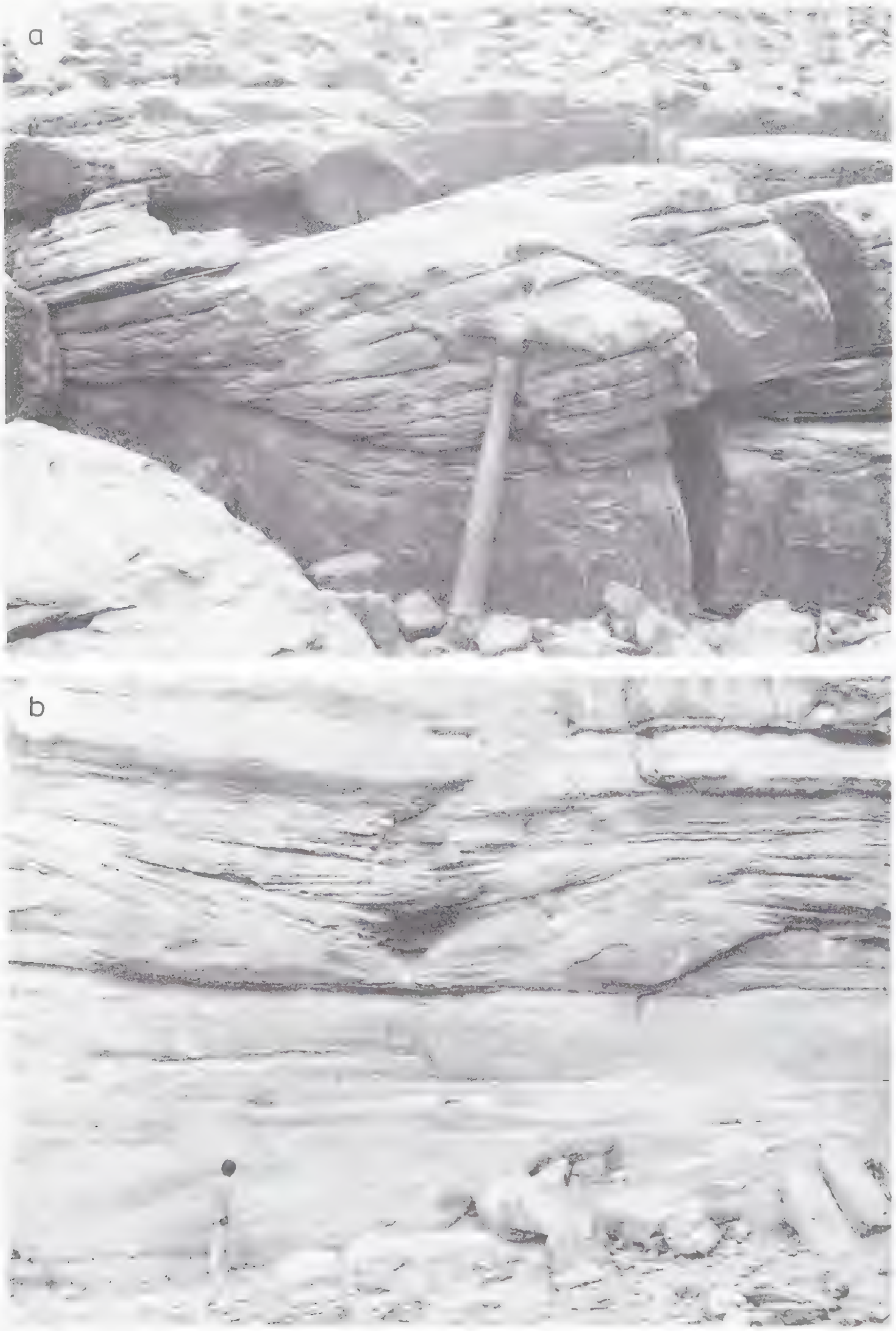

Fig. 10. (a) Sigmoidal lobe in sandstone of Lower Acacus Formation; inferred flow direction is right to left (95 km S of Ghāt). (b) Cut view of fluvial channel, Upper Acacus Formation (105 km S of Ghāt, near Jabal Tādrārt).

ble age. Bearing in mind the above reasoning and the diachronous character of the lithostratigraphic boundaries, the age range can change depending on the more landward or basinward position.

Ouan Kasa Formation (Early Devonian — Emsian)

The Ouan Kasa Formation was first described by Borghi and Chiesa (1940) in Wādī Wān Kāsā. In Klitzsch's type section at Takharkhouri it reaches a thickness of 43 m. Castro *et al.* (1985) reported thin coarsening-upward sequences with wavy-lenticular and flaser-bedded, occasionally bioturbated siltstones and fine-grained sandstones, grading to tabular cross-bedded sandstones at the top. An abundant marine fauna of brachiopods and tentaculites is found. The separation of the Ouan Kasa from the Tadrart in the subsurface is not evident. Electric logs from wells A1-76 and H1-NC58 suggest a rapid transitional passage of the estuarine Upper Tadrart to the shallow marine-neritic Ouan Kasa sandstones and siltstones (tidal bar facies).

In the subsurface of Al Ḥamādah basin a rich assemblage of palynomorphs indicates an Emsian age (Massa and Moreau-Benoit, 1976) for the Ouan Kasa. As for the Murzuq basin, Fürst and Klitzsch (1963) give a possible Eifelian age. The regional erosional event (Early–Middle Devonian unconformity) separates the Lower from the Middle–Upper Devonian sequence. Due to the lack of direct palaeontological dating from subsurface samples, an Emsian age seems to be an appropriate assumption until further data indicate otherwise. Indications that its upper contact may be in part conformable with the overlying Aouinet Ouenine Formation were provided by Bellini and Massa (1980) and Castro *et al.* (1985).

Middle–Upper Devonian System

The Middle-Upper Devonian sequence of SW Libya can be regarded as the result of a major transgressive cycle which began in the Early Devonian (Ouan Kasa "facies") and progressed into the Carboniferous with brief regressive stages, reaching a maximum during the Late Mississippian. The marine encroachment was widespread. In Murzuq its thickness ranges from 40 m to 270 m, generally increasing towards the western part of Al Qarqaf high and into Al Ḥamādah basin. The Middle–Upper Devonian formations can be considered attractive targets for hydrocarbon exploration as they exhibit fair quality reservoir and source beds.

Aouinet Ouenine Formation (Middle/Late Devonian — Couvinian to Strunian)

The Aouinet Ouenine Formation was named by Lelubre (1946) after a well in western Jabal al Qarqaf. Massa and Moreau-Benoit (1976) raised the formation to the rank of a group, splitting it into four informal units: Aouinet Ouenine Formations I to IV. This same subdivision is not feasible for the subsurface of Murzuq basin. Bellini and Massa (1980) described a type section reaching 225 m in the western Al Qarqaf area, appointing four units of chronostratigraphic significance. Vos (1981) and Castro *et al.* (1985) recognized three cycles, whose lithological and electrical-log similarities do not warrant formal subdivisions. The subsurface thickness of the Aouinet Ouenine ranges from 20 m to about 210 m. It has the basal contact with older rocks provided by the so-called Early–Middle Devonian unconformity which is time-related to the onset of the Hercynian orogenic phase and a gentle ENE shift of the basin's depocentre. The Formation is conformably overlain by the Tahara Formation.

Its depositional setting suggests marine conditions were predominant, but fluvial-deltaic deposits occur in its middle and upper parts. Castro *et al.* (1985) reported two types of deltaic facies in outcrops: fine-grained suspension deposits (delta front) and coarse-grained tractive sediments (fluvial-distributary channels), all of them intensely reworked by tide (tidal channels and bars, Fig. 11) and storm waves ("tempestite" cycles, Fig. 12). Conspicuous burrowing (*Spyrophyton*) and common Coquina beds (brachiopod fragments) occur associated with calm-water

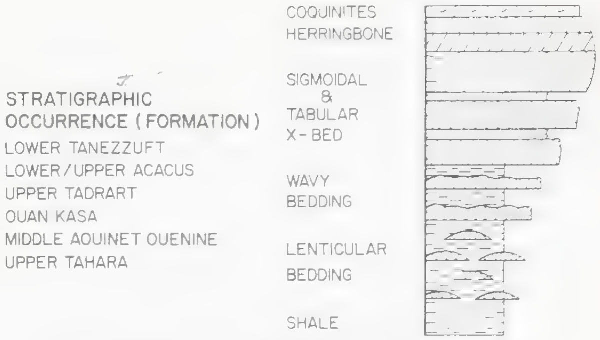

Fig. 11. Typical depositional stacking of a tidal bar.

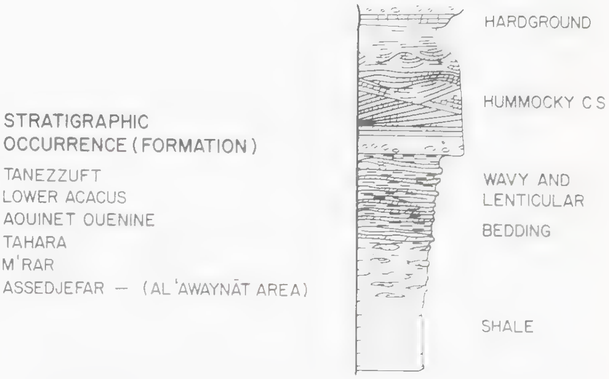

Fig. 12. Typical depositional stacking of a tempestite cycle.

phases ("hardgrounds"); *Skolithos* and *Cruziana* were also reported by Seilacher (1969). The faunistic assemblages found in the Aouinet Ouenine are numerous. Several authors have appointed ages ranging from Couvinian to Strunian; palynological analyses carried out on samples from Braspetro wells (Millepied, 1979, 1984; Uesugui, 1984) confirm the same age range.

Tahara Formation (Late Devonian — Famennian to Strunian)

The Tahara Formation was defined in well B1-49 located in Wādī Taḥārah in Al Ḥamādah basin (Massa and Moreau-Benoit, 1976). Despite some controversy over its age (Sanchez-Barreda, 1977; Bellini and Massa, 1980), it has been placed within Devonian units, but its basal contact cannot easily be picked out in the subsurface because of the extreme lithological similarities with the underlying Aouinet Ouenine Formation. The formation crops out primarily in the W Al Qarqaf area. Its contact with the transgressive Mrar Formation is conformable. Massa and Moreau-Benoit (1976) suggested a possible faunistic distinction between the two formations. The formation reaches 50 m in thickness in outcrops, and 20–60 m in the subsurface.

The lower Tahara displays thin bedsets with lenticular/wavy-bedded shale and very fine sandstone at the base grading upwards in a cyclic fashion into hummocky to cross-bedded sandstones; each cycle is no more than a few metres thick and is marked by intense bioturbation (*Skolithos*) and oxidized levels (commonly bearing ferruginous oolites) in the top part. The upper Tahara is quite similar; topping the cycles are massive and sigmoidal to tabular cross-bedded sandstones. The overall facies pattern suggests that suspension deposits poured into the marine basin by fluvial channels (tidal-dominated deltas, Fig. 13) were reworked and re-deposited as offshore tidal bars and further by storm waves; as the storm ceased, normal "fair-weather" conditions were re-established and organisms thrived, until the next storm came to remobilize the sediment. The Tahara shales have a rich marine fauna. Famennian to Strunian (Massa and Moreau-Benoit, 1976; Millepied, 1979; Uesugui, 1984) is the most probable age.

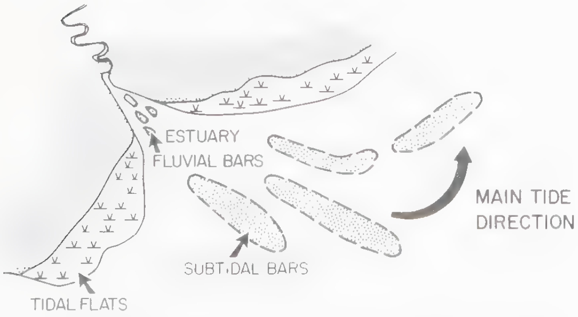

Fig. 13. Schematic map view of tide-dominated delta.

Lower Carboniferous System

The Lower Carboniferous System (Assedjefar and Mrar Formations) represents the last fully marine cycle in the Palaeozoic of southwestern Libya. It exceeds 1000 m in thickness in the outcrops of W Al Qarqaf (Al Ḥamādah basin); in the subsurface of Murzuq basin thicknesses range from almost zero to 380 m. The overall transgressive signature is quite evident in the electric logs.

Mrar and Assedjefar Formations (Early Carboniferous — Tournaisian to Visean?)

The Mrar Formation in subsurface is a thick section (180–240 m) of interbedded shales and sandstones of marine origin. The lower part contains fine to locally coarse-grained, kaolinitic sandstones of cyclic appearance (Massa *et al.*, 1974), interbedded with dark grey to black, finely laminated, carbonaceous shales and siltstones, which become predominant in the upper and middle parts. The informal "Collenia Beds" unit (Fig. 3) is recognized in outcrops in the west, as well as in boreholes drilled in the north-northwest, but is missing in the eastern, central and southern portions of the basin. In wells C1-, E1- and F1-NC58, the Mrar/Assedjefar sequence thins abruptly, due to uplifting of an expressive regional high of NW-SE orientation.

The cyclic nature of the Mrar and Assedjefar Formations is evident. Whitbread and Kelling (1982) mapped and described fifteen coarsening-upward cycles from outcrops in the western Al Qarqaf high (Fig. 14) to wells as far as 250 km into Al Ḥamādah basin, having interpreted them as deltaic to shallow marine, suggesting a sediment supply from NE to SW. Castro *et al.* (1985), studying the same sequence, related these cycles to offshore sandbars which migrated southwards with time (reporting no typical deltaic progradation). According to them, the upper Mrar cycles are characteristically tempestites (coarsening and shoaling-upward sequences up to 50 m thick with the ever-present and diagnostic hummocky cross-stratification, Fig. 15a, b). Basin-wide correlations and the lateral/vertical facies organization sug-

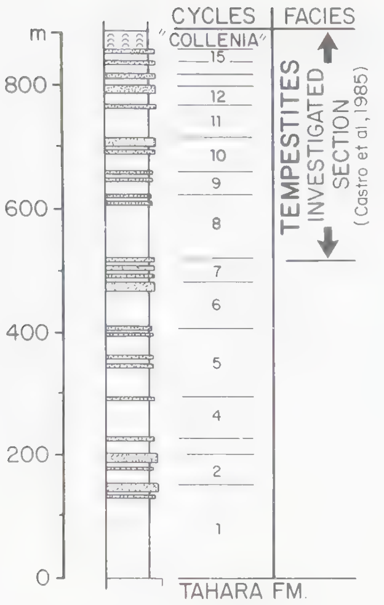

Fig. 14. Depositional cycles in the Mrar Formation (modified from Whitbread and Kelling, 1982).

gest an epicontinental seaway connecting Murzuq and Al Ḥamādah basins in those times.

The same facies distribution was noted for the Mrar and Assedjefar Formations in Al 'Awaynāt area. The "Collenia Beds" unit would represent brief-regressive intertidal sediments deposited by the end of the Mrar sequence.

The Assedjefar Formation is a sequence of dark grey to black shales interbedded with siltstones and fine to very fine-grained, argillaceous sandstones forming thin lenses, to beds up to some tens of metres thick. The same characteristics mentioned for the Mrar Formation apply to the Assedjefar. Their lithological and facies similarities are outstanding. According to Bellini and Massa (1980) the age of Mrar and Assedjefar together is Tournaisian to Early Bashkirian. Palynological analyses on samples from some Braspetro wells give a Visean to Tournaisian age.

Middle Carboniferous to Lower Permian System

This depositional system is the last widespread marine sequence of the Murzuq basin. The Dembaba carbonates, displaying a clear onlapping character on seismic sections, represent the final stages of the Carboniferous transgression, followed by the stillstand phase of the Late Mississippian (Vail *et al.*, 1977) and the prograding continental Tiguentourine Formation.

Dembaba Formation (Middle/Late Carboniferous — Namurian to Westphalian)

The Dembaba Formation is a marine to transitional sequence of white to cream-coloured, argillaceous and dolomitic calcilutites, interbedded with varicoloured, marly claystones which grade downwards to shales; occasionally thin beds of very fine to fine-grained sandstones are intercalated. The thickness in the subsurface is in the range of 35–55 m. Electric logs and seismic evidence suggest that the Dembaba rests unconformably upon older rocks.

Burollet (1960) divided the Dembaba Formation into three informal subunits: an "upper limestone" bearing a rich fauna of productids and gastropods; a "middle shale member" with occasional sandy/dolomitic beds and rare gypsum; and a"lower limestone/marl member" with some intercalations of dolomite and green shales. At least one of these subunits is present in most wells drilled in Murzuq basin. A palaeogeographic reconstruction of the depositional Dembaba lithofacies (Fig. 16) suggests that waning marine conditions in the Namurian gave way to the progradation of a continental setting of fluvio-alluvial plains, brackish-water lagoons and small evaporitic basins. This setting is probably related to the increasingly drier climatic conditions of the Permian. A Namurian to Moscovian (Westphalian) age is indicated by Banerjee (1980) for the Dembaba; this is corroborated by palynological and seismic data gathered by Braspetro.

Tiguentourine Formation (Middle/Late Carboniferous to Early Permian?)

The Tiguentourine Formation consists of a monotonous sequence of brownish to brick-red, plastic and soft claystones bearing calcareous and dolomitic layers, and thin intercalations of very fine to medium-grained, calcareous sandstones. A characteristic sharp drop in electric log resistivities marks the unconformable contact with the overlying Post-Tassilian Formation. Thicknesses between 130 m and 520 m are encountered in the subsurface.

A significant easterly thickening of the lower Tiguentourine occurred concomitantly with the eastward shift of the basin's depocentre in the Middle–Late Devonian (Hercynian orogenic movements); with the ongoing marine transgression, Carboniferous sediments onlap older rocks progressively westwards. The lithological boundaries are, therefore, diachronous and the onlapping character is clearly

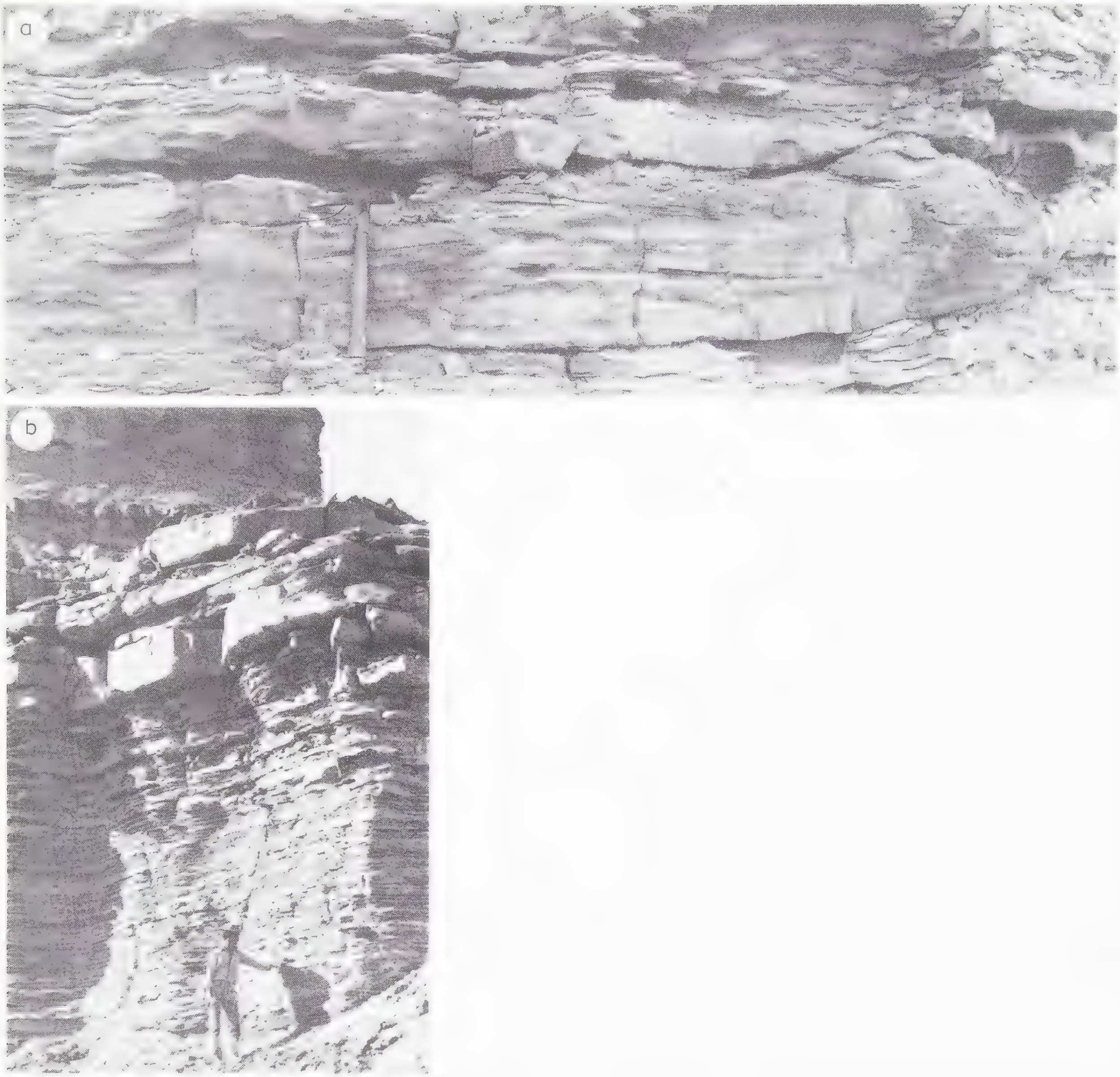

Fig. 15. (a) Detail of hummocky cross-stratification, uppermost part of a tempestite cycle; notice low-angle truncations and sharp base of each bed (Mesa al Mrār, 219 km NW of Idrī).
(b) Typical vertical profile of tempestite cycle; wavy/lenticular siltstone and shale interbeds are sharply cut by sandstone hummocky beds at top part (same location as in (a)).

demonstrated in seismic lines. The presence of some anhydrite in the upper half of the Tiguentourine suggests evaporitic deposition and restricted sea-water circulation, probably combined with an increasingly drier climate.

Correlations based on seismic and well data permit dating of the marine lower Tiguentourine as Middle to Late Carboniferous. The upper transitional to continental section has a poor microfossil record, but some of the spore assemblages obtained suggest an undivided Permian age (Uesugui, 1984).

Permian to Jurassic and Cretaceous Systems

Post-Tassilian and Nubian Formations (Late Permian to Early Cretaceous)

The Post-Tassilian Formation is a thick package (270–630 m in the subsurface) of continental sand-

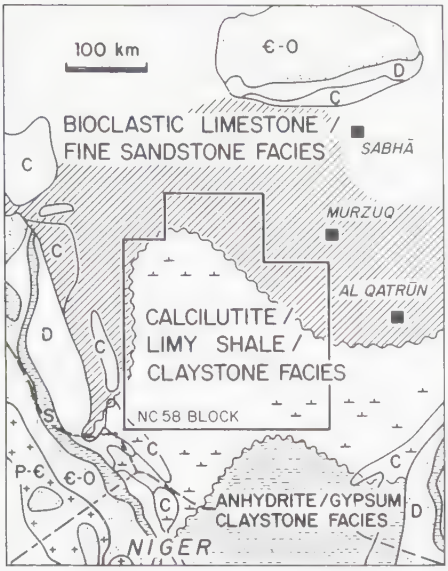
100 km
Є-O
D
C
BIOCLASTIC LIMESTONE / FINE SANDSTONE FACIES
SABHĀ
C
MURZUQ
C
AL QATRŪN
CALCILUTITE / LIMY SHALE / CLAYSTONE FACIES
D
C
NC 58 BLOCK
S
C
P-Є
Є-O
C
ANHYDRITE / GYPSUM CLAYSTONE FACIES
D
NIGER

Fig. 16. Lithofacies map of Dembaba Formation. *P-C* = Precambrian, *C-O* = Cambro-Ordovician, *S* = Silurian, *D* = Devonian, *C* = Carboniferous).

stones and interbedded claystones of characteristic electric log patterns. The sandstones are quartzose, medium- to coarse-grained, conglomeratic and ferruginous in some levels; the claystones are soft and red/brown-coloured. Thin lenses of lignite may locally occur below the erosional contact with the Nubian sandstones. The lowermost Post-Tassilian is characterized by blanket conglomeratic sands lying unconformably over the Tiguentourine claystones; the advent of coarse-clastics deposition from high-energy episodes (fluvial channels and alluvial fans) contrasts with the low-energy conditions prevailing before.

Lithologically, the Nubian and Post-Tassilian formations are very similar to each other. The Lower Nubian (over 100 m thick) shows a sequence of massive, ferruginous, medium- to very coarse-grained/conglomeratic sandstones interbedded with varicoloured, soft claystones; the sandstones are usually poorly consolidated. The upper Nubian (180–760 m) bears conspicuous conglomeratic levels. Very good permo-porosities are characteristic of these excellent freshwater aquifers.

The Nubian and Post-Tassilian sandstones resulted from a continental depositional setting in which overloaded braided streams separated by flood plains formed various fluviatile, alluvial, and possibly lagoonal systems continuously overlying each other. This interpretation finds support in well logs: bell-shaped sand beds with fining-upward terminations into claystones suggest the abandonment of a channel overtaken by the flood-plain claystones and siltstones, whose upper boundaries show sharp cut-and-fill by the next successive channel. The palaeontological content of the entire section is very poor. Palynological analyses in well E1-NC58 revealed a mostly barren section except for a thin interval with scarce spores (*Allisporites* sp., *Protohaploxipinus* sp.; Uesugui, 1984) which date the Upper/Middle Post-Tassilian as Juro-Triassic (undivided). A Late Permian age is inferred for the lower part by comparison with the Tiguentourine Formation; as for the Nubian sandstones, an Early Cretaceous age is generally assumed.

Recent Dune Sands

A great part of Murzuq basin is covered by Recent aeolian sands forming dune systems separated by deflation valleys. The highest dunes reach over 300 m above the valley floors, and are concentrated in the basin's central portions. The sand grains show polished surfaces, are well sorted and lack bounding cement; the presence of conglomeratic pavements indicates ephemeral fluvial systems (flash-flood "playas"). The characteristic longitudinal dune systems trend NE–SW. The long and continuous interdune valleys are usually pebbly and firmer, as they are covered by lag deposits.

CONCLUSIONS

The sedimentary fill of the Murzuq basin is typical of Palaeozoic basins of other parts of the world. The depositional history is relatively uncomplicated, with some conspicuous characteristic facies patterns. Events of a stratigraphic nature throughout the basin's sedimentary column are intimately related to tectonic phases and to major transgressive and regressive cycles of sea-level changes which are documented worldwide. Braspetro's extensive exploratory campaign yielded vast amounts of new subsurface data for the central parts of the basin. There appear to be no remaining crucial points still to be clarified on the stratigraphy of the basin.

The basement complex underlying the sedimentary basin seems to be highly heterogeneous in composition. The lateral and vertical extent of the Cambro-Ordovician sandstones (the main prospectable hydrocarbon reservoir in Murzuq) is remarkable. Field studies indicated that the Early–

Middle Cambrian section (Hassaouna Formation) has a continental origin, the remaining part of the Eo-Palaeozoic section being predominantly marine, with an important periglacial contribution in the Late Ordovician and Early Silurian. Typical deltaic sediments do not seem to occur in the Eo-Palaeozoic section of the basin. The occurrence of storm-wave deposits (tempestites) of very typical outcrop and electric log patterns characterize most of the Silurian, Devonian and Carboniferous sequences.

The Silurian System of Murzuq (the main potential oil-source interval) represents a classic example of a transgressive and regressive depositional cycle. Rhythmic alternations of shales and siltstones to very fine sandstones occurring in the Tanezzuft and lower Acacus Formations show characteristics of turbidity deposition over a broad marine platform; the constant influx of terrigenous material could have diluted the organic matter accumulated in the bottom sediment, thus precluding good quality source rocks from being formed over large portions of the basin during the Silurian.

The basin-wide Early–Middle Devonian unconformity marks a major change in the basin's sedimentary and tectonic history; older sediments were uplifted and the basin's depocentre began to shift eastwards, creating a differentiated subbasin whose filling occurred mostly in the Late Carboniferous and Early Permian. From this time onwards tectonic quiescence marks the whole basin and fluvio-continental conditions prevailed.

ACKNOWLEDGEMENTS

The whole of this work was based on a regional petroleum evaluation report on Murzuq basin prepared for the National Oil Corporation – NOC, to whom the author is indebted for permission to release pertinent information. Profound thanks are due to geologists J.C. Castro and J.C. Della Favera for valuable insights during discussions in the field; geologist R. Porto and office staff members for liberal exchange of technical viewpoints; geologist E.M. Meister who collaborated closely in the critique and review, editing and processing of the original text; draftsmen P.C. Egues and A.R. Vianna and colleagues for the illustrations. Finally, the author acknowledges the various contributions given directly or indirectly by several other Brazilian and Libyan colleagues during the many years of Braspetro's work in the Great Socialist People's Libyan Arab Jamahiriya.

REFERENCES

AMERICAN OVERSEAS PETROLEUM LTD. (1959). Composite Log, Well A1-73. Int. Rept.

BANERJEE, S. (1980). Stratigraphic Lexicon of Libya. *Ind. Res. Cent.*, Bull, **13**, 300 p.

BELLINI, E. and MASSA, D. (1980). A stratigraphic contribution to the Palaeozoic of the southern basins of Libya. *In: The Geology of Libya (eds* M.J. Salem and M.T. Busrewil). Academic Press, London, **I**, 3–56.

BEUF, S., BIJU-DUVAL, B., DE CHARPAL, O., ROGNON, P., GARIEL, O. and BENNACEF, A. (1971). Les grès du Paléozoïque inférieur au Sahara. *Sci. Tech. Pétrole*, No. 18, TECHNIP, Paris, 464 p.

BORGHI, P. and CHIESA, C. (1940). Cenni geologici e paleontologici sul Paleozoico dell'Egghidi Uan Caza nel deserto di Taita (Fezzan Occidentale). *Ann. Mus. Libico Stor. Nat.*, **2**, 123–137.

BULGARIAN OIL CO (BOCO) OF LIBYA (1981–1984). Composite well logs — NC101 area (Various Unpubl. Repts.).

BUROLLET, P.F. (1960). Lexique stratigraphique international, 4, Afrique, Pt. 4a, Libye. *Comm. Strat.*, *Cent. Nat. Rech. Sci.*, 62 p.

BUROLLET, P.F., BRENNAN, P.F., SOMMER, M.P., TEMPLETON, R.S.M., GOUDARZI, G.H. and JORDI, H.A. (1963). A discussion of Libyan stratigraphy. *Rev. Inst. Fr. Pétrole*, **18**, 1323–1326.

BUROLLET, P.F. and BYRAMJEE, R. (1969). Sedimentological remarks on lower Paleozoic sandstones of south Libya. *In*: Geology, Archaeology and Prehistory of Southwest Fezzan, Libya (*ed.* W.H. Kanes). *Petrol. Explor. Soc. Libya*, 11th Annu. Field Conf., 91–101.

BUSSON, G. and BUROLLET, P.F. (1970). La limite Permian-Trias sur la platforme Saharienne (Algérie, Tunisie, Libye). *In*: The Permian and Triassic Systems and their Mutual Boundary, 74–88.

BRENCHLEY, P.J. (1985). Storm-influenced sandstone beds. *In: Mod. Geol.*, **9** (40) 369–396.

CASTRO, J.C., DELLA FAVERA, J.C. and EL-JADI, M. (1985). Paleozoic sedimentary facies, Murzuq basin, SPLAJ. Int. Rept. Braspetro-Petrobras, Rio de Janeiro, 117 p.

COLLOMB, G.R. (1962). Étude géologique du Jebel Fezzan et de sa bordure paléozoïque. *Notes Mém. Comp. Fr. Pétrole*, **1**, 35 p.

CONANT, L.C. and GOUDARZI, G.H. (1977). Geological map of Libya; 1 : 2 000 000. (2nd edition). *Ind. Res. Cent.*, Tripoli.

DELLA FAVERA, J.C. (1984). Eventos de sedimentacao episodica nas bacias braslleiras, uma contribulcao para atestar o carater pontuado do registro sedimentar (in Portugese). *Anals 33° Brasil. Geol.*, Rio de Janeiro, 489–501.

DESIO, A. (1936a). Riassunto sulla constituzione geologica del Fezzan. *Boll. Soc. Geol. Ital.*, **55**(2), 319–356.

DESIO, A. (1936b). Prime notizie sulla presenza del Silurico fossilifero nel Fezzan. *Boll. Soc. Geol. Ital.*, **55**(1), 116–120.

DESIO, A. (1942). Ubersicht über die Geologie Libyens. *Geol. Rundsch.*, **33**(4–6), 415–421.

DESIO, A. (1943). L'esplorazione mineraria della Libia. *Coll. Doc. Sci. Cura Min. Afr. Ital.*, **10**, 333 p.

DOTT, R.H., JR. (1983). The 1982 SEPM presidential address: Episodic sedimentation: How normal is average? How rare is rare? Does it matter? *J. Sedimentol. Petrol.*, **53**(1), 5–23.

FÜRST, M. and KLITZSCH, E. (1963). Late Caledonian paleogeography of the Murzuq basin. *Rev. Inst. Fr. Pétrole*, **18**(10), 1472–1484.

Greigert, J.R. and Pougnet, R. (1985). Carte géologique, République du Niger, 1:2000000. *Bur. Rech. Géol. Min.*, Nantes.

Havlicek, V. and Massa, D. (1973). Brachiopodes de l'Ordovicien supérieur de Libye occidental: Implications stratigraphiques régionales. *Geobios*, **6**(4), 267–290.

Hecht, F., Furst, M. and Klitzsch, E. (1964). Zur Geologie von Libyen (Contribution à la géologie de la Libye). *Geol. Rundsch.*, **53**(2), 413–470.

Hoen, E.W. (1968). Geology of the Murzuq basin. Unpubl. Rept. Amoseas Ltd, 85 p.

Karasek, R.M. (1981). *Structural and Stratigraphical Analysis of the Paleozoic Murzuq and Ghadames Basins, Western Libya*. Ph.D. Thesis, Univ. S. Carolina, 146 p.

Klitzsch, E. (1963). Geology of the northeast flank of the Murzuq basin (Djebel Ben Ghnema–Dor El Goussa area). *Rev. Inst. Fr. Pétrole*, **18**(10-11), 1411–1427.

Klitzsch, E. (1965). Ein Profil aus dem Typusgebiet gotlandischer und devonischer Schichten der Zentralsahara (Westrand Murzukbecken, Libyen). *Erdöl. Kohle*, **18**(8), 605–607.

Klitzsch, E. (1966). Comments on the geology of the central parts of southern Libya and northern Chad. *In*: South-Central Libya and Northern Chad (*ed.* J.J. Williams). *Petrol. Explor. Soc. Libya*, 8th Annu. Field Conf., 1–17.

Klitzsch, E. (1968). Die gotlandium Transgression in der zentral Sahara. *Z. Dt. Geol. Ges.*, **117**(2), 492–501.

Klitzsch, E. (1969). Stratigraphic section from the type areas of Silurian and Devonian strata at western Murzuq basin (Libya). *In*: Geology, Archaeology and Prehistory of the Southwestern Fezzan, Libya (*ed.* W.H. Kanes). *Petrol. Explor. Soc. Libya*, 8th Annu. Field Conf., 83–101.

Lelubre, M. (1946). Sur le Paléozoïque du Fezzan. *C.R. Hebd. Séanc. Acad. Sci.*, **222**(24), 1403–1404.

Massa, D. and Collomb, G.R. (1960). Observations nouvelles sur la région d'Aouinet Ouenine et du Djebel Fezzan (Libye). *Proc. 21st Int. Geol. Congr.* (Norden), **12**, 65–73.

Massa, D. and Moreau-Benoit, A. (1976). Essai de synthèse stratigraphique et palynologique du Système Dévonien en Libye occidentale. *Rev. Inst. Fr. Pétrole*, **31**(2), 287–333.

Massa, D., Termier, G. and Termier, H. (1974). Le Carbonifère de Libye occidentale, stratigraphie et paléontologie. *Notes Mém. Comp. Fr. Pétrole*, **11**, 139–206.

Millepied, P. (1979). Palynological Study of the Braspetro A1-NC58 Onshore Well, Libya. Total-CFP, Unpubl. Rept. No. 1808, 6 p.

Millepied, P. (1984). Palynological study of the Braspetro C-NC58 Well, Libya. Total-CFP, Unpubl. Rept. No. 3166, 8 p.

Occidental Of Libya Inc. (1977). Composite Well Log, A1-NC34. Int. Rept.

Oliveira, M.A.M., Arruda, A.A., Ortiz, E.F., Meister, E.M. and Pierobon, E.S.T. (1985). Regional Petroleum Exploration Evaluation Report of Murzuk Basin. Unpubl. Rept. Braspetro, Tripoli/Rio de Janeiro, 105 p.

Pan American Libya Oil Co. (1959). Composite Well Log, A1-76. Int. Rept.

Petrobras Internacional S/A - Braspetro (1978–1985). Composite well logs and final well reports (various) — NC58 area. Unpubl. Repts.

Petropar/CFP (1964). Composite Well Logs: Kouana-1, Kourneida-1. Unpubl. Rept.

Petropar-Prepa (1962). Rapport du fin de sondage: Kourneida-1 (Kr-1). Unpubl. Rept., Petropar-Prepa, Niger, 22 p.

Pierobon, E. (1984). Regional Distribution of Reservoir Quality of Upper 100 metres Cambro-Ordovician Formation, Murzuq Basin, Libya, Tripoli. Unpubl. Tech. Rept.

Quadros, L.P. (1985). Palynological Report of Well H1-NC58. Int. Rept. Cenpes-Petrobras, Rio de Janeiro.

Rompetrol Of Libya (1984). Composite Log, Well A1-NC115. Int. Rept.

Sanchez-Barreda, M. (1977). Palaeoenvironmental Reconstruction of the Tahara Formation of Northwestern Libya. Int. Rept. NOC, Tripoli.

Seilacher, A. (1969). Sedimentary rhythms and trace fossils in Paleozoic sandstones of Libya. *In*: Geology, Archaeology and Prehistory of Southwestern Fezzan, Libya (*ed.* W.H. Kanes). *Petrol. Explor. Soc. Libya*, 11th Annu. Field Conf., 117–123.

Uesugui, N. (1984). Palynological Study of Well E1-NC58, Murzuq Basin. Int. Rept. Cenpes-Petrobras, 7 p.

Vail, P.R., Mitchum, R.M. and Thompson, S. III (1977). Seismic stratigraphy and global changes of sea level from coastal onlap. 4: Global cycles of relative changes of sea level. *In*: Seismic Stratigraphy — Applications to Hydrocarbon Exploration (*ed.* C.E. Payton). *Mem. Am. Assoc. Petrol. Geol.*, **26**, 83–98.

Van Eysinga, F.W.B. (1975). Geological Time Table (Global). 3rd ed. Elsevier, Amsterdam.

Vos, R.G. (1981). Deltaic sedimentation in the Devonian of western Libya. *Sediment. Geol.*, **29**, 67–88.

Whitbread, T. and Kelling, G. (1982). Mrar Formation of western Libya; evolution of an Early Carboniferous delta system. *Bull. Am. Assoc. Petrol. Geol.*, **66**(8), 1091–1107.

Neogene to Pleistocene Continental Deposits in Northern Fazzān and the Central Sirt Basin

LUDĚK DOMÁCÍ[1], PAVEL RÖHLICH[1] AND PAVEL BOSÁK[1]

الرسوبيات البرية من النيوجين إلى عصر البلايستوسين بشمال ووسط حوضي مرزق وسرت

د. دوماشي وب. روليخ وب. بوساك

الخلاصــة

يعطي تتابع من رسوبيات الصخور القارية للحين النيوجيني والعصر البلايستوسيني مساحات شاسعة بشمال ووسط حوض مرزق. فقد سادت الرواسب الرضخية (حجر رملي وحجر غريني) في المرحلة الأولى. أما تراكم الرسوبيات الجيرية (تكوين المحروقة) فقد تراكم في المرحلة الأخيرة، حيث كان هناك اتصال بالترسيب في المناطق الواقعة إلى الشمال والشمال الشرقي. ويتضح من طبيعة الصخور ومن المستحاثات أن بيئات الترسيب كانت بحيرات أو بيئات مويلحة إلى مالحة تماماً. أما المستحاثات الفقارية فتدل على عمر جيولوجي يتراوح بين عصر البلايوسين والحين الرابع.

هذا. وقد تمت مضاهاة رواسب البلايوسين والبلايستوسين في حوض مرزق برواسب تكويني الهيشة وقارة ودة في حوض سرت. وقد اعتبرت الوحدات التي تمت مضاهاتها في المنطقتين على أنها ناتجة عن فترة رطبة خلال البلايوسين والبلايستوسين انتهت في البلايستوسين المبكر.

أما التقلبات المناخية خلال البلايستوسين المبكر والمتوسط فقد تسببت في ثلاثة مراحل من ترسيب البحيرات في وسط حوض سرت. وتتفق العوامل المناخية المتحكمة في ترسيب البحيرات مع تقلباتّ النشاط الحركي.

وتعكس صخور البحيرات الجيرية، الممثلة لعدة عوامل، تركيباً صخرياً مميزاً ومتشابهاً في كلا المنطقتين (الجير الوحلي الكريي والجير الوحلي العضوي والرمل الجيري العضوي والدولوميت). وبعد الترسيب إلتحمت الصخور وأعيد تبلرها عن طريق عدد من عمليات التسبخ تحت ظروف متغيرة من مستوى المياه العام، وبظاهرة التكلس القوي [التصلب وإعادة التبلر والتفتت (التبرش) وتكون الفجوات وما إلى ذلك].

Abstract. A sequence of Neogene to Pleistocene continental deposits covers large areas in northern and central Murzuq basin. Clastic sedimentation prevailed in the early phases of deposition; carbonate sediments (Al Maḥrūqah Formation) were mainly deposited in the final phase which was connected with an extension of the sedimentation area towards the north and northeast. Both lithological and palaeontological data testify to a lacustrine, brackish to saline environment. Invertebrate fossils indicate a late Pliocene to Quaternary age. A stratigraphic correlation is made between the Plio-Pleistocene deposits in the Murzuq basin and the Al Hīshah/ Qārat Weddah Formations in the Sirt Basin. The correlated units in the two regions are considered to be products of a humid Plio-Pleistocene period which ended in the Early Pleistocene. Climatic oscillations during the Early and Middle Pleistocene resulted in three stages of lacustrine sedimentation in the central part of the Sirt basin; the climatic control of the lacustrine sedimentation was combined with oscillations of the diastrophic activity. Lacustrine carbonate rocks of various stages show remarkable analogies with each other in terms of petrology (pelletoid micrites and biomicrites, fine biocalcarenites and dolomites). After deposition, the rocks were affected by recrystallization and cementation by a wide variety of paludal processes under changing water-table conditions and by strong calichification (hardening, recrystallization, brecciation, origin of vadoids, etc.).

---

[1] Industrial Research Centre, P.O. Box 3633, Tripoli, Libya, G.S.P.L.A.J.
Present address: Geoindustria, U průhonu 32, 17004 Praha 7, Czechoslovakia.

INTRODUCTION

The regional geological mapping programme in central Libya (Wādī ash Shāṭi'–Sabhā–Al Fuqahā sector) organized by the Industrial Research Centre in 1981–1984 has revealed new lithological, stratigraphic and palaeontological data about the Neogene to Pleistocene continental deposits in the northern part of the Murzuq basin (sheets NG 33-1 Idrī, NG 33-2 Sabhā, NG 33-3 Al Fuqahā, NG 33-5 Awbārī, NG 33-6 Tanahmū, and NG 33-7 Tmassah). The mapping of the central Sirt basin (Marādah-Zallah sector) has contributed to a better knowledge of the Pleistocene lacustrine sediments in the area of map-sheets NH 34-9 Marādah, NH 34-10 Sabkhat Ghuzayil, NH 34-13 Abú Na'īm, and NH 34-14 Bi'r Zalṭan (Fig. 1).

The aim of the present contribution is to summarize the acquired information and to consider it in the broader context of the geological and climatic development of Libya. The first part (by P. Röhlich) is focussed on the clastic (sandstones, siltstones) and carbonate continental deposits widely developed in the northern part of the Murzuq basin and their correlation with the Plio-Pleistocene continental deposits in the Sirt basin. The main topic of the second part (by L. Domácí) is the Pleistocene lacustrine sediments in the central Sirt basin with special regard to their morphological control. P. Bosák participated in the survey of both regions as a petrologist; the results of his study are mainly incorporated in the first part of this contribution.

NORTHERN FAZZĀN (MURZUQ BASIN)

In the northern and central parts of the Murzuq basin there are widely developed clastic and carbonate continental deposits unconformably overlying the Palaeozoic and Mesozoic formations. Parts of the deposits are outliers, namely those north of Wādī ash Shāṭi' and in Sarīr al Qaṭṭūsah, but a major part is covered with aeolian sands of the Awbārī and Murzuq sand seas and are exposed only along the margins of the sand seas or as small inliers.

Opinions on the age of the deposits in question, including the so-called Murzuk Limestone (Desio, 1936), have differed considerably. Pagni (1938, p. 73) attributed a Jurassic age to the Murzuk Limestone, but Bellair (1944) was the first to conclude its Quaternary, or, at the oldest Pliocene, age. Lelubre (1949) considered the age of the sequence to be between the Eocene and Mio-Pliocene. The deposits in the Wādī ash Shāṭi' area were classified as Miocene lacustrine deposits by Collomb (1962); however, Klitzsch (1974) suggested a Late Cretaceous age for this unit. A review of this controversy has been given in the Stratigraphic Lexicon of Libya by Banerjee (1980, pp. 185–186) who reasonably proposed abandoning the term "Murzuk Limestone" because of its poor definition and vague usage.

The new investigation has resulted in classifying the sequence, or at least the bulk of it, as Plio-Pleistocene continental deposits (Seidl and Röhlich, 1984; Koráb, 1984, among others).

Lithology

The new geological mapping has distinguished two facies of the continental sequence: (1) the carbonate facies having only locally developed subordinate clastics (usually a basal conglomerate); (2) the mixed facies, generally with clastics (sandstone, siltstone) predominating over carbonates.

The carbonate facies is confined to the N and NE margin of the Murzuq basin (table hills N of Wādī ash Shāṭi', and Sarīr al Qaṭṭūsah). This facies appears as a clearly definable lithostratigraphic unit and has therefore been named Al Maḥrūqah Formation (Seidl and Röhlich, 1984, p. 89). The name is derived from the village Al Maḥrūqah, 25 km W of Brāk, where the formation is typically developed and reaches its maximum thickness of 12 m. The bulk of the formation consists of whitish limestone, dolomitic limestone or dolomite. The carbonate rocks are more or less sandy, mostly non-bedded with bouldery disintegration. Most of the sections investigated contain a bed of basal conglomerate of variable thickness, usually with calcareous cement, or a bed of poorly sorted sandy/silty sediment. A characteristic feature of the whole formation is a more or less abundant admixture of quartz sand grains, some of which are reddish. Clastic quartz is medium- to fine-grained, poorly sorted and subangular to subrounded. Limestones have a mainly micritic matrix with streaks of microsparite to fine pseudosparite; allochems make up 1–12%; bioclasts are represented by ostracodes and small gastropods and bivalves and fine organic detritus. Among the limestones, strongly altered types occur. These are more or less sparitized and often pseudobrecciated, with a cloddy texture and with vadose pisoids and such like.

A mixed facies of continental deposits is developed in the major part of the study area, namely south of Wādī ash Shāṭi' and in the Tmassah sheet

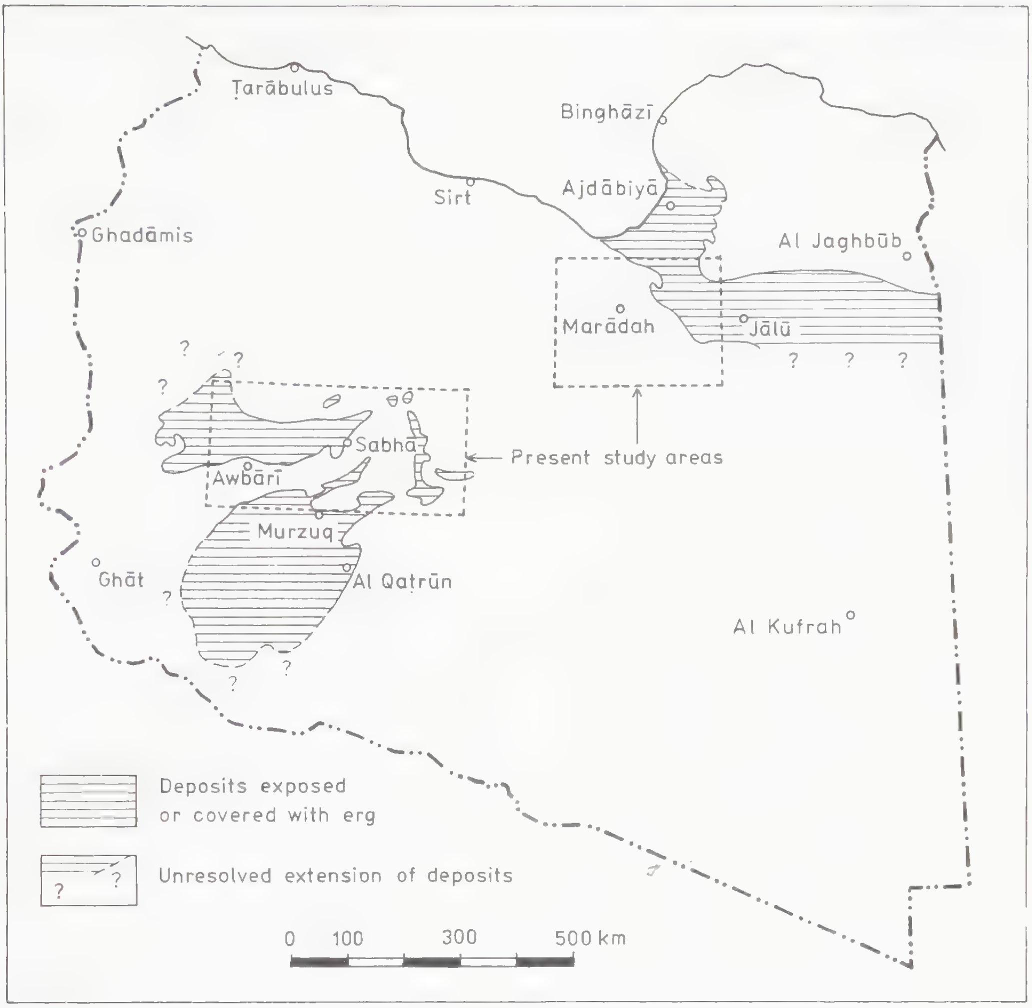
Ṭarābulus
Binghāzī
Ajdābiyā
Sirt
Ghadāmis
Al Jaghbūb
Marādah
Jālū
Sabhā
Present study areas
Awbārī
Murzuq
Ghāt
Al Qaṭrūn
Al Kufrah
Deposits exposed or covered with erg
Unresolved extension of deposits
0 100 300 500 km

Fig. 1. Approximate extent of the Plio-Pleistocene continental deposits in Libya.

area. The area north of Tmassah provides a unique opportunity to observe the contact between the predominantly clastic facies and Al Maḥrūqah Formation. The Al Maḥrūqah limestone overlies the calcareous sandstones and siltstones which are exposed in the northern vicinity of Tmassah and in two small endorheic depressions (qarārats) further to the north. Along the eastern and western margins of its occurrence, however, Al Maḥrūqah Formation directly overlies the Mesāk Formation (Jurassic–Lower Cretaceous). This overlap is due to a depression (shallow palaeovalley) running N–S, which was filled with clastics before deposition of Al Maḥrūqah Formation which covered a wider area (see Fig. 3).

The widespread clastic sequence of continental deposits has a variable composition in particular areas. The best outcrops are along the northern margin of Ramlat az Zallāf, where the maximum observed thickness is about 25 m. The basal layer is built of conglomerate, pebbly sandstone, or microconglomeratic argillaceous sandstone. The succession continues with yellowish-green or yellowish-white argillaceous to calcareous sandstone. The upper part is rich in carbonate rock layers: sandy limestone, organodetrital limestone, dolomite and/or dolomitic limestone. Some structures of the carbonate rocks are strongly reminiscent of Al Maḥrūqah Formation, which is probably partly equivalent to the upper part of this sequence. A remarkable rock type is a thinly bedded to laminated dolomite, with desiccation cracks in some layers, which yielded poorly preserved plant fossils and small fish remains. Other fossils, found in the organodetrital limestone are gastropods (*Melania* sp.) and ostracodes (*Cyprideis torosa*). Bioclasts

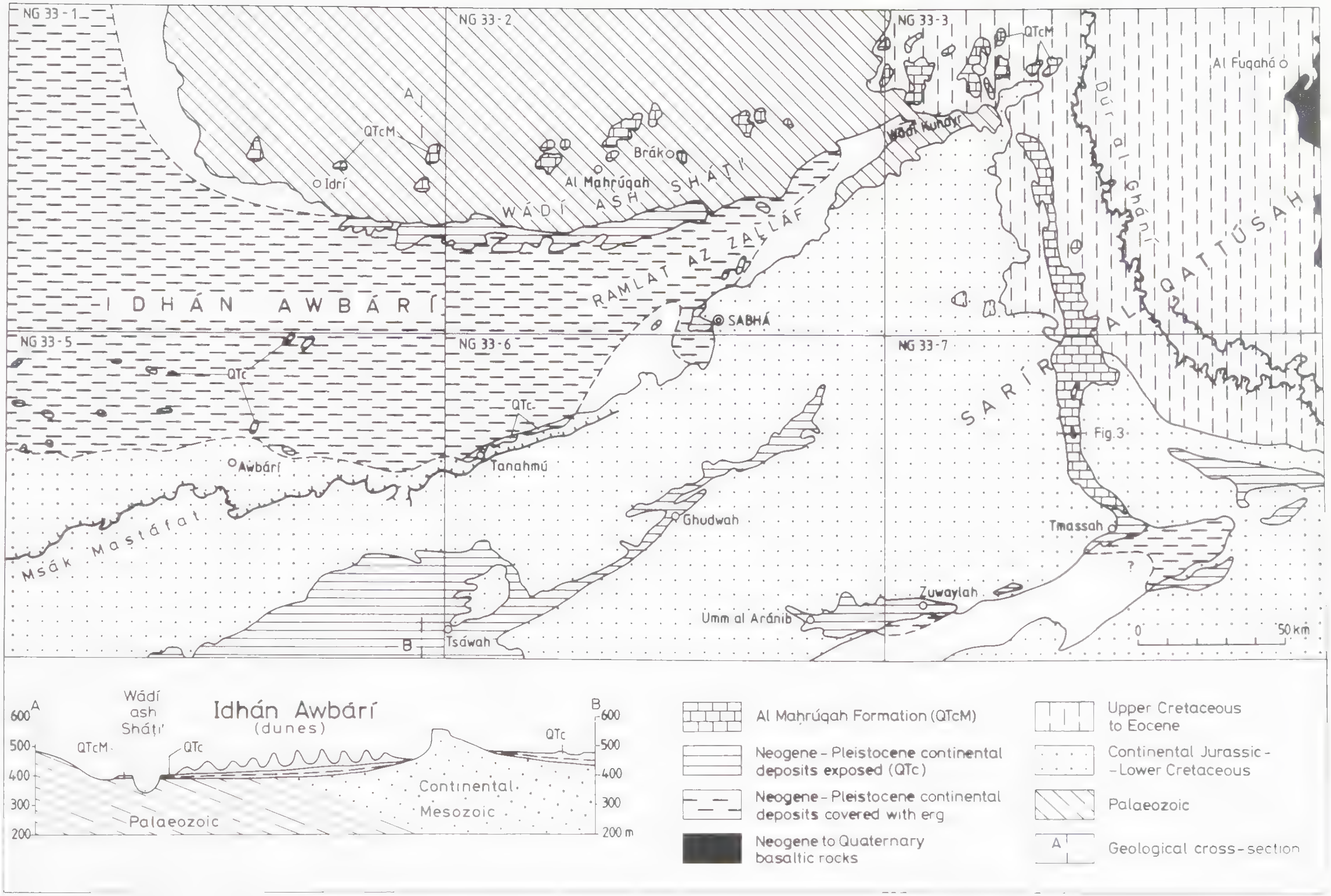
NG 33 - 1
NG 33 - 2
NG 33 - 3
NG 33 - 5
NG 33 - 6
NG 33 - 7
A
QTcM
QTcM
Idrí
Bráko
Al Mahrúqah
WÁDÍ ASH SHÁTI'
Wádí Kuhayr
Al Fuqahá
Dúr al Ghání
AL QATTÚSAH
SARÍR
RAMLAT AZ ZALLÁF
SABHÁ
IDHÁN AWBÁRÍ
QTc
QTc
Awbárí
Tanahmú
Msák Mastáfat
Ghudwah
Tsáwah
B
Umm al Aránib
Zuwaylah
Tmassah
Fig. 3
?
0
50 km
Wádí ash Sháţi'
Idhán Awbárí (dunes)
QTcM
QTc
QTc
Continental Mesozoic
Palaeozoic
600
500
400
300
200
200 m
Al Mahrúqah Formation (QTcM)
Neogene - Pleistocene continental deposits exposed (QTc)
Neogene - Pleistocene continental deposits covered with erg
Neogene to Quaternary basaltic rocks
Upper Cretaceous to Eocene
Continental Jurassic - - Lower Cretaceous
Palaeozoic
Geological cross - section

Fig. 2. Geological sketch map of the study area in northern Fazzān.

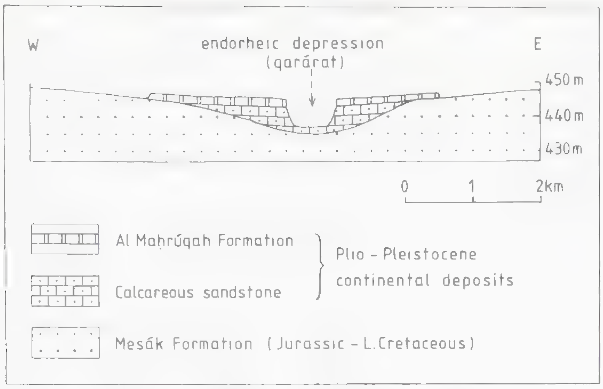

Fig. 3. The relation between Al Maḥrūqah Formation and the underlying Plio-Pleistocene clastics in the north of Tmassah (for location of the section see Fig. 2).

consist of ostracodes, bivalves, gastropods and charophytes.

The maximum verified thickness of the clastic sequence in question is more than 40 m (exploratory oil well B 1 near Umm al Ḥamām, outside the map area). The maximum preserved thickness probably does not exceed 50 m in the study area.

In summary, lithological data from the whole study area suggest that the continental sequence originated in a flat lowland with lakes of changing salinity, brackish to saline (glauconite grains; dolomite, gypsum and halite cement of sandstones). Clastic material, washed off the neighbouring areas, was probably a mixture of first, second and later cycle material (from the Palaeozoic to the Cretaceous). An admixture of aeolian clastic material cannot be ruled out. Carbonate rocks indicate sedimentation in a shallow lake.

Palaeontological Data

The most important fossil found in the sequence examined is the ostracode *Cyprideis torosa* (Jones). This species indicates a brackish to slightly saline environment and a late Pliocene to Quaternary age. (Determination and evaluation of ostracodes by R. Jiříček, Moravian Oil Wells, Hodonín, Czechoslovakia.) *Cyprideis torosa* has been found in calcareous sandstones of the Ramlat az Zallāf and Tmassah areas. The other fossils, *Leptocythere* sp., *Ammonia beccarii* (Linné), *Melania* sp., *Limnaea* sp., *Planorbis* sp., *Bulimus* sp., small fish of the family *Centropomidae* (*Ambassidae*), fully corroborate the above conclusion but do not contribute to a more exact dating. The invertebrate fossils are closely related — some of them even identical — with fossils found in the younger, indisputably Quaternary lacustrine deposits of the study area (Wādī ash Shāṭi', Wādī Darmān, Tmassah sheet).

Floral remains are mostly represented by indeterminable oogonia of charophytes. Among sporadic remains of angiosperms, *Phragmites* sp. indicates a Late Tertiary to Quaternary age. Palynological investigations of clastics yielded assemblages of pteridophyte spores, gymnosperm and angiosperm pollen, especially from the Tanahmū and Awbārī sheet areas. The spore and pollen assemblages are indicative of a xerophytic environment close to savannah which may correspond to a broad regional framework.

Geomorphology and Palaeotopography

The thinness of the Cenozoic continental sequence (50 m max.) when considered in context with the vast area of deposition, testifies to a senescent, rather pediplanated surface at the beginning of the sedimentary cycle. This is also proof of a negligible rate of differential subsidence during the deposition. The study area is divided into two large basins by the Msāk Mastāfat escarpment (Fig. 2). The two basins were connected only in the later phase of deposition which corresponded to Al Maḥrūqah Formation. The area of connection was in the east; this is shown by the continuous strip of Al Maḥrūqah Formation stretching approximately N–S over Sarīr al Qaṭṭūsah.

The low variability of elevations and their regional distribution suggest that the relief of the basins has not been deformed by tectonic movements, or at least not to an appreciable extent. A very gentle general sloping down towards the NNE, observable in the area of the basin studied, might be primary, but more probably it is due to subsequent epeirogenic movements. In this connection, the overlap of Al Maḥrūqah Formation on the NE and N basin margin suggests a slight shift of the sedimentation in the same direction and may be due to an earlier phase of the same movement.

In spite of all subsequent modifications, the landforms delimiting the basins are still preserved:

(1) The southern slope of Al Qarqaf uplift formed the northern margin of the whole basin area. The base of Al Maḥrūqah Formation is nowhere higher than 475 m; along Al Qarqaf uplift it is only 460 m. The present elevation of the uplift is generally over 500 m in the study area and still higher towards the north.

(2) The Dūr al Ghānī escarpment with altitudes generally exceeding 500 m, and its southern extension Dūr al Masīd exceeding 600 m, represent the well-defined eastern margin of the basin area.

(3) The Msāk Mastāfat escarpment and the adjoining strip of Ḥamādat Murzuq formed the barrier, or cuesta, between the northern and southern basins as defined above.

The age of the landforms controlling the basin development can best be estimated on the eastern margin of the basin. Here a new cycle of erosion started after the regression of the Eocene sea, that is in the Oligocene. The development of the Msāk Mastāfat escarpment, however, probably began as early as during the Cretaceous period. This is suggested by the low pre-Maastrichtian escarpment observable in the Wādī Kunayr area, as described by Klitzsch (1974, p. 113). The Maastrichtian transgression and shallow marine sedimentation covered this "embryonic" escarpment and precluded its further development in the eastern part of the study area.

The deposition of Al Maḥrūqah Formation and equivalent carbonate rocks preceded the termination of the cycle of erosion which had started in the Oligocene. The lacustrine sedimentation completed the planation by levelling the basin bottom. This was followed by a drying up of the basin and a new cycle of erosion started. This began in the Early or Middle Pleistocene and continues to the present. The main manifestation of the new cycle is the distinct downward erosion with prevailing aeolian activity (deflation). The greatest downward erosion has been observed in the Wādī ash Shāṭi' area.

Wādī ash Shāṭi' is the deepest and largest Quaternary endorheic depression in the study area; its origin is due to combined fluvial and aeolian erosion. The depression stretches E–W for more than about 140 km and is about 10–20 km wide. The edges of escarpments framing the northern side of Wādī ash Shāṭi' are at about 400–410 m a.s.l. The deepest point of the depression (289 m) is located south of the village of Al Maḥrūqah. The bottom is covered with sabkha deposits. In this area, the relief was eroded to a depth of some 110–120 m below the surface of Al Maḥrūqah Formation (Fig. 4).

The gradual deepening of the depression was interrupted in the relatively humid periods from which the denudation relics of lacustrine coquinas were preserved. Petit-Maire *et al.* (1980) and Gaven (1982) presented isotope dates of the coquinas, among which the values obtained by the ionium–uranium method have a frequency peak between 130 000 and 140 000 years (Gaven, 1982). The coquinas of this age occur in medium levels between the top of Al Maḥrūqah Formation and the present bottom of the depression; some of them are still closer to the bottom level. This shows that the new (post-Maḥrūqah) cycle of erosion started earlier, probably in the Early Pleistocene. Late Acheulian artifacts recorded by Aumassip and Petit-Maire (1982) also confirm the Middle Pleistocene existence of the deeply and widely developed Shāṭi' depression.

In the other areas with lacustrine deposits of both cycles, there was less dramatic downward erosion. This mainly applies to the southern half of the study area where the late Quaternary (Middle Pleistocene to Holocene?) lacustrine deposits lie on the eroded surface of the Plio-Pleistocene sediments. Such conditions may be expected in the whole central part of the Murzuq basin. The correlations between the Quaternary of Tejerhi (Bellair, 1949) and similar deposits in the surroundings of Murzuq, including the southern part of the study area, should therefore be considered with extreme caution. At least two sedimentary cycles may be involved, being separated by important stratigraphic hiatuses. Employment of radiometric dating is needed to resolve the problem.

Correlation with Neighbouring Basins

Di Cesare *et al.* (1963), when studying the Neogene to Quaternary deposits between Al Jaghbūb and Jālū, were the first to point out the similarity between the young continental deposits in NE Libya and in the Murzuq basin. The Garet Uedda (Qārat Weddah) Formation, defined in the above work, yielded fossils indicating a Pliocene to Quaternary age and a continental environment with calm, shallow, fresh or brackish water. The Qārat Weddah Formation is a succession of quartzose sands to sandstones, with intercalations of sandy clays, somewhat gypseous and salty, and marly-sandy limestones, overlain by a limy-sandy calcrete with cherts. In the type area, the Qārat Weddah represents a cycle of sedimentation unconformably or disconformably overlying the Middle Miocene Al Jaghbūb Formation. The Qārat Weddah has left numerous residual hills, less than 30 m high, gradually disappearing below the Great Sand Sea towards the south.

Recent geological mapping in the NE part of the Sirt basin by the Industrial Research Centre (Giglia, 1984; Pertusati and Innocenti, 1984; Kodym, 1985; Maštera, 1985) has revealed new data on the Plio-

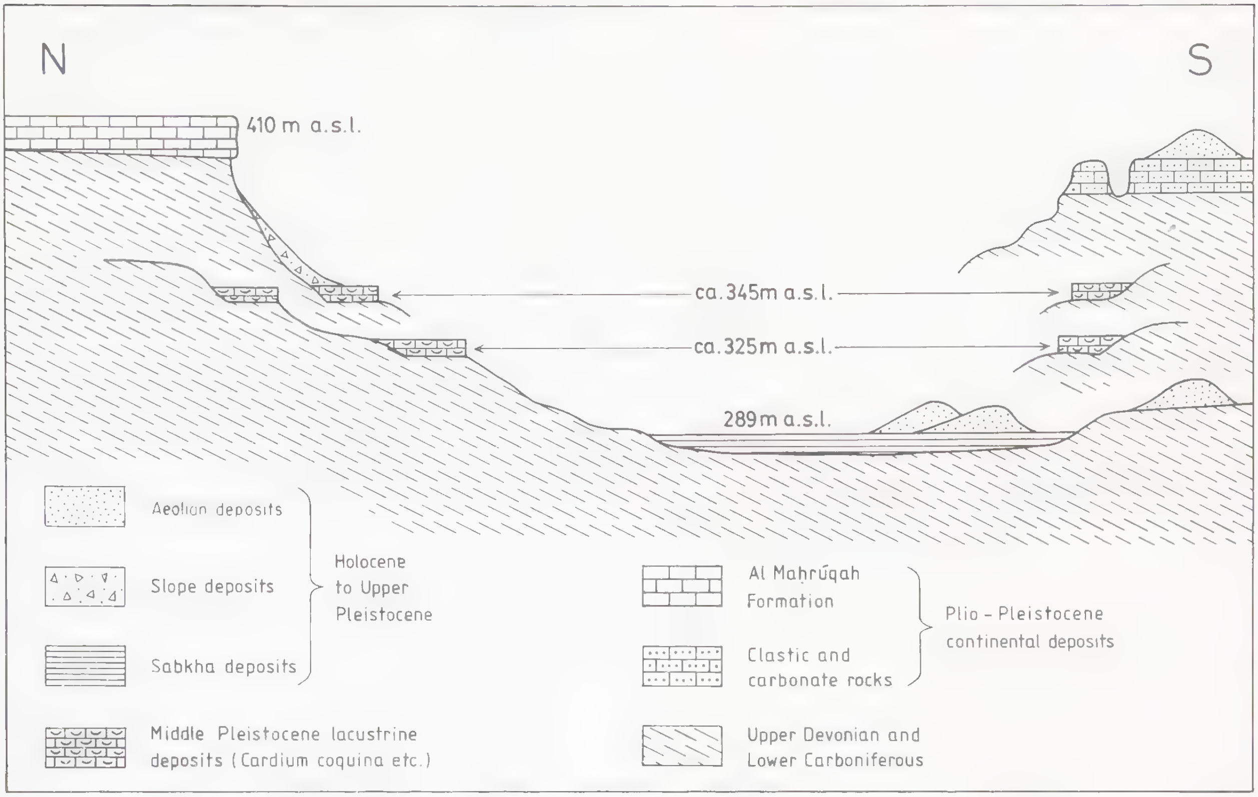
N
S
410 m a.s.l.
ca. 345m a.s.l.
ca. 325m a.s.l.
289m a.s.l.
Aeolian deposits
Slope deposits
Sabkha deposits
Holocene to Upper Pleistocene
Middle Pleistocene lacustrine deposits (Cardium coquina etc.)
Al Maḥrūqah Formation
Clastic and carbonate rocks
Plio-Pleistocene continental deposits
Upper Devonian and Lower Carboniferous

Fig. 4. Scheme of development of the endorheic Shāṭi' depression (after Seidl and Röhlich, 1984).

Pleistocene deposits. In this area, the Qārat Weddah Formation overlies Al Hīshah Formation defined by Mijalković (1977) in a more northwesterly area. Both formations comprise one cycle of sedimentation but Al Hīshah Formation contains typically marine faunal elements, especially in the area west of long. 20°E.

The present state of knowledge permits a stratigraphic correlation to be made between the Plio-Pleistocene continental deposits in the Murzuq basin and Al Hīshah/Qārat Weddah Formations. The correlated units in both regions represent distinct cycles of sedimentation, having certain analogies, above all in their geological history. Their sedimentation was preceded by erosion, planation and duricrust formation. The lacustrine sedimentation which extends over vast areas testifies to a relatively humid period.

The termination of lacustrine sedimentation closely preceded the last great cycle of erosion which had an impact on the landforms comparable to, and probably connected with, the formation of the great sand seas. All these circumstances suggest that the sedimentation of the Qārat Weddah and Al Maḥrūqah Formations was terminated by the same climatic change.

Last but not least, it should be mentioned that the occurrence of a Plio-Pleistocene lacustrine phase has also been concluded from stratigraphic and geomorphological data in Tunisia (Coque, 1962) and the Algerian Sahara: the Villafranchian pluvial (Conrad and Conrad, 1983). The Pliocene–Pleistocene development outlined by Conrad and Conrad (*op. cit.*, pp. 172–173) corresponds very well with our observations in northern Fazzān.

Conclusions

The above data testify to a humid period covering a part of the Pliocene–Pleistocene transitory interval which accounted for extensive lacustrine sedimentation in the Murzuq basin. In terms of quantity of sediments and area of deposition, this period is much more impressive than the later Quaternary lacustrine periods recorded in Libya. Unfortunately, the dating of the deposits is far from accurate. Radiometric dating is needed to further our knowledge.

CENTRAL SIRT BASIN

The study area corresponds to four sheets of the geological map on a 1:250000 scale: sheets Marādah, Sabkhat Ghuzayil, Abū Na'īm, and Bi'r Zalṭan (Fig. 1). Pleistocene lacustrine sediments have been found in the broad vicinity of Marādah and Jabal Zalṭan. Further small occurrences lie at the southern margin of the study area, and in the southern part of the map-sheet Sabkhat Ghuzayil. Based on the geological and geomorphological analyses, the sediments have been classified into three developmental stages of the fluvio-lacustrine system. Formation of Pleistocene lakes was preceded by several phases of denudation which have affected Palaeogene and Neogene sediments in the study area (Fig. 5). The main stages of the development from the Upper Miocene are represented in palaeogeological sketch maps (Figs 6–9).

Pleistocene Lacustrine Deposits

Pleistocene lacustrine sedimentation took place in broad fluvial valleys and, later, in endorheic depressions which had developed in the valleys. Lacustrine sediments, which had originally covered larger areas, now occur as erosional relics at three distinct levels, the lowest, i.e. the youngest ones, being the most frequently preserved. The type section (Fig. 10) was described by Domácí (1985, pp. 58–59) at Bi'r Zalṭan (lat. 28°08′08″N, long. 19°52′13″E) and represents the youngest development stage. The lower contact has been set on the erosional surface of whitish to pinkish, fine- to coarse-grained, unsorted, purely quartzose sand with isolated pebbles, up to 1 cm in size. This layer is exposed in an incomplete thickness of 4 m and belongs to the Oligocene. It is overlain by a similar but more argillaceous sand with numerous manganese oxide dendrites and schliers, conspicuously laminated, with layers of arenaceous green claystones several tens of centimetres thick. The layer is 0.8 m thick. Above this, there is a light green, finely arenaceous claystone with abundant dendrites of manganese oxides and with secondary gypsum in joints. The claystone displays cuboidal jointing and is cracked. This layer occurs between 4.8 and 5.9 m. Overlying this is a thicker layer (5.9–12.5 m) of subhorizontally layered and 1–10 cm laminated, whitish chalky limestone, and evaporite (gypsum) with 1–3 cm laminae of green silty claystone and gypsiferous claystone, typically undulated and vertically jointed in places. The sequence overlies the underlying Oligocene sands along a well-defined boundary and is marked by dark Mn oxide films. The surface is covered with a brown-patinated calcrete.

The sequence of rocks in this type section is repeated, with minor variations, in the other residual hills in the broad vicinity of Bi'r Zalṭan. Towards the south, higher members can also be found in the residual hills formed by lacustrine deposits: the overlying laminated sediments are organogenic limestones with a typical content of stalks and roots of reed vegetation, and even small intercalations of carbonaceous claystone and siltstone. On the top of the residual hills is the genetically interesting grey calcrete which is up to 40 cm thick; it may be considered to be the last stage of the duricrust formation in the Pleistocene.

An equivalent of the lacustrine deposits is also represented by the relics of sediments located quite far to the south in the area between lat. 28°05′N, long. 20°04′E and lat. 28°01′N, long. 19°54′E. The first example involves a small platform within a sand-sheet which is formed by grey-white porous fossiliferous limestone with a crust on its surface. It contains small *Cardium* shells.

The second example is a low residual hill which has pinky-grey sandstones, coarse-grained, conspicuously bimodal, thinly stratified, developed in its lower part. The sandstones are overlain by a 0.5 m thick layer of white porous chalky limestone of the *alm* type, which is horizontally stratified or undulated and slightly arenaceous.

It is also worth mentioning the occurrence of lacustrine sediments immediately beyond the southern boundary of the area described, near lat. 27°50′N, long. 19°54′E, where apart from carbonates and green claystones, lenses of silicilites have also developed.

Lacustrine sediments have also been found in the form of residual hills in the Marādah oasis (Maštera, 1985). Ochreous yellow, strongly evaporitic-saturated siltstone forms a massive layer, 3 m thick, at the foot of the residual hills. It belongs to the Qārat Jahannam Member. A layer 3 m thick overlies it and makes a well-defined, uneven boundary with it. This second layer is formed of irregularly alternating whitish calcareous siltstones and ochreous rusty to yellow gypsiferous siltstones. In the upper part, strongly cavernous carbonates with rusty coated cavities predominate. The cavities were generated by leaching of plant remains, as is evidenced by their imprints. The top of the residual hill is covered by a

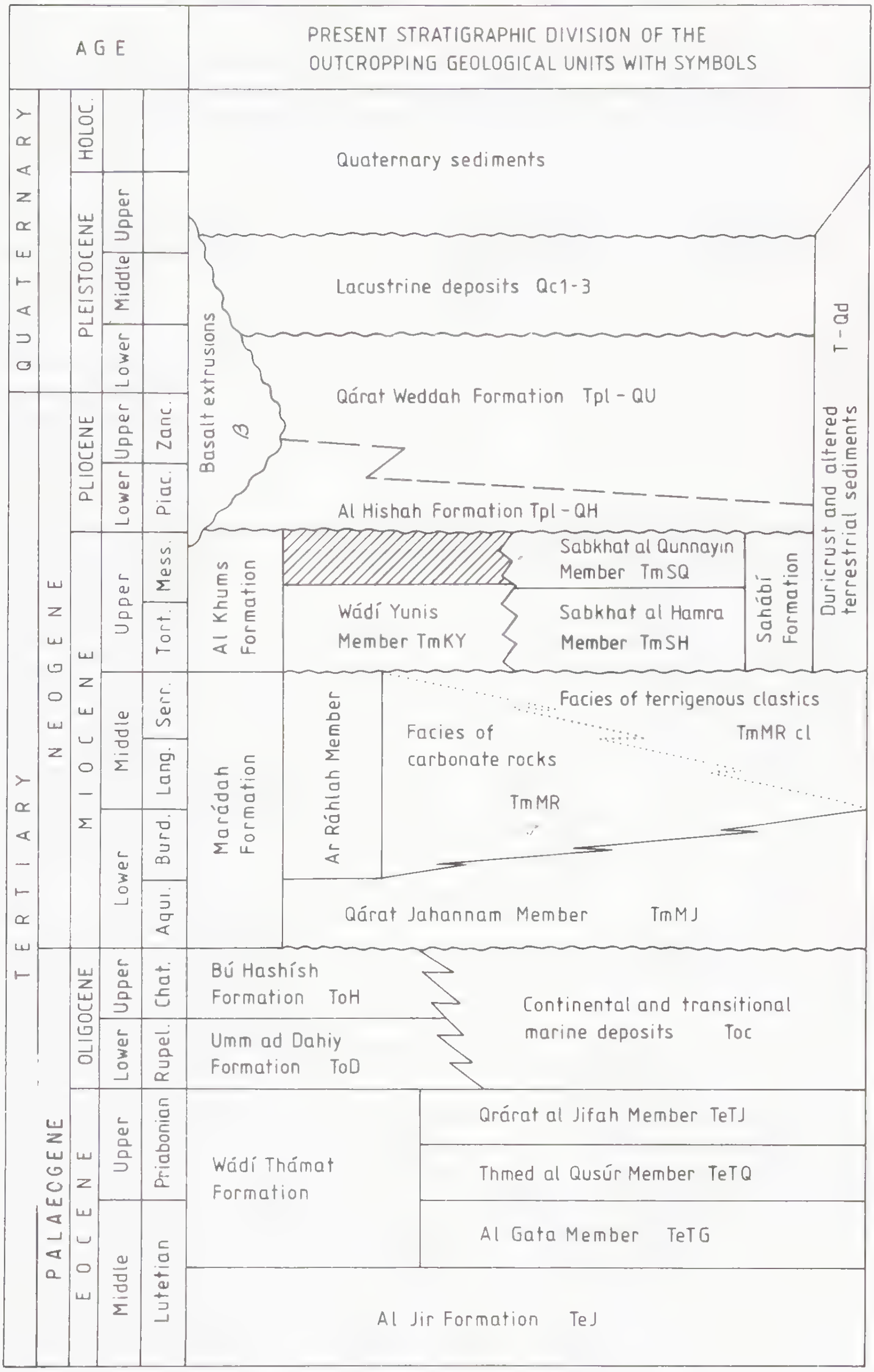
AGE
PRESENT STRATIGRAPHIC DIVISION OF THE OUTCROPPING GEOLOGICAL UNITS WITH SYMBOLS
QUATERNARY
TERTIARY
NEOGENE
PALAEOGENE
HOLOC.
PLEISTOCENE
PLIOCENE
MIOCENE
OLIGOCENE
EOCENE
Upper
Middle
Lower
Zanc.
Piac.
Mess.
Tort.
Serr.
Lang.
Burd.
Aqui.
Chat.
Rupel.
Priabonian
Lutetian
Quaternary sediments
Lacustrine deposits Qc1-3
Qárat Weddah Formation Tpl - QU
Al Hishah Formation Tpl - QH
Basalt extrusions β
T - Qd
Duricrust and altered terrestrial sediments
Al Khums Formation
Wádí Yunis Member TmKY
Sabkhat al Qunnayın Member TmSQ
Sabkhat al Hamra Member TmSH
Sahábí Formation
Marádah Formation
Ar Ráhlah Member
Facies of terrigenous clastics
TmMR cl
Facies of carbonate rocks
TmMR
Qárat Jahannam Member TmMJ
Bú Hashísh Formation ToH
Umm ad Dahiy Formation ToD
Continental and transitional marine deposits Toc
Wádí Thámat Formation
Qrárat al Jifah Member TeTJ
Thmed al Qusúr Member TeTQ
Al Gata Member TeTG
Al Jir Formation TeJ

(Adapted from : Domácí 1985, Kodym 1985, Maštera 1985, Zikmund 1985)

Fig. 5. Review of the exposed stratigraphic units in the central part of the Sirt basin. Key to the indexes used in Figs 6–9.

table of crusted grey carbonate about 0.5 m thick.

Similar sections are also preserved in a number of other, more extensive residual hills in the immediate vicinity. The sediments in the group of small residual hills near the road of the Marādah oasis belong to the same sequence. The lower part is formed by a layer 3 m thick, in which marly siltstones alternate with claystones. These sediments belong to

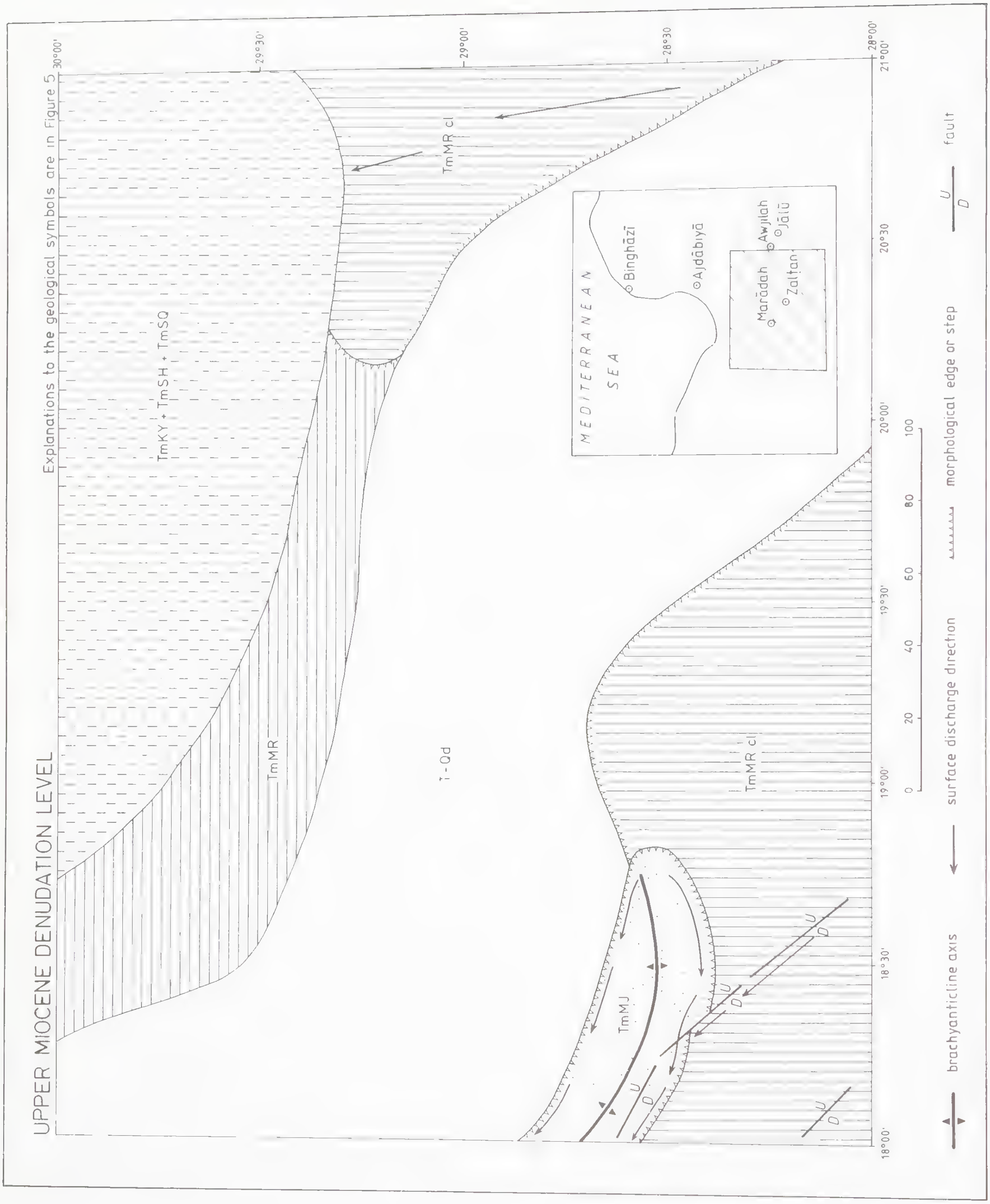
UPPER MIOCENE DENUDATION LEVEL
Explanations to the geological symbols are in Figure 5
TmKY + TmSH + TmSQ
TmMR
TmMR cl
TmMR cl
T - Qd
TmMJ
U
D
MEDITERRANEAN SEA
Binghāzī
Ajdābiyā
Awjilah
Jālū
Marādah
Zalṭan
30°00'
29°30'
29°00'
28°30
28°00'
18°00'
18°30'
19°00'
19°30'
20°00'
20°30
21°00'
0
20
40
60
80
100
brachyanticline axis
surface discharge direction
morphological edge or step
fault

Fig. 6. Palaeogeological sketch map of the Upper Miocene denudation level in the central part of the Sirt basin.

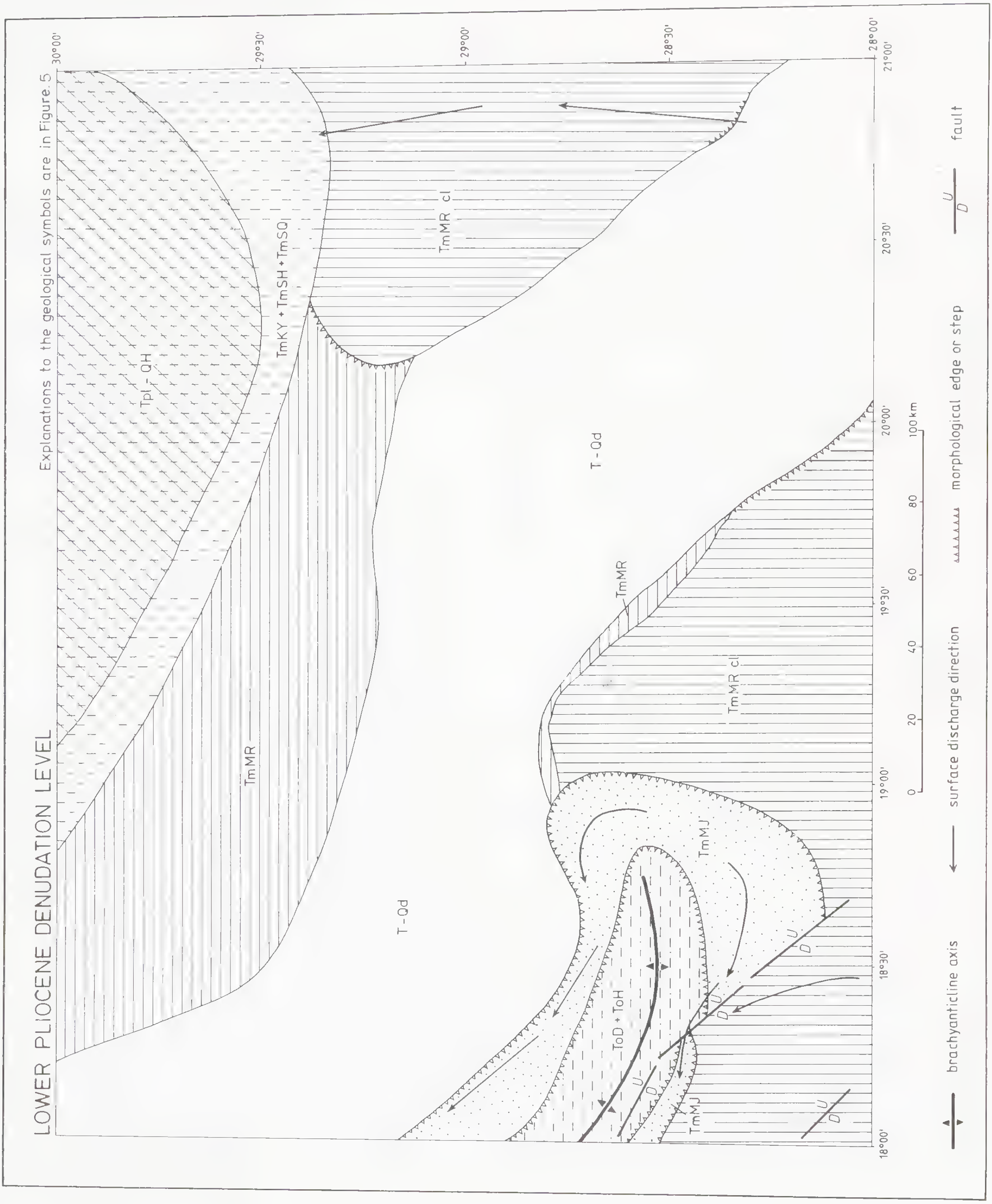
LOWER PLIOCENE DENUDATION LEVEL
Explanations to the geological symbols are in Figure 5
30°00'
29°30'
29°00'
28°30'
28°00'
21°00'
20°30'
20°00'
19°30'
19°00'
18°30'
18°00'
Tpl - QH
TmKY + TmSH + TmSQ
TmMR cl
TmMR
T - Qd
TmMJ
ToD + ToH
U
D
0
20
40
60
80
100 km
brachyanticline axis
surface discharge direction
morphological edge or step
fault

Fig. 7. Palaeogeological sketch map of the Lower Pliocene denudation level in the central part of the Sirt basin.

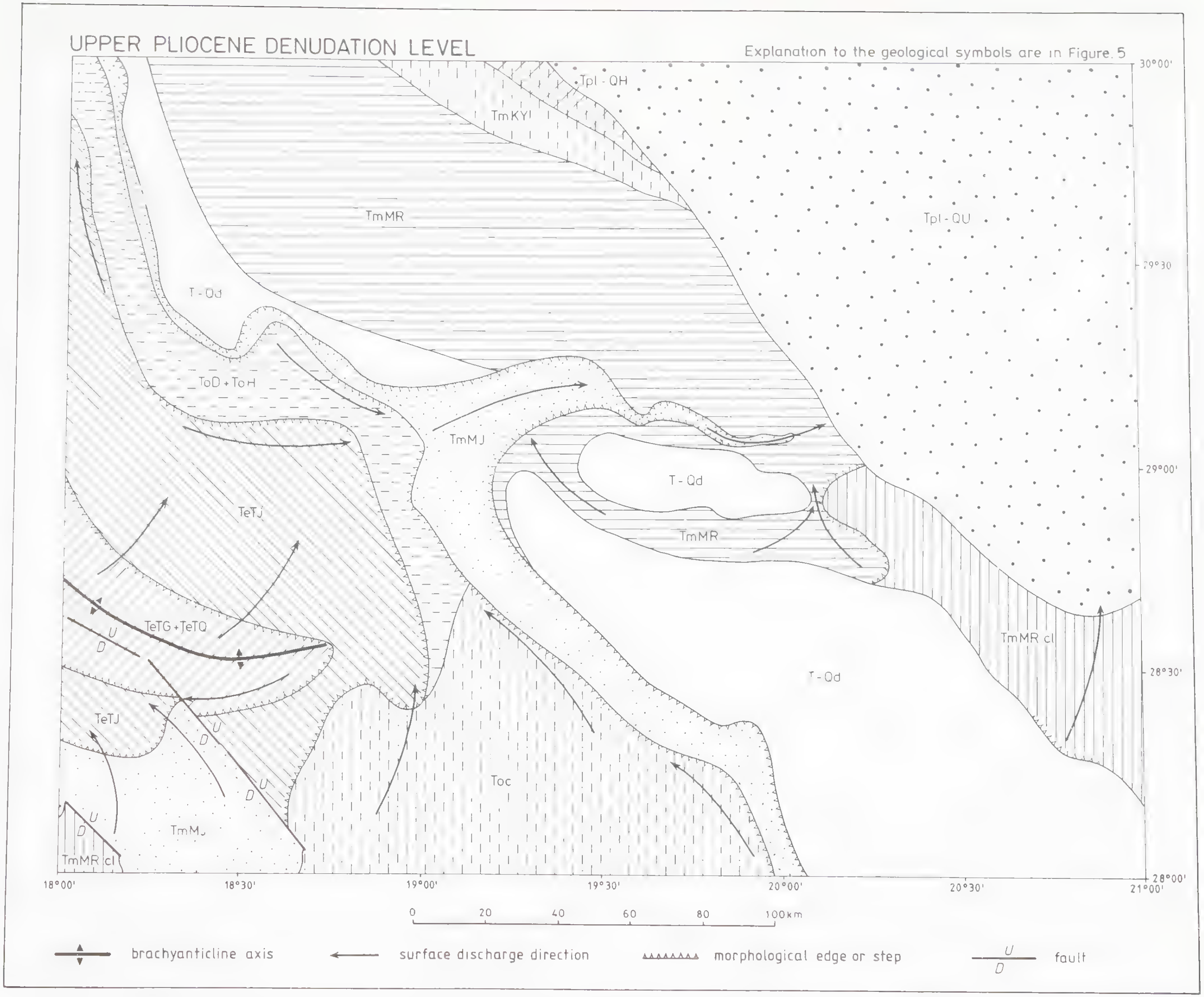
UPPER PLIOCENE DENUDATION LEVEL
Explanation to the geological symbols are in Figure. 5
Tpl - QH
TmKYl
Tpl - QU
TmMR
T - Qd
ToD + ToH
TmMJ
T - Qd
TmMR
TeTJ
TeTG + TeTQ
TeTJ
TmMJ
TmMR cl
Toc
T - Qd
TmMR cl
U
D
30°00'
29°30
29°00'
28°30'
28°00'
18°00'
18°30'
19°00'
19°30'
20°00'
20°30'
21°00'
0
20
40
60
80
100km
brachyanticline axis
surface discharge direction
morphological edge or step
fault

Fig. 8. Palaeogeological sketch map of the Upper Pliocene denudation level in the central part of the Sirt basin.

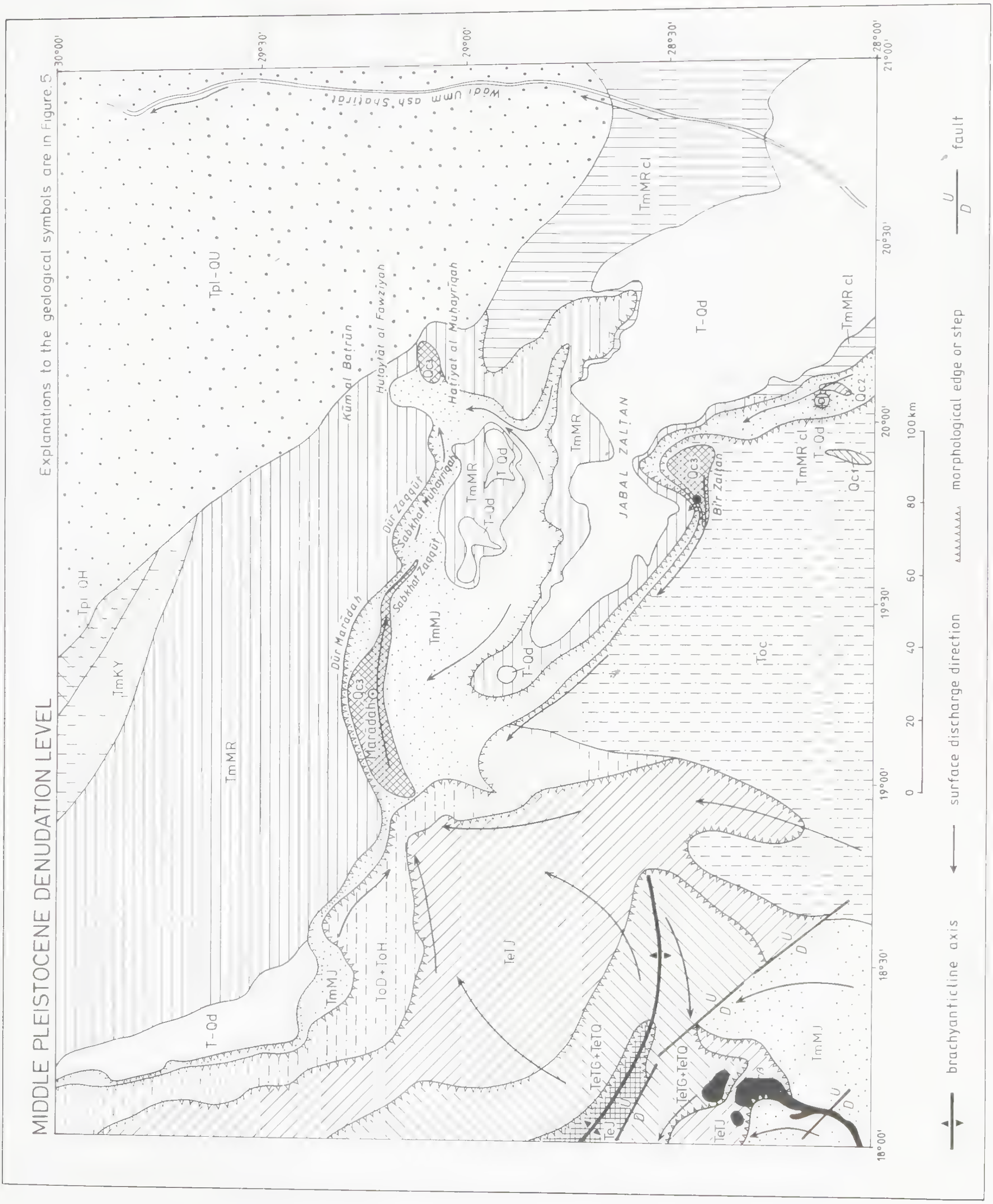
MIDDLE PLEISTOCENE DENUDATION LEVEL
Explanations to the geological symbols are in Figure 5
30°00'
29°30'
29°00'
28°30'
28°00'
18°00'
18°30'
19°00'
19°30'
20°00'
20°30'
21°00'
Wadi Umm ash Shatirat
Tpl-QU
Tpl QH
TmKY
TmMR
T-Qd
TmMJ
ToD+ToH
TeIJ
TeTG+TeTQ
TeJ
Dūr Marādah
Marādah
Qc3
Sabkhat Zaqqūt
Dūr Zaqqūt
Sabkhat Muhayriqah
Kūm al Batrūn
Hutaylāt al Fawziyah
Hatiyat al Muhayriqah
Qc1
TmMR cl
JABAL ZALTAN
Bir Zaltan
Toc
Qc2
U
D
0
20
40
60
80
100 km
brachyanticline axis
surface discharge direction
morphological edge or step
fault

Fig. 9. Palaeogeological sketch map of the late Middle Pleistocene denudation level in the central part of the Sirt basin.

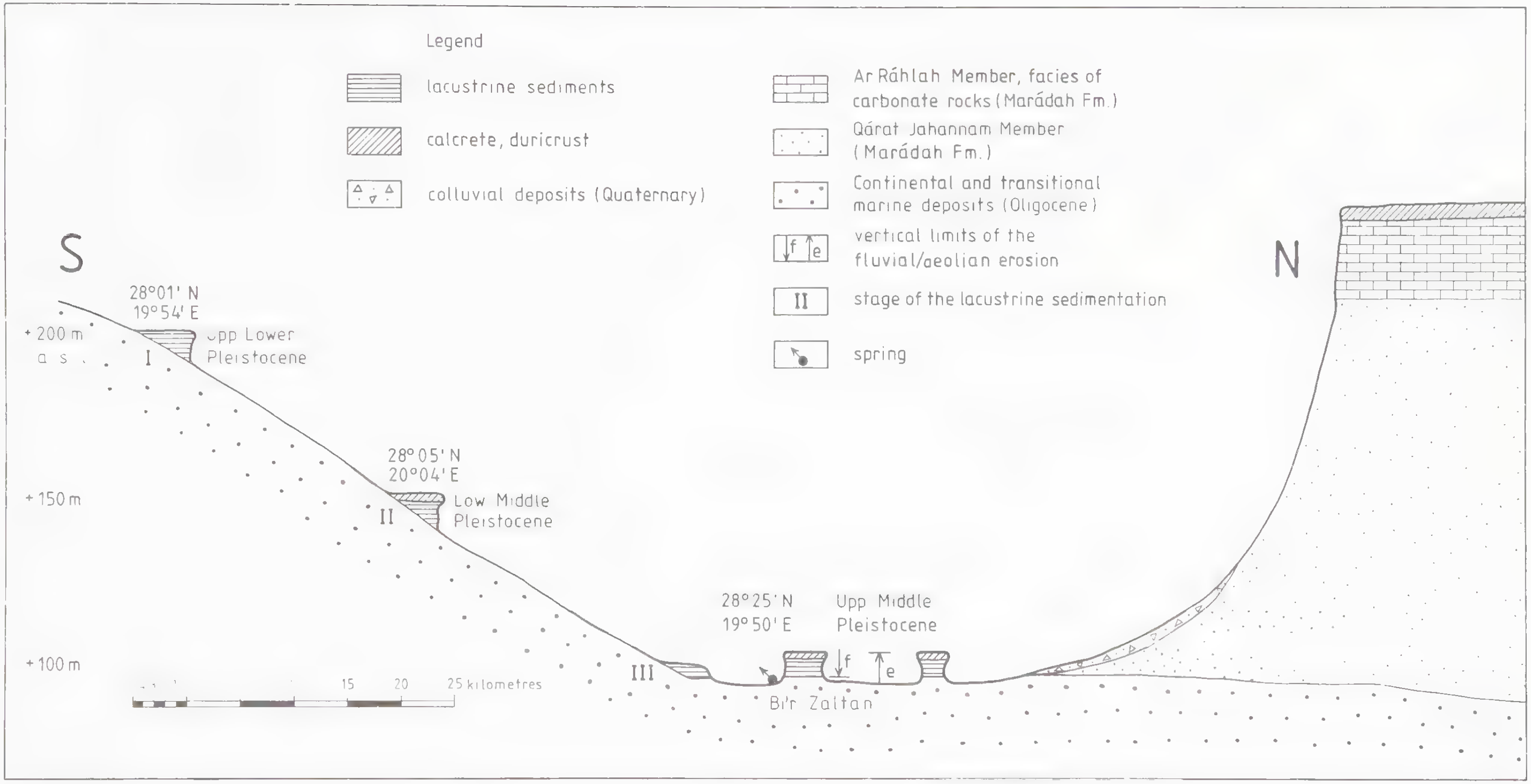
Legend
lacustrine sediments
calcrete, duricrust
colluvial deposits (Quaternary)
Ar Ráhlah Member, facies of carbonate rocks (Marádah Fm.)
Qárat Jahannam Member (Marádah Fm.)
Continental and transitional marine deposits (Oligocene)
vertical limits of the fluvial/aeolian erosion
f
e
II
stage of the lacustrine sedimentation
spring
S
N
+200 m a.s.
+150 m
+100 m
28°01' N 19°54' E
Upp Lower Pleistocene
I
28°05' N 20°04' E
Low Middle Pleistocene
II
III
28°25' N 19°50' E
Upp Middle Pleistocene
Bi'r Zaltan
15
20
25 kilometres

Fig. 10. Three stages of the Pleistocene lacustrine sediments and the origin of the endorheic depression near Bi'r Zalṭan.

the Qārat Jahannam Member; their eroded surface is overlain by fine- to coarse-grained creamy calcareous sandstone with tabular cross-bedding, attaining a thickness of 0.8 m; it has, however, been eroded. Then follow 2 m of chalky lutitic limestones containing grey calcareous claystones with laminae up to 5 mm thick. The whole layer has a brecciated character with grey intraclasts of marlstones. Intensive jointing has enabled the crystallization of very coarse-grained aggregates of gypsum in the joints.

A small relic of lacustrine deposits was found by O. Kodym (pers. comm.) near lat. 29°15′N, long. 19°30′30″E. A remnant of sediments resembling those described at Marādah (Maštera, 1985) overlies the Pleistocene slope deposits covering the flank of an endorheic depression. Another miniature relic, at lat. 29°06′30″N, long. 20°14′30″E, is formed of fluviolacustrine sediments reminiscent of the basal layers of the lacustrine deposits at Marādah. This relic lies on Ar Rāhlah Member of the Marādah Formation. Neither of these relics could be mapped, and so they are missing from the map on 1 : 250 000 scale Sabkhat Ghuzayil sheet (Kodym, 1985); however, they are important from the palaeogeographic point of view.

All the above-mentioned occurrences of Pleistocene lacustrine sediments are similar in terms of petrology and sedimentology; their thickness does not exceed 10 m; usually only 2–4 m are preserved.

Climatic Factors

During the Late Miocene a warm climate prevailed giving a semiarid character to the Messinian. The prevailing evaporation resulted in the rising of groundwater which deposited its mineral content in the form of duricrust (calcrete). This type of climate persisted till the Early Pleistocene. The incision of fluvial valleys at the end of the Miocene (Barr and Walker, 1973) shows that the rivers coming from the south had enough water, at least seasonally.

In the Pliocene, the extensive fluvial and lacustrine sediments of the Qārat Weddah Formation were deposited; their sedimentation gradually shifted towards the north and replaced the marine sedimentation of Al Hīshah Formation. A warm, humid climate is indicated by the recorded fauna (Kodym, 1985). The rivers had enough water for adequate transportation. The Qārat Weddah sediments testify to the transport of coarse sands with pebbles exceeding 1 cm in size (Domácí, 1985).

The warm and humid climate continued in the earliest period of the Pleistocene. The development of the river system and a conspicuous degree of erosion is consistent with this climate. The average temperature was probably lower but sufficient for the development of palm vegetation (Domácí, 1985).

Both long-term and seasonal humidity and temperature oscillations are documented by three stages of lacustrine sedimentation. Each stage began with fluvial and lacustrine sediments in the flow-through system, continued with typical lacustrine sedimentation, probably in isolated lakes, and ended with swamp drying up, with reed vegetation and brackish water. The seasonal oscillations resulted in lamination of the lacustrine sediments (clay, evaporitic clay, and lake marl).

A warm period with prevailing evaporation at the beginning of the Late Pleistocene is indicated by the calcrete, up to 0.5 m thick, developed on the lacustrine sediments (Domácí, 1985).

During the Late Pleistocene, arid climatic phases were strong enough to lower the groundwater level and to stop capillary rising; the formation of aeolian deposits was enhanced. These sediments were, however, partly destroyed later by water and reworked in the subsequent period of aeolian activity. The relics of the Late Pleistocene aeolian sands probably include the sand sheets overlain by the younger dunes in the south of the study area.

In the Holocene, the arid climate prevailed; aeolian activity became stronger whereas fluvial erosion had ceased. This is shown by: (1) the conspicuous development of the endorheic depressions, sometimes stopped by the development of sabkhas; (2) the development of escarpments, and (3) the formation of dune fields. The groundwater level sank deeply (e.g., in As Sarīr area 20–80 m below the surface); so conditions for the duricrust formation no longer existed; only thin desert crusts (a few mm to one cm thick) developed locally.

Geomorphological Development

The geomorphological development of the study area was essentially controlled by the above-mentioned geological and climatic factors. The maps of the denudation stages (Figs 6–9) show the progress of denudation from the Late Miocene to the Middle Pleistocene.

Sedimentation of the Qārat Weddah Formation was completed in the Early Pleistocene; then followed the first stage of the lacustrine sedimentation (Qc1) in the south of the study area (lat. 28°01′N,long. 19°54′E) near the Jabal Zalṭan escarpment of that time (Fig. 9), at an altitude of about 200 m a.s.l. The second stage of the lacustrine sedimentation (Qc2), approximately at the beginning of the Middle Pleistocene, took place again below the former SW escarpment of Jabal Zalṭan (lat. 28°05′N, long.20°04′E). This sedimentation was controlled by the former fluvial valley lying about 150 m a.s.l.

The third stage of the lacustrine sedimentation (Qc3) took place during the Middle Pleistocene and left numerous relics covering a large area: at the S margin of Jabal Zalṭan (lat. 28°25′N, long. 19°50′E) at an altitude of about 100 m a.s.l.; in the close vicinity of Marādah at an altitude of 75 m a.s.l. Isolated relics are found near lat. 29°14′N, long. 19°30′30″E (ca. 70 m a.s.l.) and lat. 29°06′30″N, long. 20°14′30″E (ca. 50 m a.s.l.).

As a result of climatic and endogenetic factors, local changes of the stream gradient took place. Flow-through lakes formed at first, in which fluviolacustrine clastic sediments accumulated. Communication between the lacustrine depressions gradually ceased and typical varved lacustrine sedimentation took place. Eventually the lake became dry. A further change of the gradient curve, together with climatic oscillation, resulted in the next fluvial phase being accompanied by erosion. Following the third lacustrine stage (Qc3) the climate became arid and fluvial erosion was replaced by aeolian erosion. The wadis became the main site for this and so shaping of the present escarpments and endorheic depressions began.

The present endorheic depressions of the study area follow, essentially, the main Middle Pleistocene fluvial valleys and some rock steps of that time (Fig. 9): in the broad vicinity of Marādah, along Dūr Zaqqūt and Dūr Marādah, as far as between longitudes 20°00′E and 20°15′E. Other endorheic depressions are at the foot of Jabal Zalṭan. The flat depression in the vicinity of Bi'r Zalṭan deserves special note because it bears numerous relics of the third stage of lacustrine sedimentation (lat. 28°25′N, long. 19°50′E). The deepening of this depression by aeolian activity is beyond doubt. The central part of the depression bears residual hills having a sequence of lacustrine deposits, including calcrete, in their upper parts; the lower parts (5–10 m) are built of Oligocene clastics. This testifies to the deflation of clastic sediments, up to 10 m thick, from the centre of the depression. The groundwater table has reached the surface in the immediate vicinity of Bi'r Zalṭan which is why aeolian erosion cannot continue to a greater depth.

Conclusions

In general, the Pleistocene lacustrine sediments in the central Sirt basin are an integral part of a denudation–accumulation megacycle consisting of the following phases:

(1) fluvial erosion and sedimentation (origin of fluvial valleys, denudation and accumulation of fluvial sediments, e.g. the Qārat Weddah Formation);
(2) lacustrine sedimentation (Pleistocene lacustrine sediments in the fluvial valleys);
(3) aeolian erosion and accumulation (origin of endorheic depressions, escarpments, residual hills; formation of dune fields);
(4) formation of sabkhas (after the groundwater table had been reached by aeolian erosion); and, in some cases,
(5) extinction of sabkhas (as a result of aeolian accumulations).

REFERENCES

AUMASSIP, G. and PETIT-MAIRE, N. (1982). Les industries préhistoriques de la vallée du Shati. *In*: Le Shati. Lac pléistocène du Fezzan (Libye) (*ed.* N. Petit-Maire). *Cent. Nat. Rech. Sci.*, 89–97.

BANERJEE, S. (1980). Stratigraphic lexicon of Libya. *Ind. Res. Cent.*, Tripoli, Bull. **13**, 300 p.

BARR, F.T. and WALKER, B.R. (1973). Late Tertiary channel system in northern Libya and its implications on Mediterranean sea level changes. *In: Initial Rep. Deep Sea Drill. Proj.* (*eds* W.B.F. Ryan, K.S. Hsü *et al.*) **13**(2), 1244–1251.

BELLAIR, P. (1944). Sur l'âge du Calcaire de Mourzouk (Fezzan). *C. R. Somm. Séanc. Acad. Sci. Paris*, **219**, 490–491.

BELLAIR, P. (1949). Le Quaternaire de Tejerhi (Fezzan). *C. R. Somm. Séanc. Sci. Soc. Géol. Fr.*, **9**, 160–162.

COLLOMB, G.R. (1962). Etude géologique du Jebel Fezzan et de sa bordure Paléozoïque. *Notes Mém. Comp. Fr. Pétrole*, **1**, 26 p.

CONRAD, G. and CONRAD, J. (1983). L'histoire néogène et quaternaire du Sahara algérien. *In: Lexique stratigraphique international*, N.S., 1. Afrique de l'Ouest, 171–174.

COQUE, R. (1962). *La Tunisie pré-saharienne, étude géomorphologique.* Colin, Paris, 476 p.

DESIO, A. (1936). Riassunto sulla costituzione geologica del Fezzan. *Boll. Soc. Geol. Ital.*, **55**, 2, 319–356.

DI CESARE, F., FRANCHINO, A. and SOMMARUGA, C. (1963). The Pliocene–Quaternary of Giarabub erg region. *Rev. Inst. Fr. Pétrole*, **18**(10), 1344–1362.

DOMÁCÍ, L. (1985). Geological map of Libya, 1 : 250 000. Sheet: Bi'r Zaltan NH 34-14. Explanatory Booklet. *Ind. Res. Cent.*, Tripoli, 106 p.

GAVEN, C. (1982). Radiochronologie isotopique ionium-uranium. *In*: Le Shati. Lac pléistocène du Fezzan (Libye) (*ed.* N. Petit-Maire). *Cent. Nat. Rech. Sci.*, 44–54.

GIGLIA, G. (1984). Geological map of Libya, 1 : 250 000. Sheet: Ajdabiya NH 34-6. Explanatory Booklet. *Ind. Res. Cent.*, Tripoli, 93 p.

KLITZSCH, E. (1974). Bau und Genese der Grarets und Alter des Grossreliefs in Nordostfezzan (Libyen). *Z. Geomorph.*, **18**, 1, 99–116.

KODYM, O. (1985). Geological map of Libya, 1:250 000. Sheet Sabkhat Ghuzayil NH 34-10. Explanatory Booklet. *Ind. Res. Cent.*, Tripoli, 104 p.

KORÁB, T. (1984). Geological map of Libya, 1:250 000. Sheet: Tmassah NG 33-7. Explanatory Booklet. *Ind. Res. Cent.*, Tripoli, 87 p.

LELUBRE, M. (1949). Géologie du Fezzan oriental. *Bull. Soc. Géol. Fr.*, Ser. **5**(19), 251–262.

MAŠTERA, L. (1985). Geological map of Libya, 1:250 000. Sheet: Marādah NH 34-9. Explanatory Booklet. *Ind. Res. Cent.*, Tripoli, 121 p.

MIJALKOVIČ, N. (1977). Geological map of Libya, 1:250 000. Sheet: Al Qaddahiyah NH 33-3. Explanatory Booklet. *Ind. Res. Cent.*, Tripoli, 66 p.

MRÁZEK, P. (1984). Geological map of Libya, 1:250 000. Sheet: Tanahmū NG 33-6. Explanatory Booklet. *Ind. Res. Cent.*, Tripoli, 72 p.

PAGNI, A. (1938). Sull'eta dei 'Calcari di Murzuch' (Fezzan). *Atti Soc. Ital. Sci. Nat.*, **77**, 73–78.

PAŘÍZEK, A., KLEN, L. and RÖHLICH, P. (1984). Geological map of Libya, 1:250 000. Sheet: Idrī NG 33-1. Explanatory Booklet. *Ind. Res. Cent.*, Tripoli, 108 p.

PERTUSATI, P. and INNOCENTI, F. (1984). Geological map of Libya, 1:250 000. Sheet: Al Aqilah NH 34-5. Explanatory Booklet. *Ind. Res. Cent.*, Tripoli.

PETIT-MAIRE, N. (1982). Conclusions générales. *In*: Le Shati. Lac pléistocène du Fezzan (Libye) (*ed.* N. Petit-Maire). *Cent. Nat. Rech. Sci.*, 98–99.

PETIT-MAIRE, N., CASTA, L., DELIBRIAS, G. and GAVEN, CH. (1980). Preliminary data on Quaternary palaeolacustrine deposits in the Wādī ash Shāṭi' area, Libya. *In: The Geology of Libya* (*eds* M.J. Salem and M.T. Busrewil). Fac. Sci., Univ. Al-Fateh, Tripoli, **III**, 797–807.

SEIDL, K. and RÖHLICH, P. (1984). Geological map of Libya, 1:250 000. Sheet: Sabhā NG 33-2. Explanatory Booklet. *Ind. Res. Cent.*, Tripoli, 138 p.

SELLEY, R.C. (1969). Near-shore marine and continental sediments of the Sirte Basin, Libya. *Q. J. Geol. Soc. Lond.*, 124 (1968), **4**, 496, 419–460.

ŠTEFEK, V. and RÖHLICH, P. (1984). Geological map of Libya, 1:250 000. Sheet: Awbārī NG 33-5. Explanatory Booklet. *Ind. Res. Cent.*, Tripoli, 69 p.

WOLLER, F. (1984). Geological map of Libya, 1:250 000. Sheet: Al Fuqahā NG 33-3. Explanatory Booklet. *Ind. Res. Cent.*, Tripoli, 123 p.

ZIKMUND, J. (1985). Geological map of Libya, 1:250 000. Sheet: Abū Nā'im NH 34-13. Explanatory Booklet. *Ind. Res. Cent.*, Tripoli, 114 p.

Advanced Palaeoclimate Weathering in Soils of the Fazzān Area of Libya

GILANI M. ABUDELGAWAD [1] AND K. BEN MAHMOUD [1]

تجوية متقدمة الأطوار لمناخ قديم في تربة منطقة فزان بليبيا

ج. م. عبد الجواد وخ. بن محمود

الخلاصــــة

لقد تم تقصى التجوية القديمة المتقدمة في تربة فزان بدراسة خصائص عدة مجموعات من التربة. وتبين الخصائص السطحية والكيميائية والمعدنية أن المنطقة قد مرت بثلاثة فترات على الأقل من المناخ الرطب، خلف أولها تجوية شديدة في منطقة العوينات صاحبها تكوين نطاق ب$_2$ت ب. والمكون الرئيسي لمعادن الطفلة في هذه الأنواع من التربة هي معادن الكاولينيت والجبسيت والمايكا. وقد أدت الفترة الثانية الرطبة إلى تكوين ب$_2$لب في منطقة العوينات أيضاً وكانت المكونات الرئيسية في معادن الطفلة هي كاولينيت، وجبسيت والفيرميكيوليت والسميكتيت والمايكا البينطبقية. وتشكل الفترة الرطبة الثالثة المساطب في مناطق تراغن وأم الأرانب وزويلة وسهول الفيضان في وادي تهالة وفي العوينات. وقد تركت الفترة الثالثة تغيرات كبيرة في معادن الطفلة حيث شكل معدن الباليَجورسكيت في معظم الحالات المكون الرئيسي لأنواع التربة التي تمت دراستها. في مناطق تراغن وأم الأرانب وزويلة يتركز معدن الباليجورسكيت في تربة زويلة التي توجد في المناطق المنخفضة بينما يتركز معدن السميكتيت في المناطق المرتفعة في تربة أم الأرانب ويتكون معدن الباليجورسكيت في تربة وادي تهالة عند الحد الفاصل بين أنواع الصخور. وللباليجورسكيت مظاهر شكلية مميزة مثل الفتائل الطويلة أو الرزم. وحيث أن الصخور الأم لهذا النوع من التربة خالية تماماً من معدن الباليجورسكيت، فإن العينات المختارة من هذه التربة غالباً ما تكون غنية بعنصر الماغنسيوم. وبناء على هذه العوامل مجتمعة وحسب المعلومات المنشورة حول إستقرار الباليجورسكيت، فإن تواجد الباليجورسكيت في هذه الأنواع من التربة يعتبر ذا نشأة مستمدة من أصل التربة نفسها. أما دراسة معادن الغرين والرمل لمعظم أنواع التربة التي تناولها البحث فتدل على تغلب الفلسبار والجبس والكالسيت والكاولينيت والكوارتز والجبسيت التي تتواجد في حصة الغرين للنطاقات المدفونة من تربة العوينات. وقد تسببت عوامل الجفاف التي تمر بها المنطقة في ترسب نطاقات ملحية وجبسية وذلك نتيجة لتذبذب المستوى العام للمياه بالمنطقة.

Abstract. Advanced palaeoweathering in soils of Fazzān was monitored by studying the properties of several soil series. The morphological, chemical and mineralogical properties reveal that the area passed through at least three humid periods. The first led to intensive weathering of soils of Al ʻAwaynāt area to form B2tb horizon. The major components of the clay fraction in these soils are kaolinitic, gibbsite and mica. The second humid area resulted in the formation of B22b also in Al ʻAwaynāt area. The major components in the clay fraction are kaolinite, gibbsite, vermiculite, smectite and kaolinite, and interstratified micas. The third humid period formed terraces in the Trāghan, Umm al Arānib and Zuwaylah area, and flood plains in the area of Tahala and Al ʻAwaynāt. This period caused a significant change in the mineralogy of the clay fraction in that, in most cases, palygorskite is the major component of the soils studied. In the Trāghan, Umm al Arānib and Zuwaylah areas the palygorskite is concentrated in the Zuwaylah soils which are at a lower elevation while smectite is concentrated at a higher elevation in the soils of Umm al Arānib. The palygorskite in the soils of Tahala is formed at the boundary of the lithologic discontinuity. The palygorskite throughout the region occurs in a variety of habits, such as long fibres and bundles. Since the parent material of the soils is devoid of palygorskite, their soil extracts are generally high in magnesium. Based upon this observation and published data regarding the stability field of palygorskite, the existence of palygorskite in the soils is considered to be of pedogenic origin. In all cases the palygorskite

---

[1] Department of Soils & Water Science, Faculty of Agriculture, University of Al-Fateh, Tripoli, Libya, G.S.P.L.A.J.

is accompanied by pedogenic gypsum. The silt and sand mineralogy of most of the soils studied is shown to be dominated by feldspar; gypsum, calcite, kaolinite, quartz with gibbsite occurring in the silt fraction of the buried horizons of Al ʻAwaynāt soils. The present arid climatic conditions have caused formation of salic (a horizon of salt accumulation) and gypsic horizons in response to water table fluctuation.

INTRODUCTION

The distribution of silicate minerals in the clay fractions of arid soils has been postulated as reflecting the mineralogy inherent in the material (Buol, 1965; Elgabaly and Khader, 1962). Others have suggested that desert soil-forming processes exert a considerable influence in the form of mineralogical transformation which results in a smectite-rich clay fraction (Barshad, 1962; Jackson, 1959; Vanden Heuvel, 1966). Under conditions of very low rainfall, deep water table and severe erosional and/or depositional regimes, mineralogical transformation would be extremely slow, so that soil mineralogy would tend to be controlled by the nature of the parent material. However, the situation in arid and semi-arid conditions where mineralogy may in fact reflect pedogenic processes, has not been reflected in certain cases in this study.

In arid, semi-arid, and, in extremely arid regions where water tables are close to the surface (in coastal/or undrained interior basin areas), there is a strong possibility that distinctive mineralogical suites may be developed by processes of transformation and/or neoformation. Bases and silica, released by weathering from highland soils, and brought to closed basins by surface run-off, groundwater flow and groundwater uprising, play a highly significant role in the development of pedogenic mineral suites (Cooke and Warren, 1973).

Concentration of the groundwater by evaporation, leading to precipitation of salts and silicate minerals, together with the re-equilibration of detrital minerals in response to saline soil solutions, may result in distinctive mineralogical associations (Millot, 1970; Kovda, 1973). Silicate minerals such as smectite, palygorskite, sepiolite, mica, zeolites and feldspars, and non-silicates such as gypsum, calcite, anhydrite, epsomite and other soluble salts, are postulated to have formed in response to such conditions (Abtahi, 1977; Al-Rawi and Sys, 1967; Elprince *et al.*, 1979; Millot, 1970; Singer and Norrish, 1974). Smectite and palygorskite, in particular, have been postulated to form in an enclosed basin environment. Some workers have proposed smectite formation from palygorskite, while others have proposed the opposite (Millot, 1970; Bigham *et al.*, 1980). The presence of calcite, dolomite, gypsum and the more soluble salts in arid soils is controlled by climate, topography and nature of parent material, and groundwater movement upward and downward. Aridity is a necessary condition for formation as well as preservation of the relatively soluble compounds in soil. Actual quantities and types of salts formed can vary widely.

Large concentrations of calcite, gypsum and more soluble salts in soils are generally the result of both factors; the breakdown of the primary minerals during a palaeoclimatic event, together with addition or inheritance from parent materials. Materials may be added to the soil system via groundwater movement such as occurs in sabkhas, or movement and redistribution of calcite, gypsum and other salts might, on the other hand, be due to aeolian processes, a common phenomenon of the arid environment (Cooke and Warren, 1973; McNeal *et al.*, 1972).

Our knowledge of present day and past soil-forming processes in the Sahara Desert remains extremely scanty. Localized pedological investigations have been made in Algeria to the west (Kubiena, 1955); in the southern Sahara (Beaudet, 1976); part of the central Sahara (Kubiena, 1963); and in the Nile Valley to the east (Elgabaly and Khader, 1962). However, much of the central and southeastern Sahara is virtually uninvestigated except in the area of Al Kufrah (Abudelgawad *et al.*, 1974; Atkinson and Waugh, 1979). Here both authors reported the inheritance of mineralogical properties of these soils from the parent material (Nubian Sandstone), thus highlighting a significant gap in our knowledge of both contemporary and relict pedological processes in arid regions. Although significant evidence has accumulated for climatic changes in the Sahara from studies of landforms (Beaudet, 1976); prehistoric remains (Klitzsch and Pesce, 1966); and hydrology (Pallas, 1978), studies of soil properties have been generally lagging behind these disciplines in terms of detail and extent of investigations. This lack of soil studies appears to be one reason for several controversies that exist concerning important aspects of pedogenesis in arid areas in general, and in the Sahara particularly. One such controversy, explored in the present paper, concerns the origin and significance of specific clay mineral suites in the desert soils of the Fazzān region of Libya.

The purpose of this paper is, in effect, to evaluate the soil properties (morphological, chemical and mineralogical) of the major soil series in Fazzān in terms of palaeoclimate weathering, and on past and recent environmental changes and, in particular, to emphasize the pedogenic origin of palygorskite in the area.

MATERIALS AND METHODS

Description of the Study Area

The Fazzān area occupies the southwestern part of Libya between 23° and 28.5°N lat., between 10° and 16°E long. The total area is 725 000 km^2, and lies within the Murzuq basin. The soil profiles studied represent the soils of the Murzuq area (Umm al Arānib, and Trāghan and Wādī Tanezzuft (Tahala and Al 'Awaynāt), (Fig. 1).

The annual rainfall of the areas of the study ranges from zero to 10 mm. Evapotranspiration ranges from 4.2 to 3.8 m annually. The mean annual temperature is 30°C with maximum temperatures as high as 45°C, and minimum temperatures as low as 4.5°C. The mean annual relative humidity is 32%.

The soils of Trāghan, Umm al Arānib, and Zuwaylah (1, 2, 3), occurring at elevations 435, 350, 310 and 280 m a.s.l., are developed on alluvial terraces bordering a playa-like depression. Soils of Tahala and Al 'Awaynāt are developed on flood plain deposits occurring at 630 m a.s.l. The alluvium is largely the product of weathering of the Acacus and Tadrart sandstones.

The Reconnaissance Soil Survey was done by Regwa in 1972, 1973 and 1974. The groundwater quality in the area of the study ranges from 150 to 800 ppm. Generally this water is an acid water with relatively high magnesium concentration. Major agricultural projects have been under development in this area for the last ten years.

Stratigraphic Units and Lithologies of the Substrate

Geological aspects of the area have been studied and discussed by a number of investigators (Klitzsch, 1966a, b; Vittimberg and Cardello, 1963; Lessar, 1961; Pallas, 1978; Goudarzi, 1970; W.S. Kloss, pers. comm., 1982). The rocks range from Cambrian to Devonian in age, and have been subdivided into a number of formations.

The Acacus sandstone, Cambrian to Ordovician in age, is comprised of approximately 345 m of marine and continental sandstones which are typically white, grey and brown. It is mainly fine-grained, thin- to thick-bedded, quartzitic near the top and with shale beds in the lower part. Frequent trace fossils,

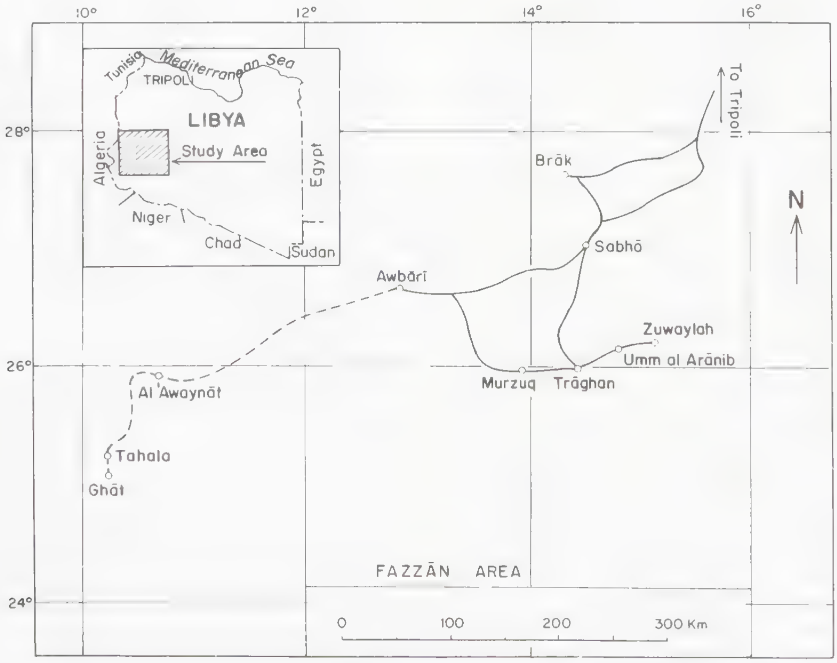

Fig. 1. Location map showing the location of the Fazzān area, and locations of the soil sampling sites.

occurring on thin-bedded sandstone units, indicate a shallow-water deposition. The Acacus sandstone is Middle to Late Silurian in age. The dominant minerals are quartz, feldspar, mica and goethite.

The Tanezzuft shale of Early Silurian age is composed of approximately 400 m of grey marine shale, which is partly silty, with sandstone lenses and some thin sandstone beds in the lower part. The sediments are comprised largely of mica, traces of kaolinite, quartz, plagioclase and orthoclase feldspars.

The Tadrart sandstone of Devonian age is composed of approximately 317 m of continental to marine, white to light brown, and ferruginous dark to red brown sandstone. The lower part is thick-bedded and cross-stratified with rare plant remains. The upper part is thinly bedded with abundant marine trace fossils. It is mainly composed of mica, quartz and feldspar. The Ouan Kasa Formation is composed of approximately 43 m of grey partly silty shale interbedded with clay and siltstone. The formation is Middle Devonian in age. The mineralogy of the formation was studied by Burollet and Byramjee (1969). The dominant minerals in the sand, silt and clay factions are quartz, feldspar, mica and traces of kaolinite and smectite (W.S. Kloss, pers. comm., 1982).

In the area of Trāghan, Zuwaylah, Umm al Arānib, the geology of these areas, as summarized from Goudarzi (1970) and map of the Industrial Research Centre (IRC) 1985, consists of Tertiary lacustrine deposits which are underlain in the north by Lower Cretaceous rocks, comprising conglomerate siltstone and subordinate amounts of grey to purple clay and claystone. Characteristically, cross-bedded quartzite and common, silicified wood, are found in the area. In the south, the Tertiary lacustrine deposits are covered with Quaternary aeolian deposits and Quaternary sabkhas.

PHYSICAL, CHEMICAL AND MINERALOGICAL ANALYSIS

Analysis of Fine Earth Fraction

Soil samples were air dried and crushed to pass through a 2 mm sieve. Calcium carbonate was determined by a manometric method (Williams, 1948); gypsum by extraction with water and precipitation with acetone (Richards, 1954); and organic carbon was estimated by wet oxidation using acid dichromate (Allison, 1965). Soil pH was determined on a 1:1 suspension after 1 hour equilibration. The electrical conductivity and Na, K, Ca and Mg were measured in the saturated paste extract. Na and K were measured by flame photometry; electrical conductivity measured in the saturated paste extract, using Beckman conductivity bridge. Ca and Mg were measured by a complexometric titration with versenate. Silicate was determined by heteropoly blue method. Aluminium was determined colorimetrically by the haematoxylin method of Dalal (1972); Fe by 420 Perkin Elmer atomic absorption; cation exchange capacity by the method of sodium acetate at pH 8.2 (Black, 1965). Particle size analysis was carried out according to the method of Jackson (1969). Preparation of the soil for mineralogical analysis included removal of carbonates with *N* NaOAc at pH 5. Removal of organic matter with H_2O_2, removal of free iron oxides with dithionite, citrate, bicarbonate and fractionation by wet sieving, sedimentation and centrifugation (Jackson, 1969).

Analysis of Clay Fraction

The <2 μm size fractions were saturated with Mg and K. Out of the Mg-saturated samples and K-saturated samples, 50–60 mg of both the K- and Mg-saturated samples were pipetted as a thick suspension on the glass slides and air dried and equilibrated at 54% relative humidity for 24 hours. The oriented samples were X-rayed by using Krestalloflex Siemens X-ray diffraction instrument with copper radiation at 35 kV and 18 mA. The potassium-saturated samples were X-rayed after air-drying and after heating to 300 and 550°C. 2–20 μm of silt fraction were X-rayed in random orientation as a powder in box mounts. The Mg-saturated samples were X-rayed after air-drying and after equilibrium in aluminium pan with ethylene glycol-vapour for 48 hours. 15 mg of the Na-saturated <2 μm fraction from selected samples were equilibrated over a saturated solution of Mg $(NO_3)_2$ and used for differential thermal analysis. Ground-ignited Al_2O_3 was used as a reference in R.L. Stone DTA apparatus and the heating rate was set at 12°C/l min.

Droplets of diluted suspension of Na-saturated <2 μm fractions were dried on 300 mesh formvar coated copper grids and examined using Hitachi HU-11E Transmission Electron Microscope. Triplicate 100 mg samples of the <2 μm size fraction were used to measure the Ca/Mg and K/NH_4 exchange capacities for the soils that show smectite and vermiculite following Jackson (1969). Total K analysis of the 2 μm of the clay fractions was carried out according to the method of Bernas (1968).

Estimation of Minerals in the <2 μm Fraction

Estimates of the smectite and vermiculite contents of the $<2\ \mu m$ fractions were made using Ca and K exchange according to the method of Alexiades and Jackson (1965). The mica content was estimated from the total K_2O content, assuming mica with a composition of 10% K_2O. Kaolinite was estimated from relative peak areas of the $(001)_{\mathrm{Kaol}}$ and $(001)_{\mathrm{Smec}}$ for the Mg-glycerol treated samples, and the % smectite estimated from cation exchange according to the following relationship:

$$\%\,\text{Kaolinite} = (\%\,\text{Smectite})\left(\frac{(001)_{\mathrm{Kaol}}}{(001)_{\mathrm{Smec}}}\right) \times 1.6 \qquad (1)$$

where $(001)_{\mathrm{Kaol}}$ and $(001)_{\mathrm{Smec}}$ refer to the peak areas of the kaolinite and smectite, respectively. The estimate of the (001) kaolinite intensity was made using the intensity ratios of (002) (3.57 Å) and (004) chlorite 3.54 Å peak according to the following (John *et al.*, 1954):

$$(001)_{\mathrm{Kaol}} = (7.2\ \text{Å peak area}) \times (002)_{\mathrm{Kaol}}(002_{\mathrm{Kaol}} + (004)_{\mathrm{Chl}})$$

The estimates of peak areas at 3.57 and 3.54 Å were made from diffraction patterns obtained at the rate of ¼°. The factor 1.6 in the equation (1) was determined by W.F. Bradley as quoted in Scafes and Kunze (1971). The chlorite content was estimated from the kaolinite content.

Estimation of palygorskite was based on the relative increase in the (110) peak intensity (10.5 Å) when heated to 150–170°C (Nathan, 1970; Hayashi *et al.*, 1969). The determination of different charged smectite was carried out as follows: 50 mg of soil clay reacted with dodecylamine HCl according to the method of Lagaly and Weiss (1969).

RESULTS

Physical and Chemical Properties of Soil

Table 1 shows some selected morphological properties of the soils studied and their classification. In most cases these soils showed minimum development of their profiles, except in Al 'Awaynāt soils 2 and 3. One characteristic of the soils studied is the presence of surface pebble gravel or desert pavement (Dregne, 1976), especially in soils of Trāghan, Umm al Arānib, and Zuwaylah, and in the surface horizons of the palaeosoils in Al 'Awaynāt. In certain cases the gravel distribution through the soil profiles indicates there has been more than one erosion cycle, in which removal of the fine materials (Table 1) is due to a combination of both wind and water erosion. Fluctuation of the water table has played an important role in forming specific subsurface horizons in some of the soils studied. These are salic horizons of salt accumulation, and gypsic horizons. The salic horizons exist in soils of Trāghan, Wādī Tanezzuft and Al 'Awaynāt 1 and 2. Gypsic horizons exist in soils of Al 'Awaynāt 2.

Study of the morphological properties of the soils shown in Table 1 and field observation, lead to the conclusion that four climatic events occurred in the Fazzān region of Libya. The first, a humid climate, led to the formation of the IIB2tb horizon in soils of Al 'Awaynāt 3.

The second period led to the formation of the IIB22b horizon in soils of Al 'Awaynāt 2. A third humid period led to the deposition of alluvial deposits in terraces and flood plains of Umm al Arānib, Zuwaylah, Tahala and Al 'Awaynāt, forming Al 'Awaynāt 1 and burying the Al 'Awaynāt 2 and 3 above the palaeosoils. The fourth period corresponds to the present. The soils of Trāghan, Umm al Arānib and Zuwaylah areas are developed at the following elevations: 435, 350, 310, 280 m a.s.l. The direction of slope is towards Zuwaylah 3 which is like a centre of the playa. The soils studied have been classified according to Soil Taxonomy (1975) as follows: three soil series as Typic Salorthids; two soil series as Lithic Torriorthents; two soils as Typic Torriorthents; one soil as Typic Torrifluvents and one soil series as Salic Gypsiorthid.

Table 2 shows some of the selected chemical properties and particle size analysis. The pH data show most of the soil as neutral to calcareous in reaction, except in the soils of palaeosoils. The pH of the latter is in the acid region and can be as low as 3.6. The CEC (Cation Exchange Capacity) of the soils varies from one to another, mainly depending on the type of layer silicates present. The highest values are reported from the Tahala soils. The lowest is also from the Tahala soils at the lower horizon of IICR. Pedogenic lime varies from one soil series to another; the highest values are recorded from Zuwaylah 3 soil, where they reach as high as 21%. Soils of Al 'Awaynāt 2 and 3, IIB22b and IIB2tb, are devoid of $CaCO_3$. Pedogenic gypsum is highest in the soils of Al 'Awaynāt 2 and Tahala soils (Table 2). The gypsum occurs both in nodular and

Table 1. Morphology and classification of soils studied

Soil series	Family	Horizon	Depth (cm)	Munsell Colour		Texture	Structure	Consistency			Boundary	Parent material
				Moist	Dry			Dry	Moist	Wet		
Typic Salorthids												
Trāghan	Sandy, mixed, thermic	C_1	0– 20	7.5YR 5/6	7.5YR 6/6	gS	Sg	Lo	Lo	SS,PS	CS	Alluvium over glauconitic sandstone
		C_2	20– 23	7.5YR 5/6	7.5YR 6/6		m	eh	fi	S,P	CS	
		IIC_3	28– 45	7.5YR 5/6	7.5YR 6/6	LS	m	Lo	Lo	SS,PS	CS	
		$IIIC_4$	45– 80	7.5YR 5/6	7.5YR 5/8	gLS	Sg	Lo	Lo	SO,PO	CS	
Umm al Arānib	Coarse, loamy, mixed, thermic	C_{1sa}	0– 25	10YR 5/4	10YR 7/6	SL	m	SO	Vfr	SS,SP	CS	Alluvium
		C_{2sa}	25– 40	10YR 6/6	10YR 7/6	SL	m	SO	Vfr	SS,SP	CS	
		C_{3sa}	40– 75	10YR 6/4	10YR 7/4	LS	m	SO	Vfr	SS,SP	CS	
		C_4	75–110	10YR 6/6	10YR 7/6	SL	m	Sh	fr	S,P	CS	
Al ‘Awaynāt 1	Coarse, loamy, mixed, thermic	C_{1sa}	0– 15	5YR 4/6	5YR 6/6	SL	Sg	Lo	Lo	SS,SP	CS	Alluvium and aeolian mixed
		C_{2sa}	15– 30	5YR 4/4	5YR 5/6	SL	m	Sh	fr	S,P	A.W.	
		IIC_3	30– 75	5YR 6/6	7.5YR 6/6	SL	m	Sh	fr	N.St.H.P.	CS	
		IIC_4	75–130	5YR 4/6	5YR 6/6	SL	m	Sh	fr	N.St.N.P.	CS	
Lithic Torriorthents												
Zuwaylah 2	Sandy, loamy, mixed, calcareous, thermic	C_{1p}	0– 25	7.5YR 6/6	10YR 7/4	gSL	m	Sh	fi	SO,PO	CS	Alluvium over breccia
		C_2	25– 40	7.5YR 6/6	10YR 7/4	gSL	m	Sh	fi	SS,PS	CS	
		IICR	>40		5Y 8/2							
Zuwaylah 1	Sandy, mixed, calcareous, thermic	C_1	0– 20	7.5YR 5/6	7.5YR 6/6	gLS	Sg	Lo	Lo	SO,PS	CS	Alluvium over breccia

Typic Torriorthents												
Zuwaylah 3	Coarse, loamy, mixed, calcareous	A_p	0– 30	7.5YR 5/6	7.5YR 6/6	gSL	Sg	Lo	Lo	SO,PO	CS	Alluvium over breccia
		C	30– 75	7.5YR 5/6	7.5YR 6/6	gSL	Sg	Lo	Lo	SO,PO	CS	
		IICR	75–100		5Y 8/2							
Al 'Awaynāt 3	Coarse, loamy, mixed, thermic	C_1	0– 70	7.5YR 4/4	10YR 6/4	SL	m	Lo	Lo	SS,PS	CS	Aeolian over sandstone and kaolinite
		C_2	70–105	5YR 4/6	5YR 5/6	SL	m	Lo	Lo	SS,PS	CS	
		IIA_{1b}	105–150	7.5YR 4/4	7.5YR 5/6	SL	m	Lo	Lo	SS,PS	CS	
		IIB_{2tb}	150–165	7.5YR 4/4	7.5YR 6/4	gSL	m	Lo	Lo	S,P	CS	
		IIICR	>165		7.5YR 6/6							
Typic Torrifluvents												
Tahala	Fine silty over sandy, mixed, thermic	C_1	0– 35	10YR 6/4	10YR 8/4	SiCL	PL	Sh	fr	VS,VP	CS	Alluvium
		C_2	35– 52	10YR 5/4	10YR 7/4	SiCL	m	Sh	fr	VS,VP	CS	
		C_3	52– 78	10YR 5/4	10YR 7/4	SiCL	m	Sh	fr	VS,VP	CS	
		IIC_4	78– 95	5YR 5/6	5YR 6/6	gS	Sg	SO	lo	SO,PO	CS	
		IICR	>95	5YR 5/6	5YR 6/6	St S	m	SO	Lo	SO,PO	CS	
Salic Gypsiorthids												
Al 'Awaynāt 2	Coarse loamy, mixed, thermic	C_{1saCS}	0– 40	7.5YR 4/4	7.5 YR 6/6	SL	Sg	Lo	Lo	SO,PO	CS	Aeolian over sandstone and kaolinite
		C_{2sa}	40– 52	7.5YR 4/4	7.5YR 6/6	StSil	Sg	Lo	Lo	SO,PO	A.W.	
		C_3	52– 70	7.5YR 4/4	7.5YR 6/6		Sg	Lo	Lo	SO,PO	CS	
		C_4	70–105	5YR 4/6	7.5YR 6/6	SL	Sg	Lo	Lo	SS,PS	CS	
		IIB_{21b}	105–125	10YR 6/4	10YR 6/4	L	m	Sh	fr	S,P	CS	
		IIB_{22b}	125–150	10YR 5/4	10YR 7/4	gSCL	m	Sh	fr	SS,PS	CS	
		IIIR	150–160		2.5YR 8/0							
		IVR	>160									

Table 2. Particle size distribution and selected chemical properties of soils studied

Soil Series	Family	Horizon	Depth (cm)	Sand 2–0.05	Silt 0.05–0.002 (PCT of 2 mm)	Clay <0.002	O.M. (%)	C.E.C (meq/100 g)	pH of saturated soil	E.C (mmho/cm at 25°C)	Lime (%)	Gypsum (%)
Typic Salorthids												
Trāghan	Sandy, kaolinitic, thermic	C_1	0– 28	93.84	2.82	3.34	0.72	2.6	7.8	125		
		IIC_2	28– 45	86.67	6.64	6.69	1.3	4.5	8.9	130	1.7	0.1
		$IIIC_3$	45– 80	88.02	2.83	9.15	1.20	3.7	9.5	66.2	2.0	0.2
		IVR	>80							13.5	0.6	0.02
Umm al Arānib	Coarse loamy, mixed, thermic	C_{1sa}	0– 25	79.29	6.04	14.67	0.9	8	8.4	60	1.9	0.2
		C_{2sa}	25– 40	79.52	5.6	14.89	1.0	8.5	7.3	50	1.4	0.3
		C_{3sa}	40– 75	83.91	4.49	11.58	0.8	7.2	6.9	55	1.2	0.4
		C_4	75–110	78.57	5.24	16.2	0.5	9	7.0	2	1.0	0.2
Zuwaylah 3	Coarse loamy, mixed, calcareous, thermic	A_p	0– 30	74.05	14.82	11.12	1.45	8.17	7.7	7.8	18.05	3.0
		C	30– 75	74.35	14.37	11.27	1.45	7.52	8.0	2.5	21.32	3.4
		IICR	75–100									
Lithic Torriorthents												
Zuwaylah 2	Coarse loamy, mixed, calcareous, thermic	C_{1p}	0– 25	63.08	23.95	12.97	1.29	8.7	8.1	1.36	18.62	3.2
		C_2	25– 40	61.96	19.75	18.29	1.45	13.39	8.0	6.6	18.2	3.7
		IICR	>40									
Zuwaylah 1	Sandy, mixed, calcareous, thermic	C_1	0– 20	83.98	9.83	6.18	1.32	6.96	7.7	11.0	10.5	0.01

Typic Torrifluvents												
Tahala	Fine silty	C_1	0– 35	8.83	53.18	37.99	0.81	28.7	6.3	17.0	0.56	0.14
	over sandy,	C_2	35– 52	4.02	59.55	36.43	0.81	31.96	6.6	19.6	0.5	0.48
	mixed, thermic	C_3	52– 78	10.6	60.61	28.79	0.72	13.39	6.5	24.2	0.56	2.0
		IIC_4	95	89.28	4.62	6.10	0.33	2.58	7.1	15.0	0.38	2.1
		IIC_r	95	89.28	4.62	6.10	0.33	2.58	7.1	15.0	0.38	0.76
Al 'Awaynāt	Coarse loamy,	C_{1sa}	0– 15	63.97	26.53	9.51	1.0	6.9	7.7	51.5	0.9	1.1
	mixed, thermic	C_{2sa}	15– 30	69.89	19.15	10.96	1.12	6.3	7.6	18.0	1.1	3.6
		IIC_3	30– 75	61.96	29.15	8.89	0.80	8.1	7.5	3.5	1.1	1.2
		IIC_4	75–130	66.46	23.98	9.56	0.3	8.4	7.3	2.3	1.6	1.3
Salic Gypsiorthids												
Al 'Awaynāt 2	Coarse loamy,	C_{1sa}	0– 40	67.48	24.29	8.23	1.6	9.9	7.3	151	1.34	7.1
	mixed, thermic	C_{2sa}	40– 52	43.95	51.31	4.74	0.8	14.7	7.4	3.8	1.0	1.3
		C_3	52– 70				0.6	15.3	7.5	7.8	1.7	1.3
		C_4	70–105	51.85	46.22	1.93	0.6	21.3	7.7	3.5	0.7	1.3
		IIB_{21b}	105–125	47.48	33.33	19.19	1.8	10.8	4.0	3.1	0.0	0.2
		IIB_{22b}	125–150	52.79	25.61	21.6	1.3	10.4	3.6	3.5	0.0	1.0
		IIIR	150–160									
Typic Torriorthents												
Al 'Awaynāt 3	Coarse loamy,	C_1	0– 70	61.16	31.58	7.26	1.45	13.39	7.6	5.3	1.69	1.4
	mixed, thermic	C_2	70–105	62.77	32.14	5.08	0.64	16.87	7.1	0.68	1.03	1.3
		IIA_{1b}	105–150	66.31	20.09	13.6	1.4	9.3	4.3	4.25	0.0	tr
		IIB_{2tb}	150–165	68.99	14.6	16.4	1.3	6.09	4.1	0.30	0.0	tr
		IIICR	165									

Table 3. Exchangeable cations and soluble anions and cations of the soils studied

Soil Series	Horizon	Exchangeable cations (meq/100 g)				Soluble cations and anions (meq/l)							
		Ca	Mg	Na	K	Ca	Mg	Na	K	CO_3^{2-}	HCO_3^-	SO_4^{2-}	Cl^-
Trāghan	C_1	1.7	0.6	0.8	0.5	6.4	29.2	160	1.4	–	0.3	135	100
	IIC_2	2.1	0.4	1.1	0.8	11.4	40.1	120	1.1	–	0.3	120	60
	$IIIC_3$	1.8	0.2	1.0	1.0	5.5	76.0	50	2.0	–	0.5	7.30	120
Umm al Arānib	C_{1sa}	5.0	0.8	1.5	0.7	18	40	220	1.0	–	0.2	140	120
	C_{2sa}	4.5	0.9	1.8	0.8	16	60	240	1.2	–	0.2	130	140
	C_{3sa}	4.0	0.6	2.0	0.8	18	70	230	1.1	–	0.2	110	120
	C_4	6.0	0.8	0.9	0.6	4	12	4	0.8	–	0.4	8	10
Zuwaylah 2	C_{1p}	4.1	1.4	0.5	2.2	0.8	50	3.6	0.1	–	0.3	3.8	242
	C_2	5.0	1.6	1.0	3.7	9.7	76.7	26.8	0.1	–	0.4	13.17	38.0
	IICR	–	–	–	–	–	–	–	–	–	–	–	–
Zuwaylah 3	A_p	3.7	0.9	0.7	1.3	10.2	33	32.1	0.1	–	0.2	5.5	6.7
	C	2.1	0.6	0.3	1.5	2.5	35.1	12.6	0.1	–	0.3	6.7	3.0
	IICR	–	–	–	–	–	–	–	–	–	–	–	–
Zuwaylah 1	C_1	2.5	0.8	1.6	1.3	11.4	110.0	56	0.07	–	0.07	6.6	114.7
Tahala	C_1	13.5	10.6	4.7	0.4	11.4	116	63	0.1	–	0.5	67.4	114
	C_2	24.5	10.5	3.5	0.4	8.9	164	63	0.1	–	0.9	97.0	101
	C_3	4.0	11.2	3.6	0.3	10.2	169	71	0.1	–	0.7	80.0	211
	IIC_4	1.2	2.0	0.4	0.2	9.3	224	44	0.1	–	0.5	76.0	50.1
	IIC_r	1.3	0.8	0.4	0.1	8.6	180	40.1	0.1	–	0.18	68.0	51.0
Al 'Awaynāt 2	C_{1sa}	8.0	2.1	2.0	1.8	21.5	65.0	1231	2.1	–	0.5	103	1160
	C_{2sa}	9.0	0.6	2.5	1.4	12.7	48.5	10	0.1	–	0.9	2.8	38.0
	C_3	11	0.4	3.0	0.8	13.7	52.5	31.8	0.1	–	0.3	24.1	38.2
	C_4	12	0.4	0.8	0.9	12.2	28.5	0.4	0.1	–	0.5	21.1	37.0
	IIB_{21b}	6.9	0.8	0.2	0.6	7.4	28.3	2.4	0.1	–	0.5	12.2	25.6
	IIB_{22b}	5.0	0.4	0.1	0.5	8.9	26.7	2.4	0.1	–	0.5	11.1	38.1
	IIIR	–	–	–	–	–	–	–	–	–	–	–	–
Al 'Awaynāt 3	C_1	11.4	0.8	0.5	1.6	15.3	40.8	24	0.1	–	0.7	22	63.8
	C_2	7.4	3.0	0.4	1.3	1.3	65.0	0.1	0.1	–	0.7	7.8	25.5
	IIA_{1b}	1.7	1.8	0.1	0.7	5.0	20.5	0.2	0.2	–	0.2	1.7	25.4
	IIB_{2tb}	1.1	0.8	0.1	0.3	3.5	16.8	0.1	0.1	–	0.2	4.5	25.5
	IIICR	–	–	–	–	–	–	–	–	–	–	–	–
Al 'Awaynāt 1	C_{1sa}	4.5	2.0	0.7	0.5	11.4	126	319	0.8	–	0.3	162	191
	C_{2sa}	4.0	1.5	0.4	0.8	15.9	290	1343	2.5	–	0.7	211	395
	IIC_3	5.6	1.2	0.30	1.0	11.4	29	2.4	0.1	–	0.3	17.6	25
	IIC_4	4.8	0.7	0.4	0.6	12.7	56.6	1.1	0.1	–	0.9	18.5	25

fibrous form. In certain cases the gypsum fibres are as long as 5–8 cm.

Organic matter content varies from one depth to another reflecting variation in depositional environments and palaeoclimate conditions. It should be noted that the buried horizons have relatively higher values of organic matter in comparison to the other soil series.

Magnesium and sodium are the dominant cations in the soluble soil extracts (Table 3). Magnesium concentration ranges from 8 to 264 meq/litre, while sodium concentration is as high as 1000 meq/litre for some saliorthids. Sulphate and chloride (Table 3) are the dominant anions in all soils studied. The available potassium as determined by IN NH_4OAc, ranges from 10 to 260 ppm. Thus, most of the soils in the area of the study do not need potassium fertilizer. The chloride, sodium, magnesium and the high EC_e (electrical conductivity of soil extract) values of some of the soils studied will be one problem affecting their productivity, as is shown in Tables 2 and 3.

Mineralogy of Sand and Silt Fractions

Both coarse and fine sand fractions consist mainly of quartz with traces of muscovite and feldspar, mainly orthoclase. The silt mineralogy of 2 to 50 μm is shown in Table 4. In all the soils studied, quartz and potassium feldspar are the dominant minerals. In most of the soils, the amounts of quartz and potassium feldspar of the C horizons are quite uniform.

Table 4. Mineralogical composition of the 2 to 50 μm silt fraction of the soils studied

Soil Series	Horizon	Q	KF	Pla	Gy	Do	Cal	Gib	Goe	Kao	Anh	Arag	Eps
Trāghan	C_1	7X	–	4X	X	3X	4X	–	X	3X	–	–	–
	IIC_2	7X	4X	2X	2X	3X	2X	–	2X	2X	–	–	–
	$IIIC_3$	7X	4X	2X	X	2X	2X	–	X	4X	–	–	–
Umm al Arānib	C_{1sa}	6X	3X	2X	–	–	–	–	–	2X	–	–	–
	C_{2sa}	6X	4X	2X	–	–	–	–	–	2X	–	–	–
	C_{3sa}	6X	4X	2X	–	–	–	–	–	3X	–	–	–
	C_4	6X	4X	2X	–	–	–	–	–	2X	–	–	–
Zuwaylah 2	C_{1p}	7X	3X	2X	–	2X	4X	–	X	3X	–	–	–
	C_2	7X	3X	3X	2X	3X	4X	–	X	3X	–	–	–
Zuwaylay 3	A_p	7X	4X	2X	X	–	4X	–	X	3X	–	–	–
	C	7X	4X	3X	–	–	5X	–	X	3X	–	–	–
Tahala	C_1	X	3X	2X	X	–	2X	–	2X	2X	–	–	–
	C_2	6X	3X	2X	2X	–	2X	–	X	2X	–	–	–
	C_3	6X	3X	2X	3X	–	2X	–	X	2X	–	–	–
	IIC_4	7X	2X	3X	3X	–	2X	–	X	X	–	–	–
	IICR	7X	2X	4X	X	–	2X	–	X	X	–	–	–
Al 'Awaynāt	C_{1sa}	7X	3X	2X	3X	–	X	–	X	X	–	–	–
	C_{2sa}	7X	3X	2X	X	–	X	–	X	X	–	–	–
	C_3	7X	3X	2X	X	–	X	–	X	X	–	–	–
	C_4	7X	3X	X	X	–	X	–	X	X	–	–	–
	IIB_{21b}	4X	4X	2X	X	–	–	–	X	2X	–	–	–
	IIB_{22b}	4X	4X	X	X	–	–	–	X	2X	–	–	–
Al 'Awaynāt 3	C_1	7X	3X	3X	X	–	2X	–	X	X	–	–	–
	C_2	7X	3X	3X	–	–	X	–	X	X	–	–	–
	IIA_{1b}	6X	2X	–	–	–	–	–	X	2X	–	–	–
	IIB_{2tb}	6X	2X	–	–	–	–	–	X	2X	–	–	–
Al 'Awaynāt 1	C_{1sa}	7X	–	3X	2X	–	X	–	X	2X	–	–	–
	C_{2sa}	7X	–	3X	3X	–	2X	–	X	2X	–	–	–
	IIC_3	6X	2X	2X	2X	–	2X	–	X	2X	–	–	–
	IIC_4	6X	2X	2X	2X	–	2X	–	X	2X	–	–	–

Minerals: Q = quartz, KF = potassium feldspar, Pla = plagioclase, Gy = gypsum, Do = dolomite, Cal = calcite, Gib = gibbsite, Goe = goethite, Kao = kaolinite, Anh = anhydrite, Arag = aragonite and Eps = epsomite.
7X = >50%, 6X = 25–50%, 5X = 15–25%, 4X = 8–15%, 3X = 3–8%, 2X = 1–3%, X = <1%, –= not detected.

Lesser amounts of potassium feldspar are found in the IIB2b of Al 'Awaynāt 3, as compared to the soils of Al 'Awaynāt 2 (Table 4).

Plagioclase feldspar, present in minor amounts in Al 'Awaynāt 2, is absent from Al 'Awaynāt 3 (Table 4), underlining its low stability. The other mineral which occurs in the buried soil horizons of Al 'Awaynāt 2 and 3 is gibbsite. The silt fraction, under the optical microscopic, shows a soft white material which, following X-ray and DTA analyses, was found to be mainly kaolinite and gibbsite. Relict fabrics of primary feldspar indicate that the kaolinite is mainly formed from the alteration of feldspar during the palaeoclimate weathering. Feldspars have been reported as weathering directly to an amorphous phase (Fields, 1966; Garbumov, 1969); to halloysite (Sand, 1956; McCaleb, 1959; Bates, 1960; Uehara *et al.*, 1966; Parham, 1969); to kaolinite (McCaleb, 1959; Exley, 1976); to gibbsite or boehmite (Helgeson *et al.*, 1969; Lodding, 1972); or to muscovite, mica or illite (Sand, 1956; Exley, 1976). The soil solution chemical composition has a great effect upon the product weathering of feldspar. The other minerals found in the silt fraction are calcite, dolomite, gypsum and goethite in varying amounts. For the non-treated soil samples, epsomite and halite are present in appreciable amounts, especially in soils with salic horizons.

Mineralogy of the Clay Fractions

X-ray diffractograms for the <2 μm clay fraction obtained for all the soils studied are present in Table 5. The data shows various suites minerals such as: (1) smectite, mica, kaolinite, (2) smectite, mica, palygorskite, kaolinite, (3) smectite, mica, palygorskite, kaolinite/mica interstratified, (4) kaolinite, micas, mica/kaolinite interstratified, gibbsite. Figures 2, 3, 4 and 5 show details of X-ray analysis.

The data for all the soils is summarized in Table 5. Kaolinite is, in most cases, the dominant clay mineral, followed by mica and palygorskite for soils of Trāghan, Umm al Arānib, Zuwaylah 1, 2 and 3.

Figure 2 shows the X-ray pattern of Umm al Arānib soils. The dominant clay minerals are kaolinite, mica, smectite and palygorskite. The kaolinite, as shown by X-ray diffractograms and TEM micrograph (Figs 2, 7c), is coarsely crystalline. It is also a high charged type, as indicated by the X-ray pattern which shows a 22 Å reflection (Fig. 2), and the fact that it collapses to 10 Å at room temperature following potassium saturation and air drying (data not shown). Table 5 shows that smectite increases with depth as determined by Ca/Mg CEC. The Umm al Arānib soils show no quartz in the clay fraction although it is a dominant mineral in the sand and silt fraction (Table 4). The palygorskite shows only as traces during regular X-ray analysis, but upon heating the sample to 150°C (Nathan, 1970), the 10.5 Å is enhanced and its amount was estimated at between 4 and 8% (data not shown).

The Trāghan soils show a similar mineralogy except that there is an increase in the amount of palygorskite (Table 5, Fig. 3), more kaolinite, and less mica and smectite. Quartz is also present as indicated in Fig. 3 by 4.26 Å reflection (Fig. 3). The palygorskite is well defined by X-ray diffraction. Peaks at 10.5 and 6.44 Å for palygorskite, and for kaolinite at 7.14 and 3.57 Å disappeared upon heating to 550°C. Kaolinite displays a well-developed crystalline habit with hexagonal plates (Fig. 7b). Lesser amounts of mica were determined by total K_2O.

Since there is no evidence of potassium feldspar on X-ray analysis, it was found that, in general, mica increases with depth. Palygorskite also increases with depth. Morphologically it is comprised of coarse fibres which, in certain cases, occur as bundles. Vermiculite/mica, interstratified, is also present, as is shown by 11.9 Å peak and its collapse to 10 Å reflection upon heating to 300°C.

The Zuwaylah soils' mineralogy is represented by Zuwaylah 3 in X-ray diffractograms (Fig. 3), and by TEM micrographs for the C horizon (Fig. 7a). The data, summarized in Table 5, shows that palygorskite and kaolinite are the dominant clay minerals with lesser amounts of mica and smectite. The smectite has a broad reflection between 2 and 5° indicating the presence of interstratified mica/smectite. Also, there is a trace of quartz. The TEM micrographs show that there is an abundance of palygorskite existing in bundles and coarse fibres (Fig. 7a, b). Figure 7d shows palygorskite from northern Libya for comparison.

The mineralogical properties of the <2 μm clay fraction of Tahala soil, shown in Fig. 4, and summarized in Table 5, show that kaolinite is the dominant clay mineral followed by mica in the C_2 and C_3 horizons. Vermiculite decreases with depth, and palygorskite increases with depth (Fig. 4). The TEM micrographs for C_2, C_3, IIC_4 and IICR, shown in Fig. 8a, b, c and d, indicate palygorskite concentration at C_3, IIC_4 and IICR.

In effect, it would appear to be concentrated at the lithological discontinuity (further clarified in

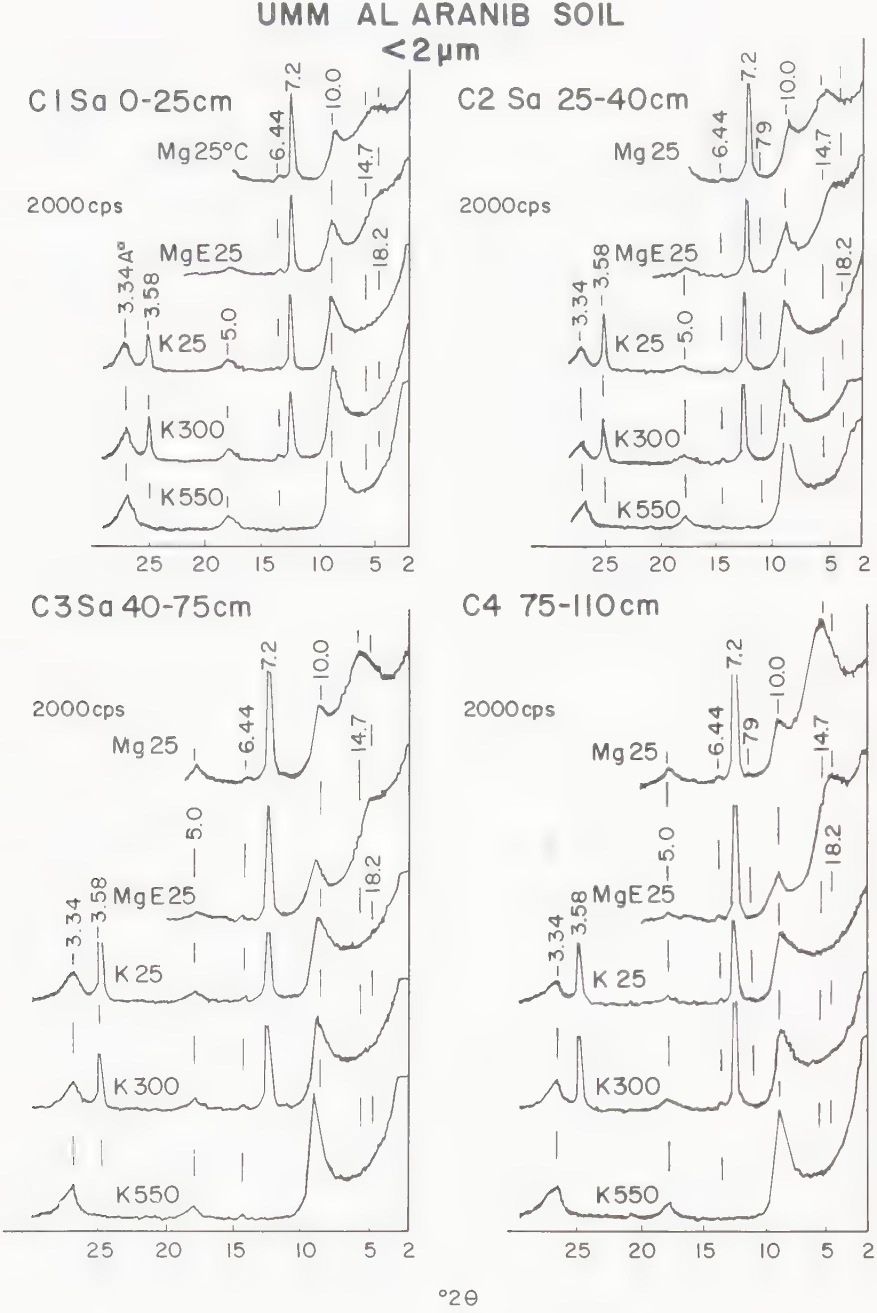

Fig. 2. X-ray diffractograms of the <2 µm clay fractions of the Umm al Arānib soil.

Fig. 9), accompanied by an increase in gypsum content (Table 2). The other minerals, existing in trace amounts, are chlorite and mica/kaolinite interstratified.

The soils of Al ʻAwaynāt area are represented by three soil types, referred to as Al ʻAwaynāt 1, 2 and 3. The clay mineralogy of these soils is presented in Table 5, and X-ray diffractograms for a few horizons, C_2Sa, Al ʻAwaynāt 1, IIB22b, Al ʻAwaynāt 2, IIA1b, IIB2tb, and Al ʻAwaynāt 3 are shown in Fig. 5, and TEM micrographs of IIB22b and IIB2tb(a, b) in Fig. 5, and of Al ʻAwaynāt 2 and Al ʻAwaynāt 3 in Fig. 10a, b. The data in all cases show kaolinite as the dominant clay mineral fol-

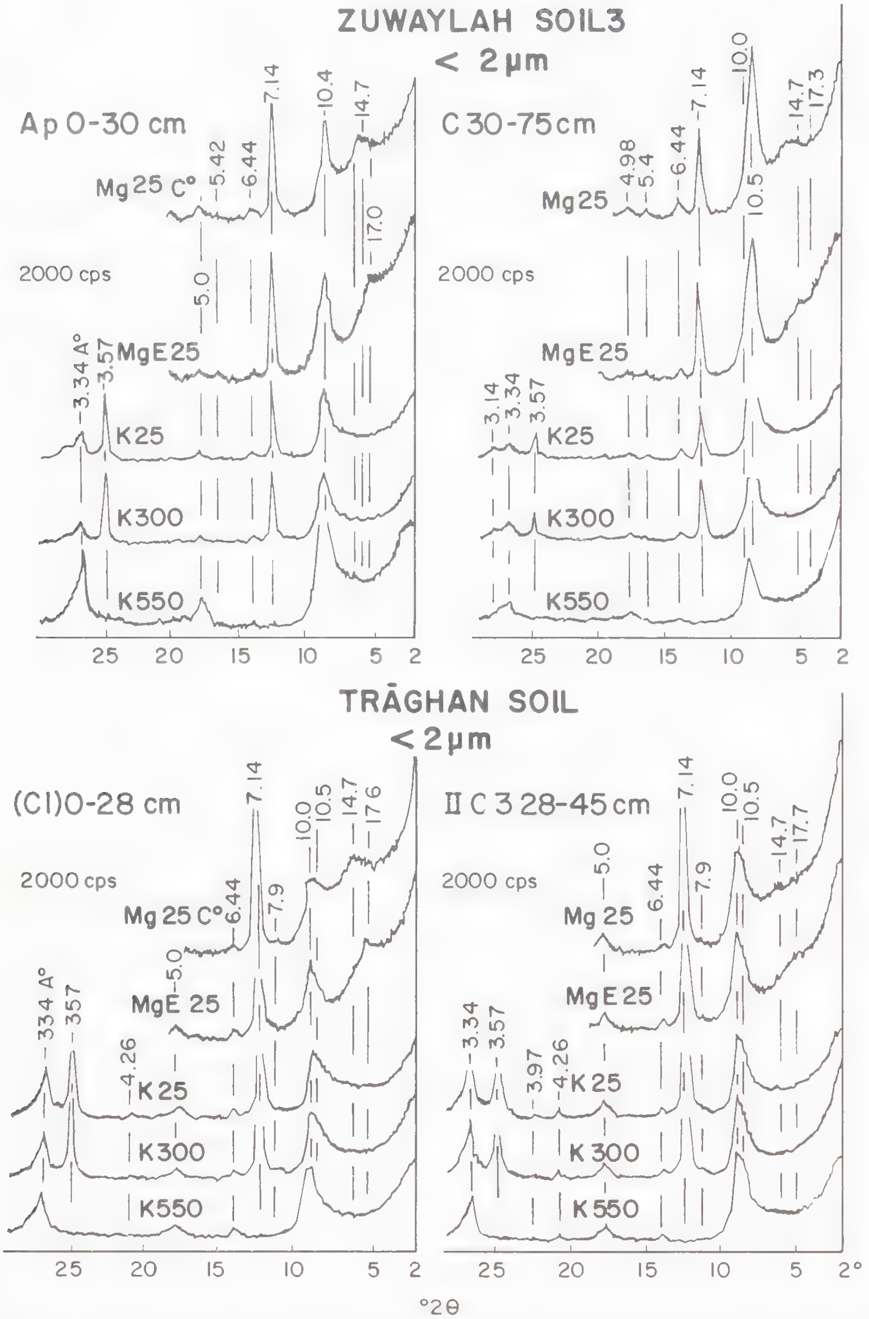

Fig. 3. X-ray diffractograms of the <2 μm clay fractions of Zuwaylah soils (top two) and Trāghan soils (bottom).

lowed by mica, smectite, palygorskite, mica/kaolinite interstratified and gibbsite. Palygorskite occurs in the alluvial soils of the third climatic era. The kaolinite is a product of weathering of micas and feldspars of the Acacus Sandstone. It is interpreted as having formed from the *in situ* alteration of micas and feldspars, on the grounds that it is coarsely crystalline, and unlikely therefore to have been able to withstand transport. Similar findings were reported by Millot (1970), for the weathering of the Cambro-Ordovician sandstone in the area of Hassi Messoud and Hassi El Gassi in Algeria.

The other minerals in the area of the study are muscovite, as determined by its 060 spacings, and or-

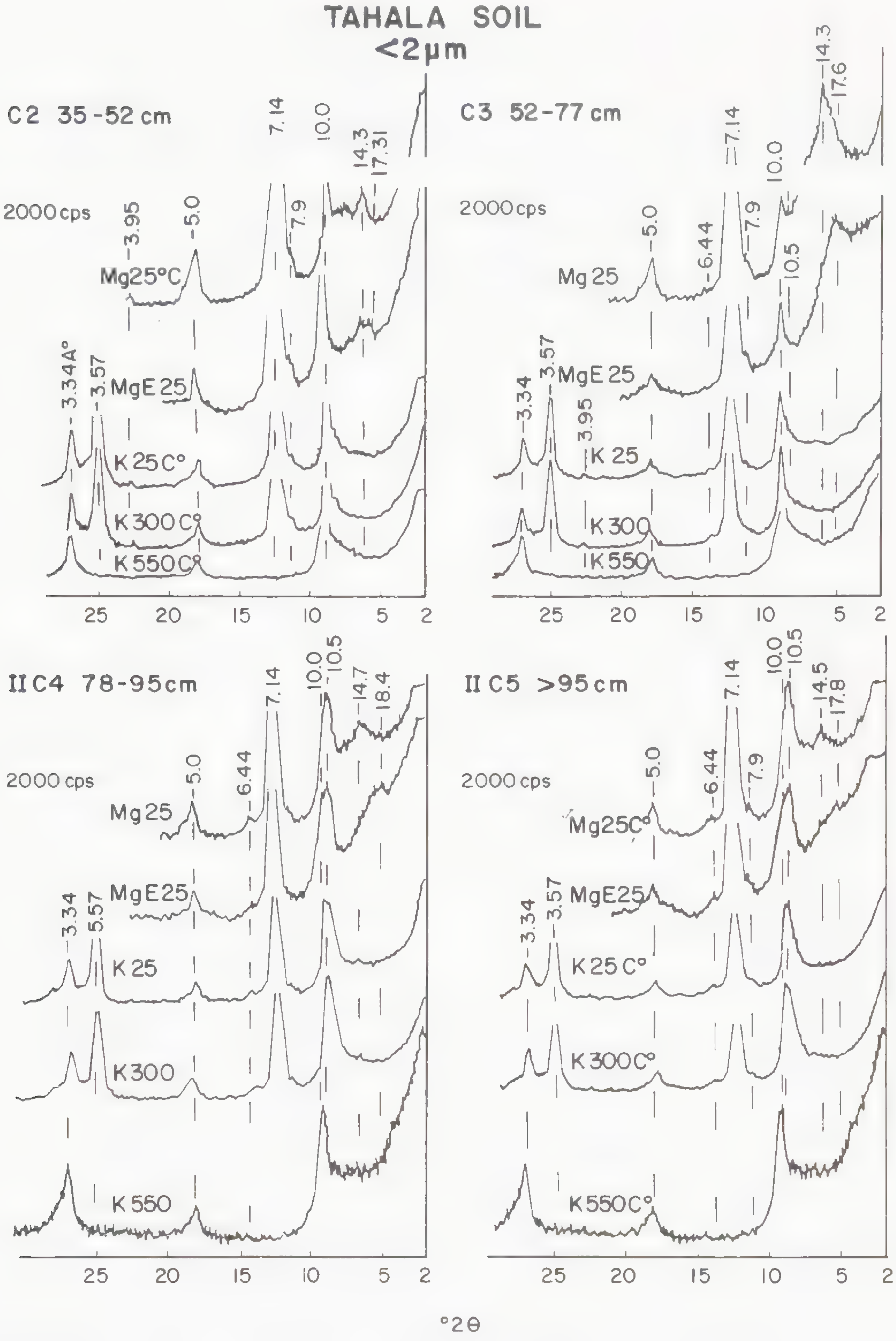

Fig. 4. X-ray diffractograms of the <2 µm clay fraction of the Tahala soil.

thoclase. The kaolinite in this case is mostly formed from weathering of feldspars, since it is abundant in the parent material and in the silt fraction of the soils studied. Kaolinite content is highest in Al ‘Awaynāt 3 and less in Al ‘Awaynāt 1, indicating the palaeoclimatic effect of weathering of Acacus Sandstone upon the B21b. Gibbsite occurs only in the IIB22b, IIA1b and IIB2b of Al ‘Awaynāt 2 and 3

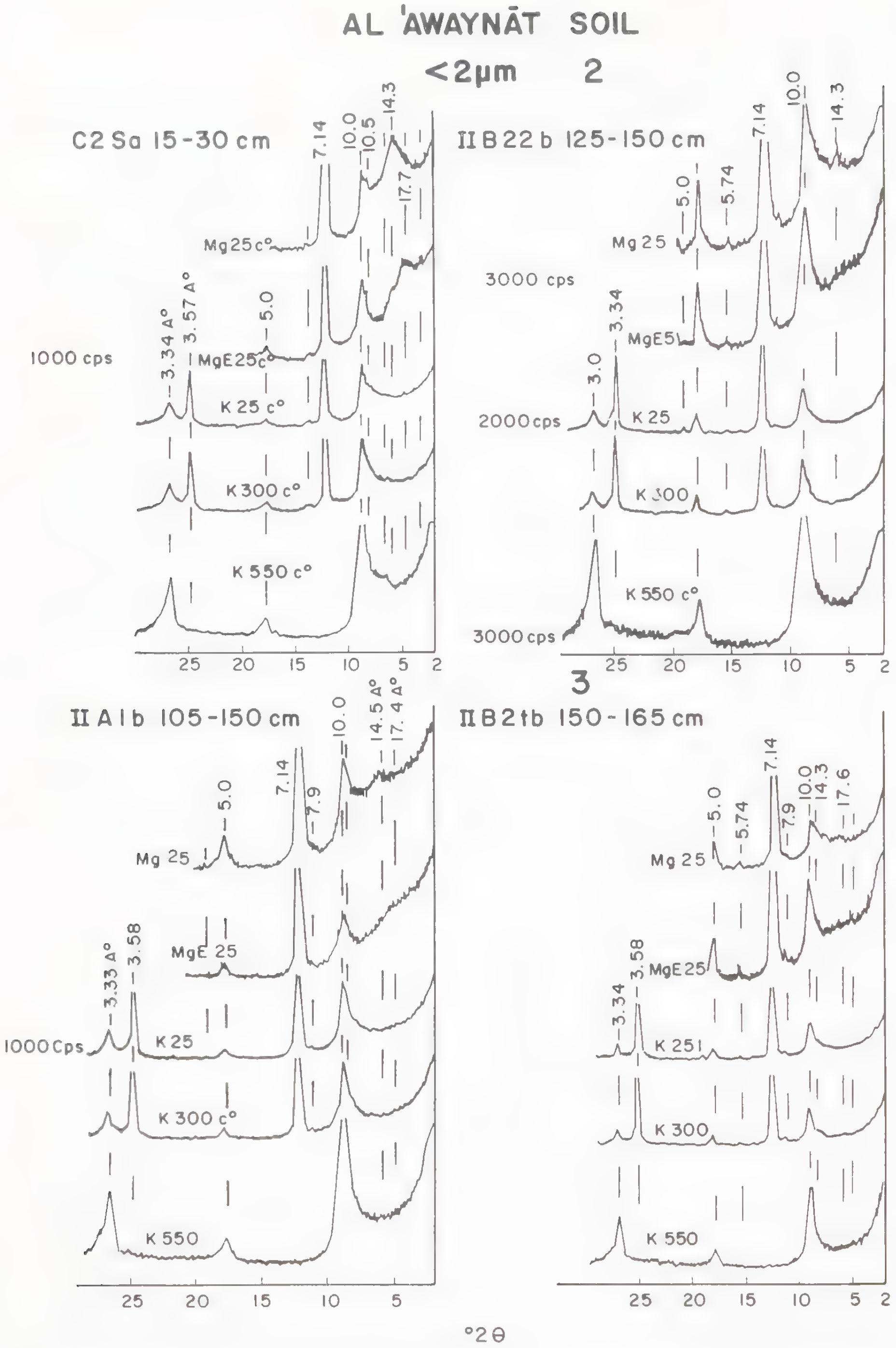

Fig. 5. X-ray diffractograms of the <2 μm clay fraction of Al 'Awaynāt soil 2 (top), and Al 'Awaynāt soil 3 (bottom).

(Figs 5, 6, 10). Gibbsite is confirmed by its DTA endotherm peak at 308°C (Fig. 6). It is worthy of note that the gibbsite IR study absorbence pattern is different to that of gibbsites reported in the literature (Ahlrichs *et al.*, 1986). It shows a strong absorbence band only at 3490 cm^{-1} suggesting that there might be gibbsite with a considerable magnesium substitution.

Table 5. Mineralogical composition of the <2 μm fraction of the soils studied

Soil Series	Horizon	Ka (%)	Sm (%)	Pa (%)	Mi (%)	Ver (%)	Chl (%)	Other minerals
Trāghan	C_1	58	7	12	20	–	–	
	IIC_2	53	2	14	23	–	–	Mica/kaolinite interstratified
	$IIIC_3$	48	–	15	35	–	–	Quartz
Umm al Arānib	C_{1sa}	44	3	4	39	–	–	
	C_{2sa}	48	4	6	30	–	–	
	C_{3sa}	49	10	8	30	–	–	Interstratified
	C_3	58	18	8	12	–	–	Mica/kaolinite
Zuwaylah 2	C_{1p}	15	5	36	26	–	3	Mica/vermiculite interstratified
	C_2	15	2	40	44	–	2	Mica/vermiculite interstratified
Zuwaylah 3	A_p	40	4	30	20	–	3	Quartz
	C	34	2	40	18	–	1	Mica/smectite interstratified
Zuwaylah 1	C_1	27	6	30	30	–	–	Degraded
	IICR	–	–	–	–	–	–	Chlorite
Tahala	C_1	70	1	4	10	10	–	Chlorite
	C_2	75	2	2	14	4	–	Mica/kaolinite interstratified
	C_3	67	2	15	12	2	0	
	IIC_4	60	4	20	8	–	–	
	IICr	50	2	28	12	–	–	
Al ʻAwaynāt 3	C_1	60	12	4	20	–	–	Mica interstratified
	C_2	50	8	10	25	–	–	Kaolinite
	IIA_{1b}	75	5	–	16	–	–	
	IIB_{2tb}	80	4	–	8	–	–	
Al ʻAwaynāt 2	C_{1Sa}	40	11.7	9	30	2.3	–	Mica/kaolinite interstratified and gibbsite
	C_{2Sa}	56	4.2	12	20	–	–	Mica/kaolinite interstratified and gibbsite
	C_3	54	3.1	14	25	–	–	Mica/kaolinite interstratified and gibbsite
	C_4	54	3.1	6	30	–	–	
	IIB_{21b}	60	4.2	–	20	–	–	
	IIB_{22b}	60	3.1	–	18	–	–	
Al ʻAwaynāt 1	C_{1sa}	60	10	3	18	–	–	Degraded chlorite
	C_{2sa}	55	7	8	16	–	–	Mica/kaolinite interstratified
	IIC_3	55	6	3	20	–	–	Mica/vermiculite interstratified
	IIC_4	60	4	4	18	–	–	

Minerals: Ka = kaolinite, Sm = smectite, Pa = palygorskite, Mi = mica, Ver = vermiculite, Chl = chlorite.

DISCUSSION

Study of field relationships, morphology, and chemical and mineralogical properties, provide considerable evidence that previous humid episodes led to the formation of a number of different soil types in the soils of the Fazzān region. These episodes led to the formation of horizons IIB21b and IIB2tb in Al ʻAwaynāt area, and alluvial soils (terraces and flood plains) in the area of Tahala and Trāghan, Zuwaylah and Umm al Arānib. The last and present dry periods led to the formation of salic and gypsic horizons. The morphological, pedological, chemical and mineralogical properties observed agree with the conclusions of Rognon and Kubiena (1976), that relict soils of the central Sahara were formed during humid periods.

Although it is at present impossible to give a general chronology of climatic changes for the Sahara, given the considerable regional variations which occurred, more humid climatic phases are thought to have existed in southern Libya from 40 000 to 20 000 B.P., from 12 000 to 9000 B.P., and from 7000 to 5000 B.P. (Klitzsch and Pesce, 1966; Rognon and Kubiena, 1976; Pallas, 1978; W.S. Kloss, pers. comm., 1982).

These humid palaeoclimate episodes led to the formation of several soil mineralogical suites such as (1) kaolinite, mica, smectite; (2) kaolinite, mica,

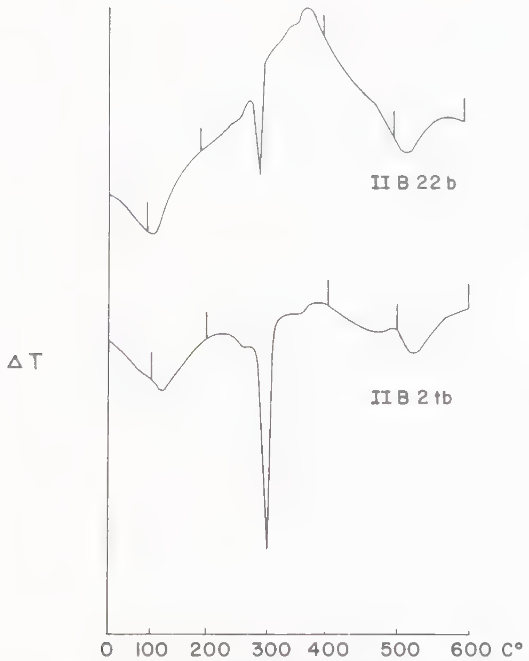

Fig. 6. Differential thermal analysis of the <2 μm of IIB22b horizon of Al 'Awaynāt 2 and IIB2tb of Al 'Awaynāt 3.

gibbsite; (3) kaolinite, mica, smectite, vermiculite; (4) kaolinite, mica, smectite, palygorskite (Figs 7, 8).

Kaolinite is mainly a product of weathering of feldspar and micas. The coarse habit of the kaolinite crystals, as shown by TEM micrographs and X-ray diffraction patterns, suggest that they are *in situ* since it is most unlikely that the kaolinite would have been able to withstand much transport.

Gibbsite occurs only in the IIB21b, IIB22b and IIA1b, IIB2tb of Al 'Awaynāt 2 and 3. Its preservation for such a long period of time in the Saharan soils is surprising. The gibbsite is thought to be mainly a product of weathering of feldspars, since the silt fraction of these soils shows mainly kaolinite and gibbsite with preservation of crystal structure of orthoclase. TEM micrographs of the clay fraction of the B2tb horizon (Fig. 10b) show particle shapes indicating gibbsite and kaolinite as dominant clay minerals.

The other important suite of minerals is the kaolinite/mica interstratification in horizons IIB2tb and IIB22b (Fig. 5). These interstratifications show 7.9 and 3.45 Å, and in most cases occur as a plateau between 7.2 and 10 Å (Fig. 5). The K-saturated clay heated to 550°C, and samples subjected to selective dissolution of kaolinite, gave a diffractogram which did not exhibit this plateau of reflections. These findings substantiate the presence of irregular interstratification of kaolinite with non-expandable 2:1 layer silicates, which in this case are micas. The presence of kaolinite/mica interstratified in soils of Al 'Awaynāt could be due to one or other of three processes: (1) incomplete weathering of micas to kaolinite; Lee *et al.* (1978) and Lim and Jackson (1980) observed, by ultra-microtomy, micaceous occlusions in kaolinite, and attributed this to the stripping of one silicate sheet due to acidic environment during a palaeoclimate, leaving a mixed structure of 1:1 with some occlusions of 2:1 layer silicates; (2) an alternative mechanism is illitization of kaolinite; a phenomenon observed by Millot (1970) in studies of Cambro-Ordovician sandstone in Algeria. This process is doubtful in the present case due to the presence of kaolinite traces in the sandstone of the area; (3) the third possible mechanism is incomplete transformation of feldspar–mica–kaolinite, as proposed by Lim and Jackson (1980).

One of the most striking phenomena of these soils is the high concentration of magnesium in their soil extract. The magnesium most probably comes from weathering of the Tanezzuft Shale, which has a high dolomite content (W.S. Kloss, pers. comm., 1982). During the humid periods dolomite was weathered and/or dissolved by acid water, which migrated to lower lying areas.

The pH of the ground water in such areas is around 6, and in certain cases as low as 5. The products of weathering of the Tanezzuft Shale and other

Table 6. Selected chemical composition of soil water extract of 1:1 soil water ratios of the soils having appreciable amounts of palygorskite

Soil Series	Horizon	pH	Mg (meq/l)	SiO_2 (ppm)	Al (ppm)	Fe (ppm)
Trāghan	IIC_2	8.9	40	25	0.25	<0.1
	IIC_3	7.8	76	52	0.1	–
Zuwaylah 1	C	8.0	70	25	–	–
Zuwaylah 2	C_{1p}	8.1	50	24	–	–
	C_2	8.0	77	27	–	–
Zuwaylah 3	C	7.7	110	55	0.16	<0.1
Tahala	C_3	6.5	164	98	–	–
	IIC_4	7.1	180	45	0.14	–
	IIC_r	7.2	224	40	0.14	–
Al 'Awaynāt 1	C_{2Sa}	7.6	290	50	0.14	–

– = not detected.

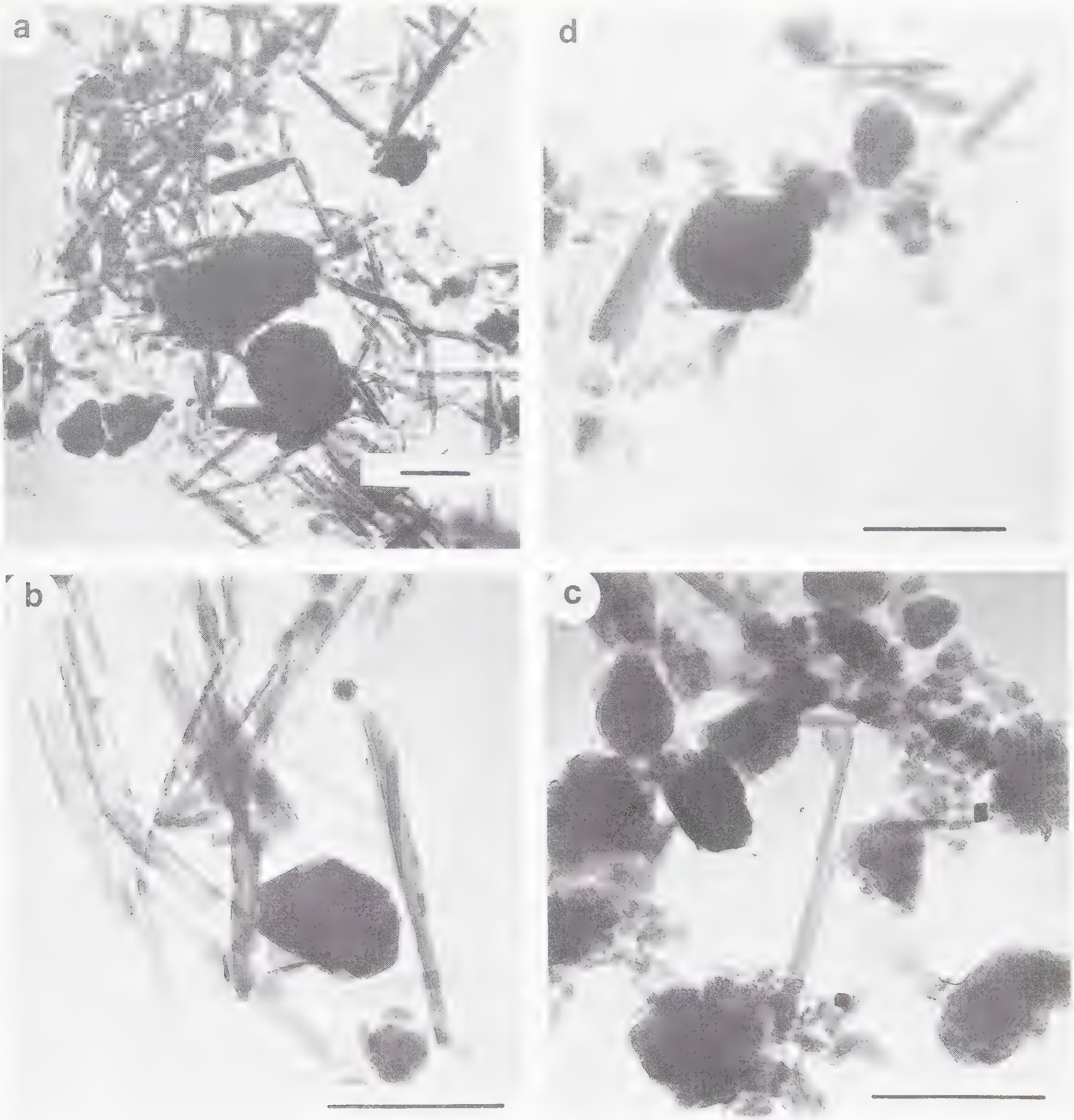

Fig. 7. Transmission electron micrographs of the <2 μm clay fraction of Ap and C horizons of Zuwaylah soil (a, b); C2Sa horizon of Umm al Arānib soil (c); and clay fraction of B21 horizon from Rhodozeralf soils of northern Libya (d). Dark bars represent 0.5 μm.

formations had an important effect on development of other soil minerals such as palygorskite.

Although palygorskite is present in all the soils of Trāghan, Zuwaylah, Umm al Arānib, Tahala, and in Al 'Awaynāt 1 (Fig. 9), it is totally absent in the geological formations which make up the sub-strata (W.S. Kloss, pers. comm., 1982). As a consequence, it is proposed that the existence of pedogenic palygorskite in the Fazzān area of Libya is due to the following reasons: Tables 3 and 6 show pH and the concentrations of soluble silica, aluminium, iron and magnesium (Table 6) in the soil extract and 1 : 1 soil water ratios. The fact that the positions of the soil water extract and the saturation extract component lie within the stability field for palygorskite and solution composition (Singer and Norrish, 1974), and for palygorskite and smectite stability (Elprince, *et al.*, 1979), is one line of evidence for pedogenic palygorskite. This data also shows that all the soils are alkaline in reaction; magnesium concentrations

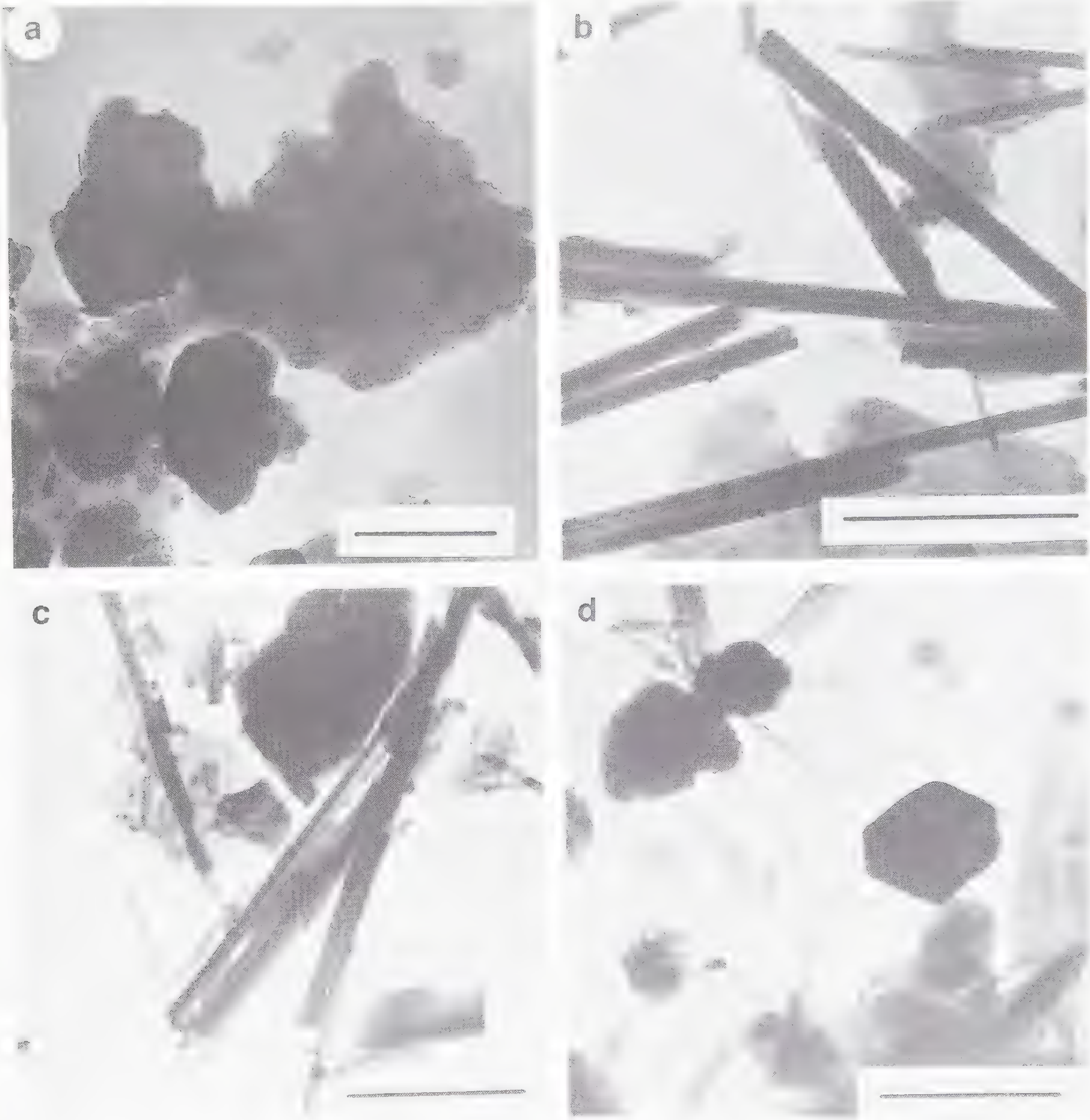

Fig. 8. Transmission electron micrographs of the <2 μm clay fraction of horizons C2 (a), C3 (b), IIC4 (c), and IICR (d) of Tahala soils. Dark bars represent 0.5 μm.

range from 40 to 264 meq/litre; soluble silica ranges from 24 to 89 ppm.

The silica content of soil solution of most soils studied is higher than the average Si content of soil solution which is reported to be 15–20 ppm (Wilding *et al.*, 1977). Aluminium is low as well as iron. This is in accordance with the slightly calcareous nature of the soils which tend to maintain a very low aluminium and iron concentration, but a relatively high magnesium level.

Not only lake water, but soil water with suitable composition, can satisfy the conditions necessary for formation of palygorskite. Waters containing high magnesium concentrations from weathering of Tanezzuft Shale drain into the depositional basins of Zuwaylah, Tahala and Al 'Awaynāt flood plain, where evaporation exceeds precipitation. This causes concentration of ions up to values which allow the precipitation of palygorskite.

Further evidence is found in the association of

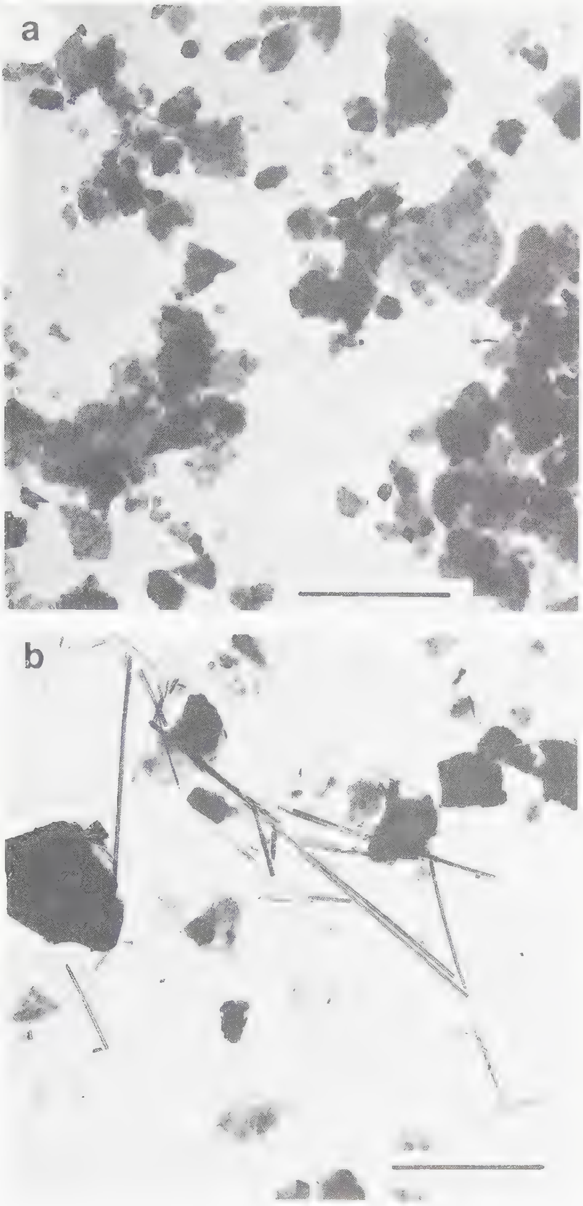

Fig. 9. Transmission electron micrographs of the <2 μm clay fraction of Tahala soils, C2 (a) and IIC4 (b) showing palygorskite concentrated at the lithologic discontinuity. Dark bars represent 0.5 μm.

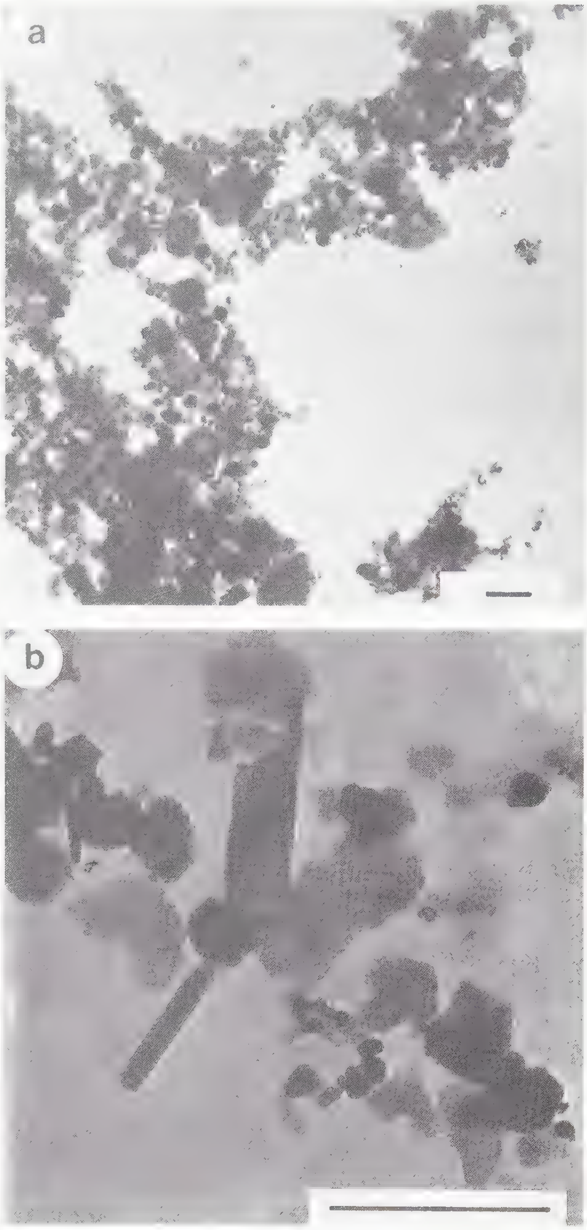

Fig. 10. Transmission electron micrographs of the <2 μm clay fraction of IIB21b (a) and IIB2tb (b) horizons of Al 'Awaynāt 2 and 3 showing a crystal of gibbsite appearing to be hexagonal in shape at the bottom. Dark bars represent 0.5 μm.

pedogenic gypsum with soils containing palygorskite (Tables 2 and 4), as seen in Zuwaylah and Tahala soils, and Al 'Awaynāt 1. Formation of the gypsum enhances the concentration of magnesium, and in consequence, facilitates the precipitation of palygorskite. Similar findings are recorded by Hassouba and Shaw (1980). It should also be noted that the occurrence of the quantitative data represented in Table 5 shows that there is a trend in which a decrease in the amount of smectite is accompanied by an increase in palygorskite. The decrease in the montmorillonite component could provide additional magnesium, which in turn would enhance palygorskite neoformation.

In conclusion, it is proposed that the palaeoclimate conditions had an important effect on the morphological, chemical and mineralogical properties of soils of the Fazzān region of Libya (Fig. 1). Several climatic episodes led to the formation of several mineralogical suites. Pedogenic formation of palygorskite seems to have occurred in some of the soils of the region as a result of dolomite weathering, gypsum crystallization, and lithologic discontinuity.

ACKNOWLEDGEMENTS

The authors would like to thank Dr. Werner Smykatz-Kloss for help provided during the field work; and Mr. A. Raba for his help with the morphology and classification of soils. Special thanks are due to Professor J.B. Dixon, Department of Soil and Crop Science, Texas A&M University, U.S.A. for reading the manuscript, and for his valuable comments.

REFERENCES

ABUDELGAWAD, G.M., PAGE, A.L. and LUND, L.J. (1974). Chemical and mineralogical properties of Kufra Sahara soils. *Libyan J. Agric.*, **3**, 1–6.

ABTAHI, ALI, (1977). Effect of a saline and alkaline ground water on soil genesis in semi-arid southern Iran. *Soil Sci. Soc. Am. J.*, **41**, 583–588.

ABTAHI, ALI (1980). Soil Genesis as affected by topography and time in highly calcareous parent materials under semi-arid conditions in Iran. *Soil Sci. Soc. Am. J.*, **44**, 329–336.

AHLRICHS, J.L., ABUDELGAWAD, G.M. and DIXON, J.B. (1986). A rapid glass slide technique for survey of clays containing kaolinite and gibbsite. (In review).

ALEXIADES, C.A. and JACKSON, M.L. (1965). Quantitative determination of vermiculite in soils. *Soil Sci. Soc. Am. Proc.*, **29**, 522–527.

ALLISON, L.E. (1965). Total carbon. *In*: Methods of soil analysis (*ed.* C.A. Black) Pt. 2. *Am. Soc. Agron.*, Madison, Wisc., 1367–1378.

AL-RAWI, G.J. and SYS, C. (1967). A comparative study between Euphrates and Tigris sediments in the Mesopotamian Flood Plain. *Pedology*, **17**, 187–211.

ATKINSON, K. and WAUGH, B. (1979). Morphology and mineralogy of Red Desert Soils in the Libyan Sahara (*Int. Geogr. Mag.*), 1–10.

BARSHAD, I. (1962). Soil development. *In: The Chemistry of the Soil* (*ed.* F.E. Bear). Reinhold, N.Y. 2nd ed., 1–52.

BATES, T.F. (1960). Rock weathering and clay formation in Hawaii. *Mineral Industries*, **29**, 1–6. Coll. Mineral Ind., Penn. State Univ.

BEAUDET, G.A. (1976). Former Formations, Superficielles et Variation Climatiques récentes du Sahara Occidentale. *Rev. Géogr. Phy. Géol. Dyn.*, **18**, 157–173.

BERNAS, B.L. (1968). A new method, for decomposition and comprehensive analysis of silicates by atomic absorption spectrometry. *Analyt. Chem.*, **40**, 1682–1688.

BIGHAM, J.M., JAYNES, W.F. and ALLEN, B.L. (1980). Pedogenic degradation of Sepiolite and Palygorskite on the Texas High Plains. *Soil Sci. Soc. Am. J.*, **44**, 159–167.

BLACK, C.A. (1965). Methods of soil analysis, Pt. 1. *Am. Soc. Agron.*, Madison, Wisc.

BOLTZ, D.F. and MELLON, M.G. (1947). Determination of phosphorus, germanium, silicon and arsenic by Heterophy Blue method. *Analyt. Chem.*, **19**, 873–877.

BORDET, P.M. (1951). Présence de Laterites Fossiles dans L. Atakor du Hoggar. *C. R. Soc. Géol. Fr.*, **1**, 97–99.

BUOL, S.W. (1965). Present soil-forming factors and processes in arid and semi-arid zones. *Soil Sci.*, **99**, 45–49.

BUROLLET, P.F. and BYRAMJEE, R. (1969). Sedimentological Remarks on Lower Paleozoic Sandstones of South Libya. *In*: Geology, Archaeology and Prehistory of the Southwestern Fezzan, Libya (*ed.* W.K. Kanes). *Petrol. Explor. Soc. Libya*, 11th Annu. Field Conf., 91–101.

COOKE, R.V. and WARREN, A. (1973). *Geomorphology in Deserts*. Univ. Calif. Press, Berkeley, 234 p.

DALAL, R.C. (1972). Colorimetric determination of aluminum in soil extracts using Haematoxylin. *Plant Soil*, **34**, 223–231.

DIXON, J.B. (1977). Kaolinite and serpentine group minerals. *In*: Minerals in Soil Environments (*eds* J.B. Dixon and S.B. Weed). *Soil Sci. Soc. Am.*, Madison, Wisc.

DREGNE, H.E. (1976). *Soils of Arid Regions*. Elsevier, N.Y. 237 p.

DREVER, J.I. and SMITH, C.L. (1978). Cyclic wetting and drying of the soil zone as an influence on the chemistry of ground water in arid terrains. *Am. J. Sci.*, **278**, 1448–1454.

ELGABALY, M.M. and KHADER, M. (1962). Clay mineral studies of some Egyptian Desert and Nile alluvial soils. *J. Soil Sci.*, **13**, 333–342.

ELPRINCE, A.M., MASHHADY, A.S. and ABA-HUSAYN, M.M. (1979). The occurrence of pedogenic palygorskite (Attapulgite) in Saudi Arabia. *Soil Sci.*, **128**, 211–218.

ESWARAN, H. and BARZANJI, A.F. (1974). Evidence for the neoformation of attapulgite in some soils of Iraq. *Trans. 10th Int. Cong. Soil Soc.* (Moscow), **7**, 154–160.

EUGSTER, H.P. and JONES, B.F. (1979). Behavior of major solutes during closed basin brine evolution. *Am. J. Sci.*, **279**, 609–631.

EXLEY, C.S. (1976). Observation on the formation of kaolinite in the St. Austell granite. *Cornwall Clay Miner.*, **11**, 51–63.

FIELDS, M.A. (1966). The nature of allophane in soils. Pt. 1. Significance of structural randomness in pedogenesis. *N. S. J. Soil Sci.*, **9**, 599–607.

GARBUMOV, V.V. (1969). Genesis and transformation of minerals in soils. *Sov. Soil Sci.*, **1**, 201–213.

GEOLOGICAL MAP OF LIBYA (1985). Compiled by Industrial Research Centre, Geologic Research and Min. Department, Tripoli, Libya, 1985.

GOUDARZI, G.H. (1970). Geology and Mineral Resources of Libya. A Reconnaissance. *U.S. Geol. Surv. Prof. Pap.*, **660**.

HASSOUBA, H. and SHAW, H.F. (1980). The occurrence of palygorskite in Quaternary sediments of the Coastal Plain of north-west Egypt. *Clay Minerals*, **15**, 77–83.

HAYASHI, H., OTSUKA, R. and IMAI, N. (1969). Infra-red study of sepiolite and palygorskite on heating. *Am. Mineral*, **53**, 1613–1624.

HELGESON, H.C., GARRELS, R.M. and MACKENZIE, F.T. (1969). Evolution of irreversible reactions in geochemical process involving minerals and aqueous solution — II. *Geochim. Cosmochim. Acta*, **33**, 455–481.

JACKSON, M.L. (1959). Frequency distribution of clay minerals in major great soil groups as related to the factors of soil formation. *Clays Clay Miner.*, **6**, 133–143.

JACKSON, M.L. (1969). *Soil Chemical Analysis — Advanced Course*. 2nd ed., 9th printing. Published by the author. Madison, Wisc., 53705.

JOHN, W.D., GRIM, R.E. and BRADLEY, W.F. (1954). Quantitative estimations of clay minerals by diffraction methods. *J. Sediment. Petrology*, **24**, 242–251.

KLITZSCH, E. (1966a). Geology of the northeast flank of the Murzuk Basin. *In*: South Central Libya and Northern Chad (*ed.* J.J. Williams). *Petrol. Explor. Soc. Libya*, 8th Annu. Field Conf., 19–32.

KLITZSCH, E. (1966b). Comments on the geology of the central parts of Southern Libya and Northern Chad. *In*: South Central Libya and Northern Chad (*ed.* J.J. Williams). *Petrol. Explor. Soc. Libya*, 8th Annu. Field Conf., 1–17.

KLITZSCH, E. (1969). Stratigraphic section from the areas of Silurian and Devonian strata at western Murzuk Basin (Libya). *In: Archaeology and Geology of Fezzan*. Published by Netherland Publishing Co., 250 p.

KLITZSCH, E. and PESCE, A. (1966). Remarks about pre-historical sites in southern Libya and Tibesti. *In*: South Central Libya and Northern Chad (*ed.* J.J. Williams). *Petrol. Explor. Soc. Libya*, 8th Annu. Field Conf., 69–74.

KOVDA, V.A. (1973). Origin of Saline Soils and their Regime. Program for scientific translation, Jerusalem.

KUBIENA, W.L. (1955). Uber die Braunlehm Relikte der Atakor. *Erdkunde*, **9**, 115–132.

KUBIENA, W.L. (1963). Paleosoils as indicator of paleoclimates. *In: Arid Zone Research Symp. XX-Changes of Climate*. UNESCO, 207–209.

LAGALY, A. and WEISS, A. (1969). Determination of the layer charge in mica type. *Proc. Int. Clay Conf. Tokyo*. **1**, 61–80.

LEE, S.Y., JACKSON, M.L. and BROWN, J.L. (1978). Micaceous occlusion electron microscopy. *Clays Clay Miner.*, **28**, 125–129.

LESSAR, L. (1961). Les séries primaires du Tassili Ouan A. Haggar au sud du Haggar Emyre l'Air et l'Adrar des Horhas (Sahara Méridional). *Bull. Soc. Géol. Fr.*, Sér. III, **5**, 501 p.

LIM, C.H. and JACKSON, M.L. (1980). Polycomponent interstratified phyllo silicates in dolomite residuum and sandy till of central Wisconsin. *Soil Sci. Soc. Am. J.*, **44**, 868–872.

LODDING, W. (1972). Conditions for the direct formation of gibbsite from K-feldspar. Discussion. *Am. Mineral.*, **57**, 292–294.

MCCALEB, S.B. (1959). The genesis of red-yellow podzolic soils. *Soil Sci. Soc. Am. Proc.*, **23**, 164–168.

MCNEAL, S.A., ALLEN, B.L. and CRAIG, J.R. (1972). The occurrence of sepiolite and attapulgite on Southern High Plain. *Clays Clay Miner.*, **20**, 143–149.

MILLOT, A. (1970). *Geology of Clays*. Springer-Verlag, New York, N.Y., 429 p.

NATHAN, Y. (1970). An improved X-ray method for detecting small quantities of palygorskite in clay mineral mixtures. *Clays Clay Miner.*, **18**, 363–365.

PALLAS, P. (1978). *Water resources of the Socialist People's Libyan Arab Jamahirya.* Bull. Secretariat Dams Wat. Resour., Tripoli, 80 p.

PARHAM, W.E. (1969). Formation of halloysite from feldspar. Low temperature, artificial weathering versus natural weathering. *Clays Clay Miner.*, **17**, 13–22.

REGWA (1972, 1973, 1974). Hydrogeological, geochemical studies on Wadi Ajal, Wadi Elshatti, and Tragen for agricultural development. Unpublished Rep. Agric. Dev. Council, Tripoli.

RICHARDS, L.A. (ed.) (1954). Diagnosis and improvement of saline and alkali soils. *U.S. Dep. Agric.*, *Agric. Handbook.*, No. 60.

ROGNON, P. and KUBIENA, D. (1976). Oscillations Climatiques au Sahara depuis 40,000 ans. *Rev. Géogr. Phys. Géol. Dyn.*, **18**, 147–282.

SAND, L.B. (1956). On the genesis of residual kaolins. *Am. Mineral.*, **41**, 28–40.

SCAFES, D.W. and KUNZE, A.W. (1971). A clay mineral investigation of six cores from the Gulf of Mexico. *Mar. Geol.*, **10**, 69–85.

SINGER, A. and NORRISH, K. (1974). Pedogenic palygorskite occurrence. *In: Soil Sci. Australia Am. Miner.*, **59**, 508–517.

SOIL TAXONOMY (1975). Soil survey staff 1975. Soil taxonomy — a basic system of soil classification for making and interpreting soil surveys. *U.S. Dep. Agric.*, *Agric. Handb.*, No. 436.

TARDY, Y. (1971). Characterization of the principal weathering types by the geochemistry of waters from some European and African crystalline massifs. *Chem. Geol.*, **7**, 253–271.

UEHARA, A., IKAWA, H. and SHERMAN, A.D. (1966). Desilication of halloysite and its relation to gibbsite formation. *Pacific Sci.*, **20**, 119–124.

VANDEN HEUVEL, R.C. (1966). The occurrence of sepiolite and attapulgite in the calcareous zone of a soil near Las Cruces, New Mexico. *Clays Clay Miner.*, **13**, 193–207.

VITTIMBERG, A.P. and CARDELLO, R. (1963). Sédimentologie et pétrographie du paléozoïque du Bassin de Kufra 1st Saharan Symposium of Tripoli. *Rev. Inst. Fr. Pétrole*, **18**, 1546–1557.

WALLAST, T.R. (1967). Formation of Red beds in modern and ancient deserts. *Geol. Soc. Am.*, **78**, 353–368.

WALLAST, R.E., MACKENZIE, E.T. and BRICKER, O.P. (1968). Experimental precipitation and genesis of sepiolite at earth surface conditions. *Am. Mineral.*, **53**, 1645–1662.

WILDING, L.P., SMECK, N.E. and DREES, L.R. (1977). Silica in soils. *In*: Minerals in Soil Environments (*eds* J.B. Dixon and S.B. Weed). *Soil Sci. Soc.*, Madison, Wisc., 471–552.

WILLIAMS, D.E. (1948). A rapid manometric method for the determination of carbonate soils. *Soil Sci. Soc. Am. Proc.*, **13**, 127–129.

YAALON, D.H. and WIEDER, M. (1973). Pedogenic palygorskite in some arid brown (calciorthid) soils. *Clay Mineralogy*, **11**, 73–79.

Cyclic Transgressive and Regressive Sequences and their Association with Hydrocarbons — Ghānī Field, Sirt Basin, Libya

SULAIMAN A. ABUSHAGUR [1]

الدورات التجاوزية والانحسارية وعلاقتها بالنفط – حقل الغني، حوض سرت، ليبيا

س . أ . أبو شاقور

الخلاصــــة

لقد تم اكتشاف حقل الغني سنة 1978 . ويبلغ الإنتاج اليومي لهذا الحقل 100,000 برميل من ثلاثة مستويات نفطية . بخزان الفرود الذي يعد مكمناً تركيبياً وطبقياً في آن واحد .

هناك سبعة وحدات صخرية — طبقية تمثل دورات تجاوزية وانحسارية متعالية قد تم التعرف عليها في صخور الباليوسين لهذا الحقل وفي الحقول المحيطة . وهذه الوحدات بالترتيب من الأقدم فالأحدث هي : حجر الحقفة الطيني ، حجر ثاليث الجيري ، حجر الرابية الجيري ، والطيني ، حجر الفرود الدولوميتي والجيري والأنهيدريتي (بما في ذلك عضو المبروك) ، حجر الظهرة الطيني ، حجر زلطن الجيري ، وحجر الخير الجيرى . وقد ترسبت هذه الصخور الجيرية والطينية في بحار ضحلة فوق قارية امتدت عبر حوض سرت . ويعد تكوين الفرود (مكافيء الجزء الأعلى من تكوين البيضاء) المنتج الرئيس في حقل الغنى .

ويدل تحليل خزان الفرود على تتابع السحنات الثمانية الآتية : (1) الفتات الحياتي الحزازي (حيوانات طحلبية) ، (2) حجر وحلى ، (3) طحالب داسيكلاداسي ، (4) فتات حياتي ، (5) طحلبي ، (6) هيكلي الكريّات ، (7) حجر دولوميتى ، (8) الأنهيدريت .

وتمثل تجمعات المستحاثات وكذلك الأنواع الصخرية بيئات بحرية ضحلة جداً . وقد قدر عمق المياه الضحلة بحوالي 3 - 9 أمتار ، كما تدل عليه أنواع المستحاثات النباتية والحيوانية . كما أن الظروف المناخية السائدة قد فسرت على أنها ظروف استوائية إلى شبه استوائية . وقد دلت النسبة الكبيرة للوحل الجيري على أن نشاط الأمواج كان محدوداً إلى متوسط (طاقة منخفضة) . ولكن وجود قطع لمستحاثات كبيرة في مواقع من السحنات يدل على وجود نشاط متقطع للأمواج (طاقة مرتفعة) أحياناً .

أما صخور المصدر في حقل الغنى فقد استحدث من حجر طيني تجاوزي غني بالمواد العضوية . وتوصف المسامية بأنها من أنواع القوالب والشبكية والبينحبيبية . أما النفاذية فقد نشأت جزئياً بعمليات التدلمت والتشقق والإذابة في كلا السحنات الجيرية المتعالية والمؤدية إلى المكامن التركيبية والطبقية الممتازة لحقل الغني النفطي . وقد تجمع النفط في هذه الخزانات تحت سقف من صخور الأنهيدريت الذي ترسب في بيئات بحرية فوق نطاق المد والجزر .

Abstract. The Ghānī Field was discovered by Mobil Oil Libya in 1978. The average daily production of this field is about 100 000 barrels from three producing zones. Al Fūrūd reservoir is a combination of both a structural and stratigraphic trap.

Seven lithostratigraphical units representing two transgressive and regressive prograding cycles are recognized in the Palaeocene of this field and peripheral areas. From older to younger, they are the Hagfa shale; the Thalith limestone; the Rabia limestone and shale; Al Fūrūd dolomite, limestone, and anhydrite (including Al Mabruk Member); Dahra shale; Zelten limestone; and Kheir limestone. These carbonates and shales were deposited in an epeiric sea which extended across the Sirt basin.

Al Fūrūd Formation (equivalent to Upper Beda) is the principal producing zone in the Ghānī Field. Facies analysis of Al Fūrūd reservoir indicated the occurrence of the following sequence of eight facies: (1) bryozoan

---

[1] Department of Geological Sciences, University of Texas at El Paso, El Paso, TX 79968, U.S.A.

bioclastic, (2) mudstone, (3) dasycladacean algae, (4) bioclastic, (5) algal, (6) pelloidal–pelletal skeletal, (7) dolostone and (8) anhydrite.

The faunal assemblages and lithologies apparently reflect a very shallow-water marine environment of deposition. From the environmental parameters of the accompanying flora and fauna, water depth is inferred to be less than 3–9 m. Deposition occurred under tropical to subtropical conditions. The high recorded content of lime mud suggests low to moderate wave action and current activity (low energy). However, the presence of some fossil fragments in portions of the facies may indicate sporadic, vigorous current activity (high energy).

Source rocks of the field are primarily developed in organic-rich, transgressive shales. Moldic, fenestral, and intraparticle porosities are the most common types recognized in the carbonate reservoirs of Al Fūrūd reservoir. Permeability developed in part by such processes as dolomitization, fracturing, and leaching in the two progradational, regressive carbonate facies resulting in the exceptional structural/stratigraphic traps of the Ghānī Field. Hydrocarbons were entrapped in these reservoirs due to the presence of a supratidal, anhydrite cap rock.

INTRODUCTION

The study area is located in the western part of the Sirt basin (Concession 11) about 200 km south of the Libyan coast (Fig. 1). The Ghānī Oil Field is located in the vicinity of lat. 28°57′N and long. 17°27′E on the western shelf of the Sirt basin. The area studied in detail is about 180 km^2. Regional consideration is given to the entire Palaeocene sequence across the basin.

The Sirt basin developed in North Africa in the area between the Tethys Sea and the Saharan shield during the Late Cretaceous. The basin was the site of mixed siliciclastic and carbonate deposition throughout the Tertiary. A series of bioclastic limestones and shales was deposited around the basin rim; in some areas, these can be traced laterally into a continental clastic facies (Selley, 1969). It is in these marginal limestone facies that much of Libya's oil has been found.

Previous investigations of the Palaeocene section were largely limited to local geologic studies. This paper is oriented to both the local and regional depositional history of the Palaeocene suite. The most

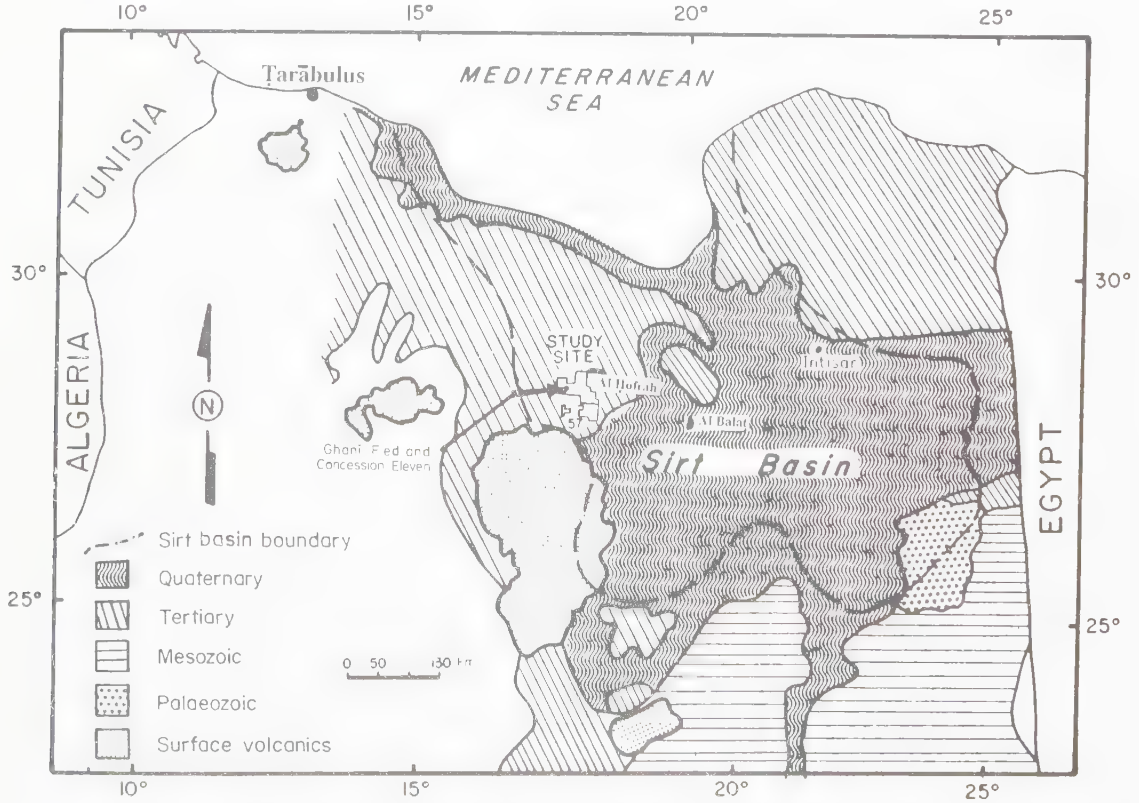

Fig. 1. Generalized geologic map of the Sirt basin (modified after Roberts, 1970; Goudarzi, 1978).

significant Palaeocene studies would include Fraser (1967), Terry and Williams (1969), Conley (1971), Bebout and Pendexter (1975), Brady *et al.* (1980), Abushagur (1983a, b, 1984a, b, 1986), Abuzekri (1984) and Gumati and Kanes (1985).

PALAEOCENE DEPOSITIONAL HISTORY

Palaeocene rocks crop out almost continuously along the SW and W margins of the basin (Fig. 1). Rapid changes in the lateral facies occurred between the platform areas and the deeper parts of the basin. The carbonates, evaporites and shales of the Palaeocene series were deposited in an epicontinental sea which extended across the Sirt basin. This heterogeneous series shows considerable variation in formation thickness which is interpreted as being related to the residual effect of the oil structures rather than renewed tectonic activity (Brady *et al.*, 1980). This is also documented by the isopach map of the Palaeocene in the Ghānī Field which shows a thickening Palaeocene section of about 980 m towards the limbs of the structural closure and a thinner section of about 882 m on the structural highs (Fig. 2).

The Palaeocene section of the Sirt basin was controlled by a segment of transgressions and regressions of an epeiric sea across a deep and persistent shale basin (Terry and Williams, 1969; Abushagur, 1986). Two transgressive and regressive cycles (Fig. 3) during Palaeocene and Eocene time were recognized in the Ghānī Field (Abushagur, 1983b, 1986). These two depositional episodes are traceable and extend throughout much of the basin (Fig. 4).

The first cycle is represented by the deposition of the Hagfa transgressive shale in the western and central parts of the basin during Danian time. This sequence was followed by the deposition of a shallowing upward, regressive carbonate and evaporite sequence (Thalith, Al Fūrūd, and Al Mabruk lithofacies) during Montian time. Farther east, shelf carbonate deposition (Defa and lower Sabil carbonates) took place along the shelf during Danian and Montian times.

The second cycle is represented by a deeper depositional environment during the early Landenian. This is represented by the deposition of a transgressive shale sequence along the western (Dahra shale), central (Khalifa shale), and eastern (Shterat shale) parts of the basin. During the middle and upper Landenian, progressive shallowing of the sequence occurred. During this time, the western and central parts of the basin were dominated by the deposition of calcilutitic limestones and dolomites (Zelten facies) within a restricted shelf, while basinal and near-basinal deposition (marls–limestone) with reef-type carbonates (Intisār A, B, C, D and E) dominated the eastern parts of the basin. During the last stages of the Landenian, the general depositional environment became even more shallow than that represented by the underlying unit along the western part of the basin.

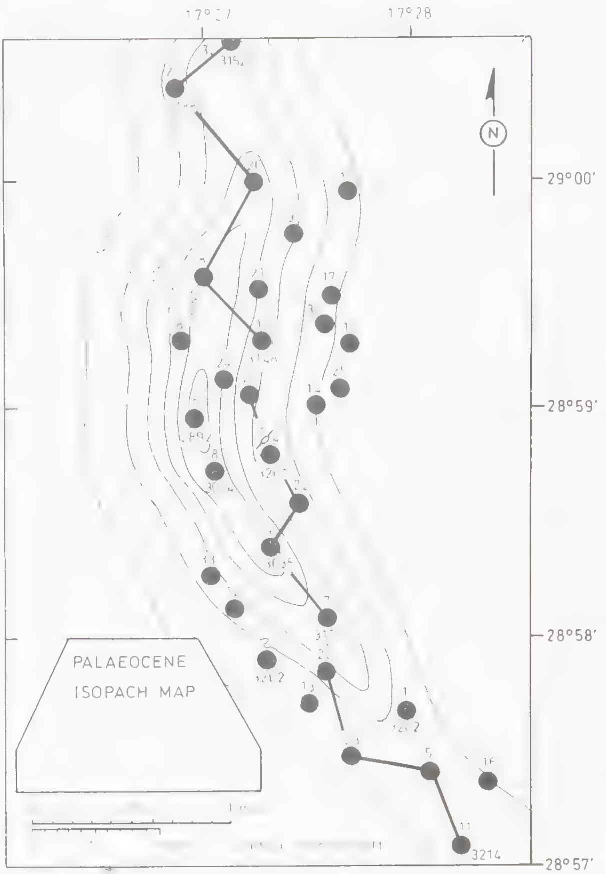

Fig. 2. Palaeocene sequence isopach map, Ghānī Field, Sirt basin; numbers above well symbols represent well numbers (RRR-10 to RRR-29). Depths are in feet.

Alternating cycles of transgression and regression of open marine water continued throughout the Middle and Late Miocene.

DEPOSITIONAL ENVIRONMENT

The interpretation of the depositional environment of the different Al Fūrūd facies recognized in this study is based on a combination of the microfossil content and lithology (Fig. 5). Three cores were recovered from wells RRR-1, RRR-10 and RRR-29.

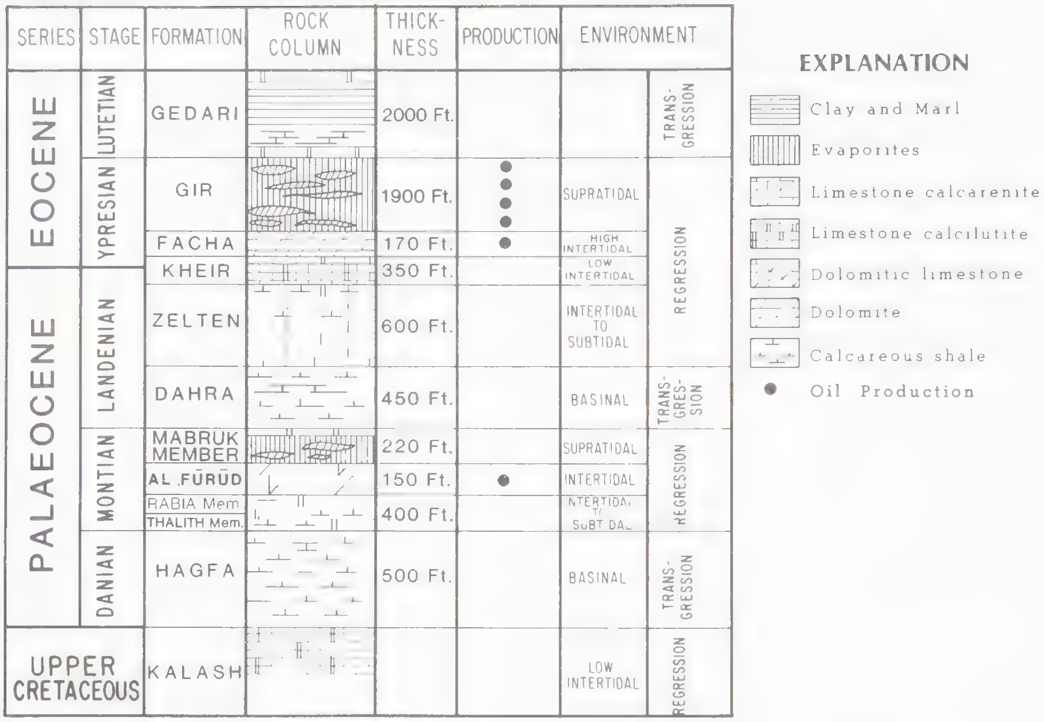
SERIES
STAGE
FORMATION
ROCK COLUMN
THICKNESS
PRODUCTION
ENVIRONMENT
EOCENE
LUTETIAN
YPRESIAN
PALAEOCENE
LANDENIAN
MONTIAN
DANIAN
UPPER CRETACEOUS
GEDARI
GIR
FACHA
KHEIR
ZELTEN
DAHRA
MABRUK MEMBER
AL FŪRŪD
RABIA Mem.
THALITH Mem.
HAGFA
KALASH
2000 Ft.
1900 Ft.
170 Ft.
350 Ft.
600 Ft.
450 Ft.
220 Ft.
150 Ft.
400 Ft.
500 Ft.
SUPRATIDAL
HIGH INTERTIDAL
LOW INTERTIDAL
INTERTIDAL TO SUBTIDAL
BASINAL
SUPRATIDAL
INTERTIDAL
INTERTIDAL TO SUBTIDAL
BASINAL
LOW INTERTIDAL
TRANSGRESSION
REGRESSION
TRANSGRESSION
REGRESSION
TRANSGRESSION
REGRESSION
EXPLANATION
Clay and Marl
Evaporites
Limestone calcarenite
Limestone calcilutite
Dolomitic limestone
Dolomite
Calcareous shale
Oil Production

Fig. 3. Generalized stratigraphic column of the Palaeocene section in the Ghānī Field showing the depositional environment, production, and thicknesses.

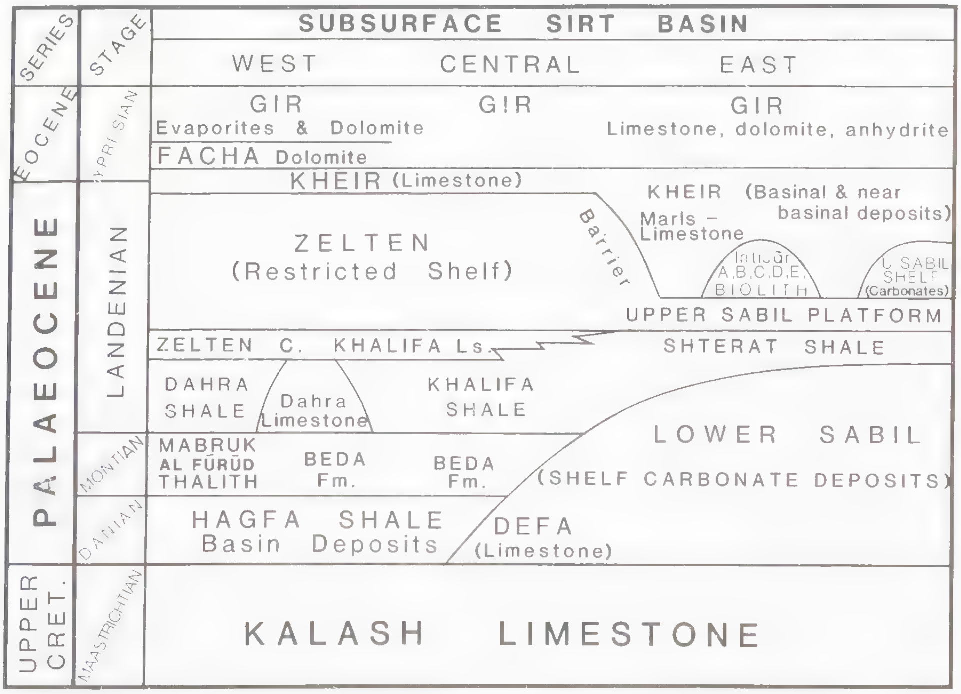
SERIES
STAGE
SUBSURFACE SIRT BASIN
WEST
CENTRAL
EAST
EOCENE
YPRESIAN
PALAEOCENE
LANDENIAN
MONTIAN
DANIAN
UPPER CRET.
MAASTRICHTIAN
GIR
Evaporites & Dolomite
GIR
GIR
Limestone, dolomite, anhydrite
FACHA Dolomite
KHEIR (Limestone)
KHEIR (Basinal & near basinal deposits)
Marls – Limestone
Barrier
ZELTEN (Restricted Shelf)
Intisar A,B,C,D,E, BIOLITH
U. SABIL SHELF (Carbonates)
UPPER SABIL PLATFORM
ZELTEN C. KHALIFA Ls.
SHTERAT SHALE
DAHRA SHALE
Dahra Limestone
KHALIFA SHALE
LOWER SABIL
(SHELF CARBONATE DEPOSITS)
MABRUK
AL FŪRŪD
THALITH
BEDA Fm.
BEDA Fm.
HAGFA SHALE Basin Deposits
DEFA (Limestone)
KALASH LIMESTONE

Fig. 4. Generalized stratigraphic chart of the Palaeocene in the Sirt basin (modified after Barr and Weegar, 1972; and Brady *et al.*, 1980).

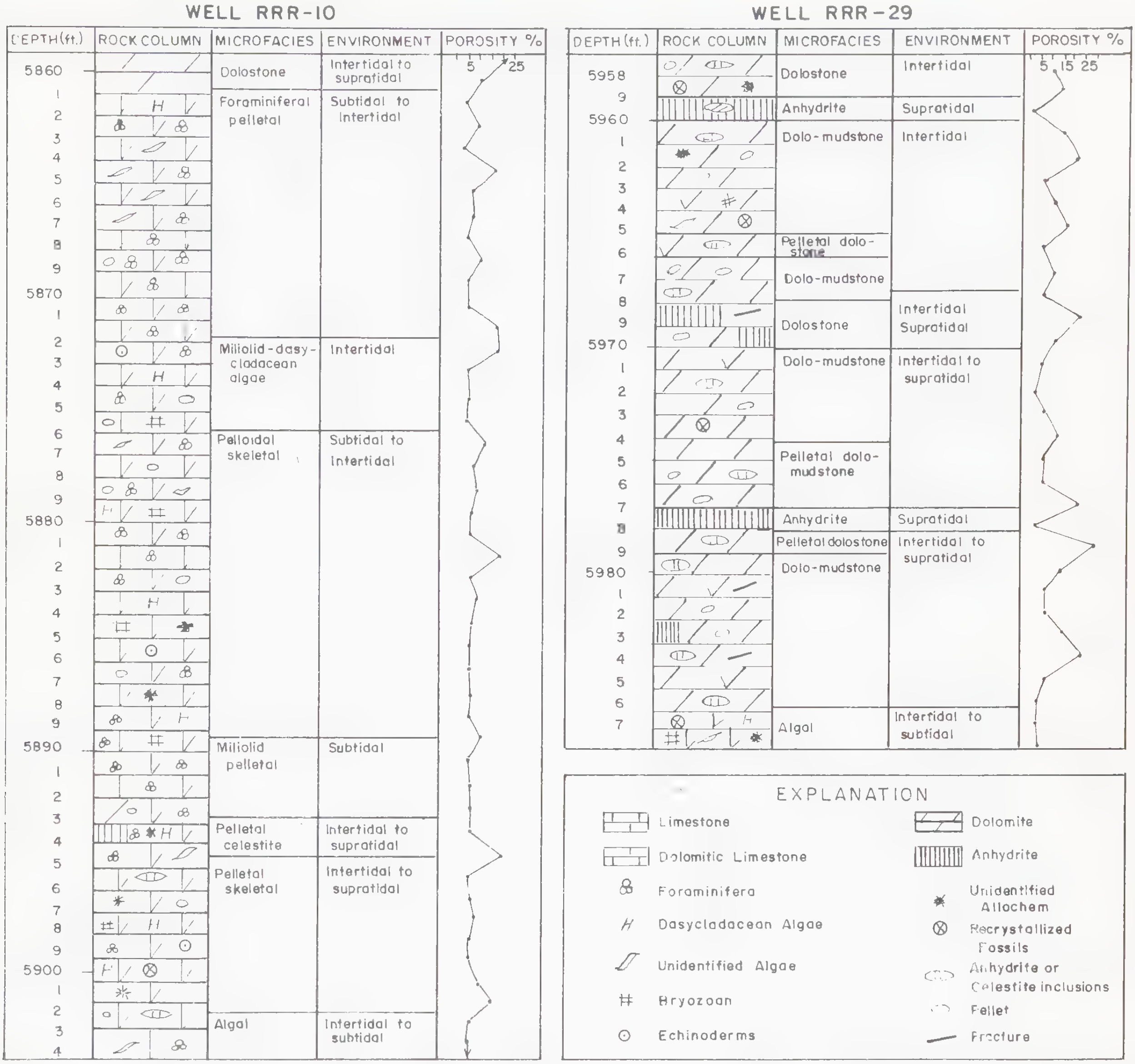
WELL RRR-10
DEPTH(ft.)
ROCK COLUMN
MICROFACIES
ENVIRONMENT
POROSITY %
Dolostone
Intertidal to supratidal
Foraminiferal pelletal
Subtidal to Intertidal
Miliolid-dasycladacean algae
Intertidal
Pelloidal skeletal
Subtidal to Intertidal
Miliolid pelletal
Subtidal
Pelletal celestite
Intertidal to supratidal
Pelletal skeletal
Intertidal to supratidal
Algal
Intertidal to subtidal
WELL RRR-29
Dolostone
Intertidal
Anhydrite
Supratidal
Dolo-mudstone
Intertidal
Pelletal dolostone
Dolo-mudstone
Dolostone
Intertidal Supratidal
Dolo-mudstone
Intertidal to supratidal
Pelletal dolo-mudstone
Anhydrite
Supratidal
Pelletal dolostone
Intertidal to supratidal
Dolo-mudstone
Algal
Intertidal to subtidal
EXPLANATION
Limestone
Dolomite
Dolomitic Limestone
Anhydrite
Foraminifera
Unidentified Allochem
Dasycladacean Algae
Recrystallized Fossils
Unidentified Algae
Anhydrite or Celestite inclusions
Bryozoan
Pellet
Echinoderms
Fracture

Fig. 5. Microfacies, depositional environment, and porosity distribution, Al Fūrūd Formation, wells RRR-10 and RRR-29, Ghānī Field, Sirt basin.

Wilson's (1975) standard microfacies (SMF) classification is utilized in this study. The observed microfacies are arranged in a sequence from older to younger:

Facies 1: Bryozoan Bioclastic (Wackestone)

This facies is recognized in the northern area of the Ghānī Field (well RRR-29) at the interval 1832–1835 m, but has not been recognized in the southern area (well RRR-10). The combined presence of bryozoans, echinoderms, benthonic foraminifers, and dasycladacean algae indicates shallow, warm, normal marine shelf deposition (Fig. 6). Wave and current activity (energy) is considered to be low to moderate on the basis of a high content of lime mud matrix. Water depth and temperature can be inferred to be less than 5 m and tropical to subtropical on the basis of the dasycladacean algae observed in this facies. This facies occurs in an environment similar to Wilson's (1975) facies belt 7 or 8, SMF 8, and 9 (Standard Microfacies).

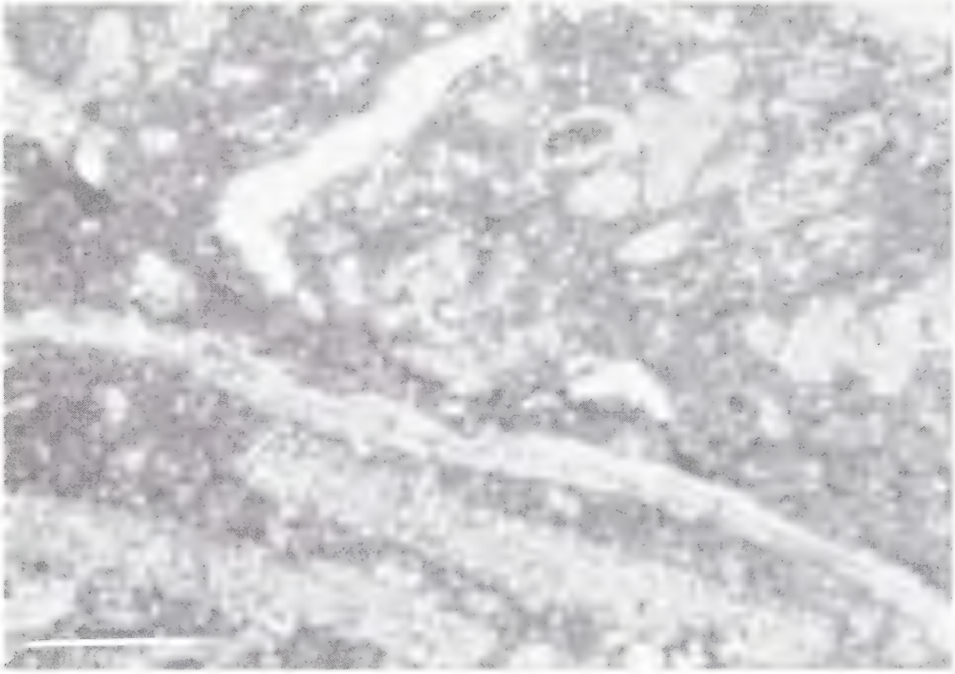

Fig. 6. Photomicrograph of thin section (cross nicols and stained) illustrating the bryozoan bioclastic facies. Bar represents 0.5 mm.

Facies 2: Mudstone

This facies is about 2 m thick in the northern area, but has not been cored in well RRR-10. The inferred depositional environment of this facies is a low-energy, restricted circulation shelf. The presence of some green algae indicates a very shallow marine environment of deposition. This facies would be similar to Wilson's belts 8 or 9, SMF 23.

Facies 3: Dasycladacean (Wackestone–Rudstone)

This facies is about 3 m thick in the northern area, but it was not recovered from well RRR-10. The depositional environment is interpreted as being very shallow marine, based on the abundant dasycladacean algae and minor amount of echinoderms, bryozoans, and benthonic foraminifers (Fig. 7). The presence of echinoderms indicates a normal marine salinity. Water depth is inferred to be less than 3–9 m in tropical to subtropical conditions as indicated by the common dasycladacean algae. Wave action and current activity are considered to be low to moderate on the basis of the high content of lime mud. This facies is similar to Wilson's belt 7 or 8, SMF 8 and 9.

Facies 4: Bioclastic (Wackestone–Rudstone)

This facies is recognized in cores from both wells (RRR-10 and RRR-29). The allochems range in size from a few millimetres to 2 cm. The inferred environment of deposition of this facies is a shelf lagoon with open circulation. The presence of bivalve fragments, benthonic foraminifers, dasycladacean algae, echinoderms, and bryozoans indicates a normal, very shallow marine environment (Fig. 8). Current activity and wave action is inferred to be moderate to vigorous, as indicated by the presence of fragmented thick- and thin-shelled bivalves (molluscs) and minor unidentified allochems. The diverse fauna and the occurrence of echinoderm fragments indicate a probable normal marine salinity rather than brackish water. Water depth is inferred to be less than 3–9 m in tropical to subtropical conditions as indicated by the common occurrence of dasycladacean algal fragments. This facies is similar to Wilson's belts 7 or 8, SMF 8, 9, 18, and 24(?).

Facies 5: Algal (Wackestone)

This facies has been observed in both wells. Its thickness is about 4 m in the southern area and about 3 m in the northern area. The depositional environment is interpreted as being shallow marine in a shelf lagoon with open circulation. Current activity and wave action is inferred to be moderate to high

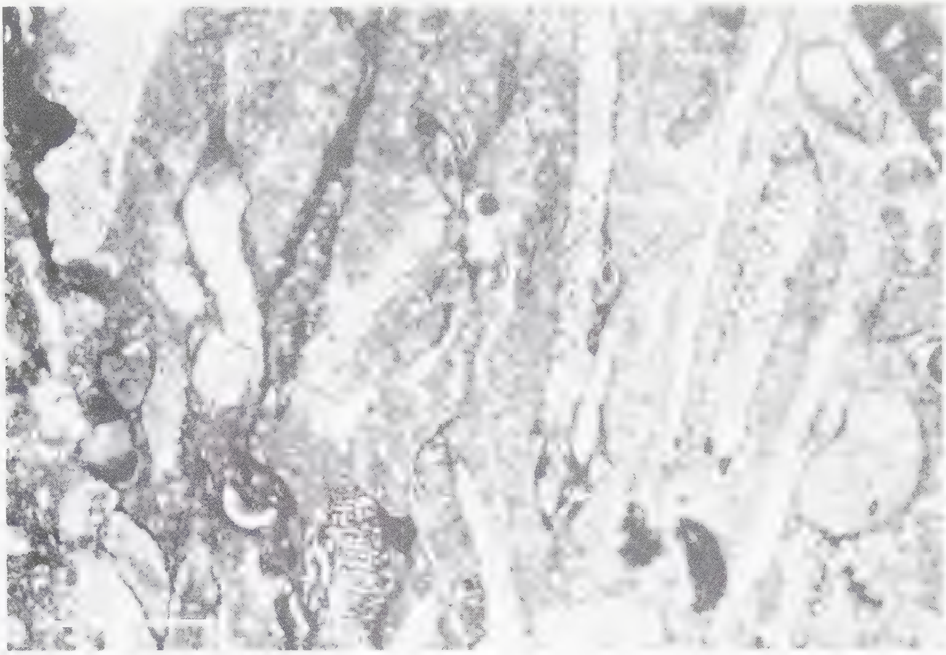

Fig. 7. Photomicrograph of thin section (cross nicols and stained) illustrating the dasycladacean facies. Bar represents 0.5 mm.

Fig. 8. Photomicrograph of thin section (cross nicols and stained) illustrating the bioclastic facies. Bar represents 0.5 mm.

as indicated by the presence of fragmental allochems (Fig. 9). This facies is similar to Wilson's belts 7 or 8, SMF 8 and 9.

Facies 6: Pelloidal–Pelletal Skeletal (Wackestone–Packstone)

This facies is recognized in the southern area and has a thickness of about 9 m. In the northern area it is not recognized because of intense dolomitization. It consists primarily of pellets, peloids, benthonic foraminifers, and dasycladacean algae (Fig. 10). Foraminiferal tests and pellets suggest deposition within slightly agitated water of a sheltered shelf lagoon. The hardened fecal pellets with minor intraclasts and scattered small foraminifers show a winnowed aspect due to water movement on a shallow restricted shelf–lagoonal environment. The pellets are elliptical to rounded, about 0.10 mm in size. Some of these pellets show internal structure (proba-

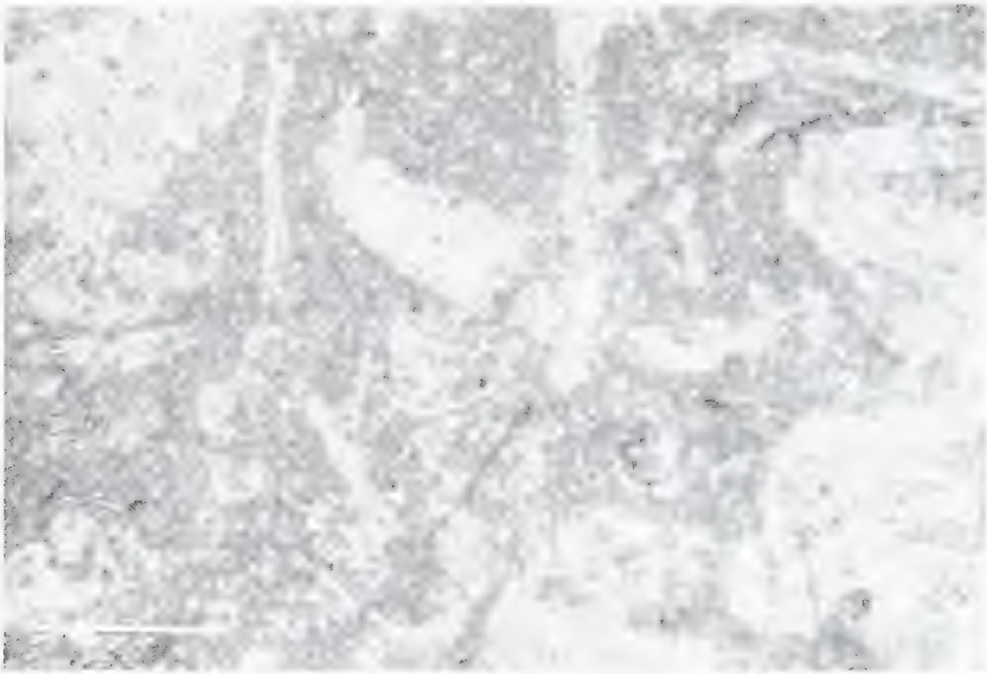

Fig. 9. Photomicrograph of thin section (cross nicols and stained) illustrating the algal facies. Bar represents 0.5 mm.

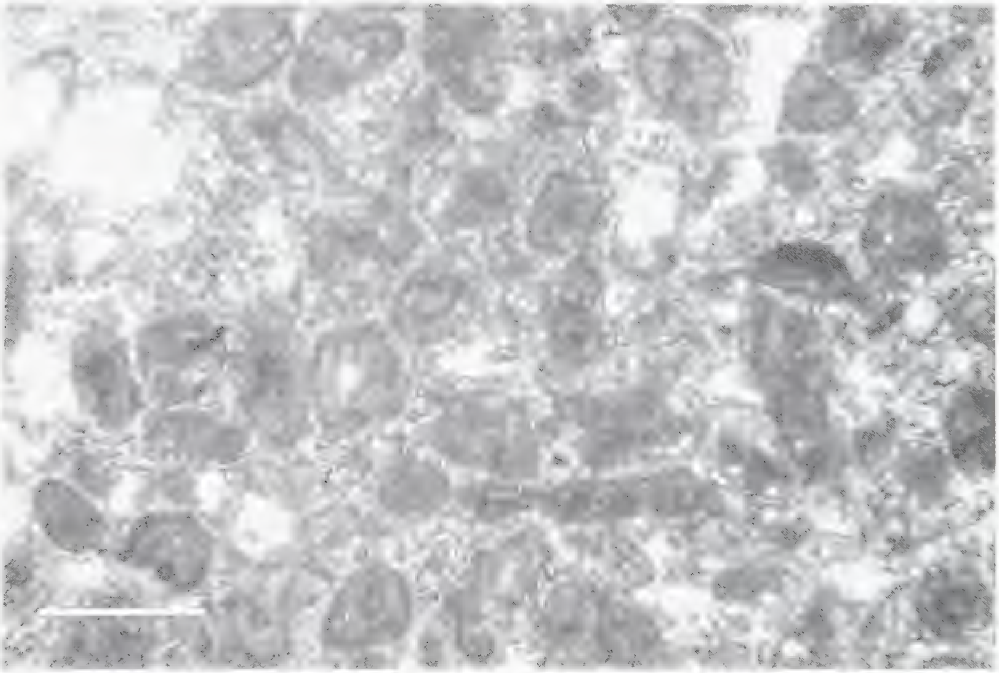

Fig. 10. Photomicrograph of thin section (cross nicols and stained) illustrating the pelletal–skeletal facies. Bar represents 0.5 mm.

bly foraminiferal fragments). The abundance of lime mud, however, indicates low to moderate current activity. The occurrence of some echinoderm fragments may indicate normal water salinities. Water depth is inferred to be less than 3–9 m in tropical to subtropical conditions as indicated by the occurrence of dasycladacean algae. This facies is similar to Wilson's belt 7 or 8, SMF 16, 17, 18, and 19.

Facies 7: Dolostone

This facies is observed in the northern area of the field and has a thickness of about 9 m of secondary dolomite interbedded in part with anhydrite. In the southern area, on the other hand, only the upper 0.6 m reveals this microfacies, as dolomitization in this well was not very intense. The dolomitized micrite indicates low-energy or calm water deposition (Abushagur, 1984b). A few recrystallized fossils (probably dasycladacean algae) were recovered. These would seem to reveal a shallow, warm environment, and normal marine salinities in which the water depth is inferred to be less than 3–9 m. The anhydrite inclusions scattered in this microfacies indicate that it was deposited in a high intertidal to supratidal environment. This facies is similar to Wilson's belt 8 and 9, SMF 16, 17, 18, and 19.

Facies 8: Anhydrite and Celestite

Anhydrite is recognized in the northern area as either beds about 0.3 m thick or as anhydrite and celestite inclusions (Fig. 11). In the southern area only some anhydrite inclusions and a 0.6 m celestite (strontium sulphate) were recognized (Abushagur, 1984a). The celestite is revealed by X-ray diffraction analysis and is common as a minor mineral in the pelletal skeletal calcarenite and limestone calcilutite facies in well RRR-10. This facies clearly reflects a supratidal environment of deposition. It is similar to Wilson's facies in belt 9.

DISCUSSION

There were two major marine transgressions and regressions across the Sirt basin shelves during Palaeocene time (Figs 4, 12). Shales were confined to the very low-energy zones in the basin during transgressive phases, whereas carbonates were deposited on the shelf areas during regressive phases (Terry and Williams, 1969). The two depositional cycles are discussed in detail below:

I. Lower Palaeocene Depositional Cycle

The Danian Shale (Hagfa Shale in the Ghānī and Al Balaṭ Field areas) changes facies to carbonates (Lower Sabil in the Intisār Field area) in the eastern part of the basin. The Hagfa transgressive shale contains varied fauna of planktonic foraminifers, as well as less abundant ostracods, molluscs, bryozoans, echinoderms; very rare benthonic foraminifers are present at the top of the formation (Lehman, 1964;

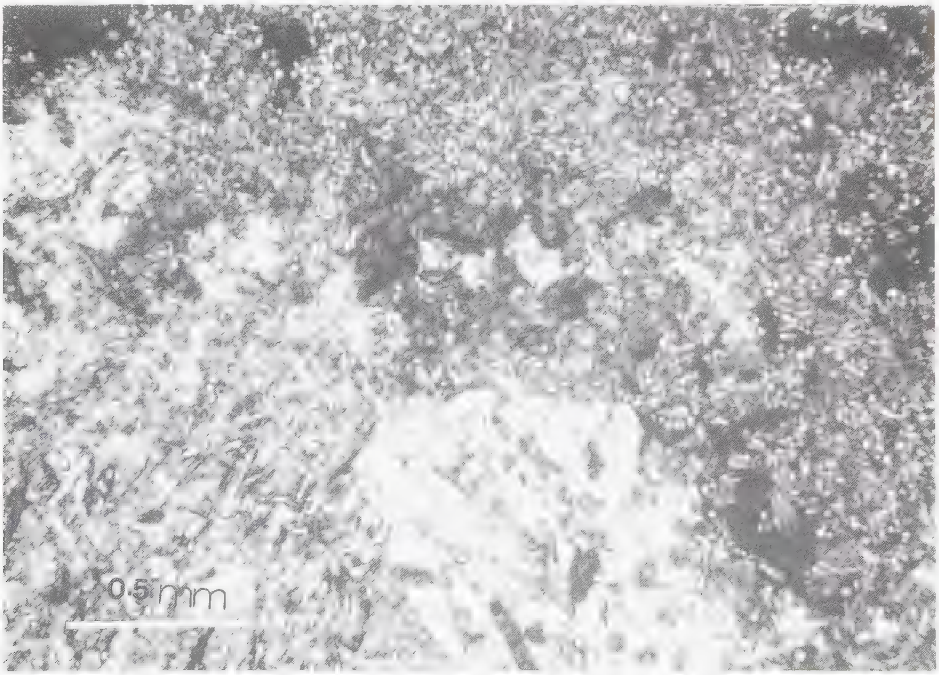

Fig. 11. Photomicrograph of thin section (cross nicols and stained) illustrating the dolo-mudstone and anhydrite facies. Bar represents 0.5 mm.

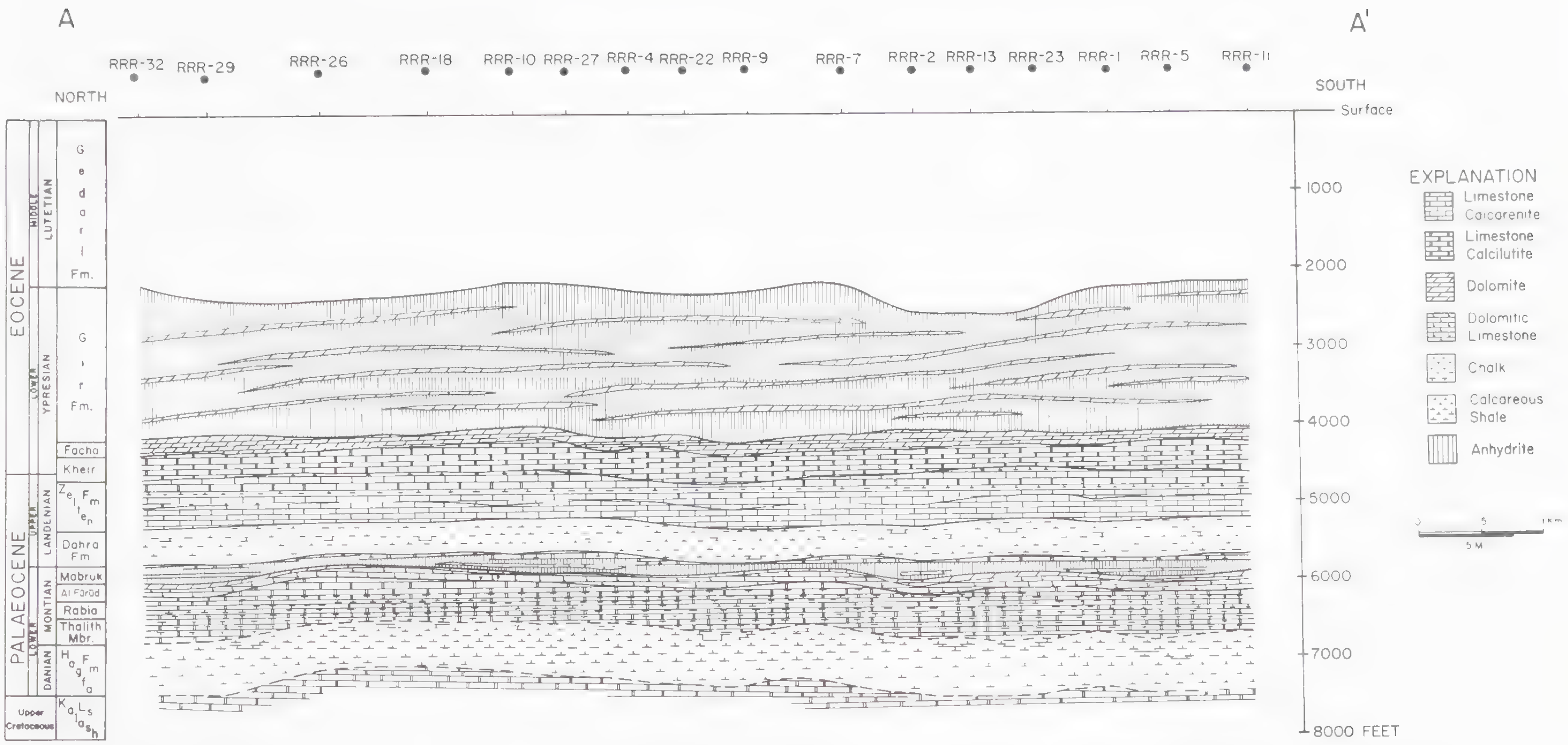
A
A'
RRR-32
RRR-29
RRR-26
RRR-18
RRR-10
RRR-27
RRR-4
RRR-22
RRR-9
RRR-7
RRR-2
RRR-13
RRR-23
RRR-1
RRR-5
RRR-11
NORTH
SOUTH
Surface
1000
2000
3000
4000
5000
6000
7000
8000 FEET
EOCENE
PALAEOCENE
Upper Cretaceous
MIDDLE
LOWER
UPPER
LOWER
LUTETIAN
YPRESIAN
LANDENIAN
MONTIAN
DANIAN
Gedari Fm.
Gir Fm.
Facha
Kheir
Zelten Fm
Dahra Fm
Mabruk
Al Faråd
Rabia
Thalith Mbr.
Hagfa Fm
Kalash Ls
EXPLANATION
Limestone Calcarenite
Limestone Calcilutite
Dolomite
Dolomitic Limestone
Chalk
Calcareous Shale
Anhydrite
0
5
1 Km
5 M

Fig. 12. Stratigraphic cross-section across the Ghānī Field showing the two transgressive and regressive cycles. Depths are in feet. See Fig. 2 for location.

Berggren, 1974). These fauna suggest a deep marine environment of deposition with open sea circulation (Conley, 1971). The presence of interbedded clayey calcilutite suggests intermittent reduction in the rate of supply of terrigenous detritus to the basin (Conley, 1971).

Hagfa shales were probably the source of hydrocarbons which migrated updip and were trapped mainly in Palaeocene reservoirs. Palaeocene shale sequences on the basis of 214 measurements have an average organic matter content of about 0.95% (Parsons *et al.*, 1980).

Al Fūrūd Formation (equivalent to Beda) is the primary reservoir rock in the Ghānī Oil Field (Fig. 13) with porosity ranging from 10 to 25%, mainly moldic, fenestral, intraparticle and fracture.

The various facies of Al Fūrūd Formation can be interpreted as being those deposited in three types of environments: (1) open shelf environments which are mostly subtidal; (2) shallow-water shelf intertidal and shallow-water subtidal environments; and (3) supratidal environments.

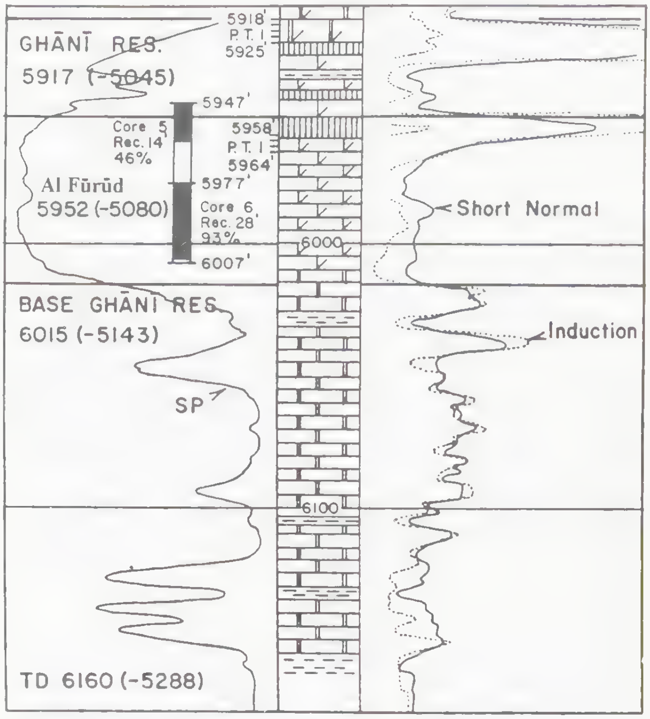

Fig. 13. Detailed well log of Al Fūrūd reservoir, showing typical facies, cored section and perforations. Depths are in feet.

Open Shelf Subtidal Environments

Open shelf conditions imply an unrestricted circulation of marine waters. Al Fūrūd skeletal microfacies attest to these conditions by containing a variety of open marine organisms. In the following discussion, each of the open shelf skeletal facies types is related to its specific environment of deposition.

(1) The bryozoan bioclastic wackestone facies can be interpreted as an open shelf possibly low-relief mound deposit. Bryozoans provided a baffling effect in which fine-grained sediments were trapped. The sediments accumulated in the absence of high wave energy as suggested by the abundance of mud matrix. The reservoir potential of such a facies is very low, which is substantiated by the fact that no significant porosity has been recognized (Fig. 2).

(2) The mudstone facies stratigraphically overlies the bryozoan–bioclastic wackestone and can be interpreted as having been deposited in a very shallow subtidal environment. This facies is tight and consequently has a very low reservoir potential.

Shallow Shelf Environments

Shallow shelf environments dominated in the inner shelf area during the regressive phases that terminated this depositional sequence. Only unwinnowed shallow shelf environments are recognized in the Ghānī Field area; however, winnowed shallow shelf environments have been recognized in the eastern parts of the basin (Barr and Weegar, 1972; Abuzekri, 1984).

Unwinnowed shallow shelf environments of the inner shelf are dominated by low-energy conditions. Al Fūrūd deposits that affirm this condition include the dasycladacean algal wackestone–rudstone facies and the pelloidal–pelletal skeletal facies. The deposition of each of the above facies can be attributed to unwinnowed subenvironments that include nonrestricted, restricted, and sabkha–tidal flat environments as follows:

(1) The deposition of dasycladacean algae has generally been ascribed to protected lagoonal environments. The algal facies may have accumulated in such an environment. Based on the available data, it can only be suggested that the algal facies of the Ghānī Field reveals deposition in a shallow-water subtidal to intertidal environment. Thin algal wackestone deposits accumulated in a quiet water area, while algal–pelloidal packstone and grainstone units clearly reflect deposition in a slightly higher energy area.

(2) Stromatolitic fenestral facies are typical of unwinnowed tidal flat environments. Stromatolites occasionally are found in some of the algal or bioclastic

packstone–grainstone facies. These thin stromatolitic zones indicate a gradual regression accompanied by a decrease in tidal current energy. Their intertidal–supratidal conditions probably caused the development of fenestral facies.

The reservoir potential of both the dasycladacean algal and pelloidal skeletal facies is very low in the southern area of the Ghānī Field; however, the pelletal–dolostone facies in the northern area has a high reservoir potential with porosity averaging about 20%, and is mainly moldic while some is interparticle.

(3) Supratidal environments dominated the area of the Ghānī Field as a result of regression of the sea. These environments are represented by the thick dolomite and anhydrite facies. They exhibit the following depositional and diagenetic features which provide overwhelming evidence of a sabkha supratidal deposit:

(a) The scarcity of fossils, absence of burrows and the abundance of mud indicate accumulation in a quiet depositional environment.

(b) The abundance of anhydrite and celestite strongly supports the sabkha interpretation. The reservoir potential of the dolostone facies is very high. Porosity ranges between 15 and 25%, and is mainly moldic and fenestral.

In Al Balaṭ Field area (Fig. 1), the Beda (equivalent to Al Fūrūd Formation) dasycladacean oolitic limestone of Montian age represents the first shallowing cycle of the Palaeocene and is composed of skeletal micrites, oolitic-rich calcilutites, dasycladacean and miliolid calcarenites. The upper Beda Formation is producing oil in Al Balaṭ Field area with porosity averaging about 29% (Abuzekri, 1984).

Farther to the east (Intisār Field area), the prevailing environment of deposition for the Lower Sabil carbonates is interpreted as a low-energy, shallow marine environment based on the echinoderms, gastropods, green algae, miliolids, rotalids, and arenaceous and calcareous benthonic foraminifers (Brady *et al.*, 1980).

II. Upper Palaeocene and Lower Eocene Depositional Cycle

The reflux of transgressive shale (Dahra, Khalifa and Shterat) occurred during early Landenian time (Fig. 4). Occasional periods of clear water conditions allowed a resurgence of biotic activity in the vicinity of the shelf edge resulting in limestone/shale interfingering (Brady *et al.*, 1980). The Dahra Shale is considered as the main source rock for hydrocarbons found in the Facha and other Gir dolomite members (Early Eocene) in the western parts of the Sirt basin (Abushagur, 1983b).

Regression of the sea occurred during Middle and Late Landenian time, resulting in deposition of the Zelten carbonates in the western and central parts of the basin. No oil production occurs from the Zelten Formation in the Ghānī Field area; however, oil shows have been reported from some members of the Zelten Formation (Zelten "B"). In the Zalṭan Field area (central part of the basin), the Upper Palaeocene shelf limestone of the Zelten Member is producing oil, with porosities ranging from 2 to 40% (averaging 30% in the highly leached zones) of both primary intergranular and intragranular and secondary leached types (Bebout and Pendexter, 1975). The depositional history of the Zelten Member (Late Palaeocene) was described in detail by Bebout and Pendexter (1975).

The eastern parts of the basin were dominated by the growth of reef-type carbonates (Intisār "A, B, C, D, and E"), shelf carbonates (Upper Sabil), and basinal and near-basinal deposits (Kheir marls and limestones) during Late Palaeocene time. The return of clear water conditions initiated the formation of widespread, open marine, mud-supported biomicrites of the upper Sabil Formation, while areas such as those at Intisār "D" and "E" were able to support a biota that included echinoids, red algae, and scarce corals (Brady *et al.*, 1980). Intisār "A" and "D" are producing oil with estimated reserves of about 2 billion and 1.1 billion barrels of oil, respectively (Terry and Williams, 1969; Brady *et al.*, 1980).

CONCLUSIONS

Al Fūrūd Formation is the main reservoir rock in the Ghānī Field and western Concession 11. Eight facies are recognized in Al Fūrūd Formation in the Ghānī Oil Field area. These eight facies are (1) bryozoan–bioclastic, which indicates shallow, warm, normal marine shelf deposits; (2) mudstone, which suggests quiet, low-energy conditions such as may have existed in a well-protected lagoon; and the lack of microfauna in this lime mudstone also suggests that the lagoon may have been at least hypersaline during part of its existence, with times of normal to brackish conditions; (3) dasycladacean facies, which indicate a very shallow, normal marine environment of deposition; (4) bioclastic facies, which suggest a very shallow, normal marine environment with moderate to vigorous energy; (5) algal facies, which reflect a very shallow, normal marine environment in a shelf lagoon with moderate to high energy; (6) pelloidal–pelletal skeletal calcarenite, which suggests deposition within slightly agitated waters of a sheltered lagoon with restricted circulation; (7) dolostone facies, with fenestrate structures (algal) that indicate a high intertidal environment of deposition; and (8) anhydrite facies which reflect a supratidal environment of deposition.

The Palaeocene suite of Al Fūrūd Formation generally shows a shallowing-upward prograding, regressive sequence of three main facies:

(1) Supratidal facies: characterized by nonfossiliferous anhydrite, dolomite, and dolomitic pelletal carbonate mudstone. Dolomitization was penecontemporaneous or very early after deposition.
(2) Intertidal facies: characterized by fossiliferous, pelletal, carbonate mudstone and skeletal calcarenite. Benthonic foraminifers, dasycladacean and stromatolitic algae, and fossil fragments of bryozoans, echinoderms, and molluscs (bivalves) are the most common organisms recognized in this facies.
(3) Subtidal facies: characterized by a skeletal, pelletal, carbonate mudstone. Selected units in this facies have some clays.

The observed and interpreted matrix of these facies apparently consists of lime mud which suggests an absence of strong current action which would remove fine particles. However, the abraded and broken fossils indicate that there must have been at least sporadic, vigorous current action.

Palaeocene cyclic transgressive and regressive sequences combined with the structural configuration in the western parts of the Sirt basin, should yield economically viable exploration targets. The Palaeocene transgressive shales (Hagfa and Dahra) represent the main source rocks for hydrocarbons trapped in the lower and upper regressive cycles in most parts of the basin.

ACKNOWLEDGEMENTS

I sincerely thank Philip Goodell, Calvin James, David V. LeMone, David Eby, F.E. Hill, Don G. Bebout, Gordon Baker, and Nicholas E. Pingitore for their helpful criticism and valuable suggestions. I also thank Mobil Oil Libya, particularly Lutfi Buruin for providing enough data for this study. I am also very grateful to Margaret Cota, Julieta R. Aguirre, Sandy Ladewig and Palmira Hart for typing the manuscript and to Cecil Rounsaville for drafting some of the figures.

REFERENCES

ABUSHAGUR, S.A. (1983a). Paleocene lithofacies and microfacies of the Ghani Field, Sirte Basin, Libya. *New Mexico J. Sci.*, **23**(1), 3 (abstract).

ABUSHAGUR, S.A. (1983b). *Microfacies Analysis of the Farrud Lithofacies in the Ghani Field, Sirte Basin, Libya*. M.S. Thesis, Univ. Texas, El Paso, 185 p.

ABUSHAGUR, S.A. (1984a). Anhydrite and celestite in the Farrud Formation (Paleocene) Sirte Basin, Libya. *New Mexico J. Sci.*, **24**(2), 8 (abstract).

ABUSHAGUR, S.A. (1984b). Dolomitization of the Farrud Suite (Paleocene), Sirte Basin, Libya. *New Mexico J. Sci.*, **24**(2), 9 (abstract).

ABUSHAGUR, S.A. (1986). Cyclic transgressive and regressive sequences, Paleocene Suite, Sirte Basin, Libya. *Bull. Am. Assoc. Petrol. Geol.*, **70**(5), 558 (abstract).

ABUZEKRI, S. (1984). *Microfacies Analysis of the Upper Beda Formation in the Balaṭ Field, Sirte Basin, Libya.* M.S. Thesis. Univ. Texas, El Paso, 194 p.

BARR, F.T. and WEEGAR, A.A. (1972). Stratigraphic Nomenclature of the Sirte Basin, Libya. *Petrol. Explor. Soc. Libya*, 1–6.

BEBOUT, D.B. and PENDEXTER, C. (1975). Secondary carbonate porosity as related to early Tertiary depositional facies, Zelten Field, Libya. *Bull. Am. Assoc. Petrol. Geol.*, **59**(4), 665–693.

BERGGREN, W.A. (1974). Paleocene benthonic foraminiferal biogeography and palaeoecology of Libya and Mali. *Micropaleontology*, **20**, 449–465.

BRADY, T.J., CAMPBELL, N.D. and MAHER, C.E. (1980). Intisar "D" Oil Field, Libya. *In*: Giant Oil Fields (*ed.* M. Halbouty). *Mem. Am. Assoc. Petrol. Geol.*, **30**, 543–564.

CONLEY, C.D. (1971). Stratigraphy and lithofacies of lower Paleocene rocks, Sirte Basin, Libya. *In: Symp. Geol. Libya* (*ed.* C. Gray). Fac. Sci., Univ. Libya, Tripoli, 127–140.

DUNHAM, R.J. (1962). Classification of carbonate rocks according to depositional texture. *In*: Classification of Carbonate Rocks (*ed.* W.E. Ham). *Mem. Am. Assoc. Petrol. Geol.*, **1**, 108–121.

FOLK, R.L. (1962). Spectral subdivision of limestone types. *In*: Classification of Carbonate Rocks (*ed.* W.E. Ham). *Mem. Am. Assoc. Petrol. Geol.*, **1**, 62–84.

FRASER, W.W. (1967). Geology of the Zelten Field, Libya, North Africa. *In: 7th World Petrol. Congr.*, **2**, 259–264.

GOUDARZI, G.H. (1980). Structure-Libya. *In: The Geology of Libya* (*eds* M.J. Salem and M.T. Busrewil). Fac. Sci., Univ. Al-Fateh, Tripoli, **III**, 879–892.

GUMATI, Y.D. and KANES, W.H. (1985). Early Tertiary subsidence and sedimentary facies-Northern Sirte Basin, Libya. *Bull. Am. Assoc. Petrol. Geol.*, **69**(1), 39–52.

LEHMAN, E.P. (1964). Tertiary-Cretaceous boundary facies in the Sirte Basin. *In: 22nd Inst. Geol. Congr.*, New Delhi, **3**, 56–73.

PARSONS, M.G., ZAGAAR, A.M. and CURRY, J.J. (1980). Hydrocarbon occurrence in the Sirte Basin, Libya. *In*: Facts and principles of World Petroleum Occurrence. *Mem. Can. Soc. Petrol. Geol.*, **6**, 724–732.

ROBERTS, J.M. (1970). Amal Field, Libya. *In*: Geology of Giant Petroleum Fields. *Mem. Am. Assoc. Petrol. Geol.*, **14**, 438–448.

SELLEY, R.C. (1969). Nearshore marine and continental sediments of the Sirte Basin, Libya. *Q. J. Geol. Soc. London*, **124**, 4 (496), 419–460.

TERRY, C.E. and WILLIAMS, J.J. (1969). The Idris "A" bioherm and Oil Field, Sirte Basin, Libya; its commercial development, regional Paleocene geologic setting and stratigraphy. *In*: Exploration for Petroleum in Europe and North Africa. *Inst. Petrol. London*, 31–68.

WILSON, J.L. (1975). *Carbonate Facies in Geologic History*. Springer-Verlag, New York, 471 p.

Petrography and Lithofacies of the Satal Formation in Northwestern Sirt Basin, Libya

AHMED J. MOUZUGHI[1]

دراسة الشرائح الصخرية والسحنات التكوينية لتكوين السطل ، شمال غربي حوض سرت الترسيبي بليبيا

أ. ج. المزوغي

الخلاصــة

يوجد تكوين السطل تحت السطح غربي حوض سرت الترسيبي. ويشغل التكوين معظم مرتفعي الظهرة والبيضاء، كما أنه يغطي طبقياً حافة الحد الفاصل بين الحينين الكريتاسي والثالث. ولقد أمكن هنا التعرف على سبعة سحنات هي:

رضاخي فتاتي، جير دقيق الحبيبات، صخور حبيبية اخراجية، صخور دولوميتية، صخور حبيبية حياتية رضاخية، صخور حبيبية مرجانية طحلبية. وصخور عوينية.

لم تستمر عملية تدلمت عضو السطل العلوي تجاه الأجزاء السفلى والخارجية من المرتفع، وعليه فان التتابع كما ورد هنا يقدم مفهوماً لأنسب البيئات الترسيبية.

وحيث أن عضو السطل السفلي فتاتي عند القاعدة فهو عموماً عبارة عن صخور ردغة وواكستون في معظمه. ومثل هذه السحنات تحدث لها عملية تحوير بعد الترسيب، مما أدى إلى توزيعها على رقعة واسعة كما أدى إلى التنوع في سحناتها نتيجة لعوامل البيئة المتعددة.

وقد ترسبت هذه السحنات في بيئة بحرية محمية جزئياً. وقد تحكمت تراكيب المنطقة في البيئات الترسيبية، أي أن عملية هبوط ورفع المنطقة قد نشأ عنها إزاحة في أحزمة السحنات.

Abstract. The Satal Formation occurs in the subsurface of the western Sirt basin. The formation occupies most of the Az Ẓahrah and Al Bayḍā' platforms, and stratigraphically it straddles the Cretaceous–Tertiary boundary. Seven facies have been recognized; these are terrigenous clastic, fine-grained carbonate, peloidal grainstone, dolostones, bioclastic grainstones, coralgal grainstones, oolite grainstone.

The dolomitization of the Upper Satal Member cannot be sustained towards the lower and outer parts of the platform. Thus, the sequences as described here offer a better understanding of the depositional environment.

The Lower Satal Member, being terrigenous at the base, is for the most part mudstone–wackestone; such a facies is modified by ensuing diagenesis and environmental conditions resulting in wide distribution and variation of the facies.

These different facies have been deposited in a partly protected shallow neritic environment. The depositional environments were structurally controlled so that subsidence and uplift resulted in shifting of the facies belts.

INTRODUCTION

The Satal Formation is a carbonate succession occurring in the subsurface of the western Sirt basin, Libya. This formation is confined in areal distribution to the limits of the platform areas of the northeast-trending elements of the Aẓ Ẓahrah and Al Bayḍā' platforms (Fig. 1).

This study is concerned with the petrography and facies analysis of carbonate formations of Maastrichtian to Danian age. The study has been restricted to Al Bayḍā' platform and the southeastern parts of the Aẓ Ẓahrah platform.

[1] National Oil Corporation, P.O. Box 2655, Tripoli, Libya, G.S.P.L.A.J.

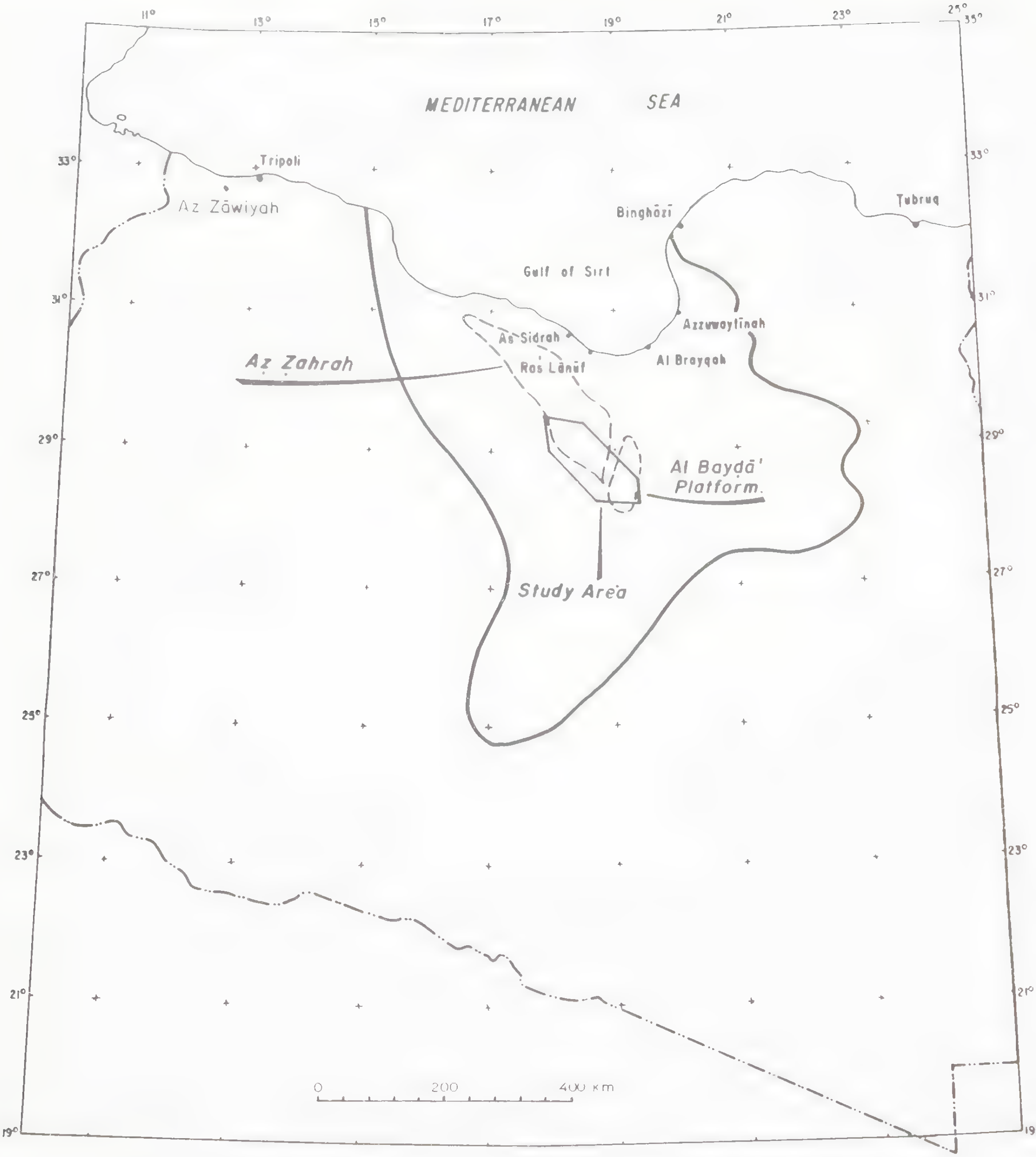
11°
13°
15°
17°
19°
21°
23°
25°
35°
33°
31°
29°
27°
25°
23°
21°
19°
MEDITERRANEAN SEA
Tripoli
Az Zāwiyah
Binghāzī
Tubruq
Gulf of Sirt
As Sidrah
Ras Lānūf
Al Brayqah
Azzuwaytīnah
Az Zahrah
Al Baydā' Platform
Study Area
0
200
400 km

Fig. 1. Location of the area showing the location of Az Zahrah and Al Baydā' platforms in the Sirt basin.

Barr and Weegar (1972) distinguished two members in the Satal Formation: an Upper member of Danian age and a Lower member of Maastrichtian age. This division of the formation as it occurs in the type well (B2-32) on the Az Ẓahrah platform cannot be applied to Al Bayḍā' platform as no lithologic break can be distinguished straddling the Cretaceous–Tertiary boundary in the latter. Thus, a degree of variation from the type section had to be accepted.

The facies described here may be different from those that occur in the subsurface of the northern Az

Ẓahrah platform, where the depositional palaeoenvironment might have differed from Al Bayḍā' platform area.

METHODS OF STUDY

This study was conducted using the limited material available, mostly in the form of cuttings and well logs. The nature of the samples did not permit detailed petrographic analysis; however an attempt was made to describe the various facies units in order to reconstruct the palaeogeography of the area.

Representative cuttings from the boreholes that penetrated the Satal Formation were picked at intervals of 6 m. These cuttings were thin sectioned and stained by Alzarine Red S and Turner's blue. The thin sections were examined under a light microscope and specific intervals which showed predominance of micrite to skeletal constituents were chosen for scanning electron microscopy.

STRATIGRAPHY AND PREVIOUS WORK

The Satal Formation, of Maastrichtian–Danian age, occurs in the subsurface of the western Sirt basin. It has been encountered in boreholes located in Aẓ Ẓahrah and Al Bayḍā' platforms (Fig. 2).

Carbonate sequences were first recognized by petroleum geologists during exploratory activities in the basin and were described by Conley (1971) who did not propose any formal stratigraphic terminology for the carbonates. Barr and Weegar (1972) suggested the name Satal Formation and described the type section from B2-32 borehole in the Aẓ Ẓahrah Field, located at lat. 29°28′09″N and long. 17°47′20″E at a subsea depth of 2593′ to 3622′.

In this type section, the Satal Formation is subdivided into two members (Barr and Weegar, 1972).

The Lower member (Maastrichtian) consists of argillaceous calcilutite and calcarenite and is mainly chalky with sandstone while the Upper member (Danian) is composed of light grey to white fine-grained calcarenite and calcilutite which becomes dolomitic. The boundary is placed at the change from dominantly chalky to dolomitic (Barr and Weegar, *op. cit.*). The contact between the two members also defines the Cretaceous–Tertiary boundary.

The Lower member may overlie the Sirt Shale Formation as in the type section, or it may overstep older Cretaceous or lower Palaeozoic formations. The contact with the underlying formation is usually disconformable. The upper member is conformably overlain by the Al Bayda Formation (Montian).

Where interdigitation of Hagfa Shale Formation (Danian) with other formations occurs in the marginal areas of the platforms, Al Bayda Formation may be separated from the upper member by a tongue of the Hagfa Shale Formation (Fig. 3).

DISTRIBUTION OF THE SATAL FORMATION

The Satal Formation occurs in the subsurface of the Aẓ Ẓahrah and Al Bayḍā' platforms in the western Sirt basin (Fig. 2). It is not known to crop out within the Sirt basin proper, although carbonates of similar age were reported from the western flank of the basin by Furst (1968). The relationship of these exposed carbonates to those of the Satal Formation is not precisely known. However, it is possible to trace and correlate these carbonate formations over relatively long distances despite intervening grabens and structural lows (Fig. 3).

During late Upper Cretaceous (Maastrichtian) most of the Sirt basin received carbonates and shales of the Kalash Formation. The Kalash Formation practically blankets all troughs and some parts of the platforms. However, over the Aẓ Ẓahrah and Al Bayḍā' platforms the Kalash is restricted to the outer platform areas, while the inner structurally higher parts received carbonates of the Satal Formation (Fig. 3).

Deposition of the Lower member of the Satal Formation occurred on the eroded surfaces of the quartzitic Gargaf sandstones or, where the latter are absent, the Satal Formation unconformably overlies basement.

STRUCTURAL SETTING

The Sirt basin is a complex of horsts and grabens that have resulted from rifting of the North African continental margin. The dominant trend of the fault patterns runs in a NW–SE direction. In the west Aẓ Ẓahrah platform is the most dominant feature. The contiguous Al Bayḍā' platform is separated from Aẓ Ẓahrah platform by a NE–SW trending graben. Aẓ Ẓahrah platform extends to the northwest where it is approximately parallel to the present-day coastline of NW Libya. Aẓ Ẓahrah and Al Bayḍā' platforms are separated from adjacent platforms in the east, Zalṭan and Jahamah, by the Marādah trough; and to the west from Wadān uplift by Dūr al 'Abd trough (Fig. 4).

However, Al Bayḍā' and Aẓ Ẓahrah platforms have been built on a complex of smaller highs and

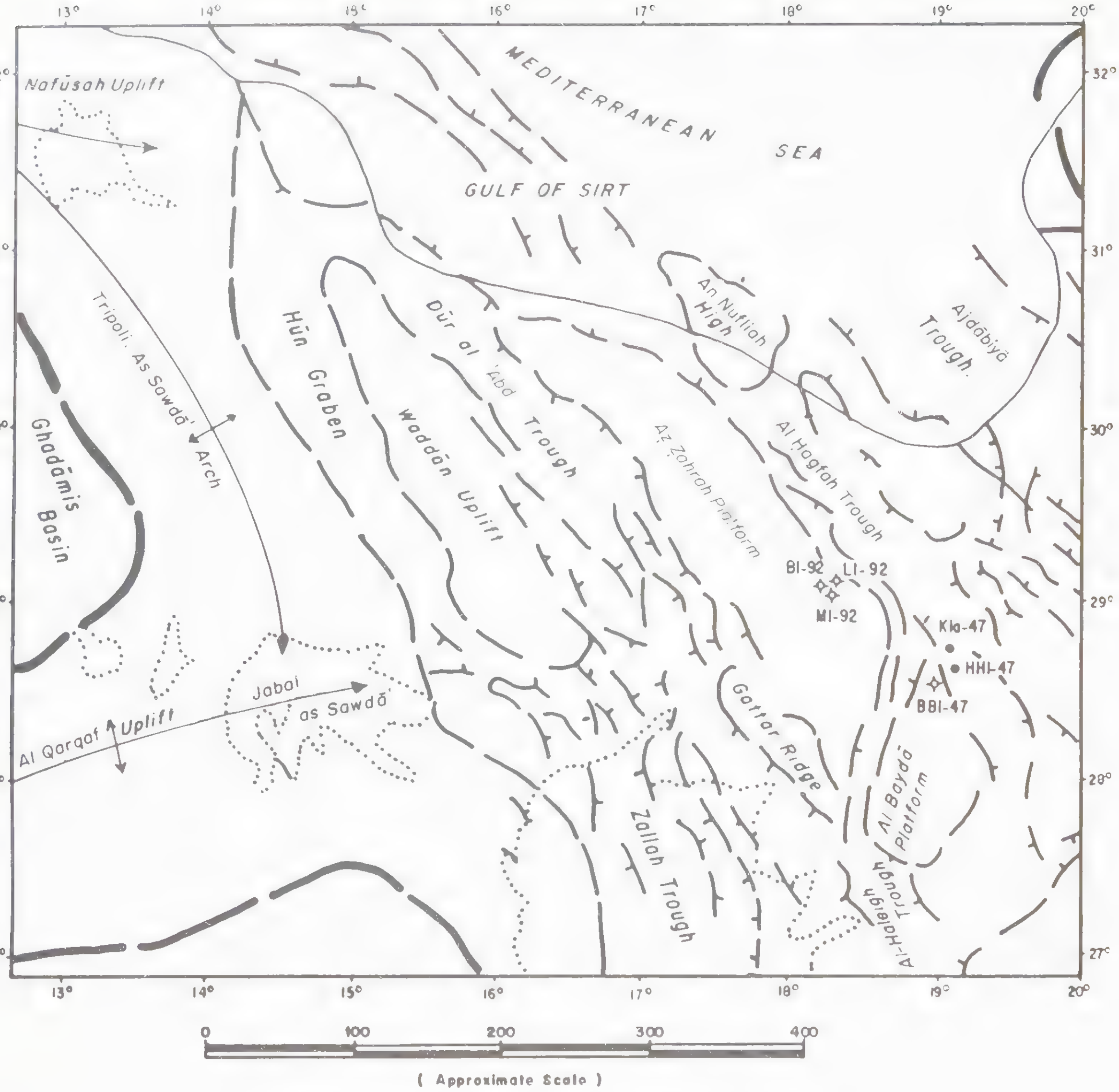
13°
14°
15°
16°
17°
18°
19°
20°
32°
31°
30°
29°
28°
27°
Nafūsah Uplift
MEDITERRANEAN SEA
GULF OF SIRT
Tripoli: As Sawdā' Arch
Hūn Graben
Dūr al 'Abd Trough
Waddān Uplift
Az Zahrah Platform
An Nufliah High
Ajdābiyā Trough
Al Hagfah Trough
BI-92
LI-92
MI-92
Kla-47
HHI-47
BBI-47
Ghadāmis Basin
Jabal as Sawdā'
Al Qarqaf Uplift
Gattar Ridge
Zallah Trough
Al Baydā Platform
Al-Haleigh Trough
0
100
200
300
400
(Approximate Scale)

Fig. 2. Borehole location in Aẓ Ẓahrah and Al Bayḍā' platforms.

lows whose dominant trends are in a NW–SE and N–S direction. Minor faults show no preferred orientation. These faults may have modified the pattern of sedimentation.

ECONOMIC CONSIDERATION

The most prolific reservoirs in the Sirt basin are those of the Cretaceous and Palaeocene. Several fields have been discovered in Aẓ Ẓahrah and Al Bayḍā' platforms, although the Upper Satal Formation has produced oil only in Aẓ Ẓahrah, Almas and Ali oil fields. The fields are located in Aẓ Ẓahrah platform. To date no oil has been discovered in the Satal Formation in the fields located in Al Bayḍā' platform.

LITHOFACIES

Seven lithofacies are recognized in the Satal Formation (Fig. 5). These are terrigenous clastic, fine-grained carbonates, peloidal grainstone, dolomite, bioclastic grainstone, coralgal, and oolitic grainstone. Any of these units may re-occur, alternate with one another, or be missing completely. Such variations are particularly common in the marginal areas.

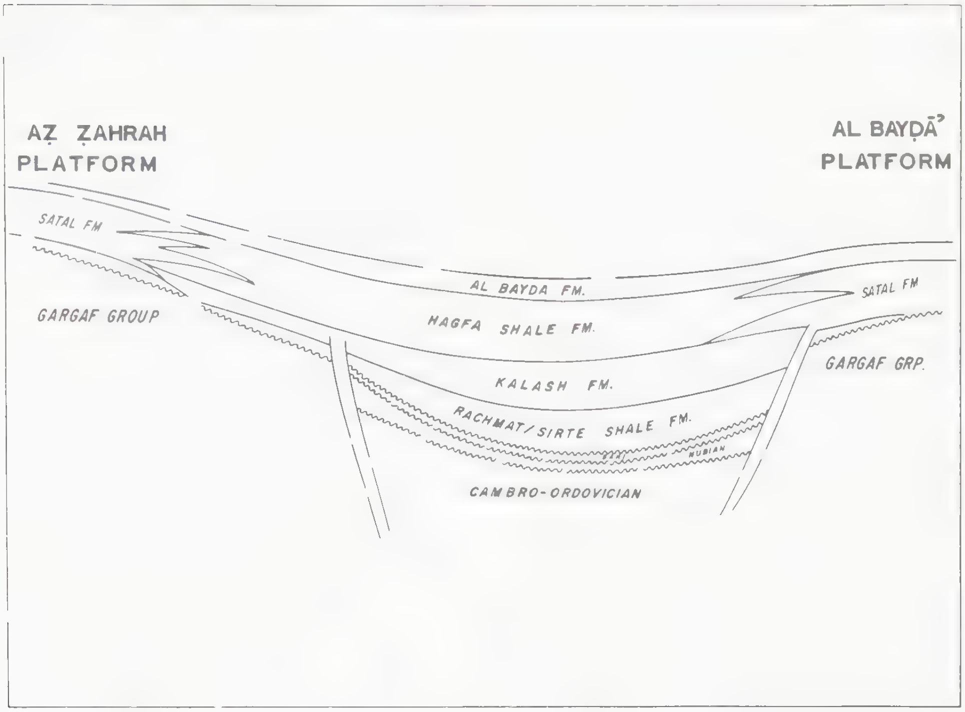

Fig. 3. Schematic diagram showing stratigraphic intercorrelations of Aẓ Ẓahrah and Al Bayḍā' platforms, and El Haleigh graben.

Terrigenous clastic facies

Occurrence: This facies unit commonly occurs in the lowermost beds of the succession although sandy carbonates do occur at other stratigraphic levels.

Description: Two main components are immediately apparent in this facies, the high quartz content and the high percentage of carbonate mud. The quartz grains range from angular to subrounded, poorly sorted silt and fine sand sizes are most common along with small amounts of coarse quartz grains. The interstitial pores are filled with carbonate mud material which includes rare skeletal fragments (Fig. 6).

No particular diagenetic features have been noted and the quartz grains appear to have suffered little or no diagenesis.

Interpretation: The environmental conditions which prevailed in early Maastrichtian time must have been sufficient for carbonate mud to be deposited. Influx of quartz sands occurred sporadically, possibly during periods of storm conditions. The quartz sand may have resulted from weathering of the underlying Gargaf Formation.

Fine-Grained Carbonate

Occurrence: This facies unit occurs abundantly in various parts of the area. It is most common in the inner parts of the Aẓ Ẓahrah and Al Bayḍā' platforms, particularly in the topographically low areas. The unit also occurs at various stratigraphic levels.

Description: The mudstone–wackestone facies comprises a range of sedimentary constituents in which carbonate mud is dominant. The skeletal content of the mudstone–wackestone varies from nil to 30%. The skeletal elements include unidentifiable microbioclasts and large molluscan shell fragments. Ostracods and foraminifera are also common. The foraminiferal assemblage is dominated by benthonic forms. Bryozoa and echinoderms are also present (Fig. 7).

Where the mudstone has not been completely compacted pellet packstone replaces the mudstone facies.

Ellipsoidal-shaped grains, possibly faecal in origin, may have become dominant. In places individual pellets are smeared or coalesced, giving rise to patches of apparently homogeneous micrite. A notable feature of this microfacies is the paucity of bioclastic material (10%).

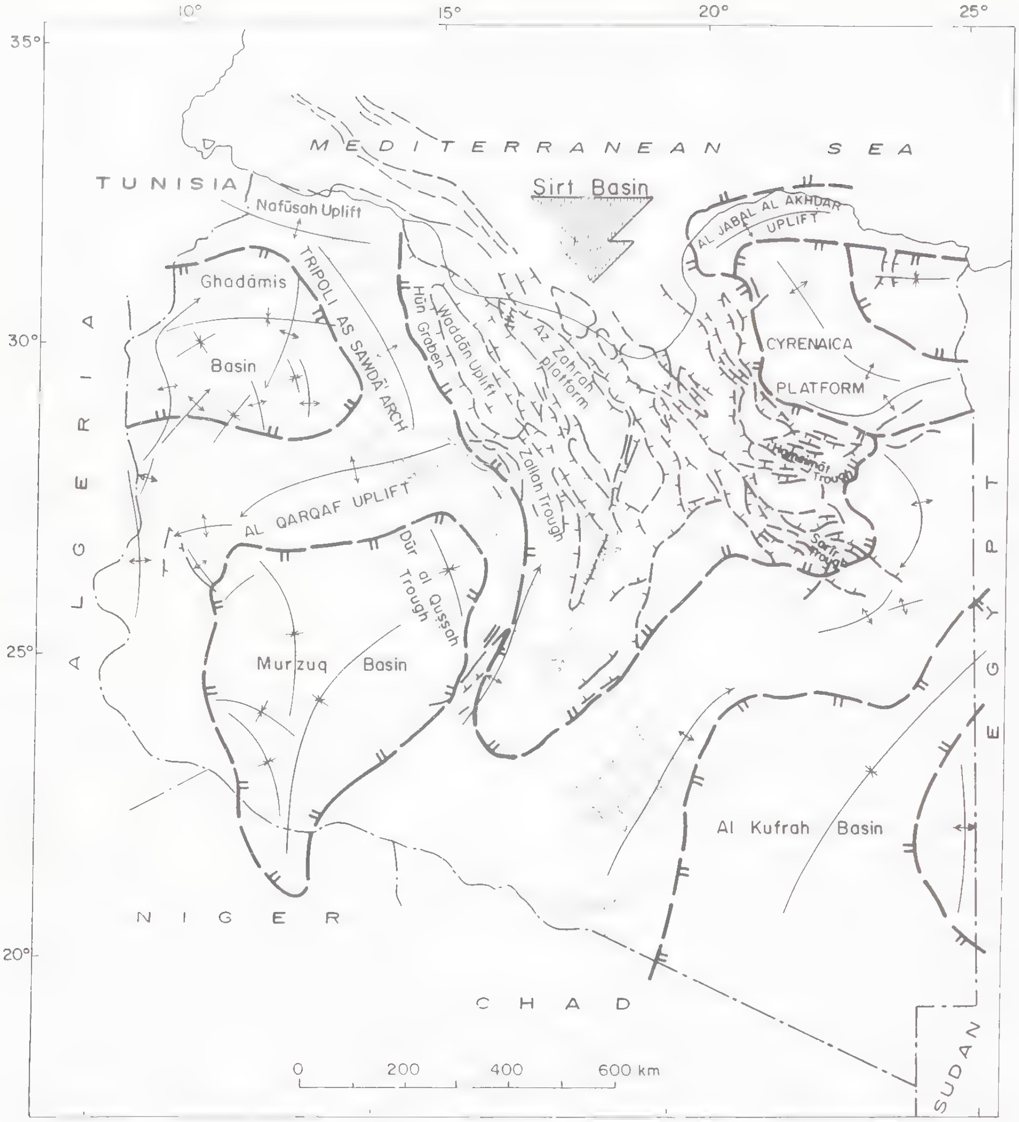
10°
15°
20°
25°
35°
30°
25°
20°
MEDITERRANEAN SEA
TUNISIA
Sirt Basin
Nafūsah Uplift
AL JABAL AL AKHDAR UPLIFT
Ghadāmis Basin
TRIPOLI AS SAWDĀ' ARCH
Hūn Graben
Waddān Uplift
Az Zahrah Platform
Zallah Trough
CYRENAICA PLATFORM
Hameimat Trough
Sarir Trough
AL QARQAF UPLIFT
Dūr al Qussah Trough
Murzuq Basin
ALGERIA
EGYPT
Al Kufrah Basin
NIGER
CHAD
SUDAN
0 200 400 600 km

Fig. 4. Tectonic elements of the Sirt basin.

The bioclastic packstone is distinguished by a relatively high percentage of bioclastic material and a low mud content in the interparticle space. The biota include algae, mostly dasycladacean fragments, ostracods, bryozoa and unidentifiable microclasts.

The calcisilites are distinguished on the basis of the coarser texture of the matrix and the presence of bioclastic material within interparticle fossil pores. Diagenetic alteration of the different fine-grained facies includes recrystallization and stylolitization.

Interpretation: The fine-grained facies blankets most of the area with the exception of the marginal parts of the horsts. The various features described from the facies invite comparison to lagoonal sequences described by Khoja (1971) from Aẓ Ẓahrah Field area. The faunal association being limited to a small number of species suggests deposition in a quiet, restricted environment — such conditions could have existed in the lagoons of the southern and northern parts of Al Baydā' platform and the southeastern parts of Aẓ Ẓahrah platform.

Peloidal Grainstone

Occurrence: The fine-grained facies are commonly overlain, and in a few instances pass laterally into peloidal grainstones. These are distinguished from the fine-grained facies in general and the pellet packstone in particular by larger peloids, an absence of carbonate mud, and the presence of sparry calcite cement.

Description: The microfacies is dominated by peloids of various sizes. The size ranges from 0.12 to 0.6 mm. Most peloids have a grain size range between 0.3 and 0.4 mm. Individual peloids are in contact or cemented by calcite spar. Quartz sand is absent but fine silty quartz grains occasionally occur within the peloids.

Amalgamation of the peloids also occurs. These amalgamated grains show signs of deformation and partial fusing. Where the sparry calcite is absent micrite pellets dominate the microfacies; they can be distinguished by their micrite matrix.

The most common diagenetic effect on the peloidal grainstone is the cementation and amalgamation of the peloids.

Interpretation: The peloidal grainstone facies are limited to the southern part of Al Bayḍā' platform. This restricted areal distribution to a topographic low suggests proximity to a lagoonal environment. This interpretation is further indicated by the paucity of skeletal material.

Dolostones

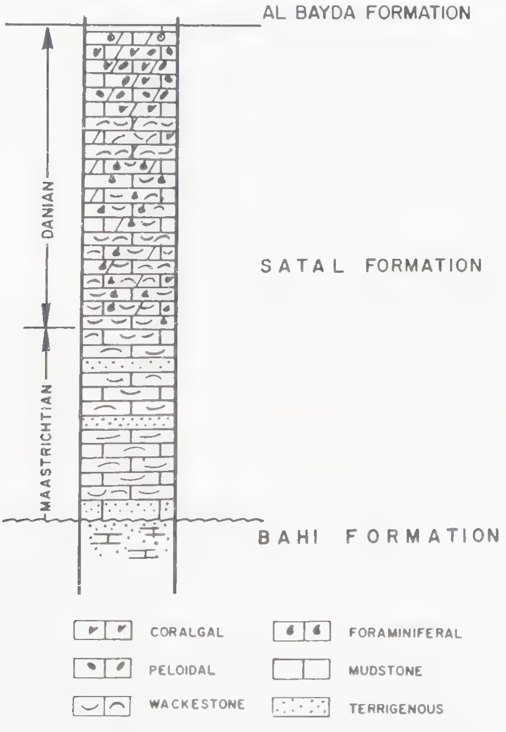

Fig. 5. Lithofacies units of the Satal Formation.

Occurrence: This facies unit occurs in Aẓ Ẓahrah and Al Bayḍā' platform areas. It occupies the structural highs and upper flanks of the ridges.

Description: Two types of dolomites are recognizable in the dolostone facies.

(1) Euhedral dolomite rhombs up to 300 μm in length; commonly the rhombs are uniform in size — their centres may be clear or clouded (Fig. 8).
(2) Anhedral dolomite rhombs ranging in length from 6 to 15 μm. This type is often vuggy. The shape of the vug suggests that they were created by solution of non-skeletal allochems (Fig. 9).

The coarse crystals and the presence of ghost structures suggest that the dolostones are diagenetic in origin.

Interpretation: The occurrence of the dolostones over parts of the platforms where sediments of the fine-grained facies and the peloidal grainstones appear to pass laterally into dolomites suggests that the dolostones originated through dolomitization of lime muds deposited in lagoonal supratidal environments. The former conditions possibly prevailed in Al Bayḍā' platform area while the latter are likely to have occurred on parts of Aẓ Ẓahrah platform. High rates of evaporation due to a high temperature and concentration of brines with high Mg/Ca ratio probably caused dolomitization of the carbonate mud.

Bioclastic grainstone

Occurrence: This facies unit is common along the margins of the platforms and over the topographic features on the platforms. Foraminifera and molluscs are among the most abundant skeletal components. The foraminifera are dominated by nummulites.

Description: This facies is predominantly a bioclastic grainstone. Changes on a microfacies scale are common. These are indicated by variations in texture and the type of skeletal constituents. The bioclasts consist mostly of large foraminiferal tests up to 4 mm in length. Fragmented mollusc shells and bryozoa are also present. Foraminifera make up 50% of the skeletal elements. The gastropods dominate the molluscan shell percentage. Only 5% of the constituents are algae, mainly dasycladacean. Diagenetic minerals are absent, and sparry calcite is rare, occurring mostly as cavity fill in the foraminiferal tests (Fig. 10).

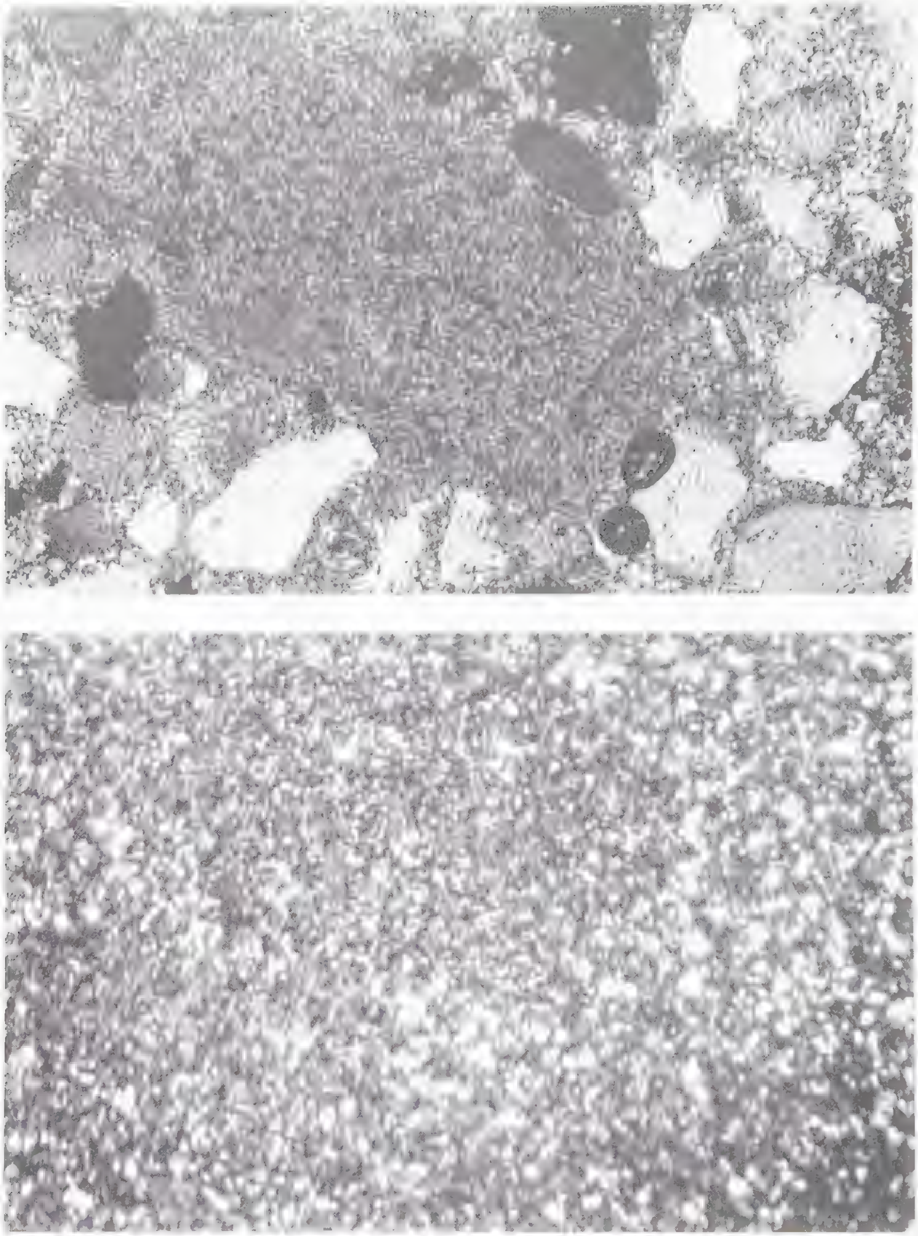

Fig. 6. Terrigenous clastic facies, top figure ×40, bottom figure ×16.

Interpretation: The bioclastic grainstones are deposited in a high-energy, marginal marine and outer lagoon environment.

Coralgal grainstone

Occurrence: The coralgal facies is restricted to the outer western margin of Al Bayḍā' platform and part of the southeastern Aẓ Ẓahrah platform. The facies was encountered at only two locations in the subsurface of the Amin high (DD1-47 and B7-47 boreholes); coral-bearing grainstones also occur at several horizons, interbedded with other facies.

Description: The coralgal facies is characterized by an abundance of scleractinian corals in association with coralline algae. Other bioclasts include foraminifera, molluscs and various other skeletal fragments of unknown affinity (Fig. 11). Recrystallization and dolomitization are the most common

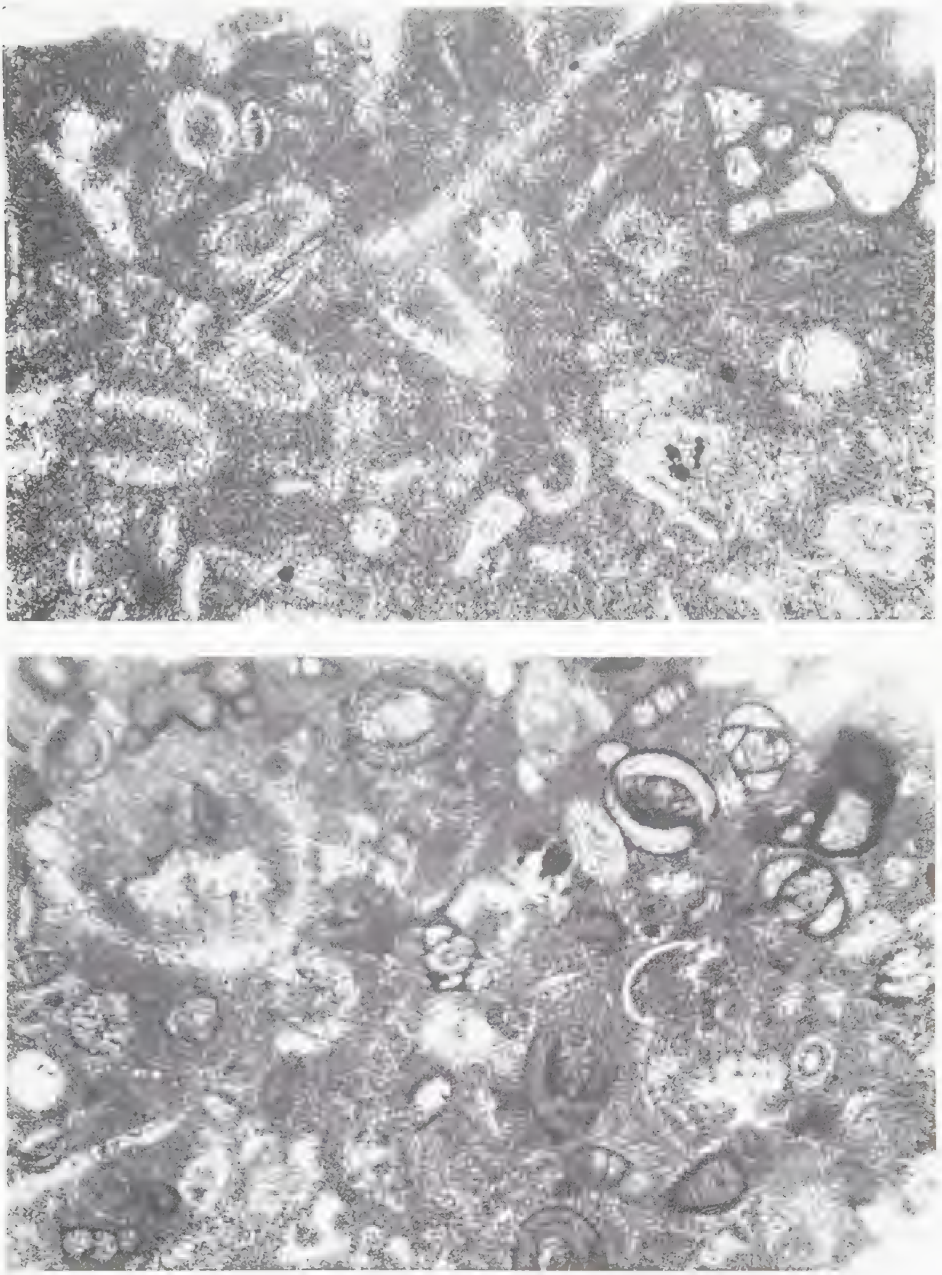

Fig. 7. Fine-grained carbonate; top figure ×64, bottom figure ×40.

diagenetic features of the coralgal facies. In addition, variations from the type of the microfacies do occur — dolomites, oolitic grainstones and intraclasts are associated with this facies.

Interpretation: The coralgal grainstones and their subfacies, along with their areal distribution and occurrence along the outer platform areas suggest deposition in a narrow belt where favourable open marine conditions existed. Such conditions probably initiated the growth of fringing reefs along this margin. Because of the nature of the subsurface data it is impossible to ascertain the presence and dimensions of such build-ups.

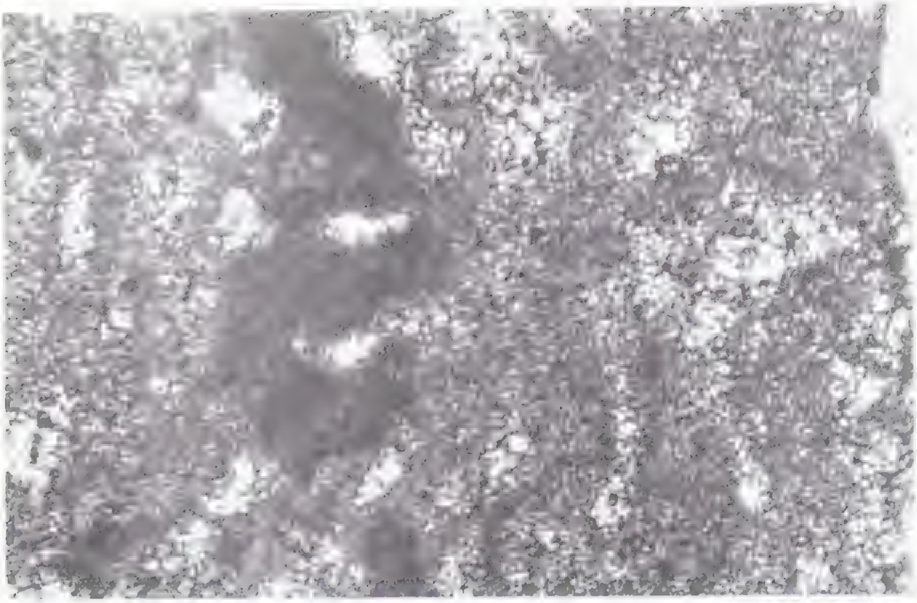

Fig. 8. Euhedral dolomite, scale ×40

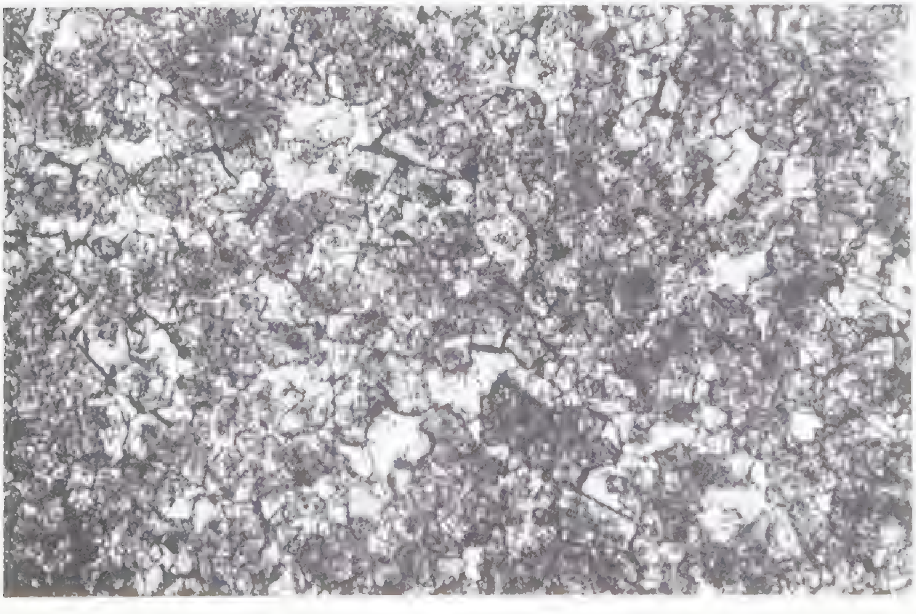

Fig. 9. Anhedral dolomite, scale ×56.

Oolitic grainstone

Occurrence: This facies has been encountered only on the northern Al Bayḍā' platform.

Description: The oolitic grainstones are composed of ooids in a ground mass of sparite. Two distinct shapes have been recognized, well-rounded (in thin section) ooids and elongated bodies some of which enclose a relatively large nucleus. The former normally have nuclei that are either small or have been recrystallized with the cortices and the two cannot be distinguished. Both bryozoa and echinoderm fragments occur as nuclei. Oomicrite is the most common varitype of the facies. It is distinguished by an abundance of micrite material. Skeletal grains are

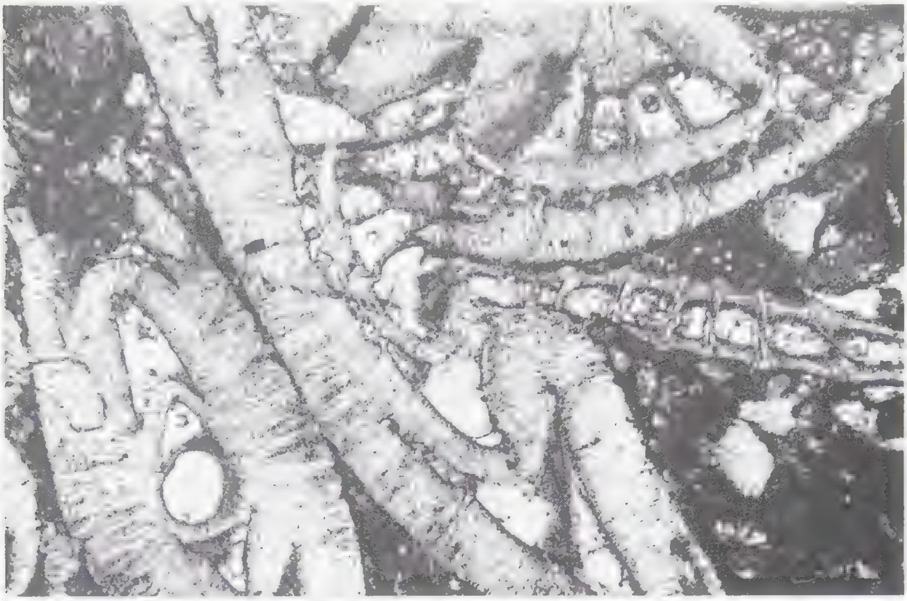

Fig. 10. Bioclastic grainstone, scale ×40.

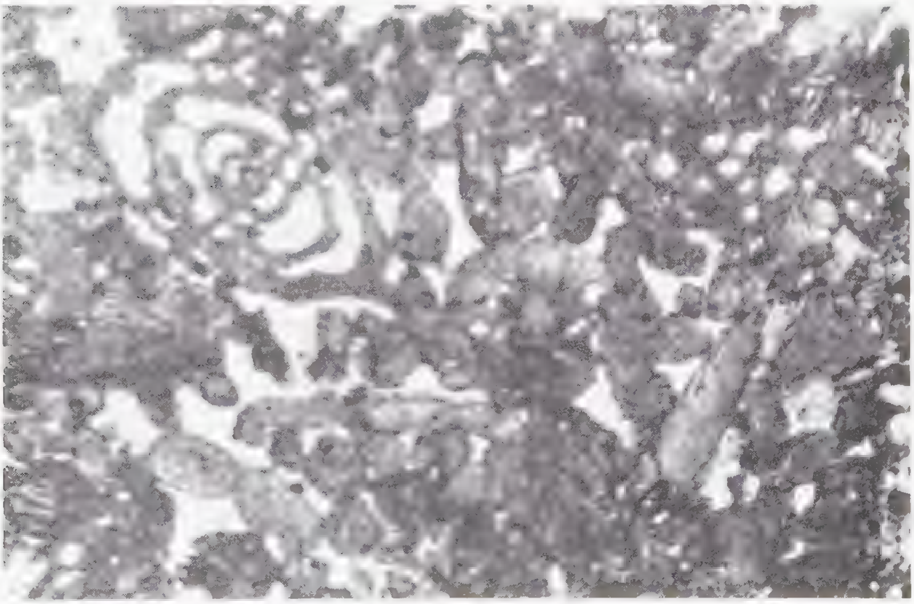

Fig. 11. Coralgal grainstone, scale ×16.

extremely rare. Stylolitization occurs in this facies and affects both grainstones and oomicrites. Recrystallization and cementation of the oolitic facies are also common (Fig. 12).

Interpretation: The oolitic facies are restricted to the area adjacent to the coralgal facies with which they are interbedded. This invites comparison with the oolitic tidal deltas and tidal channels in the landward side of the coralgal reefs in the Bahamas (Purdy, 1963) and the tidal deltas of the Abu Dhabi lagoon, UAE (Loreau and Purser, 1973).

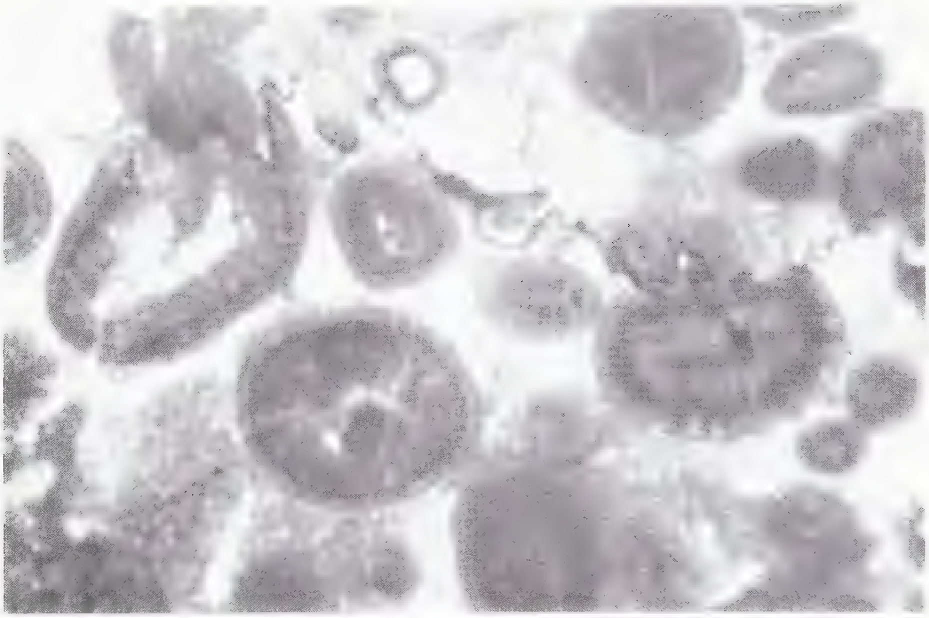

Fig. 12. Oolitic grainstone, scale ×64.

DEPOSITIONAL HISTORY

The Upper Cretaceous marine transgression covered the Sirt basin for the first time in its history during the Cenomanian although the horsts were not transgressed until late in the Maastrichtian. This resulted in the deposition of thick shale sequences and relatively deep-water carbonates in the grabens and shallow-water carbonates over the horsts (Lehman, 1964; Conley, 1971; Hea, 1971) (Fig. 13).

In the northwestern Sirt basin the structural elements controlled the depth of water. During the Cenomanian, sedimentation in the area was restricted to the graben separating Al Bayḍā' and Aẓ Ẓahrah platforms. During the Turonian the shallow-water conditions were replaced by deep-water conditions throughout the remainder of the Upper Cretaceous and early Tertiary but in the grabens, shales and deep-water argillaceous limestone became dominant (Lehman, 1964). Only small areas of the horsts were transgressed during the Cenomanian, mainly the lower flanks. The higher and crestal parts remained emergent on Al Bayḍā' platform.

The slow retreat of the late Cretaceous seas is manifested in the distribution of the carbonate sediments and development of platforms over the horsts. On the western margin of Al Bayḍā' high the conditions were ideal for reef building organisms to flourish; open conditions dominated the Marādah and Dūr al 'Abd troughs to the east and west of the high. The line of fringing reefs may have created a semiprotected lagoonal area with carbonate mud deposition on the inner parts of Al Bayḍā' high; ultimately, as circulation was further restricted carbonate mud deposition extended to the northeast and north of Al Bayḍā' high. Over the southeastern Aẓ Ẓahrah area topographically low areas occurred and these were natural sites for carbonate mud deposition. These carbonate muds were subsequently dolomitized.

Small islands remained emergent on Al Bayḍā' and Aẓ Ẓahrah highs and were structurally important in initiating and controlling deposition of shell sand (bioclastic grainstones) particularly in the outer parts (marginal zones) of Al Bayḍā' and Aẓ Ẓahrah highs.

The transition from the Cretaceous into the Tertiary was marked by an influx of fine-grained sediments, mainly clays and silts, into the grabens of the Sirt basin (Terry and Williams, 1969). This episode of sea-level rise was in keeping with the eustatic change of sea level. However, over the highs, no lithologic break occurs — sedimentation seems to have continued uninterrupted, although variations in thickness are common. Shallow-water conditions are suggested by the formation of oolites in tidal deltas over the northwest area of Al Bayḍā' high and an increase

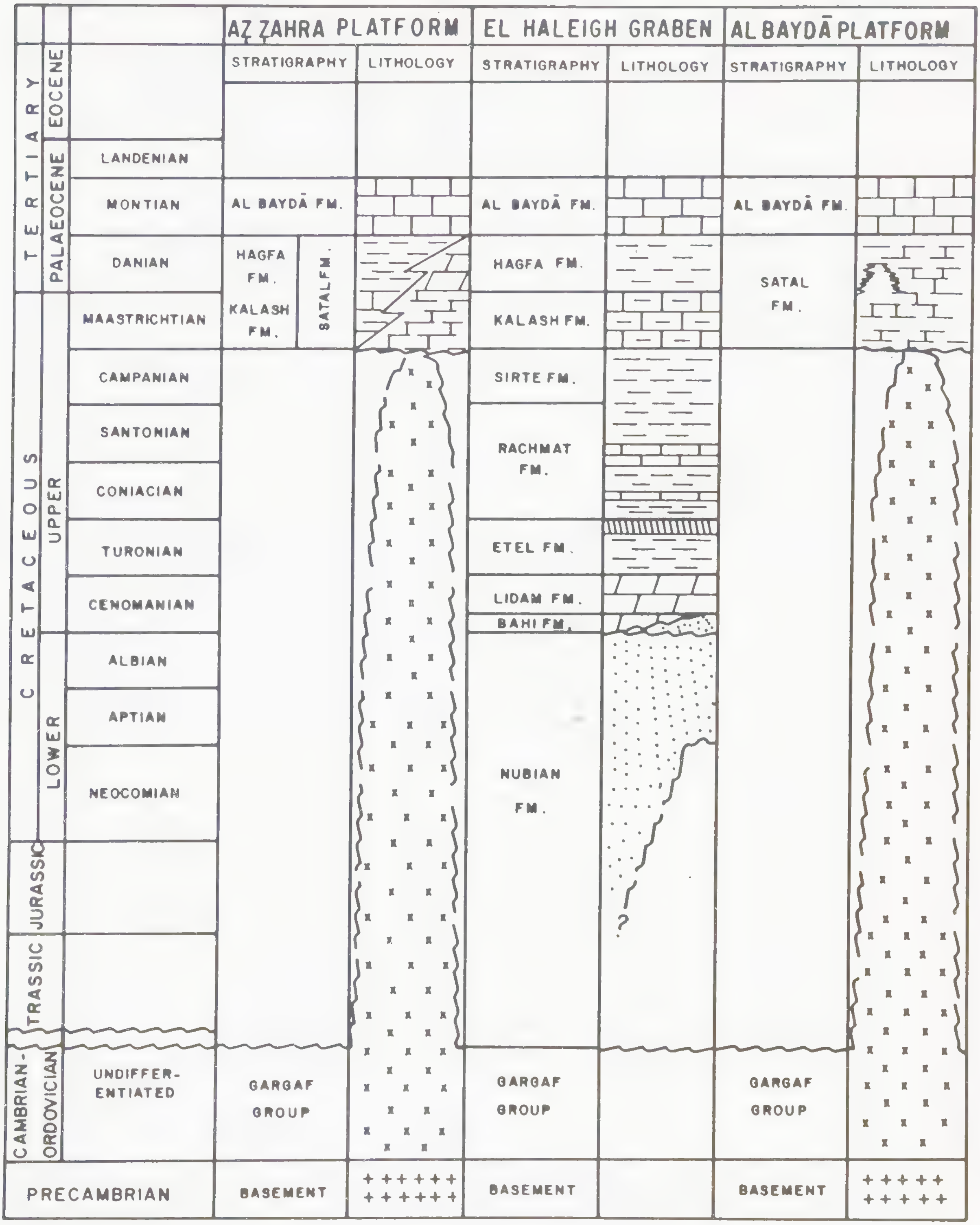
AZ ZAHRA PLATFORM
EL HALEIGH GRABEN
AL BAYDĀ PLATFORM
STRATIGRAPHY
LITHOLOGY
TERTIARY
EOCENE
PALAEOCENE
LANDENIAN
MONTIAN
DANIAN
CRETACEOUS
UPPER
LOWER
MAASTRICHTIAN
CAMPANIAN
SANTONIAN
CONIACIAN
TURONIAN
CENOMANIAN
ALBIAN
APTIAN
NEOCOMIAN
JURASSIC
TRASSIC
CAMBRIAN-ORDOVICIAN
UNDIFFERENTIATED
PRECAMBRIAN
AL BAYDĀ FM.
HAGFA FM.
KALASH FM.
SATAL FM.
SIRTE FM.
RACHMAT FM.
ETEL FM.
LIDAM FM.
BAHI FM.
NUBIAN FM.
?
GARGAF GROUP
BASEMENT

Fig. 13. Schematic diagram showing progressive development of Aẓ Ẓahrah and Al Bayḍā' areas.

in dolomitization of the marginal lagoonal sediments in northern Al Bayḍā' platform and southeastern Aẓ Ẓahrah platform.

CONCLUSIONS

The depositional history of the northwest and west of the Sirt basin indicates a gradual rise in sea level during the Cenomanian. Sedimentation was limited to the grabens and topographic low areas until the Campanian.

Carbonate deposition on the highs occurred concurrently with the shallow-water conditions resulting from a eustatic change of sea level during the Maastrichtian. During the Danian a rise in sea level resulted in the deposition of silts and clays in the trough areas (grabens) while on Aẓ Ẓahrah and Al Bayḍā' platforms, carbonate sedimentation continued without interruption. Seven facies were deposited during the Maastrichtian and Danian. These facies were deposited in a wide range of environments. The environment of deposition was structurally controlled.

ACKNOWLEDGEMENTS

I wish to thank Dr. Max Dobson for his assistance during the research period. I would also like to thank Mr. D. Baird for reading the manuscript. The work has been carried out as part of a research programme for a Ph.D. degree.

REFERENCES

BARR, F.T. and WEEGAR, A.A. (1972). Stratigraphic Nomenclature of the Sirte Basin, Libya. *Petrol. Explor. Soc. Libya*, 179 p.

CONLEY, C.D. (1971). Stratigraphy and lithology of lower Paleocene rocks, Sirte basin, Libya. *In: Symp. Geol. Libya* (*ed.* C. Gray). Fac. Sci., Univ. Libya, Tripoli, 127–140.

FÜRST, M. (1968). The Paleocene-Eocene transgression in South Libya. *Geol. Rundsch.*, **58**, 296–313.

HEA, J.P. (1971). Petrography of Paleozoic-Mesozoic sandstones of the southern Sirte Basin, Libya. *In: Symp. Geol. Libya* (*ed.* C. Gray). Fac. Sci., Univ. Libya, Tripoli.

KHOJA, E.F. (1971). *Petrography and Diagenesis of Lower Paleocene Carbonate Reservoir Rocks, Dahra Field, Sirte Basin, Libya.* Ph.D. Thesis, Rice Univ.

LEHMAN, E.P. (1964). Tertiary-Cretaceous Boundary Facies in the Sirte Basin, Libya. *Proc. 22nd Int. Geol. Congr.*, (India), **7**(3), 56–73.

LOREAU, J.P. and PURSER, B.H. (1973). Distribution and ultrastructure of Holocene ooids in the Persian Gulf. *In: The Persian Gulf: Holocene Carbonate Sedimentation and Diagenesis in a Shallow Epicontinental Sea* (*ed.* P.H. Purser). Springer-Verlag, Berlin, 299–328.

PURDY, E.G. (1963). Recent calcium carbonate facies of the Great Bahama Bank. 2: Sedimentary Facies. *J. Geol.*, **71**(4), 472–497.

TERRY, C.E. and WILLIAMS, J.J. (1969). The Idris "A" bioherms and oil fields, Sirte Basin Libya. Its commercial development, regional Paleocene geological setting and stratigraphy. *In*: The Exploration for Petroleum in Europe and North Africa (*ed.* P. Hepple). *Inst. Petrol. London*, 31–48.

Sedimentology and Geochemistry of the Jir Formation in Jabal al Jīr and the Western Sirt Basin

MOKHTAR I. LASHHAB[1] AND IAN M. WEST[1]

دراسة ترسيبية وجيوكيميائية لتكوين الجير بجبل الجير والجزء الغربي من حوض سرت

م. أ. الأشهب وإ. م وست

الخلاصـــة

يتألف تكوين الجير ذي العمر الإيوسيني من صخور الجبس والأنهيدريت والهاليت والدولوميت. وقد ترسب أكثر التتابع سمكاً في غرب حوض سرت ومحاذياً لنظام منخسف كبير. وقد بدأ هذا المنخسف خلال العصر الإيوسيني وهو يتخذ إتجاهاً موازياً لتصدع البحر الأحمر ذي الأصل الميوسيني. ويوجد القطاع النموذجي لتكوين الجير في وادي الفرس بمنطقة جبل الجير. ويعد هذا التكشف تكشفاً قليل السمك على حافة الحوض من الجبس ثانوي التبلر تتخلله طبقات من الدولوميت. أما تحت السطح في منخسف ميلاغ فيصل سمك التكوين إلى كيلومتر واحد ويتألف من الإنهيدريت والهاليت مع الدولوميت. وقد نشأت بخريات وادي الفرس في بحار ضحلة وأهوار وأسباخ مع صخور جيرية غنية بالمنخربات مما يدل على طغيان البحار من آن لآخر. أما الإنهيدريت الرقائقي المترسب داخل المنخسف فربما نشأ في هور كبير تحت مستوى قاع الأمواج. أما الهاليت فقد ترسب في بحيرة ملحية مغلقة احتلت الجزء الأوسط فقط من الحوض. وقد انتهى ترسيب البخريات خلال الأيوسين المتأخر عندما غمرت المياه الحوض بأسره وترسبت صخور بها مستحاثات المنخَرْبات والكوكوليثات. وتشبه صخور الدولوميت في تكوين الجير مثيلاتها في تكويني رواقة وبشيمة. فهي متجانسة غير حديدية وتحتوي على الصوديوم. ويدل تركيبها الكيميائي وتوزيعها على أن الدولوميت قد ترسب من محاليل غنية بالماغنيسيوم. وقد أدت عمليات التحور إلى تراكمات محلية من أملاح السترونشيوم في الجزء الأعلى من التتابع التبخري والجزء الأسفل من الطبقات التي فوقها. وهناك تركيزات محلية من عنصر الفنيديوم في المواقع التي يحل فيها الجيوثيت محل البيريت وربما نشأت هذه عن طريق التفاعلات التحورية مع بلورات الفنيديوم.

Abstract. The Jir Formation, of Eocene age, consists of gypsum, anhydrite, halite and dolomite. The thickest sequence is developed in the western Sirt basin in and adjacent to a major graben system. This originated in the Eocene but is parallel to the trend of the Miocene Red Sea rift. The type section of the Jir Formation is at Wādī Faras, in the Jabal al Jīr area. This is a thin, basin margin exposure of porphyrotopic secondary gypsum with dolomite beds. In the subsurface of the Meulagh graben, the formation attains 1 km and consists of anhydrite and halite with dolomite. The evaporites at Wādī Faras are of shallow-water lagoonal and sabkha origin, with foraminifera-rich carbonates indicating periodic marine influx. Laminated anhydrite within the graben was probably formed in a large lagoon below wave-base. Halite was deposited in a closed salt-lake which occupied only the central part of the basin. Evaporite deposition ended in the late Eocene when marine water flooded the basin and brought in coccoliths and foraminifera. The dolomite of the Jir and underlying Rawāghah and Bishīmah Formations is similar. It is stoichiometric, non-ferroan and with high Na content. Its composition and distribution indicate that the dolomite has been formed from Mg-rich brines of evaporitic origin. Diagenetic processes included the local accumulation of Sr^{2+} in the upper part of the evaporite sequence and the lower part of the overlying strata. Local concentrations of vanadium occur in goethite replacements of pyrite and these may have been formed by diagenetic reactions with vanadium porphyrins.

---

[1] Department of Geology, Southampton University, Southampton, SO9 5NH, England.

INTRODUCTION AND STRATIGRAPHIC FRAMEWORK

The term "Jir Formation" is used here for a major evaporite formation of Eocene age. This is extensively developed in the subsurface of the Meulagh graben (Zallah trough) in the western part of the Sirt basin and exposed in the southeastern edge of the Hūn graben (Fig. 1). The early history and origin of the Sirt basin has been discussed recently by Gumati and Kanes (1985) who gave references to previous work.

The unit, originally called the "Gir Gypsum", at outcrop (Burollet, 1960) was subsequently classified as the "Hun Evaporite Member" of the "Gir Formation" in the subsurface (Barr and Weegar, 1972). It was then termed the "Al Jir Formation" at the surface (Mijalković, 1977; Banerjee, 1980). In this paper the authors use the spelling "Jir Formation" (and avoid the use of two definite articles "the" and "Al") for both surface and subsurface evaporites. In the Meulagh graben this unit is very thick (Fig. 1) and consists of anhydrite and halite with thin beds of dolomite. The evaporites of the surface and subsurface are clearly linked as one lithological unit.

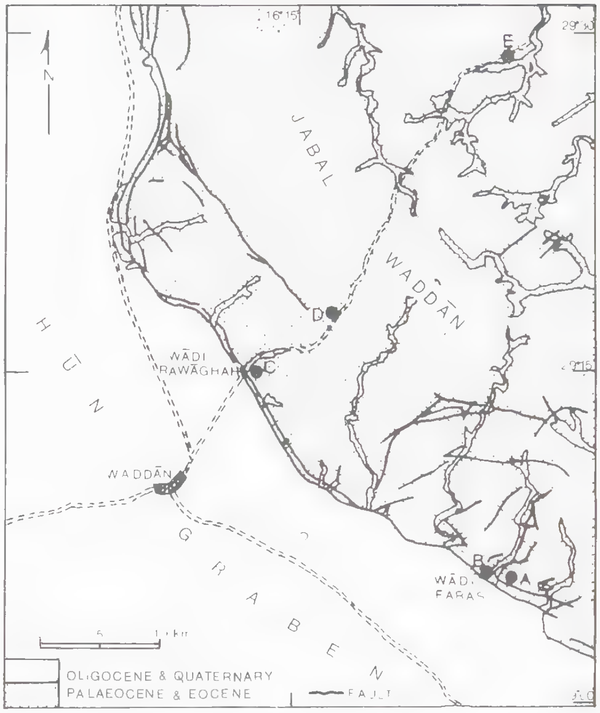

Fig. 2. Location map, with very simplified geology, showing the Wādī Faras (*A*, *B*) and Wādī ar Rawāghah (*C*) exposures and two additional sampling sites, *D* and *E* (Jahanāt Sīdī al Muntasar). The positions of wādīs on Jabal Waddān are shown. For details see the geological maps of Shakoor and Shaqroni (1984, Figs. 4, 5 and 22) and the Geological Map of Libya: Sheet Hūn, NH 33-11 on which this is broadly based.

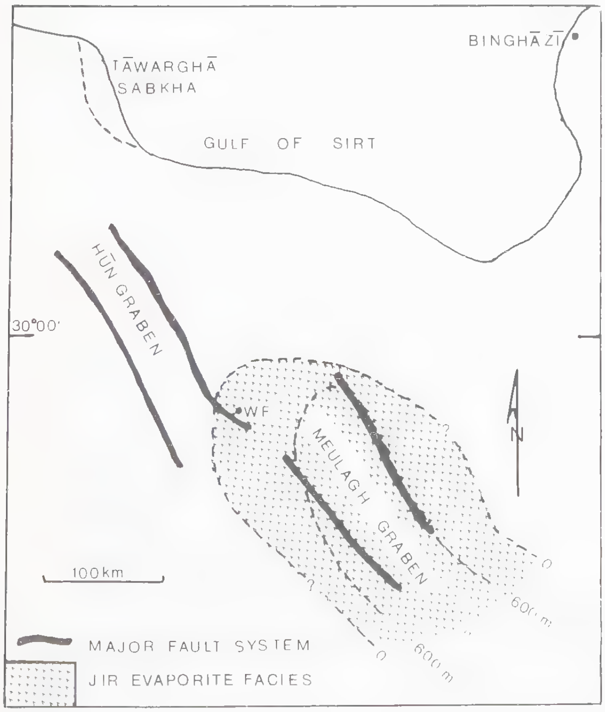

Fig. 1. Generalized distribution and thicknesses of Jir evaporites in the Sirt basin. Details of the complex pattern of faults are not shown, only the locations of the major graben boundary faults. Lack of borehole information means that there is uncertainty about the extent of the evaporites towards the southeast.

Problems exist about the location of the type section of the Jir Formation. Barr and Weegar in 1972 designated Oasis well Y1-59 (28°09′14″ N: 18°36′15″ E) as the type section of the Gir Formation. A surface type section of the "Al Jir Formation" was, however, designated by Shakoor and Shaqroni (1980) at Wādī Faras in Jabal al Jīr (Fig. 2) where it consists of 52 m of gypsum and dolomite. The question arises as to whether the surface section or the well is the true type section. Hedberg (1976) stated that subsurface stratotypes can be established if adequate sections are lacking but that preference should generally be given to the surface unit as the type. In the present case the surface exposure is adequate (although not ideal because the sequence is thin) and a more readily available source of samples. The section at Wādī Faras in Jabal al Jīr is thus regarded here as the type section. The Oasis well Y1-59 is taken as the hypostratotype, or major reference section, for the subsurface of the Meulagh graben.

The Jir Formation underlies the Wādī Thamat Formation (Burollet, 1960; Barr and Weegar, 1972; Shakoor and Shaqroni, 1980). The evaporites overlie the porous dolomite which has been referred to as the "Rawāghah Member" (of the Bishīmah Formation) at the surface (Barr and Weegar, 1972; Shakoor and Shaqroni, 1980) and the "Facha Dolomite Formation" in the subsurface (Gumati and Kanes, 1985). It is a major reservoir in several oil fields. Two separate names are not justified and thus in the present paper the member is raised to "Rawāghah Formation" and used for both surface and subsurface. As a consequence the Bishīmah Formation is restricted here so as to consist only of the underlying Khayir and Wādī Zākīm Members. The type section for the Rawāghah Formation is, as designated by Shakoor and Shaqroni (1980) for the member, at Wādī ar Rawāghah at the eastern edge of the Hūn graben (Fig. 2).

The lateral continuity and relative position in the sequence of these lithostratigraphic units is clear. There is, however, some uncertainty about the age of the Jir Formation at the surface and in the subsurface. At the surface the evaporites have been dated as Middle Eocene (Barr and Weegar, 1972; Shakoor and Shaqroni, 1980; Megerisi and Mamgain, 1980) but in the Meulagh graben as Lower Eocene (Steele, 1984). The underlying dolomite formation (Rawāghah) is regarded as of Lower Eocene age in both areas (Burollet, 1960; Barr and Weegar, 1972; Banerjee, 1980 and Steele, 1984). Further investigation is needed. If the evaporites in the subsurface also prove to be Middle Eocene then an anomalous increase in subsidence rates in the area for the early Eocene (Gumati and Kanes, 1985) is partly smoothed.

TECHNIQUES

All samples were thin-sectioned and stained by a modification of Dickson's (1965) technique. Mineral composition was determined by X.R.D., using the method of Norrish and Taylor (1962). X.R.F. was undertaken on pellets of powdered rock samples for major and trace elements. Selected samples of dolomite were analyzed by atomic absorption.

JIR FORMATION AT WĀDĪ FARAS AND IN THE SUBSURFACE

Field studies were concentrated on the Wādī Faras type section (29°05′44″ N, 16°26′29″ E). Here the Jir Formation is well exposed and consists of white to grey secondary gypsum and dolomite. The main section is in the west-facing scarp of the prominent Jabal southeast of the dry river bed. To some extent weathering and hydration have obscured sedimentary structures. Some of the gypsum is massive and some of it is laminated and it usually contains much dispersed dolomite. Some gypsum nodules occur in dolomite beds (Fig. 6) but most of the gypsum is not nodular.

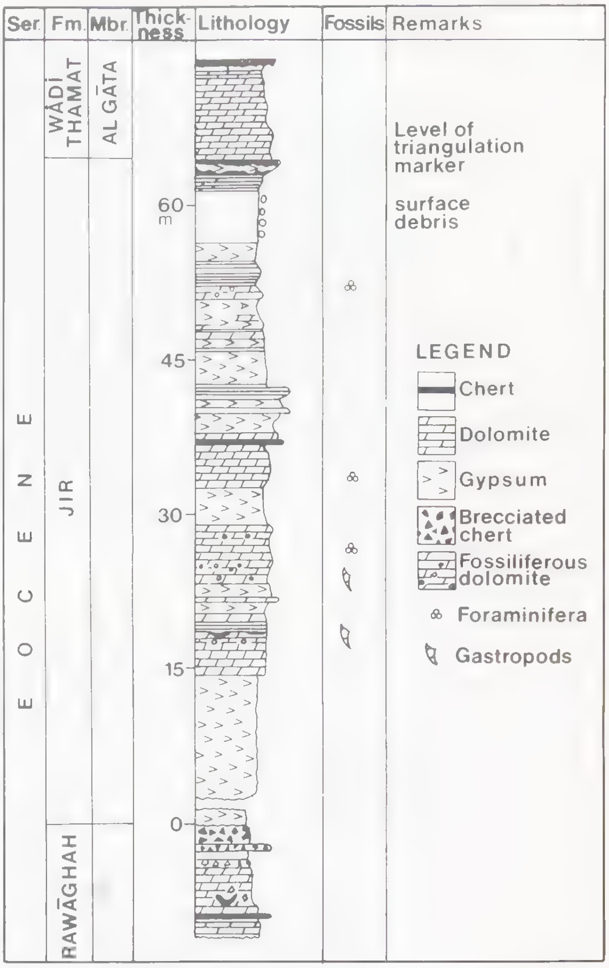

Fig. 3. Summary log of the type section of the Jir Formation at Wādī Faras. This is based on more detailed bed by bed measurements.

The thin dolomite beds are of chalky appearance and mostly structureless. Some, however, are well laminated (Fig. 6). Macrofossils are rare or absent. Chert beds occur at the top of the Jir Formation and form useful markers (Fig. 4). Some of the chert contains foraminifera (Fig. 11). The overlying Wādī

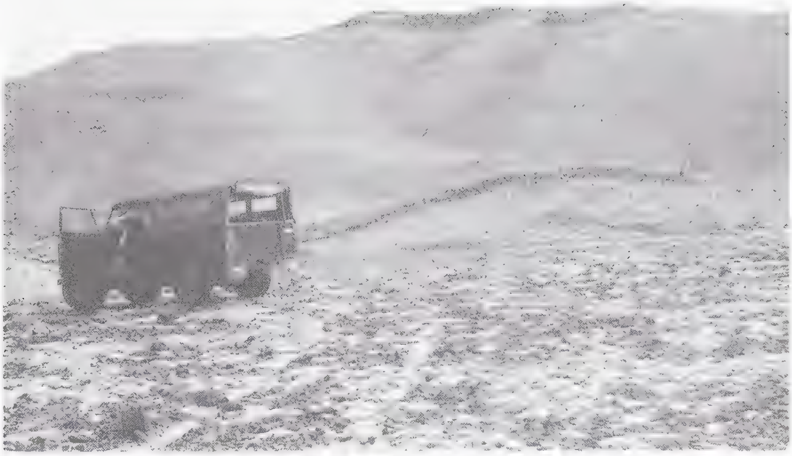

Fig. 4. The main Wādī Faras type section of gypsum and dolomite. At the top of the hill chert bands occur beneath a triangular marker, useful for location purposes.

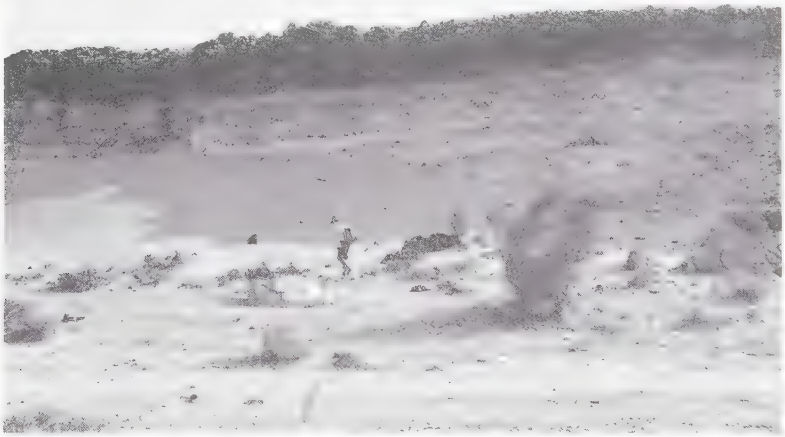

Fig. 5. A thick chert bed at the base of the Jir Formation exposed in the side of the dry stream bed of Wādī Faras.

Thamat Formation crops out on the Jabal near the summit of the hill and northeast of the type section.

An important additional exposure is provided by the northeast side of the dry stream bed of Wādī Faras (Fig. 5). Here the junction between the underlying Rawāghah Formation and the Jir Formation is marked by a thick bed of brecciated chert (Fig. 3).

In the Meulagh graben the Jir Formation is 492 m at Oasis Y1-59 well and it increases to 1067 m in the central part of the graben (Barr and Weegar, 1972). It consists here of anhydrite, with major development of halite in some areas. Much of the anhydrite is imperfectly laminated (Fig. 8). Thin beds of dolomite occur at frequent intervals and small quantities of calcite, quartz and pyrite are present.

RAWĀGHAH FORMATION AND UNDERLYING STRATA

The Rawāghah Formation and the underlying Bishīmah (Khayīr Members and Wādī Zākīm Members) and Shurfah Formations (Ammūr Member etc.) are well exposed at Wādī ar Rawāghah (Fig. 2). At the surface the Rawāghah Formation consists

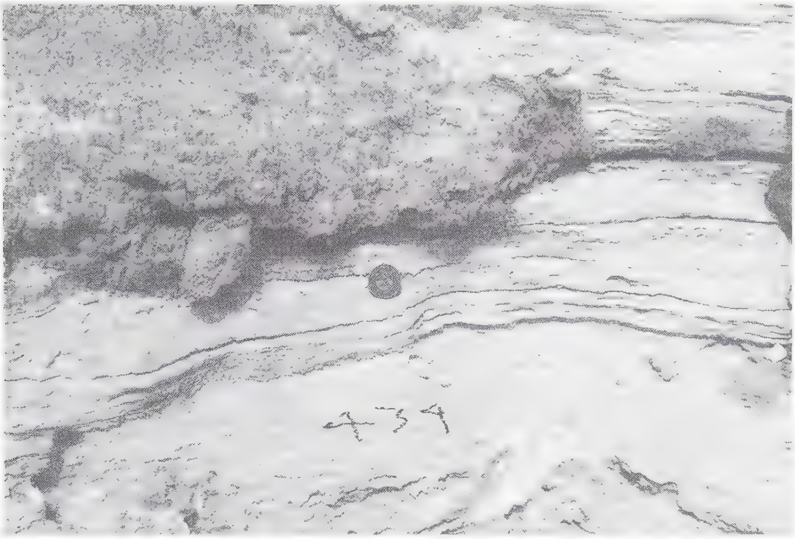

Fig. 6. Laminated dolomite interbedded with the gypsum at Wādī Faras. This contains gypsum nodules.

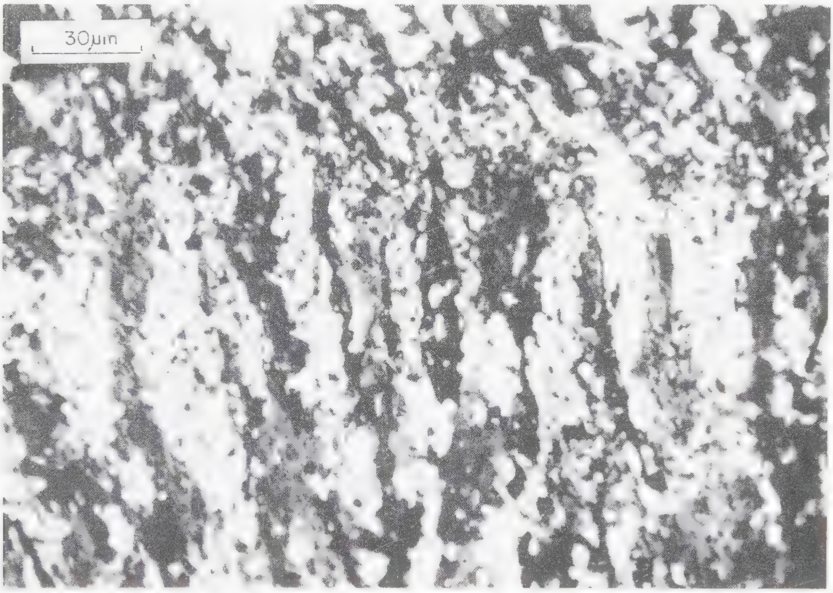

Fig. 7. Elongate xenotopic secondary gypsum crystals, Jir Formation, Wādī Faras.

of dolomite with some conspicuous beds of chert (Figs 3 and 5). In the subsurface it is mainly dolomite, with some interbeds of limestone and some of anhydrite. It attains 95 m at Oasis Y1-59 well (Barr and Weegar, 1972).

The underlying strata are also dominated by dolomites. They contain molluscs and foraminifera. The Khayīr Member consists of argillaceous dolomites with nodules of goethite in the lower part. The morphology of the goethite nodules suggests that they are replacements of pyrite nodules and they show interesting geochemical features, discussed below.

PETROGRAPHY AND MINERALOGY OF THE JIR GYPSUM

At Wādī Faras the Jir Formation consists of gypsum and dolomite with some calcite and quartz in places. The gypsum at Wādī Faras is of a secondary

Fig. 8. Laminated anhydrite from a borehole core in the Meulagh graben. Jir Formation.

type, much of it porphyrotopic, some equant (granotopic). It does not contain lenticular crystals or other typical primary features. Relics of anhydrite and the presence of gypsum pseudomorphs after anhydrite show that it is the result of hydration of anhydrite. Most of the gypsum contains abundant dolomite crystals, many of which are poikilotopically included in secondary gypsum crystals (Figs 9 and 14). Similar dolomite crystals occur in the anhydrite of the subsurface. Some foraminifera, replaced by dolomite, are present in secondary gypsum.

Fibrous displacive gypsum of satin-spar type is commonly developed (Fig. 7) and, as is usually the case, this is probably a late feature. There has been much fracture and displacement by secondary gypsum.

PETROGRAPHY AND GEOCHEMISTRY OF THE DOLOMITE

The gypsiferous dolomite of the Jir Formation and the dolomite of the underlying strata such as the Rawāghah, Bishīmah and Shurfah Formations was examined. The dolomite occurs mainly as subhexagonal crystals (Fig. 9) like those described by Pièrre *et al.* (1984). The subhexagonal crystals are syntaxially overgrown rhombs (Fig. 9). Some of the dolomite crystals are hollow, some micrite-filled and some cored by an opaque mineral, probably pyrite. Some

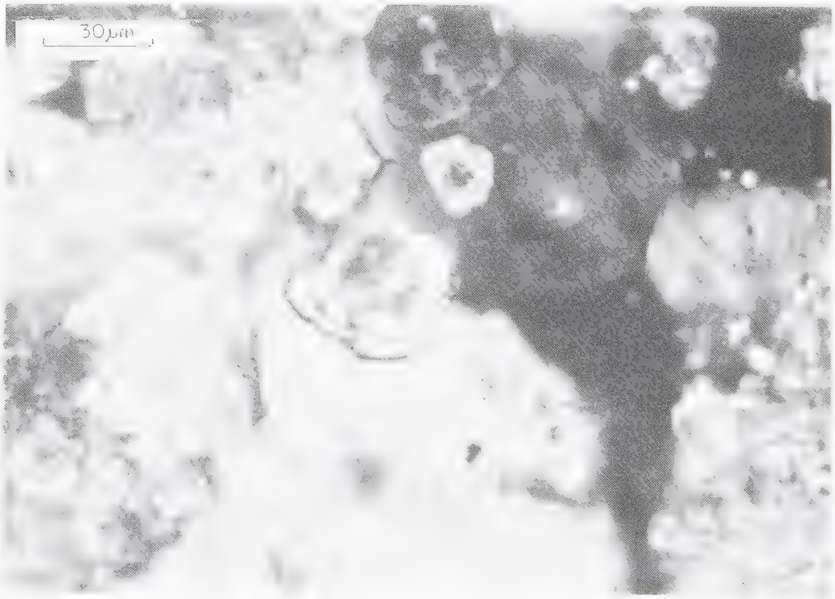

Fig. 9. Subhexagonal dolomite in secondary gypsum. Jir Formation, Wādī Faras.

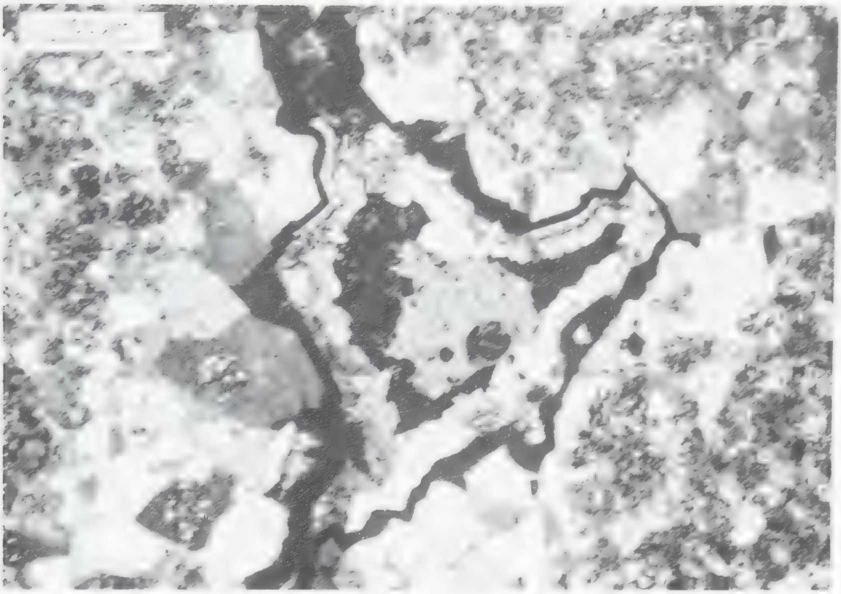

Fig. 10. Brecciated chert with quartz crystals. Oxidized pyrite (goethite) occurs as opaque void and fracture linings. Jir Formation, Wādī Faras.

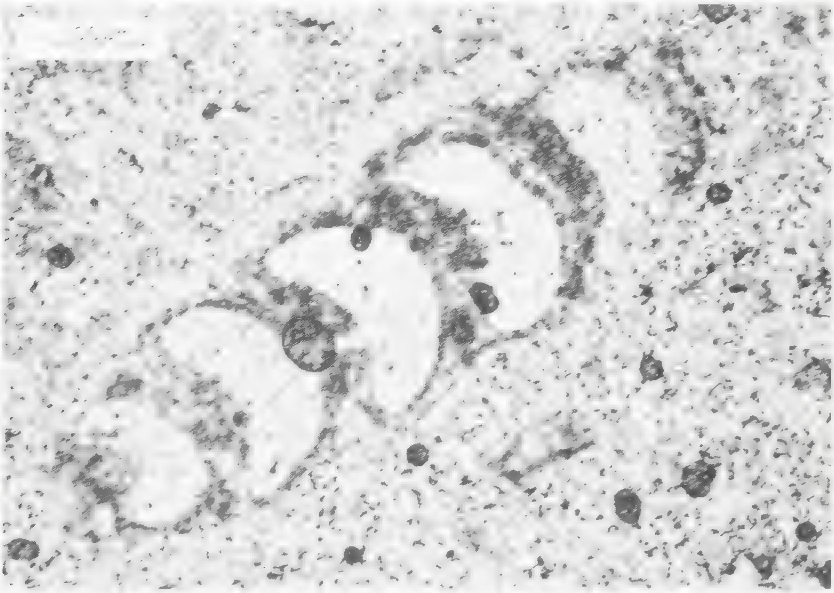

Fig. 12. Foraminifera in chert. Jir Formation, Wādī Faras.

limpid dolomite crystals were observed and many dolomite crystals are zoned. Very fine to coarse-grained rhombs also occur but are less common. Benthic foraminifera, particularly miliolinid forms are abundant in certain beds of dolomite in the Jir Formation at Wādī Faras (Fig. 12).

Minute spheroidal crystals of dolomite have been described from the Rawāghah Formation ("Facha Member") by Amiri-Garrousi (1988). These are of penecontemporaneous origin.

Samples of dolomite from the Jir and the underlying Rawāghah, Bishīmah and Shurfah Formations were investigated for content of Mn, Sr, Na, Fe, CaO and MgO (Table 1). The dolomite has very low Fe and is of "non-ferroan" type. The amount of HCl-soluble Sr (i.e. excluding celestite) in the dolomite is

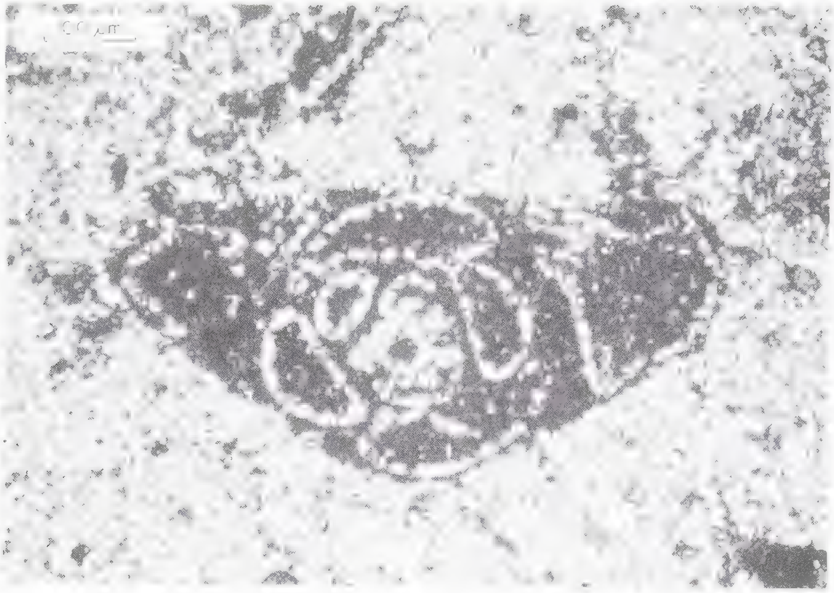

Fig. 12. Miliolinid foraminifer, Jir Formation, Wādī Faras.

Table 1. Atomic Absorption Analysis of samples of dolomite known to be almost pure and not to contain substantial quantities of other minerals (except perhaps for some pyrite in M.L. 27)

Sample No.	Formation	Location *	Mn (ppm)	Sr (ppm)	Na (ppm)	Fe (ppm)	CaO (%)	MgO (%)
M.L. 1	Bishīmah	W.R.	40	69	485	160	31.48	21.55
M.L. 12	Rawāghah	W.R.	54	68	365	200	30.08	21.55
M.L. 19	Shurfah	W.R.	77	112	420	240	30.08	20.73
M.L. 27	Bishīmah	W.R.	264	129	295	>1100	29.38	19.90
M.L. 36	Bishīmah	W.R.	74	93	540	220	29.38	19.90
M.L. 44	Bishīmah	W.R.	29	67	550	110	31.48	21.55
M.L. 70	Jir	W.F.	107	98	275	330	27.28	20.73
M.L. 85	Jir	W.F.	21	56	230	100	29.38	21.55
M.L. 89	Jir	W.F.	85	52	335	300	29.80	21.89
M.L. 131	Jir	W.F.	47	305	460	500	28.68	18.74
M.L. 145	Jir	W.F.	43	122	335	460	27.98	20.06
M.L. 186	Jir	W.F.	73	88	350	145	29.66	20.06
M.L. 193	Jir	W.F.	45	85	480	135	30.08	20.39
Mean			76	103	394	>316	29.60	20.39

* W.R.=Wādī ar Rawāghah, W.F.=Wādī Faras.

usually about 100 ppm (Table 1). Sodium averages about 400 ppm and ranges up to 550 ppm. Using a procedure of Lumsden (1979) the percentage of Ca atoms in the cations of $CaMg(CO_3)_2$ was found to range from about 49.5% to about 51.5% (Tables 2 and 3) and the dolomite is stoichiometric.

ORIGIN OF THE DOLOMITE

These geochemical characteristics are typical of dolomite of an evaporite-related type (Quest, 1985). The stratigraphic position of the dolomite within and beneath an evaporite sequence points to an origin from Mg-rich evaporitic brines. Early, probably penecontemporaneous, dolomitization is indicated by the cryptocrystalline type of dolomite found by Amiri-Garrousi (1988) in thin beds in cyclical sequences within the Rawāghah Formation in proximity to evaporites. The thin dolomite beds, in many cases with foraminifera, which occur in the Jir Formation were probably aragonitic sediments resulting from salinity reductions associated with periodic in-

Table 2. Ca% in $CaMg(CO_3)_2$ in samples from the Bishīmah Formation at Wādī ar Rawāghah

Sample No.	CaO (wt.%)	MgO (wt.%)	Ca atoms (%) in $CaMg(CO_3)_2$
M.L. 1	31.48	21.55	51.19
M.L. 12	30.08	21.55	50.06
M.L. 19	30.08	20.73	51.05
M.L. 27	29.38	19.90	51.49
M.L. 36	29.38	19.90	51.49
M.L. 44	31.48	21.55	51.19
Mean	30.31	20.86	51.08

flux of seawater. Mg-rich brines would have caused penecontemporaneous dolomitization. The syntaxially overgrown dolomite crystals, present within impermeable evaporites suggests a second phase of dolomite formation from Mg with a very local source. Perhaps a relatively unstable Mg mineral was originally also present and released Mg^{2+} on diagenesis. A replacement origin for much of the dolomite of the Rawāghah and Bishīmah Formations is shown by the fauna, mostly of foraminifera but also of some macrofossils (Shakoor and Shaqroni, 1980).

Most of these dolomites of the underlying Bishīmah and Rawāghah Formations were probably marine aragonitic sediments that were dolomitized by reaction with descending brines with high Mg^{2+}/Ca^{2+} ratios. These would have been generated by the extensive $CaSO_4$ precipitation of the Jir Formation. Clearly, a very Mg-rich environment existed because very little calcite has persisted in a large volume of dolomitized strata.

Dolomite similarly occurring beneath a lower evaporitic sequence in the same area supports the theory of dolomitization by downward percolation of evaporite brines.

Table 3. Ca% in $CaMg(CO_3)_2$ in samples from the Jir Formation at Wādī Faras

Sample No.	CaO (wt.%)	MgO (wt.%)	Ca atoms (%) in $CaMg(CO_3)_2$
M.L. 85	29.38	21.55	49.48
M.L. 89	29.80	21.89	49.44
M.L. 131	28.68	18.74	52.33
M.L. 145	27.98	20.06	50.06
M.L. 186	29.66	20.06	51.51
M.L. 193	30.08	20.39	50.40
Mean	28.98	20.50	50.54

OCCURRENCE AND ORIGIN OF CELESTITE

Small quantities of celestite occur in the Jir Formation at the top of the Wādī Faras section (Fig. 14). It is more abundant in the overlying Wādī Thamat Formation. X.R.F. bulk-rock analyses reveal high Sr^{2+} (Table 4) where celestite is present. Significant quantities of this mineral occur elsewhere around the basin. The Industrial Research Centre has published information in the explanatory booklets for the geological maps of Zallah, Wādī Abū ash Shāykh, Sabkhat Ghuzayyil and Marādah areas (NH 33-16, NH 33-12, NH 34-10 and NH 39-9). Celestite is usually a replacement of evaporites (West, 1973; West *et al.*, 1968). Sr^{2+} ions derived from overlying carbonates, particularly of aragonite, has been transported down in ground water to the upper boundary of the evaporites. Here the selective removal of strontium ions from the ground water has taken place by reaction with deposits of calcium sulphate (West, 1973). Much of the calcite and quartz in the evaporites at the surface is probably also a replacement of calcium sulphate.

VANADIUM CONCENTRATIONS

Vanadium concentrations occur in slightly radioactive goethite nodules of the Khayīr and Ammūr Members (Table 5). Goethite associated with chert within the Jir Formation is also rich in V (Table 4, Fig. 10). The association of vanadium with the seal of a hydrocarbon-bearing basin suggests that it has originated from diagenetic processes involving reactions with vanadium-bearing organic compounds, vanadium porphyrins.

SEDIMENTARY FACIES AND ENVIRONMENTS

Much of the Eocene of Libya consists of carbonates formed in an extensive shallow-water platform area (Shakoor and Shaqroni, 1980). The evaporite basin occurs southwest of an area of extensive carbonate facies and above and below shallow carbonate shelf facies. Lithological and palaeontological features of the Jir Formation at Wādī Faras indicate evaporation of water of marine origin. The presence of benthic organisms, particularly the miliolinid foraminifera (Fig. 12), suggests that the water was shallow. The lack of clastics shows that the margins of the graben were not greatly uplifted above sea level during the Eocene. The occurrence of sabkha

Table 4. Trace element composition of samples from the Jir Formation at Wādī Faras in ppm. These are in stratigraphical order and each consists of various proportions of gypsum and dolomite, with the exception of samples M.L. 153, M.L. 177b, M.L. 188 and M.L. 191 which are of chert. Sample M.L. 132 is an example of dominant dolomite (98%) and M.L. 165 of dominant gypsum (92%). High Sr values usually indicate the presence of celestite

Sample No.	TiO_2	MnO	V	Cr	Ni	Zn	Rb	Sr	Zr	Ba	Ce
M.L. 194	29	67	10	6	12	4	3	609	(1)	(0)	22
M.L. 193	36	79	31	12	9	6	3	126	5	(0)	15
M.L. 192	6	78	34	14	11	6	3	114	4	(0)	28
M.L. 191	4	45	6	26	25	(0)	3	30	5	28	(0)
M.L. 190	218	146	217	19	21	15	6	166	9	(0)	17
M.L. 189	144	103	101	20	11	9	4	354	10	(0)	(9)
M.L. 188	2	45	11	14	41	(0)	3	29	5	22	(0)
M.L. 186	(0)	119	38	11	8	4	3	119	4	(0)	33
M.L. 185	12	135	30	9	6	6	2	109	4	(0)	(6)
M.L. 182	89	32	(0)	9	5	6	2	4183	(0)	(5)	23
M.L. 180	179	48	(0)	7	5	8	3	8522	(0)	20	(3)
M.L. 179	409	51	6	6	6	5	6	272	22	14	(3)
M.L. 177b	6	85	11	14	6	(0)	2	901	(0)	20	(0)
M.L. 177a	23	91	21	11	7	5	2	1989	(0)	(1)	37
M.L. 176	93	91	23	10	9	8	(1)	17890	(0)	137	47
M.L. 175	54	70	20	8	10	6	2	2677	(0)	(8)	21
M.L. 173	97	68	19	10	8	7	4	209	5	(0)	(11)
M.L. 172	40	27	(0)	9	5	4	2	1121	(0)	(0)	(1)
M.L. 171	79	79	31	11	13	5	3	371	8	(0)	(7)
M.L. 170	1	66	23	6	8	5	2	1296	(0)	(0)	18
M.L. 169	28	48	23	11	8	5	2	262	4	(0)	20
M.L. 168	198	39	(0)	5	4	6	4	2989	(0)	10	18
M.L. 167	230	59	17	8	11	7	5	1559	(0)	(6)	16
M.L. 165	133	28	(0)	8	4	6	2	1275	31	(0)	16
M.L. 163	44	37	10	12	6	5	2	1635	(0)	(0)	(6)
M.L. 161	7	35	12	7	5	3	2	1556	(0)	(0)	(14)
M.L. 160	10	35	14	8	7	3	2	1424	(0)	(0)	(13)
M.L. 159	32	42	13	6	7	5	(1)	5500	(0)	13	(11)
M.L. 158	18	34	9	8	4	4	2	2008	(0)	(4)	(12)
M.L. 155	53	4	(2)	13	4	6	3	2382	(0)	(0)	(4)
M.L. 154	(0)	41	10	9	4	4	2	261	2	(0)	(5)
M.L. 153	(0)	63	(1)	13	19	1	2	47	4	(2)	(6)
M.L. 152	17	57	7	9	6	5	3	166	6	(0)	(5)
M.L. 149	12	52	20	11	9	5	2	345	(1)	(0)	(10)
M.L. 148	28	47	10	10	10	15	3	500	28	(0)	17
M.L. 147b	93	31	10	14	3	0	4	78	8	21	(0)
M.L. 147a	129	54	23	11	10	7	3	2146	(0)	(0)	31
M.L. 146	343	67	27	18	8	6	7	932	5	(0)	22
M.L. 145	336	82	25	9	9	7	7	161	11	(1)	(8)
M.L. 144	626	49	23	16	9	9	11	3320	(0)	13	(4)
M.L. 143	87	34	34	25	10	6	2	1299	11	(0)	25
M.L. 142	12	26	(0)	(7)	3	7	2	1483	(0)	(0)	13
M.L. 139	(1)	57	23	10	8	25	3	244	3	(0)	(14)
M.L. 138	21	48	12	9	7	5	2	736	2	(0)	18
M.L. 137	27	26	(0)	5	5	4	2	1087	(0)	(0)	(0)
M.L. 136	55	31	4	23	3	4	2	1125	(0)	(0)	(8)
M.L. 134	136	76	34	14	7	8	4	1436	5	(0)	(13)
M.L. 133	19	95	31	9	10	6	2	301	3	(0)	20
M.L. 132	32	81	21	13	9	5	3	187	4	(0)	(8)
M.L. 131	377	86	19	35	8	8	8	362	9	(0)	24
M.L. 130	165	187	22	12	23	8	5	489	3	(0)	(11)
M.L. 128	69	10	16	15	5	6	4	2223	7	15	(10)
M.L. 127	30	83	17	10	10	6	3	177	4	(0)	(2)
M.L. 126	12	36	(0)	17	3	4	2	530	(1)	(0)	20
M.L. 125	27	53	5	6	9	5	2	443	2	(0)	(1)

Table 4 (continued)

Sample No.	TiO_2	MnO	V	Cr	Ni	Zn	Rb	Sr	Zr	Ba	Ce
M.L. 124	26	73	5	10	10	4	3	188	4	(0)	21
M.L. 123	(0)	70	16	14	25	4	3	350	(1)	(0)	29
M.L. 122	(0)	47	(2)	7	62	5	(0)	493	(0)	(0)	33
M.L. 119	12	60	(0)	6	6	4	2	132	4	(0)	(1)
M.L. 118	(0)	45	(0)	10	7	4	2	225	3	(0)	(7)
M.L. 117	11	59	6	10	14	5	2	209	4	(1)	(12)
M.L. 116	50	55	8	12	18	3	3	198	6	10	(0)
M.L. 115	28	66	10	11	5	5	3	121	5	(0)	26
M.L. 114	7	71	22	5	9	4	3	330	2	(0)	20

Figures in parentheses are below the detection limits. Analysis by PW 1400 X-ray spectrometer with 3 kW rhodium anode X-ray tube and 40 s count on background.

environments during deposition of the Jir Formation is suggested by the presence of gypsum nodules in the marginal facies at Wādī Faras. Gypsum nodules are well-known features of Recent sabkhas (Shearman, 1966) and occur in such environments on the present Mediterranean coast (Ali and West, 1983). Associated non-nodular gypsum is probably of shallow-water origin.

The laminated anhydrite (Fig. 8) of the Meulagh graben is similar to that present in the Permian Castille Formation of the Delaware basin (Anderson, 1982; Anderson *et al.*, 1972), the Zechstein of Germany (Richter-Bernberg, 1957) and the "poker chip" anhydrite of the Salina Formation of the Michigan basin (Huh *et al.*, 1977).

These and other similar occurrences have been attributed to relatively deep-water origins. Laminated gypsum and aragonite occur in the sediments of the Pleistocene precursor of the Dead Sea, Lake Lissan (Neev and Emery, 1967) and was formed at a time of appreciable water depth. It should be noted, however, that lamination is also developed in the present, mainly carbonate, sediments of the Dead Sea, where the bottom is below the depth of wave action (Neev and Emery, 1967). Thus the laminated anhydrite may only imply a depth exceeding about 10 or 20 m, not necessarily any great depth. Thick halite is confined to the Meulagh graben. This halite implies complete or almost complete restriction of the water body. Presumably periodically marine access was closed and halite was precipitated in a salt lake occupying only the basin centre. The modern

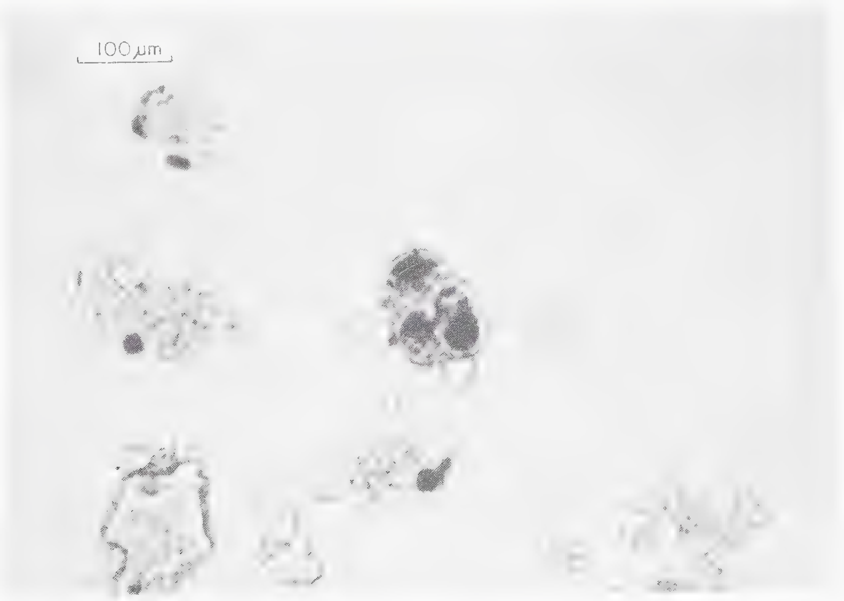

Fig. 13. Globigerinid foraminifer from marl above Jir Formation, Meulagh graben.

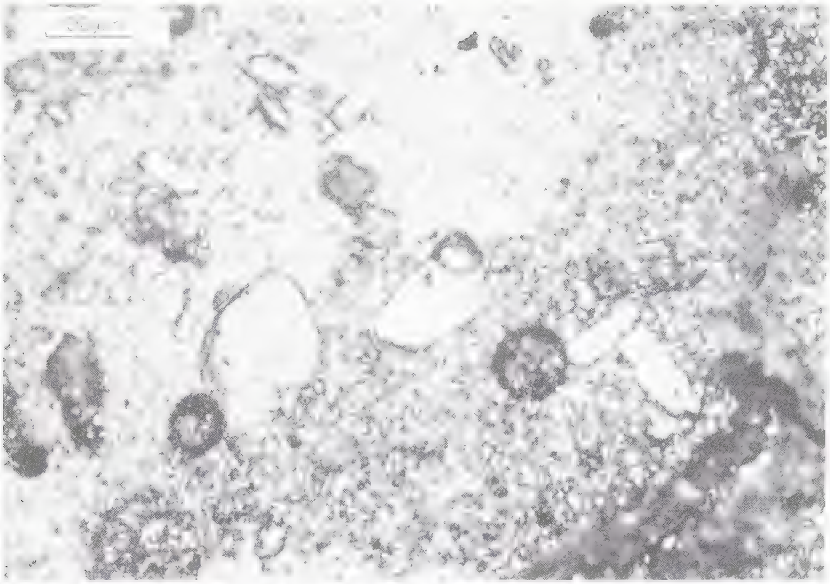

Fig. 14. Celestite crystals in coarse-grained secondary gypsum which poikilotopically includes dolomite crystals. Upper part of the Jir Formation (M.L. 180), Wādī Faras.

halite-precipitating and fault-bounded Dead Sea has this relationship to the previous calcium sulphate precipitating lake, the much larger Lake Lissan of Pleistocene age. There are major differences from this model, as noted below.

The thick anhydrite and halite of the Jir Formation at subsurface here imply the evaporation of the equivalent of many kilometres of sea water. The frequent resupply necessary was probably marked by the dolomite beds with foraminifera.

At the end of the Middle Eocene, marine water flooded the basin and carbonate sedimentation with coccoliths and foraminifera followed (Fig. 13).

The major thickness difference in the Jir Formation between the Meulagh Graben and Jabal al Jīr is a consequence of major fault movement which started at the commencement of evaporite deposition in Eocene times (Steele, 1984). Kinsman (1975) pointed out that times of initiation of new continental rifting may be periods of major evaporite formation. Although the Sirt basin rifting did not continue to the next stage, that of a proto-ocean with oceanic crust, an evaporite basin more than 150 km wide was formed. It should be noted that the rifting is very complex in detail and not necessarily a simple extensional structure. Some volcanicity was associated with it.

By the end of deposition of the Jir Formation, differential movement had attained one kilometre. The lack of clastics in the Jir Formation suggests that the upthrown sides of the grabens were not greatly uplifted above sea level. This is evidence against continued precipitation in a deep isolated basin with a water surface well below sea level like the present Dead Sea. The evaporites represent the fillings of troughs progressively downfaulted and downwarped in an extensive carbonate shelf. Periodic transgression is suggested by the frequent cyclicity of calcium sulphate and dolomite.

Comparable evaporite basins have also been produced by Palaeogene faulting on the other side of the Mediterranean Sea in southeastern France (Truc, 1980). As in the Libyan case, halite and anhydrite is localized in the strongly subsident grabens whereas on the platforms halite is absent and gypsum is dominant. The Liassic Aquitaine basin of southwestern France is another major evaporite basin that similarly contains halite, anhydrite and dolomite with hydrocarbons (Curnelle *et al.*, 1982) and this too results from large-scale extensional tectonics.

CONCLUSIONS

A preliminary depositional model has been derived. One major control on the type of sediment deposited was probably the relative sea level (Clark and Tallbocka, 1980). There was a major and widespread offlap event at or about the lower/middle Eocene

Table 5. Trace element composition in ppm of samples from the Bishīmah and Shurfah Formations which underlie the Jir Formation at Wādī ar Rawāghah. Figures in parentheses are below the detection limit

Sample No.	TiO_2	MnO	V	Cr	Ni	Zn	Rb	Sr	Zr	Ba	Ce
Rawāghah Formation (dolomites):											
M.L. 14	67	95	7	10	5	5	3	94	6	(0)	31
M.L. 13	19	107	11	10	7	6	3	184	4	(0)	19
M.L. 12	30	90	16	8	7	5	2	87	5	(0)	29
M.L. 11	22	101	3	5	6	4	2	99	5	8	11
M.L. 10	108	107	(0)	9	4	5	3	69	7	(0)	73
M.L. 9	41	134	5	10	5	6	2	98	6	(0)	35
M.L. 7	17	106	20	12	7	4	2	125	4	2	31
M.L. 6	9	79	11	12	6	5	3	80	5	(0)	17
Rawāghah Formation (chert):											
M.L. 8	8	111	4	10	19	1	2	38	5	35	(0)
Bishīmah Formation — Wādī Zakim Member (dolomitic limestones):											
M.L. 44	19	60	14	14	5	7	3	91	5	(0)	25
M.L. 43	29	75	11	10	10	5	4	107	5	(0)	36
M.L. 41	14	83	14	7	6	6	2	99	5	(0)	21
M.L. 40	62	80	11	11	5	8	4	102	5	(0)	22
M.L. 39	38	89	5	5	7	6	3	118	5	(0)	17
M.L. 38	56	109	14	10	6	5	3	125	6	(0)	25
M.L. 37	16	93	8	5	6	6	3	149	5	(0)	18
M.L. 36	79	119	13	9	5	5	5	126	6	12	(13)
M.L. 35	16	101	29	18	6	7	4	87	5	(0)	(11)
Bishīmah Formation — Khayīr Member (argillaceous dolomites):											
M.L. 34	64	85	36	14	6	7	4	97	6	(0)	19
M.L. 33	432	204	25	22	9	9	5	262	11	(0)	15
M.L. 32	197	276	36	20	10	35	5	56	7	23	15
M.L. 30	640	393	49	24	12	8	9	52	15	27	29
M.L. 29	667	480	37	30	10	11	9	30	15	(0)	29
M.L. 27	597	458	23	27	7	20	7	155	13	(0)	15
M.L. 26	1969	581	82	43	30	17	17	40	34	28	31
M.L. 25	1415	501	46	30	10	9	15	30	24	12	35
M.L. 17	279	365	29	16	10	11	6	40	9	(0)	39
M.L. 16	546	270	44	27	15	9	13	85	71	8	(7)
Bishīmah Formation — Khayīr Member (goethite nodules):											
M.L. 31	113	228	1495	95		1516	(0)	97	7	(0)	49
M.L. 28	552	410	579	77	221	132	(0)	258	10		32
Shurfah Formation — Ammūr Member (dolomites, some with molluscs):											
M.L. 18	263	452	25	13	12	14	4	158	8	52	55
M.L. 24	292	360	28	18	13	22	5	82	9	(0)	30
M.L. 23	261	242	28	20	4	8	4	117	7	12	34
M.L. 20	1060	287	82	33	16	18	11	129	20	63	25
Shurfah Formation — Qaltah Member (dolomitic carbonates):											
M.L. 18	345	175	36	27	9	7	7	69	10	(0)	(11)
M.L. 19	42	117	53	13	14	6	2	150	4	(0)	14
Ammūr Member (goethite nodules):											
M.L. 22	212	306	124	26	24	41	5	91	8	3	19
M.L. 21	608	319	3380	150	643	381	(0)	310	26	163	34

boundary (Aubry, 1985) and if this was of eustatic origin it could have caused evaporite precipitation. The other major controlling factor was major faulting and graben formation. The margins were not raised much above sea level. The basin of deposition was in the northern hemisphere arid zone.

The dominant evaporite was $CaSO_4$, nodular and of sabkha origin in some cases at the basin margin.

This was laminated in the basin centre. During burial any unaltered primary gypsum was converted to anhydrite. Recently with subaerial exposure at the basin margins secondary gypsum developed by hydration. The laminated dolomite beds suggest primary calcium carbonate sediment with foraminifera that has been diagenetically replaced. Carbonate accumulation alternated with extensive $CaSO_4$ precipitation as evaporation took place. Mg-rich brines caused dolomitization.

The thick beds of halite in the Meulagh graben indicate the evaporation of sea water in a closed or very restricted basin occupying only the downwarping centre of the whole evaporite basin. Finally sea water of near-normal marine salinity flooded the basin again bringing in coccoliths and foraminifera.

ACKNOWLEDGEMENTS

Research by M.L. has been funded by Al-Fateh University and the authors express their gratitude. Thanks are due to the staff of the Geological Engineering and Earth Science Departments, Al-Fateh University, especially Mr. Mohammed Menai, Mr. Refai Taher, Dr. M.T. Busrewil and Mr. S. Lagha for their help. The authors thank the staff of the Exploration Department of the Industrial Research Centre, Tripoli, particularly Mr. Bashir Youshah. They are very much obliged to the Occidental Oil Company of Libya, Tripoli for valuable help and to staff in the Exploration Department, particularly Mr. Mohammed El-Majdub and Mr. Mustafa Lashhab. The authors thank the staff and technicians of the Geology Department, Southampton University, particularly Mr. T. Clayton and Dr. I. Croudace. They record their gratitude to the hospitable people of Waddān town. Thanks are extended to Mr. Taib Lashhab of Zlīṭan for his help in many respects.

REFERENCES

Ali, Y.A. and West, I.M. (1983). Relationship of modern gypsum nodules in sabkhas of loess to composition of brine and sediments in northern Egypt. *J. Sediment. Petrology*, **53**, 1151–1168.

Amiri-Garrousi, K. (1988). Eocene spheroidal dolomite from the western Sirte Basin, Libya. *Sedimentology*, **35**, 577–585.

Anderson, R.Y. (1982). A long geoclimatic record from the Permian. *J. Geophys. Res.*, **87**, 7285–7294.

Anderson, R.Y., Dean, W.E., Kirkland, D.W. and Snider, H.I. (1972). Permian Castile varved anhydrite sequence, west Texas and New Mexico. *Bull. Am. Geol. Soc.*, **83**, 59–86.

Aubry, M.P. (1985). Northwestern European Palaeogene magnetostratigraphy, biostratigraphy and palaeogeography: calcareous nannofossil evidence. *Geology*, **13**, 198–202.

Banerjee, S. (1980). Stratigraphic Lexicon of Libya. *Ind. Res. Cent.*, Tripoli, Bull. **13**, 300 p.

Barr, F.T. and Weegar, A.A. (1972). Stratigraphic Nomenclature of Sirte Basin, Libya. *Petrol. Explor. Soc. Libya*, 179 p.

Burke, K. and Dewey, J. (1974). Two plates in Africa during the Cretaceous? *Nature*, **249**, 313–316.

Burollet, P.F. (1960). Lexique Stratigraphique International, 4, Afrique, Pt. 4a, Libye. *Comm. Strat., Cent. Nat. Rech. Sci.*, 62 p.

Clark, D.N. and Tallbacka, L. (1980). The Zechstein deposits of southern Denmark. *Contrib. Sedimentology*, **9**, 205–231.

Curnelle, R., Duboiso, P. and Seguin, J.C. (1982). The Mesozoic–Tertiary evolution of the Aquitaine Basin. *Philos. Trans. R. Soc.* London, A, **305**, 63–84.

Dickson, J.A.D. (1965). A modified staining technique for carbonates in thin-sections. *Nature*, **205**, 587–588.

Gumati, Y.D. and Kanes, W.H. (1985). Early Tertiary subsidence and sedimentary facies — northern Sirte Basin, Libya. *Bull. Am. Assoc. Petrol. Geol.*, **69**, 39–52.

Hedberg, H.D. (1976). *International Stratigraphic Guide: A Guide to Stratigraphic Classification, Terminology and Procedure*. John Wiley and Sons, New York, N.Y., 200 p.

Huh, J.M., Briggs, L. and Gill, D. (1977). Depositional environments of the Niagara–Salina pinnacle reefs in the northern shelf of the Michigan Basin. *In*: Reefs and Evaporites (*ed.* J. Fischer). *Am. Assoc. Petrol. Geol., Studies in Geol.*, **15**, 1–21.

Jordi, H.A. and Lonfat, F. (1963). Stratigraphic subdivision and problems in Upper Cretaceous and Lower Tertiary deposits in northwestern Libya. *Rev. Inst. Fr. Pétrole*, **18**, 1428–1436.

Kinsman, D.J.J. (1975). Salt floors to geosynclines. *Nature*, **255**, 375–378.

Lumsden, D.N. (1979). Discrepancy between thin-section and X-ray estimates of dolomite in limestone. *J. Sediment. Petrology*, **49**, 429–436.

Magnier, P. and Langhe, R. (1960). Carte Géologique Bu-Ngem Giofra, scale 1 : 500 000. *Ind. Res. Cent.*, Tripoli.

Megerisi, M. and Mamgain, V.D. (1980). The Upper Cretaceous–Tertiary Formations of northern Libya. *In*: *The Geology of Libya* (*eds* M.J. Salem and M.T. Busrewil). Academic Press, London, **II**, 393–418.

Mijalković, N. (1977). Explanatory Booklet of Geological Map of Libya (Al Qaddahiyah Sheet). *Ind. Res. Cent.*, Tripoli, 121 p.

Neev, D. and Emery, K.O. (1967). *The Dead Sea: Depositional Processes and Environments of Evaporites*, 147 p.

Norrish, K. and Taylor, R.M. (1962). Quantitative analysis by X-ray diffraction. *Clay Mineralogy*, **5**, 98–109.

Pièrre, C., Ortlieb, L. and Person, A. (1984). Supratidal evaporitic dolomite at Ojo de Liebre lagoon: mineralogical and isotopic arguments for primary crystallization. *J. Sediment. Petrology*, **54**, 1049–1061.

Quest, M. (1985). *Petrographical and Geochemical Studies of the Portland and Purbeck Beds of Dorset, England*. Ph.D. Thesis, *Univ. of Birmingham, England*, 199 p.

Richter-Bernberg, G. (1957). Isochrone Warven im Anhydrite des Zechstein 2. *Dtsch. Geol. Landesanst. Geol. Jahrb. Bd.*, **74**, 601–610.

Shakoor, A. and Shaqroni, Y. (1980). Explanatory Booklet of Geological Map of Libya (Hūn Sheet), *Ind. Res. Cent.*, Tripoli, 117 p.

SHEARMAN, D.J. (1966). Origin of marine evaporites by diagenesis. *Trans. Inst. Ming. Metall.*, **75**, B208–215.

STEELE, A.D. (1984). Southwest Sirte Basin Study, Gir Formation (Hun Member), Interim Report, Occidental Oil Company of Libya, Inc. Tripoli, 13 p.

TRUC, G. (1980). Evaporites in a subsident continental basin (Ludian and Stampian of Mormoiron-Pernes in southeastern France): sequential aspects of deposition, primary facies and their diagenetic evolution. *In*: *Evaporite Deposits: Illustration and Interpretation of Some Environmental Sequences.* (*eds* Commité des Technicians). Editions Technip, Paris, 266 p., 61–71.

VAN HOUTEN, F.B. (1983). Sirte Basin, north-central Libya: Cretaceous rifting above a fixed mantle hotspot? *Geology*, **11**, 115–118.

WEST, I.M. (1973). Vanished evaporites — significance of strontium minerals. *J. Sediment. Petrology*, **43**, 278–279.

WEST, I.M., BRANDON, A. and SMITH, M. (1968). Tidal flat evaporitic facies in the Viséan of Ireland. *J. Sediment. Petrology*, **38**, 1079–1093.

Depositional Facies and Diagenesis as a Guide to Correlating Porosity Zones — Al Fūrūd Formation, Ghānī Field, Sirt Basin, Libya

SULAIMAN A. ABUSHAGUR[1] AND DAVID V. LEMONE[1]

السحنات الترسيبية والتحور كدليل لمضاهاة نطاقات المسامية — تكوين الفرود ، حقل الغني ، حوض سرت ، ليبيا

س . أ. أبو شاقور ود. لومون

الخلاصـــة

يُمثل تكوين الفرود الباليوسيني الخزان الرئيسي (مكمن تركيبي — طبقي) في حقل الغني النفطي. كما أن تكويني الفاشا والجير (عصر الأيوسين) هما منتجين للنفط في نفس المنطقة. ويبلغ متوسط انتاج النفط من حقل الغني حوالي 100,000 برميل من النفط من النطاقات الثلاثة.

وقد تغير التركيب النسيجي والمعدني لتكوين الفرود تغيراً ملحوظاً عن طريق التحور. ومن عمليات التحور التي تم التعرف عليها في صخور «الفرود» الجيرية الإذابة الثانوية والتدلمت والتهدرت ، والتشقق والتلصق والتعرق. ودالات التحور الأكثر شيوعاً والأهم ، التي تحكمت في المسامية والنفاذية وتوزيعها في الصخور، هي الإذابة والتدلمت والتهدرت.

وتتراوح المسامية في تكوين الفرود بين 5 و25٪ ونوعيتها عادة قالبية وشبكية وبينحبيبية وداخل حبيبية وشقوقية. ويمكن أن تعزى المسامية والنفاذية في هذا التكوين إلى السحنات الترسيبية الأولية وإلى نوع التحور اللاحق. وقد تناقصت المسامية الأولية والثانوية باحلال الأنهيدريت والتلصّق. كما أنها في مواقع أخرى قد زادت بسبب الإذابة والتدلمت.

ويعزى التوزيع غير المنتظم للمسامية والنفاذية في تكوين الفرود بحقل الغني إلى أنواع ودرجات التغير التحوري الثانوي واللاحق للترسيب. كما يعزي كذلك لأنماط ترسيب الصخور الرسوبية الجيرية.

Abstract. Al Fūrūd Formation (Palaeocene) is the main reservoir (a structural/stratigraphical trap) in the Ghānī Oil Field. The Facha and Gir (Eocene) Formations are also producing oil in the same area. Average daily production of the Ghānī Field is about 100 000 barrels of oil from the three pay zones.

The original textural and mineralogical composition of Al Fūrūd Formation has been altered intensively by diagenesis. The most important diagenetic processes that have been recognized in Al Fūrūd carbonates are secondary dissolution, dolomitization, anhydritization, fracturing, cementation, and stylolitization. The most common, and apparently most important diagenetic parameters that controlled porosity and permeability distribution were leaching, dolomitization, and anhydritization.

Porosity in Al Fūrūd Formation ranges between 5 and 25%, and typically is moldic, fenestral, intraparticle, interparticle, and fracture. Porosity and permeability in this formation can be related to primary depositional facies and to the type of diagenesis. Primary and secondary porosities have been reduced by anhydrite replacement and cementation and enhanced by dissolution and dolomitization.

The heterogeneous distribution of porosity and permeability in Al Fūrūd Formation in the Ghānī Field is attributable to the types and intensities of secondary, post-depositional, diagenetic alterations as well as to the primary depositional patterns of the carbonate sedimentary rocks.

---

[1] University of Texas at El Paso, Department of Geological Sciences, El Paso, TX 79968, U.S.A.

INTRODUCTION

The study area is located in the western part of the Sirt basin (Concession 11) about 200 km south of the Libyan coast (Fig. 1).

This study has focused on the determination of the diagenetic changes that took place in Al Fūrūd Formation. Six cores were recovered from this formation from wells RRR-10 and RRR-29. One hundred and twenty-five (125) thin sections (1″ × 3″) were prepared and then stained with Alizarin Red-S to differentiate between dolomite and calcite. These thin sections were examined using a Zeiss petrographic research microscope. Selected samples were cut into 1-mm plaquettes, polished, and examined using Scanning Electron Microscope techniques. In order to better comprehend the mineralogy and diagenetic processes of Al Fūrūd Formation X-ray diffraction analyses of selected samples were made.

These data, in combination with the recognition of the microfauna and microflora, aid in the determination of depositional environments and, consequently, the reservoir characteristics of Al Fūrūd Formation.

DIAGENESIS OF AL FŪRŪD FORMATION

The early diagenetic processes that are recognized in Al Fūrūd Formation were associated with two types of environment: supratidal and intertidal. On the supratidal flats, temperature, evaporation rates, and salinity were high enough so that early diagenesis of evaporite and carbonate minerals was widespread. Late diagenetic alteration in the supratidal deposits probably resulted in the conversion of gypsum to anhydrite as well as continued cementation and selective replacement by anhydrite. While the supratidal sequences are typified by exhibiting early diagenetic events, the intertidal deposits are characterized by somewhat later diagenetic events. The major diagenetic processes altering these shallow, intertidal deposits and open shelf deposits include dolomitization, leaching, anhydritization, fracturing, stylolitization, and pyritization.

Dissolution has significantly increased secondary porosity and permeability, especially in the grainstone facies in both wells (Abushagur, 1983). Most of the original, fossil allochems of the dolo-mudstone facies in well RRR-29 have been leached out, resulting in excellent secondary porosity (Fig. 2). The allochems in the equivalent facies (pelletal–skeletal grainstone) in well RRR-10 have been leached only partially. This fact suggests that the allochems in well RRR-29 had not been chemically stabilized, since grain molds were formed by fabric-selective dissolution; conversely, allochems in well RRR-10 must already have been relatively chemically more stable with respect to formation fluids since there was very limited development of grain molds formed by fabric-selective

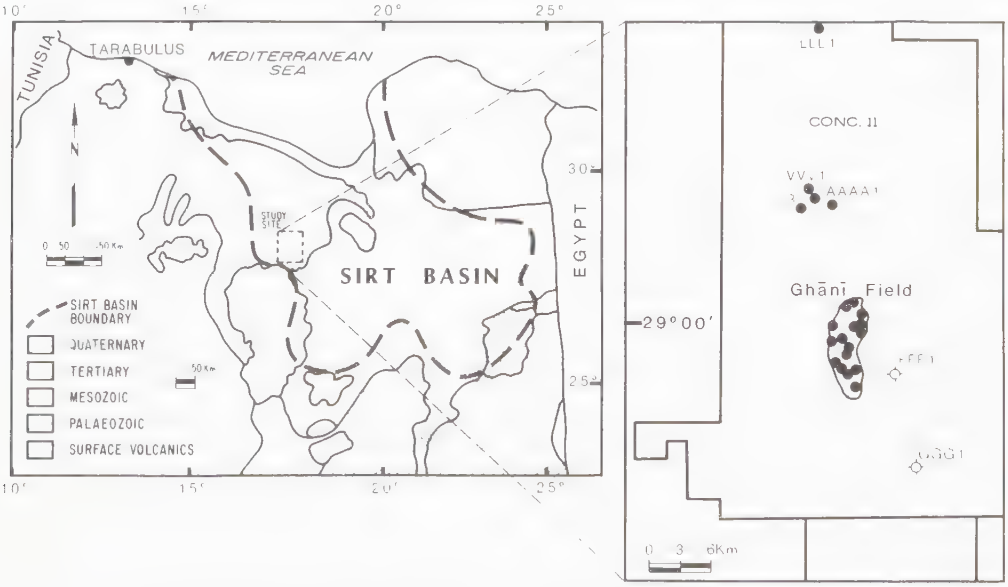

Fig. 1. Generalized geologic map and Ghānī Field location mp (modified after Roberts, 1970; Goudarzi, 1980; and Abushagur, 1983).

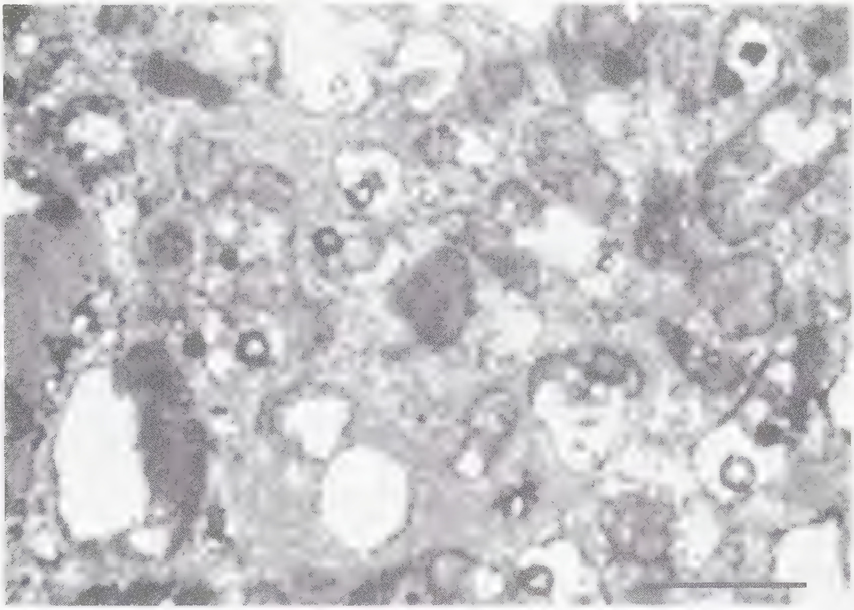

Fig. 2. Photomicrograph (cross nicols and stained) illustrating the leaching moldic porosity, intraparticle porosity and interparticle porosity. Al Fūrūd lithofacies, well RRR-29, at a depth of 1797 m. Bar scale represents 0.5 mm.

dissolution. The fluids which caused this porosity enhancement are interpreted as having been undersaturated with respect to calcium carbonate, possibly as a result of hydrocarbon maturation releasing volatile gases and fluids which were then added into connate waters in the hydrocarbon source and reservoir areas. A combination of these gases and fluids in solution should have been at least mildly corrosive to pore walls. The concept of relating secondary porosity to the arrival of oil was first developed by Chepikov *et al.* (1961). They suggested that the arrival of oil in the reservoir leads to cement dissolution and improves reservoir properties. The concept of carbonate mineral dissolution by carbon dioxide released from maturing organic matter was introduced by Schmidt and McDonald (1979).

Features suggesting sediment compaction apparently are lacking in Al Fūrūd carbonates. The absence of such features has often been taken as evidence that cementation and lithification must have developed early in carbonate grainstones, prior to significant compaction. Contradictory evidence, however, shows that fine-grained limestones may undergo considerable compaction without experiencing responses such as shell breakage (Shinn *et al.*, 1965). Pressure solution between grains is not recognized. Stylolites, conversely, are very common, especially in the bioclastic facies in both wells (Fig. 3). The stylolites that are observed in the lower facies of Al Fūrūd carbonates are oriented parallel to the bedding and have a dark-brown dead-oil stain or organic matter. Probably chemical compaction resulted in grain-to-grain microstylolites and in stylolites which cut across the whole rock fabric.

Fracturing is recognized in the lower part of the dolo-mudstone facies in well RRR-29, but is not very common in well RRR-10. Some of these fractures show good porosity, which would increase the reservoir properties of this formation (Fig. 4).

The ORTEC analysis (X-ray fluorescence) revealed the presence of iron in Al Fūrūd Formation. A reasonable origin for the pyrite in Al Fūrūd carbonates is the reduction of the anhydrite by hydrocarbons, producing the sulphur ions which in turn reacted with the soluble iron compounds to form pyrite later in the diagenetic history. Production of the pyrite may represent the beginning of significant changes in the water chemistry in the area.

Celestite (strontium sulphate) has been documented by X-ray diffraction analysis and is common as a minor accessory mineral in the pelletal–skeletal grainstone facies in well RRR-10 (Abushagur, 1984a). The presence of celestite suggests that the source of anhydrite was probably the gypsum, which was partially dissolved, transported by descending brines, and precipitated as void fillings.

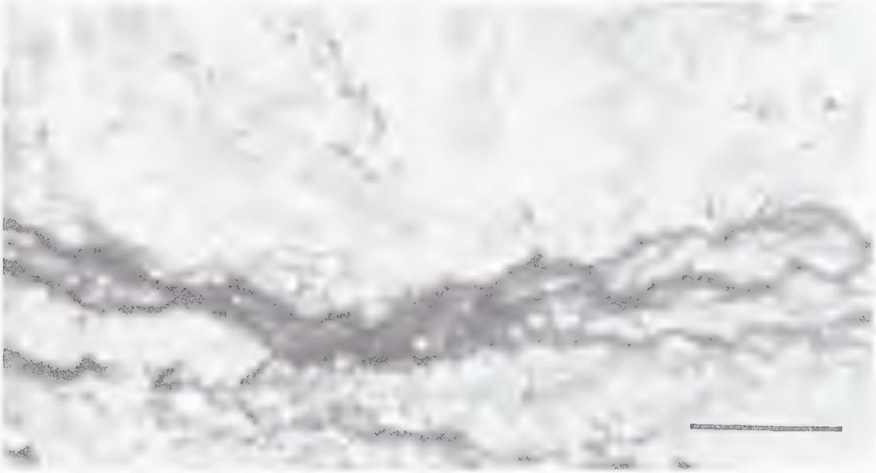

Fig. 3. Photomicrograph (cross nicols and stained) illustrating the stylolitization. Al Fūrūd lithofacies, well RRR-29, at a depth of 1828 m. Bar scale represents 0.5 mm.

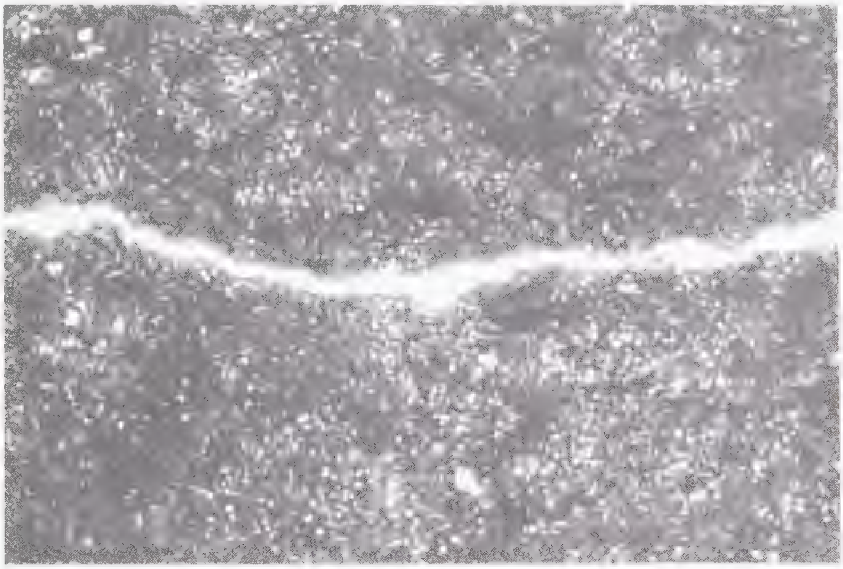

Fig. 4. Photomicrograph (cross nicols and stained) illustrating the fracture porosity. Al Fūrūd lithofacies, well RRR-29, at a depth of 1824 m. Bar scale represents 0.5 mm.

Both the anhydrite (Fig. 5) and celestite are developed typically in a supratidal environment of deposition.

DOLOMITIZATION OF AL FŪRŪD FORMATION

Intense early dolomitization is recognized in the upper Al Fūrūd Formation in the northern part of the Ghānī Field. This dolomite facies is about 10 m thick. It is associated with anhydrite inclusions throughout the entire dolomitic section. However, only 0.6 m of dolomite with anhydrite and celestite were recognized in the cored section of the similar facies in the southern area of the Ghānī Field.

Various authors have advocated a variety of possible origins for dolomite, including primary precipitation from sea water, penecontemporaneous alteration of calcium carbonate, etc. A selection of the more typical hypotheses on the secondary origin of dolomite would include such examples as dolomitization by gravity-driven seepage refluxion (Adams and

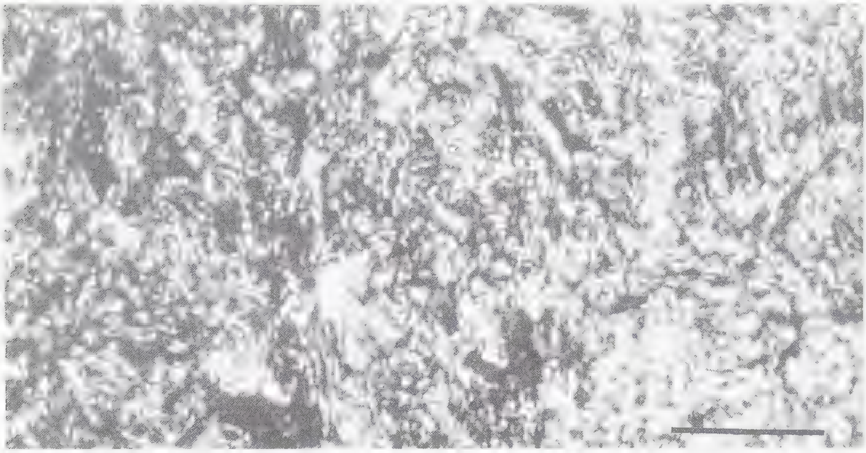

Fig. 5. Photomicrograph of thin section (plane light) at a depth of 1823 m illustrating the anhydrite microfacies Al Fūrūd lithofacies, well RRR-29. Bar scale represents 0.5 mm.

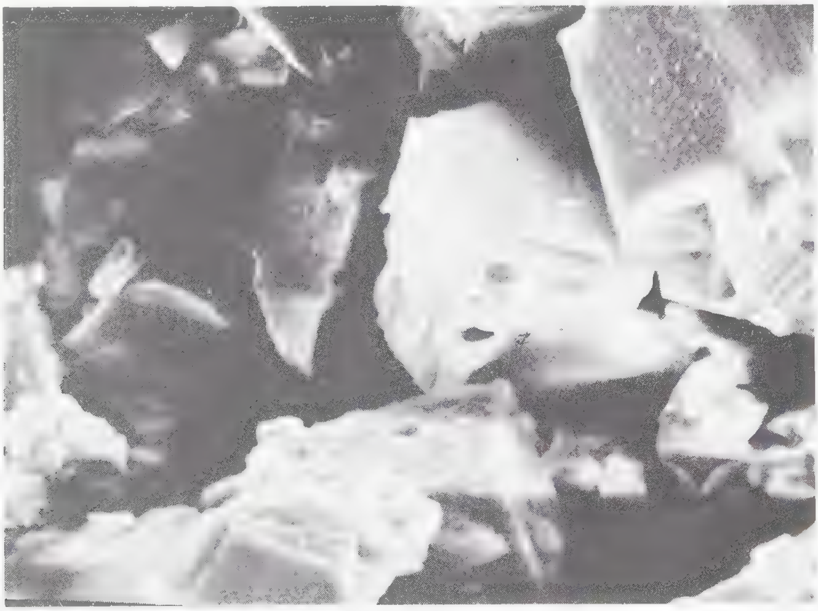

Fig. 6. SEM photomicrograph at 3000×, illustrating the euhedral to subeuhedral dolomite crystal with pore spaces. Al Fūrūd lithofacies, well RRR-10, at a depth of 1795 m.

Rhodes, 1960; Deffeyes *et al.*, 1965), by capillary concentration (Friedman and Sanders, 1967), by evaporative pumping (Hsü and Siegenthaler, 1969), and by seawater–meteoric water mixing (Land, 1973).

Dolomitization of Al Fūrūd limestones probably began with the partial replacement of the porous lime mud matrix by subeuhedral rhombohedrons (Abushagur, 1984b). It secondarily affected the coarse, pelletal–skeletal grain allochems (which are generally indicated by their cast outlines). Probably because of an original high fluid content, carbonate muds altered easily to a cryptocrystalline to microcrystalline, anhedral to subhedral dolomite (Fig. 6). Lime wackestones in Al Fūrūd Formation in the southern area of the Ghānī Field probably resisted dolomitization because they were semilithified, whereas dolomitization of wackestones in the upper Al Fūrūd Formation of the northern area probably occurred because they were less lithified and/or contained more unstable high-magnesium calcite.

Al Fūrūd dolomite is characterized by a dense

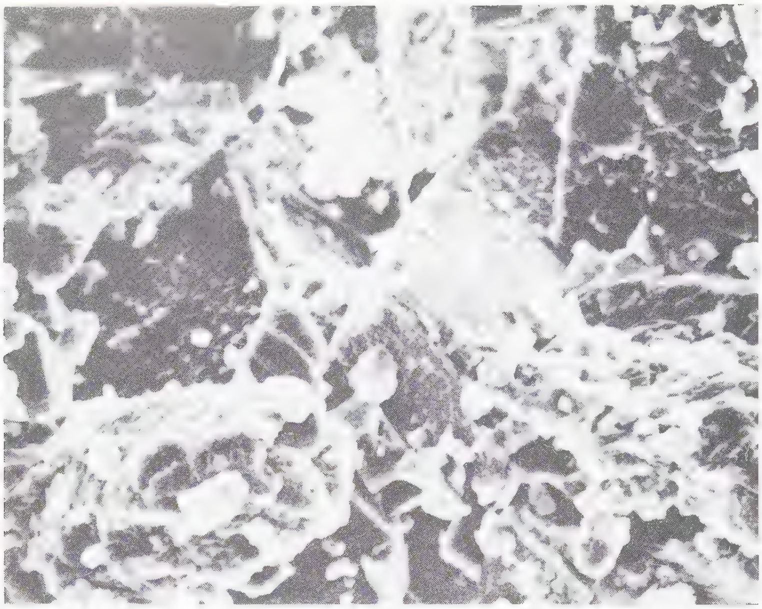

Fig. 7. SEM photomicrograph at 2000×, illustrating the dolomite crystals with high corrosion surfaces, and high porosity. Al Fūrūd lithofacies, well RRR-29, at a depth of 1824 m.

fabric and some fenestral porosity. Some dolomite crystals display planar crystal faces and sharp terminations (Fig. 6), whereas others show signs of corrosion and dissolutions (Fig. 7). The microcrystalline dolomite in the mudstone sequence consists mainly of loosely intergrown, euhedral rhombs 5–20 μm, averaging just under 10 μm.

Replacement dolomitization is interpreted as having been the main diagenetic process affecting the original calcium carbonate grains, pellets, and muds of these sequences. The relationship of the dolomite to other diagenetic features and textures (porosity occlusion) indicates that dolomite replacement took place after deposition but before significant compaction could produce either stressed carbonate grains or overly close packing in the grain-supported fabrics.

The ORTEC qualitative analysis from well RRR-10 and well RRR-29 shows that the highest strontium values are in the dolomite facies, whereas the lowest values are recorded in the limestone facies (Tables 1 and 2, Appendix I). High strontium values in dolomite, in addition to the presence of anhydrite, may indicate that the dolomite was created by the interaction of limestone with hypersaline connate brine. Kinsman (1969) reported that $(Sr^{2+})/(Ca^{2+})P$ ratios in such brines are higher than in fresh water. It might be expected that dolomitization by such a brine would raise the Sr^{2+} concentration in the dolomite to a value similar to that of dolomite in equilibrium with sea water. This could account for the fact that there are higher recorded strontium values in the dolomites than in the limestones.

The presence of anhydrite thin beds and anhydrite and celestite inclusions in a shoaling upward, prograding, regressive carbonate sequence indicates that the dolomites were formed by reaction with hypersaline brines. This would seem to suggest that Al Fūrūd dolomite probably originated by seepage refluxion.

DISCUSSION

The areas of greatest porosity preservation in the Ghānī Field area can be related to sedimentological factors and structural position (Fig. 8). The grainstone facies in well RRR-29 has the highest porosity. Single facies units, however, typically exhibit alternating porous and non-porous intervals as the result of modification by leaching, dolomitization, and occasionally by cementation (including anhydrite filling). The matrix in these two porosity units is either a dolomitized or undolomitized lime mud. The ratio of grains to lime mud may have played an important role in the later development of the secondary (leaching) porosity in Al Fūrūd Formation. Based on lime mud matrix characteristics, three porosity zones are recognized in Al Fūrūd Formation:

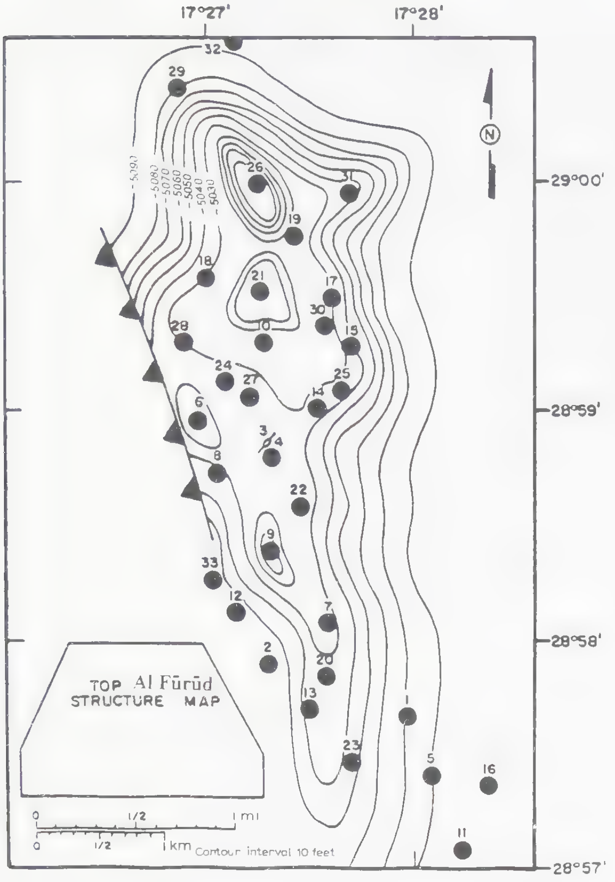

Fig. 8. Top Al Fūrūd map, Ghānī Field, Sirt basin. Numbers above well symbols represent well numbers (well RRR-32). Depths are in feet.

I. Allochems with Dolomitized Lime Mud Matrix

The effective reservoir characteristics (porosity and permeability) of Al Fūrūd Formation occur mainly in the dolomitized and partially leached facies which are equivalent to an originally coarse, pelletal–skeletal grainstone facies (Fig. 2). This high porosity zone (10–25%) is recognized in both wells. In well RRR-10, it has been observed only in the upper 0.6 m; in well RRR-29, it has been recognized in the dolo-mudstone facies. Dolomitization probably began with partial replacement of the porous granular matrix by subeuhedral rhombohedrons shortly after deposition. Leaching, evidenced by moldic porosity, was selective and, probably, vadose. Fracturing of the dolomite combined with consequent interconnected moldic porosities resulted in dramatically increased permeability and the development of an excellent reservoir rock. The most common porosity types recognized in this zone, are moldic, intraparticle, fracture, and fenestral (Fig. 9).

II. Partially Leached Allochems with Both Dolomitized and Undolomitized Lime Mud Matrix

The porosity zone is very common in the pelletal–skeletal grainstone facies (Fig. 10). Porosity ranges between 10 and 20% in well RRR-10. Porosity is not recognized in well RRR-29 because of the intense dolomitization.

Allochems in this porosity zone are partially leached. Some of the constituents are preserved and were originally probably cemented by low-magnesium calcite which is verified by staining and X-ray diffraction analysis.

Dolomitized lime mud matrix and undolomitized lime mud matrix were recognized in this zone. Porosity control in this zone is unclear as both high and low porosities were recognized in both the dolomitized lime mud matrix units and the undolomitized lime mud (micritic) units. The most common porosity types that are recognized are the moldic, intraparticle and interparticle. Minor fracture porosity, which is critical in the development of selective permeability, is recognized also.

III. Allochems with Undolomitized Lime Mud Matrix

Porosity in this zone is very low, averaging less than 5% and tight in some units. This low porosity zone is recognized in both wells (RRR-10 and RRR-29). The only significant type of porosity observed in this zone is interparticle.

Reservoir Analysis

Secondary (leaching) porosity probably developed very early after deposition and is related to depositional facies and structural position. Overlaying the Al Fūrūd pay porosity map (Fig. 11) on the top of Al Fūrūd isopotential map (Fig. 12) illustrates the fact that generally the highest porosity and oil production are associated with the structurally high areas. This may indicate that post-depositional folding resulted in the development of fractures which consequently increase reservoir quality of Al Fūrūd Formation in the western part of the Sirt basin. Moldic porosity (leaching) is abundant in the pelletal dolo-mudstone facies (equivalent to the original pelletal–skeletal grainstone facies). Low permeability values usually are associated with moldic poros-

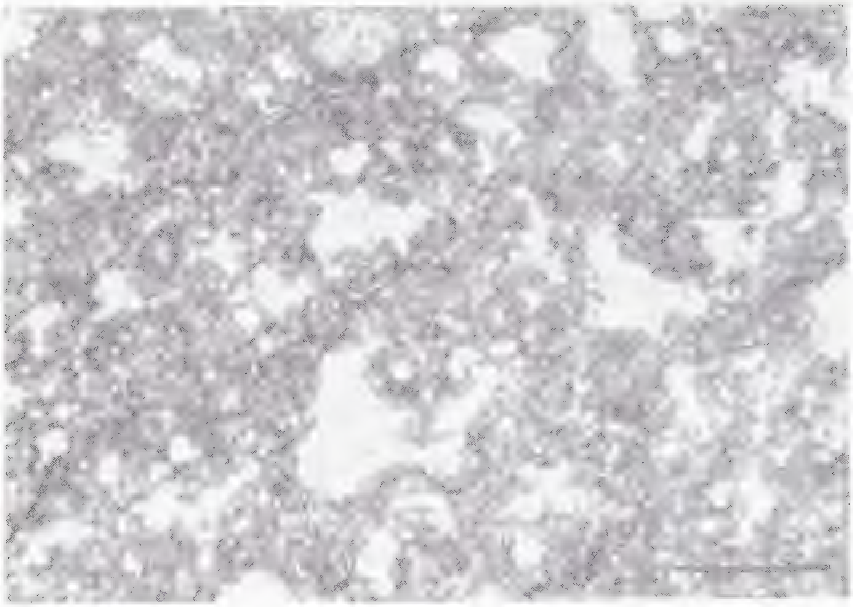

Fig. 9. Photomicrograph (cross nicols and stained) illustrating the fenestral porosity of Al Fūrūd lithofacies, well RRR-29, at a depth of 1818 m. Bar scale represents 0.5 mm.

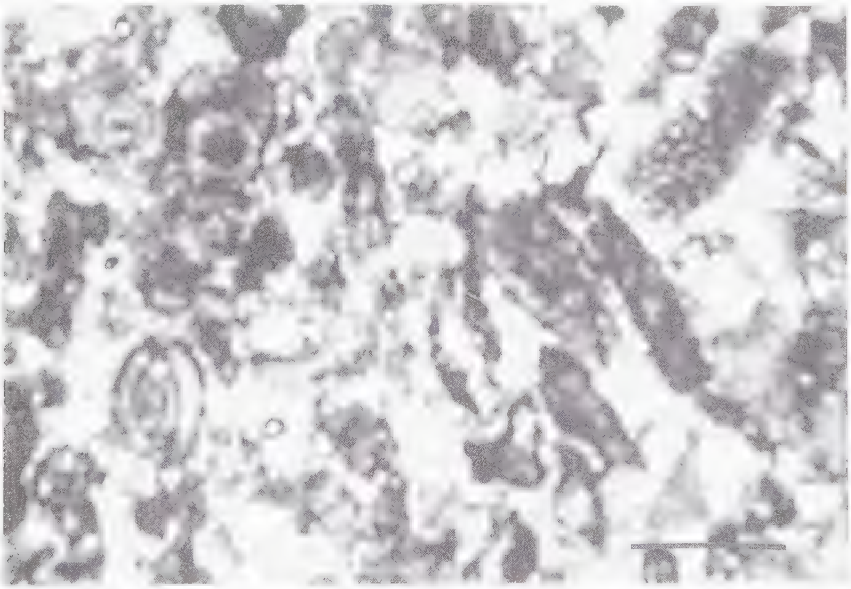

Fig. 10. Photomicrograph (cross nicols and stained) illustrating the partially leached facies with both dolomitized and undolomitized lime mud matrix. Al Fūrūd lithofacies, well RRR-29, at a depth of 1798 m. Bar scale represents 0.5 mm.

ity; however, the occurrence of fracture porosity in association with moldic porosity can dramatically increase the reservoir potential of a formation. Fenestral porosity is present in the supratidal facies (Fig. 9), whereas interparticle porosity is associated with the foraminiferal grainstone, algal, and bioclastic facies (wells RRR-10 and RRR-29). Bebout and Pendexter (1975) have concluded that the porosity in the Zalṭan Field area is related to the original depositional fabric and inversely proportional to the degree of post-depositional packing. Al Balaṭ Field in the central part of the basin and Intisār "A" & "D" Fields in the eastern part of the basin, are producing oil from Palaeocene units. In these fields secondary

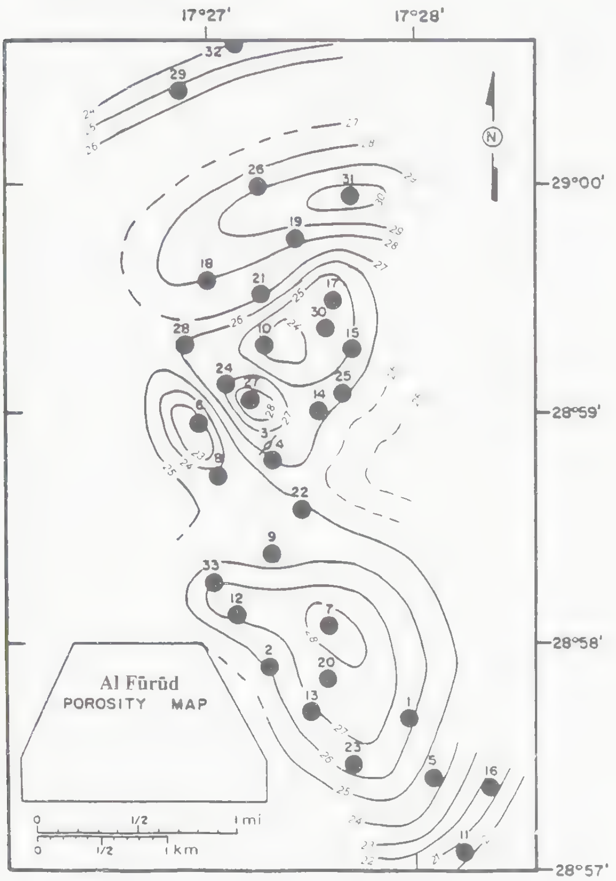

Fig. 11. Al Fūrūd porosity map, Ghānī Field, Sirt basin, Libya.

(leaching) porosity is the most important type (Terry and Williams, 1969; Brady *et al.*, 1980; Abuzekri, 1984). These studies combined with the results of this study suggest that secondary (leaching) porosity is the most common and, apparently, most important type of porosity in most parts of the basin. In the study area secondary porosity was probably developed very early after deposition and is related to depositional facies.

CONCLUSIONS

Al Fūrūd (Palaeocene) Formation in the Ghānī Oil Field generally shows a prograding, regressive sequence of three main facies:

(1) Supratidal facies: characterized by high reservoir potential. Porosity ranges between 10 and 25%, and is primarily fenestral, moldic, and fracture.
(2) Intertidal facies: characterized by high reservoir potential. Porosity averages about 15%, and is primarily moldic, intraparticle, and interparticle.
(3) Subtidal facies: reservoir potential is very poor, with porosity of less than 5% and of the interparticle type.

Development of porosity and permeability in this formation is directly related to the response of depositional facies, structural position, and subsequent diagenetic histories (leaching, dolomitization, and anhydritization). Ancient shoaling areas are typified by high porosity and extensive dolomitization whereas the intershoal areas are less porous and exhibit less dolomitization. Anhydrite infilling and cementation apparently were not a major factor in the destruction of the porosity. The pelletal dolo-mudstone facies and the foraminiferal grainstone facies, which originally possessed high porosities and permeabilities, were more affected by leaching and dolomitization, resulting in very favourable reservoir characteristics. On the other hand, mudstone–wackestone units (lime mud, algal, and bioclastic facies), which originally were characterized by low porosity and

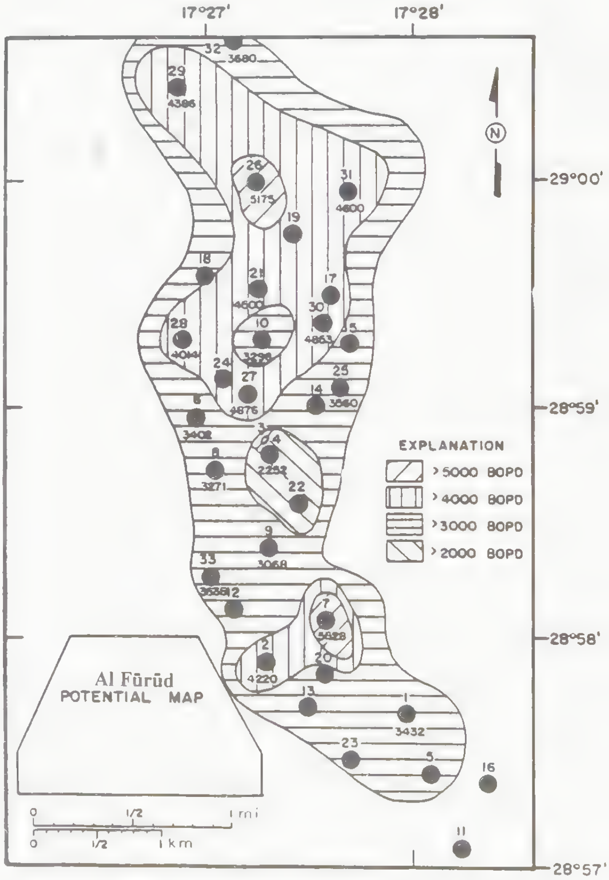

Fig. 12. Al Fūrūd isopotential map, Ghānī Field, Sirt basin.

APPENDIX I

X-ray diffraction and ORTEC (X-ray fluorescence) qualitative analysis of four samples from wells RRR-10 and RRR-29 in Al Fūrūd Formation.

Table 1. X-ray diffraction and ORTEC qualitative analyses of Al Fūrūd Formation at depths of 1786 m and 1789 m

Sample depth 1786 m (5861 ft)					Sample depth 1789 m (5870 ft)				
ORTEC qual. analysis		X-ray diffraction analysis			ORTEC qual. analysis		X-ray diffraction analysis		
Element	I	Element	I	KA	Element	I	Element	I	KA
Co (KA)	32	Dolomite	100	2.895	Ni (KA)	43	Calcite	100	
N	30	Dolomite	30	2.196	Se	42	Calcite	25	
Se	32	Dolomite	15	1.790	Br	56	Dolomite	25	
Na	37	Dolomite	13	2.018	Na (KA)	–	Calcite	24	
Mg	39	Dolomite	10	1.805	Mg	–	Calcite	20	
Al	39	Dolomite	8	2.408	Al	–	Calcite	20	
Si	56	Dolomite	5	2.676	Si	54	Calcite	10	
S	62				S	106	Dolomite	8	
Cl	59				Cl	–			
Ar	126				K	75			
K	121				Ar	47			
Ca (KA)	13136				Ca (KA)	23781			
Ca (KB)	2258				Ca (KB)	3668			
Ti	34				Ti	–			
Mn	80				Mn	–			
Fe (KA)	252				Fe (KA)	114			
Fe (KB)	92				Fe (KB)	57			
Cu	126				Cu	54			
Zn	95				Zn	38			
As	93				As	942			
Sr (KA)	2243				Sr (KA)	241			
Sr (KB)	520				Sr (KB)				

Table 2. X-ray diffraction and ORTEC qualitative analyses of Al Fūrūd Formation at depths of 1826 m and 1828 m

Sample depth 1826 m (5989 ft)					Sample depth 1828 m (5998 ft)				
ORTEC qual. analysis		X-ray diffraction analysis			ORTEC qual. analysis		X-ray diffraction analysis		
Element	I	Element	I	KA	Element	I	Element	I	KA
Au (KA)	1013	Dolomite	100	2.891	Au (KA)	665	Calcite	100	3.026
Hg	506	Calcite	50	3.034	Hg	429	Calcite	30	2.279
Na (KA)	273	Dolomite	20	2.193	Na	292	Calcite	30	1.910
Mg	305	Dolomite	15	1.789	Mg	296	Calcite	30	1.873
Al	192	Dolomite	10	2.012	Al	269	Calcite	25	2.091
Si	466	Dolomite	10	1.808	Si	547	Calcite	23	2.496
S	409	Calcite	8	1.872	S	436	Calcite	20	3.847
Cl	381	Dolomite	6	2.405	Cl	521			
Ar	426	Calcite	5	2.093	Ar	553			
K	712	Calcite	5	1.912	K	1215			
Ca (KA)	71479	Calcite	5	1.545	Ca (KA)	87399			
Ca (KB)	10843	Dolomite	3	2.669	Ca (KB)	16812			
Ti (KA)	214	Calcite	2	3.839	Ti	202			
Mn	227				Mn	107			
Fe (KA)	2038				Fe (KA)	1980			
Fe (KB)	447				Fe (KB)	451			
Ni	364				Ni	475			
Cu	342				Cu	283			
Zn	335				Zn	246			
Sr (KA)	1950				Sr (KA)	302			
Sr (KB)	520				Sr (KB)	195			

Explanation: KA = Strong X-ray peak; KB = Second X-ray peak; I = Intensity.

permeability due to the abundance of matrix, were less affected by leaching and dolomitization and have resulted in relatively poor reservoir potential.

ACKNOWLEDGEMENTS

We thank Philip Goodell, Calvin James, Laura Gavaldon, Gordon Baker, F.E. Hill, and David Eby for their valuable suggestions. We also thank Margaret Cota, Julieta R. Aguirre, Sandy Ladewig and Palmira Hart for typing the manuscript.

REFERENCES

ABUSHAGUR, S.A. (1983). *Microfacies Analysis of the Farrud Lithofacies in the Ghani Field, Sirte Basin, Libya*. M.Sc. Thesis. Univ. Texas, El Paso, Texas, 185 p.

ABUSHAGUR, S.A. (1984a). Anhydrite and celestite in the Farrud Formation (Paleocene), Sirte Basin, Libya. *New Mexico J. Sci.*, **24**(2), 8 (abstract).

ABUSHAGUR, S.A. (1984b). Dolomitization of the Farrud suite (Paleocene) Sirte Basin. *New Mexico J. Sci.*, **24**(2), 9 (abstract).

ABUZEKRI, S.K. (1984). *Microfacies Analysis of the Upper Beda Formation in the Balat Field, Sirte Basin, Libya*. M.Sc. Thesis. Univ. Texas, El Paso, Texas, 194 p.

ADAMS, J.E. and RHODES, J.L. (1960). Dolomitization by seepage refluxion. *Bull. Am. Assoc. Petrol. Geol.*, **44**(12), 1912–1920.

BEBOUT, D.B. and PENDEXTER, C. (1975). Secondary carbonate porosity as related to early Tertiary depositional facies, Zelten Field, Libya. *Bull. Am. Assoc. Petrol. Geol.*, **59**(4), 665–693.

BRADY, T.J., CAMPBELL, N.D. and MAHER, C.E. (1980). Intisar "D" Oil Field, Libya. *In*: Giant Oil Fields. *Mem. Am. Assoc. Petrol. Geol.*, **30**, 543–564.

CHEPIKOV, K.P., YERMOLOVA, U.P. and ORLOVA, N.A. (1961). Corrosion of quartz grains and examples of the possible effect of oil on the reservoir properties of sandy rocks. *Dokl. Akad. Nauk USSR*, Ser. Geol., **140**, 1111–1113 (in English).

DEFFEYES, K.S., LUCIA, F.J. and WEYL, P.K. (1965). Dolomitization of Recent and Plio-Pleistocene sediments by marine evaporite waters on Bonaire, Netherlands Antilles. *In:* Dolomitization and Limestone Diagenesis. *SEPM Spec. Publ.*, **13**, 71–87.

FRIEDMAN, G.M. and SANDERS, J.E. (1967). Origin and occurrence of dolostones. *In: Carbonate Rocks. Part A: Origin , Occurrence, and Classification*. Elsevier, Amsterdam, 267–348.

GOUDARZI, G.H. (1980). Structure-Libya. *In: The Geology of Libya* (*eds* M.J. Salem and M.T. Busrewil). Fac. Sci., Univ. Al-Fateh, Tripoli, **III**, 879–892.

HSÜ, K.J. and SIEGENTHALER, C. (1969). Preliminary experiment and hydrodynamic movement induced by evapotranspiration and their bearing on the dolomite problem. *Sedimentology*, **12**, 11–25.

KINSMAN, D.J.J. (1969). Interpretation of Sr^{2+} concentrations in carbonate minerals and rocks. *J. Sediment. Petrology*, **39**, 486–508.

LAND, L.S. (1973). Holocene meteoric dolomitization of Pleistocene limestones, North Jamaica. *Sedimentology*, **20**, 422–424.

ROBERTS, J.M. (1970). Amal Field, Libya. *In*: Geology of Giant Petroleum Fields. *Mem. Am. Assoc. Petrol. Geol.*, **14**, 438–448.

SCHMIDT, V. and MCDONALD, D.A. (1979). The role of secondary porosity in the course of sandstone diagenesis. *In*: Aspects of Diagenesis. *SEPM Spec. Publ.*, **26**, 175–207.

SHINN, E.A., GINSBURG, R.N. and LLOYD, R.M. (1965). Recent Supratidal dolomite from Andres Island, Bahamas. *In*: Dolomitization and Limestone Diagenesis. *SEPM Spec. Publ.*, **13**, 112–123.

TERRY, C.E. and WILLIAMS, J.J. (1969). The Idris "A" bioherm and Oil Field, Sirte Basin, Libya; its commercial development, regional Paleocene geologic setting and stratigraphy. *In*: Exploration for Petroleum in Europe and North Africa. *Inst. Petrol. London*, 31–68.

Sedimentary History of the Āṣiyah Formation — Upper Eocene of Al Ḥufrah Area, Western Sirt Basin, G.S.P.L.A.J.

J.M. Anketell[1] and S.M. Kumati[2]

التاريخ الترسيبي لتكوين العصيّة لرسوبيات الأيوسين الأعلى بمنطقة الحفرة غربي حوض سرت ، الجماهيرية

ج . م . أنكتيل وص . القماطي

الخلاصـــة

لقد تصدعت صخور ما قبل الأيوسيني الأعلى غربي حوض سرت بصورة واسعة . وذلك قبل تراكم رسوبيات الأيوسين العلوية . ويوجد بمنطقة الحفرة رسوبيات مميزة ترجع إلى العصر الأيوسيني الأعلى سميت هنا بتكوين العصيّة . ويقع هذا التكوين بسطح عدم توافق واضح فوق عدة تكاوين ترجع إلى العصر الأيوسيني الأوسط . وعموماً فإن سطح عدم التوافق مستو فيما عدا بعض المنحدرات التي يصل إرتفاعها إلى 5 أمتار والتي يرجع أصل تكوينها إلى عمليات التصدع . وتتميز أسطح عدم التوافق المستوى منها والمنحدر بثقوب حفرتها أنواع من مستحاثات ، *Trypanites* ، وذلك إلى جانب حصى كبيرة وجلاميد صخرية عند قاعدة منحدرات الصدوع . وفيما عدا هذه الرسوبيات الخشنة المحدودة الإنتشار فان سطح عدم التوافق يفتقر إلى مثيلاتها مما قد يشير إلى أن هذا السطح يمثل رصيف قطع أمواج قد جرفت أو كشطت كل رسوبياته عدى الخشن منها . وفيما عدا رسوبيات الجرف فإن الرسوبيات القاعية من العصر الأيوسيني الأعلِى هي عبارة عن صخور ردغة وصخور رسوبية جيرية ميكريتية رفيعة السمك هورية الصفات . وتلي هذه الرسوبيات سحنات لمرتفعات مرمّلة من الكلكرنايت ذي الطبقية المتقاطعة . ويلي إرتفاعات المرملة البحرية رسوبيات مسطحات المد والجزر التي تتضح بها جلياً القنوات المد جزرية والطبقية المتقاطعة التي تشبه عظام أسماك الرنكة والطبقية المتقاطعة وطبقات رقيقة من الستروماتوليت . وفي إتجاه قمة تتابع مسطحات المد والجزر يصحب الصخور الطينية الحمراء رسوبيات الجبس في صورة عجيرات ورقائق . وبالقرب من جرف الحبارة على طول خط صدع الجداري تتحول الطينة الحمراء وعجيرات الجبس إلى تراكمات خاصة دقيقة ذات طابع بري . وقد تكونت هذه على هيئة رقع على طول الجرف الذي يبدو جلياً أنه قد عمل كجرف شاطئ أثناء العصر الأيوسيني الأعلى . وهناك دليل على عمق مياه البحر تجاه الغرب متمثلاً في تحول رقائق وعجيرات الجبس إلى حجر جيري بالمنطقة الواقعة غرب أبو شوش . وإلى الشرق من منطقة الحفرة تبرز مرة ثانية تكشفات تكوين العصيّة بوادي بومراس بسطح عدم توافق واضح. وبالرغم من عدم العثور على رسوبيات شاطئية هنا فإننا نعتقد بأنها قد أزيلت بواسطة عوامل التعرية ، حيث أنه من المرجح أن منطقة الضهرة — الحفرة كانت عبارة عن جزيرة خلال معظم أو كل العصر الأيوسيني العلوي .

ومن القاعدة إلى أعلى ، تسجل السحنات المؤلفة لتكوين العصيّة تتابعاً طبقياً لرواسب معكوسة التعالي متغيرة إلى رواسب متعالية مع طور نهائي محدود معكوس التعالي . وقد تم تفسير هذه العلاقات واعتبار تقدم وانحسار البحار الناشيء عن ارتفاع وانخفاض مستوى سطح البحر كظاهرة عالمية ، فإن ذلك يرجع إلى العلاقة بين معدل إنخفاض وإرتفاع سطح البحر وبين معدلات الرفع والخفض الناشيء عن الحركات المحلية .

Abstract. Pre-Upper Eocene deposits of the western Sirt basin were extensively faulted prior to the deposition of Upper Eocene sediments. A distinctive development of these Upper Eocene deposits in Al Ḥufrah area is here formally designated as the Āṣiyah Formation. The formation rests with clearly defined unconformity on a variety of Middle Eocene deposits. The surface of unconformity is in general planar but is locally interrupted by fault-related cliffs up to 5 m in height. Both the planar areas and cliff faces are extensively bored by *Trypanites* ichnofauna as are cobble and boulder deposits found at the bases of some of the cliffs. With the exception of these local developments of coarse detritus and occasional concentrations of reworked large molluscan casts, the

---

[1] Department of Geology, University of Manchester, Manchester M13 9PL, England.

[2] National Oil Corporation, P.O. Box 2655, Tripoli, Libya, G.S.P.L.A.J.

surface of unconformity is clear of debris. It is suggested that the surface represents a wave-cut or wave-dominated platform from which all but the coarsest materials were swept away. Following the development of coarse residual deposits by reworking of Middle Eocene rocks, Upper Eocene sedimentation continued with the deposition of mudstones and shales with thin micritic limestones of lagoonal and/or restricted marine character. These were succeeded by cross-bedded, coarse calcarenite barforms with *Thalassinoides* formed by migrating offshore shoals and indicating an overall deepening of the region. A return to shallower conditions of deposition is recorded in the overlying sequence which is dominated by finer calcarenites and shales displaying well developed tidal channels, herring-bone cross-stratification and stromatolites. Towards the top of this tidal flat sequence, a change in lithology to red shales and mudstones, is accompanied by units of nodular and laminated gypsum deposited in supratidal flats and salinas. Immediately to the west of the Ḥabārah escarpment, along the line of the Gedārī fault zone, the red and green shales with gypsum pass abruptly into fine breccias of terrestrial character. These breccias are developed patchily along the length of the escarpment and it is proposed that the escarpment acted as a cliff-line throughout Upper Eocene times. Evidence that marine environments lay to the west is seen in the passage of the laminated and nodular gypsums into marine, bioclastic limestones in the region west of Qārat Ash Shush.

To the east of Al Ḥufrah area, the Āṣiyah Formation crops out extensively in the west facing scarps of Wādī Abū Marās, resting with strong unconformity on formations low within the Middle Eocene. Although no shoreline deposits have been recognized here, they were almost certainly removed by erosion, it would appear that the Dahra–Al Ḥufrah platform was emergent throughout the greater part, if not all, of Upper Eocene times.

From the base upwards, the facies making up the Āṣiyah Formation record a sequence of retrogradational deposits passing into progradational deposits with a final, minor retrogradational phase. Interpretation of these relationships in terms of transgression and regression against a background of global fall in sea level is explained as an interplay between rate of sea level fall and rates of uplift and downwarp consequent upon local tectonism.

INTRODUCTION

The Āṣiyah Formation, comprised of limestones, shales and evaporites of Upper Eocene age was first described by Kumati (1981) following a study of Al Ḥufrah region in the western Sirt basin. The formation is of particular importance in the evaluation of the geological history of the region since it rests with marked unconformity on a variety of Middle Eocene formations, and is demonstrably younger than a major episode of faulting which juxtaposes these older beds (Anketell and Kumati, 1991). It is characterized by rapid facies variation which, although making systematic description difficult, allows interpretation of the depositional history of the area in terms of an interplay between tectonism and sea-level rise and fall.

STRATIGRAPHY

Regional stratigraphy of west Sirt

Sediments of the western Sirt region range from Eocene to Miocene in age and are presently classified as shown in Fig. 1A (Banerjee, 1980; Megerisi and Mamgain, 1980). The type areas for these formations lie to the W and NNW of Al Ḥufrah area (Fig. 2). The succession is dominated by light grey to yellow limestones and marls with green shales and evaporites, mainly gypsum. Subordinate developments of terrigenous sediments occur in the Oligocene and Miocene.

Banerjee (1980, p. 113), states that resedimentation continued uninterrupted from the Palaeocene to the Oligocene in northwestern and central Libya, but shows hiatus both below and above the Eocene rocks in Al Jabal al Akhḍar region of Cyrenaica. A study of the Eocene to Miocene rocks of Al Ḥufrah region (Kumati, 1981) demonstrates, however, that here also the succession is interrupted by episodes of tilting and erosion of previously deposited sediments. The unconformities so produced are, with the exception of the major break at the base of the Āṣiyah Formation, not immediately apparent at outcrop, however, their angular nature is clearly obvious from regional mapping (Kumati, 1981, figs 5, 14) and Fig. 3.

The unofficial stratigraphic subdivisions and nomenclature proposed by Kumati (1981) for Al Ḥufrah region and their proposed correlation with the scheme presented in Banerjee (1980) are shown in Fig. 1B. The correlations are based on faunas and lithologies.

The Jaf Jaf and Wādī Abū Marās Members of the Ḥabārah Formation are equivalent to Al Gata and Thamad al Quṣūr Members of the Wādī Tāmet Formation respectively. The correlation is particularly clear between the Wādī Abū Marās and Thamad al Quṣūr Members and the chalk of which they are comprised makes this unit the most easily recognized in the region. Correlation throughout the rest of the succession is, however, less clear. Banerjee (1980, p. 272) gives the age range of the Qararat al Jifah

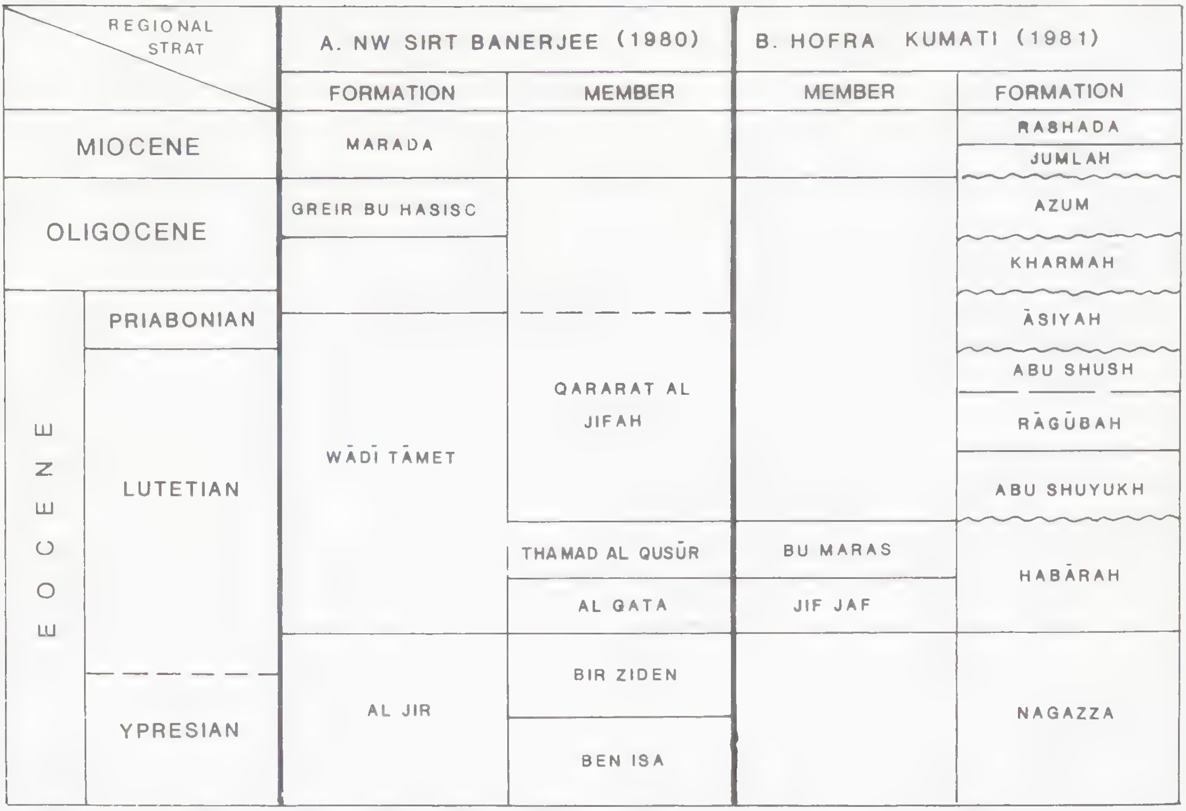

REGIONAL STRAT		A. NW SIRT BANERJEE (1980)		B. HOFRA KUMATI (1981)	
		FORMATION	MEMBER	MEMBER	FORMATION
MIOCENE		MARADA			RASHADA
					JUMLAH
OLIGOCENE		GREIR BU HASISC			AZUM
					KHARMAH
EOCENE	PRIABONIAN	WĀDĪ TĀMET	QARARAT AL JIFAH		ĀSIYAH
	LUTETIAN				ABU SHUSH
					RĀGŪBAH
					ABU SHUYUKH
			THAMAD AL QUSŪR	BU MARAS	HABĀRAH
			AL GATA	JIF JAF	
	YPRESIAN	AL JIR	BIR ZIDEN		NAGAZZA
			BEN ISA		

Fig. 1. Comparison of Tertiary stratigraphic sequences derived from studies in A. Northwest Sirt (Banerjee, 1980) and B. Al Ḥufrah region (Kumati, 1981).

Member of the Wādī Tāmet Formation as Lutetian to Priabonian and the Dor el Abd Formation as Upper Eocene to Oligocene (1980, p.102). As such, the Abū Shuyūkh and Rāqūbah Formations of Al Ḥufrah region are equivalent to only the lowermost part of the Qararat al Jifah Member and the Āṣiyah Formation would thus be equivalent to the remainder of that member plus the lower part of the Dor el Abd Formation. The remainder of the Dor el Abd Formation is equivalent to the Kharmah and Azum Formations (Fig. 1B). It is obvious that study of the areas between Al Ḥufrah and Wādī Tāmet is needed to clarify the relationships between the successions and to refine the stratigraphic nomenclature of the western Sirt.

Āṣiyah Formation — Definition

The formation displays rapid facies variations so that no one section can be taken as typical, however, Fig. 4B illustrates the main characteristics and serves as a type section to which reference may be made.

The formation is divisible into five members, each of which displays appreciable lateral facies variation across the region.

Description of the Āṣiyah Formation

Named and defined by: Anketell, J.M. and Kumati, S.M. (this paper).

See also: Kumati, S.M. Āṣiyah Formation. The Geology of (the) Al Ḥufrah Region, Sirte Basin, Libya (S.P.L.A.J.). Unpublished Ph.D. Thesis, (1981), Manchester University, England.

Named from: The Wādī Āṣiyah (17°20′00″, 29°20′00″) which lies at the foot of the Dūr Mukhaybīsh al Ḥabārah escarpment some 15 kilometres west of Al Ḥufrah (Fig. 3).

Holostratotype locality: Cliff section on the east flanks of the Jabal Qārat Ash Shush. Ref: 17°43′30″, 29°19′20″.

Definition: The Āṣiyah Formation consists of buff, bioclastic grainstones and packstones, green to

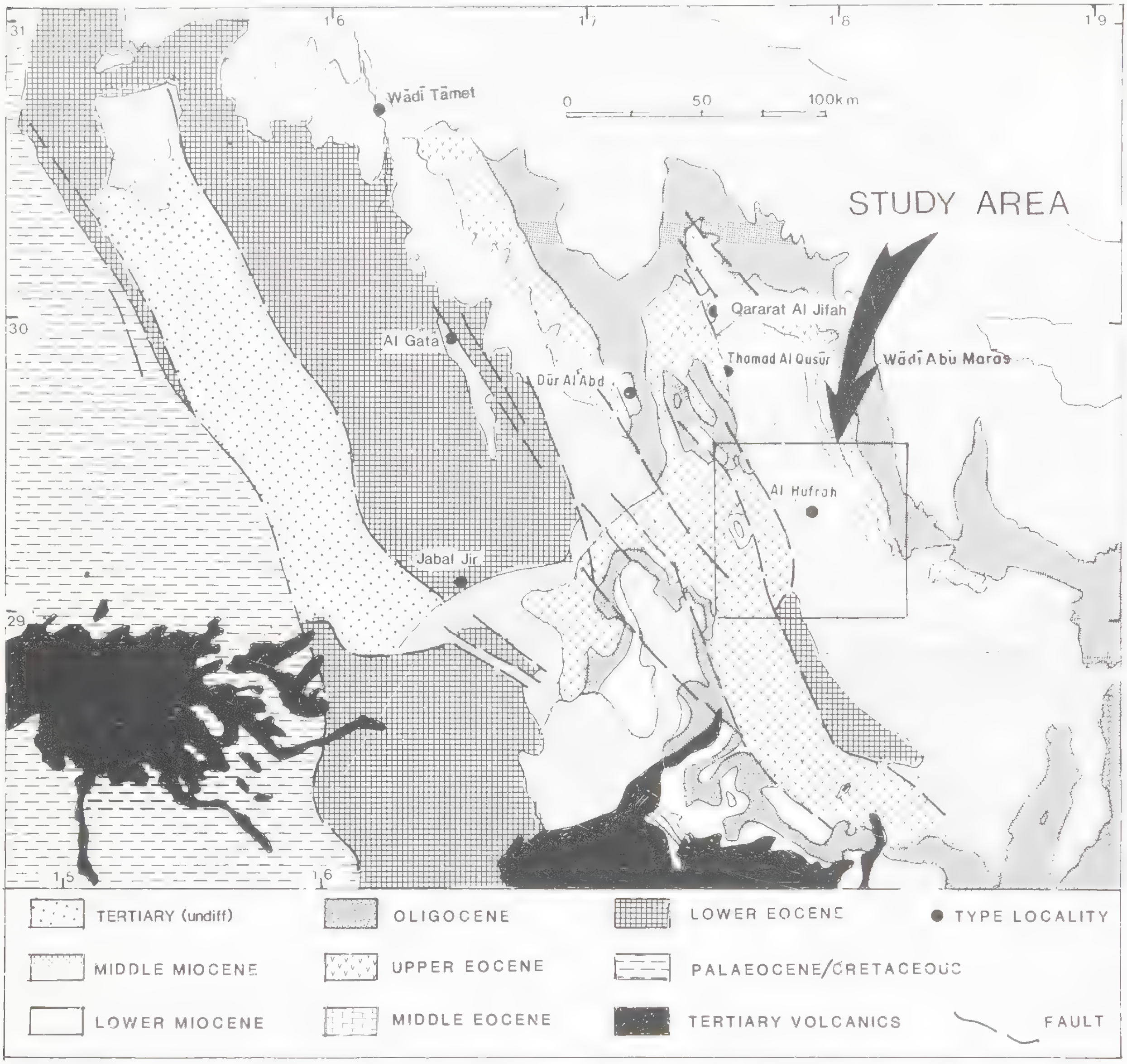
31
16
17
18
19
Wādī Tāmet
0
50
100km
STUDY AREA
Qararat Al Jifah
30
Al Gata
Thamad Al Qusūr
Wādī Abu Maras
Dūr Al Abd
Al Hufrah
Jabal Jir
29
15
16
TERTIARY (undiff)
OLIGOCENE
LOWER EOCENE
TYPE LOCALITY
MIDDLE MIOCENE
UPPER EOCENE
PALAEOCENE/CRETACEOUS
LOWER MIOCENE
MIDDLE EOCENE
TERTIARY VOLCANICS
FAULT

Fig. 2. Regional Geology of northwest Sirt basin showing location of Al Hufrah area and type areas for some Upper Tertiary formations (based on Conant and Goudarzi, 1964; Geological Map of Libya, 1 : 2 000 000).

khakhi laminated shales with interbedded argillaceous limestones and, towards the top of the succession, nodular and laminated gypsum beds passing into gypsified limestones.

Holostratotype section: Comprises 37 m of interbedded limestones, shales and evaporites which can be divided into five members for convenience of description. From bottom to top these are:

– *Member 1:* Comprised of 2.8 m of dark green laminated shales with interbedded units of unfossiliferous red micritic limestone up to 3 cm in thickness. These limestone units commonly display a *Trypanites* ichnofacies (Frey and Seilacher, 1980) indicating development of hardgrounds. Discrete nodules of fossiliferous, micritic limestones with a distinctive ochre yellow colour occur some 1.8 m above the base and occasionally coalesce to form nodular layers. The nodules are irregular and reach up to 35 cm in longest diameter.

– *Member 2:* Comprises 10 m of bioclastic grainstones and packstones interbedded with thin units

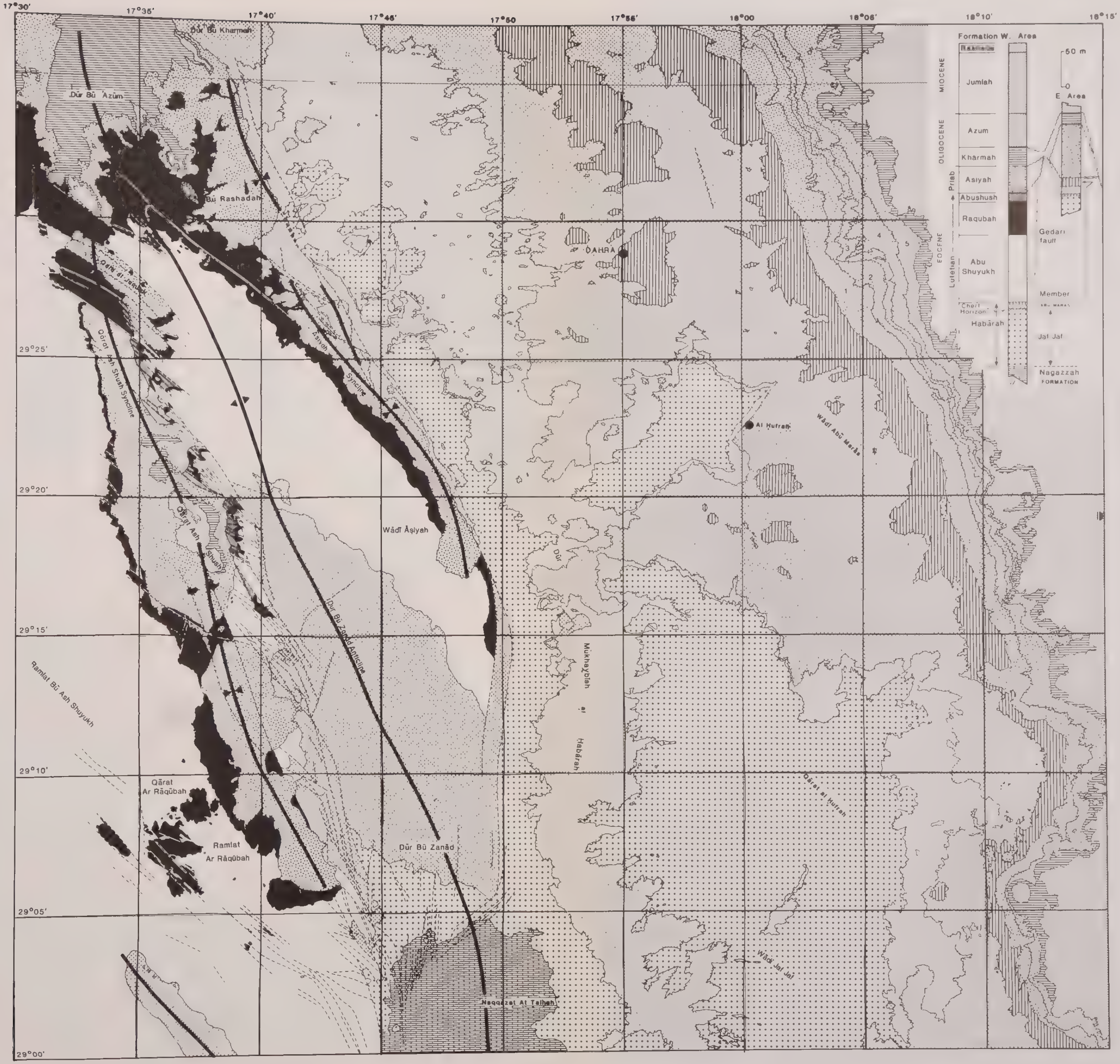
17°30'
17°35'
17°40'
17°45'
17°50'
17°55'
18°00'
18°05'
18°10'
18°15'
29°25'
29°20'
29°15'
29°10'
29°05'
29°00'
Dūr Bū Kharmah
Dūr Bū Azūm
Bū Rashadah
Qārat Ash Shush Syncline
Āṣiyah Syncline
DAHRA
Al Hufrah
Wādī Abū Marās
Wādī Āṣiyah
Dūr
Dūr Bū Zanād Anticline
Mukhayzlah al Habārah
Ramlat Bū Ash Shuyukh
Qārat Ar Rāqūbah
Ramlat Ar Rāqūbah
Dūr Bū Zanād
Qārat al Hufrah
Wādī Jaf Jaf
Naqqazat At Talhah
1
2
3
4
5
Formation W. Area
MIOCENE
OLIGOCENE
EOCENE
Priab
Lutetian
Jumlah
Azum
Kharmah
Asiyah
Abushush
Raqubah
Abu Shuyukh
Chert Horizon
Habārah
50 m
0
E Area
Gedari fault
Member
Jaf Jaf
Nagazzah FORMATION

Fig. 3. Geological Map of Al Ḥufrah region.

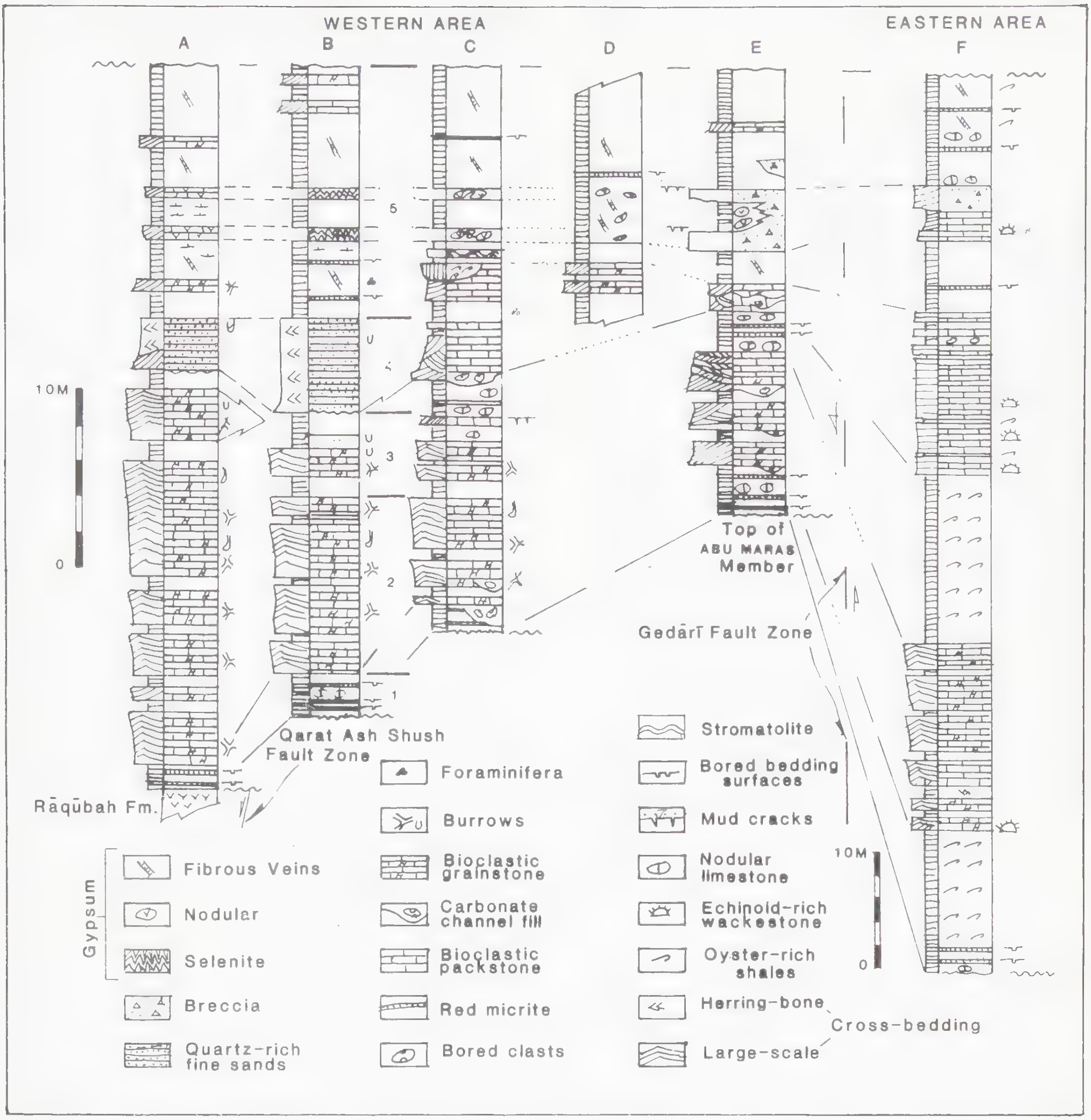
WESTERN AREA
EASTERN AREA
A
B
C
D
E
F
10M
0
5
3
2
1
Top of ABU MARAS Member
Gedārī Fault Zone
Qarat Ash Shush Fault Zone
Rāqūbah Fm.
Gypsum
Fibrous Veins
Nodular
Selenite
Breccia
Quartz-rich fine sands
Foraminifera
Burrows
Bioclastic grainstone
Carbonate channel fill
Bioclastic packstone
Red micrite
Bored clasts
Stromatolite
Bored bedding surfaces
Mud cracks
Nodular limestone
Echinoid-rich wackestone
Oyster-rich shales
Herring-bone
Large-scale
Cross-bedding
10M
0

Fig. 4. Type Section for the Āṣiyah Formation (B) in comparison with other sections recorded from a west to east transect across Al Ḥufrah region.

of olive green to khakhi shales. Individual limestone units range up to 2 m in thickness and show an upper layer of grey, cross-bedded grainstone resting on buff to yellow packstone. Complex *Thalassinoides* burrow systems are well-developed and are particularly well displayed at the interface between the packstone units and the shales.

– *Member 3:* Approximately 5 m thick, this unit is comprised of olive green and khakhi shales with one unit of bioclastic grainstone/packstone 1.4 m thick. The shales succeeding the grainstone contain several thin, fine sandy limestone units. Both these and the top of the grainstone unit are burrowed by *Diplocraterion* and *Arenicolites*.

– *Member 4:* This member is characterized by quartz-rich silty limestones with well-developed flaser bedding and rare herring-bone cross-lamination. The base of this unit is sharp and the deposits cut into the underlying shales in broad, shallow channels up to 30 cm deep.

– *Member 5:* The lowermost 3 m of this unit are characterized by lithologies similar to those of Member 1, but with the addition of thin, gypsum-filled cracks. These basal beds are succeeded by shales with three units of gypsum up to 80 cm thick. The gypsum beds are pale brown to white in colour and display a pervasive cleavage resulting from the orientation of selenite crystals at right angles to the bedding. The crystals display wavy and chevron internal lamination parallel to the bedding surfaces. Occasional thin silt layers in the intervening shales contain mudcracks with coarser silt infills. The topmost gypsum bed is succeeded by shales with cracks filled with fibrous gypsum. Towards the top of the formation these shales contain two beds of tabular cross-bedded grainstone closely comparable to those developed in Member 2.

Boundaries:

– *Base:* The contact between the formation and the underlying beds is poorly exposed and locally covered by cliff scree. The junction is sharp and shows the basal green shales resting with apparent conformity on the interbedded shales and limestones of the underlying Abu Shush Formation (Kumati, 1981) (Fig. 2). The strongly unconformable nature of this junction is, however, clearly seen on the regional scale (see below).

– *Top:* The top of the formation is in sharp contact with the succeeding Kharmah Formation, the basal beds of which fill channels which are locally eroded deeply into the shales and gypsum beds of Member 5 (Kumati, 1981, figs 5–13).

Regional extent: In Al Ḥufrah area the Āṣiyah Formation crops out in two main areas lying to the east and west of a gentle NNW–SSE trending arch (Fig. 3). To the east the formation can be followed continuously for 30 km in the scarps which flank the eastern margins of Wādī Abū Marās (Fig. 3). In the western region the formation crops out immediately to the west of the Dūr Mukhaybīsh escarpment from where it can be followed around the gentle north northwesterly plunging nose of the Dūr Bū Zanād anticline into Qārat Ash Shush syncline where it is preserved in two gently dipping ovate basins (Fig. 3). It is not known how far outside the present region the formation extends, however, the presence of shoreline deposits show that the east and west regions were separated by a land area. This area, interpreted as a tilted fault block, probably formed an "island" or a promontory of Lower to Middle Eocene rocks within an Upper Eocene sea. It is likely that the eastern and western developments of the Āṣiyah Formation were originally connected to the north and possibly to the south of Al Ḥufrah region. The present distribution of Lower and Middle Eocene rocks to north and south of Al Ḥufrah (Fig. 2) may roughly delineate the original extent of the Upper Eocene land area.

Geologic age: The formation is in general deficient in whole fossils and the limestones in particular are comprised of strongly abraded, finely comminuted shell debris. In the Wādī Abū Marās sections, however, the limestones of Members 2 and 4 contain a rich fauna of echinoids and these, together with microfaunal assemblages from the shales have formed the basis for dating the deposits. The microfaunas yielded by the samples collected were, however, poorly preserved and it generally proved difficult to identify the material to specific level.

Eastern area — Wādī Abū Marās:

Member 1.

Foraminifera: *Discorbis* cf. *finlayai* Doreen; *Pararotalia* cf. *inermis* Terquem; *Quinqueloculina*; *Tritaxia;*: *Tristix*; *Elphidium*; *Sagrina*.

Ostracoda: *Loxoconcha*; *Bairdia*; *Hermanites*; *Leguminocythereis*; *Brachcythere*.

Member 2.

Echinodermata: *Eupatagus* sp.; *Breynia meslei* Gautier; *Echinolampus africanus*; *Thagastea wetterlei* Pomel; *Schizaster meslei* Cotteau; *Echinolampus crameria* de Loriol; *Echinolampus* cf. *mokattamensis* or *E. globulus*; *Echinocyamus luciani* de Loriol; Cidaroid spines.

Member 3.

Foraminifera: *Clavulina*; *Ramulina*; *Cibicides*.

Ostracoda: *Cytherella*; *Cytherelloidea*; *Occultocythereis*.

Member 5.

Foraminifera: *Discorbis*; *Pararotalia*; *Tritaxia*; *Quinqueloculina*; *Cibicides*; *Elphidium*.

Western area:

Locality 17°43′30″, 29°25′50″.

Foraminifera: *Elphidium*; *Pararotalia*; *Triloculina*; *Quinqueloculina*; *Pyrgo*; *Glandulina*; *Ramulina*; *Tristix*; *Bolivina*; *Cycloloculina*; *Cibicides*; *Sagrina*;

Nonionella; *Gavelinella*; *Tritaxia*; *Discorbis*.

Ostracoda: *Paijenborchella*; *Bairdia*; *Cytherella*; *Cytherelloides*; *Hermanites*; *Pterygocythere*; *Brachcythere*; *Leguminocythereis*.

The echinoderm fauna contains several species, notably *Breynia meslei*; *Thagastea wetterlei*; *Schisaster meslei*; *Echinolampus crameria*; and *Echinocyamus luciani* which strongly indicate an Upper Eocene age (Airaghi, 1939). The foraminifera and ostracoda, although not identified to specific level, strongly support this as does the fact that the underlying and succeeding formations yield Middle Eocene and Lower to Middle Oligocene faunas respectively (Kumati, *ibid*).

Regional variation

Throughout the western and eastern areas the basic five-fold subdivision of the Āṣiyah Formation can be recognized; nevertheless, there are appreciable changes in thickness and lithology across an overall west to east trend (Fig. 4). In the western area the formation thins from 42 m west of Qārat Ash Shush to 25.5 m near the Dūr Mukhaybīsh al Ḥabārah escarpment before rapidly pinching out in the escarpment foothills. In the eastern region it reaches a maximum of 110 m to the west of Al Ḥufrah at 18°07′, 29°25′, thinning both to the north and south. To the north the thinning is accomplished by a gradual decrease in thickness of each member but to the south, the change is brought about by erosion and overstep at the base of the succeeding Kharmah Formation with the removal of members 4 and 5 (Fig. 3).

In the western area the W–E thinning of the formation is accompanied by a change from interbedded limestones and shales to shales with gypsum and less limestone near to a contemporaneous shoreline marked by the general trend of the Dūr Mukhaybīsh al Ḥabārah escarpment (Fig. 3). In the eastern area, where the shoreline probably lay between Al Ḥufrah and Wādī Abū Marās, there is a general increase in limestone content to the SSE. These relationships are discussed in the following section.

SEDIMENTARY FACIES AND PALAEOENVIRONMENTS

The type section (Fig. 4B) provides a convenient frame of reference for subdivision of the succession into facies types based on lithology, sedimentary structures and biological attributes. The various characteristics and the environmental interpretations of these facies are as follows:

Facies 1. Laminated Shales and Silts

Description. Laminated shales form the background sedimentation to the Āṣiyah Formation being interbedded with all other facies and predominating the lithology of Members 1, 3 and 5. The most common type is olive green to khakhi in colour occurring in units which range from 0.1 to 4.5 m thick. Individual laminae are on the scale of 2 mm and less and range from very fine calcareous silt to mud in composition. Locally the shales contain thin seams of coarser calcareous silt and fine sand displaying ripple cross-lamination. Large body fossils are absent, however, as noted above, the shales yield a microfauna of shallow marine affinities. Bioturbation occurs locally, particularly as the base of a succeeding bioclastic carbonate unit of Facies 4 is approached. The most common trace fossil appears to be *Thalassinoides*, however, the burrows do not extend deeply into the shales but instead, are confined largely to the limestone–shale interface and within the limestone bed. *Diplocraterion* is found in Member 3 in association with thin sandy limestone units. Disruption of laminae by desiccation cracks filled with fine silt, and cracks filled with fibrous gypsum are particularly common in the middle part of Member 5. Thin layers up to 10 cm in thickness containing rootlets are also found at this level. A further notable variation in the shale facies in the central part of Member 5 occurs in a narrow zone trending NNW to SSE near the Ḥabārah escarpment. Here the olive green shales pass into, and are locally interbedded with, red shaley mudstones with well developed desiccation cracks. The "redbeds" occur at the same stratigraphic level as the main gypsum horizons found not far to the west (Fig. 4).

Interpretation. The fine laminae characteristic of the greater part of this facies and the nature of the microfauna argues for deposition in a shallow marine environment, however, it is clear that the shales were laid down in a variable if limited range of depth and energy conditions. Desiccation cracks, reddening of the sediments, rootlets and the presence of trace fossils such as *Diplocraterion* and *Thalassinoides* argue for very shallow environments with periods of subaerial exposure while the regular undisturbed laminae imply deposition in somewhat deeper standing water. The evidence for occasional subaerial exposure implies an overall shallow marine, nearshore setting, however, the range and nature of the shale environments becomes clearer on consideration of the associated carbonate and evaporite facies.

Facies 2. Argillaceous Limestone Facies

Description. Two sub-facies can be recognized:

(1) Red, occasionally buff coloured, argillaceous limestone in units ranging from 0.5 up to 8 cm in thickness. Beds are sheet-like and display only minor variation in thickness over distances of 100 to 150 m, the maximum extent of individual outcrop. Although occasionally smooth and planar on both top surface and sole, the top surfaces more commonly display either, irregular polygonal cracks or they are extensively bored and display a *Trypanites* ichnofacies. Flask-shaped borings of *Gastrochaenolites* are most common but some surfaces display closely packed circular pits up to 1.5 cm in diameter which compare closely with those formed by regular echinoids (Warme and McHuron, 1978). The cracks display a range of forms comparable to those produced by both desiccation and synaeresis and it appears that both types are present.

Interpretation. The limestones were obviously deposited during periods of decreased clay input and/or, increased carbonate formation. The *Trypanites* ichnofauna developed in some of the units indicates the formation of hardgrounds, due to synsedimentary lithification (Bromley, 1975b). These surfaces of non- or restricted deposition can occur at a wide range of depths (Jenkyns, 1978) and are very commonly present on shallow marine carbonate platforms (Wilson, 1975). The *Trypanites* ichnofacies suggests a shallow water environment with a marked reduction in clay input (Ekdale *et al.*, 1984). The reddening of the limestone units, in marked contrast to the associated green shales, reflects different oxidation states of the iron content of the sediments. Red-stained zones due to oxidation are not uncommon in the substrate at surfaces of discontinuity (Wilson, 1975). Concentration of iron at such surfaces is related to the pronounced slow-down in sedimentation which leads to their formation and the reddening results from oxidation of the iron on subsequent weathering (Wilson, 1975). The association of the red limestones with features resulting from desiccation suggests strongly that they may have undergone such an alteration in a subaerial environment following their initial deposition in shallow, clean marine waters during times of decreased clay deposition and increased carbonate formation.

(2) Buff to khakhi, and occasionally reddened argillaceous limestone occurring as discrete nodules or coalesced to form nodular beds within an envelope of laminated shale facies. The nodules are generally irregular elongate, commonly 15 to 20 cm in length parallel to the depositional plane but may range up to 40 cm. Thicknesses vary from 5 to 30 cm. They are packed with casts of partly fragmented and occasionally whole gastropods and bivalves. The fauna is restricted to a limited number of species not as yet identified.

Interpretation. It seems clear that the nodules formed by cementation around isolated patches of shell debris which acted as loci for the accumulation of calcium carbonate. The derivation of the shell material is more problematic. It was either derived by erosion from underlying sediments or was introduced into the area from an adjacent depositional environment. It is obvious from the state of preservation that the shells suffered little prolonged abrasion suggesting that the event which led to their concentration was either low energy or short-lived. The absence of similar fauna in life positions, indeed the absence of any large shell material in the surrounding shales, strongly suggests that they were introduced into the area in which they are now found. Considering the size of most of the material it is unlikely that a low energy current would have been capable of distributing the shells over the distances involved and a stronger current necessary to do so would undoubtedly have caused much more fragmentation. A more likely explanation is that the material was ripped up from adjacent shell beds and swept into the area during a storm. Such a rapid translation and dumping of potentially fragile material into a normally low energy environment would provide optimum conditions for its preservation. Following deposition, the patches of shell material provided the nuclei necessary for deposition of calcium carbonate to form the nodules.

Facies 3. Echinoid-rich Bioclastic Wackestones

Description. Two subfacies may be recognized;

(1) The first is a coquina comprised predominantly of very strongly abraded echinoid debris ranging from highly fragmented material to whole fossils along with fragments of crustacea, most notably pieces of crab claw. The deposit is weakly cemented, very porous and characteristically light yellow to white in colour. In the western region it occurs in

irregular lenses on surfaces of erosion some of which seem to have a channel form.

(2) The second type is characteristic of the limestone making up Members 2 and 4 in the eastern region. Units, up to 2 m in thickness, grade upwards from bioclastic wackestones with echinoid and oyster fragments and extensive *Thalassinoides* burrow systems into a slightly more porous layer with a much greater abundance of whole echinoids. The shell material is altogether much less abraded than that seen in the western area.

Interpretation. The deposits of the eastern region compare closely with those described from Pennsylvanian shelf sediments by Wilson (*ibid*) and can be assigned to Standard microfacies 9, i.e. deposits formed in shallow neritic water of open circulation at or just below wave base. The coquinas of the western region have obviously suffered a much higher energy regime and accumulated either as channel or storm lag deposits.

Facies 4. Bioclastic Packstone to Grainstone Facies

Description. Composed of strongly abraded bioclasts in units up to 2.6 m in thickness. Individual units pinch out over a distance of 50 to 200 m defining the shape of the bodies as thin lenses separated from adjacent units by thin beds of laminated green shale or, more rarely, wackestone. Basal contacts are generally sharp and locally erosional but in general the contact is obscured by bioturbation. Beds are cream to pale grey in colour. Petrographically the units vary from the base to the top. The topmost part of the units is essentially a pale grey grainstone with a sparite cement and has a higher porosity than the lower part of the unit which is a cream to pale yellow packstone. The junction between the two is commonly sharp and often clearly erosional. Large-scale planar and less commonly, trough or cuspate cross-bedding units, varying from 50 cm up to 1.2 m in thickness can be quite clearly seen in the upper parts of the units. Gently dipping cross-beds are occasionally seen in the lower parts but normally, intense bioturbation by *Thalassinoides* has destroyed depositional sedimentary structures. Cross-beds display two main directions of dip, to the east and to the west. It is notable, however, that the west-facing dips are much gentler than those to the east averaging 6° as opposed to east-facing dip values of 20° to 25°.

Interpretation. The lenticular or barform geometry of these units suggests that they were deposited as mega-ripples or shoals. Closely comparable deposits were described from the Miocene Marada Formation by Selley (1966, 1970) and by El-Hawat (1980a) and interpreted in terms of migrating offshore and/or onshore bars. Such bodies commonly display opposing dips in which steeper lee-side dips face onshore and gentle stoss-side dips face seawards (Selley, 1970). In the present situation there is ample independent evidence of the position of the shorelines relative to the shoal deposits and it can be seen that the steeper dips do indeed face onshore. The basal bioturbated packstone facies is interpreted by El-Hawat (1980a) as the result of "rapid deposition of high-energy or storm conditions below the wave base" (1980a, p. 436) in contrast to the cross-bedded facies which would have accumulated in more turbulent conditions at or above wave-base. In the Āṣiyah Formation, however, the basal packstone lacks the strong evidence for erosion recorded by El-Hawat and it appears to be the product of a quieter depositional regime. They are interpreted as bottomset deposits laid down in calmer waters in the lee of the advancing barforms.

Facies 5. Carbonate Channel Fill

Description. Channels filled with limestone debris are developed at several horizons in the western area particularly at the base of and within Member 2 in the region east of the Qārat Ash Shush hills. They vary in width from a few metres up to 30 m or more and reach as much as 2.5 m in depth. The narrower channels tend to be much steeper sided than the broader ones. Channel fill is composed of trough and festoon cross-bedded bioclastic grainstone and packstone which display an overall upwards fining. Lag deposits comprised of red to khakhi limestone pebbles, similar to that making up Facies 2, and rare fragments of silicified wood, are well developed in the narrower channels. The argillaceous limestone pebbles are rounded and generally their total surface is bored by a *Trypanites* ichnofauna in which *Gastrochaenolites* predominates. From the associated sediments and infill it would appear that two types of channel are present. There are those which are cut into and through units of Facies 4 and there are those, narrower in width and more steep sided, which cut into Facies 1. Transport directions within the channels are typically bi-polar. Since the channels are generally exposed only in cross-section in wādī cliffs it is difficult to evaluate trends in detail, however, their general orientation is roughly E–W.

Interpretation. There is no question that these erosional-based accumulations are channel fills. The question is as to their origin. The fact that they are closely associated with marine deposits and display a bi-polar transport pattern strongly suggests that they are tidally influenced. The absence of exotic clasts, other than fragments of silicified wood, further suggests that there is no fluvial influence and that their origin is entirely marine. The association of the broader shallower channels with Facies 4 and their orientation sensibly at right angles to the trend of the shoals allows their interpretation in terms of subtidal channels cutting through the subaqueous shoals. The narrower deeper channels associated with Facies 1 are more likely to have developed in the intertidal zone and may be continuous with the shallow subtidal type.

Facies 6. Calcareous Sandstone and Siltstone

Description. Yellow, fine, quartz-rich calcareous sandstones and siltstones are well developed in Member 4 in the area both east and west of Qārat Ash Shush although they die out as the Ḥabārah escarpment is approached. Sand units range from 0.5 cm up to 4 cm in thickness and are interbedded with thin units of olive green to ochre mudstone. The beds typically display flaser bedding and show a strong bi-polarity in current direction. Symmetrical ripple marks are common in thin more persistent sand sheets while herring-bone cross-lamination is locally well developed. Trace fossils are not common within these beds. Faint vertical and U-shaped burrows suggest the presence of a *Skolithos* ichnofacies association.

Interpretation. The predominance of flaser bedding associated with symmetrical ripples and herring-bone cross-stratification strongly indicates that these deposits were laid down in tidal sand-flats (Reineck and Singh, 1975). The increase in quartz content relative to all other facies in the succession may be interpreted in terms of source control and/or depositional and transportational processes leading to grain size sorting.

Facies 7. Oyster Reef Facies

Description. Linear bodies comprised of *Crassostrea* in life position are well developed in Member 5. The bodies are lenticular in cross-section and are cut into thinly laminated calcareous shales with rootlets and thin layers of finely comminuted shell material. The oyster banks are generally flanked by mounds of partially disarticulated shells.

Interpretation. The oyster reefs are closely similar to those described by Frey and Basan (1978) from modern coastal salt marsh environments in Georgia where *Crassostrea* is seen to build large discontinuous beds along the margin of large creeks and to floor smaller tributaries. Disarticulated shells are due to reworking of the reefs to give local shell pavements both on creek banks and channel bottoms.

More continuous, sheet-like shell deposits comprised of articulated and disarticulated oysters are common in the eastern Al Ḥufrah region interbedded with the echinoid limestone facies. These beds range from a highly porous coquina to shells set in a clay matrix. They generally rest directly on the limestones and are usually succeeded by thin laminated clays. Although no oysters are actually found in life position it would seem that the shells have suffered only restricted transport and may have been reworked from sheet-like oyster colonies such as occur in open bays or lagoons (Frey and Basan, 1978) by storms.

Facies 8. Limestone Breccia

Description. This facies is composed of angular fragments of older limestones set in an orange-red silty clay matrix. The limestone fragments are coated with a black to dark purple patina of manganese oxide. Small, thin-shelled terrestrial gastropods occur sporadically within these deposits. Bedding is irregular and poorly defined. The breccias are found only in the western area where they form the most easterly facies of the formation resting with strong unconformity on older rocks along the base of the Ḥabārah escarpment south of Al Ḥufrah–Facha road. They crop out as a number of small isolated hills with westerly dipping top surfaces and invade the underlying limestones along cracks and hollows. Away from the escarpment the beds thin abruptly although locally, thin units and lenses of breccia are seen within the laminated green shale facies.

Interpretation. The breccia deposits are similar in every way to "beach rock" deposits described by Shinn (1973) from the Persian Gulf and they represent the only truly terrestrial deposits within the formation. The isolated pockets and thin layers occasionally found within the shales are interpreted as storm deposits.

Facies 9. Limestone Conglomerate

Description. There are two types of conglomerate composed of limestone clasts, both of which are found resting on the surface of unconformity at the base of the formation. The first is composed of fossil casts of large gastropods and bivalves derived from the underlying Middle Eocene formations. The casts, which are abraded and often extensively invaded by *Entobia* and more rarely, *Trypanites*, are buried by the green clays of Facies 1. The deposits are patchy, thin and rarely more than one cast thick. The second type is much coarser and is comprised of boulders ranging from 20 cm up to 2 m in diameter. They form irregular lenses stacked against steep steps on the surface of unconformity. Both the boulders and the steep faces against which they are piled are extensively bored by *Gastrochaenolites*.

Interpretation. These sediments were derived from the underlying formations during the erosional phase which accompanied formation of the unconformity and represent lag or residual deposits too heavy to be swept away by the process which carved the platform. Preservation of the shell casts argues for the infilling material having had a greater mechanical durability and chemical stability than the matrix in which they were originally enclosed, properties most likely related to cementation of the lime mud infills in response to biochemical/chemical interplay between the muds and the enclosing shell material. The boulder beds were formed by cutting back of cliffs in the underlying limestones and denote a high-energy regime. The *Trypanites* ichnofacies which were developed both on the clasts and the substrate on which they lay indicate a wave-washed, high-energy rocky shore and shallow rock platform. Following their formation on the rock surface both the boulder gravels and the casts were eventually buried by green muds settling out in a low energy environment. The nature of these deposits will be discussed further below in conjunction with a discussion on the nature of the surface of unconformity.

Facies 10. Evaporite Facies

Description. The evaporite facies occurs either as beds of coarsely crystalline gypsum or as gypsum nodules and nodular layers. The coarsely crystalline gypsum forms beds up to 80 cm thick which consist of several units of selenite crystals oriented with apices pointed downwards at right angles to the bedding planes. The crystals, up to 30 cm in length, display a well developed "wavy" to chevron-pattern internal lamination which is picked out by the interbedding of clear to milky bands of gypsum, with thin bands containing inclusions of carbonate and clay particles. The detritus-rich seams are stained to a rust colour by iron oxides and this staining commonly pervades the rest of the deposit. The presence of the detrital layers does not break the optical continuity of the gypsum crystals and this produces a pervasive cleavage which is broken only where thin seams of limestone have formed within the unit. It is noticeable, however, that even where such seams occur, the gypsum crystals on either side display very similar orientations. Despite being thin the beds of gypsum can be followed for as much as ten kilometres north to south in the Qārat Ash Shush area. Their periodic disappearance in this region is the result of interformational erosion as opposed to facies change (Kumati, 1981). To the east, however, they pass into the nodular gypsum commonly in association with the red muds noted above in the discussion on Facies 1. The nodules comprise single gypsum crystals which have grown displacively in the host sediment. They range up to 15 cm in longest diameter and occur both in isolation and packed together to form nodular layers.

Interpretation. The coarsely crystalline, banded gypsum deposits are closely similar to those described by Hardie and Eugster (1971), Schreiber (1978), Kendall (1979b) and El-Hawat (1980b). The gypsum crystals are considered to be primary in origin and to have grown poikolitically to include the thin seams of clay and carbonate inclusions which serve to delineate successive stages of growth. The lamination records alternation of periods of precipitation with periods of partial solution and deposition of fines brought about by seasonally controlled evaporation and dilution of the waters in the salina. Schreiber and Kinsman (1975) note that continued growth of the gypsum to produce poikolitic crystals is possible after the deposition of the detrital layer if that layer is less than 100μ. Thicker seams cause interruption of growth and lead to a new phase of nucleation with the production of a new bed. Schreiber (1978) suggests that the depths of water in the salinas depositing gypsum of this type is shallow and commonly less than 5 m. The nodular gypsum is similar to that developed in the supratidal sabkha environment (Butler, 1970; Kendall, 1979a) and the lateral change from laminated to nodular deposits is thus interpreted as recording the passage from salina into sabkha environment of deposition.

DEPOSITIONAL HISTORY

Although the successions developed in the eastern and western regions are closely similar, the eastern succession is essentially two dimensional in outcrop and shows relatively little lithological variation. In contrast, both lateral and vertical variation in the western area is rapid and complex providing ample data for its evaluation in terms of depositional history. It is convenient therefore to treat the two areas separately starting with the western region.

Stage 1. Upper Eocene Transgressive Phase — Nature of the Surface of Unconformity

The initial stage of the Upper Eocene transgression was the cutting of the unconformity, the nature of which is of prime importance in the evaluation and interpretation of the depositional history of the formation.

Figure 3 shows that the Āṣiyah Formation rests on a number of older formations which were tilted and extensively faulted before upper Eocene sedimentation commenced. Throughout the region, however, the basal Āṣiyah sediments are dominated by green shales with thin seams of red argillaceous limestone (Facies 1 and 2) irrespective of the lithology of the underlying rocks. The shales step over the limestones, shales and gypsum beds of the older formations without obvious change in lithology. Lithological variation within the basal beds of the Āṣiyah Formation is, therefore, rare and developed only locally in response to changes in the topography of unconformity. The contact between the Āṣiyah shales and the underlying units, no matter what their lithology, is abrupt. In contrast, the junction within shale sequences is seldom clear and is difficult to place with any degree of certainty.

The commonest relationship (Fig. 5A), shows a planar surface extensively bored by *Gastrochaenolites*. The borings are infilled by green muds and silts and occasionally fine carbonate sand. These bored surfaces are best developed where the substrate is comprised of the chalk of the Wādī Abū Marās Member of the Ḥabārah Formation. They are much more rarely developed on the more granular limestones of the Rāqūbah Formation. The widespread development of *Gastrochaenolites* indicates that the substrate was not only hard but that the waters were generally devoid of suspended clays.

Another expression of the unconformity which occurs near to the Ḥabārah escarpment is also shown in Fig. 5A, Loc: 17°48′00″, 29°28′10″. Here the limestone surface displays irregular mushroom-shaped pillars isolated one from the other by irregular hollows and pits up to 30 cm in depth. Both tops and sides of the pillars are bored. The succeeding sediments range from Facies 1 to Facies 9 the last being commonly well developed on these surfaces. Worn casts of gastropods and bivalves, displaying a polished patina of iron and manganese oxide and *Entobia* borings lie in the hollows and are buried by the green shales. The fauna is identical with that of the underlying chalk and was obviously derived from it during development of the unconformity. The rock pillars and concentration of derived material are similar to the biokarst topography described by Schneider (1976) and Ekdale *et al.* (1984) from the intertidal zone of rocky coasts.

Although change in lithology of the substrate has little effect on the composition of the basal beds of the Āṣiyah Formation, it may, due to variation in resistance to erosion of the different lithologies, affect the geometry to a greater or lesser degree.

Figure 5B (Loc: 17°43′30″, 29°26′10″) shows the base of the formation stepping across a major fault which brings gypsum beds of the Rāqūbah Formation into contact with Wādī Abū Marās chalk. It can be seen that neither the planar nature of the unconformity nor the lithology of the succeeding beds is much affected by the change in lithology. The difference in levels across the fault is a matter of less than 10 cm indicating that both rock types must have reacted in a very similar manner to the erosional processes which sculpted the surface. In addition, the laminated green shales of the Āṣiyah beds step across from the chalk to the gypsum with no change in lithology. The only notable difference in the surface from one side of the fault to the other is that the limestone surface is extensively invaded by *Gastrochaenolites* borings, whereas, the gypsum surface is not.

A contrasting relationship is seen at Loc: 17°37′30″, 29°15′09″ in the Qārat Ash Shush region where the Āṣiyah Formation overlies a complex fault zone (Fig. 5C) (Anketell and Kumati, 1991). Here, Members 1 and 2 of the Āṣiyah Formation are in steep contact with the Rāqūbah gypsum in what su-

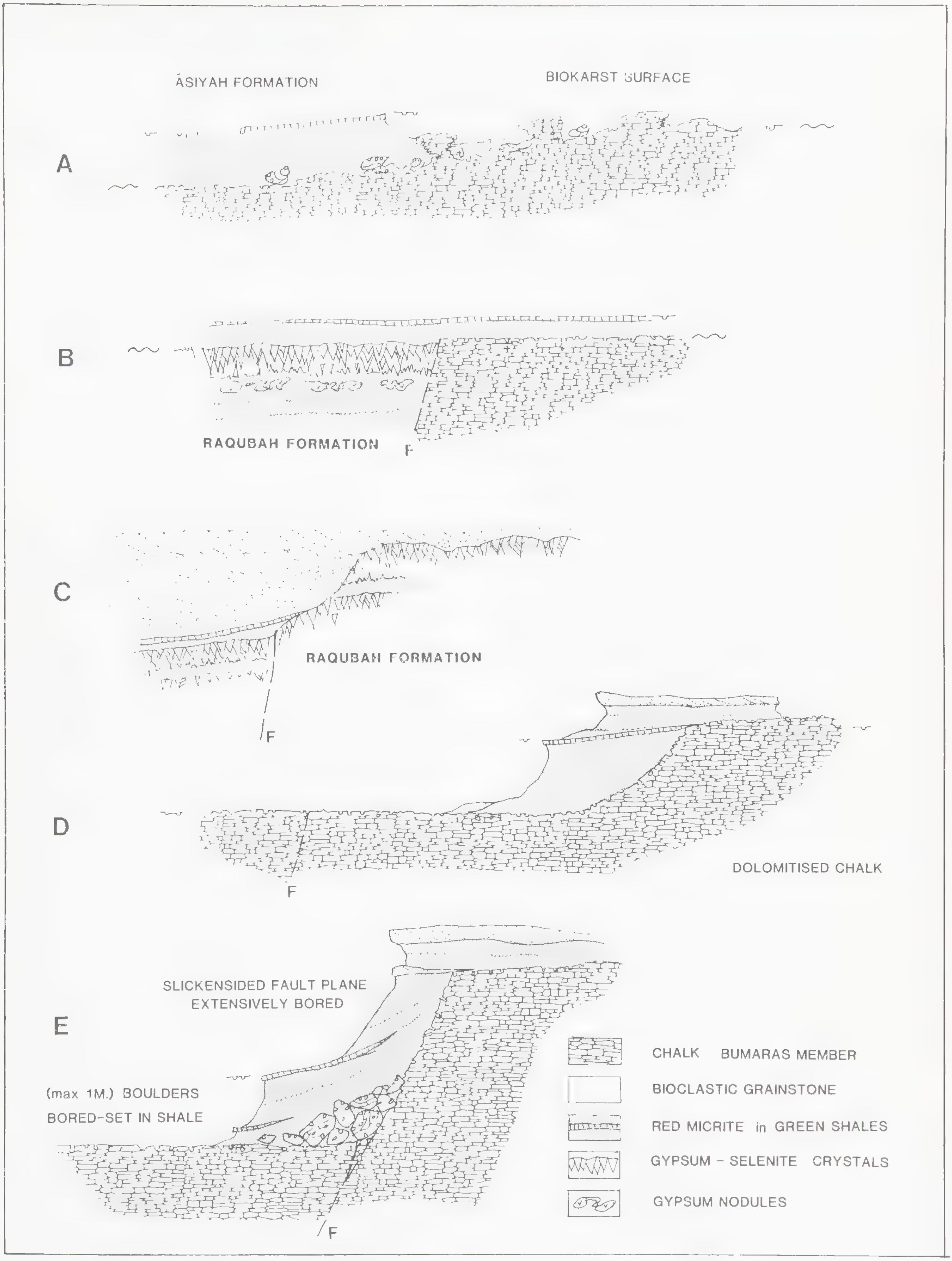
ĀSIYAH FORMATION
BIOKARST SURFACE
A
B
RAQUBAH FORMATION
F
C
RAQUBAH FORMATION
F
D
F
DOLOMITISED CHALK
E
SLICKENSIDED FAULT PLANE
EXTENSIVELY BORED
(max 1M.) BOULDERS
BORED–SET IN SHALE
F
CHALK BUMARAS MEMBER
BIOCLASTIC GRAINSTONE
RED MICRITE in GREEN SHALES
GYPSUM – SELENITE CRYSTALS
GYPSUM NODULES

Fig. 5. Sketch diagrams showing features developed on the pre-Āṣiyah Formation surface of unconformity.

perficially appears to be a faulted relationship. It can be shown, however, that the shales and limestones are banked against the gypsum and that the limestones of Member 2 overlap the shales of Member 1 onto the gypsum which they eventually overstep and bury. Many similar examples are found throughout the fault zone along the eastern flanks of the Qārat Ash Shush region, where pre-Āṣiyah faulting of the Rāqūbah Formation has resulted in the juxtaposition of thick gypsum and shale beds. Differential erosion of the softer shales during erosion of the surface of unconformity produced an irregular topography which was subsequently buried by the sediments of the Āṣiyah Formation. Shales of Member 1 accumulated in the downfaulted and erosional lows causing complete or partial burial which was completed by the gradual advance of the bioclastic limestone facies of Member 2. There is no evidence that the topography of this area exerted a control on the facies of the Āṣiyah Formation for both Members 1 and 2 exhibit exactly the same characteristics in adjacent areas where the geometry of the unconformity is planar.

A closely comparable situation seen at Loc: 17°47′10″, 29°27′20″ shows green shales and red argillaceous limestones of Facies 1 step over a fault cutting through strongly dolomitized chalks of the Abū Marās Member (Fig. 5D). The fault has little effect on the geometry of the unconformity which is again essentially planar. Some 25 m back from the fault, however, the surface steps up abruptly at an angle of 50° to 60° forming a scarp some 3 m in height. The shales lap up over this scarp and are succeeded by limestones near the top. Both the scarp and the dolostone pavement are intensely bored by *Gastrochaenolites*. It seems likely that the scarp was formed by erosional retreat of the original fault scarp. There is, however, no coarse debris which might be expected from such erosion and the shales rest with sharp contact on the dolostones. The absence of coarse detritus may be explained by the nature of the dolostone which is granular and would erode to form a fine to medium sand easily removed from the immediate vicinity.

In marked contrast to this relationship is the situation seen at Loc: 17°46′50″, 29°27′00″. Here, a scarp in the Abū Marās limestone is partially buried by a conglomerate of rounded boulders up to 1 metre in diameter (Fig. 5E). These, and the upper part of the scarp, are buried under green clays and shales with red argillaceous limestone units. The scarp face, the boulders, and the platform on which they lie are all bored in the manner seen elsewhere. The deposit is closely similar to those described by Radwanski (1970) and obviously represents a cliff shore deposit. The origin of this scarp is again due to faulting, however, it differs from that developed in the dolostones in that it has not suffered any retreat as is shown by the preservation of slickensides on the fault face. This raises questions as to the origin of the boulders since it is clear that they cannot have been derived from that part of the cliff against which they lie. Instead they must either have been eroded from the upper part of a once higher cliff or have been transported from nearby. It is clear from the size of the boulders that if they were transported by marine agencies then this must have occurred during storms. Alternatively, the boulders may have been formed as a cliff scree during subaerial erosion of a once higher cliff and were abraded and burrowed following marine inundation.

From the few examples cited above it is clear that, with the exception of local fault scarps and areas where softer sediments such as shales were differentially eroded, the surface on which the Āṣiyah Formation was deposited was essentially planar, intensely bored and devoid of all but the very coarsest residual deposits. The development of a *Trypanites* ichnofacies, the reworked faunas, and the clean, planar surfaces all indicate that the final characteristics of the unconformity were produced by marine erosion in shallow wave-dominated seas which would have provided ample energy for removal of the finer materials eroded from the substrate but could not transport the larger boulders and cobbles over long distances. The large, derived fossil casts of Facies 9 owe their preservation to being trapped in erosional pockets and hollows in the shore zone while the boulders of the fault scarps were simply too large to remove. The lack of coarse material also reflects the fact that the Middle Eocene rocks which underwent erosion are dominated by soft chalks, evaporites and shales which would tend to release fine detritus only. This would have been easily transported out to deeper water below wave base and the rock platform margins.

It can be seen from Fig. 3 that the amounts of material removed by erosion following the phase of faulting which affected the older formations, must have been very substantial. This is particularly true throughout the eastern region where the Āṣiyah Formation rests directly on the Abū Marās Member of the Ḥabārah Formation and in the southern parts of the Qārat Ash Shush and Gedārī fault zones where the formation steps eastwards across from Rāqūbah Gypsum in the downthrown blocks onto the older Abū Marās Member. In each of these areas, the Abū Shuyūkh and Rāqūbah Formations, with a minimum thickness of 100 m, must have been completely removed by erosion from the upthrown eastern blocks.

While it is certain that the final phase of erosion took place in a wave-dominated shallow marine environment, it is not, however, known whether marine erosion only was involved in the levelling of the block-faulted surface. The lithologies of the Rāqūbah and Abū Shush Formations (Kumati, 1981) show that shallow marine, lagoonal and supratidal environments prevailed in the region at the end of middle Eocene times. It is very possible, therefore, that during faulting, fault blocks would have been uplifted above sea level and thus subjected to subaerial weathering. Any evidence of such processes has, however, been effectively destroyed by the phase of marine erosion which ultimately sculpted the surface.

A further aspect which should be considered is the role played by solution in the development of the limestone platform. Revelle and Emery (1957) and Bird (1984) note that solution can be an important process in the marine environment despite the fact that the sea water would be effectively saturated with respect to calcium carbonate. Solution occurs due to an interplay between carbon dioxide content and variation in diurnal temperatures. Cooling of the sea water at night increases its capacity to take up more carbon dioxide and hence increases its acidity and ability to dissolve limestone. During the day, with rising temperatures, the capacity of the water to retain the dissolved bicarbonate decreases and calcium carbonate is precipitated only to be washed away by wave and current action.

In summary, the initial Upper Eocene transgression involved the formation of a wave-cut marine platform. The advance of shallow wave dominated seas would have provided ample energy for erosion and to sweep away all but the heaviest detritus such as boulders and large fossil casts. Mechanical abrasion was almost certainly accompanied by solution. The large boulders found at the base of small fault scarps may be the product of marine erosion or have formed as residual deposits during an early phase of subaerial weathering. The extent to which the sea transgressed the middle Eocene surface in the western region is clearly marked by a biokarst surface. This can be followed along the surface of unconformity in the vicinity of the Ḥabārah escarpment which must have formed a cliff preventing connection between the western and eastern regions. The position of the shoreline in the eastern region is unclear, however, it probably lay only a few kilometres to the west of Wādī Abū Marās.

Stage 2. Lagoonal–Restricted Marine Phase

The abrupt change from a clean washed, high-energy, wave cut platform environment to a low energy, lagoonal or restricted marine platform environment depositing muds and argillaceous limestones, obviously implies that the reduction in wave and current energy was sudden. The wide extent of the platform and shallowness of the water would have made it susceptible to any process which might have severely reduced the effectiveness of wave energy. Depression of the depositional surface below wave base is discounted by the frequent occurrence of desiccation cracks and development of hardgrounds bored by *Gastrochaenolites* and echinoids in the argillaceous limestones interbedded with the shales. The marked drop in wave energy was more likely brought about either by shallowing with dissipation of wave energy at the platform edge or by the build-up of sediment barriers at or near the platform margins to produce a protected shallow marine–lagoonal environment. The development of bored hardgrounds record minor periods of omission with drastically reduced clay deposition in the lagoons while the occasional patches and layers of shell debris, preserved in nodular beds, were swept in by storms either from the shelf edge or nearshore areas. The shales show minor but important variation across the western region. Near the Ḥabārah escarpment they display more nodular limestone and desiccation cracks than to the west or in the eastern region and it would appear that this area was near shore and commonly emergent, probably as a result of tidal rise and fall while to the west and in the eastern region the sediments were entirely subtidal in origin.

Stage 3. Barrier Lagoon Phase

Stage 3 is dominated by the build up of echinoid-rich limestones of shallow, open-marine character in the eastern region and by the advance of bar deposits into the western region from further westwards where they probably caused the initial isolation and restriction of the wave-cut platform. Their advance records a gradual deepening of the sea throughout the area. There is no evidence that the bars built up above sea level, however, the succession recorded in Member 2 shows appreciable variation from west to east. The unit thins from west to east concomitant with a reduction in the number of bars. There is not, however, a corresponding reduction in the shale content (Fig. 4). Throughout the Qārat Ash Shush region the interbedded bar deposits and shales display little evidence of erosion and seem to be entirely subtidal and to have advanced by the forward building of bioclastic wackestone into the restricted marine or lagoonal environment, possibly during storms. The grainstones of the upper part of the units were developed by reworking within wave base. Eastwards, near to the Ḥabārah escarpment, the bars change character and become grainstone dominated, crescent-shaped lenses with well developed trough cross-bedding. The interbedded shales display desiccation cracks and contain carbonate-filled channels the lowermost of which occasionally cut down through Member 1 to rest on the unconformity. Further east, patches of grainstone, which occasionally display planar cross-bedding dipping onshore, locally overlap the underlying shales onto the surface of unconformity. The carbonate-filled channels and associated shales represent channel and interchannel deposits of an intertidal flat environment. The crescent shaped barforms, on the other hand, accumulated in more permanent water and are interpreted as near-shore subtidal shoals largely developed within wave base. The planar cross-bedded units represent patches of fine beach deposits formed when crescentic barforms were driven onshore and possibly protected in small coves of the rocky coast.

Stage 4. Lagoonal to Intertidal Flat Phase

This stage, represented largely by Member 3, displays a return to lagoonal or restricted shelf conditions of sedimentation. In the eastern region the shales contain thin beds of oysters (Facies 7b). In the western region the beds show a similar pattern to the conditions which prevailed during deposition of Member 1 in that bored red, and concretionary limestone, commonly interbedded with the shales in the eastern part of the area, die out to the west. Towards the top of the shales, however, *Diplocraterion* becomes widespread, in contrast to the *Thalassinoides* dominated ichnofacies of the underlying barforms, and indicates a general shallowing across the whole area.

Stage 5. Intertidal Flat to Sabkha Phase

This stage, corresponding to Member 4 and the greater part of Member 5 is developed in the western region. As will be seen below the equivalent beds in the east are more marine in character. In the west this phase commences in the Qārat Ash Shush region with the deposition of flaser-bedded, sandy limestones of Facies 6. These pass eastwards into shales with lenses of planar cross-bedded bioclastic calcarenite, lenses of strongly abraded echinoid debris and channels up to 2.5 m deep filled with cross-bedded grainstones and wackes.

The influx of fine quartz sand into what had otherwise been a carbonate and mud dominated sequence of environments coincided with a time of sea-level fall. Given the tectonically unstable nature of the region at this time, it is likely that retreat was triggered by uplift and that the quartz was derived from accelerated erosion of older sediments. Its concentration in the more westerly part of the tidal flats most likely reflects areal variation in energy. Reineck and Singh (1975) and Postma (1961) show that sand size material is enriched in the intertidal zone near low water line where wave activity is strongest and active for the longest time while major mud deposition takes place near the high water line due to low wave and current energy. The low tide mark region must have been situated in the Qārat Ash Shush area where the higher energy input not only resulted in grain-size sorting but also led to a mineralogical sorting. The intertidal zone shoreward of the sand flats is mud dominated and cut by channels containing coarse bioclastic lag deposits. The lenses of strongly abraded echinoid and crustacean debris (Facies 3a) also occur in shallow channels. The strongly abraded nature of these deposits in what is a low energy environment suggests that they may have been reworked by storm wave action of higher tides from older, nearshore marine deposits such as those of Member 2, which could have been exposed along the contemporary shoreline following a drop in sea level. The trend towards shallowing continues through the base of Member 5. Rootlet beds cut by channels filled with oysters indicate the progradation of salt marsh deposits into the area near the Ḥabārah escarpment while shales with argillaceous limestones to the west probably accumulated in shallow lagoons. The final phase of the regression is indicated by the deposition of gypsum in salinas to the west of the area while stromatolites and red and green shales with nodular gypsums of a supratidal sabkha environment developed near the escarpment. The passage of the red shales into subaerial breccias with terrestrial gastropods at the base of the escarpment marks the peak of the regressive phase. The shoreline at this time lay just to the west of the Qārat Ash Shush hills. In this area, the beds which occupy the same stratigraphic level as the gypsum units are bioclastic limestones up to 1 m thick which have been replaced almost entirely by gypsum. These beds may have originally acted as barriers, partially isolating shallow lagoons from an open marine area to the west. During the subsequent saline phase of deposition, the limestones were cemented by the growth of poikolitic gypsum.

In the eastern region the phase of shallowing is less obvious than in the west and the succession is altogether more marine in character. The lowermost part is dominated by laminated shales of Facies 1 with sheets of oysters and thin sheets and nodules of Facies 2a and 2b, in contrast to the intertidal deposits on the west. These deposits are succeeded by a 2.5 m thick unit of Facies 3 which is even more marine in character and implies that as the sea shallowed in the west it was becoming a little deeper in the east. The echinoid-rich limestones are then succeeded across an erosion surface by a unit which, although it lacks red colouration, is strongly reminiscent of the breccias seen in the west. The unit, some 2 m thick, is comprised of trough cross-bedded, calcareous sand which contains many small angular grains of blackened chalk and chert and occupies a similar stratigraphic position to the breccias and gypsum beds. It is suggested that the unit was formed by reworking of beach rock which had developed along a gently shelving shoreline immediately to the west.

Stage 6. Lagoonal to Restricted Marine Deposition

The beds succeeding the topmost gypsum horizon consist largely of laminated green shales with veins of fibrous gypsum and occasional lenses of planar and trough cross-bedded, bioclastic limestones. Both the shales and the limestones are more marine in character than the underlying beds and it would appear that the final stage of the Āṣiyah Formation in the western region was one of retrogradation. A similar pattern is seen in the east where the redeposited breccia is succeeded by shales with thin limestones.

Palaeogeography of the Region

Towards the end of Middle Eocene times the area to the west of Al Ḥufrah was downthrown to the west along two major NNW to SSE trending fault zones. The throw on the more easterly Gedārī fault is estimated as 90 m while that on the Qārat Ash Shush zone appears to vary from a few metres in the north to as much as 100 m in the south. The pattern of preservation of the older formations on the pre-Āṣiyah surface displays an ENE younging within each block implying that they were tilted gently to the ENE before deposition of the Āṣiyah Formation. It is not possible to say whether this was a pre-fault attitude or a consequence of the faulting.

The post-fault topography of the region was therefore one of steep WSW facing cliffs and gently dipping ENE slopes. How much of this was submarine and how much subaerial is unknown, however, the final phase of erosion affecting the soft shales, limestones and gypsum beds making up the Abū Shuyūkh and Rāqūbah Formations was undoubtedly marine. The distribution of facies shows that the Qārat Ash Shush fault scarps were eroded to an irregular planar surface which presented little barrier to the advancing sea and had only a limited effect on facies distribution. In contrast, the development of shoreline deposits indicates that the Gedārī fault scarp formed a major cliff which must have persisted throughout Upper Eocene times and may still have been a positive feature in the early Oligocene (Kumati, 1981). From the cliff top the land must have sloped away gently to the eastern coastline, situated somewhere to the west of Wādī Abū Marās. It is not known how far to the north or south this land area stretched or whether it was an island or a promontory. What is certain, however, is that it was rapidly drowned in the Oligocene by the spread of nummulite-rich shoals which step over the Āṣiyah Formation and the Gedārī Fault to rest on the Middle Eocene (Kumati, 1981).

CONCLUSIONS AND REGIONAL IMPLICATIONS

In Al Ḥufrah region Middle Eocene sedimentation seems to have been brought to an end by earth movements which involved tilting of the beds to the ENE and the development of nett WSW downthrows across NNW trending sinistral oblique-slip faults. The resulting topography, shown in Fig. 6A, was eroded to form the surface on to which the

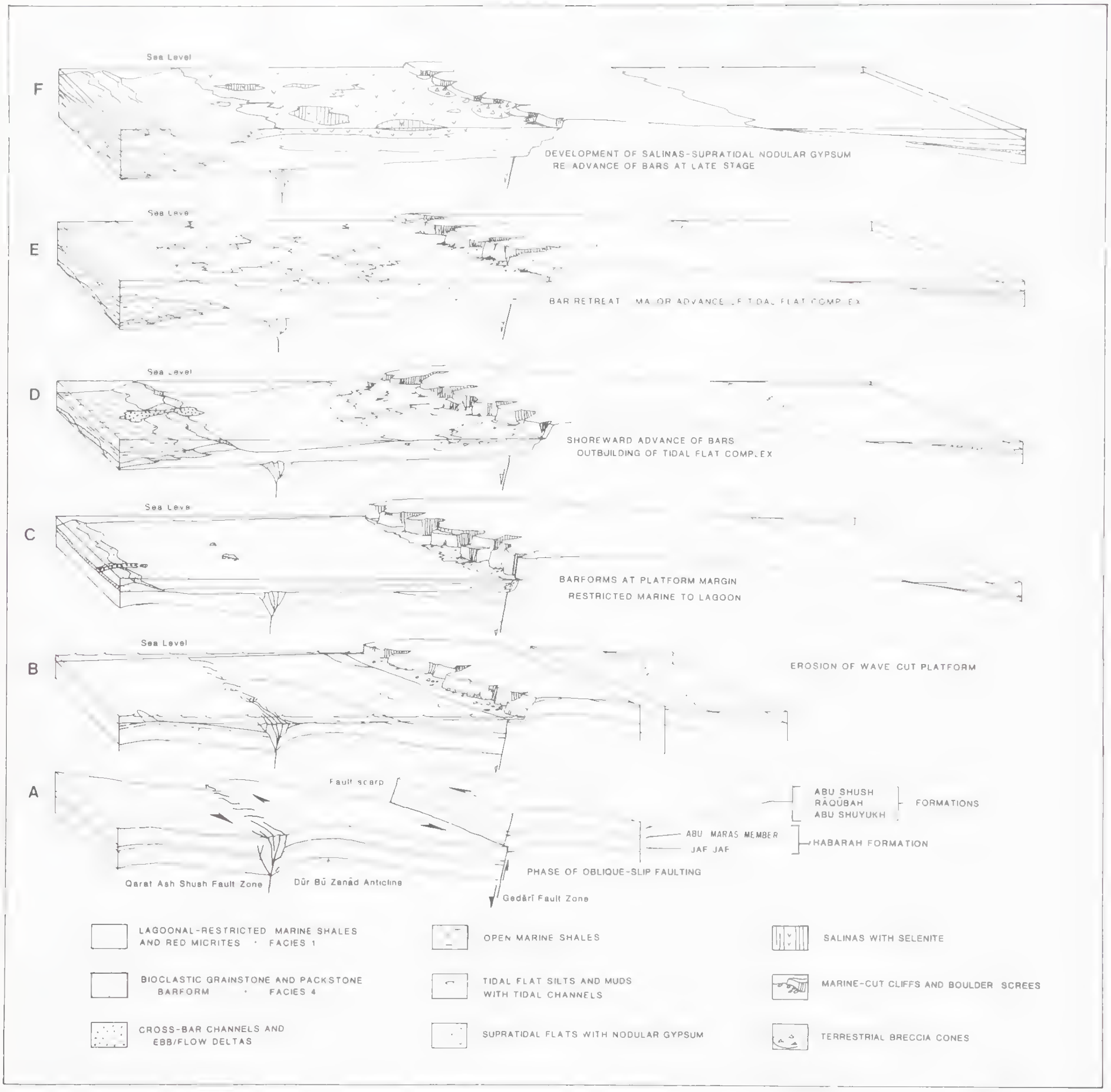
F
Sea Level
DEVELOPMENT OF SALINAS-SUPRATIDAL NODULAR GYPSUM
RE-ADVANCE OF BARS AT LATE STAGE
E
Sea Level
BAR RETREAT – MAJOR ADVANCE OF TIDAL FLAT COMPLEX
D
Sea Level
SHOREWARD ADVANCE OF BARS
OUTBUILDING OF TIDAL FLAT COMPLEX
C
Sea Level
BARFORMS AT PLATFORM MARGIN
RESTRICTED MARINE TO LAGOON
B
Sea Level
EROSION OF WAVE CUT PLATFORM
A
Fault scarp
ABU SHUSH
RĀQŪBAH
ABU SHUYUKH
FORMATIONS
ABU MARAS MEMBER
JAF JAF
HABARAH FORMATION
PHASE OF OBLIQUE-SLIP FAULTING
Qarat Ash Shush Fault Zone
Dūr Bū Zanād Anticline
Gedārī Fault Zone
LAGOONAL-RESTRICTED MARINE SHALES AND RED MICRITES · FACIES 1
OPEN MARINE SHALES
SALINAS WITH SELENITE
BIOCLASTIC GRAINSTONE AND PACKSTONE BARFORM · FACIES 4
TIDAL FLAT SILTS AND MUDS WITH TIDAL CHANNELS
MARINE-CUT CLIFFS AND BOULDER SCREES
CROSS-BAR CHANNELS AND EBB/FLOW DELTAS
SUPRATIDAL FLATS WITH NODULAR GYPSUM
TERRESTRIAL BRECCIA CONES

Fig. 6. Schematic block diagrams displaying the structural and sedimentological changes which took place during the deposition of the Āṣiyah Formation in late Eocene times in Al Ḥufrah region.

Āṣiyah Formation was deposited. The final phase, if indeed not all, of this erosiona levent, was submarine and effectively removed the "cliffs" of the Qārat Ash Shush fault zone to form a platform which continued up to the high cliff formed by the Gedārī fault (Fig. 6B). From the scarp, which formed a positive feature throughout Upper Eocene, the surface dipped gently to the east towards Wādī Abū Marās. Scouring of the substrate was effected by erosion in a turbulent marine environment such as a shallow wave-dominated sea which washed against, and eventually caused substantial retreat of the Gedārī fault scarp, preserved today as the Dūr Mukhaybīsh al Ḥabārah cliffs. To the east, the sea washed onto a gently shelving rock platform (Fig. 6B). The shorelines define a contemporaneous land area, some 20 km wide and trending NNW to SSE for at least 70 km. Deposition of the Āṣiyah Formation around the shores of this "island" proceeded as follows. The material eroded from the region by action of the sea, a considerable amount when it is considered that the whole of the Abū Shush, Abū Shuyūkh and Rāqūbah Formations were removed from the eastern area and that large amounts were eroded from the western area, was transported out below wave base. Here it provided a reservoir of sediment available for reworking to form sand bars, the development of which caused restriction of the shallow platform, giving rise to lower energy conditions and the development of broad shallow lagoons or a restricted shelf environment in which shales became the dominant deposit (Fig. 6C). This body of water was probably quite deep right up to the cliffed and steeply shelving coasts of the original wave-cut platform with the result that the shales were deposited in close proximity to the coastline, burying beach rock and boulder deposits. Tidal flat deposits did not develop until sufficient sediment had accumulated to build the depositional interface up to sea level.

The advance of carbonate barforms into the lagoon/restricted marine environment, and their subsequent retreat is documented by Member 2 (Fig. 6D, E). The prograding sequence recorded in the interplay of the upper part of Member 2 and lagoonal shales of Member 3 marked the beginning of a shallowing phase which progressed with the build up of sand and mudflats with tidal channels. This phase reached its climax in the development of sabkha with deposition of banded gypsum in salinas and nodular gypsum in the surrounding sediments of the supratidal zone (Fig. 6E). Following this, however, the final phase of sedimentation shows a return to more marine conditions of deposition with thin incursions of limestones in the more westerly areas and shales over the rest of the region.

The Āṣiyah Formation displays an initial stage of retrogradation and then a final phase of retrogradation although this is less clear in the eastern region where the prograding stage includes a minor retrograding event. It is possible to interpret the overall patterns in simple terms of transgression, regression and transgression and to extend it to the succeeding Oligocene sediments which record a regressive phase followed by a transgression. Fluctuations in sea level during the Eocene are equally marked in Cyrenaica where Barr and Berggren (1980) record a transgression starting in the Ypresian following a phase of uplift and folding. This continued through the Lutetian with the gradual inundation of the structural highs. During the Priabonian there was a gradual shallowing and advance of shallow marine facies before the Eocene "ended with a major uplift and subsequent regression of the sea from the entire region" (Barr and Berggren, 1980, p. 173).

Vail *et al.* (1977) note that there has been an overall decline in sea level through the Cenozoic. Second order cycles show that this trend is made up from a number of gradual sea level rises followed by abrupt falls. Pitman (1978) and Hallam (1980) stress that transgressive or regressive events must not simply be considered in terms of sea level rise or fall but must also be considered in terms of rate of sea level change and note that "a decrease in the rate of sea-level rise and an increase in the rate of sea-level fall may result in regressions, while an increase in the rate of sea-level rise and a decrease in the rate of sea-level fall may produce transgressions" (Hallam, 1980, p. 140).

The pattern of regression and transgression in northern Libya in the late Eocene took place against this backdrop of worldwide regression which commenced in the Palaeocene. At the same time, Hallam (1980, p. 140) notes that sea-level fell rapidly in the Palaeocene but less rapidly in the late Eocene. Given a low rate of fall, even minor downwarping or faulting could lead to local transgression.

In Al Ḥufrah region, there is ample evidence for tectonism which could have caused the land to subside at a higher rate than sea-level fall. Following the phase of uplift and faulting which caused the retreat of the sea from the land in late Middle Eocene times, a general sinking of the land at a rate higher than that at which sea level was falling would have generated the transgression which led to deposition of the Āṣiyah Formation. The development of prograding facies which followed the transgressive phase probably records a "normal" sedimentary response to sea level fall under stable tectonic conditions. The minor readvance of the sea at the end of the Upper Eocene can be related to tectonic controls also. Kumati (1981) showed that the Āṣiyah beds were folded into small *en echelon* folds due to reactivation of sinistral oblique slip movement on the faults before deposition of the Oligocene. Movements heralding this renewed tectonic activity, particularly if they caused further downwarp to the west, would have led to deepening of the depositional environment and the development of retrograde transgressive facies. In a similar fashion, the disparity in the pattern of advance and retreat of the sea in the eastern and western regions in the final stages of deposition can be explained by tilting of the fault blocks.

ACKNOWLEDGEMENTS

The authors wish to express their gratitude to Mobil Oil for financial and logistical support during the period of study and fieldwork. We would also like to thank colleagues both in Libya and in the Department of Geology of Manchester University for giving of their time in discussion. Thanks are particularly due to Dr. J.E. Pollard for his careful reading of the manuscript and giving us much helpful advice on the trace fossil content of the deposits. We are also indebted to Richard Hartley for drafting Figure 3.

REFERENCES

Airaghi, C. (1939). Echinidi Cretacei e Terziari della regioni d'Orfella e della Sirtica. *Ann. Mus. Civ. St. Nat.* Roma, 253–286.

Anketell, J.M. and Kumati, S.M. (1991). Structure of the Al Ḥufrah region, Western Sirt Basin, G.S.P.L.A.J. (Vol. VI, This Symposium).

Banerjee, S. (1980). Stratigraphic Lexicon of Libya. *Ind. Res. Cent.*, Tripoli, Bull. **13**, 300 p.

Barr, F.T. and Berggren, W.A. (1980). Lower Tertiary Biostratigraphy and Tectonics of Northeastern Libya. *In: The Geology of Libya* (*eds* M.J. Salem and M.T. Busrewil). Academic Press, London, **I**, 163–192.

Bird, E.C.F. (1984). *Coasts*. Blackwell, Oxford, 320 p.

Bromley, R.G. (1975a). Comparative analysis of fossil and echinoid bioerosion. *Palaeontology*, **18**, 725–739.

Bromley, R.G. (1975b). Trace fossils at omission surfaces. *In: The Study of Trace Fossils* (*ed.* R.W. Frey). Springer-Verlag, New York, N.Y., 399–428.

Butler, G.P. (1970). Holocene gypsum and anhydrite of the Abu Dhabi sabkha, Trucial Coast: an alternative explanation on origin. *In: Third Symposium on Salt, Northern Ohio Geol. Soc.*, Ohio, 120–152.

Conant, L.C. and Goudarzi, G.H. (1964). Geologic Map of the Kingdom of Libya; 1:2000000. *U.S. Geol. Surv. Misc. Geol. Invest.*, Map 1-350A.

Ekdale, A.A., Bromley, R.G. and Pemberton, S.G. (1984). Ichnology. The Use of Trace Fossils in Sedimentology and Stratigraphy, *SEPM Short Course*, **15**, 316 p.

El-Hawat, A.S. (1980a). Carbonate-Terrigenous Cyclic Sedimentation and Palaeogeography of the Marada Formation (Middle Miocene), Sirt Basin. *In: The Geology of Libya* (*eds* M.J.Salem and M.T. Busrewil). Academic Press, London, **II**, 427–448.

El-Hawat, A.S. (1980b). Intertidal and Storm Sedimentation from Wadi al Qattarah Member, Ar Rajmah Formation (Middle Miocene), Al Jabal Al Akhdar. *In: The Geology of Libya* (*eds* M.J. Salem and M.T. Busrewil). Academic Press, London, **II**, 449–462.

Frey, R.W. and Basan, P.B. (1978). Coastal salt marshes. *In: Coastal Sedimentary Environments*. Springer-Verlag, New York, N.Y., 101–169.

Frey, R.W. and Seilacher, A. (1980). Uniformity in marine invertebrate ichnology. *Lethaia*, **13**, 183–207.

Hallam, A. (1980). *Facies Interpretation and the Stratigraphic Record*. Freeman and Co., Oxford, 291 p.

Hardie, L.A. and Eugster, H.P. (1971). The depositional environment of marine evaporites; a case for shallow, clastic accumulation. *Sedimentology*, **16**, 187–220.

Jenkyns, H.C. (1978). Pelagic environments. *In: Sedimentary Environments and Facies* (*ed.* H.G. Reading), 314–371.

Kendall, A.C. (1979a). Continental and supratidal (Sabkha) evaporites. *In: Facies Models* (*ed.* R.G. Walker), Geoscience Canada, 145–158.

Kendall, A.C. (1979b). Subaqueous evaporites. *In: Facies Models* (*ed.* R.G. Walker), Geoscience Canada, 159–174.

Kumati, S.M. (1981). *The Geology of the Hofra Region, Sirt Basin, Libya (G.S.P.L.A.J.).* Ph.D. Thesis, Univ. Manchester, 231 p.

Megerisi, M. and Mamgain, V.D. (1980). The Upper Cretaceous and Tertiary formations of Northern Libya. *In: The Geology of Libya* (*eds* M.J. Salem and M.T.Busrewil). Academic Press, London, **I**, 68–89.

Pitman, W.C. (1978). Relationship between eustasy and stratigraphic sequences of passive margins. *Bull. Geol. Soc. Am.*, **89**, 1389–1403.

Postma, H. (1961). Transport and accumulation of suspended matter in the Dutch Wadden Sea. *Neth. J. Sea Res.*, **I**, 148–190.

Radwanski, A. (1970). Dependence of rock borers and burrowers on the environmental conditions within the Tortonian of southern Poland. *In*: Trace Fossils (*eds* T.P. Crimes and J.C. Harper). *Geol. J.*, Spec. Issue, **3**, 371–390.

Reineck, H.E. and Singh, I.B. (1975). *Depositional Sedimentary Environments*. Springer-Verlag, New York, N.Y., 439 p.

Revelle, R. and Emery, K.O. (1957). Chemical erosion of beach rock and exposed reef rock. *U.S. Geol. Surv. Prof. Pap.*, **260-T**, 699–709.

Schneider, J. (1976). Biological and inorganic factors in the destruction of limestone coasts. *Contrib. Sedimentol.*, **6**, 112 p.

Schreiber, B.C. (1978). Environments of subaqueous gypsum deposition. *In*: Notes for a Short Course on Marine Evaporites (*eds* W.E. Dean and B.C. Schreiber). *SEPM Short Course*, **4**, 43–73.

Schreiber, B.C. and Kinsman, D.J.J. (1975). New observations on the Pleistocene evaporites of Montallegro, Sicily, and modern analog. *J. Sediment. Petrology*, **45**, 465–479.

Selley, R.C. (1966). *The Miocene Shoreline of Marada, Libya.* Ph.D. Thesis, Imperial College, London.

Selley, R.C. (1970). *Ancient Sedimentary Environments*. Chapman and Hall, London, 317 p.

Shinn, E.A. (1973). Sedimentary coastal accretion in an area of longshore transport, south-east Qatar, Persian Gulf. *In: The Persian Gulf* (*ed.* H.B. Purser). Springer-Verlag, New York, N.Y., 193–209.

Vail, P.R., Mitchum, R.M., Todd, R.G., Widmier, J.M., Thompson, S., Sangree, J.B., Bubb, J.N. and Hatledid, W.G. (1977). Seismic stratigraphy and global changes in sea level. *In*: Seismic Stratigraphy — Applications to Hydrocarbon Exploration (*ed.* C.E. Payton). *Mem. Am. Assoc. Petrol. Geol.*, **26**, 49–212.

Warme, J.E. and McHuron, E.J. (1978). Marine borers; trace fossils and their significance. *In*: Trace Fossil Concepts (*ed.* P.B. Basan). *SEPM Short Course*, **5**, 67–118.

Wilson, J.L. (1975). *Carbonate Facies in Geologic History.* Springer-Verlag, New York, N.Y., 471 p.

Sedimentology, Petrography and Diagenesis of Metlaoui Group in the Offshore Northwest of Tripoli

A. BERNASCONI[1], G. POLIANI[1] AND A. DAKSHE[2]

رسوبية وبتروغرافية تحورات مجموعة المتلوى بالمنطقة المغمورة شمال غربي طرابلس

أ. برناسكوني وج. بولياني وع. الداكشي

الخلاصــة

لقد تمت دراسة مجموعة المتلوى (اليبريسى) في سبعة آبار بحقل البوري بالمنطقة المغمورة على بعد حوالي 125كم شمال غربي طرابلس.

تعلو مجموعة المتلوى تكوين الهارية (ماسترختي — باليوسين) كما يعلو هذا تكوين سوار (الأيوسين الأسفل — والأوسط).. وكل من التكوينين الأخيرين قد ترسب في ظروف بحرية مفتوحة.

ولقد تمّ التعرف على ثلاثة أعضاء بالمتلوى. وهي كما يلي من **القمة** إلى **القاعدة**

عضو نيوميوليتي يتكون من الصخر الحبيبي والباكستون النيوميوليتي. ترسب في مياه ضحلة (ضحضاح) تحت تأثير بحر مفتوح.

عضو دولوميتي يتكون من دولوميت دقيق البلورات ترسب في بيئات محصورة من رصيف ضحل و(أو) مسطح مدى جزري.

عضو ميكريتي يتكون من باكستون وواكستون. ترسب في رصيف ضحل.

ويمكن التعرف على دورتين ترسيبيتين لمجموعة المتلوى: الأولى. وهي إنحسارية. تتكون من عضو ميكريتي وعضو دولوميتي. وتتميز الثانية بعدة خصائص لتقدم وإنحسار مياه البحر، ويمثلها عضو نيوميوليتي. وقد مر المتلوى بتحورات بعد ترسبه. والتي يمكن حصرها في ثلاثة مراحل. مظاهر تحور نموذجية لبيئة ترسب سادت أثناء المرحلة الأولى، بينما عوامل يمكن أن يشار إليها ببيئة المياه الجوفية العذبة قد ميزت المرحلة الثانية. أما تأثير الدفن فقد ساد أثناء المرحلة الثالثة.

وقد وثقت الآبار من الشرق إلى الغرب التتابع العمودي والإستمرارية الجانبية للسحنات الرسوبية. وقد تمّ التوصل إلى نموذج ترسيبي خاص بمنطقة حقل البورى وذلك بناء على الإعتبارات التالية:

1 - التغير في سمك الأعضاء الثلاثة والمعلومات الزلزالية تشير إلى نشاط التكتونية أثناء ترسب المتلوى.

2 ربما كانت رسوبيات الأرصفة أكثر انتشاراً فوق المرتفعات التركيبية منه عند الجوانب.

3 - لقد نجم عن تفاعل معدلات الترسيب ومعدلات الإنخساف والتغير في مستوى المياه وعمل الأمواج الإمتداد الجانبي للأرصفة، مع خلط محتوياتها الرسوبية.

4 - لقد ساعد انحسار الماء على زيادة حجم الأرصفة.

وقد تأثرت أنواع الصخور بعمليات الترسيب والتحور بطرق مختلفة مما أدى إلى نشأة تنوع كبير في المسامية الأولية والثانوية.

Abstract. The Metlaoui Group (Ypresian, Jdeir Formation, Jirani Dolomite, Bilal Formation), has been studied in seven wells in the El Bourī Field, 125 km NW of Tripoli, in the Mediterranean Sea.

The Metlaoui Group overlies the El Haria Formation (Maastrichtian–Palaeocene, Al Jurf Formation) and is overlain by the Souar Formation (Middle–Upper Eocene, Ghalil Formation). The latter two formations are of open marine environment.

---

[1] AGIP S.p.A., Petrographic and Sedimentological Department, S. Donato Milanese, Italy.
[2] AGIP NAME, P.O. Box 346, Tripoli, Libya, G.S.P.L.A.J.

Three members have been recognized in the Metlaoui Group. From top to bottom they are:

- Nummulitic Member (Jdeir Formation), represented by nummulitic packstone–grainstone of shallow-water environment (banks) with open marine influences;
- Dolomitic Member (Jirani Dolomite, and Bilal Formation p.p.), represented by finely crystalline dolomite of restricted shallow platform and/or tidal flat complex environments;
- Micritic Member (Bilal Formation), represented by wackestone–packstone, of shallow platform environment.

Two sedimentary cycles can be recognized in the Metlaoui Group: the first, which is regressive, consists of a Micritic Member and a Dolomitic Member; the second, characterized by several transgressive and regressive pulses, is represented by the Nummulitic Member. The Metlaoui Group has undergone a diagenetic evolution which may be divided into three phases. Diagenetic processes typical of a marine depositional environment prevailed during the first phase, while processes that may be referred to freshwater phreatic and vadose environment were active during the second phase. Burial effects prevailed during the third phase.

The vertical sequence and the lateral continuity of the facies are well documented by wells in the E–W direction.

A specific depositional model in the El Bourī Field area has been reconstructed on the basis of the following considerations:

(1) The changes in thickness of the three members and the seismic data suggest that the tectonic structure was active during the deposition of the Metlaoui Group;
(2) The deposition of banks was probably more prevalent on the top of the structure than on the flanks;
(3) The interaction between rates of sedimentation, rates of subsidence, eustatic changes and wave action produced lateral migrations, reworking and "shallowing" of the banks;
(4) Regressions favoured the areal development of banks.

The sedimentary and diagenetic processes affected the lithotypes in a different way, giving rise to a wide range of combinations of primary and secondary porosities.

INTRODUCTION

The aim of this study is to trace the depositional and diagenetic history of the Metlaoui Group in the offshore NW of Tripoli, where AGIP NAME during 1970 discovered the El Bourī Field in the NC41 area and drilled several wells (Fig. 1). We have outlined in the best possible way the geometry of the porous layers in order to understand the genesis and distribution of porosity. In fact, porosity was first influenced by sedimentological factors and then by diagenetic ones.

The most porous and permeable layers are represented by the Nummulitic Member (Jdeir Formation) by the facies associated with banks of the Nummulitic Member and by the fine-grained dolomite of the Dolomitic Member (Jirani Dolomite and Bilal Formation p.p.).

In addition, a sedimentological model for the nummulitic banks has been specifically prepared for the El Bourī area.

GEOLOGICAL SETTING

The El Bourī Field is located 125 km NW of Tripoli, in the westernmost part of the gulf of Sirt. The NC41 area is located on the northern margin of the African shield, within the Gabes–Tripoli–Misṛātah basin. This basin is delimited to the north by the Medina and Lampedusa plateau and to the south by the Gafsa–Jifārah Hercynian normal-fault system.

Tripoli–Misṛātah basin was formed in the Palaeozoic (Goudarzi, 1980) and underwent four main subsidence stages coinciding with the Upper Triassic, Middle Jurassic, Upper Jurassic and Miocene–Quaternary distensive tectonic phases (Finetti, 1982).

The stratigraphic sequence crossed by the wells in the NC41 area (Fig. 2; Hammuda *et al.*, 1985) consists of carbonate and/or terrigenous sediments of relatively deep, open marine environment, with an episode of restricted water circulation in the Messinian. The wells have reached the El Haria Formation (Maastrichtian–Palaeocene).

In the Ypresian the Metlaoui Group was deposited followed by the marls and clays of the Souar Formation (Ghalil Formation) which represents the cap rock.

PALAEOGEOGRAPHY AND SEDIMENTOLOGY

In the Lower Eocene the area studied was a wide continental shelf subjected to frequent transgressions and regressions. During the Ypresian, the deposition of the Metlaoui Group (Jdeir Formation, Jirani Dolomite, Bilal Formation) took place on a substratum characterized by local topographical irreg-

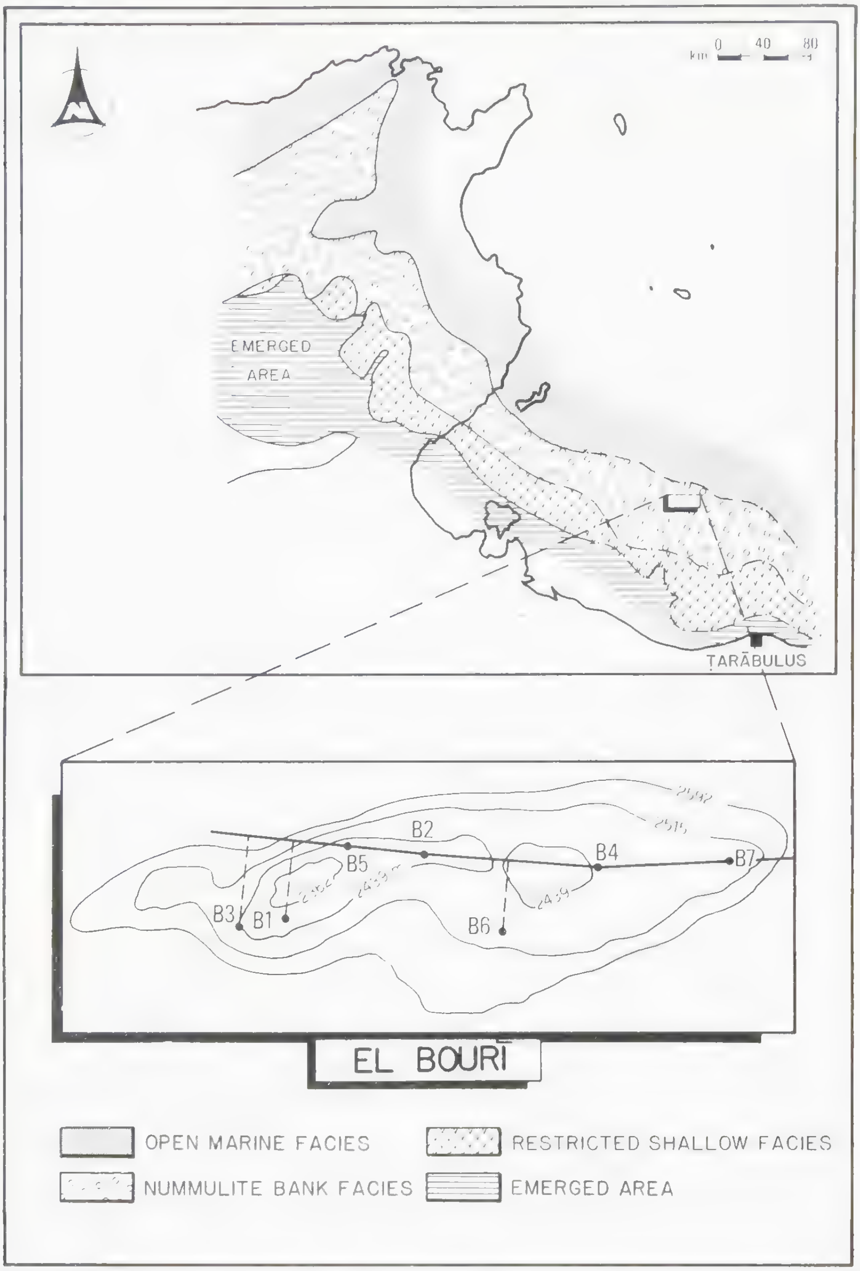
km 0 40 80
EMERGED AREA
TARĀBULUS
B2
B5
B4
B7
B3
B1
B6
2592
2515
2439
EL BOURĪ
OPEN MARINE FACIES
RESTRICTED SHALLOW FACIES
NUMMULITE BANK FACIES
EMERGED AREA

Fig. 1. Facies map, with the regional distribution of the three facies present in Metlaoui Group (Bishop, 1975; AGIP S.p.A. data); detail of the structure in the El Bourī Field (top Metlaoui Group) with the trace of the geological section of Figs 3 and 12.

ularities of tectonic origin. The coastline extended from NW to SE (Fig. 1); the emerged areas lay to the south whilst the open sea was much further to the north, beyond the wide platform. The nummulitic facies were deposited following the same NW–SE trend. The open marine micritic facies were deposited to the NE while the restricted platform facies and the dolomites were deposited to the SW. Regionally, the distribution of the facies, according to our data, complies very well with the known data (Bishop, 1975).

From a sedimentological point of view, in the NC41 area the three members of the Metlaoui Group show visible lateral changes, especially in the

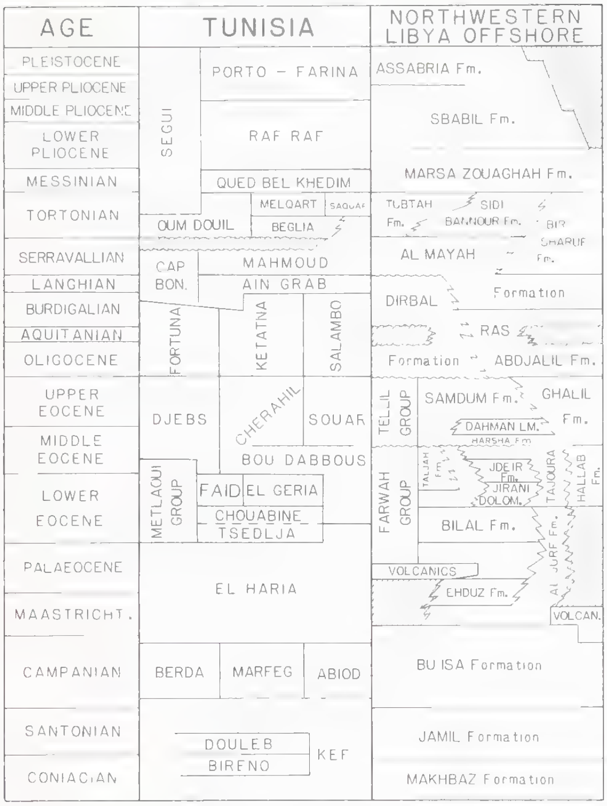
AGE
TUNISIA
NORTHWESTERN LIBYA OFFSHORE
PLEISTOCENE
UPPER PLIOCENE
MIDDLE PLIOCENE
LOWER PLIOCENE
MESSINIAN
TORTONIAN
SERRAVALLIAN
LANGHIAN
BURDIGALIAN
AQUITANIAN
OLIGOCENE
UPPER EOCENE
MIDDLE EOCENE
LOWER EOCENE
PALAEOCENE
MAASTRICHT.
CAMPANIAN
SANTONIAN
CONIACIAN
SEGUI
PORTO – FARINA
RAF RAF
OUED BEL KHEDIM
MELQART
SAQUAF
OUM DOUIL
BEGLIA
CAP BON.
MAHMOUD
AIN GRAB
FORTUNA
KETATNA
SALAMBO
DJEBS
CHERAHIL
SOUAR
BOU DABBOUS
METLAOUI GROUP
FAID
EL GERIA
CHOUABINE
TSEDLJA
EL HARIA
BERDA
MARFEG
ABIOD
DOULEB
BIRENO
KEF
ASSABRIA Fm.
SBABIL Fm.
MARSA ZOUAGHAH Fm.
TUBTAH Fm.
SIDI BANNOUR Fm.
BIR SHARUF Fm.
AL MAYAH
DIRBAL
Formation
RAS
Formation
ABDJALIL Fm.
TELLIL GROUP
SAMDUM Fm.
GHALIL Fm.
DAHMAN LM.
HARSHA Fm.
FARWAH GROUP
TALJAH Fm.
JDEIR Fm.
JIRANI DOLOM.
TAJOURA Fm.
HALLAB Fm.
BILAL Fm.
AL JURF Fm.
VOLCANICS
EHDUZ Fm.
VOLCAN.
BU ISA Formation
JAMIL Formation
MAKHBAZ Formation

Fig. 2. Generalized stratigraphic correlation chart of the formations of NW Libya offshore and Tunisia.

N–S direction. North of the El Bourī Field the Micritic Member (Bilal Formation) is well represented while the Dolomitic Member (Jirani Dolomite and Bilal Formation p.p.), represented by the dolomicrites with anhydrite and/or gypsum nodules, is missing, and the open shallow platform facies of the Nummulitic Member (Jdeir Formation) are well developed and prevail over the bank facies. South of the El Bourī area, there is a significant thickness of dolomicrites with anhydrite and gypsum nodules and associated dolomitic facies belonging to the Dolomitic Member; the Micritic Member is missing while the Nummulite bank facies of the Nummulitic Member are well developed and prevail over the open shallow platform facies with which they are usually associated.

FACIES ANALYSIS

The lithofacies analysis is based mainly on the study of cores for both the Nummulitic and the Dolomitic Members and on cuttings for the Micritic Member. The correlations are based on lithologic–petrographic criteria (Fig. 3).

The lithologic sequences of the different wells have been compared respectively with the relevant petrophysical characteristics measured. The sequence is well documented vertically, as well as laterally according to an E–W section, while in the N–S direction, forecasts are more difficult due to the distribution of the wells.

Nine lithofacies have been recognized and correlated. They can be grouped into three members:

- The Nummulitic Member (Jdeir Formation), present in the upper part of the formation. It consists of nummulitic packstone–grainstone (Fig. 4A, B, D, E) and of bioclastic, fossiliferous packstone–wackestone (Fig. 4C). The Nummulitic Member can be further subdivided into "Upper Nummulitic" and "Lower Nummulitic" (Figs 3, 4). Nummulite bank facies prevail in the "Upper Nummulitic", whereas in the "Lower Nummulitic" micritic facies of open shallow platform prevail.
- The Dolomitic Member (Jirani Dolomite and Bilal Formation p.p.), which forms the middle part of the formation, consists of dolomicrites (Fig. 4F) secondary fine-grained dolomite, and dolomitized packstone.
- The Micritic Member (Bilal Formation), which represents the lowermost part of the unit, consists of argillaceous wackestone–packstone, finely fossiliferous.

A detailed description of the lithofacies recognized, from top to bottom, follows:

Nummulitic Member: Upper Nummulitic

1. Uppermost bank with large nummulites (Figs 4A, 8A)

Packstone, rarely grainstone, with predominant large nummulites sometimes reworked or broken, fragments of pelecypods and echinoderms. Internal vadose crystal silt (Dunham, 1969; Aissoui and Purser, 1983) as well as layers cemented by sparry calcite, or uncemented, can be observed.

Dissolution phenomena as well as moldic, vuggy, intraparticle and interparticle porosity are recognizable.

2. Upper open shallow platform packstone–wackestone (Figs 4C, 8C)

Packstone–wackestone with scattered nummulites, frequent echinoderm and nummulite fragments,

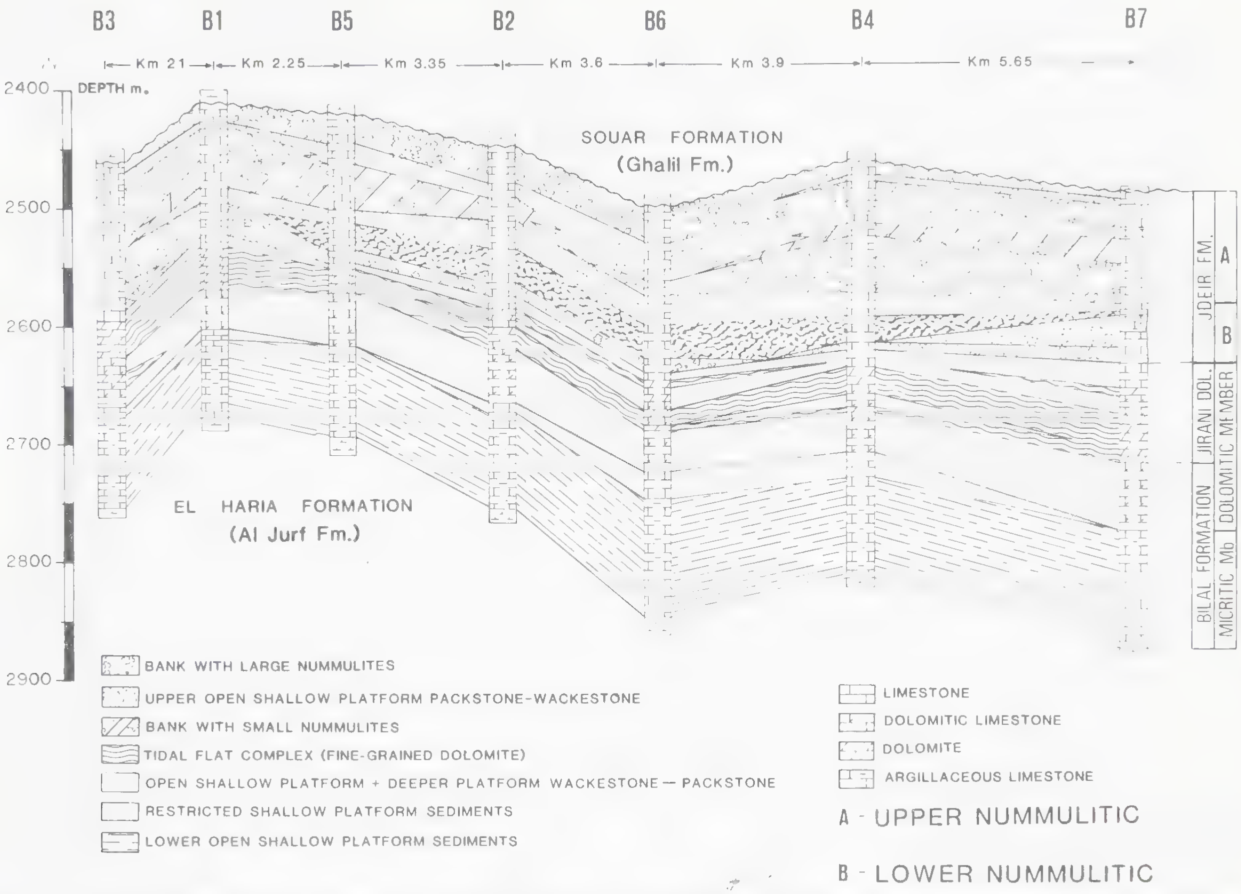
B3
B1
B5
B2
B6
B4
B7
Km 21
Km 2.25
Km 3.35
Km 3.6
Km 3.9
Km 5.65
DEPTH m.
2400
2500
2600
2700
2800
2900
SOUAR FORMATION
(Ghalil Fm.)
EL HARIA FORMATION
(Al Jurf Fm.)
JDEIR FM.
A
B
JIRANI DOL.
BILAL FORMATION
DOLOMITIC MEMBER
MICRITIC Mb
BANK WITH LARGE NUMMULITES
UPPER OPEN SHALLOW PLATFORM PACKSTONE-WACKESTONE
BANK WITH SMALL NUMMULITES
TIDAL FLAT COMPLEX (FINE-GRAINED DOLOMITE)
OPEN SHALLOW PLATFORM + DEEPER PLATFORM WACKESTONE — PACKSTONE
RESTRICTED SHALLOW PLATFORM SEDIMENTS
LOWER OPEN SHALLOW PLATFORM SEDIMENTS
LIMESTONE
DOLOMITIC LIMESTONE
DOLOMITE
ARGILLACEOUS LIMESTONE
A - UPPER NUMMULITIC
B - LOWER NUMMULITIC

Fig. 3. Lithostratigraphic section (see Fig. 1 for location) showing the E–W distribution of the nine lithofacies recognized and grouped into three members.

large pelecypods, some gastropods, other small benthonic forams, rare Alveolinidae and Miliolidae. Porosity is good, of moldic, vuggy or intraparticle type.

3. Intermediate bank with large nummulites (Fig. 8D)

Packstone–grainstone with large nummulites, echinoderm fragments, rare pelecypods. The equant calcite cement percentage increases so that porosity is progressively reduced with depth, with respect to the uppermost bank. Early dissolution features as well as internal vadose silt, as geopetal filling, can be observed.

4. Intermediate bank with small nummulites (Fig. 4E)

Packstone with small-sized nummulites, microsized nummulitic fragments (nummulitoclastic foramsiltite), echinoderm fragments with syntaxial overgrowths, and abundant micrite matrix. Good chalky microporosity and low permeability can be observed.

Nummulitic Member: Lower Nummulitic

5. Open shallow platform plus deeper platform sediments (Fig. 8E)

Finely bioclastic wackestone–packstone with benthonic forams, calcitized microscleres sponge spicules, rare radiolarians, planktonic forams; upwards they become packstone–wackestone with rare nummulites, echinoderm and mollusc fragments, and benthonic forams. Porosity is low to negligible, except for the packstone intervals, where it is fair.

6. Lowermost bank with large nummulites (Figs 4B, 8B)

Grainstone, rarely packstone, with large nummulites, echinoderm fragments, Mollusca, and rare algae. Pressure-solution phenomena as well as cementation

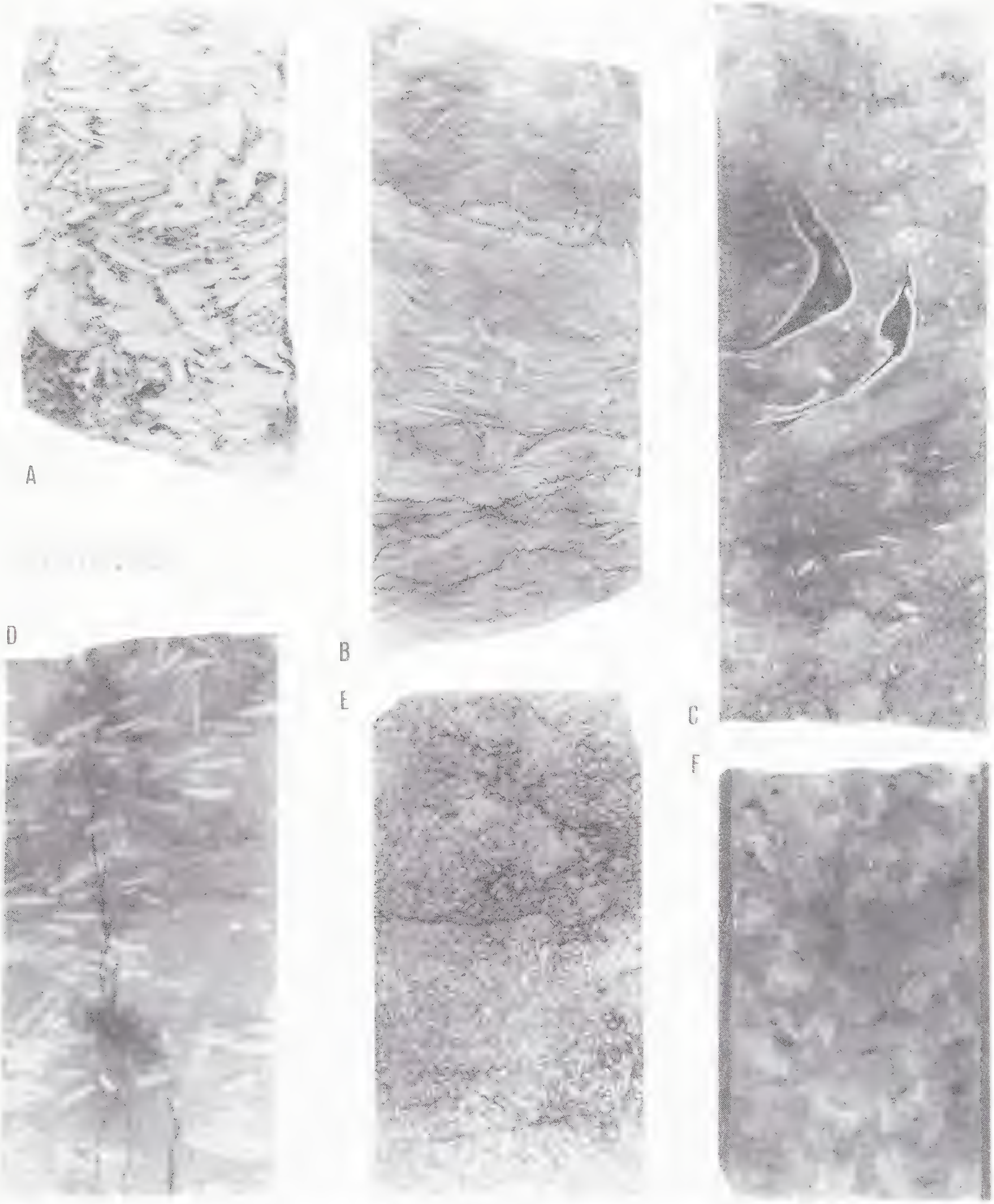

Fig. 4. Nummulitic Member: A. B6/8251–8252 ft: Packstone–grainstone with large nummulites, of bank environment. Good moldic, interparticle and intraparticle porosity ($\phi = 12\%$). B. B2/8443–8444 ft: Intensely stylolitized grainstone packstone of bank environment, with low porosity ($\phi = 4\%$). C. B3/8122–8123 ft: Fossiliferous packstone with large pelecypods, bioclasts, rare nummulites, of open shallow platform environment. Chalky porosity ($\phi = 17\%$). D. B7/8407–8408 ft: Packstone with large nummulites and finely fossiliferous bioclastic matrix. Chalky porosity ($\phi = 13\%$). E. B3/8149–8150 ft: Packstone with small nummulites and finely fossiliferous bioclastic matrix. Chalky porosity ($\phi = 14\%$).
Dolomitic Member: F. B5/8411–8412 ft: Finely crystalline, early secondary dolomite, with burrows, of tidal flat complex. Moldic and vuggy porosity ($\phi = 33\%$).

by equant calcite crystals are well developed, so that porosity is low, moldic, residual intraparticle, and interparticle type. Filling by internal vadose crystal silt as geopetal texture is recognizable.

Dolomitic Member (Jirani Dolomite and Bilal Formation p.p.)

7. Restricted shallow platform sediments (Figs 4F, 8F, 11A)

Grey to light grey packstone–grainstone, rarely wackestone, with algae, Miliolidae, Alveolinidae, Peneroplidae, Mollusca, echinoderm fragments, and phosphatic remains. Porosity is low except for the early dolomitized intervals.

8. Restricted shallow platform plus tidal flat complex sediments (Fig. 11B)

Finely crystalline, grey dolomite, sometimes intensely burrowed, with very rare anhydrite nodules, more frequent kaolinite-filled vugs, rare detrital quartz grains. Excellent vuggy and moldic porosity. Dolomicrite, grey-brownish, with rare vugs and intercrystalline porosity. Repeated interlayering of dolomicrites and finely crystalline, early secondary dolomite can be observed, giving rise to cyclic variations of the porosity curve.

Micritic Member (Bilal Formation)

9. Lower open shallow platform sediments (Fig. 11C–H).

Grey, light wackestone–packstone, argillaceous, with small Echinodermata and Mollusca fragments, rare planktonic forams and microscleres sponge spicules, small benthonic forams, phosphatic remains, rare quartz grains and glauconite nodules. Porosity is negligible to poor.

ENVIRONMENTAL INTERPRETATION OF THE SEQUENCE

In the Metlaoui Group it is possible to recognize two sedimentary cycles: regressive cycle and a transgressive–regressive cycle (Figs 5, 6).

The Metlaoui Group deposition began with argillaceous wackestone (Micritic Member, or Bilal Formation) of open shallow platform, followed by dolomitic packstone, fossiliferous packstone of restricted shallow platform and fine-grained dolomites of tidal environment (Dolomitic Member or Jirani Dolomite and Bilal Formation p.p.). It is therefore possible to recognize a former sedimentary regressive cycle which ended with the deposition of the Dolomitic Member.

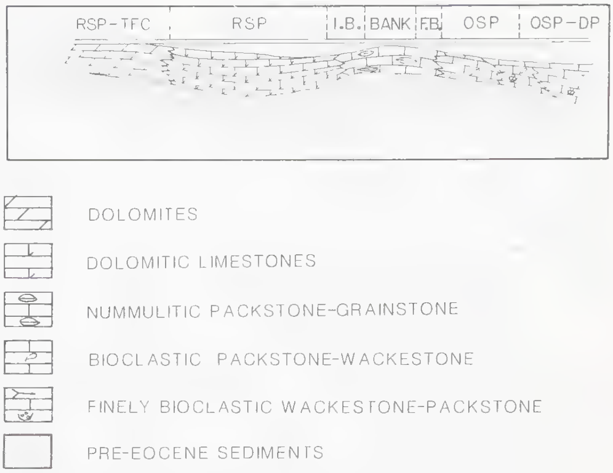
RSP-TFC
RSP
I.B.
BANK
F.B.
OSP
OSP-DP
DOLOMITES
DOLOMITIC LIMESTONES
NUMMULITIC PACKSTONE-GRAINSTONE
BIOCLASTIC PACKSTONE-WACKESTONE
FINELY BIOCLASTIC WACKESTONE-PACKSTONE
PRE-EOCENE SEDIMENTS

Fig. 5. Idealized scheme of depositional environments recognized in the El Bourī area.

Later, nummulitic packstone–grainstone of bank environment and bioclastic packstone–wackestone of shallow-water environment with open marine influence were laid down. This sequence represents the sedimentary response to the many sea-level changes that took place during the deposition of the Nummulitic Member (Jdeir Formation). Furthermore, on the basis of regional data (Vail *et al.*, 1977) and on the basis of the diagenetic evolution undergone by the formation, an emergence is hypothesized at the top of the Nummulitic Member.

We can therefore recognize a second sedimentary cycle with transgressive and regressive pulses which ended with a remarkable regression.

The regressive periods favoured the development of nummulite banks, whereas in the transgressive periods a uniform sedimentation prevailed in an open marine environment.

NUMMULITIC MEMBER AND DOLOMITIC MEMBER: DIAGENETIC HISTORY

The diagenetic evolution of the Nummulitic and Dolomitic Members may be divided into three phases (Figs 7, 8, 9, 10). The first phase is characterized by the influence of sea water present in the depositional environment, while the second phase is characterized by fresh water (Longman, 1980). Finally, processes related to burial effects prevailed during the third phase.

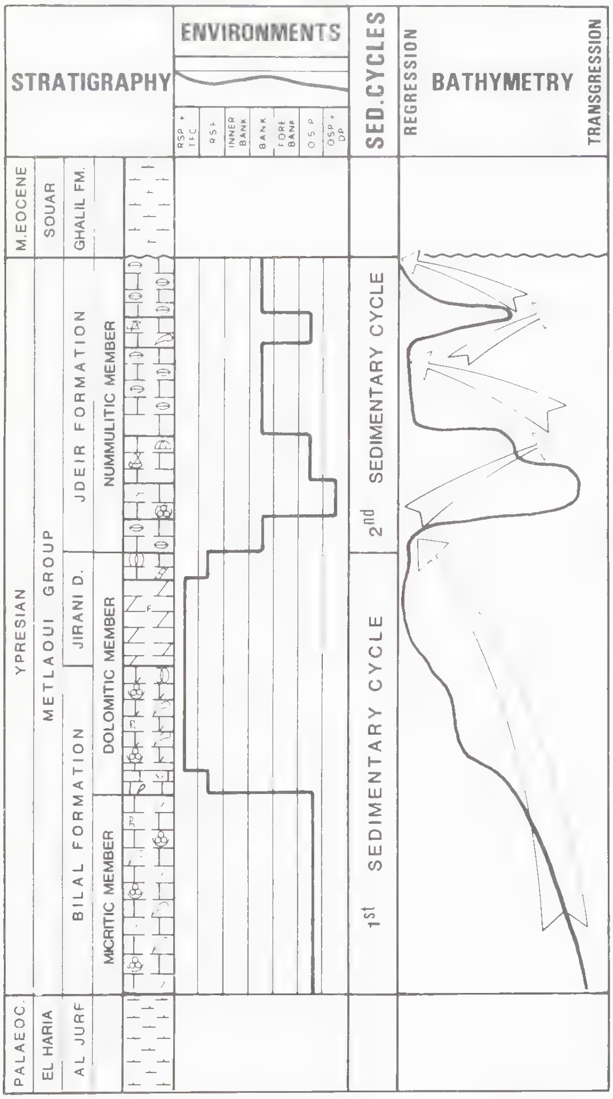

Fig. 6. Sedimentary evolution. The first sedimentary cycle is regressive; the second one shows transgressive and regressive features and ends with a regression. *TFC* = tidal flat complex; *RSP* = restricted shallow platform; *OSP* = open shallow platform; *DP* = deeper platform; *Bank* = Nummulite Bank.

Early marine diagenesis (1st phase)

In the nummulite bank facies a calcite cement which consists of thin and elongated crystals has occasionally been observed. This cement forms a fibrous coating inside the shells where it is more abundant. Its characteristics are typical of cements that are formed in the active phreatic marine zone (Bathurst, 1971; Milliman, 1974). The first diagenetic phase did not produce visible effects on the open shallow platform wackestone–packstone interbedded between the nummulite banks facies or on the restricted shallow platform facies of the Dolomitic Member (packstone–grainstone with algae, Miliolidae and Alveolinidae).

However, the dolomitization of the packstone in the Dolomitic Member must be of early formation. The interbedding of this packstone with fine-grained dolomite and dolomicrite suggests that selective dolomitization of the micritic matrix of the packstones and the formation of dolomicrites occurred concurrently. The early fine-grained secondary dolomites form low density aggregates with very high intercrystalline and vuggy porosity.

Early freshwater diagenesis (2nd phase)

The marine phreatic cement previously described is usually enclosed in a later sparry calcite cement. The nature, composition and distribution of this cement suggest that it was deposited during a diagenetic phase characterized by fresh water. The circulation of fresh water in the Metlaoui Group indicates that the El Bourī structure emerged before deposition of the marls of the Souar Formation (Ghalil Formation).

The sparry cement present in the nummulitic grainstone–packstone is irregularly distributed and concentrated in well recognizable layers. The thickness and frequency of the highly cemented layers regularly increase with depth. The distribution of these layers was probably controlled by seasonal pulse of the fresh water palaeonappe that affected the Nummulitic Member. The crystallization and growth of sparry cement, sometimes associated with the dissolution of metastable carbonates, took place in layers that progressively occurred in the saturated phreatic freshwater zone.

However, in the layers that were placed both in the vadose zone and in the undersaturated phreatic zone, dissolution phenomena prevailed.

The important moldic porosity present in all the facies of the Nummulitic and Dolomite Members was generated mainly in the vadose zone and in the undersaturated phreatic zone. Dissolution progressively affected the Lamellibranchia, Miliolidae, arenaceous forams, rotaliform forams, Alveolinidae, pellets, the micritic matrix, and finally the nummulites. Sometimes the dissolution of the tests produced molds subsequently filled by sparry calcite or internal sediments.

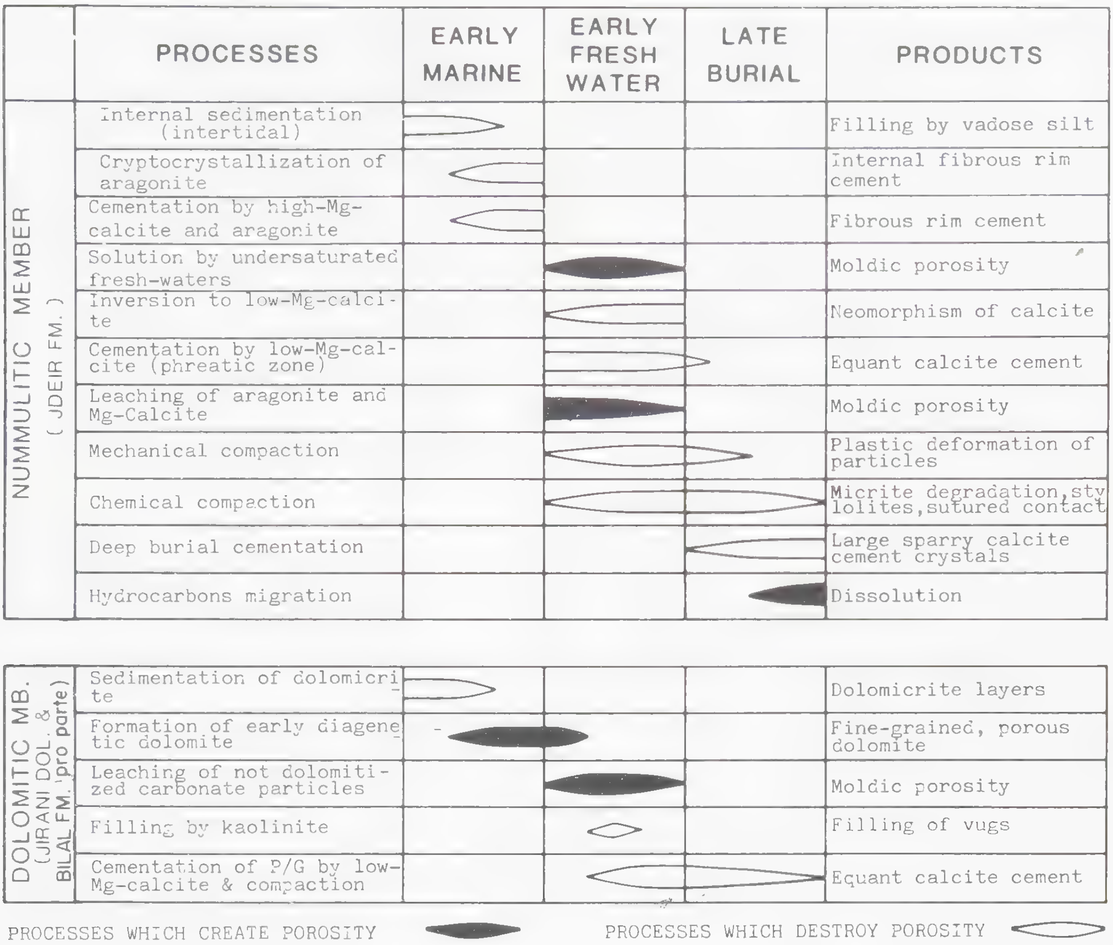
PROCESSES
EARLY MARINE
EARLY FRESH WATER
LATE BURIAL
PRODUCTS
NUMMULITIC MEMBER (JDEIR FM.)
Internal sedimentation (intertidal)
Filling by vadose silt
Cryptocrystallization of aragonite
Internal fibrous rim cement
Cementation by high-Mg-calcite and aragonite
Fibrous rim cement
Solution by undersaturated fresh-waters
Moldic porosity
Inversion to low-Mg-calcite
Neomorphism of calcite
Cementation by low-Mg-calcite (phreatic zone)
Equant calcite cement
Leaching of aragonite and Mg-Calcite
Moldic porosity
Mechanical compaction
Plastic deformation of particles
Chemical compaction
Micrite degradation, stylolites, sutured contact
Deep burial cementation
Large sparry calcite cement crystals
Hydrocarbons migration
Dissolution
DOLOMITIC MB. (JIRANI DOL. & BILAL FM. 'pro parte)
Sedimentation of dolomicrite
Dolomicrite layers
Formation of early diagenetic dolomite
Fine-grained, porous dolomite
Leaching of not dolomitized carbonate particles
Moldic porosity
Filling by kaolinite
Filling of vugs
Cementation of P/G by low-Mg-calcite & compaction
Equant calcite cement
PROCESSES WHICH CREATE POROSITY
PROCESSES WHICH DESTROY POROSITY

Fig. 7. Diagenetic evolution of the Metlaoui Group. Three diagenetic phases have been identified. During the first phase, in a marine environment, the syngenetic dolomicrites were formed and the dolomitization of restricted shallow platform facies occurred. In the Nummulitic Member, the first phase produced the crystallization of an aragonitic cement and the formation of internal sediments. During the second phase, in vadose and phreatic freshwater environments, dissolution giving rise to secondary porosity as well as sparry calcite cementation took place. During the third phase, related to burial processes, pressure solution, micrite recrystallization and cementation prevailed, causing a reduction of porosity.

Late burial diagenesis (3rd phase)

The most intensive diagenetic process of the Metlaoui Group during the burial phase is represented by the chemical compaction due to pressure solution. Both stylolitization and microstylolitization affected the cemented nummulitic grainstones as well as the uncemented ones; dissolution and cementation through pressure solution certainly occurred after the freshwater diagenetic phase. The calcite dissolved by means of pressure solution along the stylolites probably contributed to the cementation of some fractures, filled with sparry calcite, which have been observed along the cores. Moreover, some of this calcite was probably added to the preexisting freshwater cement. In very rare cases saddle dolomite crystals have been observed. They might indicate temperatures between 100° and 150°C (Radke and Mathis, 1980). Their presence in the Nummulitic Member can therefore be ascribed to the diagenesis during the burial phase.

The hydrocarbon migration represents the last diagenetic event in the Metlaoui Group in the El Bourī Field. The CO_2, originating from the maturation of organic matter, might have contributed to the increase of secondary porosity.

The difficulty in recognizing petrographically late dissolution phenomena from the intensive early dis-

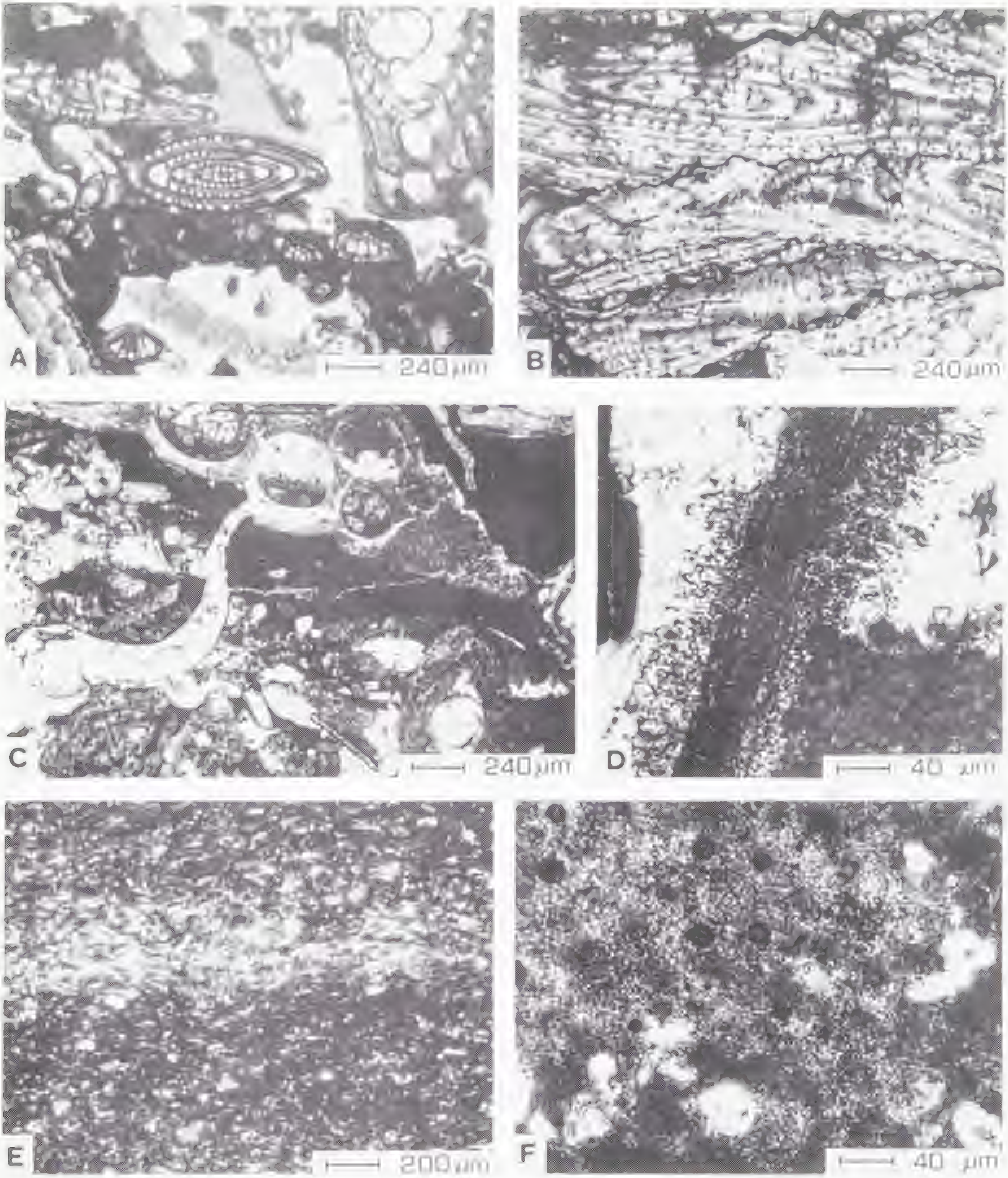

Fig. 8. Nummulitic Member: A. B4/44: Packstone with nummulites and echinoderm fragments with syntaxial overgrowths. Good intergranular and vuggy porosity. Environment: bank. B. B3/406: Strongly stylolitized and cemented nummulitic grainstone. Environment: bank. C. B2/66: Gastropod mold filled by internal vadose crystal silt. This indicates early dissolution of aragonite shells, filling by vadose silt and later cementation by sparry calcite. D. B2/54: Well-developed fibrous marine cement enclosed in a later sparry calcite cement. In the lower right corner early pelletiferous, internal vadose silt. Environment: bank. E. B6/355: Wackestone with microscleres sponges and radiolarians. Environment: Open shallow platform plus deeper platform.

Dolomitic Member: F. B3/525: Early secondary dolomites with vuggy and moldic porosity. Environment: tidal flat complex plus restricted shallow platform.

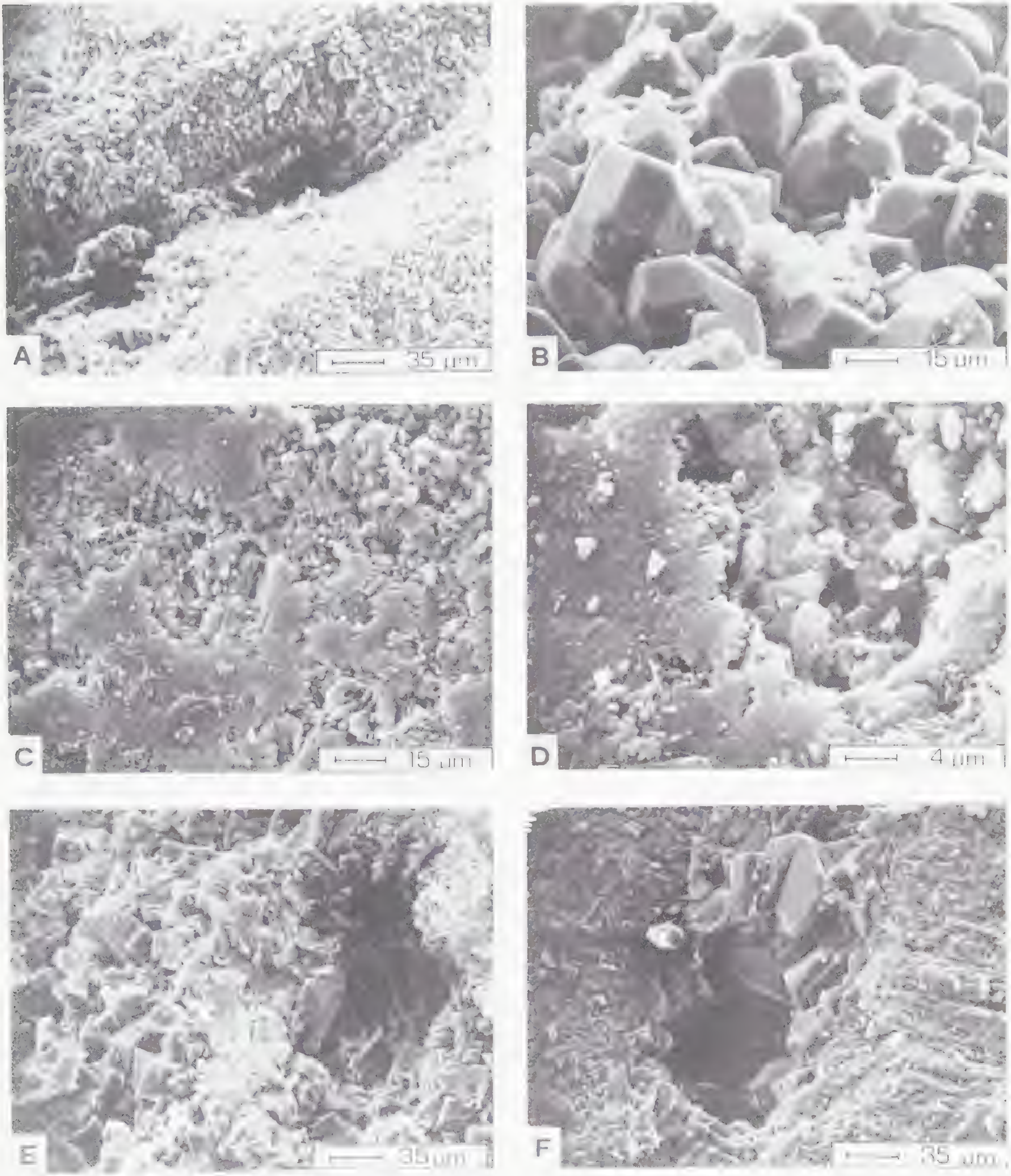

Fig. 9. Nummulitic Member: A. B7-137: Partially preserved intraparticle porosity in a nummulite shell. The chamber walls are coated by sparry calcite. B. B7-4: Well-interlocked crystals of sparry calcite. C. B2-52: Surface of a nummulite spiral lamina. Note the large corrosion figures due to post-depositional dissolution. D. B2.52: Detail of the corrosion figures. The dissolution of the lamina allows easy connection between intraparticle and interparticle porosity. The permeability is thus improved.
Dolomitic Member: E. B3-637: Secondary dolomite with vuggy porosity.
Nummulitic Member: F. B4-55: Nummulite partly filled by sparry calcite.

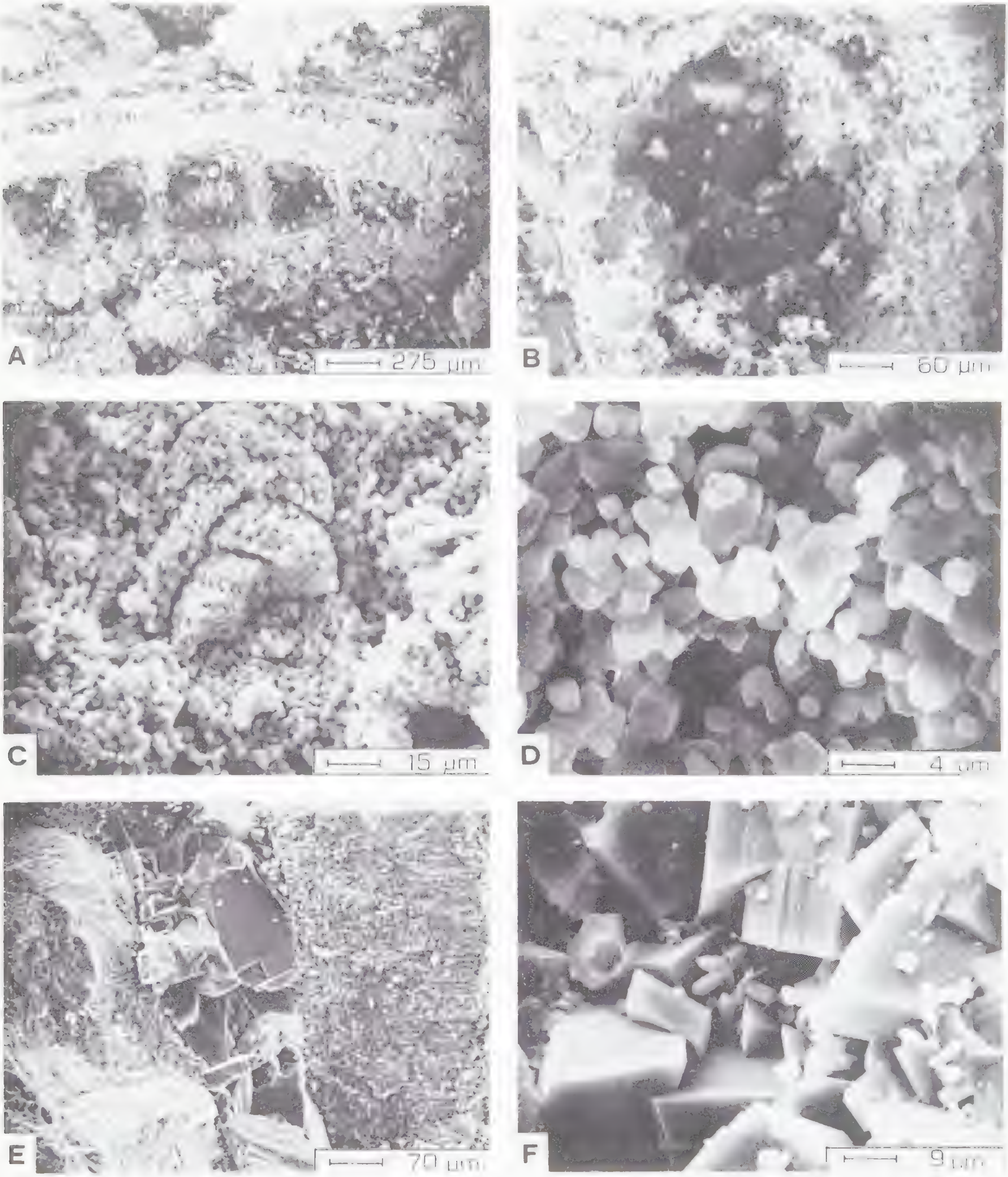

Fig. 10. Nummulitic Member: A. B3-188: Transverse section of a nummulite. B. B3-188: The chambers of the nummulite are partially coated by sparry calcite. The intraparticle porosity is rather good. C. B2-158: A mold of a biserial foraminifer; the shell has been completely dissolved giving way to moldic porosity. D. B3-278: Very good chalky porosity of the matrix. E. B2-351: Intraparticle pore in a Nummulite shell completely filled by sparry calcite.

Dolomitic Member: F. B3-637: Intercrystalline porosity in an aggregate of well interlocked euhedral secondary dolomite crystals. Note the little crystals of calcite in the centre of the photo.

solution that occurred during the second diagenetic phase has prevented us from establishing the importance of such an effect.

POROSITY–DIAGENESIS RELATIONSHIPS

In the Metlaoui Group the different types of primary and secondary porosity (Choquette and Pray, 1970) are variously distributed and combined according to the depositional facies and the diagenetic history.

The diagenetic evolution was facies-controlled, mainly due to the different initial permeabilities of the facies.

The bank facies are today the most porous and permeable layers (Table 1). In the three nummulite banks present in the Metlaoui Group the diagenesis reduced both porosity and permeability in a very variable way, because of the non-uniform distribution of its effects.

The nummulitic grainstone and packstone represents the lithotypes which were originally the most permeable and porous. Nowadays, in those nummulitic grainstones–packstones that have best retained primary and secondary porosity, porosity values above 21% and permeability values over 2000 mD have been recorded.

The diagenesis in a marine environment caused a negligible reduction of the initial porosities. Where marine cement is present the interparticle porosity reduction may be estimated at around 20%. The

Table 1. Average porosity values measured in the nine recognized lithofacies

FACIES	B2	B3	B4	B5	B6	B7	AVERAGE VALUE
1 UPPERMOST BANK WITH LARGE NUMMULITES	12.9	7.7	16.6	–	14.4	18.6	15.2
2 UPPER OPEN SHALLOW PLATFORM SEDIMENTS	20.5	15.3	20.2	–	16.4	19.9	18
4 INTERMEDIATE BANK WITH SMALL NUMMULITES	19.4	–	11.8	–	–	18.1	18.5
3 INTERMEDIATE BANK WITH LARGE NUMMULITES	–	12.9	17	–	7.6	15.8	14
5 OPEN SHALLOW PLATFORM+DEEPER PLATFORM SEDIMENTS	7.6	–	3.9	–	4.5	7.2	6
6 LOWERMOST BANK WITH LARGE NUMMULITES	5.5	–	4.9	–	4.3	5.6	5
7 RESTRICTED SHALLOW PLATFORM SEDIMENTS	8.5	7.3	6.5	–	–	–	7.5
7 DOLOMITIZED RESTRICTED SHALLOW PLATFORM SEDIMENTS	19.2	16.7	22.9	17.5	–	–	19
8 RESTRICTED SHALLOW PLATFORM PLUS TIDAL FLAT COMPLEX SEDIMENTS (FINE-GRAINED DOLOMITES)	25.7	27.1	22.7	23.9	–	–	25

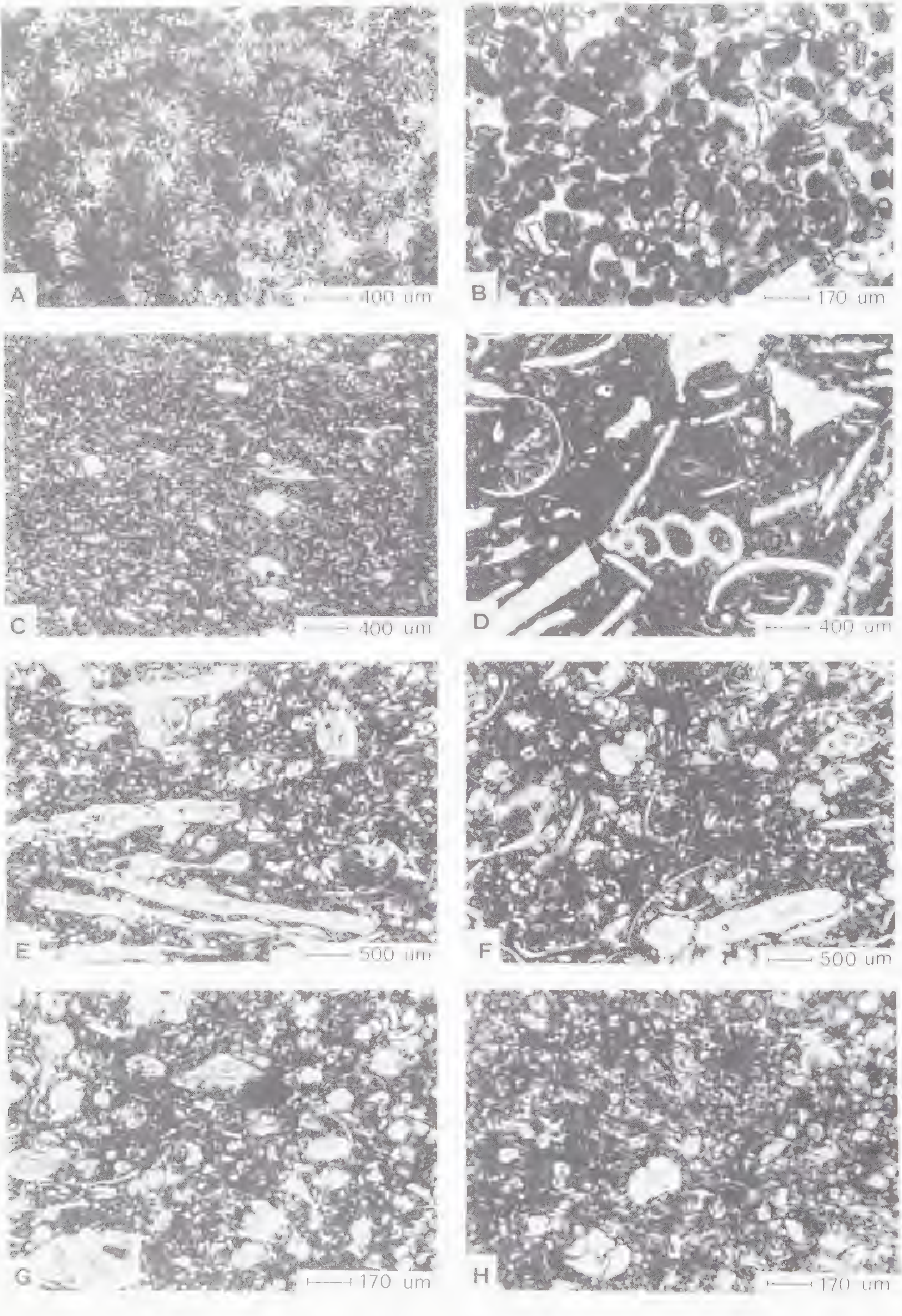
A
400 um
B
170 um
C
400 um
D
400 um
E
500 um
F
500 um
G
170 um
H
170 um

reduction of intraparticle porosity due to criptocrystallization of marine cement is greater; in rare cases, it can even be total.

The dissolution that occurred in freshwater vadose and undersaturated phreatic environments increased the porosity of all the three nummulite banks which have been recognized.

The heavier reduction of the initial porosity of some layers of the banks in general and of the lower bank in particular is due to the deposition of the sparry cement in a saturated freshwater phreatic environment; the distribution of this cement was decisive in distinguishing the characteristics of the three nummulite banks (Fig. 12; Table 1). The uppermost bank is characterized by prevailing primary and secondary porosity and very high permeability; the intermediate bank by good primary porosity, good secondary porosity and good permeability; the lowermost bank by prevailing low to fair secondary porosity and significantly lower permeability.

Wackestone–packstones of open shallow platforms are characterized by chalky and moldic porosity. The moldic porosity is interconnected through the chalky microporosity.

In some cases very high porosity values are matched by low permeability values. The dolomicrites of the Dolomitic Member retain a porosity of exclusively intercrystalline type. The porosity can be high, but the permeability is always very low. The early secondary dolomites are characterized by moldic porosity, occasionally well developed and by intercrystalline porosity which, through selective dissolution of the remaining micrite, is also well developed. The permeability of these layers is generally good; the moldic porosity is in fact well connected through the intercrystalline porosity of the dolomitic aggregates.

Fig. 11. Dolomitic Member: A. B3/506: Medium- to fine-grained dolomite, with intercrystalline and vuggy porosity ($\phi = 27\%$). B. B3/623: Well sorted grainstone-packstone, slightly dolomitic, with pellets, lithoclasts and small bioclasts ($\phi = 15\%$).
Micritic Member: C. B3/759: Wackestone with small bioclasts and rare benthonic forams ($\phi = 2\%$). D. B3/770: Wackestone with Mollusca fragments, small bioclasts ($\phi = 7\%$). E. B3/850: Wackestone–packstone with *Nummulites* sp., benthonic forams, planktonic forams, small bioclasts ($\phi = 2\%$). F. B3/858: Wackestone as above ($\phi = 2\%$). G. B3/861: Wackestone with benthonic and rare planktonic forams ($\phi = 3\%$). H. B3/931: Wackestone with rare planktonic forams ($\phi = 1\%$).

SEDIMENTOLOGICAL MODEL

Since Nummulites are a completely extinct species (Blondeau, 1972) no actual models of their ecology and sedimentation are available.

Some authors have proposed models of the formation of nummulite banks, considering Eocene sediments of different regions (Arnì, 1965; Arnì and Lanterno, 1972; Fournié, 1975; Aigner, 1983).

These models indicate that the ideal environment for the formation of nummulite banks is located in very shallow water with high energy, sometimes related to local structural highs.

Our sedimentological model, suggested for the Nummulitic Member (Jdeir Formation) in the El Bourī area, is based on the following observations:

- The seismic sections show the existence of a thinning of the seismic horizons coinciding with the Metlaoui Group toward the top of the structure. The structure was therefore active during the Ypresian and controlled the distribution of the facies.
- The scarcity of micrites in the bank facies and the presence of reworked Nummulites indicate an environment of high energy sedimentation.
- The existence of an early diagenesis in a subaerial environment, confirmed by the presence of geopetal textures with crystal silt or inversely graded micropelletal fillings, indicates the occurrence of inter-supratidal conditions.
- Well B6, located in a lower structural position, shows a cumulative minor nummulite bank facies thickness with respect to all the other wells.
- Since several reworked nummulites were observed it was assumed that a certain amount of time elapsed from the death of the Nummulite to its final deposition. During the growth of a nummulite bank an “upward shallowing” phenomenon occurred; this sedimentary process is common during the formation of coastal bars.

Thus a sedimentological model has been performed assuming the maximum development of bank facies in the highest zones of the structure and the interaction between: sedimentation rate, subsidence rate, and eustatic changes as causes of: temporary emergences of the nummulite banks, reworkings, lateral migrations of banks and anastomosis of more banks, and final regression.

The regressive periods favoured the areal migration of the banks, while during transgressive periods a minimum of nummulite bank deposits and a max-

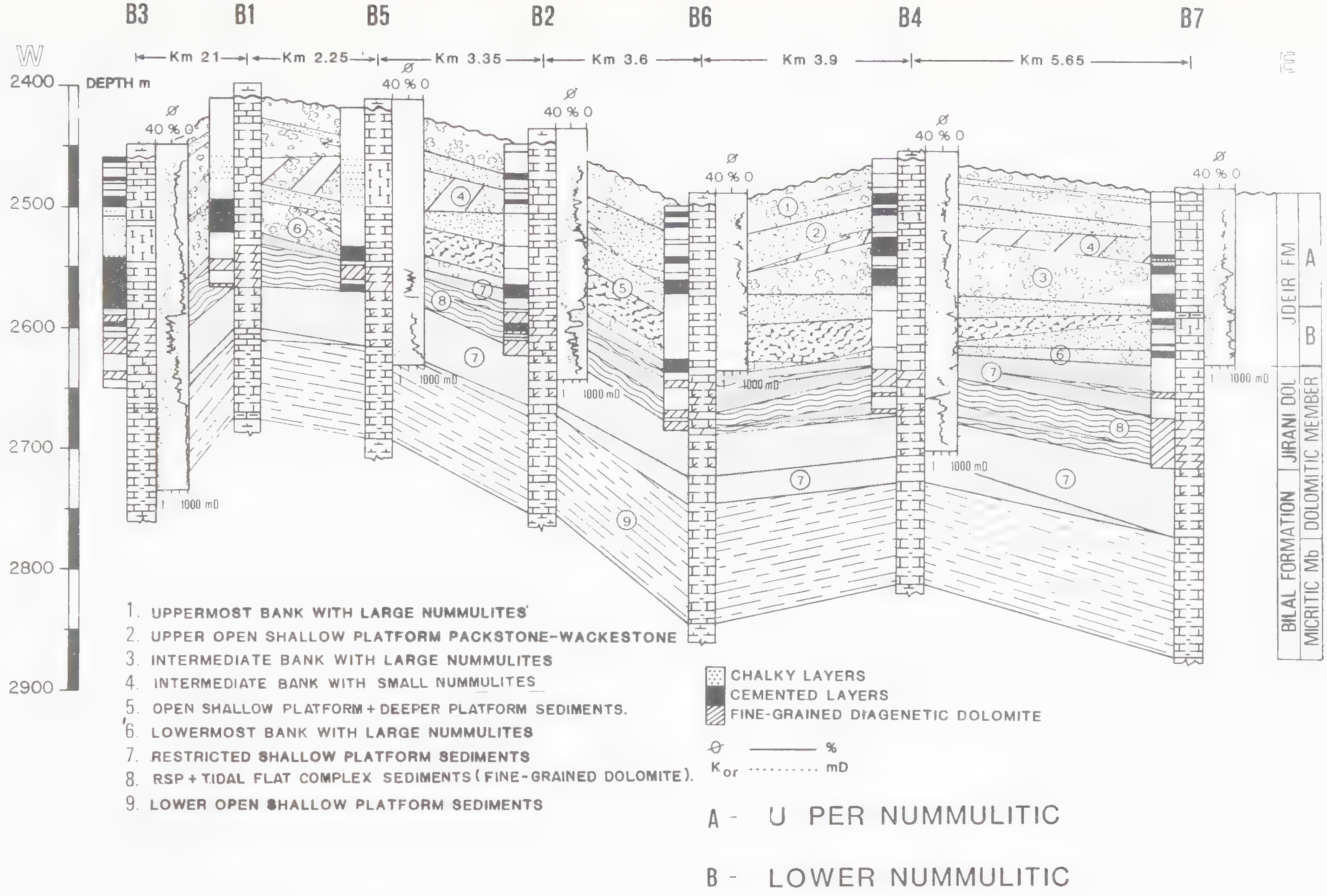
B3
B1
B5
B2
B6
B4
B7
W
E
Km 21
Km 2.25
Km 3.35
Km 3.6
Km 3.9
Km 5.65
DEPTH m
2400
2500
2600
2700
2800
2900
Ø
40 % 0
1 1000 mD
1
2
3
4
5
6
7
8
9
JDEIR FM
JIRANI DOL
BILAL FORMATION
A
B
DOLOMITIC MEMBER
MICRITIC Mb
1. UPPERMOST BANK WITH LARGE NUMMULITES
2. UPPER OPEN SHALLOW PLATFORM PACKSTONE-WACKESTONE
3. INTERMEDIATE BANK WITH LARGE NUMMULITES
4. INTERMEDIATE BANK WITH SMALL NUMMULITES
5. OPEN SHALLOW PLATFORM + DEEPER PLATFORM SEDIMENTS.
6. LOWERMOST BANK WITH LARGE NUMMULITES
7. RESTRICTED SHALLOW PLATFORM SEDIMENTS
8. RSP + TIDAL FLAT COMPLEX SEDIMENTS (FINE-GRAINED DOLOMITE).
9. LOWER OPEN SHALLOW PLATFORM SEDIMENTS
CHALKY LAYERS
CEMENTED LAYERS
FINE-GRAINED DIAGENETIC DOLOMITE
Ø ——— %
Kor .... mD
A - U PER NUMMULITIC
B - LOWER NUMMULITIC

Fig. 12. Relationships between facies, diagenesis, porosity and permeability. The Uppermost Bank with large nummulites (facies 1) underwent prevailing dissolution and therefore retains the best overall petrophysical characteristics; the Intermediate and Lowermost nummulite banks (facies 3, 4, 6) are more cemented and present lower porosity and permeability values. Facies 2 and 5 of the Nummulitic Member and the dolomitized restricted shallow platform facies (facies 7) of the Dolomitic Member have a prevailing moldic porosity interconnected through the chalky or the intercrystalline porosity. The dolomicrites (facies 8) show higher intercrystalline porosity and are characterized by lower permeability values. The Micritic Member (facies 9) shows negligible porosity and permeability values.

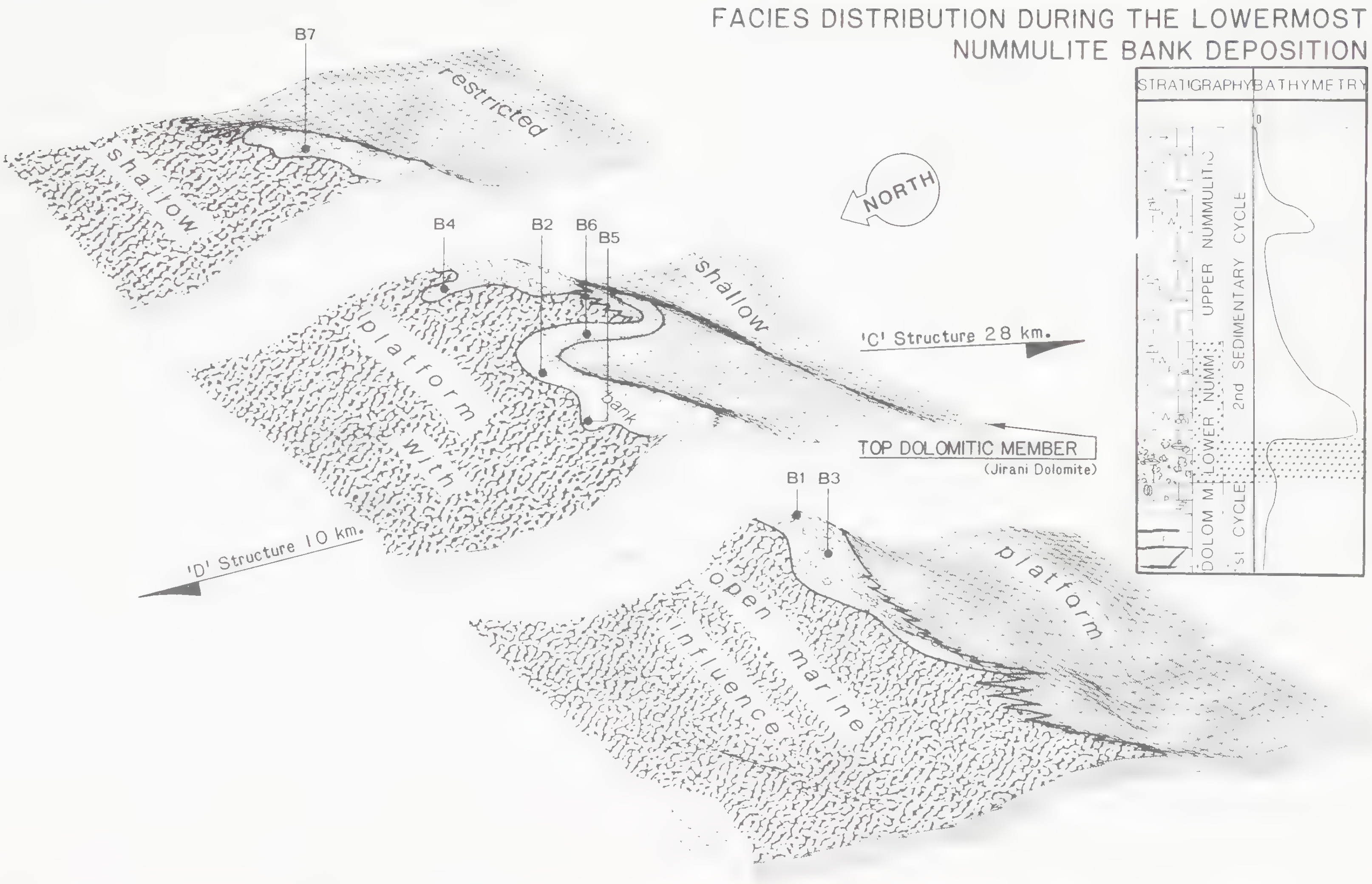
FACIES DISTRIBUTION DURING THE LOWERMOST
NUMMULITE BANK DEPOSITION
STRATIGRAPHY
BATHYMETRY
0
UPPER NUMMULITIC
LOWER NUMM.
DOLOM M.
2nd SEDIMENTARY CYCLE
1st CYCLE
NORTH
'C' Structure 28 km.
TOP DOLOMITIC MEMBER
(Jirani Dolomite)
'D' Structure 10 km.
B7
B4
B2
B6
B5
B1
B3
restricted
shallow
shallow
platform
with
bank
open
marine
influence
platform

Fig. 13. Beginning of the deposition of the "Lower Nummulitic" with the sedimentation of the lowermost nummulite bank on the top of the structure. To the south, restricted facies prevailed while to the north open shelf facies were deposited.

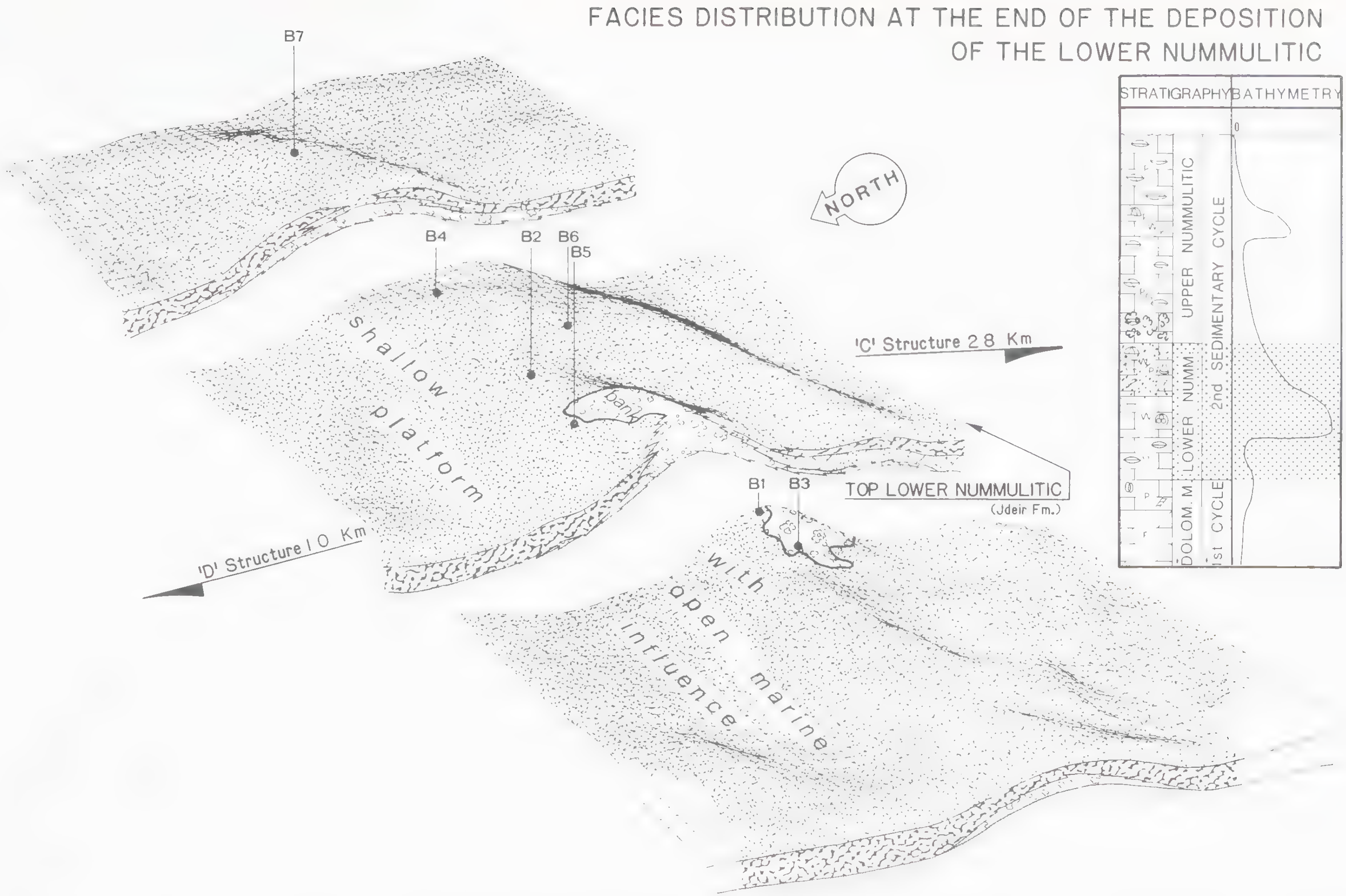
FACIES DISTRIBUTION AT THE END OF THE DEPOSITION
OF THE LOWER NUMMULITIC
STRATIGRAPHY
BATHYMETRY
0
UPPER NUMMULITIC
LOWER NUMM
DOLOM. M.
2nd SEDIMENTARY CYCLE
1st CYCLE
NORTH
B7
B4
B2
B6
B5
B1
B3
bank
shallow platform
with open marine influence
'C' Structure 2.8 Km
'D' Structure 1.0 Km
TOP LOWER NUMMULITIC
(Jdeir Fm.)

Fig. 14. Situation at the end of the deposition of the "Lower Nummulitic". The nummulite bank facies were reduced to a minimum, and partially dismantled; micritic facies prevailed over the whole area.

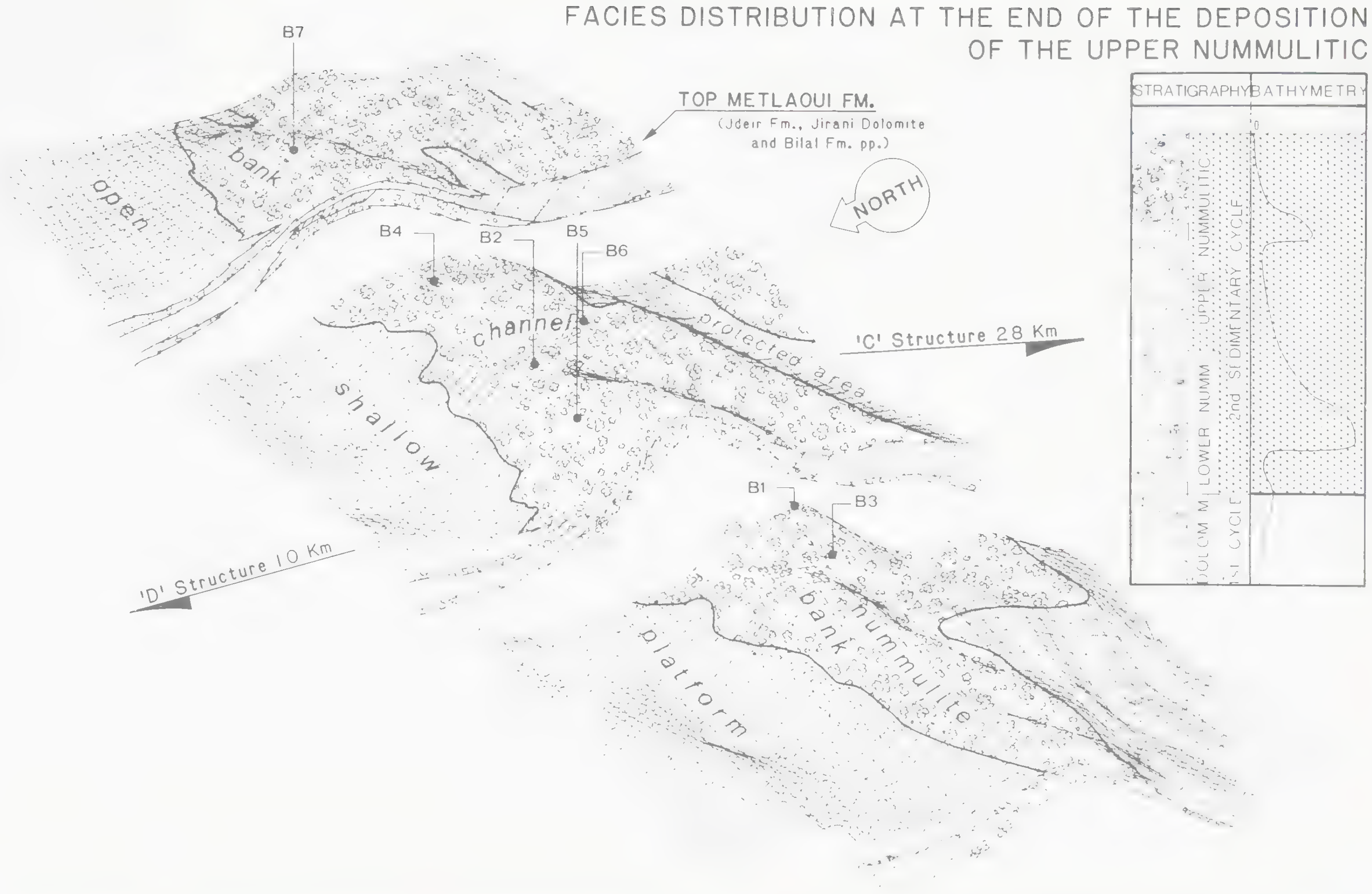
FACIES DISTRIBUTION AT THE END OF THE DEPOSITION OF THE UPPER NUMMULITIC
STRATIGRAPHY
BATHYMETRY
0
DOLOM M
LOWER NUMM
UPPER NUMMULITIC
1st CYCLE
2nd SEDIMENTARY CYCLE
TOP METLAOUI FM.
(Jdeir Fm., Jirani Dolomite and Bilal Fm. pp.)
NORTH
B7
open
bank
B4
B2
B5
B6
channel
protected area
shallow
'C' Structure 28 Km
'D' Structure 10 Km
B1
B3
nummulite
bank
platform

Fig. 15. The figure shows the idealized sedimentary situation at the end of the deposition of the "Upper Nummulitic" (top Jdeir Formation). The uppermost nummulite bank developed because of the final marine regression.

imum of micritic deposits of open marine environment occurred.

The final regression that occurred in the late Ypresian (Vail *et al.*, 1977) enabled a better development of the uppermost nummulite bank and finally determined the emergence of the Metlaoui Group. The E–W lateral continuity of the uppermost bank is better than that of the intermediate and of the lowermost banks (Fig. 3). On the other hand, the N–S lateral continuity is less predictable due to lack of data. However, it may be assumed that a reduction of the bank thickness takes place northwards, as well as southwards: northwards the decrease could be sharper, and southwards more gradual since the structure is very asymmetrical, with the northern flank more inclined than the southern one.

Our model takes into consideration three phases of the sedimentation and can be outlined as follows:

- at the beginning of the "lower Nummulitic" deposition a nummulite bank was set on the top of the structure, with very little lateral continuity. To the south facies of restricted shallow platform prevailed while to the north facies of open marine environment were present (Fig. 13);
- during the period of maximum transgression a withdrawal and a reduction of the bank facies occurred, coinciding with the maximum development of the micritic facies of open marine environment (Fig. 14);
- during the last regression the maximum areal expansion of bank facies occurred showing greater development towards the south than towards the north (Fig. 15).

The model shows both affinities and differences with other sedimentological models described in the literature.

Fournié (1975) described the nummulite bank in central Tunisia and pointed out the presence of clastic sediments and glauconite associated with them. Conversely, in the nummulite banks of the El Bourī area both glauconite and terrigenous sediments are completely missing. It is therefore likely that the nummulite banks analyzed by Fournié originated in environments of deposition less influenced by the open sea than those in the El Bourī Field.

Arnì and Lanterno (1972) indicated many coralline algae associated with Nummulites in the Eocene of the Verona area (Italy). It is likely that in the Verona area more tidal or internal environmental conditions occurred.

The Arnì model (1965) assumes a morphological change of the sea-bottom caused by the growth of the banks, while Fournié (1975) and Aigner (1983) hypothesized the formation of nummulite banks on pre-existing tectonic structures.

In the El Bourī Field, the presence of a pre-existing tectonic structure was probably the major factor in the development of nummulite banks.

CONCLUSIONS

The study of the lithofacies and of their diagenetic evolution allows us to outline a model of the distribution of the facies, to recognize the paragenesis of cements and to forecast the areal and vertical distribution of the porosity. These conclusions may be summarized as follows:

(1) According to our sedimentological model, the top of the structure coincides with the area most favourable to the development of the nummulite banks.
(2) The formation of nummulite banks was favoured by regressions. The uppermost nummulite bank is more extensive than the intermediate and lowermost ones, due to the greater width of the regression at the end of the Ypresian.
(3) The nummulite bank facies identified in the El Bourī Field probably result from the sum of several banks, so that their overall areal extension should be wider than that of a single bank.
(4) On the flanks of the structure an increase of open or restricted shallow platform micrite facies should occur, with a sudden increase toward the north and a more gradual one towards the south. Based on our model, four facies maps have been prepared which describe the evolution of the Nummulitic Member (Fig. 16).
(5) The Dolomitic Member shows a good lateral continuity since it developed in uniform sedimentary conditions. However, towards the north it tends to decline and disappear.
(6) The diagenetic phenomena that mainly modified the primary porosity occurred in a freshwater phreatic and/or vadose environment. The possibility of an extension of these phenomena on the flank of the structure depends upon the extension of the palaeonappe that permeated the Metlaoui Group. However, it is unlikely that significant variations occurred in the thickness of the palaeonappe within some hundreds of metres from the top of the structure.

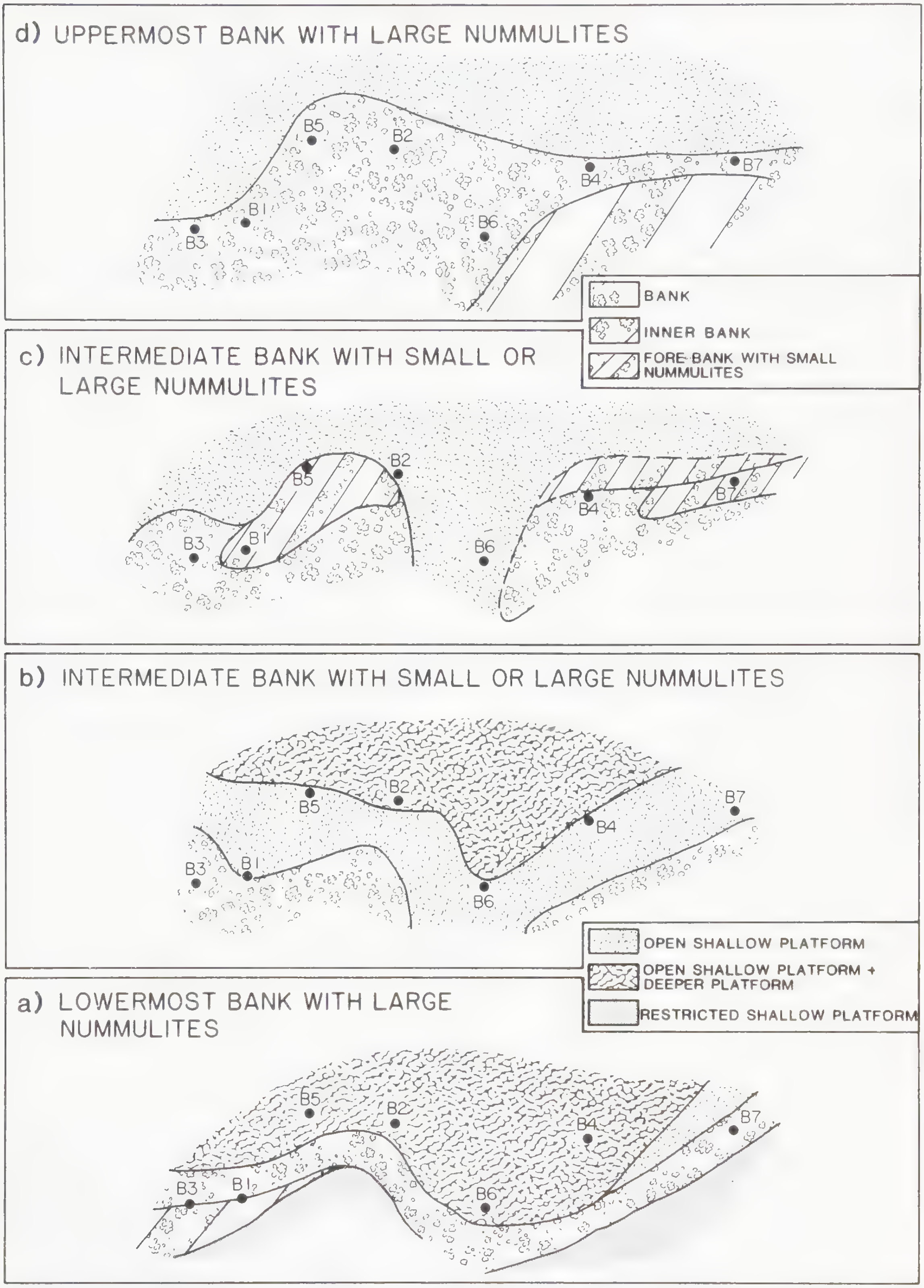
d) UPPERMOST BANK WITH LARGE NUMMULITES
B5
B2
B4
B7
B1
B3
B6
BANK
INNER BANK
FORE-BANK WITH SMALL NUMMULITES
c) INTERMEDIATE BANK WITH SMALL OR LARGE NUMMULITES
B5
B2
B4
B7
B1
B3
B6
b) INTERMEDIATE BANK WITH SMALL OR LARGE NUMMULITES
B7
B2
B5
B4
B3
B1
B6
OPEN SHALLOW PLATFORM
OPEN SHALLOW PLATFORM + DEEPER PLATFORM
RESTRICTED SHALLOW PLATFORM
a) LOWERMOST BANK WITH LARGE NUMMULITES
B5
B2
B4
B7
B3
B1
B6

Fig. 16. Facies maps of the Nummulitic Member. These four maps represent the sedimentary evolution in four successive stages and show the northward progradation of the nummulite bank facies.

(7) The Dolomitic and Nummulitic Members represent an excellent reservoir with an average porosity ranging between 10 and 15% for limestones and between 20 and 25% for dolomites, and with good permeability for both the lithotypes, which is sometimes increased by rare fractures; in particular, the nummulite banks, because of their stratigraphic position and petrophysical features, could represent similar excellent reservoirs in other parts of the wide North African continental shelf.

ACKNOWLEDGEMENTS

This study was carried out entirely for AGIP NAME at AGIP S.p.A. during a multidisciplinary study of the El Bourī oil field. We wish to thank Prof. L. Mattavelli and Dr. A. Rizzini for their help with the layout and review of the study. We would like to thank all the personnel and colleagues who were involved in this work.

REFERENCES

AIGNER, T. (1983). Facies and origin of nummulitic buildups: an example from the Giza Pyramids Plateau (Middle Eocene, Egypt). *Neues Jahrb. Geol. Paläontol. Abh.*, **166**(3), 347–368.

AISSOUI, D.M. and PURSER, B.H. (1983). Nature and origins of internal sediments in Jurassic limestones of Burgundy (France) and Fnoud (Algeria). *Sedimentology*, **39**, 273–283.

ARNÌ, P. (1965). L'évolution des Nummulites en tant que facteurs de modification des depôts littoraux. Coll. Internat. Micropal., Dakar 1963; *Mem. Bur. Rech. Géol. Min.*, **32**, 7–20.

ARNÌ, P. and LANTERNO, E. (1972). Considérations paléoécologiques et interprétation des calcaires de l'Eocène du Véronais. *Arch. Sci. Genève*, **25**, 251–283.

BATHURST, R.G.C. (1971). *Carbonate Sediments and their Diagenesis*. Elsevier, Amsterdam, 620 p.

BISHOP, F.W. (1975). Geology of Tunisia and adjacent part of Algeria and Libya. *Bull. Am. Assoc. Petrol. Geol.*, **59**, 413–450.

BLONDEAU, A. (1972). *Les Nummulites*. Librarie Vuibert, Paris, 254 p.

CHOQUETTE, P.W. and PRAY, L.C. (1970). Geologic nomenclature and classification of porosity in sedimentary carbonates. *Bull. Am. Assoc. Petrol. Geol.*, **54**, 207–250.

DUNHAM, R.J. (1969). Early vadose silt in Townsend Mound (Reef), New Mexico. *In*: Depositional Environments in Carbonate Rocks (*ed.* G.M. Friedman). *SEPM* Spec. Publ., **14**, 139–181.

FINETTI, I. (1982). Structure, stratigraphy and evolution of central Mediterranean. *Boll. Geofis. Theor. Appl.*, **XXIV**, (96).

FOURNIÉ, D. (1975). L'analyse séquentielle et la sédimentologie de l'Ypresien de Tunisie. *Bull. Cent. Rech. Pau*, SNPA, **9**, 27–75.

GOUDARZI, G.H. (1980). Structure: Libya. *In: The Geology of Libya* (*eds* M.J. Salem and M.T. Busrewil). Fac. Sci., Univ. Al-Fateh, Tripoli, **III**, 879–893.

HAMMUDA, O.S., SBETA, A.M., MOUZUGHI, A.J. and ELIAGOUBI, B.A. (1985). *Stratigraphic Nomenclature of the Northwestern offshore of Libya*. Earth Sci. Soc. Libya, 166 p.

LONGMAN, W.M. (1980). Carbonate diagenetic textures from near surface diagenetic environments. *Bull. Am. Assoc. Petrol. Geol.*, **64**, 461–487.

MILLIMAN, J.D. (1974). *Marine Carbonates*. Springer-Verlag, Berlin, 375 p.

PITTMAN, E.D. (1974). Porosity and permeability changes during diagenesis of Pleistocene corals, Barbados, West Indies. *Bull. Geol. Soc. Am.*, **85**, 1811–1820.

RADKE, B.M. and MATHIS, R.L. (1980). On the formation and occurrence of saddle dolomite. *J. Sediment. Petrology*, **50**(4), 1149–1168.

VAIL, P.R., MITCHUM, R.M. and THOMPSON, S. (1977). Global cycles of relative changes of sea-level. *In*: Seismic Stratigraphy: Application to Hydrocarbons Exploration (*ed.* C.E. Payton). *Mem. Am. Assoc. Petrol. Geol.*, **26**, 83–97.

Petrography and Facies of the Middle and Upper Eocene Rocks (Tellil Group), Offshore Western Libya

A.M. SBETA[1]

دراسة بتروغرافية وسحنات صخور الأيوسين الأوسط والأعلى – مجموعة تليل – في المنطقة البحرية بغرب ليبيا

ع . م . سبيطة

الخلاصة

خلال عصر الأيوسيني الأوسط والمبكر، كان هناك رف بحري واسع وعريض وضحل وغير محمي في المنطقة البحرية لحوض طرابلس. وقد أظهر هذا الرف قاعاً قليل الميل ودرجات متفاوتة من الحَجْر. وقد غطى هذا الرف أحزمة ضيقة من السحنات متمثلة في أوضاع سبخية إلى الجنوب على إمتداد الشاطئ الحالي، تليها، إلى الشمال، سحنات محجورة للرف القاري ثم بعد ذلك هور رفَيٌّ ممثلاً لمراحل من تجمع صدفيات الأويسترات وحواجز النيوميوليتات. وتؤدي هذه السحنات البحرية الضحلة بدورها إلى سحنات بحرية عميقة ومفتوحة.

وتتمثل صخور الأيوسين الأعلى والأوسط في تتابع انحساري لتبادلات من الحجر الجيري والحجر الطيني لمجموعة تليل. وتبدأ هذه المجموعة في أسفلها بترسيب خمسة أحزمة لتكوين الحرشة. وتتألف هذه الأحزمة من الحجر الطيني والحجر الدولوميتي والإنهيدريت التي هي رملية محلياً وتغطي معظم الجزء الجنوبي من منطقة الدراسة على إمتداد الشاطئ الحالي. وإلى الشمال، تتدرج إلى حجر الباكي وحجر الواكي والحجر الوحلي لبقايا الرخويات مع الحجر الطيني ومع وجود محلي للحجر الواكي النيوميوليتي، وكذلك الحجر الباكي النيوميوليتي. ويعلو تكوين الحرشة تكوين دحمان. وتوجد في هذا التكوين ثلاثة سحنات هي: حجر الباكي الرخوى والنيوميوليتى دالة بذلك على احتمال وجود حواجز محلية للأويسترات والنيوميوليتات خلال ترسيب هذا التكوين. وتبع ذلك ترسيب سحنات سمدون المحجورة مما يدل على أن انحسار البحار قد وصل إلى حده الأقصى خلال نهاية العصر الإيوسيني. ويتألف تكوين سمدون من أربعة سحنات محجورة هي: حجر طيني وحجر دولوميتي وانهيدريت. وهي رملية محلياً على امتداد الأجزاء الجنوبية من الحوض. وتتدرج في الشمال إلى سحنات رفيّة داخليّة الحَجْر من الحجر الوحلي والحجر الواكي مع الحجر الطيني. وتحتوي هذه السحنات على مستحاثات المنخربات القاعية والأستراكودات والأويسترات.

Abstract. During the Early and Middle Eocene a wide, broad and shallow un-rimmed shelf existed offshore of Ṭarābulus basin. This shelf had a gentle sloping surface and exhibited different degrees of restriction. In general this shelf was covered by narrow facies belts exhibiting the characteristics of a sabkha setting in the south, along the present shoreline, followed northwards by a restricted shelf and then a shelf lagoon exhibiting the different stages of oyster and nummulitic bank development. In turn these shallow water facies grade northwards into pelagic and open marine facies.

The Middle and Upper Eocene rocks are represented by the regressive sequence of the alternating limestones and shales of Tellil Group. This group started at the base with the deposition of five facies belts of Harshah Formation. They consist of shale, dolomite and anhydrite that are locally sandy and dominating the southern part of the studied area along the present coastline. Northwards they grade into molluscan packstone, wackestone and mudstone with shales and local occurrences of nummulitic wackestone and packstone. Harshah Formation is overlain by the less restricted facies of Dahman Formation. Three facies belts within Dahman are dominated by nummulitic and molluscan packstone and wackestone thus suggesting the possible occurrence of local oyster and nummulitic banks during the deposition of this formation. This was followed by the more restricted facies of Samdun Formation suggesting perhaps, that the regression reached its maximum in Late Eocene time. Samdun Formation is composed of four facies belts that are characteristically restricted. The shale, dolomite and anhydrite facies are locally sandy over the southern parts of the basin. They grade northward to inner restricted shelf facies of mudstone and wackestone with shale. These facies contain benthonic forams, ostracods and oysters.

[1] University of Al-Fateh, Geology Department, P.O. Box 13258, Tripoli, Libya, G.S.P.L.A.J.

INTRODUCTION

The area under study is located offshore of western Libya in the Pelagian block in the Continental Shelf between the Gulf of Gabes in Tunisia and the Gulf of Sirt (Fig. 1). It extends over 100 km north of Tripoli and measures over 300 km in an east–west direction. It lies between latitude 33–34°N and longitude 12–15° E. The area is divided between three operators, Agip, Aquitain and Sirt (formerly Esso). All three concessions are jointly owned by NOC and the other three operators, Agip (NC41), Aquitain (137) and Sirt (NC35A).

Exploration in the offshore began in early 1970. Over 40 wells were drilled most of which are exploratory; some 15 wells are oil and/or gas discoveries. One discovery is being developed, the El Bourī Field, jointly owned by NOC and Agip.

This paper covers part of the study conducted from 1983 to 1985 on the Eocene of the Continental Shelf offshore of Tripoli.

The objective of this work is to define the different facies, map their distribution in space and time and construct a model for the depositional environment of the Middle and Upper Eocene. It is hoped that this will result in a better picture which will aid in the definition and extension of possible good reservoir rocks and help in the understanding of Eocene depositional history.

Methods of study

Cuttings, thin sections, logs and well reports were used in the study of the Middle and Late Eocene Tellil Group. As the Middle and Late Eocene rocks are mainly interbedded limestone and shale thin sections were only prepared from the limestone beds. General descriptions of shales, including fossil content, colour, mineral composition and texture, were recorded.

Over 600 thin sections from the limestone beds and the cuttings from Tellil Group were examined from 14 wells.

The detailed petrographic data from these cut-

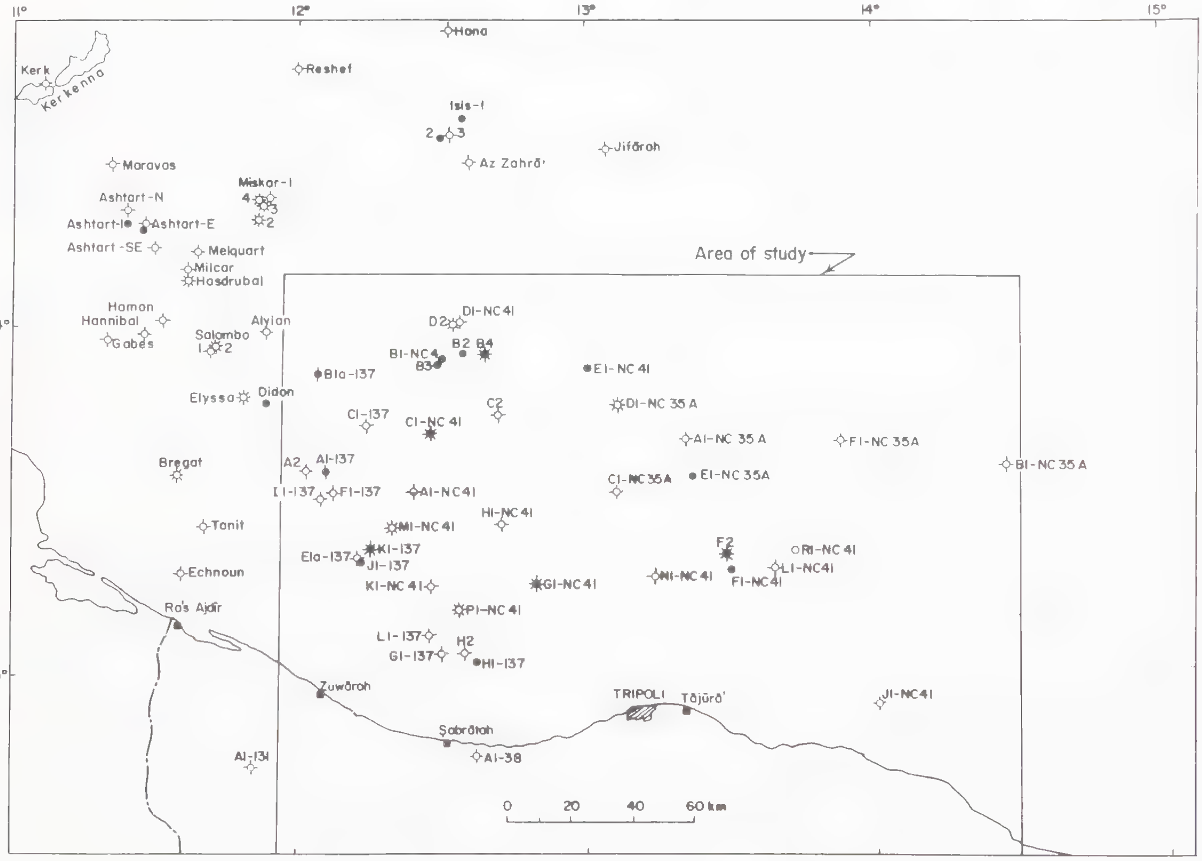
11°
12°
13°
14°
15°
34°
33°
Hana
Kerk
Kerkenna
Reshef
Isis-1
2
3
Jifāroh
Az Zahrā'
Maravas
Miskar-1
4
3
2
Ashtart-N
Ashtart-1
Ashtart-E
Ashtart-SE
Melquart
Milcar
Hasdrubal
Area of study
Hamon
Hannibal
Gabes
Alyian
Salambo
1
2
D2
D1-NC41
B1-NC4
B2
B4
B3
B1a-137
E1-NC41
Elyssa
Didon
C2
C1-137
C1-NC 41
D1-NC 35 A
A1-NC 35 A
F1-NC 35A
B1-NC 35 A
Bregat
A2
A1-137
C1-NC35A
E1-NC 35A
I1-137
F1-137
A1-NC41
H1-NC41
Tanit
M1-NC41
F2
R1-NC41
E1a-137
K1-137
J1-137
L1-NC41
Echnoun
K1-NC 41
G1-NC41
N1-NC41
F1-NC41
Ra's Ajdīr
P1-NC41
L1-137
H2
G1-137
H1-137
Zuwāroh
TRIPOLI
Tājūrā'
J1-NC41
Şabrātah
A1-131
A1-38
0
20
40
60 km

Fig. 1. Location map.

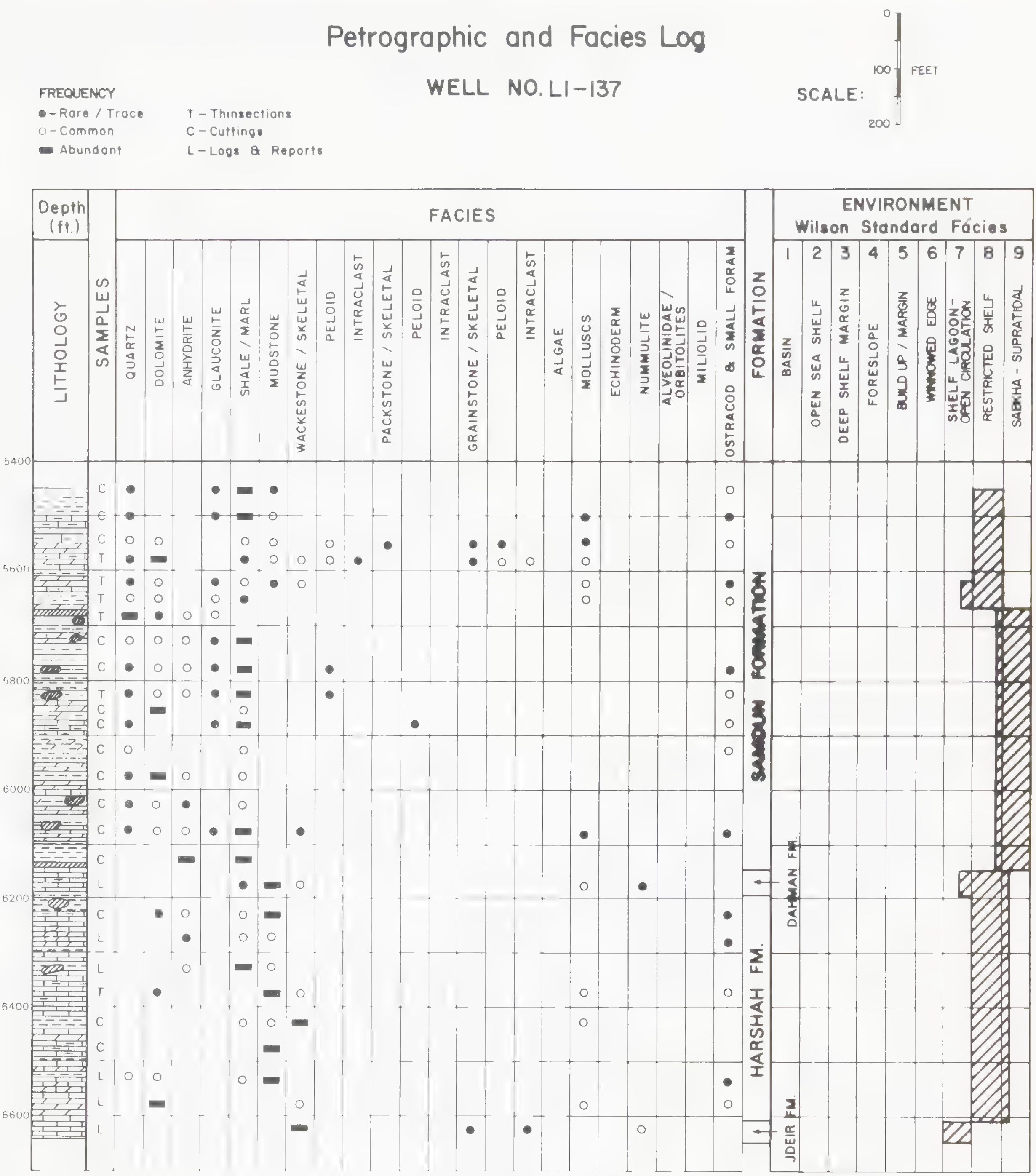

Fig. 2. Petrographic and facies log, well no. L1-137.

tings and thin sections, and in some cases from well reports and logs, are recorded on the petrographic and facies log (Fig. 2). In each case the relative abundance of the different facies and their compositional components, including biotic and non-biotic elements, were plotted. The letters T, C and L respectively are used to indicate whether the data plotted are acquired from thin sections, cuttings or logs and reports. The right hand corner of the logs was assigned for interpreting the different environmental settings, using *Wilson* facies belts if they were present (Wilson, 1975).

As no carbonate setting is exactly similar or analogous to recent or old models, a combination of many reported models are used to introduce the depositional environments of the Eocene.

IES logs are utilized for formation definition, correlation and detecting any thickness variation. In some cases, the formation tops picked by the author are different from those used by the operators thus reflecting the fact that the lithostratigraphic rather than the chronostratigraphic character of these formations was emphasized. The names used for formations and groups are those introduced by the NOC Stratigraphic Committee in their publication (Hammuda *et al.*, 1985).

GENERAL STRATIGRAPHY

The oldest rocks encountered in the offshore are of Triassic age but it is anticipated that older rocks of Permian age are present as well A1-38, drilled along the coast near Ṣabrātah, yielded rocks of Permian and Triassic age (Fig. 3). Overlying these Triassic and Permian beds sequences of Cretaceous and Tertiary rocks are encountered in many wells drilled in Ṭarābulus basin. Their stratigraphic nomenclature is published by Hammuda *et al.* (1985).

Triassic

Well L1-137 penetrated only the upper beds of Late Triassic age (Bir Alghanam Formation). Thicker and well-developed Triassic beds were reported from onshore well A1-38, 40 km south of well L1-137. The Triassic at well A1-38 is comprised of a mainly clastic sequence of sandstone and grey green, reddish shale with a few limestone beds of Al-Gudir Formation which, it is suggested, are equivalent to Ouled Chebbi Formation. This is followed by the clastics and carbonates of Kurrush Formation and the carbonates of Al-Aziziyah. Lithologically, Al-Aziziyah Formation at well A1-38 is similar to that of the Jabal Nafūsah exposure and reaches a thickness of over 2000 ft while its type section is only 525 ft thick. Al-Aziziyah is overlain by Abu-Shaybah Formation

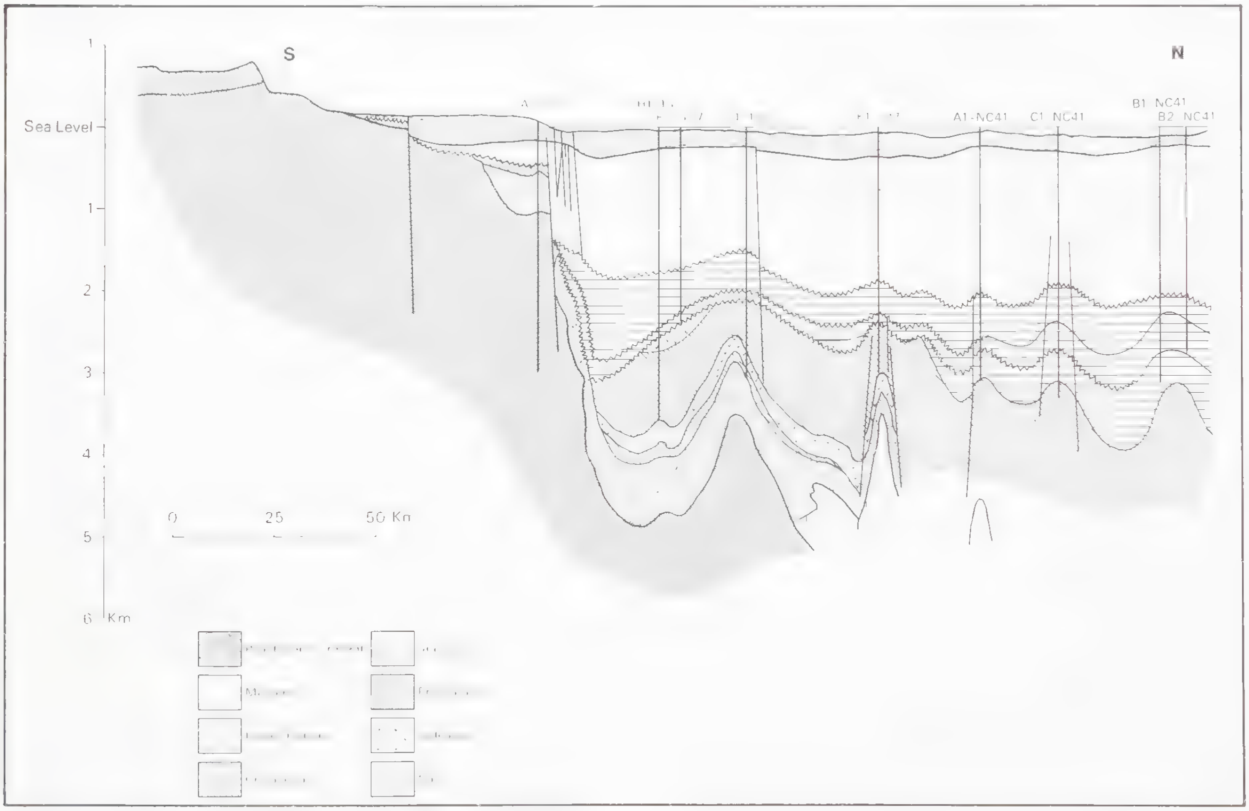

Fig. 3. Cross section of Ṭarābulus basin (after Pitman III *et al.*, 1981).

which is a multi-coloured silty, sandy shale and sandstone which becomes very thick (1169 ft) at well A1-38.

The Late Triassic is represented by the basal beds of Bir Alghanam evaporite in the offshore well L1-137, and by the lower beds of Abu-Ghaylan carbonates which grade into thick salt deposits of offshore Zuwārah.

Jurassic

The Jurassic is a mainly thick evaporite and clastics sequence. The Early and Middle Jurassic is 1252 ft thick consisting of anhydrite with shales and dolomite, as observed at well L1-137 which is one of the deepest wells drilled in the Tripoli offshore. This sequence is equivalent to Bir Alghanam Formation of Jabal Nafūsah (Banerjee, 1980). The dolomite in this formation exhibits ooids and peloidal relics suggesting an interfingering relationship with the thick sequence of Abu-Ghaylan Formation described from the onshore well A1-38. At A1-38 the Abu-Ghaylan Formation is 1100 ft thick and grades northward into the offshore evaporite of Bir Alghanam.

The Middle to Late Jurassic includes intervals of most Kiklah sandstone which reaches 1178 ft at L1-137. The lower sections are fine- to medium-grained sandstone with equal amounts of grey pyritic shale and few layers of thin brown argillaceous dolomite. The middle beds are composed of dolomite and limestone whereas the upper beds are dolomitic sandstone, siltstone and shale. The Kiklah Formation at L1-137 is unconformably overlain by a volcanic and sedimentary complex of Early Cretaceous age and is underlain by the Early Jurassic of Bir-Alghanam Formation.

Cretaceous

The Cretaceous in northwest offshore Libya is quite thick and well developed and includes the upper section of Kiklah sandstone which is thought to be of Early Cretaceous age. It is 360 ft thick and is predominantly comprised of fine dolomitic sandstone, siltstone and shale and is probably overlain by the carbonate sequence of Turghat Formation at A1-NC35A and locally by the cream to grey silty and sandy fossiliferous shale of Masid Formation at B1-NC35A. The Turghat Formation is very fossiliferous with abundant benthonic foraminifera. This shallow marine sequence includes dolomitized limestone, fossiliferous packstone, wackestone and grainstone. Locally shales predominate at the base. Laterally Turghat Formation grades into the shales and argillaceous limestones of Masid Formation. This Formation has a diverse group of fauna, including planktonic and benthonic foraminifera, and is considered to be Aptian to Albian in age.

The Late Cretaceous sequence is represented by the following formations from the base: Alalgah, Makhbaz, Jamil and Bu Isa. The Cenomanian Alalgah Formation is brown dolomicrosparite, argillaceous dolosparite with anhydrite nodules and streaks of black shale. This lithology is common in the southern edge of the Pelagian block at Concession 137. At K1-137 Alalgah Formation is conformably overlain by Makhbaz Formation which is considered to be Turonian to Coniacian in age and consists of 600 ft of mainly grey, light-grey, brown mudstone/wackestone, in places dolomitic and shaley. Only a few wells reached this level including L1-137. The thickness of Makhbaz Formation decreases towards the south and east. The Santonian Jamil Formation overlies Makhbaz conformably and mainly consists of grey to greyish brown shales. This formation has a thickness of 1242 ft at K1-137 and 1638 ft at L1-NC41.

The Campanian Bu Isa Formation consists at the southern edge of the basin of cream to light-brown mudstone, highly argillaceous wackestone, fossiliferous and glauconitic in places. Bu Isa Formation has a thickness of over 900 ft at H1-137 and thins slightly toward the east and disappears toward the west to the Tunisian offshore. Bu Isa is overlain by Al Jurf Formation and locally by Farwah Group.

The Cretaceous is terminated by the deposition of Al Jurf Formation covering almost all the Pelagian block. Al Jurf Formation ranges in age from Maastrichtian to Palaeocene and exhibits different lithologies and environments. In general it consists of dark-grey to black shale, medium hard and fissile, while locally sandstone and sandy shale occur in levels of the limestone beds: it reaches 1357 ft at C1-NC41 and only 52 ft at G1-NC41 in the south. Al Jurf Formation in the north tends to have abundant planktonic and benthonic foraminifera which indicate a deep platform environment. The formation grades laterally to Ehduz and Bilal Formations.

Tertiary

Rocks of the Palaeocene age are encountered only at the wells drilled in the northern (north of C1-NC41) and eastern sectors (east of N1-NC41). On the other hand, Early Eocene rocks unconformably

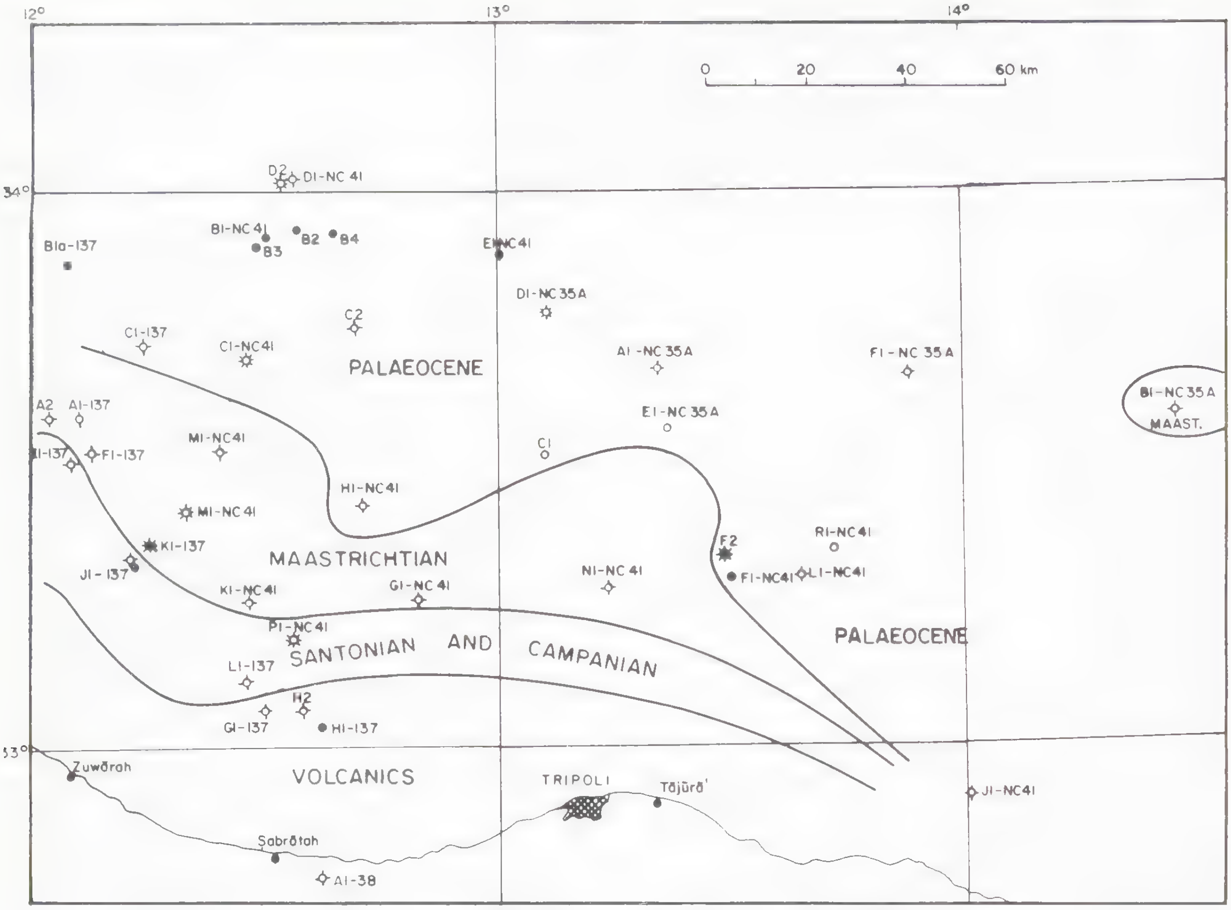
12°
13°
14°
34°
33°
0 20 40 60 km
D2
DI-NC 41
BI-NC 41
B2
B4
B3
BIa-137
EI-NC41
DI-NC35A
C2
CI-137
CI-NC41
PALAEOCENE
AI-NC35A
FI-NC 35A
BI-NC35A
MAAST.
A2
AI-137
EI-NC35A
II-137
FI-137
MI-NC41
CI
HI-NC41
MI-NC 41
KI-137
JI-137
MAASTRICHTIAN
F2
RI-NC41
NI-NC 41
FI-NC41
LI-NC41
KI-NC41
GI-NC 41
PI-NC41
SANTONIAN AND CAMPANIAN
PALAEOCENE
LI-137
H2
GI-137
HI-137
Zuwārah
VOLCANICS
TRIPOLI
Tājūrā'
JI-NC41
Sabrātah
AI-38

Fig. 4. Pre-Eocene palaeogeographic map (after Sbeta, 1990).

overlie those of Cretaceous age in the centre and the south of the Pelagian block where rocks of the Palaeocene are missing (Fig. 4). The Palaeocene is represented mainly by Al Jurf Formation and consists of shales, clay and locally, carbonates.

During the late Palaeocene and Eocene, a thick sequence of carbonate and locally dolomitic and evaporitic shales cover most of the studied area and are represented by two major transgressive–regressive units: Farwah Group and Tellil Group (Table 1). These two groups attain a maximum thickness of over 3000 ft and are marked by the Tertiary unconformity at the base and the Oligocene unconformity at the top.

Throughout most of the Libyan sector of the Pelagian block the Oligocene is characterized by the appearance of the nummulitic *vascus* bed. This marker is easily picked up from logs and is probably indicative of widespread open shallow platform influence. In the west the Oligocene is mainly carbonates and consists of wackestone, packstone, shales and marls. Locally the Oligocene is bioturbated and grades into deeper water facies of shale and marl in the north and east. The contact between the Oligocene and Miocene is gradational. The Lower Miocene is over 2800 ft thick and consists of deep shelf silty, sandy shale interbedded with wackestone and packstone with abundant planktonic forams. These Lower Miocene rocks are widespread covering the Pelagian block.

During the Middle Miocene a continuous deepening of the basin is apparent by the thick sequence of 2800 ft of deep shelf to deep marine shale, sandy silty shales and marls. These units thin westward and northward and grade into a mainly carbonate sequence of mudstone, wackestone and grainstone in the north. This is followed by over 1000 ft of Upper Miocene sediments. The Upper Miocene exhibits different lithological units, deeper water, mudstone, wackestone and packstone in the north (B1a-137).

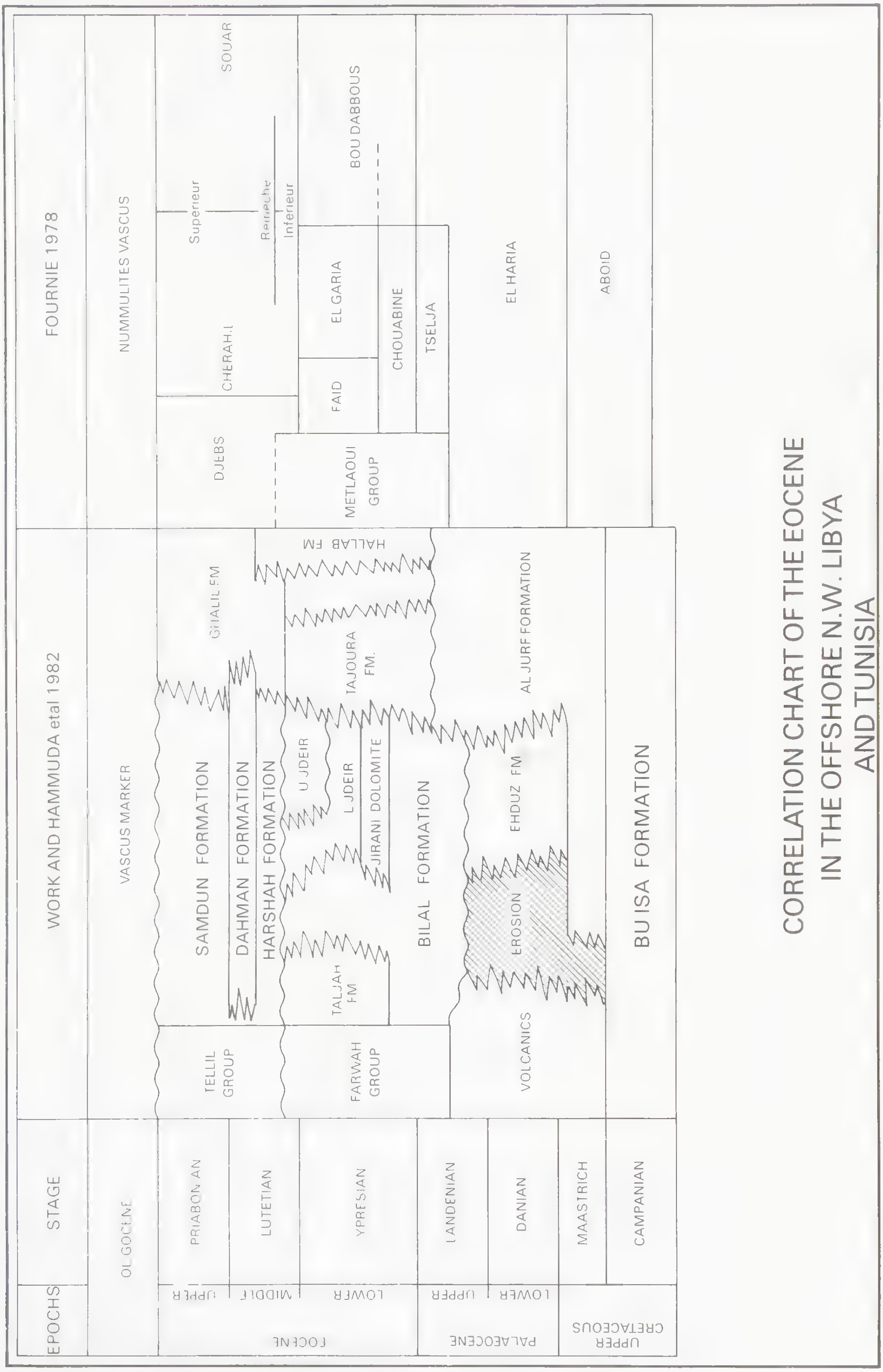
CORRELATION CHART OF THE EOCENE IN THE OFFSHORE N.W. LIBYA AND TUNISIA
EPOCHS
STAGE
WORK AND HAMMUDA etal 1982
FOURNIE 1978
OLIGOCENE
EOCENE
UPPER
MIDDLE
LOWER
PALAEOCENE
UPPER
LOWER
UPPER CRETACEOUS
PRIABONIAN
LUTETIAN
YPRESIAN
LANDENIAN
DANIAN
MAASTRICH
CAMPANIAN
VASCUS MARKER
NUMMULITES VASCUS
TELLIL GROUP
FARWAH GROUP
VOLCANICS
SAMDUN FORMATION
DAHMAN FORMATION
HARSHAH FORMATION
GHALIL FM
HALLAB FM
TAJOURA FM.
U JDEIR
L JDEIR
JIRANI DOLOMITE
TALJAH FM
BILAL FORMATION
AL JURF FORMATION
EHDUZ FM
EROSION
BU ISA FORMATION
DJEBS
CHERAHIL
Superieur
Reineche
Inferieur
SOUAR
FAID
EL GARIA
BOU DABBOUS
METLAOUI GROUP
CHOUABINE
TSELJA
EL HARIA
ABOID

Table 1. Correlation chart of the Eocene; offshore western Libya (Sbeta, 1990)

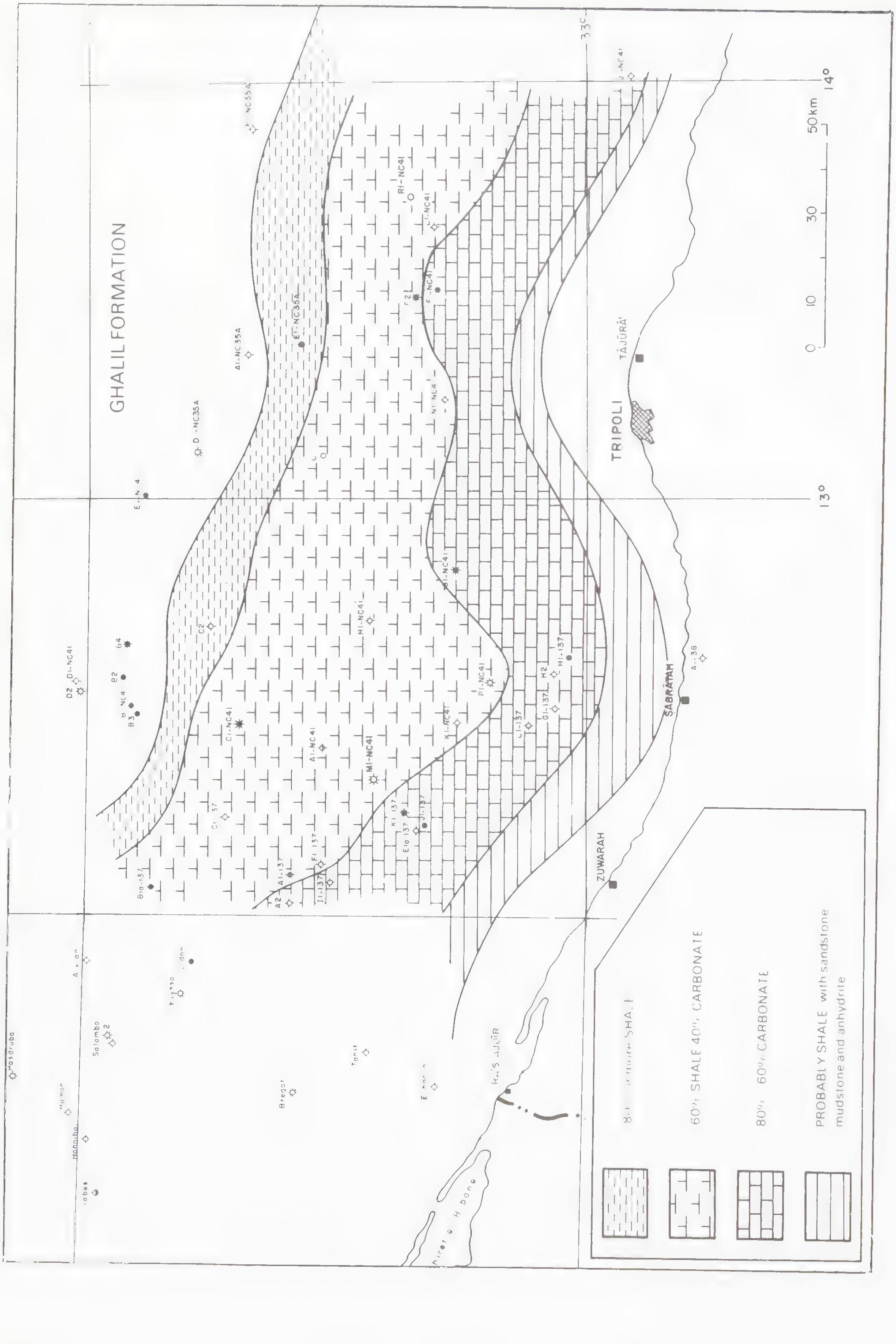
GHALIL FORMATION
TRIPOLI
TĀJŪRĀ'
ṢABRĀTAH
ZUWARAH
RA'S AJDĪR
13°
14°
33°
0 10 30 50km
D-NC35A
A1-NC35A
E1-NC35A
F-NC35A
C1-NC41
M1-NC41
H1-NC41
R1-NC41
B1a-137
C2
B3
B2
B4
D2
60% SHALE 40% CARBONATE
80% 60% CARBONATE
PROBABLY SHALE with sandstone mudstone and anhydrite

Fig. 5. Shale/carbonate percentage, Harshah Formation.

Towards the east it is mainly sandy clay. The end of the Miocene is marked by the occurrence of beds of carbonates and evaporite. At the base 90 ft of carbonate and shales are present, overlain by 250 ft of alternating anhydrite, clay and marl. This lithology clearly represents the Messinian event at the end of the Miocene.

It is probable that throughout the investigated area younger sediments of sand, shale and clay of Pliocene and Quaternary age overlie the Miocene unconformably, as a break in sedimentation is well recognized at the end of the Miocene.

STRATIGRAPHY OF MIDDLE TO UPPER EOCENE

This regressive group (Tellil Group) consists mainly of alternating shales, marls, clay and limestone, with anhydrite and sandstone occurring locally. It is clearly recognized in most of the wells drilled in the Ṭarābulus basin. However, it grades towards the north (north of B1-NC41) into the pelagic shales and marls of Ghalil Formation. The group is rich in benthonic fauna and ostracods, nummulites, pelecypods and algae.

Tellil Group is divided into three formations; these are, from the base, Harshah, Dahman and Samdun Formations.

The use of group instead of formation in the case of Tellil is practical allowing scope for redefinition and addition as a result of future detailed work. For example, detailed study of the Tellil Group has revealed two new carbonate members: Carbonate Member A within Harshah Formation and Carbonate Member B within Samdun Formation.

Harshah Formation

The lithology of Harshah Formation varies considerably. In the south it is mainly anhydrite, sandy shale and clay. Toward the north it grades to limestone along a belt extending from J1-NC47 to A2-137. At the centre shales predominate with a few limestone beds, and these grade to shale at C2-NC41 in the north as shown in Fig. 5. The formation is rich in benthonic forams, pelecypods and ostracods with local occurrences of nummulites.

Harshah Formation ranges in thickness from 700 to over 1100 ft along the central part of the basin and thins towards the south and north (Fig. 6). The formation unconformably overlies formations of Farwah Group in most of Ṭarābulus basin. On the other hand, Harshah Formation is overlain by the nummulitic facies of Dahman Formation throughout the basin with the exception of the northern and eastern edges of the studied area where Dahman Formation grades into Samdun Formation and directly overlies Harshah Formation.

Dahman Formation

Dahman Formation is mainly a limestone sequence rich in molluscs and nummulites which becomes very argillaceous containing forams towards the north, then grades into the pelagic Ghalil Formation.

The formation attains a maximum thickness of 200 ft at K1-137, then thins out northward and southward (Fig. 7). Dahman Formation has conformable contacts with the underlying and overlying formations of Harshah and Samdun.

Samdun Formation

Lithologically Samdun Formation is very similar to Harshah Formation. It consists mainly of alternating shales, clays and limestones. The shales and clays predominate in the north and centre, whereas limestone is common between F1-NC41 and L1-137 (Fig. 8). At the southern flank of the basin, a few wells show Samdun to consist of anhydritic sandy silty shales and clays locally dolomitic with lignite. The formation in places is rich in benthonic forams, ostracods, miliolids with local occurrences of nummulite and molluscs. The Samdun Formation is about 1200 ft thick at H1-NC41 then thins towards the south and north as shown in Fig. 9. This formation passes to the pelagic facies of Ghalil Formation as it does in an eastward and northeastward direction.

The Samdun is conformable with the underlying Dahman or Harshah, but the upper contact is generally unconformable.

Ghalil Formation

Ghalil Formation consists of fossiliferous shales and marls, locally silty with lenses of limestone. The formation has abundant planktonic foraminifera that suggest a deep water origin.

Ghalil overlies conformably either the Tajoura or Hallab Formation and is also conformably overlain by Oligocene rocks. In some areas, due to the facies relationship, Ghalil Formation is found overlying Tellil or Farwah Groups.

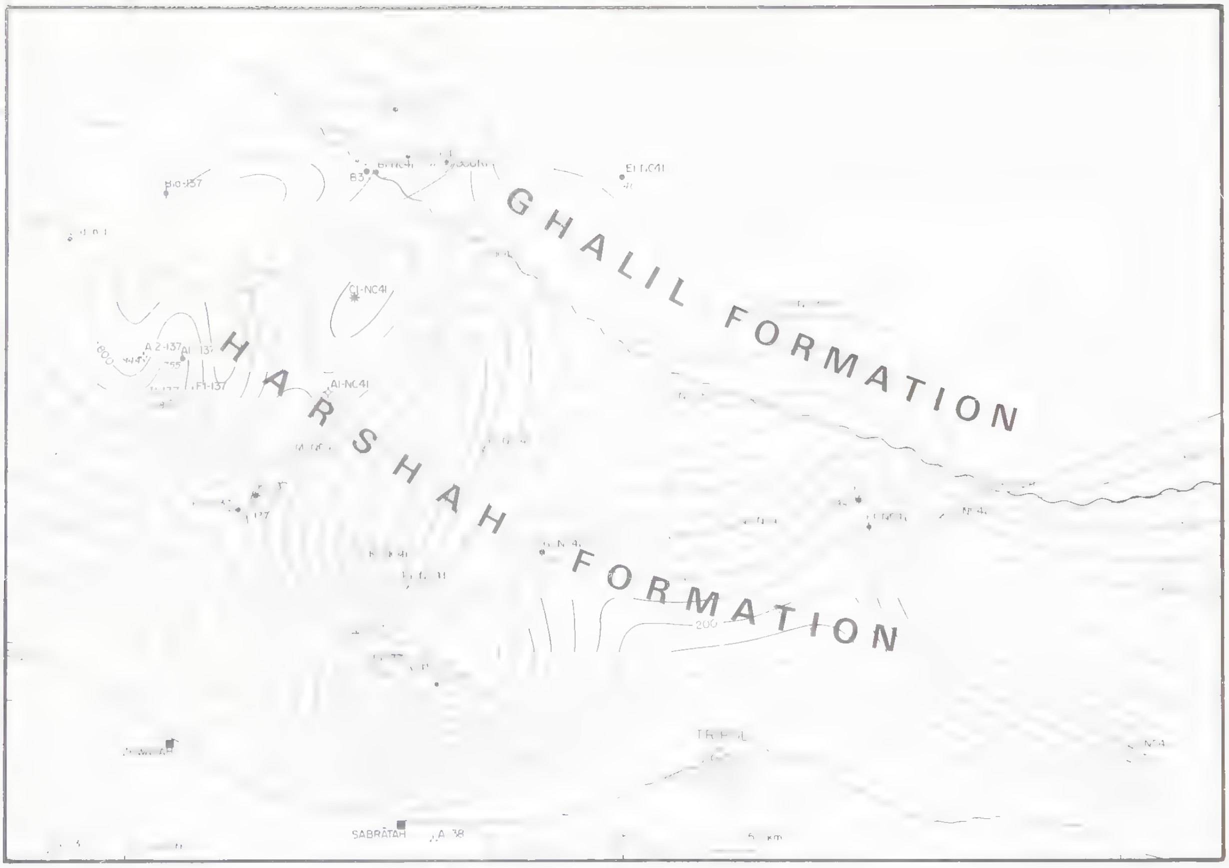
GHALIL FORMATION
HARSHAH FORMATION
B10-137
B3
E1-NC41
C1-NC41
A2-137
A1-137
800
F1-137
A1-NC41
200
SABRATAH
A1-38

Fig. 6. Isopach map of Harshah Formation.

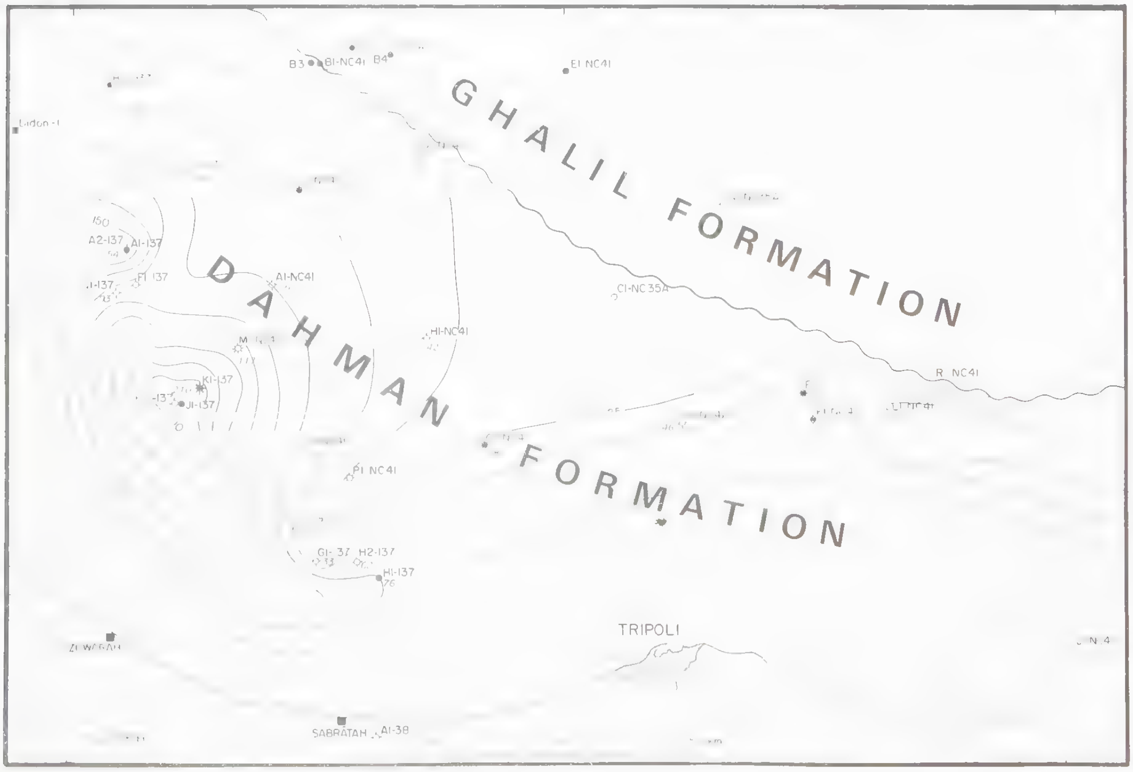
GHALIL FORMATION
DAHMAN FORMATION
B3
B1-NC41
B4
E1 NC41
150
A2-137
A1-137
F1 137
J1-137
A1-NC41
C1-NC35A
H1-NC41
K1-137
J1-137
R NC41
P1 NC41
G1-37
H2-137
H1-137
76
TRIPOLI
ZUWARAH
SABRATAH
A1-38

Fig. 7. Isopach map of Dahman Formation.

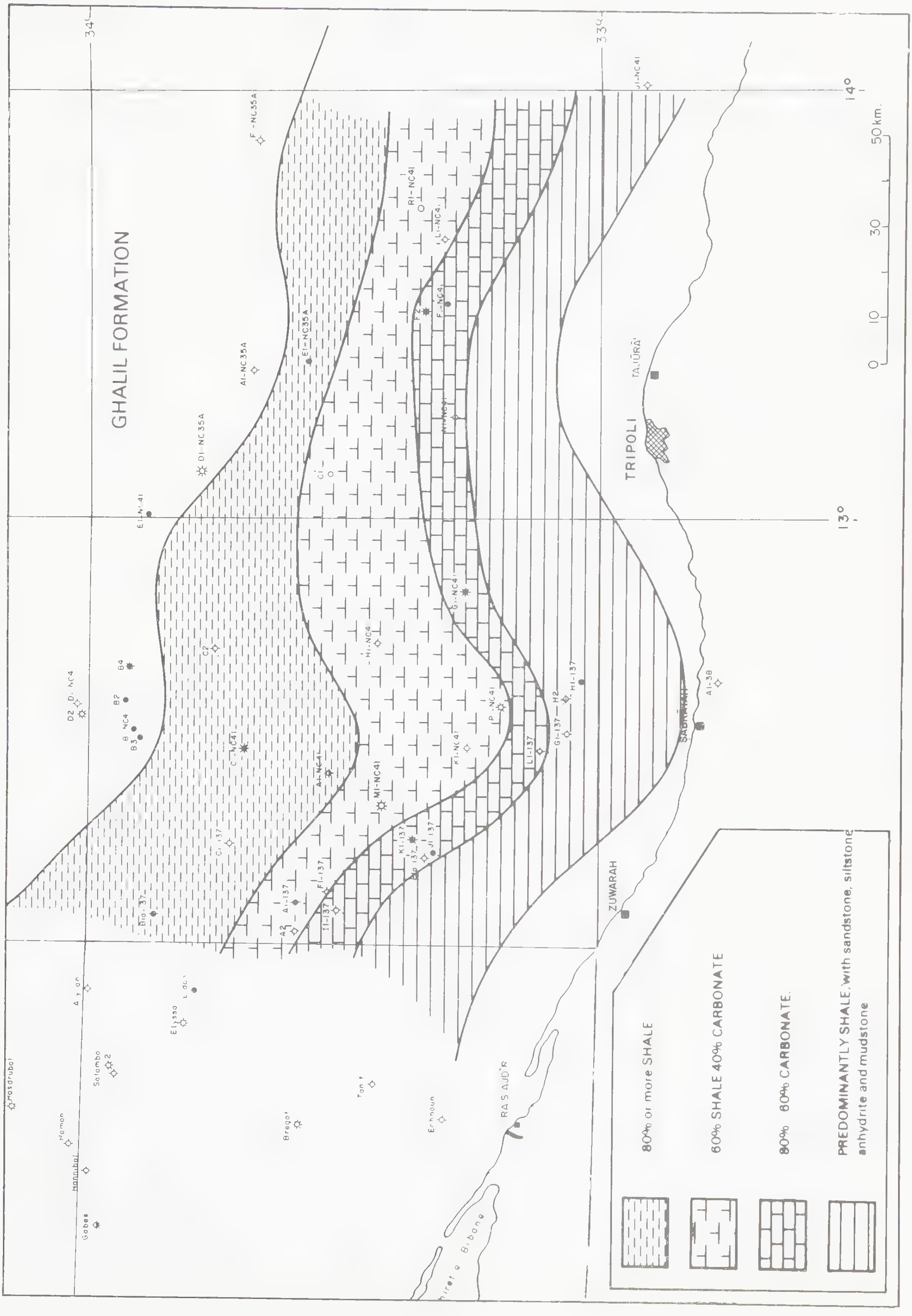
GHALIL FORMATION
34°
33°
14°
13°
TRIPOLI
TAJŪRĀ'
SABRATAH
ZUWARAH
RAS AJD'R
Bihret el Bibane
0 10 30 50 km.
Gabes
Hannibal
Hamon
Hasdrubal
Salambo 2
Ayon
Elyssa
Birsa
Ashtart
Tanit
Eshmoun
A1-NC35A
D1-NC35A
E1-NC35A
F-NC35A
E1-NC41
C1
R1-NC41
L1-NC4
F2
F1-NC4
M1-NC41
G1-NC41
H1-NC4
C2
B4
B2
B NC4
B3
D2
D. NC4
C-NC41
A1-NC41
M1-NC41
K1-NC41
P-NC41
L1-137
G1-137
H2
H1-137
A1-38
C1-137
B1a-37
A1-137
A2
F1-137
I1-137
K1-137
B1a 137
J1-137
J1-NC41
80% or more SHALE
60% SHALE 40% CARBONATE
80% 60% CARBONATE.
PREDOMINANTLY SHALE, with sandstone, siltstone anhydrite and mudstone

Fig. 8. Shale/carbonate percentage. Samdun Formation.

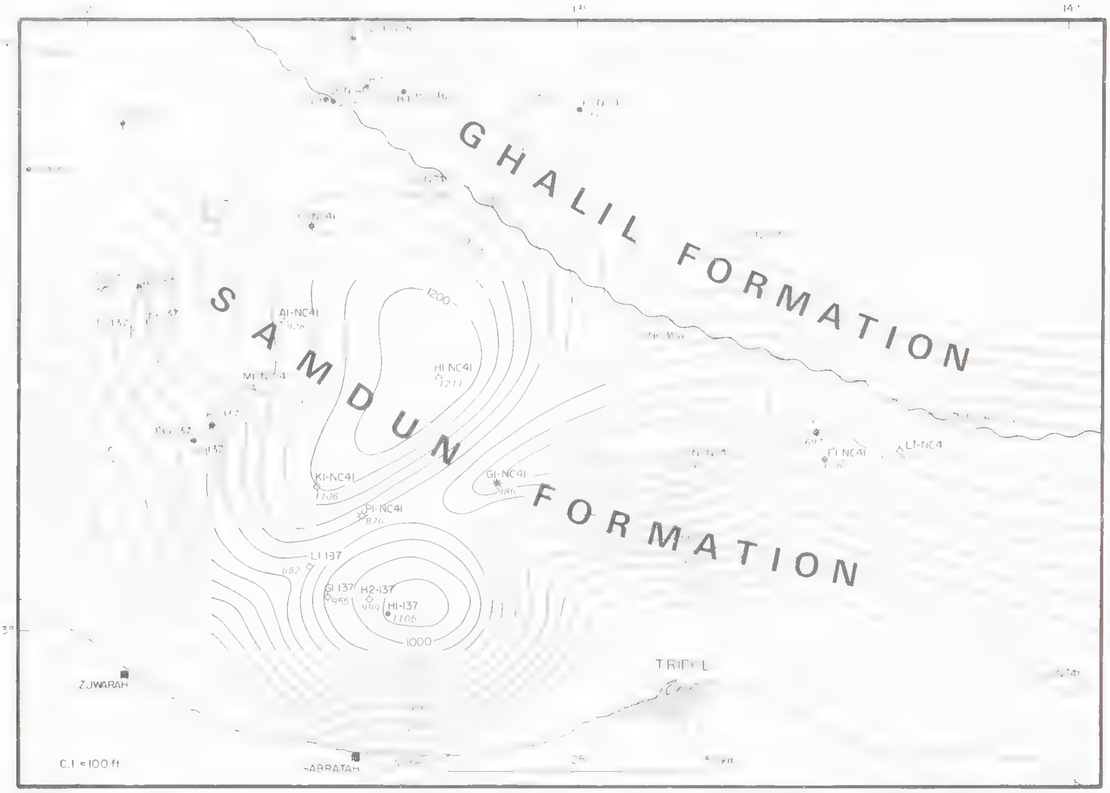

Fig. 9. Isopach map of Samdun Formation.

This formation occurs only at the northern sector of the study area, north of a line that extends from B3-NC41 to R1-NC41 and ranges in thickness from about 800 ft at B1-NC41 to 377 ft at E1-NC41, 336 ft at A1-NC35A and 384 ft at B1-NC41.

PETROGRAPHY AND FACIES OF TELLIL GROUP (MIDDLE AND UPPER EOCENE)

Facies and environment of Harshah Formation

Five major facies belts are recognized as a result of the close examination of limestone and shale cuttings and thin sections of limestone beds from eleven wells distributed throughout the three concessions.

The results of these analyses are tabulated in petrographic logs then analyzed. Each facies belt is composed of several facies that are interbedded and laterally grade into different facies belts (Fig. 10).

Facies Belt 1

This belt covers the southern edge of the Pelagian block just off the Libyan coast. This belt is inferred from the study of the two wells A2 and I1-137 and by extrapolation from the vertical sequence of H1 and G1-137 wells. The belt is composed of shale, dolomite and mudstone/wackestone. Locally the shale has lignite flakes and is sometimes silty sandy and anhydritic.

The facies of belt 1 consists mainly of dolomicrite to dolosparite, being argillaceous with mudstone/wackestone and shale. The shale is greenish grey, locally red-brown, silty and sandy with anhydrite nodules. The anhydrite nodules (Fig. 11a) show fibrous crystals (Fig. 11b). In some shale beds a few foraminifers and ostracods are present. The dolomite is very fine crystalline, slightly argillaceous, light grey to brown in colour and grades into dolomicrosparite and dolosparite which is locally anhydritic.

Locally, at well A2-137, the dolomite facies alternate with greenish grey shale with ostracods, foraminifers and lignite flakes. The limestones are mainly mudstone to wackestone with ostracod, miliolid and pelecypod fragments.

Environments: Facies belt 1 is interpreted as indicating the presence of restricted lagoon and sabkha conditions along the southern margin of Ṭarābulus basin

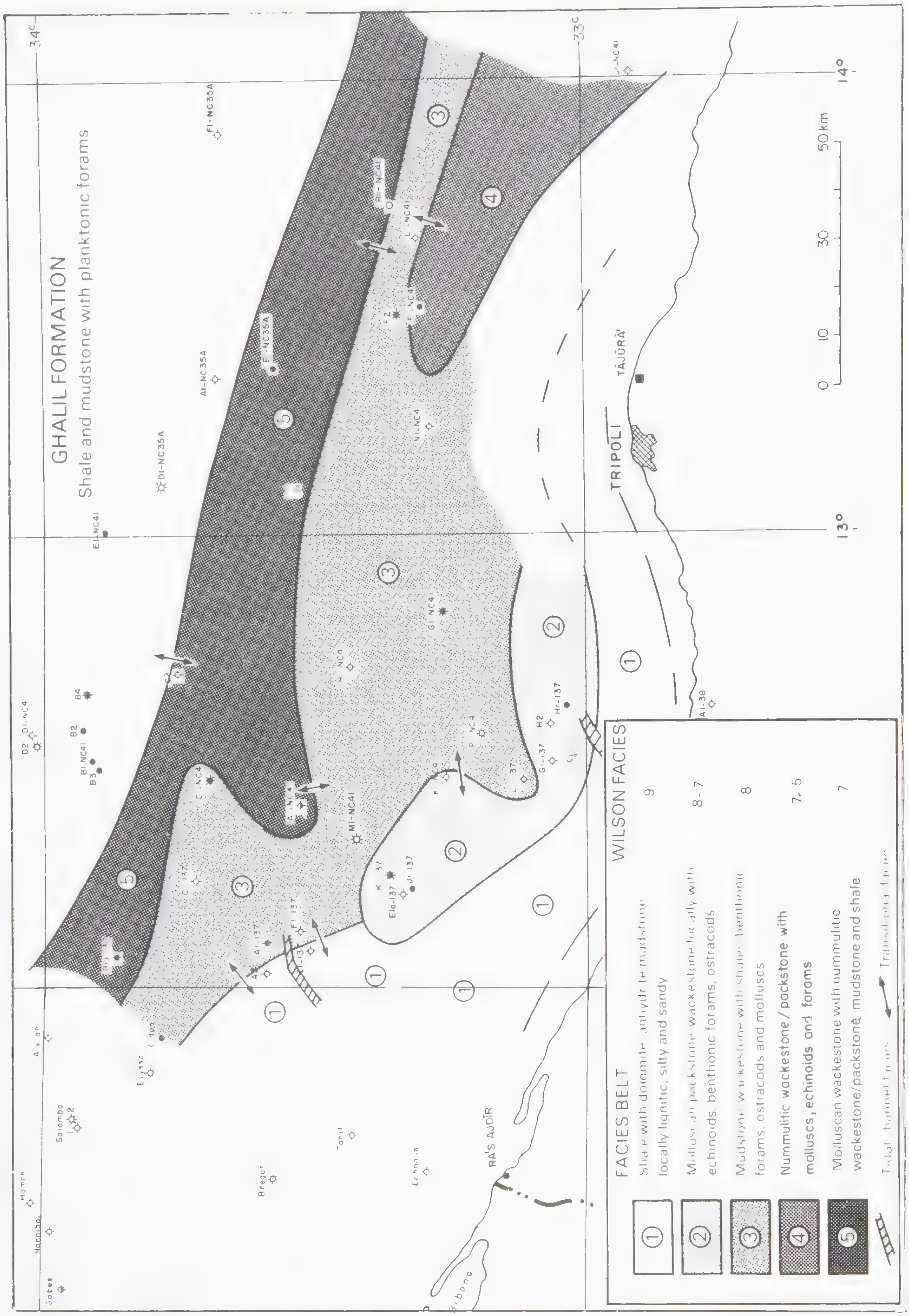
GHALIL FORMATION
Shale and mudstone with planktonic forams
TRIPOLI
TĀJŪRĀ'
RA'S AJDIR
34°
33°
13°
14°
0 10 30 50km
FACIES BELT
WILSON FACIES
① Shale with dolomite, anhydrite mudstone locally lignitic, silty and sandy 9
② Molluscan packstone wackestone locally with echinoids, benthonic forams, ostracods 8-7
③ Mudstone wackestone with sparse benthonic forams, ostracods and molluscs 8
④ Nummulitic wackestone / packstone with molluscs, echinoids and forams 7, 5
⑤ Molluscan wackestone with nummulitic wackestone/packstone, mudstone and shale 7
Tidal channel fans
Transect lines
FI-NC35A
AI-NC35A
DI-NC35A
EI-NC41
E-NC35A
RI-NC41
L-NC41
F-NC41
F2
NI-NC4
GI-NC41
H-NC4
B4
B2
BI-NC41
B3
D2
DI-NC4
C-NC4
MI-NC41
A-NC4
K-37
EIa-137
JI-137
C-137
AI-137
FI-137
HI-137
H2
GI-137
P-NC4
AI-38
JI-NC41
Gates
Hannibal
Hamon
Salambo
Bregot
Tanit
Echnoun
Bibane

Fig. 10. Facies map of Harshah Formation.

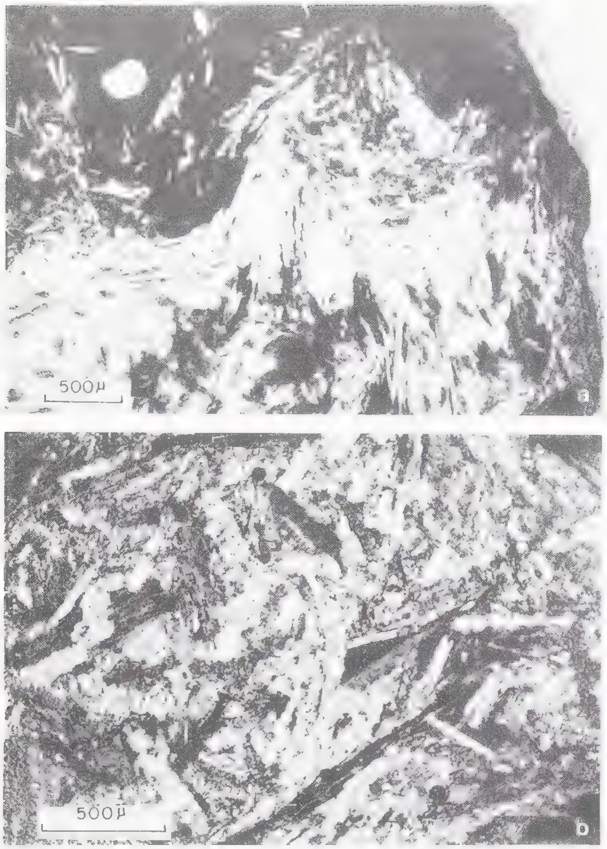

Fig. 11. (a) Anhydrite nodules growing in dark grey shale where the fibrous character is very evident. (H1-137) Harshah Formation. (b) Fibrous anhydrite characterizes most of the anhydrite in the shales. (H1-137) Harshah Formation. Cross nicols.

and covers a belt (Fig. 10) that follows the present coastline. It is suggested that a more restricted condition prevailed south of well H1-137 where sabkha sediments were deposited with local tidal channels as is indicated by the occurrence of sandy peloidal and foraminiferal wackestone and packstone (Fig. 12a, b) connecting belt 1 and belt 2. However, to the northwest near wells A2 and I1-137 the facies become less restricted and it is likely that the area was dominated by environments ranging from restricted lagoon to sabkha settings characteristic of the inner shelf conditions that covered the southern edge of Ṭarābulus basin during the Middle Eocene.

Facies Belt 2

This belt comprises several facies. They are molluscan packstone and wackestone, in places dolomitic peloidal skeletal grainstone, and silty and sandy shale with anhydrite nodules. Skeletal wackestones are widespread and sometimes grade to packstone and grainstone where peloids and skeletal debris of many kinds are the main components. This debris includes fragments from pelecypods (Fig. 13a), gastropods, nummulites, echinoids, serpulite (Fig. 13b), encrusting algae (Fig. 13c) and, in places, foraminifers are abundant (Fig. 14a). These facies become dolomitic where dolomite rhombs are clearly common (Fig. 14b) and sometimes dolomite is present as a cement in sandy horizons.

In many instances silica commonly replaces pelecypod fragments (Fig. 15a). The shales and clays which make up approximately 20% to 40% of the section are greenish-grey in colour with lignite flakes and millimetre-thin organic layers; the shales are locally silty or sandy with sporadic occurrences of anhydrite nodules which can be white or pink in colour. Ostracods and foraminifers are common in some beds.

At G1-137 this belt is more argillaceous at the

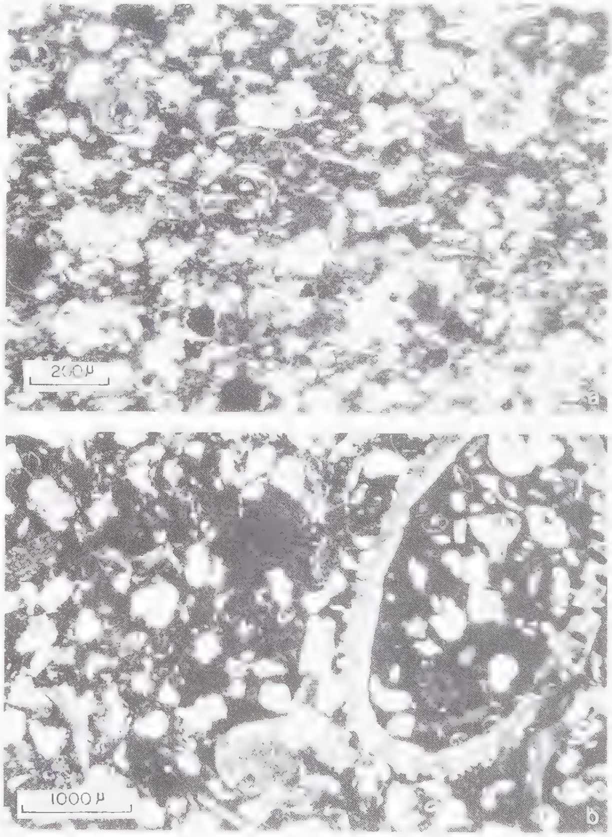

Fig. 12. (a) Sandy foraminiferal wackestone. (H1-137) Harshah Formation. (b) Sandy wackestone with glauconite grains (H1-137) Harshah Formation.

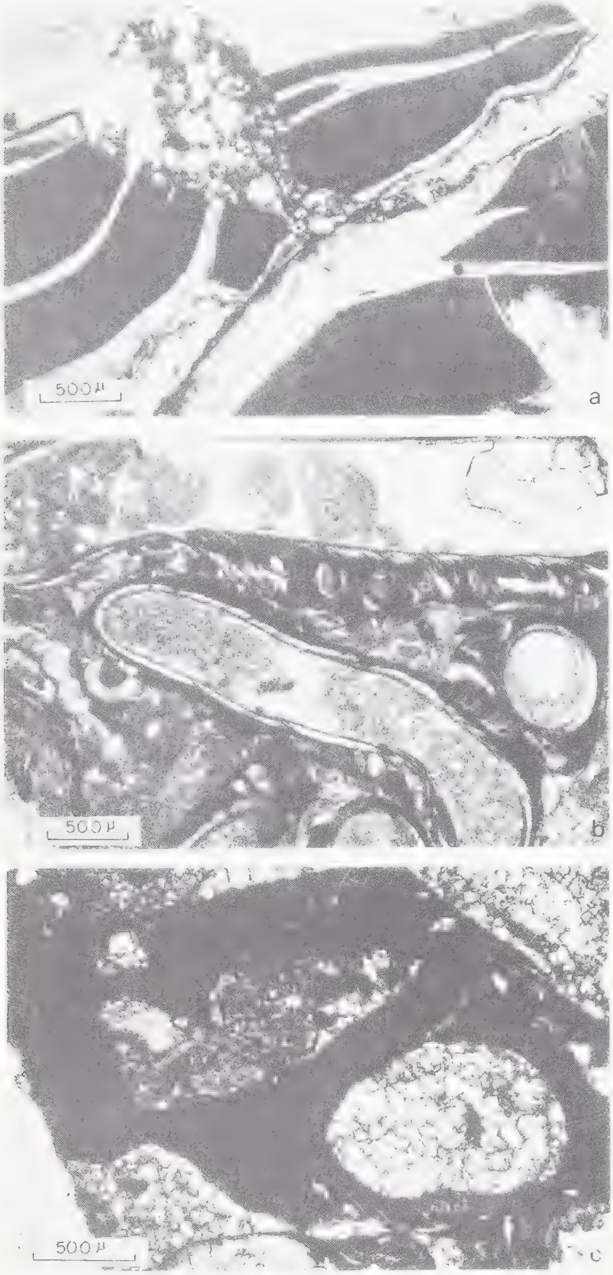

Fig. 13. (a) Thick-shelled oysters that are bored then filled by sandy mudstone. (H1-137) Harshah Formation. (b) Encrusting surpulit tubes, showing geopetal filling. (H1-137) Harshah Formation. (c) Encrusting algae(?) in coarse dolosparite facies. (H1-137) Harshah Formation.

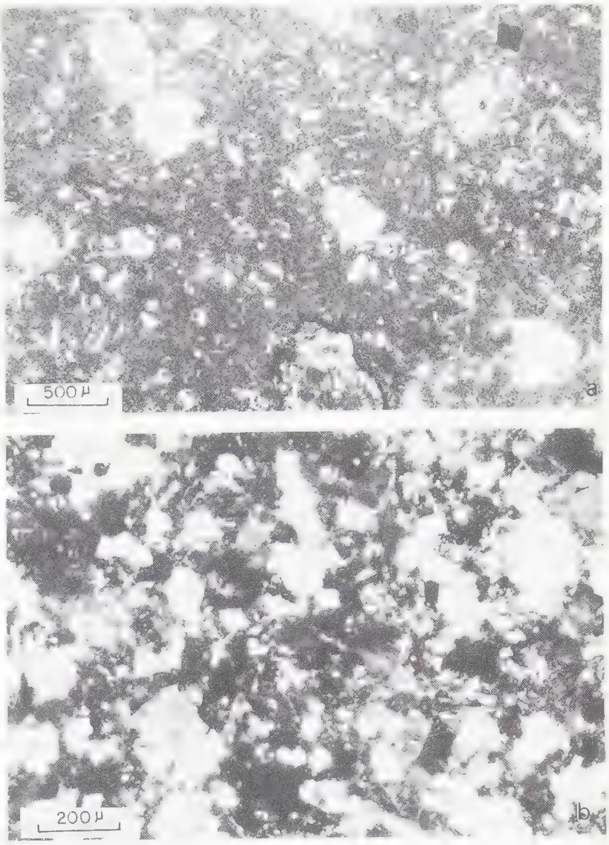

Fig. 14. (a) Foraminiferous wackestone is dominated by benthonic foraminifers (H1-137) Harshah Formation. (b) Dolomitized sandy grainstone (H1-137) Harshah Formation.

base with mudstone and wackestone facies and the skeletal debris is not as abundant and some sucrosic dolomite horizons appear. Occasionally tidal channel facies of sandy dolomitic peloidal, skeletal grainstone and packstone (Fig. 15b) occur at the base of this well. Although skeletal wackestone and mudstone dominate this section (with the exception of the carbonate member A which shows abundant and diverse skeletal fragments including nummulites and echinoids) some bryozoans, foraminifers and occasionally peloids are present (Fig. 16a). The upper beds of belt 2 at G1-137 become very argillaceous with many anhydrite levels and abundant shale and clay with no fossils and are sometimes dolomitic with anhydrite crystals and nodules. The anhydrite in places fills the open spaces of the grainstone facies which locally becomes dolomitic.

Similarly, at K1-137 the skeletal packstone and grainstone dominate the lower section with abundant molluscan debris. Then the skeletal wackestone/packstone which is locally dolomitic becomes the main facies with levels of dolomicrite with anhydrite at the top. At H1-137, however, all the facies of this belt are recognized and skeletal wackestone and packstone is the most common facies with abundant molluscs, foraminifers and ostracods. Locally nummulitic fragments are observed forming pelecypod nummulitic wackestone/packstone which represents the carbonate member A (Fig. 16b). In places peloidal packstone/grainstone facies with some calcareous algae occur (Fig. 17a) and these tend to be silty or sandy and dolomitic. Dolomicrite is present, in many cases associated with shale and anhydrite, in particular in the middle and upper beds of well H1-137. Similarly, at K1-NC41 shale beds predominate and exhibit anhydritic levels in the upper section.

Environments: The facies of belt 2, as shown in Fig. 10, occur just north of belt 1 and extend from K1-137 to H1-137 and possibly further east to connect with belt 4. The vertical and lateral distributions of these facies and their sedimentological analysis suggest an environment that ranged from inner to middle shelf. Middle shelf lagoon settings were dominant during deposition of this belt with local intermittent outer shelf influences as is exhibited by the presence of nummulitic facies with echinoids and algae (carbonate member A). At H1 and G1-137, on the other hand, wackestone and packstone facies rich in pelecypods, foraminifers and ostracods were deposited along the shelf lagoon environments where local thick accumulation of pelecypods perhaps induced the formation of oyster banks as in H1 and K1-137. It is also evident that high-energy facies of sandy peloidal grainstone/packstone are present in some wells, which very likely indicates the existence of tidal channels. In some wells, H1, G1 and K1-137, this belt shows abundant shale and dolomicrite with anhydrite nodules to be prevalent in the top of the section, thus suggesting the shallowing up of the Harshah Formation signalling the beginning of the major regression that characterizes the Tellil Group sequence. It is also possible that some sabkha facies which cover the southern belt 1 advanced northwards leaving some imprint on the middle shelf lagoon sediments.

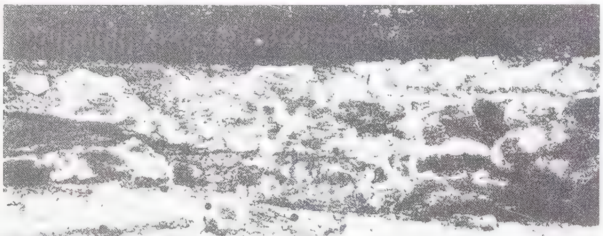

Fig. 15. (a) Silica replacing shell fragments. (H1-137) Harshah Formation. (b) Sandy peloidal skeletal packstone facies, with some phosphatic grains. (H1-137) Harshah Formation.

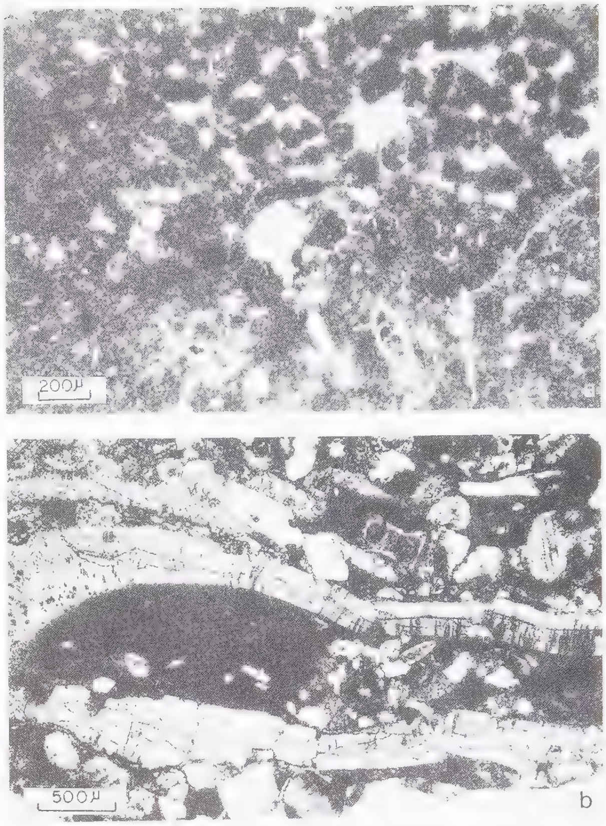

Fig. 16. (a) Peloidal texture in mudstone facies. (H1-137) Harshah Formation. (b) Skeletal wackestone to packstone facies showing compaction. (H1-137) Harshah Formation.

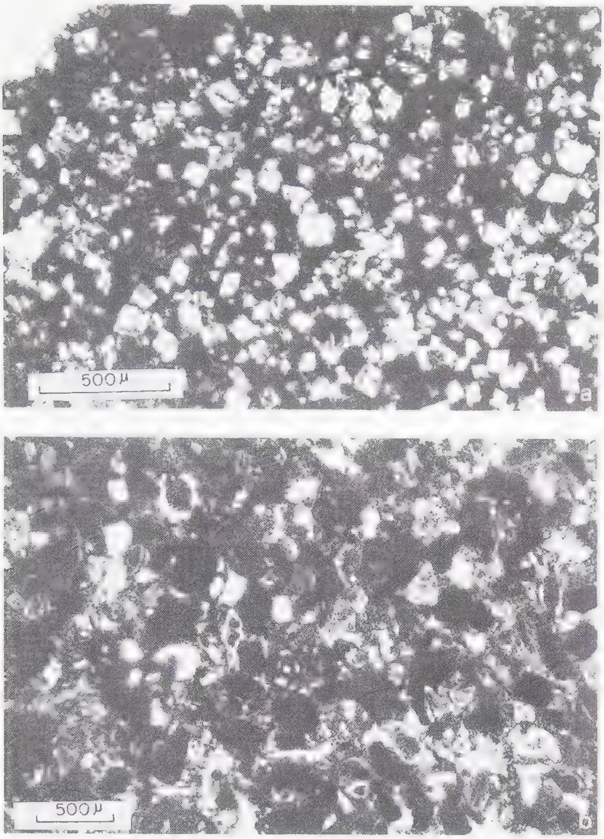

Fig. 17. (a) Packstone facies with many different fossils and skeletal fragments including calcareous algae. (H1-137) Harshah Formation. (b) Dolomite rhombs growing in argillaceous mudstone facies. (H1-NC41) Harshah Formation.

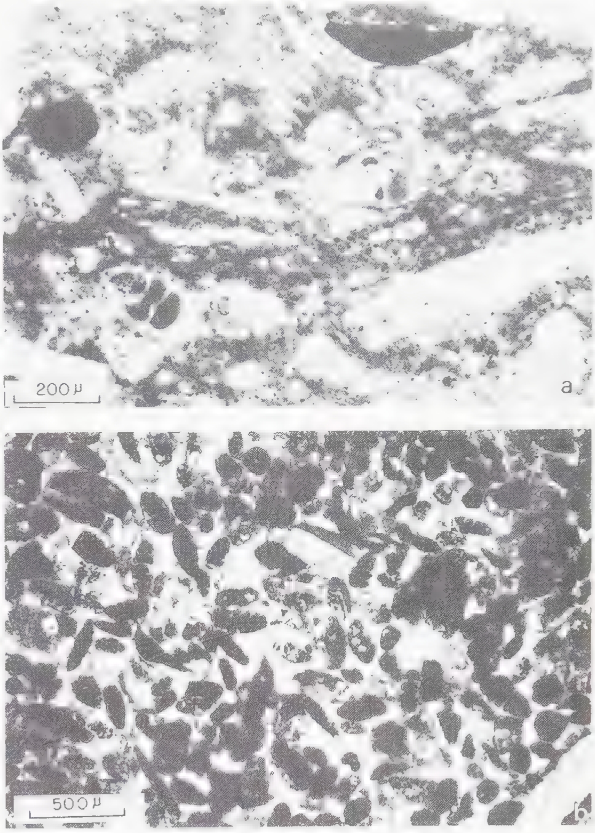

Fig. 18. (a) Shale horizon rich in microfossils that are replaced by either glauconite or pyrite. (C1-NC41) Harshah Formation. (b) Foraminiferal and ostracod grainstone. Most of the microfossils are replaced by pyrite or phosphates. (H1-NC41) Harshah Formation.

Facies Belt 3

This belt mainly comprises mudstone, wackestone and locally, packstone, however facies with shale interbeds occur. In most of the wells shale is very common and forms up to 60% of the sequence. Belt 3 is the most widely distributed in the basin and is represented by mudstone and wackestone facies with abundant benthonic foraminifers, ostracods and molluscan fragments and exhibits a wide variety of facies associations from other belts as a result of their proximity. This is clearly reflected in the lateral and vertical distributions of these facies. Locally belt 3 facies are dolomitic, sandy silty with phosphatic pyrite and silica replacement. The dolomite is common within the argillaceous mudstone (Fig. 17b).

In F1 and A1-137 wells the belt was found to contain alternating limestones and shales, the limestones ranging from mudstones to peloidal wackestones, with locally skeletal wackestone to packstone occurring; the shale is light grey, greenish grey, silty with traces of phosphatic and glauconitic grains and slightly dolomitic. Locally thin beds of calcareous sandstone are present in the upper beds. At L1-137 the limestone beds are mainly mudstone with fewer horizons of skeletal wackestones, which are dolomitic at the base and locally rich in ostracods. Shale is common and becomes anhydritic in the upper section. However, wackestone and mudstone rich in pelecypods, foraminifers and ostracods become quite common in G1-NC41 well.

At the northern edge of the belt, in H1, L1, C1-NC41 and C1-137 wells, shale dominates at the expense of limestone facies. The shale is grey to dark grey, splintery with abundant microfossils including miliolids and ostracods which in places is replaced by glauconite and pyrite (Fig. 18a). The limestones consist of mudstone to wackestone with a few levels of packstone rich in foraminifers and ostracods that

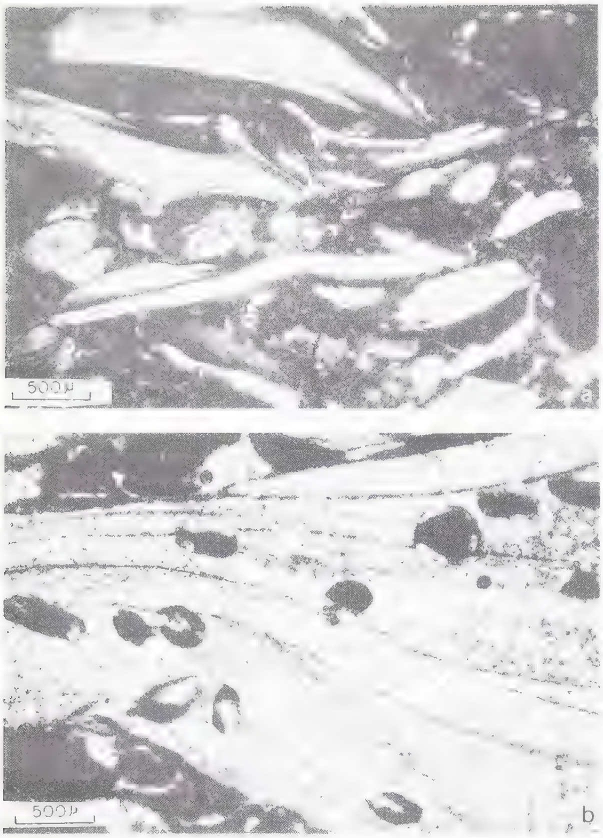

Fig. 19. (a) Pelecypod wackestone facies. Many of the shells have a well-preserved internal structure. (G1-NC41) Harshah Formation. (b) Thick-shelled pelecypods bored by smaller ones. (G1-NC41) Harshah Formation.

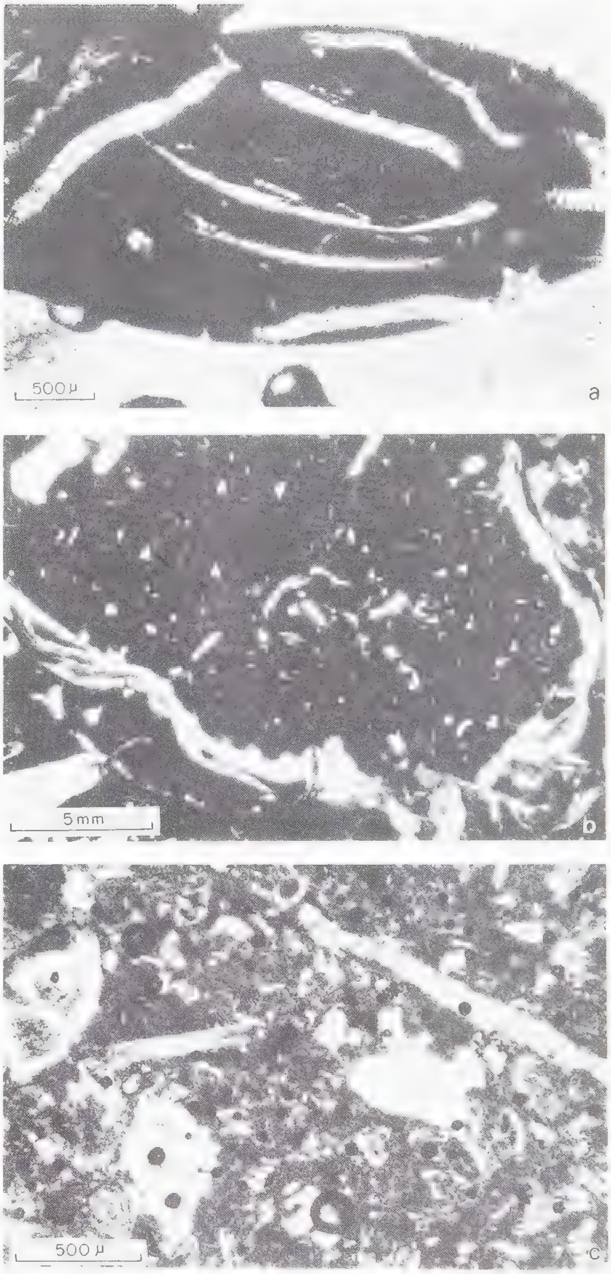

Fig. 20. (a) Thick shell, bored by smaller pelecypods and filled by mud and skeletal fragments. (G1-NC41) Harshah Formation. (b) Articulate pelecypods in wackestone facies. (G1-NC41) Harshah Formation. (c) Wackestone facies with different fossils including foraminifers, echinoid fragments and spines. (H1-137) Dahman Formation.

are sometimes filled or replaced by pyrites, phosphates (Fig. 18b), and locally at well H1-NC41 large thick-walled pelecypods and foraminifers occur. At C1-NC41 the pelecypods are so abundant that they probably formed an oyster bank. These are dominated by wackestone and packstone (Fig. 19a). Many of the pelecypod fragments are bored by smaller pelecypods (Figs 19b, 20a) and locally, articulate shells are observed (Fig. 20b). The upper beds of L1-NC41 show many nummulites thus suggesting the proximity of the nummulitic facies of belt 4 which are characterized by such facies. Many stages of replacement are observed in these facies by many minerals including phosphate, silica and dolomite.

Environments: The occurrence of wackestone and mudstone facies with abundant benthonic foraminifers and pelecypods and the predominance of fossiliferous shale, which is slightly silty and sandy, suggests deposition in a restricted shelf lagoon that was locally influenced by outer and inner shelf conditions. As such conditions covered large areas of the basin during the Middle Eocene the facies exhibit different variations in composition, reflecting their proximity to different settings surrounding the middle shelf lagoon. The conditions in this shelf were temporarily perfect for the development and growth of oyster banks which are known to flourish in shallow quiet water rich in nutrients. The middle shelf lagoon became shallower and more restricted at the end of deposition of the Harshah Formation as can be deduced from the presence of restricted lagoonal facies and sandstone horizons which again indicate the beginning of the regression as is the case in the belt 2 facies.

Facies Belt 4

The facies of belt 4 are composed mainly of wackestone, packstone, and locally, grainstone. The dominant skeletal debris are nummulites, mollusca and foraminifers; locally, however, echinoids, bryozoa, surpulite and algae are present, while in places, echinoid and pelecypod fragments become very abundant. Nummulites occur as whole tests and broken fragments, the chambers being filled by sparry calcite and occasionally by micrite. Sometimes pyrite, glauconite or dolomite fill these chambers.

Environments: These facies are recognized only in F1-NC41 well and it is suggested that they were deposited in the shallow water of the outer shelf where nummulite banks might have developed in the F1-NC41 area during the Middle Eocene. It is possible that such a nummulitic accumulation reflects local conditions which prevailed in the area and perhaps extended towards Sirt basin where similar facies of Gialo limestone (Middle Eocene) have been described. It is interesting to note that during the Early Eocene, the F1-NC41 area was the site of the reefal and high-energy facies of Tajoura Formation. This suggests that perfect conditions for carbonate build up prevailed in this area during most of the Eocene.

Facies Belt 5

This belt is dominated by shale which makes up 60% to 80% of the section (Fig. 5). The limestone bed consists of molluscan wackestone with nummulitic wackestone/packstone and mudstone. At B1a-137 the wackestone and mudstone facies have abundant ostracods, gastropods and foraminifers, locally dolomitic. Nummulitic, molluscan wackestone, locally packstone, is the main facies of the thick limestone member A. Similarly, A1-NC41 exhibits similar facies but locally traces of planktonic foraminifers are present in the marly beds. These shales, marls and mudstone beds which are rich in plankton are very common at C2-NC41 well.

Environments: Facies of belt 5 were deposited in environments that range from middle shelf to deeper water off the shelf basin. This is evidenced by the shales and marls with abundant plankton and the position of this belt in relation to the shelf setting that dominated the area and which grades to the basinal facies of Ghalil Formation. The nummulitic facies within this belt represent a shorter period of nummulite and pelecypod accumulation through the western part of the Pelagian block as the limestone member A, with similar facies, is detected in the wells located at the western section.

These facies would seem to indicate the absence of a barrier or shoal along this belt such as one would normally expect in the shelf condition. But I think we are dealing here with un-rimmed shelf.

Facies and Environments of Dahman Formation

Dahman Formation, which was encountered in most of the wells drilled is characteristically a limestone interval of more or less uniform thickness with few major facies changes. The facies are mainly wackestone with molluscan debris, foraminifers and traces of small nummulites; the facies become sandy at the southern part of the basin. The packstone facies increase northwards with the introduction of nummulites which become very common at the northern margin of the area where they become nummulite packstone. This grades to mudstone with planktonic forams at C2-NC41 which in turn changes to the basinal facies of Ghalil Formation.

Four major facies belts are recognized and each occupies a particular section (Fig. 21).

(1) Molluscan wackestone, mudstone locally packstone and sandy with traces of nummulites.
(2) Molluscan packstone: packstone with nummulites.
(3) Nummulitic packstone.
(4) Mudstone/wackestone with microfossils (planktonic).

Facies belt 1

This belt is composed mainly of wackestone and mudstone facies in different proportions. Skeletal fragments of molluscs, echinoids, foraminifers and ostracods (Fig. 20c) are common and only a few small nummulites are found. Locally at H1-137 the facies become very sandy and dolomitic with peloids and intraclasts (Fig. 22a) and in places packstone and foraminiferous wackestone occur. Mudstone facies on the other hand dominate G1-137 section. These facies are present at the wells drilled in the

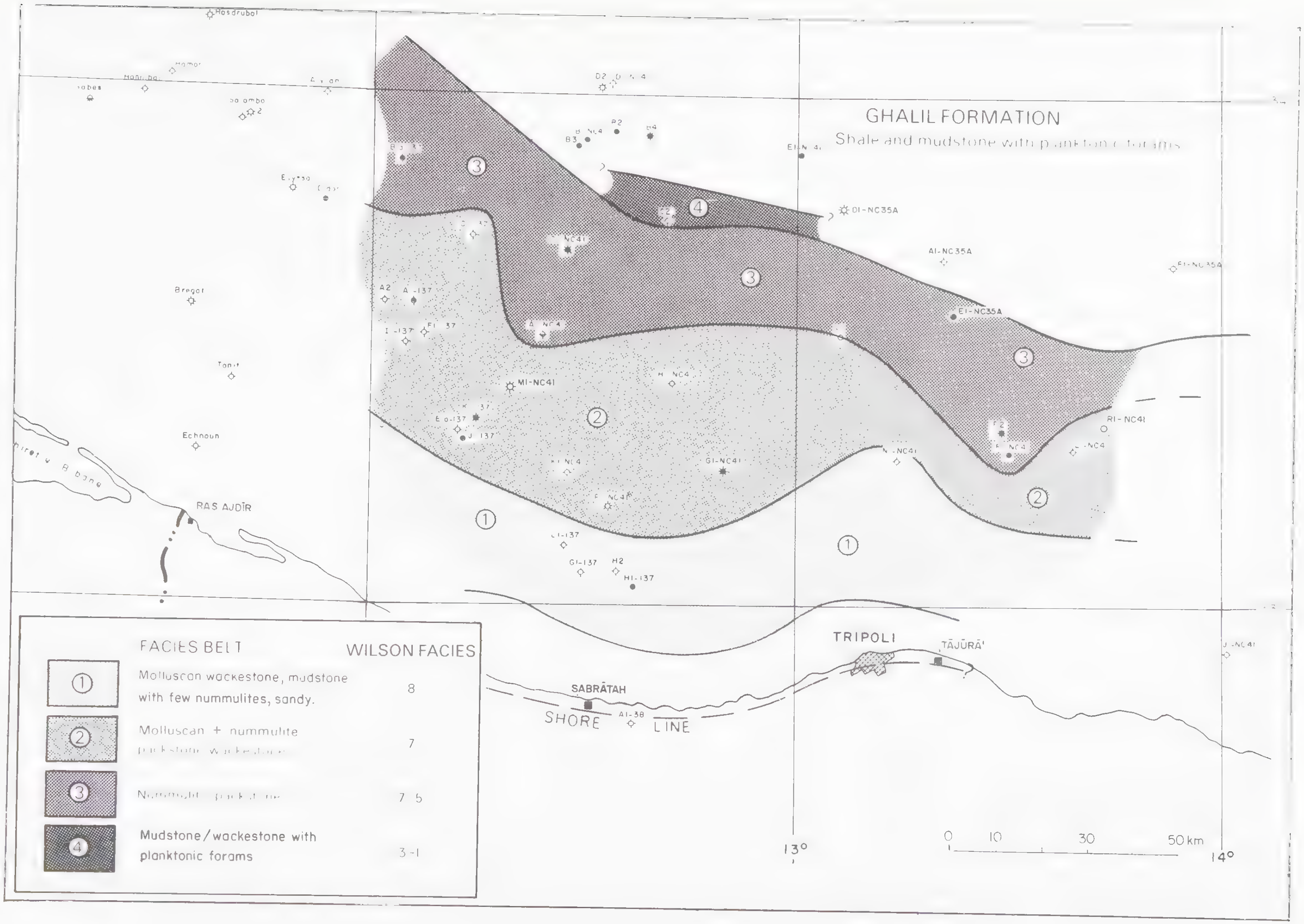
GHALIL FORMATION
Shale and mudstone with planktonic forams
TRIPOLI
TĀJŪRĀ'
SABRĀTAH
SHORE LINE
RAS AJDĪR
Hasdrubal
Bregot
Tanit
Echnoun
MI-NC41
GI-NC41
RI-NC41
DI-NC35A
AI-NC35A
EI-NC35A
A2
A -137
FI 37
I -137
E o-137
J 137
GI-137
H2
HI-137
AI-38
B3
P2
13°
14°
0
10
30
50 km
1
2
3
4
FACIES BELT
WILSON FACIES
Molluscan wackestone, mudstone with few nummulites, sandy.
8
Molluscan + nummulite packstone wackestone
7
Nummulitic packstone
7 5
Mudstone/wackestone with planktonic forams
3-1

Fig. 21. Facies map of Dahman Formation.

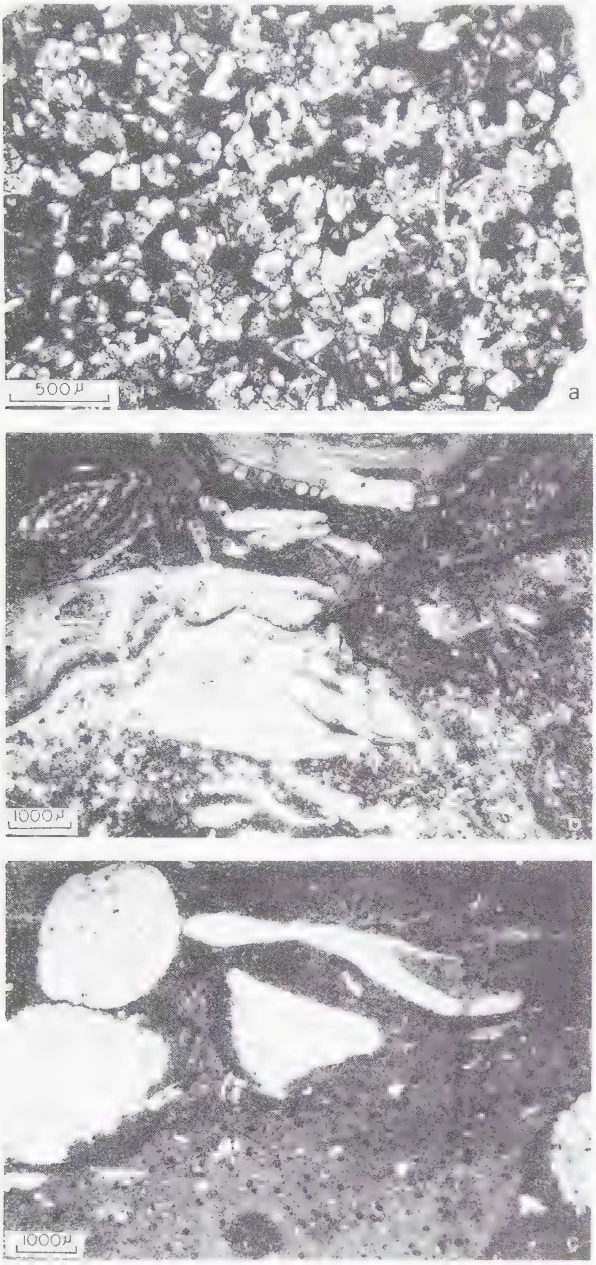

Fig. 22. (a) Dolomitic wackestone to packstone facies, slightly sandy with many fragments of echinoids and algae. (H1-137) Dahman Formation. (b) Skeletal wackestone facies where pelecypods and nummulites are common. Slightly dolomitic. (K1-NC41) Dahman Formation. (c) Nummulites and fragments of pelecypods in bioturbated wackestone facies. (K1-NC41) Dahman Formation.

south and probably extend along the present shoreline and may represent part of a middle shelf lagoon that was slightly restricted and very close to the inner shelf conditions further south where the source of the sands occur.

Facies belt 2

This belt consists predominantly of skeletal wackestone and packstone in equal proportions where molluscan and nummulitic fragments are equally important (Fig. 22b, c). However, in some sections pelecypods are very abundant thus perhaps constituting a local build up as is the case in K1-137, K1-NC41, A2-137, G1-NC41 and C1-137 wells (Fig. 23a).

Throughout the belt other fossils are present in smaller percentages such as echinoids, ostracods, miliolids and other small foraminifers; locally peloids and intraclasts are present at F1-137 and G1-NC41.

The increase of packstone facies with nummulites is evident in this belt with the common occurrence of levels rich in pelecypods. This would indicate a shelf lagoon with good circulation perhaps not far from a nummulitic bank further north. The conditions in the middle shelf meanwhile were sufficiently good for pelecypods to flourish and form a build up. The presence of both nummulite and molluscan facies suggests a fluctuation in water depth or other

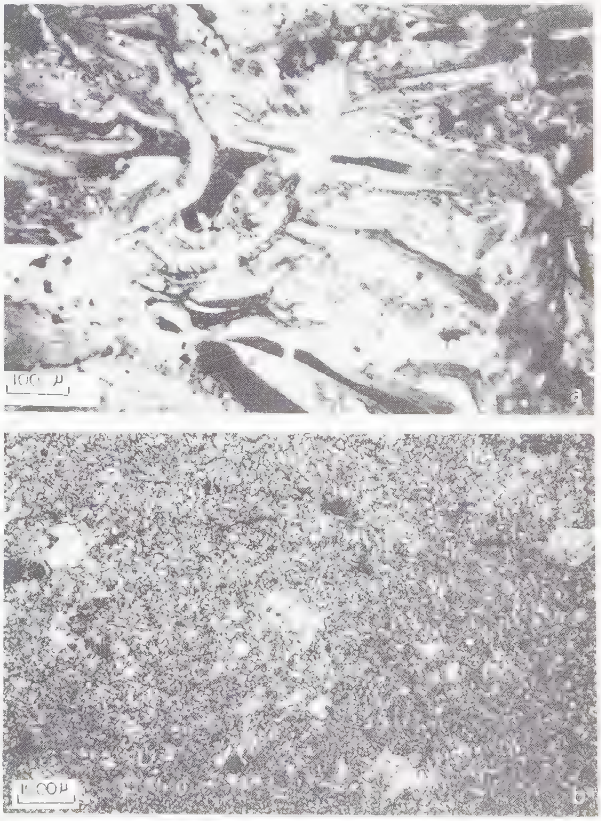

Fig. 23. (a) Pelecypod packstone to grainstone, slightly dolomitic (K1-NC41) Dahman Formation. Cross nicols. (b) Dolomicrosparite facies with relics of unreplaced calcite and pyrite inclusions. (H2-137) Samdun Formation.

factors which resulted in slight local restrictions conducive to pelecypod growth; this phase was followed by open and deeper conditions enabling nummulite accumulation. However, it is also possible that most of the nummulites in this belt were transported from a bank further north.

Facies belt 3

Nummulitic packstone is the main facies for this belt where nummulites, both large and small, are very abundant in particular *Nummulites gizehensis* with only a trace of molluscan fragments. However, locally at F1-NC41 skeletal and molluscan wackestone occurs. The facies of belt 3 are dolomitic at C1-NC41 and exhibit silica replacement at B1a-137. At A1 and C1-NC41 shale beds occur.

These facies dominate part of the northern section of the shelf and they form an irregular belt which extends from B1a-137 in the northwest to F1-NC41 in the southeast (Fig. 21).

The position and the type of facies of this belt imply the occurrence of a nummulitic bank along belt 3 covering the margin of this carbonate shelf. This bank is rather wide and may extend southwards to include the facies of belt 2.

Facies belt 4

These facies are encountered only at well C2-NC41. They are composed of mainly white argillaceous mudstone/wackestone with abundant planktonic foraminifers. This belt disappears to the north and is replaced by marls, shales and clays rich in planktonic foraminifera which belong to Ghalil Formation.

Though belt 4 facies are reported only from C2-NC41 well they are likely to be present along a narrow belt parallel to belt 3 and represent the basinal facies equivalent to the nummulitic bank facies of belts 3 and 2 which occur in the south. They indicate a transitional condition before the deep basinal facies of Ghalil Formation were dominant.

Facies and Environments of Samdun Formation

Four major facies belts are recognized, each occupying a belt more or less parallel to the present shoreline (Fig. 31). These belts cover most of the Libyan continental shelf/offshore Tripoli. They are:

Belt 1: Mainly shale with dolomite, anhydrite, mudstone locally lignitic, silty and sandy.
Belt 2: Mudstone and wackestone with shale, rich in benthonic foraminifers, ostracods and molluscs.
Belt 3: Pelecypod packstone and wackestone.
Belt 4: Wackestone, locally packstone with molluscs, benthonic foraminifers, molluscs and traces of planktonic foraminifers.

Facies Belt 1

This belt consists mainly of shale with a few levels of mudstone and wackestone, and many dolomite and dolomitic horizons where dolomite is found to replace skeletal fragments, sometimes leaving relics (Fig. 23b). The shale is dark grey to greenish grey with abundant lignite flakes and anhydrite nodules (Fig. 24b) locally red brownish clay rich in glauconite occurs. The shale is sandy, silty and dolomitic in places. The sandstones are cemented by acicular anhydrite (Fig. 24c). The limestone beds are composed of mudstone, locally wackestone with traces of peloids and mollusc debris. In general forams are absent in the limestone and shale horizon. Anhydrites as small nodules in mudstone (Fig. 25a) and thin beds are present throughout the section. At G1 and H1-137 shales predominate and become fossiliferous in the top 200 ft.; the well is otherwise barren. The fossils include a few foraminifers, ostracods and traces of molluscs which are sometimes bored or replaced by silica (Fig. 25b). The shale percentage decreases towards L1-137 and is replaced by mudstone and wackestone beds which are dolomitic in places and become more fossiliferous. Locally at L1-137 levels with peloidal packstone and grainstone with skeletal fragments occur which represent the carbonate member B. At G1 and H1-137 there are few dolomite beds but they are quite common at L1-137. The dolomicrite facies is laminated with bituminous layers which perhaps represent algal mats (Fig. 26a) and which locally have a bird's eye structure.

Environments: The facies of this belt and their distribution pattern indicate deposition in a sabkha supratidal to restricted lagoonal setting where the restricted lagoonal conditions dominate at the end of the period of deposition of this belt. This is evident from the common occurrence of fossils in the upper beds and the complete absence of fauna in the lower section, and the presence of anhydrite, dolomicrite and shale and sandstone strings which indicate a supratidal sabkha environment with perhaps some alluvial fan influence. This belt covers the southern edge of the shelf and extends parallel to the present shoreline.

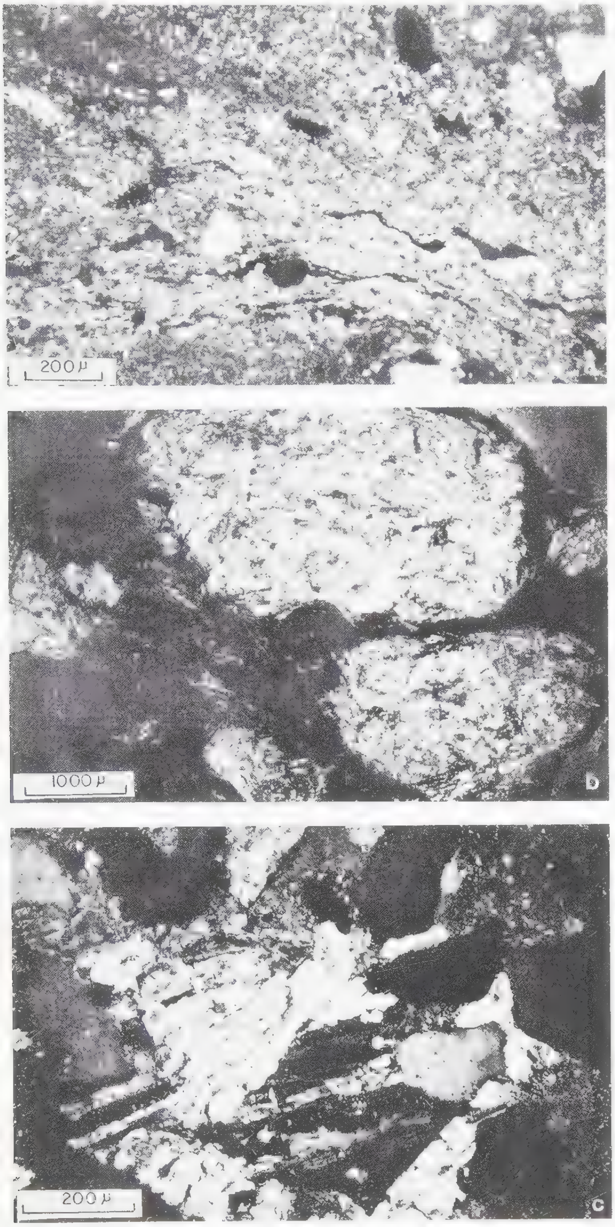

Fig. 24. (a) Shale and clay with lignite laminae, slightly sandy. (H2-137) Samdun Formation. (b) Anhydrite nodules of different sizes in shale. Note the fibrous to bladed character of the anhydrite (H2-137) Samdun Formation. Cross nicols. (c) Bladed anhydrite laths filling the cavities between sand grains. (H2-137) Samdun Formation. Cross nicols.

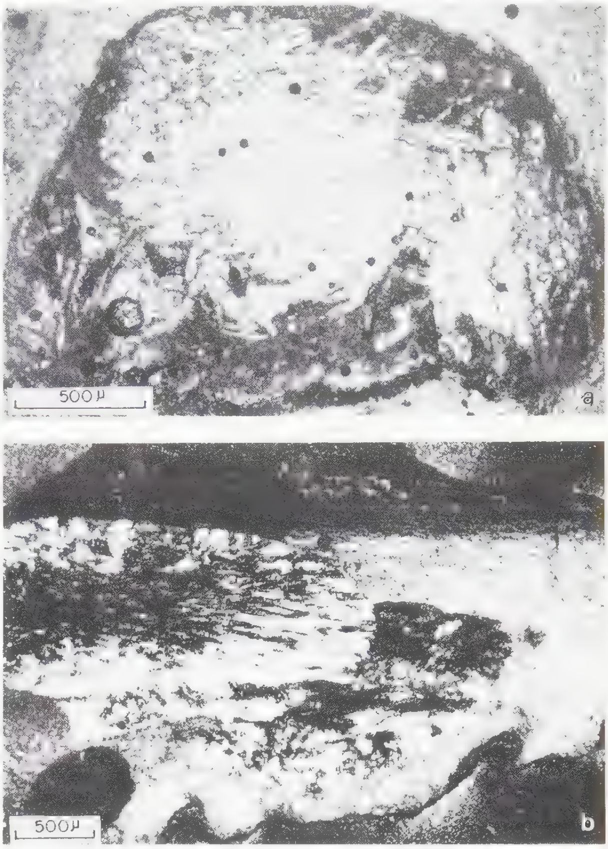

Fig. 25. (a) Anhydrite nodules in mudstone that is replaced later by dolomite and calcite. (H2-137) Samdun Formation. (b) Shell fragments bored then filled by silica (chalcedonic quartz). (H2-137) Samdun Formation.

Facies belt 2

This belt has abundant shales that comprise 40–80% of the section: the shale percentage increases from south to north. The shale is grey to dark grey, greenish in colour, slightly calcareous, fossiliferous and locally silty with glauconite and pyrite. Limestone beds are common at K1 and I1-137 and become less so in the other wells where they decrease in percentage northwards. The limestone beds consist primarily of mudstone and wackestone which is slightly dolomitic and silty and in places fossiliferous.

At K1-137 the limestones of the belt show levels that are rich in ostracods and foraminifers with a trace of pelecypods and peloids. Dolomicrite sometimes silty and dolomitized wackestone and anhydrite horizons are also present. However a well-defined carbonate unit that belongs to carbonate member (B) is clearly recognized and consists of skeletal packstones and grainstones with algae, molluscs, nummulites and foraminifers in differing proportions.

This carbonate unit is found in many wells including K1, G1-NC41 and C1 and K1-137 (Fig. 27). They differ slightly in their composition but they all clearly exhibit a normal marine fauna in contrast to the re-

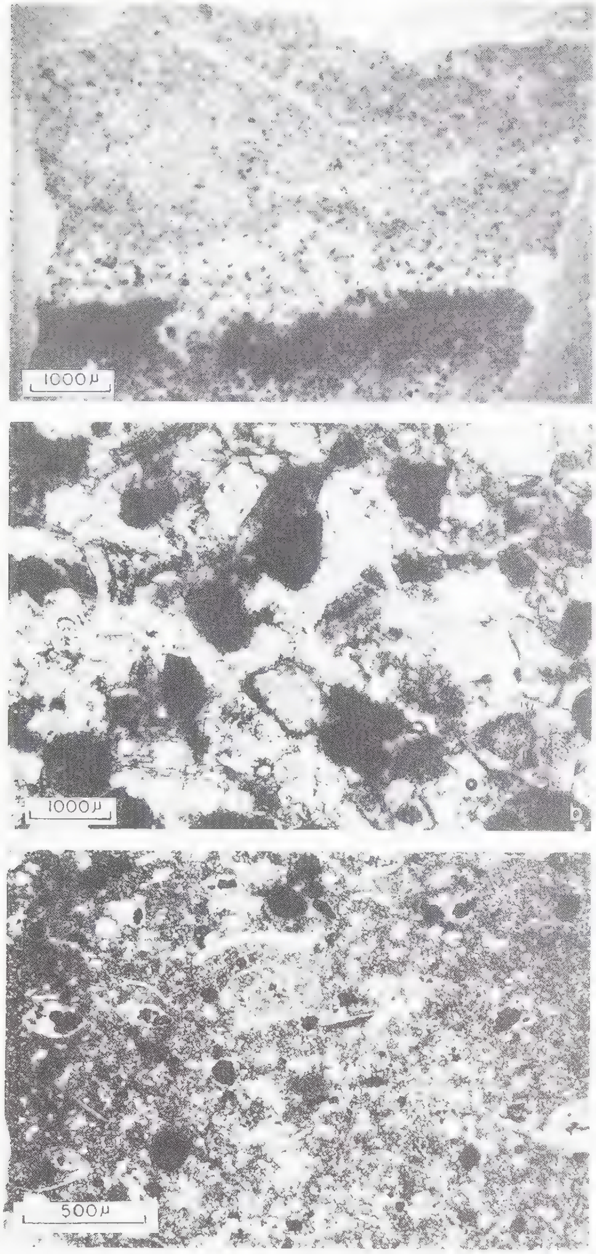

Fig. 26. (a) Thin bituminous layer with a thin laminae of quartz grains in dolomicrite and mudstone facies. This perhaps represents an algal mat layer. (H2-137) Samdun Formation. (b) Sandy peloidal, skeletal packstone to grainstone. Carbonate member B. (K1-NC41) Samdun Formation. (c) Ostracod-rich mudstone and wackestone, dolomitic with pyrite. (G1-NC41) Samdun Formation.

stricted fauna found in the shales and mudstones of this belt. This member becomes sandy peloidal skeletal packstone to grainstone at K1-NC41 (Fig. 26b) and pelecypod packstone at G1-NC41 with only a trace of echinoids and nummulites.

At K1-NC41 ostracods are very common in the wackestone and mudstone facies (Fig. 26c) which are slightly dolomitic and locally strings of argillaceous siltstones and sandstones occur. On the other hand at G1-NC41 this belt is characterized by wackestone and mudstone facies that are rich in pelecypod fragments with only a trace of nummulite and echinoid fragments. As in G1-NC41, the H1 and K1-NC41 wells are dominated by skeletal wackestone and packstone where pelecypod fragments are the main constituent. In some cases the pelecypods are so abundant that they form local pelecypod accumulations.

These pelecypod accumulations are dominated by oyster fragments in micrite that are slightly dolomitic and many of the fragments show parallel orientation suggesting perhaps a current influence (Fig. 28a). Stylolites are found to be very common throughout the pelecypod-rich facies. At G1-NC41 these facies are characterized by abundant surpulite tubes which encrust pelecypod fragments (Fig. 28b). Many types of replacement are evident within this belt, including silica (Fig. 28c), pyrite (Fig. 29a) and dolomite replacement of shell fragments (Fig. 29b).

Further northward the shales predominate in this belt replacing limestones; only a few limestone beds occur, as is the case at C1-137, where the white chalky mudstone and skeletal wackestone is rich in ostracods (Fig. 30a).

Environments: The depositional environments of this belt range from restricted lagoon to shelf lagoon settings with transitional facies at the border with facies belt 1. The restricted lagoon facies is dominated by shale, mudstone and traces of wackestone that are rich in ostracods and small foraminifers which are locally silty, sandy and dolomitic. The shelf lagoon setting has a better circulation which is indicated by the common occurrence of limestone beds of skeletal wackestone rich in normal marine fauna as is the case of the carbonate member (B). The increase in the percentage of shale and clay to the north is thought to be due to restriction, water depth, source of clay and current direction.

Facies belt 3

The typical facies of this belt occurs at well F1-NC41, where pelecypod packstone and wackestone dominate the section. Locally pelecypods become very abundant in the upper limestone beds where they probably constitute an oyster bank which covers most of the F1-NC41 area. Other fossils are common including echinoids, ostracods and foraminifers; locally a few nummulites are found in the lower beds. Similar facies are found at L1-NC41 with abundant microfossils. By correlation these facies also occur at F2 and N1-NC41 wells where wackestone becomes common. These facies are interpreted as occurring along a narrow belt which may extend in a southeast direction towards the Sirt basin (Fig. 31).

Environments: Figures 31 and 10 clearly show that belt 3 of the Samdun Formation covers almost the same area as belt 4 of the Harshah Formation. This undoubtedly suggests a close relationship between these two main facies belts. This in turn reflects a topographic feature in this area that persisted for a long time.

Thus the facies of belt 3 indicate the occurrence of an oyster bank in the area of F1-NC41 and the adjacent area, as shown in Fig. 31. The distribution of this facies (Fig. 31) is based on the correlation between wells and therefore more control is required before accurately predicting the bank location.

It is evident that there were two banks present in the same area; a nummulitic bank during deposition of Harshah Formation followed by an oyster bank development during deposition of Samdun Formation. This suggests that shallowing up took place in this area since a nummulitic bank requires relatively deeper water and less restricted conditions in contrast to pelecypods which prefer slightly restricted shallow water.

Facies belt 4

This belt is dominated by fossiliferous shales which comprise 80% or more of the Samdun section. The shale is dark grey grading to greenish grey locally very fossiliferous with pyrite and glauconite grains. The limestone intercalation consists of wackestone, mudstone locally packstone. The facies of this belt is similar to belt 2 facies but the marine fauna is more diverse and abundant in belt 4 facies; they include pelecypods, algae, corals and locally nummulites and abundant benthonic foraminifers. A trace of planktonic foraminifers is reported from C1 and C2-NC41. At B1a-137 one horizon is rich in nummulites and grainstone/packstone facies.

Environments: This belt was deposited on middle shelf lagoons which vary in restriction and was probably located adjacent to a deeper shelf to basinal environment where shale and mudstone rich in planktonic fauna were deposited as Fig. 31 suggests.

The diverse normal marine fauna, the dominance of fossiliferous shales and limestone and the local occurrence of a few beds with planktonic fauna in some wells, and in particular the location of this belt adjacent to the wells that are characterized by the shales and mudstone of Ghalil Formation, all indicate that belt 4 represents the northernmost limit of a proper shallow shelf depositional environment before the deeper basinal conditions that prevailed further northward. They also suggest that the shelf during deposition of Samdun Formation was un-rimmed as no shelf margin facies have so far been detected between C2-NC41 and B3-NC41. This conclusion is again supported by the facies of Harshah Formation.

Facies and environment of Ghalil Formation

This formation is very well defined by logs and consists mainly of shale sometimes calcareous with mainly planktonic foraminifera; locally, however, some horizons typically have Harshah and Samdun facies fauna.

The shale is greenish grey becoming darker grey higher up the section, medium hard, fissile locally grading to marl and whitish soft shale with abundant planktonic foraminifera (Fig. 30b), in places silty and exhibiting a peletoidal texture. The shales and marls are very rich in planktonic foraminifera and tend to dominate the lower beds of Ghalil Formation. The upper beds of shales and marls of wells B2, B1 and D2 are characterized by typical shallow water fauna of Harshah and Samdun Formations which indicate a lateral interfingering facies relationship with the shallower water shales and marls that prevailed on the shelf, rather than a shallowing up of the basin.

The lower beds of Ghalil Formation exhibit other shallow water characteristics, including the occurrence of levels of wackestone and mudstone facies which are locally silty and sandy and with benthonic foraminifers, ostracods, pelecypods and algae.

On the other hand at A1-NC35A no shallow water faunal assemblage is present and only a trace of benthonic fauna is reported from E1-NC41.

In general the shales and marls of Ghalil Formation are interpreted as having been deposited in the deep shelf margin or open sea shelf, such as were located off the un-rimmed shelf which dominated the Pelagian block during Middle and Late Eocene time.

THICKNESS AND DISTRIBUTION OF THE EOCENE ROCKS

From several isopach maps drawn for the individual formations and groups of the whole Eocene (Sbeta, 1984), the Upper and Middle Eocene (Fig. 32) and the thickness map of the Lower Eocene rocks (Sbeta, 1990), it is quite clear that the Ṭarābulus basin during the Eocene had an elongate shape and a general NW–SE trend and was very wide offshore Zuwārah and narrower offshore Tripoli. The Eocene sequence shows a major depocentre parallel to the shoreline where the centre of deposition is along an axis that extends from L1-NC41 in the east to B1a-137 in the west. The maximum thickness is reached at H1-NC41 where it exceeds 3500 ft. The thickness of the Eocene decreased towards the south in the direction of the present coast and in the north where it grades into the deep basinal facies of Ghalil and Hallab Formations. The thickness contours of the Eocene sequence show an irregular configuration in the western section of the basin as is reflected by the Triassic salt tectonics and pre-Eocene erosion that influenced this part of the basin. The depocentre axis is irregular and tends to exhibit pronounced deflection north of F2-NC41 well which seems to correspond to the local structures and probably to the pre-Eocene topography. Local thickening, and stretching of the basin is apparent in the centre and the western part of the basin as is indicated by the presence of local centres of thick accumulation around H1-NC41, C1-137 and H1-137. Some of these basins have secondary axes that trend NE–SW and are separated by local ridges that partially reflect salt tectonics and also erosion and non-deposition of Eocene rocks as is the case in the vicinity of K1-137.

By comparing the different isopachs of the Eocene sequence (Sbeta, 1984) it is evident that very little shifting of the depocentre has taken place, but the effect of local structures and the secondary NW–SE trending basins are quite apparent during Early Eocene time.

The thinning of the Eocene rocks to the north is probably due to a lower rate of sedimentation of which the basinal facies of marl, shales and mudstones are characteristic. On the other hand the thinning towards the south along the present coast is partially due to erosion in the area between M1-NC41 and L1-137 in the west and in the vicinity of J1-NC41. In the remaining isopachs the arbitrary zero line of the Eocene thickness is a reflection of the shoreline as is clearly suggested by the presence of shoreline facies during the deposition of Farwah and Tellil Groups.

THE DEPOSITIONAL HISTORY OF THE EOCENE

The Eocene sequence is defined by two major lithologic units, the Farwah and Tellil Groups and their equivalents Tajoura, Hallab and Ghalil Formations. These units were deposited on the continental stable shelf that was formed along the northern margin of the Cratonic African Plate. This shelf was bounded in the south by an irregular coast and in the north and northeast by a deep trough that existed throughout Eocene time and extended from north of D2-NC41 to E1-NC41 and B1-NC35A and further northwest in the Gabes basin of Tunisia. Over 3000 ft of sediments were laid down in this shelf that covers the Ṭarābulus and Gabes basins; the sediments are characterized by two major sedimentary cycles — the Late Palaeocene–Early Eocene transgressive cycle of Farwah Goup (Sbeta, 1990) followed by the thicker shallow water facies of the regressive Tellil Group.

The first cycle of Late Palaeocene to Early Eocene started with the advance of the sea over the pre-Tertiary erosional surface, overstepping older rocks that range in age from Santonian–Campanian in the south to Upper Palaeocene in the north and east-northeast (Sbeta, 1990). These two belts are characterized by shoreline and tidal flat facies and occupy the southern and southwest part of the shelf. In the centre of the shelf less restricted middle shelf lagoon conditions prevailed where the belt 3 facies of Bilal Formation were deposited. These facies grade into a deeper shelf environment in the north, as is indicated by the deposition of the basinal facies of Hallab Formation. It is evident that the shelf during the early part of the Eocene was non-rimmed as no shelf-margin facies were identified and therefore the restriction in the lagoonal waters was probably due to the damping effect of the vast expanse of the broad carbonate shelf.

The shelf water became shallower as is reflected in the sedimentation of the Taljah and Jirani dolomite type facies which indicate rather shallow and more restricted conditions than those that prevailed during deposition of Bilal Formation. This was followed by short intermittent uplifts that enhanced dolomitization and the deposition of kaolinitic clays and phosphorite horizons which characterize facies 1 of the Jirani Dolomites at B2-NC41.

While the southern edge of the shelf remained restricted and dominated by sabkha conditions, the centre and northern parts of the shelf indicate the start of a major transgression. This suggests tilting of

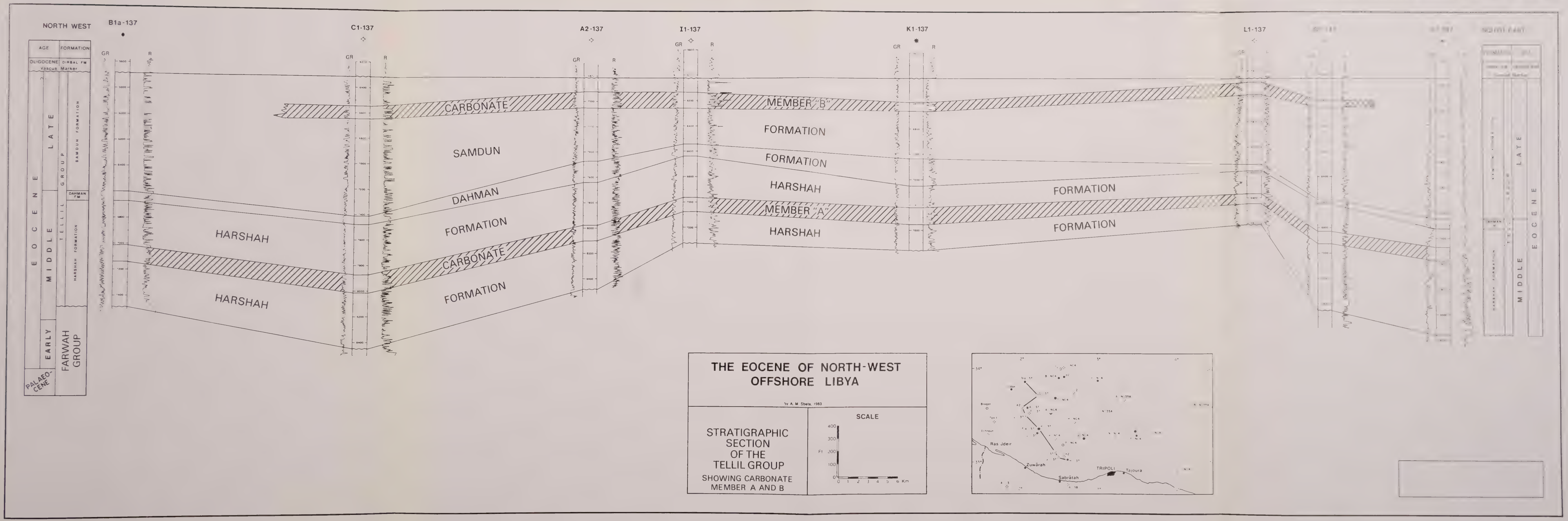
NORTH WEST
B1a-137
C1-137
A2-137
I1-137
K1-137
L1-137
AGE
FORMATION
OLIGOCENE
DIRBAL FM
Vascus Marker
EOCENE
LATE
MIDDLE
EARLY
PALAEOCENE
TELLIL GROUP
SAMDUN FORMATION
DAHMAN FM
HARSHAH FORMATION
FARWAH GROUP
GR
R
CARBONATE
MEMBER "B"
FORMATION
SAMDUN
FORMATION
HARSHAH
DAHMAN
FORMATION
MEMBER "A"
HARSHAH
FORMATION
HARSHAH
CARBONATE
FORMATION
HARSHAH
FORMATION
THE EOCENE OF NORTH-WEST OFFSHORE LIBYA
by A. M. Sbeta, 1983
STRATIGRAPHIC SECTION OF THE TELLIL GROUP
SHOWING CARBONATE MEMBER A AND B
SCALE
Ft
400
300
200
100
0
0 1 2 3 4 5 6 Km
34°
33°
2°
3°
Ras Jdeir
Zuwārah
Sabrātah
TRIPOLI
Tajoura

Fig. 27. Stratigraphic section of the Tellil Group.

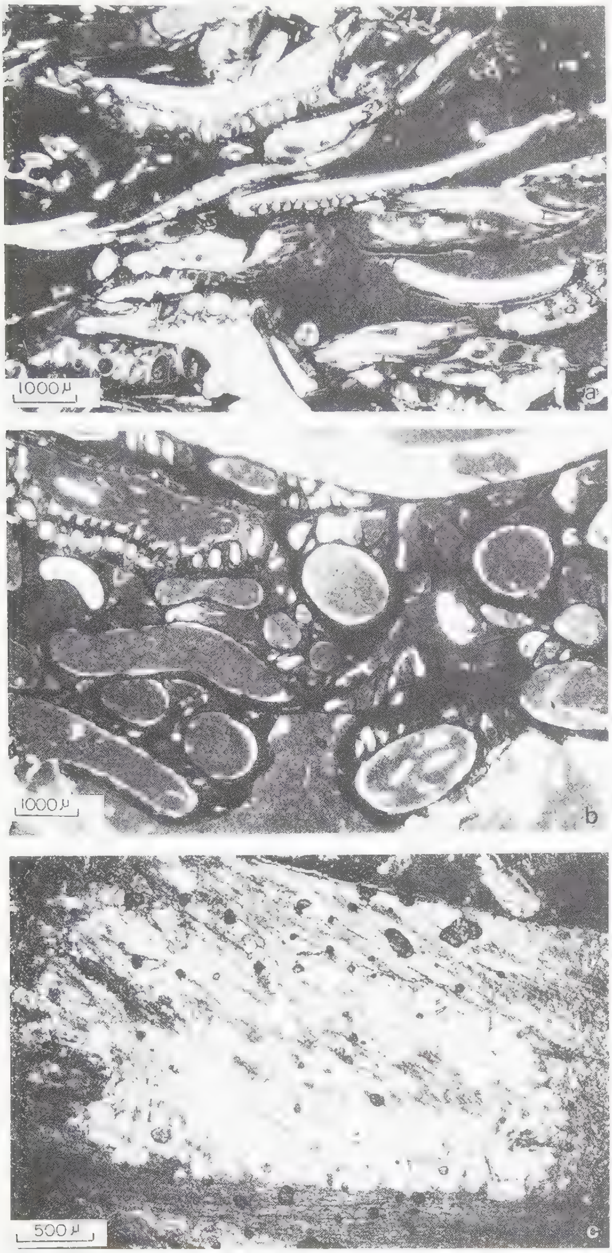

Fig. 28. (a) Pelecypod packstone and wackestone showing parallel orientation. (G1-NC41) Samdun Formation. (b) Surpulit tubes encrusting pelecypod fragments of different types. Note the articulate oyster shell in the top left corner. (G1-NC41) Samdun Formation. (c) Selective replacement of shell fragments by silica. (G1-NC41) Samdun Formation.

the shelf northwards as the sea advanced southward, and middle shelf lagoon sediments began to be deposited throughout the shelf with the exception of a narrow southern belt where Taljah sabkha-type facies were deposited.

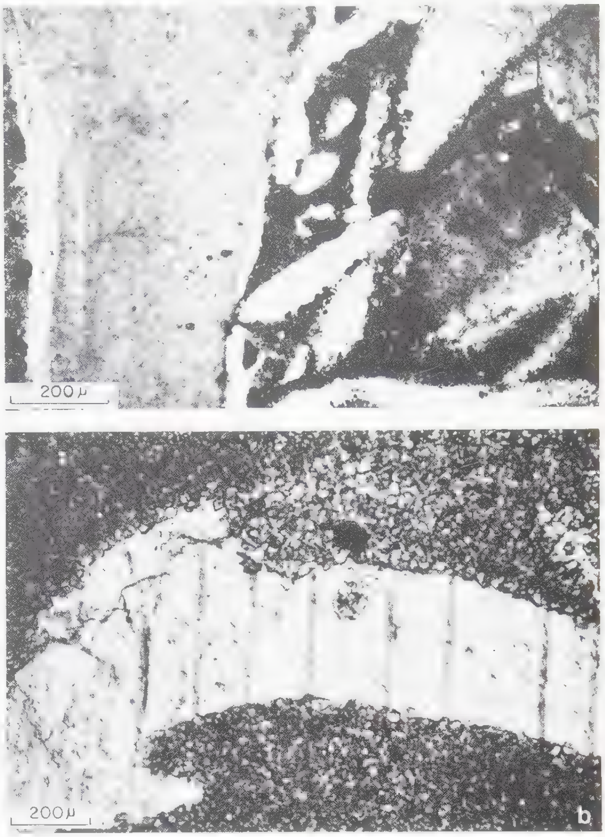

Fig. 29. (a) Selective replacement of micrite and shell fragments by pyrite. (K1-NC41) Samdun Formation. (b) Close up of dolomite replacement of shell fragments. (G1-NC41) Samdun Formation.

The termination of the Late Palaeocene–Early Eocene cycle is marked by a widespread break in sedimentation which is generally recognized and is also evident from the local occurrence of phosphates, glauconite, dolomicrite and anhydrite in the top beds of Farwah Group. This break between the Ypressian and Lutetian signalled the beginning of the Middle and Late Eocene regressive cycle. This cycle is represented by the shales and limestones of Tellil Group. During the deposition of the Harshah type facies the shelf was becoming more restricted with a gently sloping smooth surface as evidenced by the alternating beds of shales and limestones that cover the whole shelf with an increase of the shale percentage to the north (Fig. 5). The common occurrence of shale during Middle Eocene time is thought to be due to the source area and perhaps to current direction, as the source of the shale area is located to the west in Gabes basin rather than to the south where the land is very close. Currents from the northwest would have transported the shales along the coast

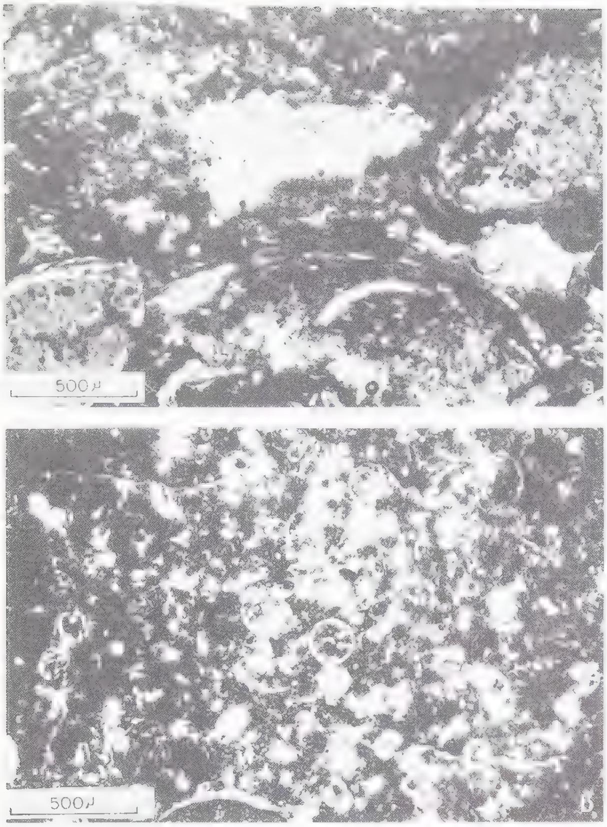

Fig. 30. (a) Ostracod-rich facies where ostracods are filled by glauconite minerals (K1-NC41) Samdun Formation. (b) Shales rich in planktonic foraminiferas. (D2-NC41) Ghalil Formation.

to be deposited in the restricted shelf along the depression, and with the increase of subsidence much thicker shale would accumulate. On the other hand the shelf continued to receive sediments from conditions that ranged from shoreline to basinal. The shale, coarse sandstone, clays and evaporite were commonly deposited along the southern edge of the shelf, followed by a belt of predominantly carbonates that are characteristically rich in molluscs and other skeletal debris and which were deposited along a shelf lagoon with some outer shelf lagoonal influence. It is possible that the conditions within the lagoon were excellent for oysters to develop and form local banks.

In the centre and on the northern margin of the shelf, shales predominate with only local limestone beds with abundant benthonic foraminifers where the conditions must have been slightly more restricted than in the adjacent belt. Shales and marls increase progressively to the north and planktonic foraminifera gradually increase till they dominate the sequence which grades into the pelagic Ghalil facies.

During the deposition of the Harshah type facies, a well-developed carbonate unit (A), well defined by its composition and log character, was deposited in the western section of the shelf (Fig. 32). This unit could represent the local influence of an outer shelf setting or else this member was generated by storm action.

Towards the end of the depositional history of Harshah Formation the shelf became shallower with the deposition of anhydrite, phosphates and coarse sandstone in the upper beds. However, within this broad shelf a nummulite bank may have developed in the eastern section starting from well F1-NC41 and extending southeastwards, where nummulitic wackestone and packstone facies were deposited (Fig. 10).

When deposition of Harshah Formation ended, the shelf water became slightly deeper as the Dahman type facies which cover the whole shelf were deposited. The limestone facies of Dahman Formation indicate a rising sea level since belts of middle and outer shelf origin overlie the slightly restricted shales and limestones of Harshah. The rising sea level is also evident in the shoreline facies that extend further south, close to the present-day coast. The shoreline thus shifted further south due to a rise in sea level and so resulted in the deposition of facies of middle and outer shelf type with perhaps a narrow sabkha-supratidal belt south of belt 1 (Fig. 21). But still these four belts which were present during deposition of Dahman Formation reflect the presence of a gently sloping shelf with both inner and middle shelf settings which grade to deep basin conditions.

During the Late Eocene conditions on the shelf were similar to those that prevailed during the Middle Eocene. The shelf was dominated by the deposition of shales. The conditions ranged from inner to middle shelf where sabkha–supratidal conditions dominated the southern edge with restricted inner shelf conditions in the centre while more marine conditions were the main influence in the belts located to the north which were adjacent to a deep basinal setting. The deep basin is characterized by the shales and marls of Ghalil Formation.

Within the middle shelf lagoon there was probably a pelecypod bank covering the western part of the shelf beginning at N1-NC41 and extending further southeast (Fig. 31). Figures 10 and 31 show that during the Middle Eocene almost that same area of the shelf was dominated first by a nummulite bank and then by a pelecypod bank. The development of

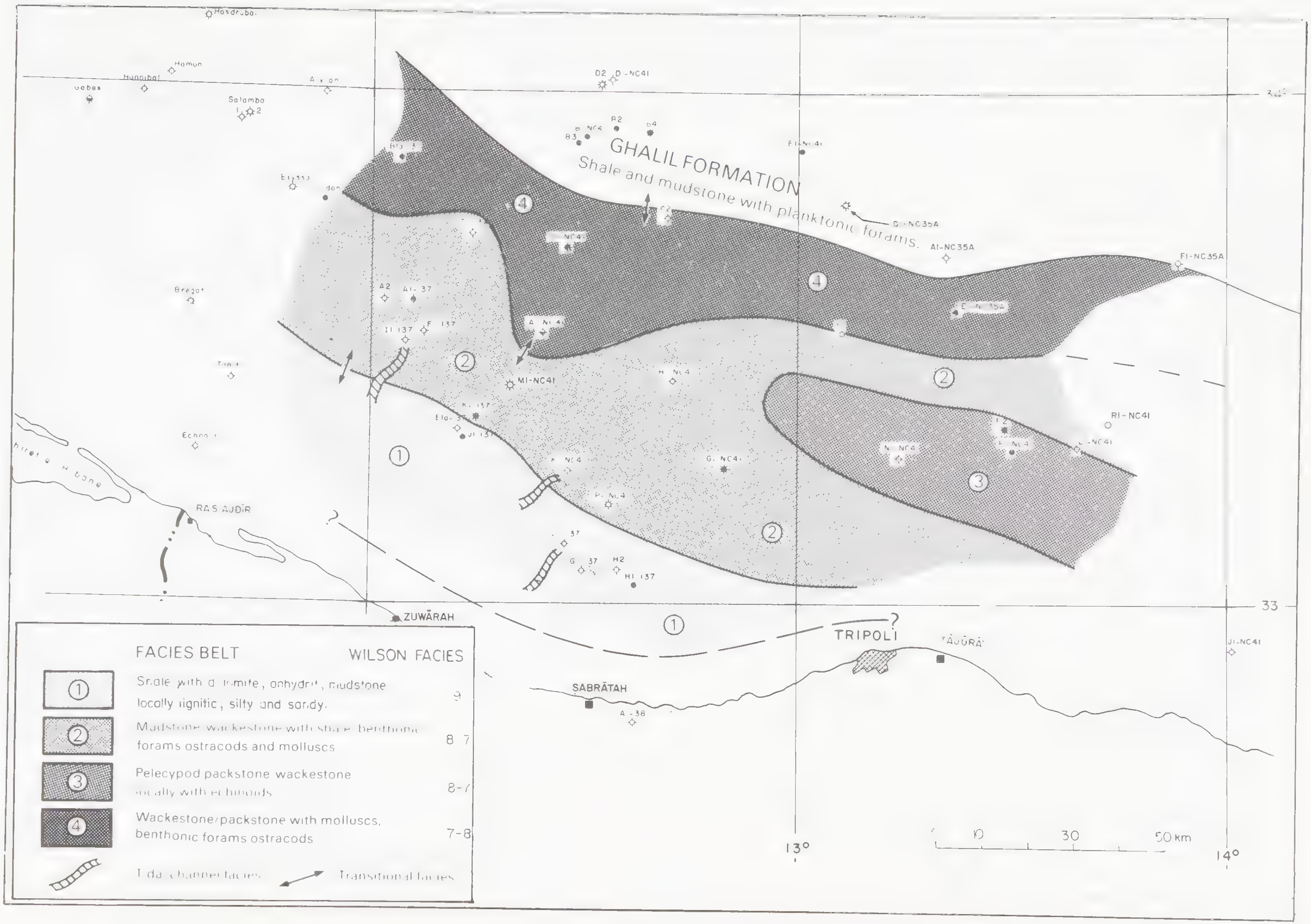
GHALIL FORMATION
Shale and mudstone with planktonic forams.
FACIES BELT
WILSON FACIES
① Shale with dolomite, anhydrite, mudstone locally lignitic, silty and sandy. 9
② Mudstone wackestone with shale benthonic forams ostracods and molluscs 8 7
③ Pelecypod packstone wackestone locally with echinoids 8-7
④ Wackestone/packstone with molluscs, benthonic forams ostracods 7-8
Tidal channel facies
Transitional facies
RAS AJDIR
ZUWĀRAH
SABRĀTAH
TRIPOLI
TĀJŪRĀ
MI-NC41
RI-NC41
FI-NC35A
AI-NC35A
D2 D-NC41
Hasdruba
Hannibal
Gabes
Salambo
Bregat
Echnos
Tanit
13°
14°
33
10
30
50 km

Fig. 31. Facies map of Samdun Formation.

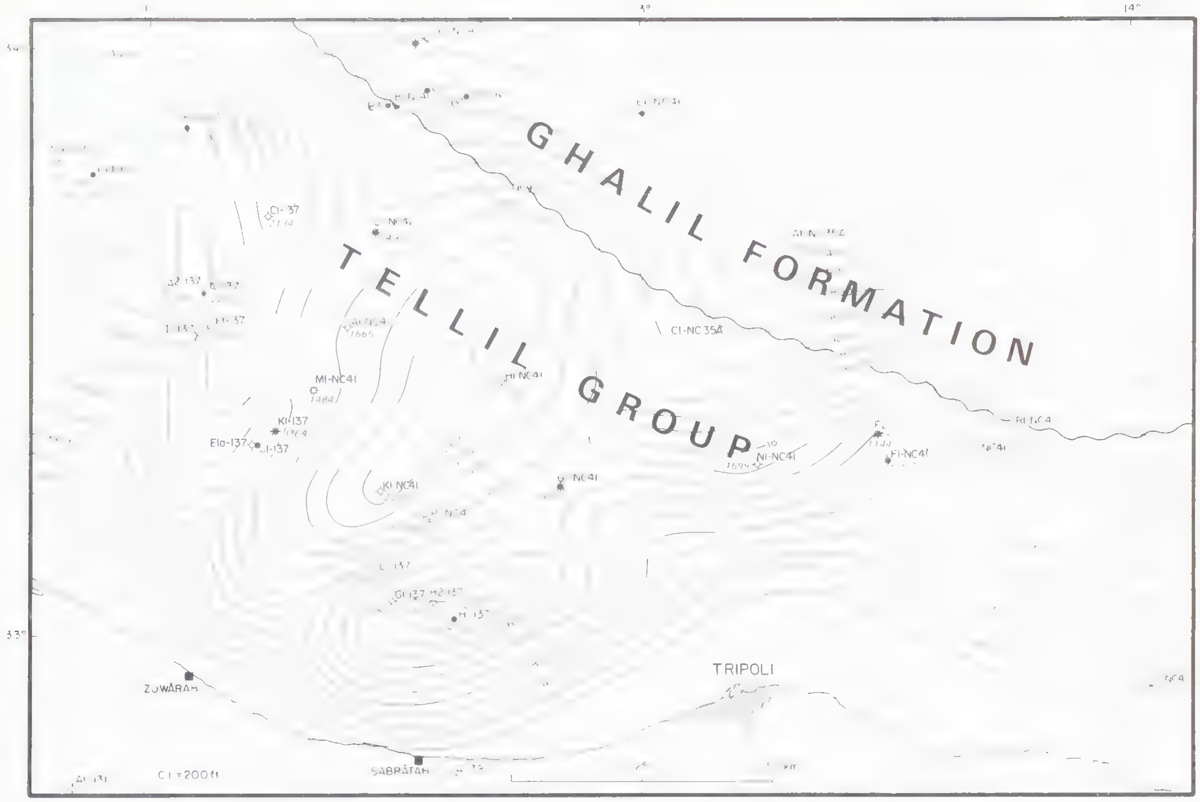

Fig. 32. Isopach map of Tellil Group and Ghalil Formation.

the pelecypod bank required shallower water and more restricted conditions than those required for nummulite accumulation. This is a further indication of the shallowing up of the shelf from Middle to Late Eocene time with a short interruption during deposition of Dahman Formation. It is also interesting to note that the area of nummulite and pelecypod accumulation was the site of reefal and high-energy facies development during Early Eocene time (Sbeta, 1990). This suggests that locally favourable conditions prevailed during the Eocene depositional history of the shelf. These conditions could be the result of positive relief and open marine influence which would have enhanced the accumulations of bryozoa, nummulites and pelecypods.

The Eocene depositional history ended with a major unconformity that is widely recognized in the offshore and this Oligocene unconformity is reported worldwide.

ACKNOWLEDGEMENTS

This study was partly supported by NOC, especially the expenses involved in the typing, drafting and preparation of most of the thin sections used. The University of Al-Fateh covered the Imperial College fees for the duration of the study. Finally I would like to express my thanks to the NOC Management for permission to publish this work.

REFERENCES

Banerjee, S. (1980). Stratigraphic lexicon of Libya. *Ind. Res. Cent.*, Tripoli, Bull. 13, 300 p.

Hammuda, O.S., Sbeta, A.M., Mouzughi, A.J. and Eliagoubi, B.A. (1985). *Stratigraphic Nomenclature of the Northwestern Offshore of Libya*. Earth Sci. Soc. Libya, 166 p.

Pitman, W.C., Cochran, J.R., Ryan, W.B.F. and Ladd, J.W. (1981). Evolution of the Libyan margin. *In*: *Proc. Int. Court Justice (Tunisia/Libya)*, III, *Libyan Memorial*.

Sbeta, A.M. (1984). Sedimentology of the Eocene sequence of the offshore Northwest Libya, Section I and Section II. Unpubl. Rept. N.O.C. Libya.

Sbeta, A.M. (1990). Stratigraphy and lithofacies of Farwah Group and its equivalent: Offshore–NW Libya. *Petrol. Res. J.*, **2**, 42-56.

Wilson, J.L. (1975). *Carbonate Facies in Geological History*. Springer-Verlag, Berlin, 471 p.

The Jifarah Formation — Aeolian and Fluvial Deposits of Quaternary Age, Jifārah Plain, G.S.P.L.A.J. A Redefinition in Terms of Composite Stratotype

J.M. Anketell[1] and S.M. Ghellali[2]

تكوين الجفارة ، رواسب رياحية ورياحية – مائية من الحين الرابع بسهل الجفارة بليبيا : إعادة تعريف على ضوء نموذج طبقي مركب

ج . م . أنكتيل وس . م . القلالي

الخلاصــة

يشكل تكوين الجفارة ، الذي يحتوي على رمال دقيقة وغرين من أصل رياحي ورياحي مائي مترسب خلال الحين الرابع ، طباقية أكثر تعقيداً مما ورد في البحوث الجيولوجية حتى الآن . والذي ساعد على تقسيم هذا التكوين إلى سبعة أعضاء هو التعرّف على أسطح طبقية مقطوعة تحدها ملامح تتعلق بالتعرية البرية والبحرية وظاهرة الذوبان ومخر الحيوانات والنشاط الحياتي وتطور نطاقات التربة . والترسيب التنازلي لهذه الأعضاء هو كما يلي :

عضو الرمان ، عضو الشريدات ، عضو الكراوة ، عضو القره بوللي ، عضو الزابين ، عضو وادي الرمل ، عضو وادي المجينين .

وقد تم التعرف على نطاقين مهمين للتربة هما : نطاق العدول المتكلس ونطاق السارية المتكلس . وقد اتضح من مضاهاة هذا النظام الطبقي بالقطاع النموذجي لتكوين الجفارة ، الذي اقترحه الحناوي وشيشيتيف (1975) في الواجهة البحرية الواقعة على بعد 10 كيلومترات غرب صبراته ، بأن القطاع النموذجي يحتوي فقط على الجزء الأعلى من عضو الشريدات ، وبذلك فهو لا يعكس إلى حد بعيد تكوين الجفارة المركب . ولذلك فإن هذا البحث يتقدم بمقترح لإعادة تعريف هذا التكوين ليحتوي على الأعضاء الطبقية السبعة المذكورة آنفاً مكوناً بذلك نموذج طبقي مركب مما يسهل عملية التخريط الجيولوجي مستقبلاً ومضاهاة هذا التكوين مع تكويني قرقارش وقصر الحاج . هذا بالإضافة إلى أن التفصيل المقترح يوفر تصوراً طبقياً لدراسة البيئات القديمة والسحنات التي تمثلها .

Abstract. The Jifarah Formation, fine sands and silts of aeolian and fluvio-aeolian origin and Quaternary age, displays a stratigraphy which is very much more complex than that which is suggested in existing literature. Recognition of surfaces of stratigraphic discontinuity defined by features related to fluvial and marine erosion, solution phenomena, bioturbation and boring, and development of soil horizons, has allowed subdivision of the formation into seven members. These, in ascending order, are: Arroman Member; Shuraydat Member; Karawah Member; Qarabulli Member; Zabayin Member; Wadi Raml Member and Wadi Megenin Member. Two important soil horizons, the Udul Calcrete and the Sariyah Calcrete are also defined. Correlation of this lithostratigraphic scheme with the type section of the Jifarah Formation as proposed by El Hinnawy and Cheshitev (1975) from coastal cliff sections six miles west of Ṣabrātah shows that the type section is composed of only the upper part of the Shuraydat Member and thus does little to portray the lithological complexities of the formation. It is proposed, therefore, that a redefinition of the formation in terms of a composite stratotype in which the members noted above constitute the component stratotypes would provide a sounder basis to future mapping of the formation and for its correlation with both the Gargaresh and the Qaṣr al Ḥaj Formations. In addition, the proposed detailed subdivision of the formation provides a convenient lithostratigraphic framework for palaeoenvironmental and facies studies.

---

[1] Department of Geology, University of Manchester, Manchester, M13 9PL, England.

[2] University of Al-Fateh, Faculty of Science, Earth Sciences Department, P.O. Box 13258, Tripoli, Libya, G.S.P.L.A.J.

INTRODUCTION

The geology of northwest Libya has, in recent years, been substantially clarified following regional geological surveys by geologists of the Industrial Research Centre (I.R.C.) of Libya with the publication of maps on the scale 1:250 000 and accompanying reports. Areas pertinent to the present study are included in sheets: NI 32-16 Ra's Ajdīr; NI 33-13 Ṭarābulus; NI 33-14 Al Khums.

The region is dominated by the broad wedge shaped Jifārah Plain which is bounded on the south by a prominent escarpment, the Jabal Nafūsah, and to the north by the Mediterranean Sea (Fig. 1). In general the area is comprised of gently dipping Mesozoic limestones with shales and sandstones overlain unconformably by Tertiary and Quaternary deposits. The Mesozoic sediments are well exposed in the Jabal Nafūsah and in isolated outcrops in the southern part of the plain (Fig. 1). South of the escarpment, late Mesozoic sediments are followed with little break by Palaeocene deposits (Antonovic, 1977). In the Jifārah Plain, however, and on the eastern part of the Jabal where it reaches the sea, the Mesozoic is followed unconformably by both Tertiary and Quaternary deposits (El Hinnawy and Cheshitev, 1975; Smetana, 1975). In general, the oldest Tertiary is Miocene in age although close offshore both Oligocene and Eocene deposits have been recorded (Hammuda and Misallati, 1980; Anketell, 1981). The Miocene deposits are predominantly limestones and shales with subordinate sands and gravels. Although upper Miocene sediments are known from offshore wells, only middle and lower Miocene deposits, overlain unconformably by Pliocene and Pleistocene deposits, are known from the Jifārah Plain where they underlie a large area north of a line trending approximately east–west through the Al 'Azīzīyah district. South of this line, which has been variously interpreted but is most commonly considered a fault of either pre- or post-Miocene age (for discussion see Ghellali, 1977, p. 256), the Miocene dies out abruptly and the Mesozoic is followed unconformably by sediments which range from Pliocene to Holocene in age. The post-middle Miocene deposits of the Jifārah region have been subdivided by the I.R.C. into four formations (Fig. 2) (El Hinnawy and Cheshitev, 1975; Smetana, 1975). The assignment of the Al Assah Formation and the lower member of the Qaṣr al Ḥaj Formation to the Plio-Pleistocene is based on the assumption that a calcrete which caps these deposits is equivalent to a calcrete dated as Villafranchian in neighbouring Tunisia (El Hinnawy and Cheshitev, 1975, p. 44). The post-Villafranchian calcrete deposits are made up of two formations which are considered lateral equivalents one of the other and of the upper members of the Qaṣr al Ḥaj Formation. This last deposit, typically alluvial fan gravels and sands, passes northwards into fluvial and aeolian fine sands and silts which comprise the Jifarah Formation. These in turn pass into the aeolian calcarenite dunes with subordinate marine sands and gravels of the Gargaresh Formation which occupies a narrow zone parallel to the present coastline. All these deposits have been assigned to the Pleistocene and Holocene and are

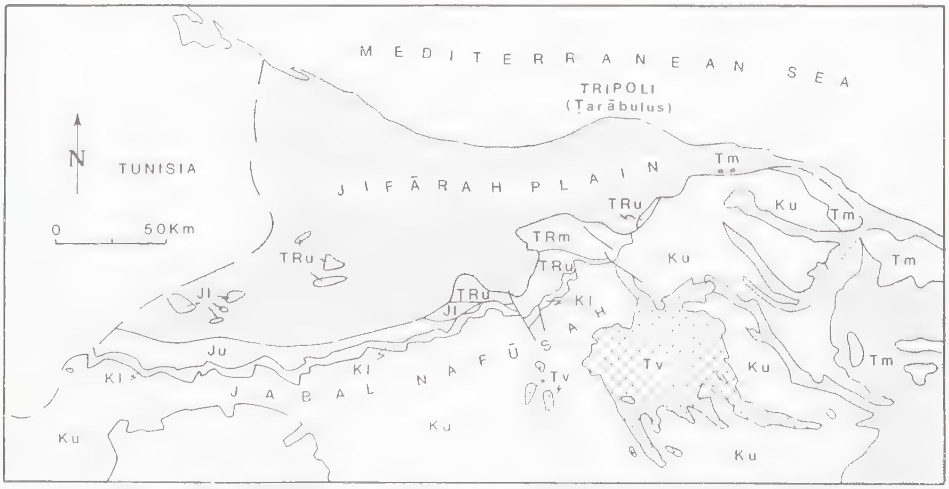

Fig. 1. Sketch geological map of the Jifārah Plain and neighbouring region.

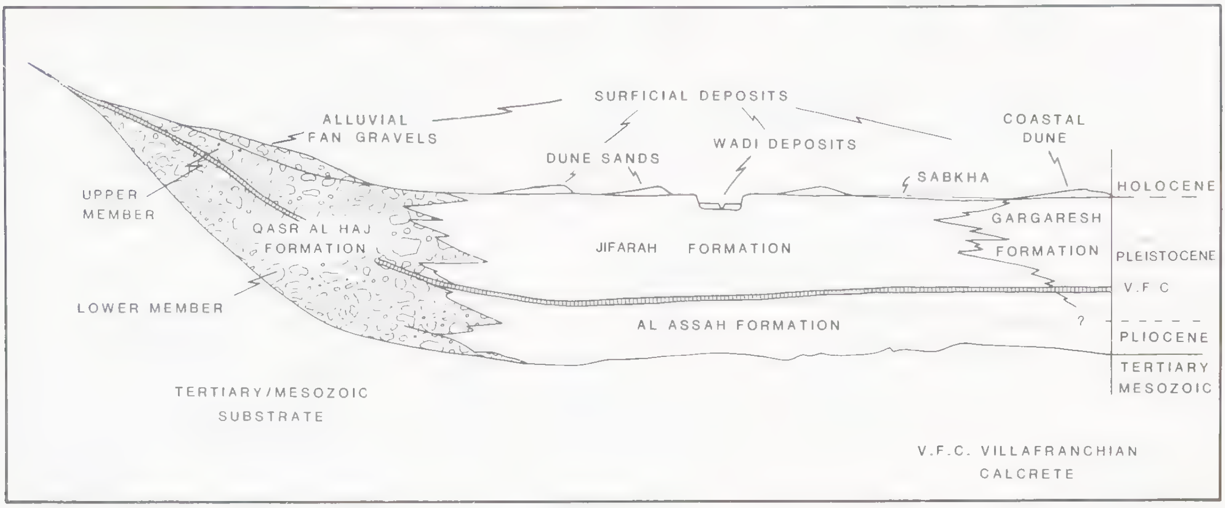

Fig. 2. Sketch cross-section showing the general relationships between the Qaṣr al Ḥaj, Jifarah and Gargaresh Formations.

capped by a veneer of superficial deposits comprising "recent" sand dunes, wadi sands and gravels and locally, evaporites of coastal and inland sabkhas all of which have been assigned to the Holocene (El Hinnawy and Cheshitev, 1975, pp. 46–48).

THE JIFARAH FORMATION — A CASE FOR REDEFINITION

Review of the present definition of the Jifarah Formation

The "floodplain" deposits of the Jifārah Plain have a complex and somewhat confusing nomenclatural history which is well summarized in Ghellali (1977), Banerjee (1980), and Anketell and Ghellali (1983). The deposits were assigned to formation status by El Hinnawy and Cheshitev (1975) and defined from a type section situated in coastal cliffs some six miles west of Ṣabrātah (Fig. 5B), with a general description as follows: "This formation was first introduced by Desio *et al.* (1963, p. 44) as Jeffara Sand and Gravels. It consists mainly of fine materials mostly silt and sand occasionally with gravel and caliche bands... It covers extensive parts of the Jeffara Plain." This brief description formed the basis for recognition of the Jifarah Formation in adjacent areas of the plain, the Ra's Ajdīr area to the west (Smetana, 1975), and the Al Khums area to the east (Mann, 1975a). The reports on both these areas in general reiterate the description given by El Hinnawy and Cheshitev (1975) and clearly show the I.R.C. geologists to conclude that the Jifarah Formation is comprised of all Quaternary sands and silts younger than the "Villafranchian calcrete" and older than the "surficial deposits" (El Hinnawy and Cheshitev, 1975, fig. 11; Smetana, 1975, fig. 10; Mann, 1975a, p. 55). The reports, however, do little to illustrate, perhaps failing to recognize, the variations in both lithology and thickness which the formation clearly displays, and instead give an impression of general lithological monotony which thoroughly masks the importance of what is a very complex stratigraphic unit. The lithostratigraphic complexity of the units is, however, clearly illustrated in the work of Ghellali (1977) and Anketell and Ghellali (1983). Detailed studies of the Quaternary floodplain deposits in the eastern Jifārah region, an area earlier studied by Mann (1975a), showed the Jifarah Formation to be comprised of several well defined stratigraphic units, units which not only have regional expression but also provide a guide to correlation with, and subdivision of, adjacent formations (Anketell and Ghellali, 1987).

Quaternary floodplain deposits of the Eastern Jifārah region: Summary of informal lithostratigraphic subdivision by Anketell and Ghellali (1983)

The eastern Jifārah region is here taken as that part of the plain east of line of latitude 13°25′ comprising a roughly triangular region which tapers rapidly to the east to die out in the vicinity of the city of Al Khums (Fig. 3). The region is cut by a number of wadis which not only expose numerous sections

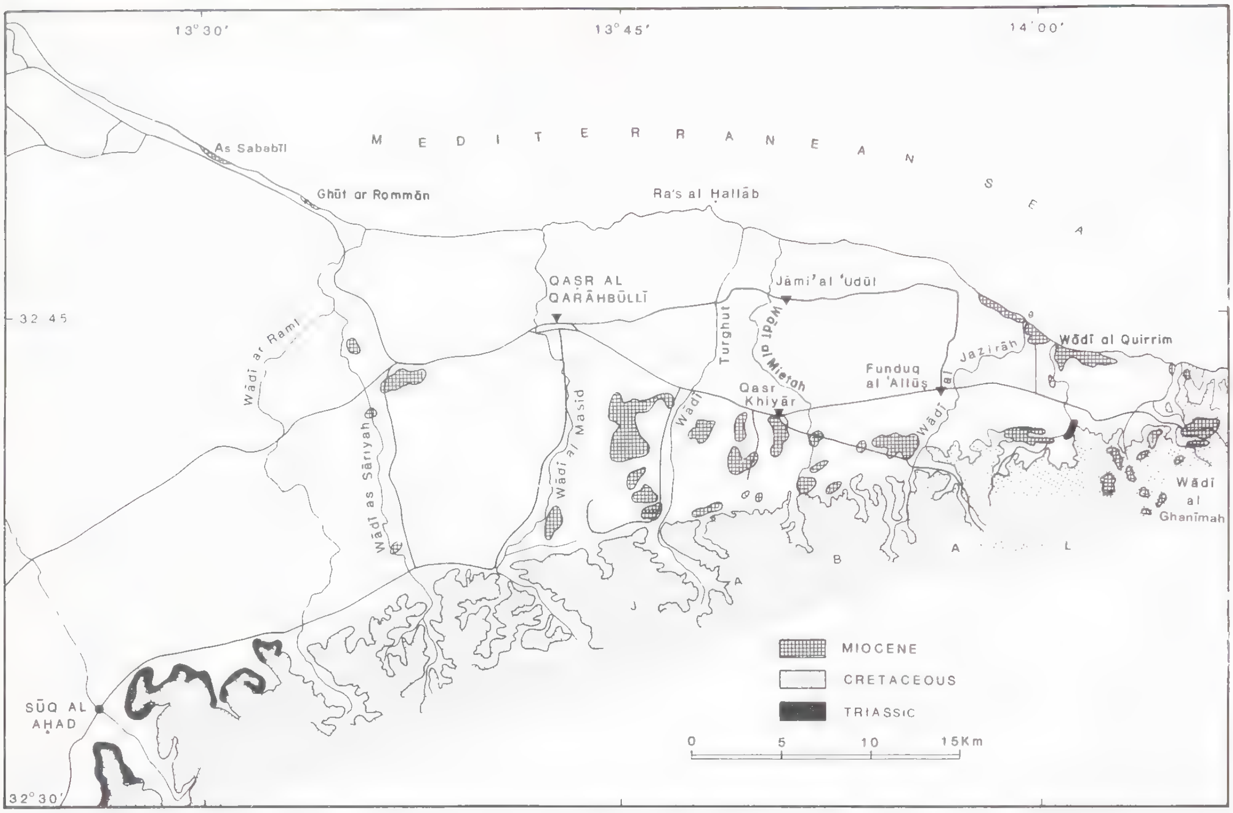
13°30′
13°45′
14°00′
32 45
32°30′
MEDITERRANEAN SEA
As Sababīl
Ghūt ar Rommān
Ra's al Hallāb
QASR AL QARĀHBŪLLĪ
Jāmi'al 'Udūl
Wādī al Quirrim
Wādī ar Ramī
Wādī as Sāriyah
Wādī al Masid
Wādī Turghut
Wādī al Mietah
Qasr Khiyār
Funduq al 'Allūs
Wādī al Jazīrāh
Wādī al Ghanīmah
J A B A L
SŪQ AL AHAD
MIOCENE
CRETACEOUS
TRIASSIC
0 5 10 15Km

Fig. 3. Sketch map of the eastern Jifārah Plain showing general geology and locations referred to in text.

within the Quaternary deposits, but also in many places cut through them to expose the contact with Miocene and/or Mesozoic bedrock. In addition, the coast is characterized by long stretches of low cliffs where marine erosion has not only exposed excellent sections in the Gargaresh Formation but has also, in places, cut through the Gargaresh Formation to expose the floodplain deposits, often in contact with bedrock. These features make the eastern Jifārah region ideal for unravelling stratigraphic relationships within the Quaternary, a situation hardly apparent from the statement by Mann (1975a, p. 62) that it is an area where "The base of the (Jifarah) Formation has not been observed". On the contrary, it is in fact one of the few areas in the whole of the Jifārah region where the relationships of this formation to bedrock can be easily observed as is clearly shown by Ghellali (1977) and Anketell and Ghellali (1983). More importantly these studies demonstrate that the area is one where the Quaternary floodplain deposits can be subdivided into a number of lithostratigraphic units separated one from the other by surfaces of stratigraphic discontinuity. The surfaces of discontinuity, which record a complex history of soil formation, solution, bioturbation and erosion are discussed in detail in Anketell and Ghellali (1983, p. 22). Six lithostratigraphic units designated Q1–Q6 were defined and described (Fig. 4). Since pene-contemporaneous erosion, coupled with depositional wedging and post-depositional erosion has produced a complexity of spatial inter-relationships between the units which effectively results in no one location showing all the units in vertical succession, the succession shown in Fig. 4 is a composite one.

Comparison and correlation of the Eastern Jifārah Floodplain succession with the Jifarah Formation as proposed by the I.R.C. — a redefinition of formation boundaries

It has been noted above that the stratigraphic scheme adopted by the I.R.C. assigns all fine-grain floodplain deposits younger than the "Villafranchian calcrete" and older than "surficial deposits" to the Jifarah Formation. Figure 5A shows a comparison of

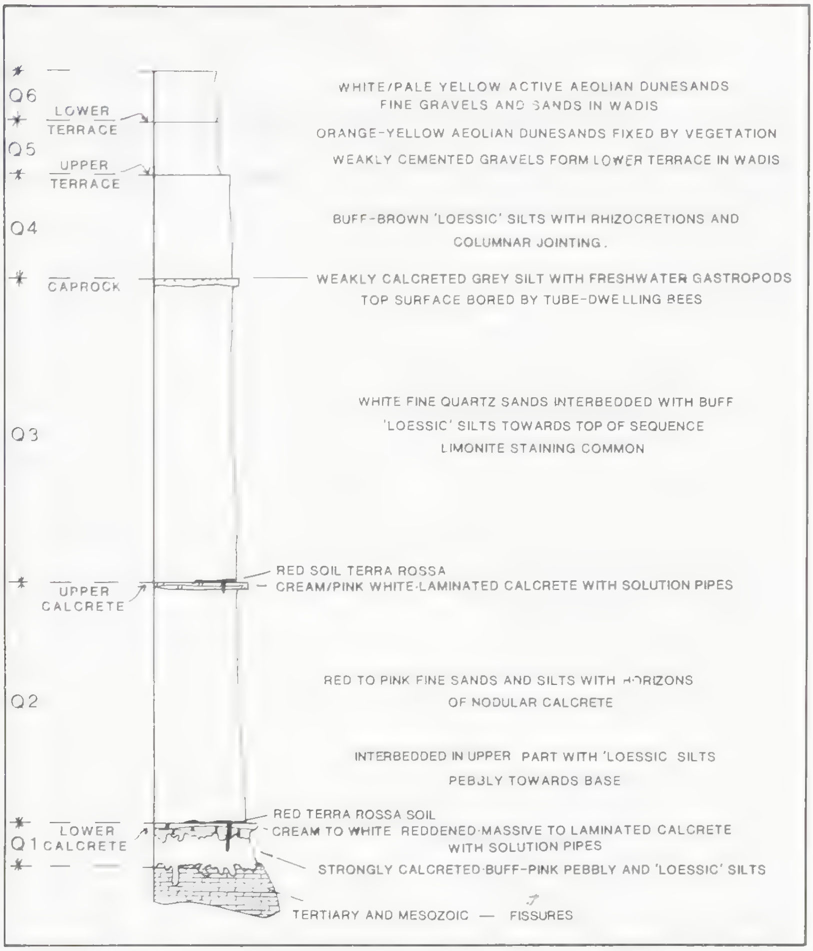
Q6
LOWER TERRACE
Q5
UPPER TERRACE
Q4
CAPROCK
Q3
UPPER CALCRETE
Q2
LOWER CALCRETE
Q1
WHITE/PALE YELLOW ACTIVE AEOLIAN DUNESANDS
FINE GRAVELS AND SANDS IN WADIS
ORANGE-YELLOW AEOLIAN DUNESANDS FIXED BY VEGETATION
WEAKLY CEMENTED GRAVELS FORM LOWER TERRACE IN WADIS
BUFF-BROWN 'LOESSIC' SILTS WITH RHIZOCRETIONS AND COLUMNAR JOINTING.
WEAKLY CALCRETED GREY SILT WITH FRESHWATER GASTROPODS
TOP SURFACE BORED BY TUBE-DWELLING BEES
WHITE FINE QUARTZ SANDS INTERBEDDED WITH BUFF 'LOESSIC' SILTS TOWARDS TOP OF SEQUENCE
LIMONITE STAINING COMMON
RED SOIL TERRA ROSSA
CREAM/PINK WHITE-LAMINATED CALCRETE WITH SOLUTION PIPES
RED TO PINK FINE SANDS AND SILTS WITH HORIZONS OF NODULAR CALCRETE
INTERBEDDED IN UPPER PART WITH 'LOESSIC SILTS
PEBBLY TOWARDS BASE
RED TERRA ROSSA SOIL
CREAM TO WHITE REDDENED-MASSIVE TO LAMINATED CALCRETE WITH SOLUTION PIPES
STRONGLY CALCRETED-BUFF-PINK PEBBLY AND 'LOESSIC' SILTS
TERTIARY AND MESOZOIC — FISSURES

Fig. 4. Generalized lithostratigraphic sequence of the Jifarah Formation illustrating dominant lithologies (based on Anketell and Ghellali, 1983).

this scheme with the lithostratigraphic subdivisions of the Quaternary floodplain deposits of the eastern area (Anketell and Ghellali, 1983). Field observation and subsurface studies (Ghellali, 1977) have shown clearly that the "Villafranchian calcrete" is the same as the calcrete which caps unit Q1 and that the surficial deposits are equivalent to Unit Q6. Thus, it follows, if the stratigraphic scheme of the I.R.C is to be applied rigorously, that only units Q2 to Q5 should be assigned to the Jifarah Formation and that units Q1 and Q6 should be excluded even though they display lithologies similar to those of the units which clearly belong to the Jifarah Formation. Examination of regional relationships, however, not only helps explain why the geologists of the I.R.C. excluded Q1 and Q6 from the formation but also provides evidence which militates for redefinition of the boundaries of the Jifarah Formation to allow their inclusion within it. Such a redefinition is acceptable on the grounds that it makes the unit both more natural and useful [Article 14(a) Code of Stratigraphic Nomenclature, 1961].

Regional surface mapping and study of subsurface data by Ghellali (1977) has shown that the units which make up the succession in the eastern Jifārah can be identified in the central Jifārah region also. He has shown that the calcrete which caps unit Q2 is the same as that which caps the Jifarah Formation at the type section (Fig. 5B). As such, the sediments making up the type section of the Jifarah Formation are older than the greater part of the formation in the eastern Jifārah and are, as far as is known at present, syndepositional with unit Q2 only. Immediately south of the type section area, as throughout the greater part of the region immediately south of the coast and west of Tājūrā', unit Q3 is absent, hav-

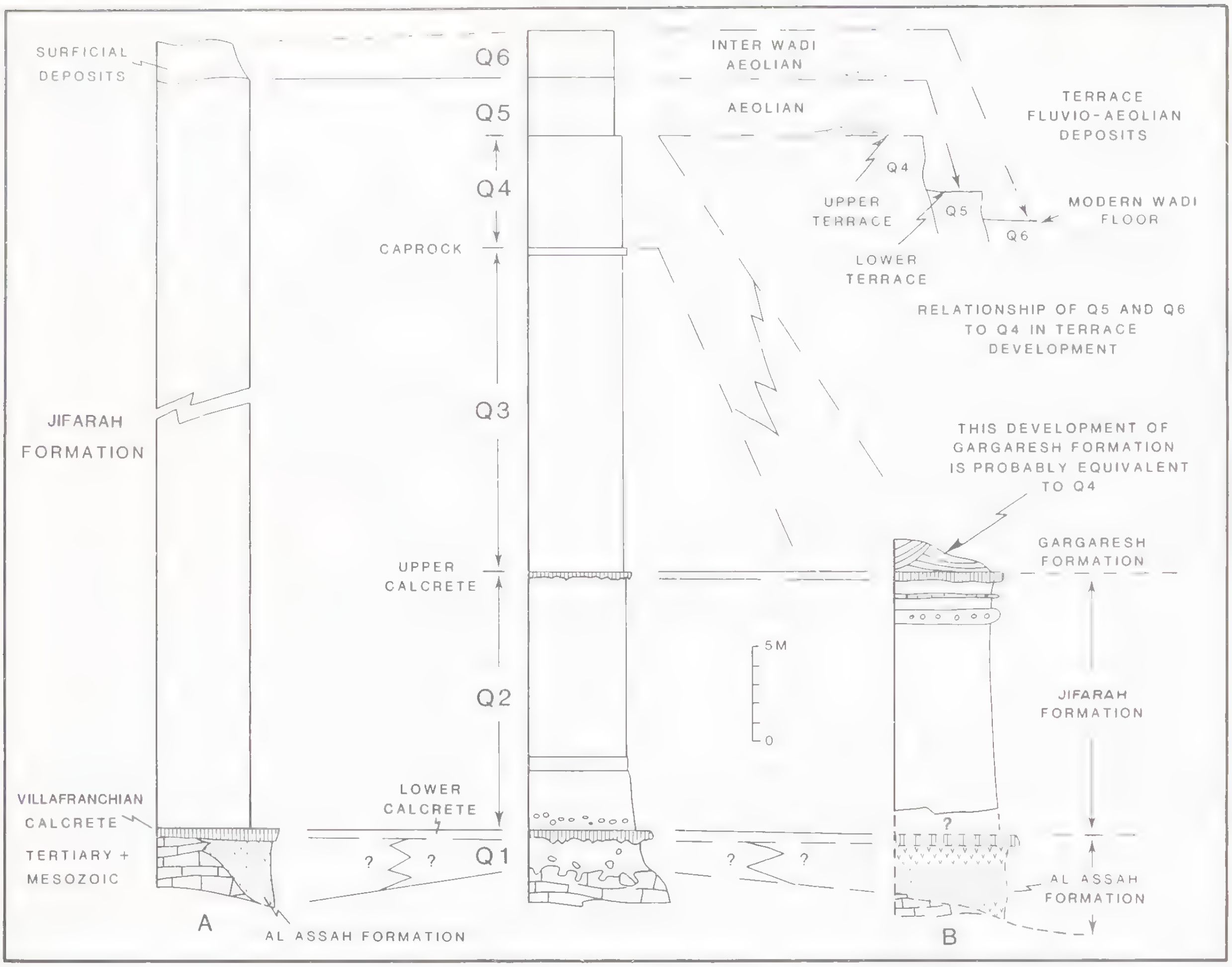
SURFICIAL DEPOSITS
Q6
INTER WADI AEOLIAN
Q5
AEOLIAN
TERRACE FLUVIO-AEOLIAN DEPOSITS
Q4
Q4
UPPER TERRACE
Q5
MODERN WADI FLOOR
Q6
CAPROCK
LOWER TERRACE
RELATIONSHIP OF Q5 AND Q6 TO Q4 IN TERRACE DEVELOPMENT
JIFARAH FORMATION
Q3
THIS DEVELOPMENT OF GARGARESH FORMATION IS PROBABLY EQUIVALENT TO Q4
GARGARESH FORMATION
UPPER CALCRETE
5M
0
Q2
JIFARAH FORMATION
VILLAFRANCHIAN CALCRETE
LOWER CALCRETE
TERTIARY + MESOZOIC
?
?
Q1
?
?
?
AL ASSAH FORMATION
A
AL ASSAH FORMATION
B

Fig. 5. Comparison of generalized lithostratigraphic sequence of the Jifarah Formation with: A. Scheme proposed by I.R.C. B. Type section as defined by El Hinnawy and Cheshitev (1975).

ing been removed by erosion prior to deposition of unit Q4 (Ghellali, 1977, fig. 26). This, in combination with localized erosion of units Q4 and Q5 prior to deposition of Q6, often results in Q6 resting with clear unconformity on the calcrete capping unit Q2. This very obvious break in sedimentation undoubtedly led the I.R.C. to exclude the surficial deposits from the Jifarah Formation. However, immediately south of the coastal zone and in the eastern Jifārah where units Q3–Q5 have not been removed from the succession by intraformational erosion, the close lithological similarity of Q6 to the preceding units lends to the succession a continuity and homogeneity which clearly argues for the inclusion of the unit Q6 in the Jifarah Formation. To exclude it on grounds of surficiality is, in the authors' opinion, unnecessary and ultimately restrictive to its use in aiding geological interpretation, correlation and mapping of the Quaternary succession.

A somewhat comparable argument can be presented in respect of unit Q1 although it differs from the case of Q6 inasmuch as the unit was never distinguished by the I.R.C. as a discrete stratigraphic unit and was simply considered part of an undifferentiated Jifarah Formation (Mann, 1975a, b). It has already been noted that the calcrete which caps unit Q1 in the eastern Jifārah based on as complete a study of boreholes as at present is possible, is stratigraphically equivalent to the "Villafranchian Calcrete" of the central region (Fig. 5A). In this area, the calcrete is taken to mark the top of Al Assah Formation, and is apparently included within it (Smetana, 1975, fig. 9). In the eastern Jifārah, however, the situation is different for here the deposit on which the calcrete is developed, i.e. the lower part of unit Q1, is lithologically closely comparable to unit Q2 which succeeds it. In instances where the calcrete has been removed by intraformational erosion prior to, or contemporaneous with, deposition of unit Q2, it is often only by identification of the erosional surface and the fact that unit Q1 is often more strongly calcreted, that the two can be separated. As with unit Q6, this degree of lithological homogeneity militates for the inclusion of this pre-calcrete deposit in the Jifarah Formation. The stratigraphic relationship of the deposit to Al Assah Formation is, however, as yet unclear. The fact that both are terminated by the same soil stratigraphic unit allows a number of possibilities. One may be younger or older than the other, the lateral equivalent having been removed in a period of erosion prior to formation of the calcrete. Alternatively, the two may be wholly or in part, equivalent in age and the difference in lithology may reflect facies change. Studies of Al Assah Formation at present underway should do much to define the relationships more clearly. Whatever the relationships may turn out to be, it is clear that there is a strong case for extending the boundaries of the Jifarah Formation to include all the floodplain deposits described by Anketell and Ghellali (1983).

A redefinition of the Jifarah Formation in terms of a composite stratotype

The proposal to extend the range of the Jifarah Formation to include all the "floodplain" sands and silts lays the basis for a formal lithostratigraphic subdivision of the formation based on the informal units Q1 to Q6. These units, although lithologically comparable are, nevertheless, clearly discrete and independently mappable. As such, it is proposed that they should, with minor modifications, be assigned to member rank. The modifications concern the fossil soils represented by the two mature calcrete horizons which precede the development of units Q2 and Q3, and the distinctive grey and black silt horizon which caps unit Q3 i.e. the "caprock" of Ghellali (1977) (Fig. 4). The calcretes, dubbed the "lower" and "upper" calcretes by Anketell and Ghellali (1983), are widely and well developed at the top of units Q1 and Q2 respectively. They are each equally well developed on older deposits and are quite independent of the lithostratigraphic succession. The units have, moreover, proved to be very persistent, easily recognized and thus easily mapped throughout the area and it is proposed that this regional expression warrants their definition as soil stratigraphic units.

The grey silt horizon, weakly calcreted and shell rich, together with the underlying thin, black clayey silt is perhaps the most distinctive lithological unit in the region. It has proved of major importance in correlation and mapping and is introduced as a member of the formation so subdividing unit Q3 into two to make up a total of seven members. Thus, the informal subdivision of the succession into units Q1 to Q6 is formally subdivided into seven members with two soil stratigraphic units (Fig. 6). These, defined, named, and described, following the guidelines of the International Subcommission on Stratigraphic Classification (I.S.S.C.), (Hedberg, 1976) are, in ascending order as follows: Arroman Member; Shuraydat Member; Karawah Member; Qarabulli Member; Zabayin Member; Wadi Raml Member; Wadi Megenin Member. The soil stratigraphic units are, the Udul Calcrete which precedes the development of the Shuraydat Member and, the Wadi Sariyah Calcrete which precedes the development of the Karawah Member.

Subdivision of the formation into members not only highlights the hitherto unrecognized complexity of the formation but also raises the question as to whether the existing definition of the formation as laid down by the I.R.C. remains adequate or is in need of revision.

It has already been noted that the nature of the deposits making up the formation, their structural attitude and degree of exposure tends to preclude the presence of the entire formation in any one section. In effect, no single section can be found which will adequately describe the formation and its boundary relationships. In such instances, common in Quaternary deposits, a comprehensive classification is, however, possible in terms of a composite stratotype (Hedberg, 1976, p. 24). Built up by combining intervals of the stratigraphic unit i.e. component stratotypes, selected from separate localities within a type area, this allows all aspects of the stratigraphic unit to be classified.

In the case of the Jifarah Formation it has already been shown that the type section of the I.R.C. corresponds to only a small part of the formation (Fig. 5B), and there is little doubt that a redefinition of the formation in terms of a composite stratotype could be more realistic and more useful.

Revision of an existing classification, however, even though it involves no change in either name

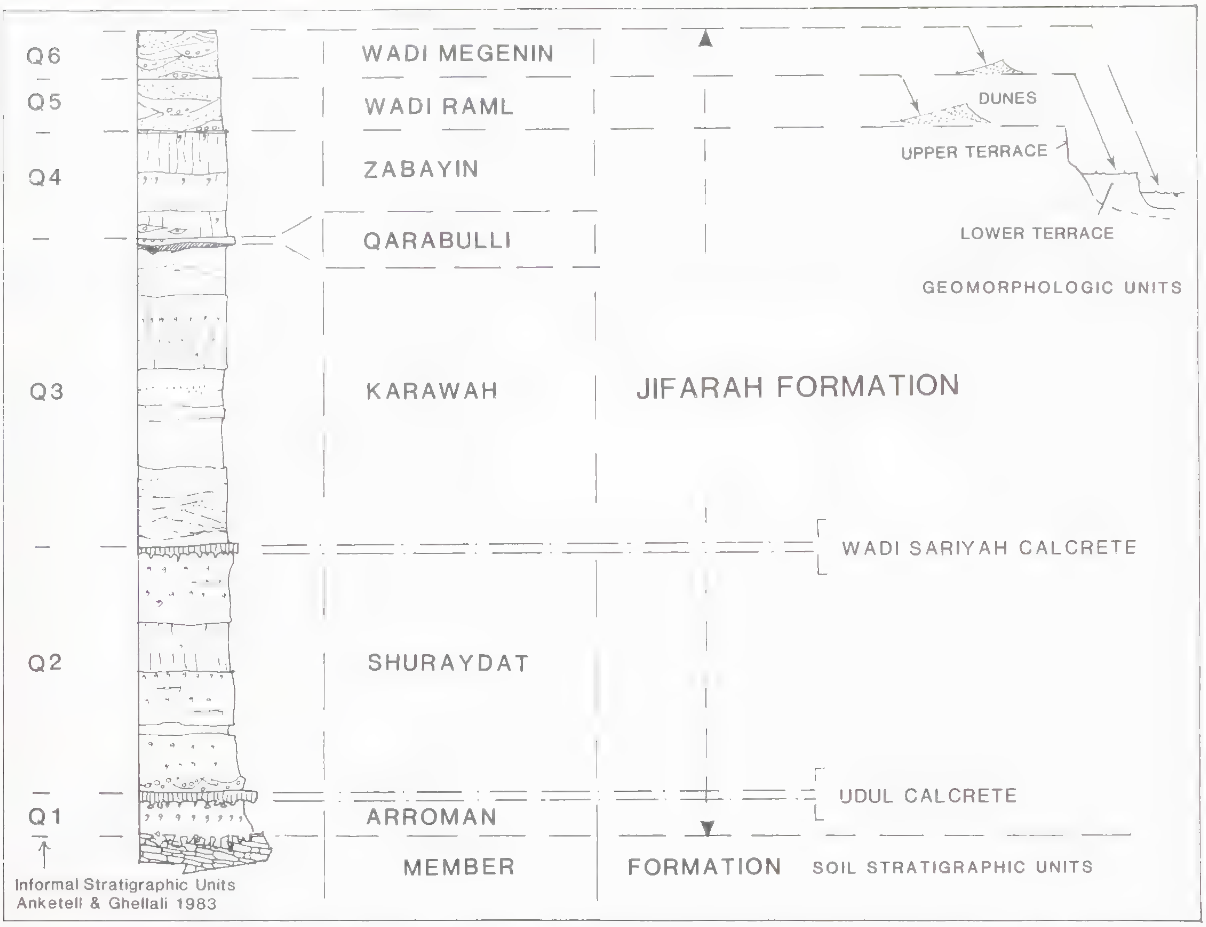
Q6
Q5
Q4
Q3
Q2
Q1
WADI MEGENIN
WADI RAML
ZABAYIN
QARABULLI
KARAWAH
SHURAYDAT
ARROMAN
MEMBER
JIFARAH FORMATION
FORMATION
DUNES
UPPER TERRACE
LOWER TERRACE
GEOMORPHOLOGIC UNITS
WADI SARIYAH CALCRETE
UDUL CALCRETE
SOIL STRATIGRAPHIC UNITS
Informal Stratigraphic Units
Anketell & Ghellali 1983

Fig. 6. Proposed stratigraphic nomenclature for members of the Jifarah Formation based on lithostratigraphic units of Anketell and Ghellali (1983).

or rank, requires as much justification as an original definition and must be approached with caution. Hedberg (1976, p. 19) states that while "Priority in publication of a properly proposed, named and defined unit should be respected ... the critical factors should always be the usefulness of the unit, the adequacy of its description, and suitability for widespread application", and notes that "redefinition may be justified to make a unit more useful or easier to recognize, map, and extend throughout the area of its development" (Hedberg, 1976, p. 20). He further states that there may never be more than one type section or stratotype and that it "In principle ... should not be altered or amended" unless "it has been found to have been established in violation of accepted stratigraphic principles" in which case "a new stratotype (neostratotype or lectostratotype) may be established, preferably in the type area." (Hedberg, 1976, p. 26).

The Code of Stratigraphic Nomenclature prepared by the American Commission on Stratigraphic Nomenclature (1961), states in Article 13a that "The proposed unit should be defined so clearly that any subsequent worker can, without doubt, recognize the same". In the case of the Jifarah Formation, both the general description and, in particular, the type section are clearly wanting in this respect (El Hinnawy and Cheshitev, 1975, p. 44). Not only is the lithological description lacking in detail but the boundaries and contact relationships are neither defined nor described anywhere in the text. Although the base of the formation is not exposed at the type locality, a condition not unexpected given the problems of exposure already noted, no reference is made to supplementary sections even though the base of the formation, in contact with the Arroman Calcrete unit, is exposed in the southern part of the Ṭarābulus region. In addition, the authors undoubtedly had access to subsurface data from the large number of boreholes drilled in the vicinity of their type section locality, data which clearly displays the relationships of the formation to the underlying deposits. The lack of supplementary sections depicting and defining the basal boundary of the formation is unfortunate and is matched by a comparable lack of definition of the upper boundary. It is felt that the brevity of the description and definition of the formation, coupled with the lack of any information on regional variation in either thickness or lithology, clearly limits its widespread application and its value in elucidating intraformational relationships, recognition of which is vital to regional mapping and interpretation of the deposits, particularly in terms of their hydrogeologic and agricultural potential.

In summary, it is proposed that the existing definition of the Jifarah Formation fulfils few of the requirements set out in Article 13a of the Code of Stratigraphic Nomenclature and there would appear to be no sound reason for retention of either the definition or the cliff section at Ṣabrātah as type section. Instead, it is proposed that the present definition should be replaced by one based on a composite stratotype which, as a new stratotype selected to replace an older one, is termed a neostratotype (Hedberg, 1976, p. 26). This composite neolithostratotype is comprised of the hololithostratotypes of the seven members which make up the component units of the formation (Fig. 6) and, unlike the older definition, has the facility to encompass all aspects of the formation, allowing its recognition over a very large area and providing a coherent and firmly based framework for investigation of interformational relationships both within and outside the Jifārah region.

The following section presents the formal definitions of the composite stratotype and the individual members or component stratotypes as well as the formal definitions of the two soil stratigraphic units in Tables 1 to 10. The order in which the component stratotypes and the soil stratigraphic units are described reflects their relationship in the field. Figure 6 shows these relationships together with the morphologic features which serve to amplify and further define the stratigraphy of the Quaternary floodplain deposits of the Jifārah region.

A COMPOSITE STRATOTYPE FOR THE JIFARAH FORMATION

Table 1. Description of the Jifarah Formation

Fluvio-aeolian sands and silts of the Jifārah Plain, G.S.P.L.A.J. — A revision and redefinition

Named and defined by: El Hinnawy, M. and Cheshitev, G., 1975, p. 44. *Explanatory Booklet for the Geological Map of Libya.* 1:250 000. Sheet Ṭarābulus N133-13.

Redefined by: Anketell, J.M. and Ghellali, S.M. (this paper).

See also: Vita Finzi, C. 1971. Alluvial History of Northern Libya since the last Interglacial. *In: Symposium on the Geology of Libya.* Tripoli.

Mann, K. 1975a pp. 55–63. *Explanatory Booklet for the Geological Map of Libya.* 1:250 000. Sheet Al Khums N133-14.

Smetana, R. 1975 pp. 33–42. *Explanatory Booklet for the Geological Map of Libya.* 1:250 000. Sheet Ra's Ajdīr N132-16.

Ghellali, S.M. 1977. On the Geology of Eastern Jeffara Plain, North West Libya. *Unpublished Ph.D. Thesis. Manchester University.*

Banerjee, S. 1980 p. 148. Stratigraphic Lexicon of Libya. *Department of Resources and Mining, Bull. No. 13.*

Anketell, J.M. and Ghellali, S.M. 1983. Stratigraphic Studies on Quaternary Floodplain Deposits of the Eastern Jeffara Plain G.S.P.L.A.J. *Journal of the Society for Libyan Studies No. 14.*

Named from: Jifārah Plain — northwest coastal plain of the Great Socialist Peoples Libyan Arab Jamahiriya.

Neostratotype locality: Composite — made up from seven member holostratotype localities in the type area — the Jifārah Plain — see Tables 2, 4 and 6–10.

Definition: The Jifarah Formation consists mainly of white, buff, pink and red to red-brown, fine sands and silts with subordinate gravels. The sediments range from weakly cemented to completely friable. Calcrete development is common, particularly in the lower part of the formation, ranging from scattered nodules to nodular layers and well-laminated mature crusts. Powder calcrete occurs but is not common. Seven members, which comprise the following stratotypes, make up the formation — in ascending order these are: Arroman Member; Shuraydat Member; Karawah Member; Qarabulli Member; Zabayin Member; Wadi Raml Member; and Wadi Megenin Member. The members are commonly separated one from the other by surfaces of stratigraphic discontinuity identified as surfaces of restricted deposition, soil formation, solution, and both marine and continental erosion (Anketell and Ghellali, 1983). The formation ranges in thickness from 0 to at least 50 m.

Neostratotype section: The composite section shown in Fig. 6 is made up from the holostratotypes of the various members, but also includes the 'Udūl and Wādī as Sāriyah soil-stratigraphic units in their most common field relationships. The various units are described and defined in Tables 2–10.

Boundaries:

– *Base:* The base of the formation is well exposed in the eastern and southern parts of the Jifārah Plain resting with strong unconformity on an irregular surface of Tertiary and/or Mesozoic sediments. Each or any of the component stratigraphic units may form the local base (see Anketell and Ghellali, 1983, Fig. 5).

– *Top:* The Jifarah Formation is at the surface over the greater part of the Jifārah Plain. The fluvio-aeolian facies of the Wadi as Sarat and Wadi Megenin Members cover by far the greatest area, however, in many places, erosion and/or non-deposition, exposes the older members to view. Locally the formation is overlain by units of the Gargaresh Formation, the Qaṣr al Ḥaj Formation and by Holocene sabkha deposits (the last are as yet stratigraphically undefined and require further study). Contacts with these overlying deposits tend to be gradational, however, the interrelationship of the Jifarah and Gargaresh Formations is complex and contacts are often strongly unconformable (Anketell and Ghellali, 1987).

Additional information: Evidence from boreholes suggests that the formation becomes enriched in gypsum in the western part of the Jifārah Plain, developing facies reminiscent of Al Assah Formation. It is unlikely that further studies will demand modification of the existing interformational stratigraphic framework proposed for this region (Smetana, 1975).

Regional extent: As already stated, the formation occurs throughout the Jifārah Plain. Similar deposits occur throughout northern Libya and in other parts of the Mediterranean littoral, however, regional stratigraphical relationships are as yet not well established.

Geologic age: Fauna is rare to absent in all the component units with the exception of the Qarabulli Member which is rich in gastropods. These are, however, all types still living at the present day and they thus do little more than assign the deposits to the late Pleistocene (Appendix). In general, dating of the deposits has, so far, largely depended on extrapolation of ages proposed for what are thought to be chronostratigraphically equivalent levels within the Gargaresh Formation, and on interpretation of the deposits in terms of glacial–interglacial cycles (for discussion see Ghellali, 1977, p. 243). In addition, there is the possibility that the Udul Calcrete, which caps the Arroman Member and the Al Assah Formation, can be correlated with a calcrete of known Villafranchian age in Tunisia. The evidence so far suggests, therefore, that the deposits range from early Pleistocene to the present. Possible ages for individual members are discussed below, but a detailed chronostratigraphy must await more detailed examination of faunas and radiometric dating.

Table 2. Description of the Arroman Member

Calcreted pink silts and conglomeratic fine sands

Named and defined by: Anketell, J.M. and Ghellali, S.M. (this paper).

See also: Ghellali, S.M. (1977) "pre-Villafranchian calcrete". Anketell, J.M. and Ghellali, S.M. (1983) "Unit Q1".

Named from: Ghūṭ ar Rommān on coast some 34 km east of Tripoli (see Fig. 3).

Holostratotype locality: Sea cliff 5 km east of Abyār as Sabābīl (Sheet 1990 I. Tājūrā'. Ref.: 3.58.65.36.34.50).

Definition: The Arroman Member consists of red, pink and buff silts, conglomeratic silts, and fine sand, well cemented by development of calcrete. Nodular calcrete is characteristic and often is coalesced to form a honeycomb structure, particularly near the junction with the succeeding Udul Calcrete. The deposit ranges from 0 m to at least 2.6 m in outcrop. Borehole data suggest it may reach up to 4.5 m.

Holostratotype section: Comprises 1.2 m of reddish pink to buff, conglomeratic silt and sand, strongly calcreted with well developed honeycomb structure towards the top (Fig. 7). Clasts are angular to sub-angular, range up to 0.35 m in longest diameter, are poorly sorted and generally display a low packing density. They are composed in the main of the underlying Tertiary limestone conglomerate and limestone assigned to the Pliocene by Ghellali (1977, Table 6), but some pebbles appear to be derived from an older calcrete.

Boundaries:

– *Base:* The member rests with strong unconformity on Tertiary limestone bedrock. The contact is highly irregular and the conglomeratic silts invade the underlying limestones along a network of interconnected fissures and solution pipes.

– *Top:* The top of the unit is sharply gradational to the Udul Calcrete and is placed at the first obvious development of laminated structure in this unit.

Parastratotype: "Dry waterfall-scarp" in floor of Wādī Turghut (1:50000 Sheet 2090 II, Qabīlat al Qalīl. Ref. 3.88.50.36.24.20) (Fig. 8). The maximum exposed thickness so far recognized in the region occurs at this locality. A small cliff, capped by the resistant Udūl calcrete, here 0.6 m thick, exposes 2.6 m of pinkish-yellow and buff silts with fine rootlet channels, a weakly developed columnar structure and abundant calcrete nodules.

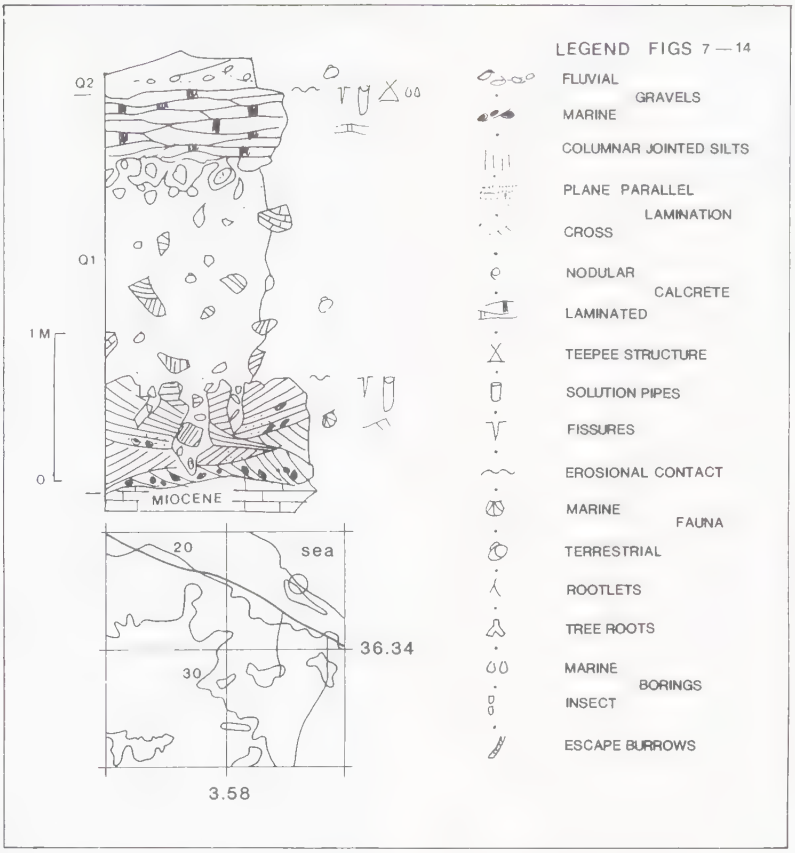
Q2
Q1
1 M
0
MIOCENE
20
sea
36.34
30
3.58
LEGEND FIGS 7—14
FLUVIAL
GRAVELS
MARINE
COLUMNAR JOINTED SILTS
PLANE PARALLEL
LAMINATION
CROSS
NODULAR
CALCRETE
LAMINATED
TEEPEE STRUCTURE
SOLUTION PIPES
FISSURES
EROSIONAL CONTACT
MARINE
FAUNA
TERRESTRIAL
ROOTLETS
TREE ROOTS
MARINE
BORINGS
INSECT
ESCAPE BURROWS

Fig. 7. Holostratotype section and location for the Arroman Member, Jifarah Formation.

Regional extent: The Arroman Member underlies most of the northern part of the eastern Jifārah region. Available evidence suggests that it is overstepped to the south by younger units, largely as a result of intraformational erosion. To the west it passes into the Al Assah Formation in the area south and southwest of Tripoli, however, details of this relationship are not as yet fully established.

Additional comments: Exposures of the member, lying at or just below sea level occur at several localities in the coastal cliffs between Abyār as Sabābīl and the mouth of Wādī al Quirrīm (Fig. 2). In many instances a succeeding cap of Udul Calcrete has been removed by intraformational erosion and the Arroman Member is overlain directly by the Shuraydat Member or by units of the Gargaresh Formation. Although lithologically very similar to the Shuraydat Member, the Arroman beds are easily recognizable by their greater proportion of calcrete nodules and honeycomb structure. Furthermore, in those areas where the Udul Calcrete is absent, the Arroman Member is almost always very deeply reddened by the development of a *terra rossa*-like soil (see Table 4).

Geologic age: El Hinnawy and Cheshitev (1975) have assigned the succeeding calcrete a Villafranchian age. If this is correct then the Arroman Member, since it rests on middle Miocene and possibly Pliocene, belongs somewhere in the age range of late Pliocene to early Pleistocene.

Table 3. Description of the Udul Calcrete

Named and defined by: Anketell, J.M. and Ghellali, S.M. (this paper).

See also: El Hinnawy and Cheshitev (1975) "Villafranchian calcrete".

Ghellali, S.M. (1977) "lower calcrete".

Anketell, J.M. and Ghellali, S.M. (1983) "lower calcrete".

Named from: The Qabīlat al Udūl of the Wādī Turghut area in the eastern Jifārah.

Holostratotype locality: In sea cliff 0.5 km west of fishing jetty at Ghūṭ ar Rommān (1 : 50 000 Sheet 2090 IV. Jamīʾ al Karāwah. Ref.: 3.66.00.36.30.60).

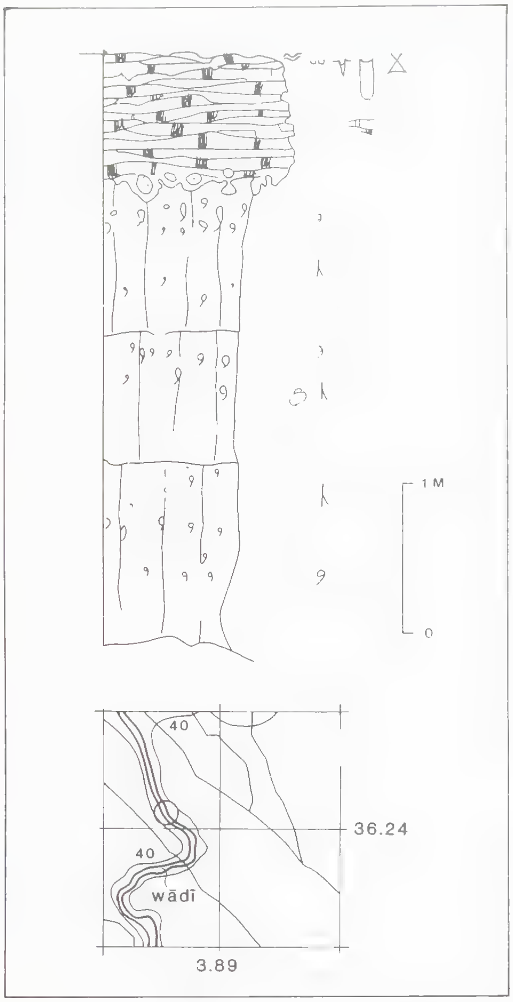

Fig. 8. Parastratotype section and location for the Arroman Member, Jifarah Formation.

Definition: A prominent, highly indurated and well laminated mature calcrete ranging from 0.5 to 1.5 m in thickness. Developed on a variety of substrates ranging from Mesozoic and Miocene limestones, sandstones and conglomerates, to the silts and gravelly silts of the Arroman Member, the calcrete reflects the nature of these sediments in itself ranging from well laminated, fine-grained limestone crust through to massive, highly indurated conglomeratic crust. Many localities display well developed tepee structure.

Holostratotype section: Comprised of 0.55 m of hard, well laminated calcrete ranging in colour from white to cream. Towards the top and along fissure walls it displays microlamination (Read, 1974, p. 263). Developed on the Arroman Member, clasts of the conglomeratic silts are preserved as ghost fragments and can only be observed with difficulty.

Boundaries:

– *Base:* The base of the unit is sharply gradational to the Arroman Member and at the type locality is placed at the onset of laminar development. On older sediments such as the Miocene, the base of the calcrete is equally sharply defined and often very irregular where it follows and blankets pre-existing topographic features.

– *Top:* The top surface is also very sharply defined by the abrupt lithological change from the calcrete to much less limey sediment and is followed unconformably by the younger members, in particular, the Shuraydat Member. In detail, the surface is patchily invaded by marine borings cf. *gastrochaenolites*, developed prior to deposition of the succeeding Shuraydat Member. These structures have been recognized at Ghūṭ ar Rommān, As Sabābīl and the Wādī Turghut but as yet, nowhere beyond 3 km south of the present coast.

Regional extent: The Udul Calcrete crops out mainly in the eastern and southern Jifārah but has been recognized in the subsurface of the central region. To the west and in the Jabal Nafūsah foothill region it can be seen capping the Al Assah Formation, the lower member of the Qaṣr al Ḥaj Formation, and both Miocene and Mesozoic bedrock.

Additional comments: The calcrete is, at many localities, invaded by large solution pipes (see Anketell and Ghellali, 1983, p. 28). Although the Udul Calcrete is often removed by intraformational erosion, it nevertheless constitutes a most important and easily recognized marker horizon. It is of prime importance in unravelling the stratigraphic relationships not only within the Jifarah Formation but also between that formation and the Qaṣr al Ḥaj and Al Assah Formations. Anketell and Ghellali (1983) have also demonstrated its value in determining an intra-Quaternary phase of faulting.

Geologic age: As already noted, El Hinnawy and Cheshitev (1975) consider this horizon to be Villafranchian in age. It should, however, be stressed that this interpretation is based only on lithological correlation with a prominent calcrete of known Villafranchian age in southern Tunisia. As yet, there is no independent evidence confirming a Villafranchian age for the calcrete in the Jifārah region. What would, however, appear to be the same calcrete occurs in the western Sirt region where it is developed on Al Hishah Formation of known Pliocene age (Mann, 1975b). Both Mann (1975a), and earlier, Hecht *et al.* (1964) maintain that the most likely age for the calcrete is Villafranchian.

Table 4. Description of the Shuraydat Member

Red to pink, fine sands and buff silts with nodular calcrete

Named and defined by: Anketell, J.M. and Ghellali, S.M. (this paper).
See also: Ghellali, S.M. (1977).
Anketell, J.M. and Ghellali, S.M. (1983) "Unit Q2".

Named from: The Qabīlat Ash Shuraydat of the Wādī Turghut area (Fig. 3).

Holostratotype locality: Cliff section in Wādī Turghut (1:50 000 Sheet 1090 II. Qabīlat al Qalīl. Ref.: 3.86.80.36.19.80).

Definition: Characteristically red to buff, fine sands and silts with abundant levels of nodular calcrete interbedded with units of columnar jointed, buff silts with abundant rootlet channels and small, irregular calcrete nodules. The rootlet channels are also commonly lined with calcium carbonate. Locally, gravel lenses are well developed, particularly in the east and to the south towards the Jabal front. The basal part of the member is also commonly conglomeratic. The red silts and fine sands with calcrete nodules often display fine plane-parallel lamination and, more rarely, cross lamination on both large and small scale. Both the sands and silts yield a sparse fauna of terrestrial gastropods cf. *Helix* sp. The maximum thickness so far recorded is 12 m.

Holostratotype section: Characteristic lithology at type section is red to pink silt and fine sand with calcrete nodules (Fig. 9). The lowermost 10 cm is conglomeratic.

Boundaries:

– *Base:* The basal contact is sharp. At the type section the thin conglomerate unit at the base of the succession rests on highly indurated, conglomeratic Udul Calcrete exposed both at the base of the wadi cliff and in the wadi floor. The strongly disconformable nature of the base is well displayed at many sections and is discussed in some detail in Anketell and Ghellali (1983).

– *Top:* The top of the member is sharply transitional to the Wadi Sariyah Calcrete and is taken at the first conspicuous development of lamination in the calcrete.

Parastratotype: Locally, the conglomeratic basal unit of the member is more thickly developed. Such is the case in cliff sections at Ghūṭ ar Rommān. Figure 10 displays a typical example from locality; 1:50 000 Sheet 2090 IV. Jamīʾ al Karāwah. Ref.: 3.66.30.36.30.50. Here the lowest part of the succession is comprised of 2 m of conglomeratic siltstones which are closely comparable to the underlying Arroman Member but which lack the strong development of calcrete typical of those deposits. Two units, separated by a 6 cm thick unit of bright red clay, display channelling (Ghellali, 1977, p. 211).

Regional extent: The Shuraydat Member is the most widespread, and best exposed member of the Jifarah Formation. The presence of calcrete nodules and the generally greater degree of cementation by calcium carbonate make it more resistant to erosion than succeeding members and it commonly forms the coastal cliffs. In addition, the strong red and pink colour makes it one of the more easily recognized members of the formation.

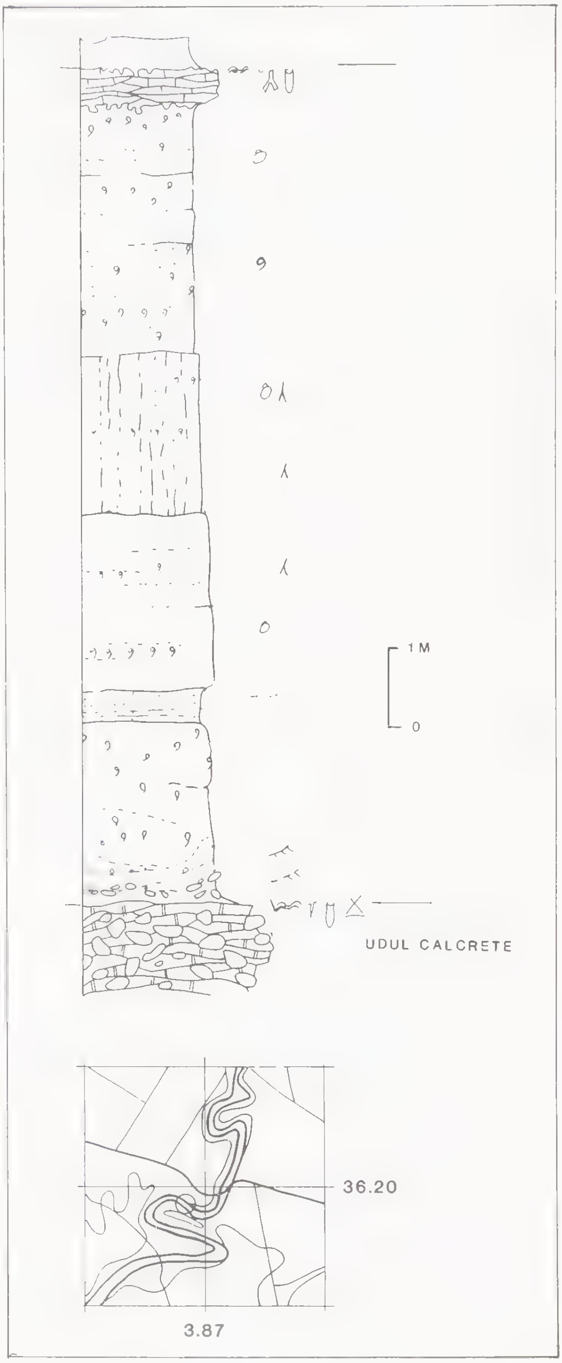

Fig. 9. Holostratotype section and location for the Shuraydat Member, Jifarah Formation.

Additional comments: A very common feature of the conglomerates which occur at the base of the member is that many of the pebbles display a black patina. This is not common in other conglomerates in the region and the presence of abundant blackened pebbles has been used

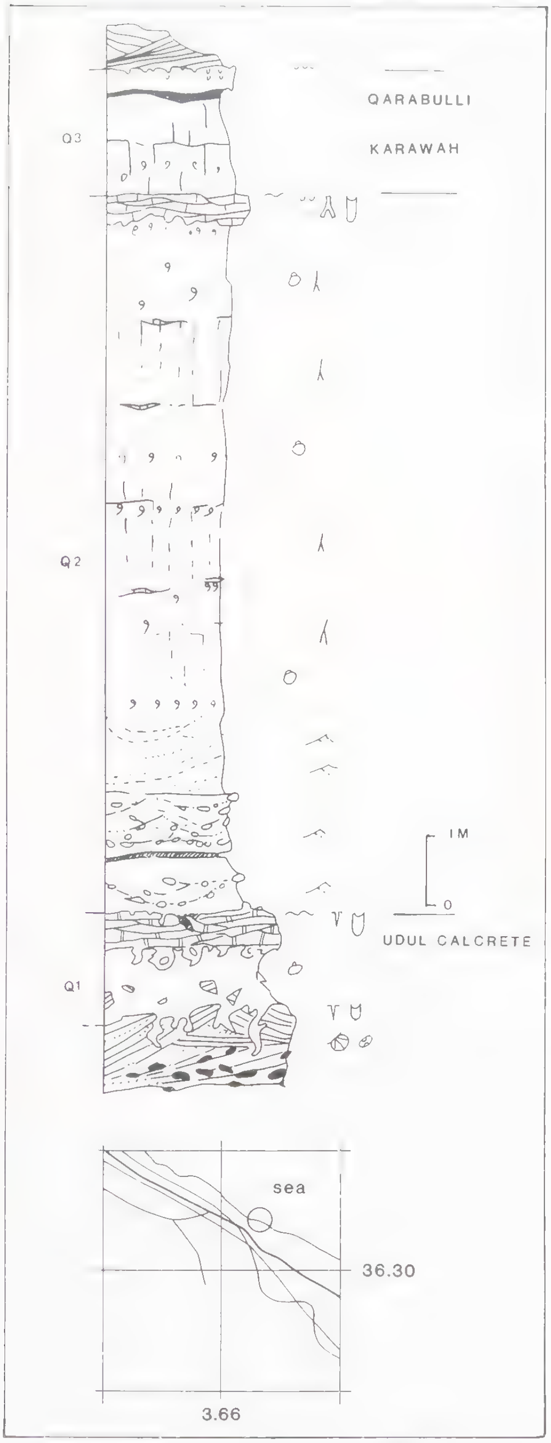

Fig. 10. Parastratotype section and location for the Shuraydat Member, Jifarah Formation.

with some success as an aid in correlation. The origin of the blackening is as yet unknown. Ghellali (1977) suggested that they may be fire-blackened and thus have accumulated from reworked hearths. Although conglomeratic silts are the most common basal lithology to the member, locally, where the conglomerate is not developed, another, earlier formed deposit is observed. This is a vivid, red clay and silty clay which both infills fissures and solution pits and forms lenticular units up to 16 cm in thickness, resting either on the Udul Calcrete or, where this is absent, directly on the Arroman Member which is, as a result, strongly reddened. The deposit has all the characteristics of a *terra rossa* and its occurrence following the Arroman Calcrete and before the development of fluvial gravels has important implications to interpretation of the geological history of the region.

Geological age: Although the silts commonly yield gastropods cf. *Helix* sp., no systematic study of the fauna has as yet been undertaken. If the member corresponds to the "red sands with Helix" of Parona *et al.* (1913), then a Wurm/Weichsel age proposed by those authors is possible. On the other hand, Ghellali (1977, Table 6), from correlation of the member with levels within the Gargaresh Formation, has proposed them as equivalent to calcarenite deposits which rest on beach gravels thought to be Palaeotyrrhenian in age. This would place the deposits in the Riss/Saale glacial period rather than in the Weichsel. There is no doubt that the question of age must remain open and await further study of associated deposits such as the Qaṣr al Ḥaj and Gargaresh Formations.

Table 5. Description of the Wadi Sariyah Calcrete

Named and defined by: Anketell, J.M. and Ghellali, S.M. (this paper).
See also: Ghellali, S.M. (1977) "upper calcrete".
Anketell, J.M. and Ghellali, S.M. (1983) "upper calcrete".

Named from: Wādī as Sāriyah of the Eastern Jifārah (Fig. 3).

Holostratotype locality: Wādī floor near junction of Wādī as Sāriyah and Wādī ar Raml (1 : 50 000 Sheet 2090 IV. Jamī' al Karāwah. Ref.: 3.66.25.36.26.75).

Definition: A hard, well laminated, mature calcrete which ranges from a few centimetres up to 0.6 m in thickness. Colour varies from white and cream to pinkish brown. The unit forms a prominent feature, capping underlying deposits and protecting them from erosion. Locally it displays spectacular development of solution pipes, filled with *terra rossa*-like soil, often with well-formed root systems.

Holostratotype section: White to pale grey, well laminated calcrete 0.30 m thick.

Boundaries:

– *Base:* Sharp although often irregular contact with older units. Most common basal contact is with the Shuraydat Member where the base is placed at first clear development of laminated calcrete.

– *Top:* Anketell and Ghellali (1983) have shown that the top surface has been much affected by erosion and solution prior to deposition of the succeeding member. The surface is, as a result, very sharply defined and constitutes an excellent mappping marker horizon.

Regional extent: The Sariyah Calcrete occurs throughout the Jifārah region and is often exposed at the surface in deflation hollows within the dune sand facies of the youngest members. In the coastal region west of Tājūrā' and south of Ṣabrātah, it is commonly exposed where intraformational erosion has removed some or all of the succeeding members. The unit is very well displayed in coastal cliff sections both east and west of Tripoli where it forms a protective cap to the deposits of the cliff face.

Additional comments: The Sariyah Calcrete is of particular importance in delineating a phase of intraformational erosion which affected the Shuraydat Member soon after its accumulation. Erosional valleys are clearly defined by the calcrete which can be seen to drape over various levels in the Shuraydat Member, often coming to rest on older units in the floors of the "fossil" valleys (see Anketell and Ghellali, 1983, Fig. 7).

Geologic age: As with the older units, the question of age of the Sariyah Calcrete must remain open until further data is available. Ghellali (1983, Table 6) suggests that the unit may have developed in late Riss/Saale times.

Table 6. Description of the Karawah Member

White, pure quartz sands and buff, loessic silts

Named and defined by: Anketell, J.M. and Ghellali, S.M. (this paper).
See also: Ghellali, S.M. (1977) "white sands".
Anketell, J.M. and Ghellali, S.M. (1983) "Unit Q3".

Named from: The Qabīlat al Karāwah of the Wādī al Masīd region in the eastern Jifārah.

Holostratotype locality: Cliff section in Wādī al Masīd (1:50 000 Sheet 2090 IV. Jamī' al Karāwah. Ref.: 3.78.75.36.28.70).

Definition: The Karawah Member is lithologically the most distinctive of the formation and is composed of clean white quartz sands and buff, columnar jointed silts, both with patchy bright yellow to orange weathering. The white sands occasionally display fine, plane parallel and gently dipping, large scale, cross lamination but are more commonly devoid of obvious sedimentary structure. Both the buff coloured silts and sands contain rootlet systems and display insect escape burrows. The member varies from zero to a maximum of 25.0 m in thickness.

Holostratotype section: The Holostratotype section is shown in Fig. 11.

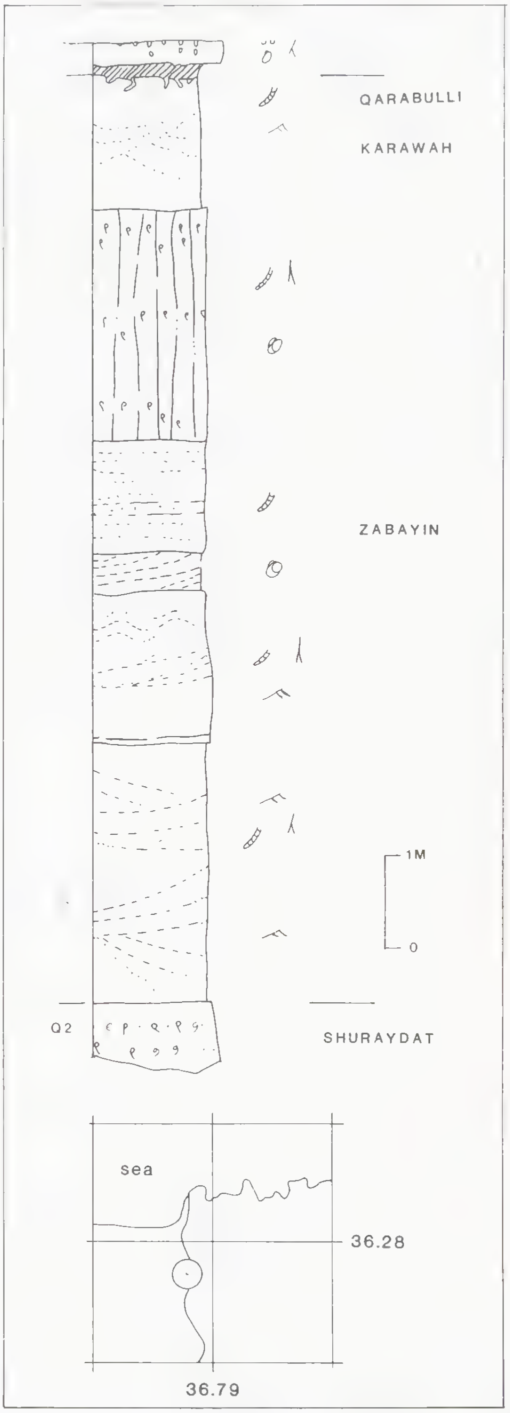

Fig. 11. Holostratotype section and location for the Karawah Member, Jifarah Formation.

Boundaries:

– *Base:* At the holostratotype locality the base of the member is in sharp contact with a horizon low in the Shuraydat Member. The rest of the Shuraydat beds and the

Sariyah Calcrete are absent due to intraformational erosion (see Anketell and Ghellali, 1983, p. 32). Elsewhere the member rests with sharp contact on the Sariyah calcrete.

– *Top:* Throughout the whole of the area, the top of the member is clearly defined at the base of a very distinctive dark grey to black, carbon-rich horizon which makes up the lower part of the Qarabulli Member. The surface commonly displays dune-like form.

Regional extent: The Karawah Member is well developed in the eastern Jifārah and can be traced into the central Jifārah where it is exposed south of Bin Ghashīr and in the Wādī al Majānīn. It is not as yet known how far to the west it extends. To the south, the member tends to thin and eventually tapers off to a feather edge (see Anketell and Ghellali, 1983, Fig. 5). North of Bin Ghashīr, in the coastal area between Tājūrā' and Ṣabrātah, the member is absent, largely due to intraformational erosion.

Additional comments: In general it would appear that the white sand facies predominates where the member is thickly developed while the buff silt facies is the more common lithology in thinner developments. The purity of the quartz sands is very high and the deposits should be investigated as a source of glass-sand.

Geologic age: Ghellali (1977, Table 6) suggests that the deposits are of Wurm/Weichsel age and certainly they are equivalent to the main development of Gargaresh Formation which Desio (1971) assigned to the Wurm/Weichsel. There is, however, no firm evidence supporting these conclusions.

Table 7. Description of the Qarabulli Member

Grey to black, weakly calcretized silts with freshwater gastropods

Named and defined by: Anketell, J.M. and Ghellali, S.M. (this paper).
See also: Ghellali, S.M. (1977) "Caprock".
Anketell, J.M. and Ghellali, S.M. (1983) "Caprock".

Named from: The town of Al Qarāhbūllī around which the member is well exposed in wādī terraces and in deflation hollows between younger dune sediments.

Holostratotype locality: Wādī bank section in Wādī al Masīd immediately west of Al Qarāhbūllī town (1:50000 Sheet 2090 III. Qaṣr al Qarāhbūllī Ref.: 3.78.10.36.24.00). Fig. 3.

Definition: The Qarabulli Member is highly distinctive, consisting of a dark grey to black, carbon-rich lower layer up to 18 cm thick capped by an upper, light grey layer comprised of weakly calcreted silt. The grey silt layer reaches up to 38 cm in maximum thickness and locally yields a rich fauna of freshwater gastropods (Appendix). The topmost part of the silts is extensively invaded by vertical, chambered borings of a type similar to those constructed by tube-dwelling bees (Anketell and Ghellali, 1984).

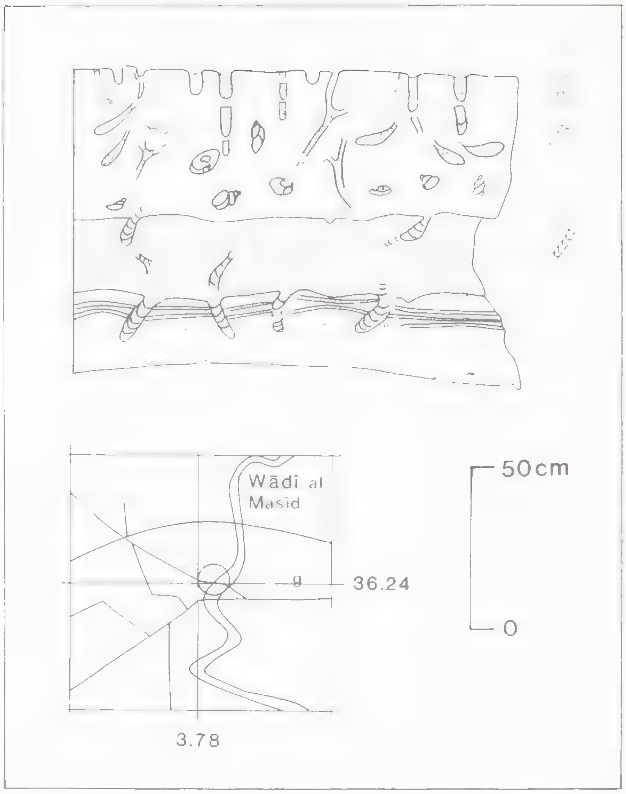

Fig. 12. Holostratotype section and location for the Qarabulli Member, Jifarah Formation.

Holostratotype section: Holostratotype section is shown in Fig. 12.

Boundaries:

– *Base:* Clearly defined contact with white sands or buff silts of Karawah Member shown by abrupt change in colour.

– *Top:* Sharp contact with all succeeding deposits. Anketell and Ghellali (1983) have shown that the junction is strongly unconformable.

Regional extent: The Qarabulli Member has been traced throughout the eastern Jifārah area and as far west and south as Bin Ghashīr and Wādī al Majānīn. To the south, where the Karawah Member feathers out, the calcreted silts with insect burrows lap over onto the older members and can be found resting on the Sariyah Calcrete and the Shuraydat beds (see Anketell and Ghellali, 1983, Figs 5 and 8a).

Geologic age: Ghellali (1977, Table 6) assigns a late Wurm age to these deposits.

Table 8. Description of the Zabayin Member

Brown to yellow-brown "loessic" silts, and gravels

Named and defined by: Anketell, J.M. and Ghellali, S.M. (this paper).

See also: Vita Finzi, C. 1971. Alluvial History of Northern Libya since the last Interglacial. *In: Symposium on the Geology of Libya.* Tripoli, "Jeffara Alluvium".

Ghellali, S.M. (1977) "upper terrace deposits".

Anketell, J.M. and Ghellali, S.M. (1983) "Unit Q4".

Named from: The Qabīlat az Zabā'in of the Wādī ar Raml area, one of the major wadis in the region providing excellent cliff sections (Fig. 3).

Holostratotype locality: In wādī cliff (1:50 000 Sheet 2090 III. Qaṣr al Qarāhbūllī Ref.: 3.63.75.36.18.40).

Definition: Characteristically mid-brown to yellow-brown and buff, "loessic" silts with pronounced columnar jointing, abundant rootlet channels, sporadic calcrete nodules and thin impersistent nodular layers of calcrete. Gravel lenses, only weakly cemented, increase in importance to the south and east. The member yields a sparse fauna dominated by *Helix* sp. White quartz sands occur locally.

Holostratotype section: The basal part of the member (Fig. 13) displays lithologies almost identical to those of the Karawah Member, from which it is separated by the Qarabulli Member (see Anketell and Ghellali, 1983, fig. 11). The junction between the white sand and the underlying formations is clearly unconformable (see Anketell and Ghellali, 1983, figs 5 and 11).

Boundaries:

– *Base:* Sharply defined and unconformable on a wide range of older deposits.

– *Top:* The top is planar with a gentle northwards dip and is excellently displayed as the top of the "upper terrace" (see Vita Finzi, 1971; Anketell and Ghellali, 1983, Fig. 5).

Regional extent: The member occurs throughout the region often forming the major part of the cliffs of the upper terrace which comprises one of the most conspicuous morphological features of the plain.

Geologic age: As with older stratigraphic units in the area, there is as yet no firm evidence as to the age of this member. Archaeological evidence from "upper terrace" deposits in Wādī Ghān (Hey, 1962) suggests a late Pleistocene age.

Table 9. Description of the Wadi Raml Member

Buff to ochre fluvial sands and gravels and dune sands

Named and defined by: Anketell, J.M. and Ghellali, S.M. (this paper).

See also: Vita Finzi, C. (1971) "younger fill", "Lebda Alluvium", *in*: *Symposium on the Geology of Libya*, Tripoli.

Ghellali, S.M. (1977) "lower terrace deposits and older dunes".

Anketell, J.M. and Ghellali, S.M. (1983) "Unit Q5".

Named from: Wādī ar Raml of the eastern Jifārah.

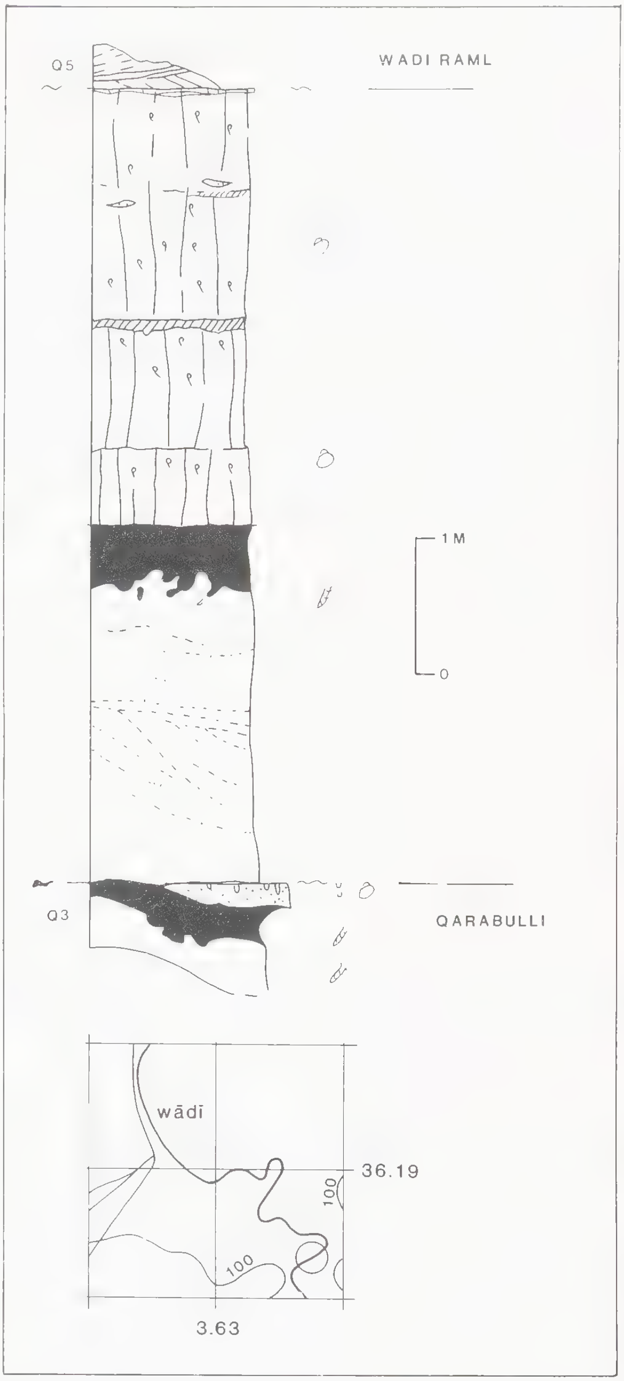

Fig. 13. Holostratotype section and location for the Zabayin Member, Jifarah Formation.

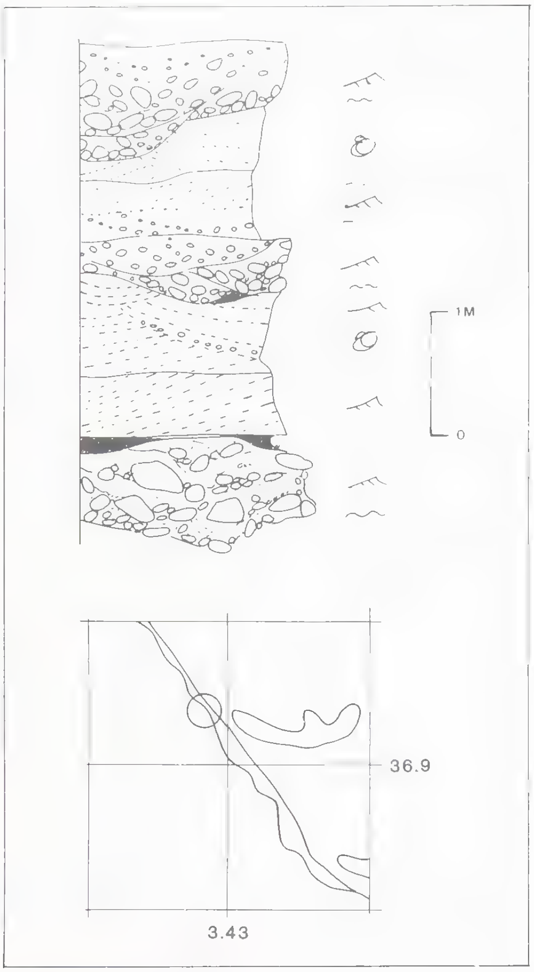

Fig. 14. Holostratotype section and location for the Wadi Raml Member, Jifarah Formation.

Holostratotype locality: Wādī bank (1:50 000 Sheet 2090 IV Jamī' al Karāwah Ref.: 3.68.60.36.28.75).

Definition: Weakly cemented sands and occasional fine gravels disposed in ribbons along wadis, interdigitated with ochreous yellow to orange, fine sands and silts in the areas between wadis. The ochreous sands and silts form well-vegetated fossil dunes.

Holostratotype section: Holostratotype section is shown in Fig. 14.

Boundaries:

– *Base:* Sharply defined, resting unconformably on all older deposits.

– *Top:* The top is sharply defined and in dune facies is hummocky. In the wadis the top is planar and corresponds to the "lower terrace" of Vita Finzi (1971).

Regional extent: The Wadi Raml Member occurs at or near the surface throughout the region. In the wadis it is exposed in cliffs of the lower terrace. The terrace deposits are generally fragmentary and in recent years have been destroyed through increased farm development. In inter wadi areas it forms an irregular blanket and forms the major agricultural soil of the area.

Geologic age: Ghellali (1977) and the I.R.C. (1975) assign the deposits to the Holocene while Vita Finzi (1971) has recorded both Roman and Arab sherds from several localities and suggests an age range from 1500 to 600 years B.P.

Table 10. Description of the Wadi Megenin Member

Fluvial sands and gravels and active sand dunes

Named and defined by: Anketell, J.M. and Ghellali, S.M. (this paper).

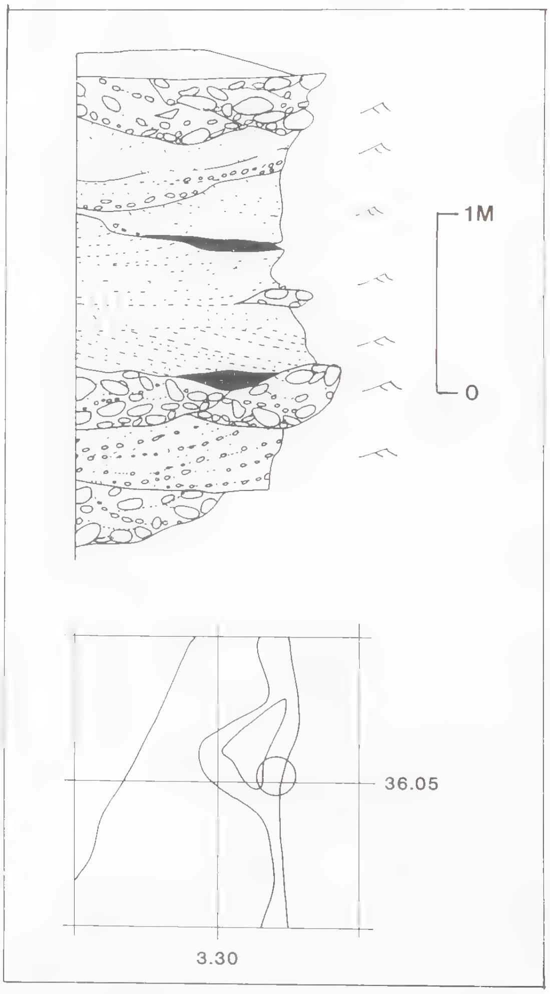

Fig. 15. Holostratotype section and location for the Megenin Member, Jifarah Formation.

See also: Ghellali, S.M. (1977).
Anketell, J.M. and Ghellali, S.M. (1983) "Unit Q6".

Named from: Wādī al Majānīn, the longest wadi of the Jifārah Plain which reaches the coast at Tripoli and exposes many sections in these most recent deposits.

Holostratotype locality: In Wādī al Majānīn (1:50000 Sheet 1990 III. Bin Ghashīr. Ref.: 3.30.40.36.05.00).

Definition: Uncemented fluvial silts, sands and rare fine gravels in wadis changing abruptly to contemporaneous fine dune sands in inter-wadi areas. The sands and fine gravels are disposed in ribbons along the wadis while the fine, inter-wadi sands are disposed in longitudinal, northeast to southwest oriented dunes up to 20 m in thickness. Fluvial sediments become coarser to the south passing into the Qaṣr al Ḥaj Formation.

Holostratotype section: Fig. 15.

Boundaries:

– *Base:* Sharply defined, resting unconformably on all other sediments.

– *Top:* Configuration of the top surface reflects shape of dunes and wadis.

Regional extent: Patchily developed over whole region.

Geologic age: These deposits are forming at the present day.

CONCLUSIONS

Definition of the Jifarah Formation in terms of a composite stratotype and its subdivision into seven members, provides a firm basis for detailed description and intraformational correlation both within and outside the immediate area of the Jifārah Plain. Subdivision in the manner proposed and regional correlation of the surface of stratigraphic discontinuity also constitute a framework for investigation of interformational relationships between the Jifarah Formation and the Gargaresh, Qaṣr al Ḥaj and Al Assah Formations.

ACKNOWLEDGEMENTS

The authors wish to express their appreciation of the financial and logistic help given over several years in the course of this research by the University of Al Fateh, Ṭarābulus, and to the Department of Geology, University of Manchester for providing laboratory facilities. Our thanks are also due to Mrs. Elaine Lock for her patience in typing the manuscript.

APPENDIX — LAND AND FRESHWATER MOLLUSCS OF THE JIFARAH FORMATION

D.T. Holyoak[1]

Four samples of shells were received for the study. The material consisted mainly of large shells collected by hand, but a few small shells were obtained from the sediment contained inside large shells.

Three samples were collected at Wādī al Mietah (32°44′N, 13°51′E). The first, from the Zabayin Member (Q4) consisted of unidentified species of Helicellinae (9 shells) and *Helix melanostoma* Drapernaud (6). These are land snails; *H. melanostoma* is widespread around the western Mediterranean and still occurs in semi-arid parts of North Africa (Bourguignat, 1864; Germain, 1908).

The other two samples from Wādī al Mietah were collected from the Qarabulli Member (upper part of Q3). Sample 25/3 was collected from *in situ* deposits. This material comprised *Lymnaea palustris* Muller (10 shells), *Planorbis planorbis* Linne (11) and unidentified Helicellinae (3). Sample 25/1 was of loose shells eroded from the Qarabulli Member and accumulated in gullies. It comprised: *Lymnaea palustris* (c. 26), *Armiger crista* Linne (1), *Cecilioides* sp. (1) and *Helix melanostoma* (2).

Most of these shells are of freshwater gastropods, and all three of the aquatic species represented (*L. palustris*, *P. planorbis*, *A. crista*) prefer shallow, richly vegetated waters. None of them is particularly tolerant of saline conditions or of water bodies that dry out seasonally. The other taxa are land snails of genera that are still widespread in the Mediterranean region.

The fourth sample was from the Qarabulli Member at Wādī ar Raml (32°41′N, 13°33′E). It comprised: *Lymnaea natalensis* Krauss (1), *Biomphalaria pfeifferei* Krauss (c. 50) and *Bulinus truncatus* Audouin (4). These are all freshwater gastropods that typically live in slow-flowing or standing water of no great depth. Presence of *B. pfeifferei* would imply occurrence of a water body more permanent than a seasonal pool, but the other two species occur in both temporary and permanent pools (Brown, 1980).

The stratigraphical distribution of Quaternary non-marine mollusca in North Africa is at present too poorly known for them to be used for detailed correlation of deposits. It is nonetheless clear from the occurrence of six species of freshwater gastropods, including several that no longer occur in the region (see below), that the deposits of the Qarabulli Member date from a period when the region had more standing water than at the present day, presumably due to higher rainfall.

---

[1] Department of Geography, Nottingham University, Nottingham, England, U.K.

Three of the freshwater gastropods recorded are of zoogeographical interest because they represent the first records from Libya, although each of the species is known in surrounding countries (cf. the recent review by Van Damme, 1984). Thus, *Lymnaea palustris* is known living in Tunisia and Egypt, *Planorbis planorbis* is known living in Algeria and Egypt, and *Armiger crista* is known living in Morocco, North Algeria and Ethiopia and as a Quaternary fossil in the Hoggar and Tībistī.

REFERENCES

American Commission on Stratigraphic Nomenclature. Code of Stratigraphic Nomenclature (1961). *Bull. Am. Assoc. Petrol. Geol.*, **45**, 546–600.

Anketell, J.M. (1981). Report on Structural and Sedimentological Trends in the Pelagian Basin and related onshore areas. *In: Proc. Int. Court Justice (Tunisia/Libya)*, **III**, Tech. Annexes 12A, 23 p.

Anketell, J.M. and Ghellali, S.M. (1983). Stratigraphic studies on Quaternary floodplain deposits of the Eastern Jeffara Plain, S.P.L.A.J. *J. Libyan Studies*, **14**, 16–37.

Anketell, J.M. and Ghellali, S.M. (1984). Nests of a tube-dwelling bee in Quaternary sediments of the Jeffara Plain, S.P.L.A.J. *J. Libyan Studies*, **15**, 137–141.

Anketell, J.M. and Ghellali, S.M. (1987). Stratigraphic aspects of the Gargaresh Formation, Tripolitania, S.P.L.A.J. *J. Libyan Studies*, **18**.

Antonovic, A. (1977). Geological Map of Libya. 1 : 250 000 Sheet Mizdah NH33-I. Explanatory Booklet. *Ind. Res. Cent.*, Tripoli.

Banerjee, S. (1980). Stratigraphic Lexicon of Libya. *Ind. Res. Cent.*, Tripoli, Bull. **13**, 300 p.

Bourguignat, J.R. (1864). *Malacologie de l'Algerie.* Paris, (2 vols.).

Brown, D.S. (1980). *Freshwater Snails of Africa and their Medical Importance.* Taylor and Francis, London.

Conant, L.C. and Goudarzi, G.H. (1976). Stratigraphic and tectonic framework of Libya. *Bull. Am. Assoc. Petrol. Geol.*, **51**, 719–730.

Desio, A. (1971). Outlines and problems on the geomorphological evolution of Libya, from the Tertiary to the present day. *In: Symp. Geol. Libya* (*ed.* C. Gray). Fac. Sci., Univ. Libya, Tripoli.

Desio, A., Ronchetti, C.R., Pozzi, R., Clerici, F., Invernizzi, G., Pisoni, C. and Vigano, P.L. (1963). Stratigraphic Studies in the Tripolitanian Jebel (Libya). *Riv. Ital. Palaeontol. Stratigr.*, **66**, 273–318.

El Hinnawy, M. and Cheshitev, G. (1975). Geological Map of Libya. 1 : 250 000 Sheet Tarabulus N133-13. Explanatory Booklet. *Ind. Res. Cent.*, Tripoli.

Germain, L. (1908). Etude sur les mollusques recueillis par M. Henri Gadeau de Kerville pendant son voyage en Khroumirie (Tunisie). *In: Voyage zoologique en Khroumirie (Tunisie).* Bailliere et fils, Paris, 129–297.

Ghellali, S.M. (1977). *On the Geology of the Eastern Gefara Plain, Northwest Libya.* Ph.D. Thesis. Manchester Univ., Manchester.

Hammuda, O.S. and Misallati, A.A. (1980). A study of the Libyan Tunisian shelf. *In: Proc. Int. Court Justice (Tunisia/Libya)*, **II**, Libyan Memorial.

Hecht, F., Fürst, M. and Klitzsch, E. (1964). Zur Geologie von Libya. (Contribution à la géologie de la Libya). *Geol. Rundsch.*, **53**, 413–470.

Hedberg, H.D. (ed.) (1976). International Stratigraphic Guide. I.U.G.S. J. Wiley and Sons, New York, N.Y., 200 p.

Hey, R.W. (1962). The Quaternary and Palaeolithic of northern Libya. *Quaternaria*, **VI**, 435–449.

Mann, K. (1975a). Geological Map of Libya. 1 : 250 000 Sheet Al Khums N133-14. Explanatory Booklet. *Ind. Res. Cent.*, Tripoli.

Mann, K. (1975b). Geological Map of Libya. 1 : 250 000 Sheet Misratah N133-15. Explanatory Booklet. *Ind. Res. Cent.*, Tripoli.

Parona, C.F., Crema, C. and Franchi, S. (1913). La Tripolitania settentrionale; descrizione fisica e geoligica della regione. *Min. Col. Comm. per lo Studio Argrocolico della Tripolitania*, Roma, **I**, 3–42.

Read, J.F. (1974). Calcrete deposits and Quaternary sediments, Edel Province, Shark Bay, Western Australia. *Mem. Am. Assoc. Petrol. Geol.*, **12**, 250–282.

Smetana, R. (1975). Geological Map of Libya. 1 : 250 000 Sheet Ra's Ajdīr N132-16. Explanatory Booklet. *Ind. Res. Cent.*, Tripoli.

Van Damme, D. (1984). *The freshwater Mollusca of Northern Africa.* W. Junk, Dordrecht.

Vita Finzi, C. (1971). Alluvial history of Northern Libya since the last interglacial. *In: Symp. Geol. Libya* (*ed.* C. Gray). Fac. Sci., Univ. Libya, Tripoli, 409–429

Quaternary Sediments of the Jifārah Plain

J.M. ANKETELL [1] AND S.M. GHELLALI [2]

رسوبيات الحين الرابع بسهل الجفارة

ج. م. انكتيل وس. م. القلالي

الخلاصــة

تمثل رسوبيات الحين الرابع بسهل الجفارة من الجنوب إلى الشمال تغيراً في السحنات من جرول المراوح المائية ومن رمال وغرين رياحية مائية إلى الرمال الجيرية الرياحية ذات الأصل البحري المصاحبة للرمال والجراول الشاطئية في المناطق الساحلية. وتمثل هذه السحنات الثلاث تكوين قصر الحاج وتكوين الجفارة وتكوين قرقارش. وهناك نطاقات مركبة للتربة وأسطح التعرية يمكن تتبعها من مكان إلى آخر ويسمح باستعمالها في تقسيم هذه التكاوين إلى ستة أعضاء من ق$_{1}$ — ق$_{6}$. وباستثناء ق$_{3}$ الذي يعد في معظمه من أصل رياحي وهو يفتقد بذلك لسحنات المراوح الركامية، فإن كل عضو من الأعضاء الأخرى يمثل تدفقاً في إتجاه الشمال وتداخلاً مع الرمال الكلسية. وينتهي كلا العضوين الأقدمين بترسب الكلس الرقائقي والذي يشكل المرحلة الأولى في تسلسل الأحداث التي تؤدي إلى نطاقات عدم التطابق. إن مثل هذا الإنطباع يبدو ضعيفاً في ق$_{3}$ ويظهر محلياً فقط في ق$_{4}$ وق$_{5}$ وينعدم تماماً في الرواسب الحديثة. ويقطع الكلس مرحلة من التعرية قبل مرحلة الإذابة أو متزامناً معها وهو مصاحب تماماً لمرحلة ثانية من تكوين التربة. مع ترسب التربة الحمراء (terra rossa). وقد انتهت هذه المرحلة من التعرية وتكوين التربة لمرحلة تعرية أساسية تتعلق باستئناف الترسيب في العضو الذي يلي ذلك إلى أعلى.

إن تفسير الرمال الكلسية على أنها تمثل رمالاً رياحية انحسارية مع اعتبار الأهمية المناخية للتربة القديمة، يسهل عملية تقييم الرواسب وأسطح التعرية على أنها تمثل ارتفاعات وانخفاضات في مستوى سطح البحر بسبب عمليات تكون انحسار الجليد فوق الكرة الأرضية. لقد حدثت تراكمات رسوبية هامة خلال مراحل الإنحسار. وقد حدّد استئناف الترسيب والتعالي للرواسب المائية المراحل الأولى للإنحسار وتقدم الجليد. كما أدّى تكشف قيعان البحار الضحلة إلى تواجد مصدر من الرمال البحرية مناسب لتكون الرواسب الرياحية التي تداخلت مع رواسب الرمال والغرين البرية المتعالية. وفي المراحل الأخيرة من الإنحسار. وربما كان للرمال الدقيقة والغرين المستمد من المناطق العميقة والذي حملته الرياح دور مهم في تكون رواسب اللوص الذي يغطي مناطق شاسعة. أما المصدر السائد للوص فربما كان في المناطق الصحراوية الجنوبية. وقد تم تعديل اللوص جزئياً عن طريق الفيضانات الواسعة مكونة رواسب لُوصِيَّةٍ. التي رغم أن بها فواصل عمودية وتكلسات جذرية. إلاّ أن حبيباتها تبدو أخشن من اللوص العادي. ويدل تكوّن مثل هذه الرواسب على أن المناخ في المراحل الأخيرة كان موسمياً رطباً.

وتدل العلاقات الطبقية للرواسب الشاطئية وكذلك التربات القديمة وأسطح التعرية التي تميز نطاقات عدم التطابق، أن الطبقات الكلسية تترسب عند الإنحسار الأقصى أو بعده مباشرة وأن أنابيب الذوبان والتربة الحمراء تتكونان في أوقات يكون فيها سطح البحر مرتفعاً ربما أثناء فترات ما بين التجلد أو بعدها مباشرة. وقد تم تفسير الترسيب المحدود للطبقات الكلسية وللتربة الحمراء فوق الأعضاء والأحدث عمراً على أساس التغيرات المناخية غير المتطرفة والتي قد تمثل حادثات بين توقفية بدلاً من حادثات بين جليدية. ترجع المستحاثات المجمعة من الرواسب الشاطئية عمر معظم صخور الحين الرابع إلى العصر التيريني ولكن قد تعود الطبقات السفلى منه إلى ما قبل عصر الفيلافرانشي وربما عادت إلى عصر البلايوسين.

Abstract. Quaternary sediments of the Jifārah Plain display a south to north change in facies from alluvial fangravels through fluvio-aeolian sands and silts to aeolian calcarenites of marine origin associated with littoral sands and gravels in the coastal region. The three facies make up the Qaṣr al Ḥāj, Jifarah and Gargaresh Formations. Complex zones of erosion and soil formation, which can be traced from one formation to the other, allow subdivision of the formations into six members Q1–Q6. With the exception of Q3 which is predominantly aeolian in origin and hence lacks an alluvial fan facies, the members each display a northward fining and

---

[1] Department of Geology, University of Manchester, Manchester M13 9PL, England.
[2] University of Al-Fateh, Faculty of Science, Earth Sciences Department, P.O. Box 13258, Tripoli, Libya, G.S.P.L.A.J.

interdigitation with calcarenites. The two oldest members are each terminated by development of laminar calcrete which forms the first phase in the series of events which give rise to the unconformable zones. This is more weakly developed on Q3, only locally on Q4 and Q5 and absent on recent deposits. The calcrete is truncated by a phase of erosion, prior to or contemporaneous with a phase of solution which is closely associated with a second phase of soil formation with development of *terra rossa*. This sequence of erosion and soil formation is terminated by a major phase of erosion related to onset of deposition of the succeeding member.

Interpretation of the calcarenites as regressional aeolianites together with the climatic significance of the palaeosols, allows evaluation of the deposits and erosional surfaces in terms of glacioeustatic sea level rise and fall. Major sediment accumulation occurred during regressive phases. Onset of deposition with progradation of fluvial deposits typified early stages of regression and ice advance. Exposure of shallow sea floor provided a source of marine sands for the aeolianites which interfingered with the prograding terrestrial sands and silts. In later stages of regression, finer sands and silts from deeper areas mobilized by wind, possibly formed a significant element of the loess which mantled the region. The dominant source of the loess was probably desert areas to the south. The loess was partially reworked by sheet wash to produce "loessic" deposits which, although displaying columnar jointing and occasional rhizocretions, are generally coarser than true loess. The formation of such deposits indicates that climate in the later stages of regression was seasonally wet.

Stratigraphic relationships of the littoral deposits with the palaeosols and erosion surfaces which characterize the zones of unconformity indicate that calcrete developed at or soon after maximum regression and that solution pipes and *terra rossa* developed at times of high sea level, possibly during and/or soon after the interglacial periods.

Limited development of calcrete and *terra rossa* on the younger members is interpreted in terms of less extreme climatic change, probably reflecting interstadial rather than interglacial events.

Faunas from the littoral deposits place the greater part of the Quaternary deposits in the Tyrrhenian, however, the lowermost beds may be pre-Villafranchian, possibly as old as Pliocene.

INTRODUCTION AND GENERAL GEOLOGICAL SETTING

The Jifārah Plain is a roughly triangular region comprised of fine sands and gravels of Quaternary age (Fig. 1). It is bounded to the north by the Mediterranean Sea and to the south by a prominent escarpment, Jabal Nafūsah, comprised of Mesozoic limestones and sandstones. From the east, where the escarpment drops to meet the coast near Al Khums, the plain widens westward over a distance of 300 km to a maximum of 100 km at the Libyan–Tunisian border. From the coast, it rises gently southward to 250 m at the base of the escarpment which in turn rises steeply to around 600 m. The plain can be subdivided into three relatively distinctive physiographic zones; a coastal zone which ranges up to 3 km in width; a medial zone with maximum width of 50 km in the west; a southern zone which runs south from the medial zone to the escarpment. The line separating the medial and southern zones which runs west southwest from the vicinity of Sūq al Aḥad to the north of Qaṣr al Waṭyah continues the strongly linear east northeast to west southwest trend which characterizes the escarpment from the coast to Sūq al Aḥad. At Sūq al Aḥad, however, the escarpment swings abruptly south to sweep in a broad arc towards the Tunisian border, forming the southern boundary of the southern zone. North of the line, the medial zone is essentially flat with only minor topographical changes related to active and stabilized dune fields and a number of wadi courses. The southern zone displays a more irregular topography due to outcrops of Mesozoic rocks which jut through the Quaternary cover (Christie, 1966). The Quaternary deposits are commonly deeply incised by wadis which rise in deep valleys cut in Jabal Nafūsah. Wadis reach the coast in the eastern Jifārah region but in the central Jifārah only Wādī al Majānīn extends from the Jabal to the sea, reaching it at Tripoli (Fig. 1).

The significance of the Sūq al Aḥad line is clear from subsurface studies which show the top surface of the Mesozoic to drop sharply across it to continue northwards at depth (Lipparini, 1940). To the south, the Mesozoic is succeeded by Pliocene and Quaternary sands and gravels. To the north, it is overlain by limestones, shales and sandstones of Lower to Middle Eocene age as well as Quaternary deposits. Miocene lithofacies variation shows that the subsurface scarp is pre-Miocene in age and formed a barrier to the southward advance of the Miocene transgressive seas (Ghellali, 1977). Its origin is complex and results from a combination of faulting pre-Miocene subaerial erosion.

Topographic subdivision of the plain is reflected in Quaternary lithofacies variation, variation which constitutes the basis for the stratigraphic subdivision of Quaternary and late Tertiary deposits of the region.

The coastal zone is characterized by calcarenite and occasionally quartz-rich aeolian dunes with lentils of shelly littoral sands and conglomerates together comprising the Gargaresh Formation. The dunes are typically well indurated and along the greater part of the coast form low cliffs, although locally both marine and fluvial erosion have cut through into the softer, less well consolidated sediments of the medial zone to form coves and bays.

These deposits, comprising the Jifarah Formation, are fine-grained and dominated by tan, brown and red silts and fine sands, commonly with layers of calcrete, both nodular and laminated. The deposits range from fluvial to aeolian in origin.

Lenses of gravel within the Jifarah Formation at the southern margins of the medial zone herald development of the characteristic deposits of the southern zone. These, which are typically conglomeratic with subordinate layers of finer sands and silts and local well-developed laminar calcrete, comprise the Qaṣr al Ḥāj Formation. The gravels and conglomerates occur both as wadi fill and as alluvial fangravels along the Jabal foothills. Interbedded finer silts and sands are both fluvial and aeolian in origin.

The Jifārah Plain is thus a northwards sloping region in which Quaternary deposits display a marked northward facies variation from coarse, alluvial fangravels near the escarpment to fluvial and aeolian fine silts and sands on the plain. In the coastal region the aeolian sands, interbedded with marine sands and gravels, are calcarenitic. Although this amply describes the gross relationship of the three formations, it is clear from previous studies that interrelationships are more complex.

STRATIGRAPHY

Previous Stratigraphic Studies of Quaternary deposits in the Jifārah Plain

Quaternary stratigraphic studies in the Jifārah region are less numerous than those on Mesozoic rocks to the south. The most important are summarized in Fig. 2 and compared with reference to the tripartite subdivision of the plain.

Earliest observations on lithologic variation within the deposits concentrated on sediments of the coastal zone. A sequence comprising "a lower arenaceous coquina" followed by "red sand with *Helix*" followed in turn by an "Upper soft sandstone" was recorded by Parona *et al.* (1913) from the region around Tripoli (Fig. 2A). The red sands with terrestrial gastropods can be assigned to the Jifarah Formation while both the upper soft sandstone and the shelly deposits comprise the two major facies of the Gargaresh Formation (Ghellali, 1977; Anketell and Ghellali, 1983). Complexity of interformational relationships in the coastal region is seen when this succession is compared with that recorded by Lipparini (1940), partly it would appear, from study of borehole data (Fig. 2B). This sequence, including an extensive list of fauna from the "detrital limestones", is quoted by Burollet (1960), Hecht *et al.* (1963) and Banerjee (1980) as representative of Quaternary stratigraphy in the coastal zone of Tripolitania. Desio (1971, p. 25) considered, however, that the "data is not in accordance with earlier accurate data collected by Parona and others". Apart from the probability that Lipparini's succession includes subsurface data, Anketell and Ghellali (1983, 1988) show that facies variation and intraformational erosion within the Quaternary deposits is considerable and that the succession changes rapidly from one area to another, with marked variation in completeness and complexity. The differences in the successions recorded by Parona and Lipparini can thus be accounted for by normal stratigraphic variation coupled with method of observation. Neither one is "inaccurate". Recent studies (Anketell and Ghellali, 1988) suggest that Lipparini's "marine dunes of Wurmian age" are equivalent to the "upper soft sandstone"; the red clayey sands with *Helicella* and hardpan correspond to the red sands with *Helix*, while the marine and foraminiferal limestones with Tyrrhenian fauna correspond to the "lower arenaceous coquina". The marine sands with terrestrial fauna which succeed the Tyrrhenian shell beds (Fig. 2B) are typical of the aeolian calcarenite facies of the coastal region and represent a development of the Gargaresh Formation not present in the sections studied by Parona *et al.* (1913). The red clayey sands with *Eremina deserterum* Forsk underlying the shell beds, comprise an older development of the Jifarah Formation. Burollet (1960) indicates that Lipparini recorded that these deposits overlie a thick calcrete which has been assigned to the Villafranchian (Hecht *et al.*, 1963).

Although these successions differ in detail, they clearly demonstrate that quartz-rich, reddened continental silts comprising the Jifarah Formation, interdigitate with aeolian calcarenites (aeolianites), and lentils of marine shelly gravels and sands, making up the Gargaresh Formation.

Recognition of southward change from Jifarah sands and silts into conglomeratic deposits, is first clearly documented by Desio *et al.* (1963) (Fig. 2C). The "Jefara Sand and Gravels" comprised of "yellowish, aeolic cross-bedded sand" with *Helix* and thin beds of pebbles at depth, pass into "fluvio aeolian" deposits comprised of alluvial fan gravels which are often superficially cemented. It is also noted that "conglomerate is grading loosely to loose gravels overlain by *Helix* sand" along the courses of the wadis. Jones (1969) (Fig. 2D) proposed the name Wadi al Hira Formation for the alluvial sands and gravels stating that "Although the Wadi al Hira is the oldest unit of Pleistocene age in much of the Gefara, the formation was deposited in part contemporaneously with the somewhat younger Gefara sand, with which it interfingers". Both Jones (1969) and Desio *et al.* (1963) clearly imply that although the two deposits are partly equivalent, the Jifarah Formation gradually succeeds the gravels throughout the southern zone.

Hey (1962) recognized that gravels and sands in the Jabal and foothill zone display two terraces (Fig. 2E), representing two major phases of aggradation recognized elsewhere in the Mediterranean region (Vita Finzi, 1969). The upper, older terrace deposits are silty with layers of pebbles towards the base and rest unconformably on strongly cemented gravels and pebbly mudstones at Wādī Ghān (Hey, 1962, p. 443). The lower terrace is fragmentary and comprised of sands and loose gravels. Vita Finzi (1971) proposed that the lower terrace deposits be termed the Lebda Alluvium and the upper terrace deposits, the Jifarah Alluvium, including not only the gravels with calcretes in the Jabal region but also the fine sand, silt and calcrete deposits of the Plain i.e. sediments which largely make up the Jifarah Formation (Fig. 2F).

It is clear that the gravels not only display important vertical variation in lithology, but that they were deposited in at least two episodes.

This was confirmed by the studies carried out by geologists of the Industrial Research Centre (I.R.C.), Libya in the course of regional geological mapping for production of the Geological Maps of Libya on the scale of 1:250000. El Hinnawy and Cheshitev (1975) defined the gravels as the Qaṣr al Ḥāj Formation recognizing two members (Fig. 2G). The lower, capped by a thick calcrete is comprised of strongly cemented conglomerates and conglomeratic mudstones. The upper, equivalent to the Wadi al Hira Formation of Jones (1969) reduced to member status, is largely unconsolidated gravel. El Hinnawy and Cheshitev (1975) correlated the thick calcrete with the Villafranchian calcrete noted above, thus placing the lower member in the Plio-Pleistocene. Given that the lower cemented member with calcrete cap can be correlated with the cemented gravels in Wādī Ghān (Anketell and Ghellali, 1988), thus subdividing the Jefara Alluvium (Vita Finzi, 1971) into two discrete phases of deposition, it is clear that interdigitation between the Gargaresh and Jifarah Formations in the coastal to medial zone is matched by that between the Jifarah and Qaṣr al Ḥāj Formations to the south.

Although El Hinnawy and Cheshitev (1975, fig. 11) imply that the three formations pass laterally one into the other, the relationships are nowhere discussed. Instead they state (1975, p. 42) that the "Pleistocene deposits ... were divided into the following rock units from top to base; Gargaresh Formation, Jeffara Formation and Qaṣr al Ḥāj Formation", implying that the Gargaresh deposits are younger than the Jifarah Formation and that this, as was also suggested by Desio (1971) and Jones (1969), is younger than the Qaṣr al Ḥāj Formation.

This interpretation was extensively modified by Ghellali (1977) (Fig. 2H). He subdivided the Jifarah Formation into a number of lithostratigraphic units that showed that each passed into penecontemporaneous Garagaresh and Qaṣr al Ḥāj deposits. An important factor in this work was the use of major calcrete horizons and bored surfaces as a means of correlation and subdivision. The sequences were further modified (Anketell and Ghellali, 1983) to produce a more refined lithostratigraphic subdivision of the Jifarah Formation and a clearer understanding of the nature of the surfaces which delimit the various units making up the Formation (Fig. 2I). Correlation of this succession with the Gargaresh Formation (Anketell and Ghellali, 1987) and the Qaṣr al Ḥāj Formation (Anketell and Ghellali, 1988) enabled their subdivision into discrete phases of distribution interrupted by periods of non-deposition, erosion and soil formation.

Correlation of the Jifarah sequence with the Gargaresh and Qaṣr al Ḥāj Formations

Jifarah Formation and Qaṣr al Ḥāj Formation

Figure 3 summarizes relationships between the Jifarah Formation and deposits exposed in the type areas of both lower and upper members of the Qaṣr al Ḥāj Formation (Anketell and Ghellali, 1988). In the Qaṣr al Ḥāj region a composite section, built up from wadi exposures east of the village, shows a closely comparable sequence to that of the Jifarah Formation although lithologies are much coarser. The

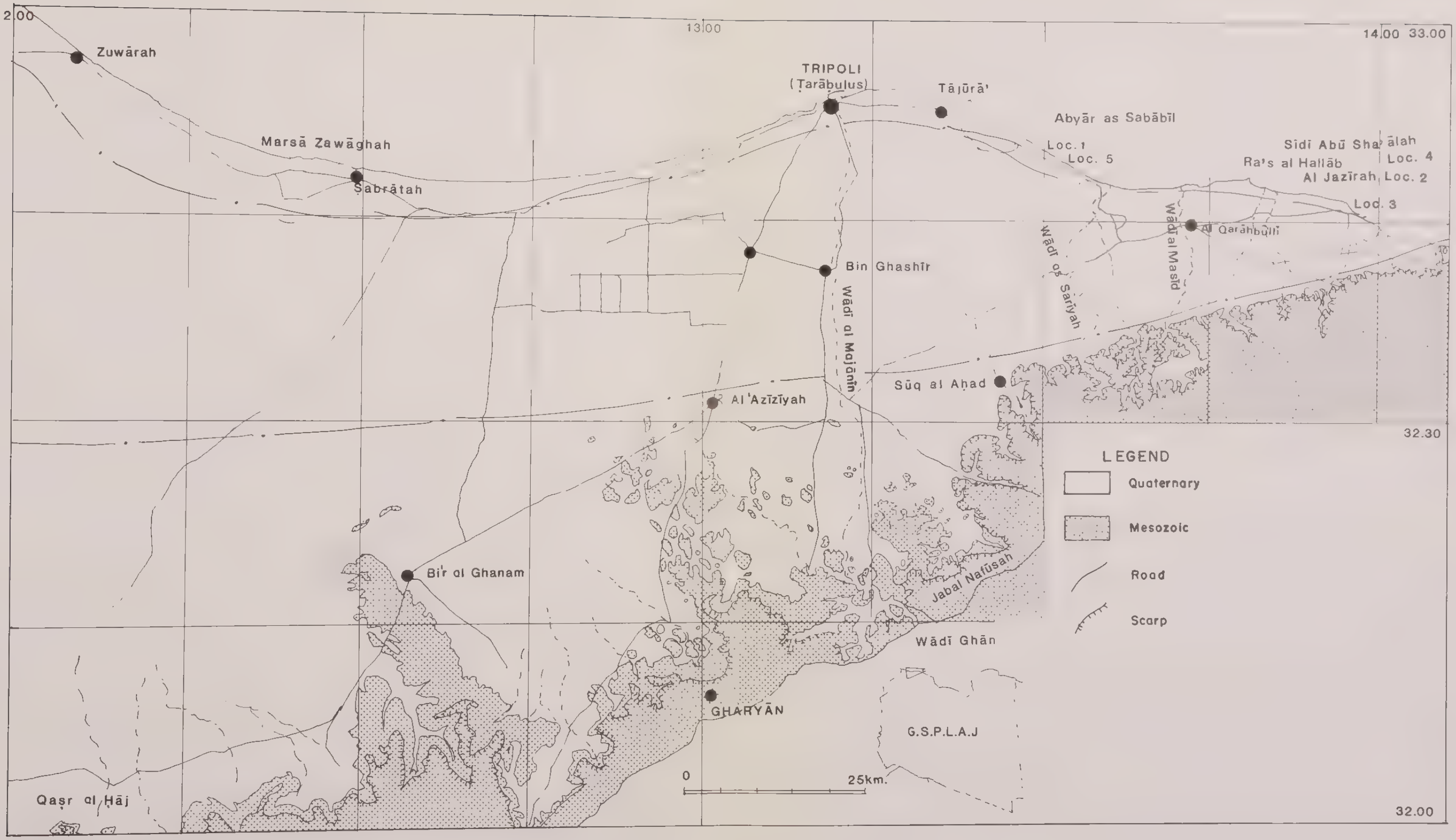
12.00
13.00
14.00
33.00
32.30
32.00
Zuwārah
Marsā Zawāghah
Şabrātah
TRIPOLI
(Ţarābulus)
Tājūrā'
Abyār as Sabābīl
Loc. 1
Loc. 5
Sīdī Abū Sha'alah
Ra's al Hallāb
Loc. 4
Al Jazīrah
Loc. 2
Loc. 3
Al Qarahbūllī
Wādī as Sāfiyah
Wādī al Masīd
Bin Ghashīr
Wādī al Majānīn
Sūq al Aḥad
Al 'Azīzīyah
Bi'r al Ghanam
Jabal Nafūsah
Wādī Ghān
GHARYĀN
G.S.P.L.A.J
Qaşr al Ḥāj
0
25km.
LEGEND
Quaternary
Mesozoic
Road
Scarp

Fig. 1. Map of the Jifārah Plain displaying general features and localities referred to in the text.

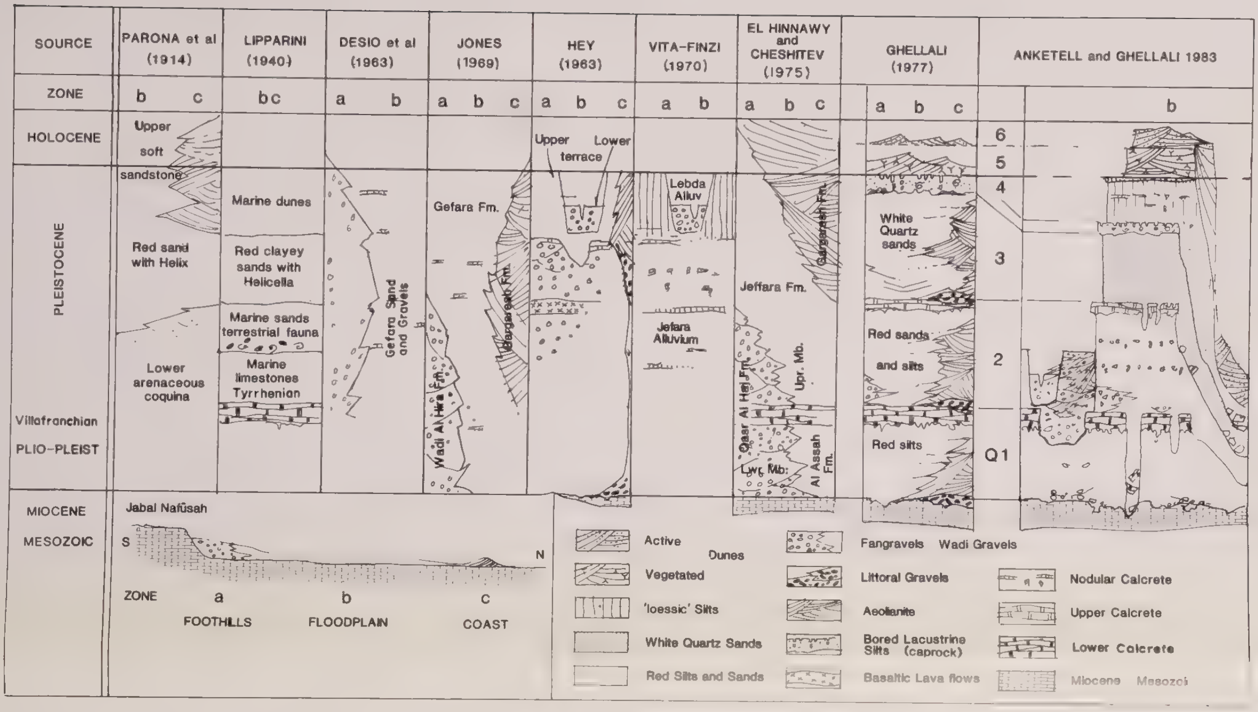
SOURCE
ZONE
HOLOCENE
PLEISTOCENE
Villafranchian
PLIO-PLEIST
MIOCENE
MESOZOIC
PARONA et al (1914)
b c
Upper soft sandstone
Red sand with Helix
Lower arenaceous coquina
LIPPARINI (1940)
bc
Marine dunes
Red clayey sands with Helicella
Marine sands terrestrial fauna
Marine limestones Tyrrhenian
DESIO et al (1963)
a b
Gefara Sand and Gravels
JONES (1969)
a b c
Gefara Fm.
Wadi Al Hira Fm.
Gargaresh Fm.
HEY (1963)
a b c
Upper Lower terrace
VITA-FINZI (1970)
a b
Lebda Alluv
Jefara Alluvium
EL HINNAWY and CHESHITEV (1975)
a b c
Jeffara Fm.
Gargaresh Fm.
Qasr Al Haj Fm.
Upr. Mb.
Lwr. Mb.
Al Assah Fm.
GHELLALI (1977)
a b c
White Quartz sands
Red sands and silts
Red silts
ANKETELL and GHELLALI 1983
b
6
5
4
3
2
Q1
Jabal Nafūsah
S
N
ZONE
a
b
c
FOOTHILLS
FLOODPLAIN
COAST
Active
Vegetated
Dunes
'loessic' Silts
White Quartz Sands
Red Silts and Sands
Fangravels
Wadi Gravels
Littoral Gravels
Aeolianite
Bored Lacustrine Silts (caprock)
Basaltic Lava flows
Nodular Calcrete
Upper Calcrete
Lower Calcrete
Miocene
Mesozoic

Fig. 2 Stratigraphic terminology of Quaternary deposits in the Jifārah–Jabal Nafūsah region — a comparative chart.

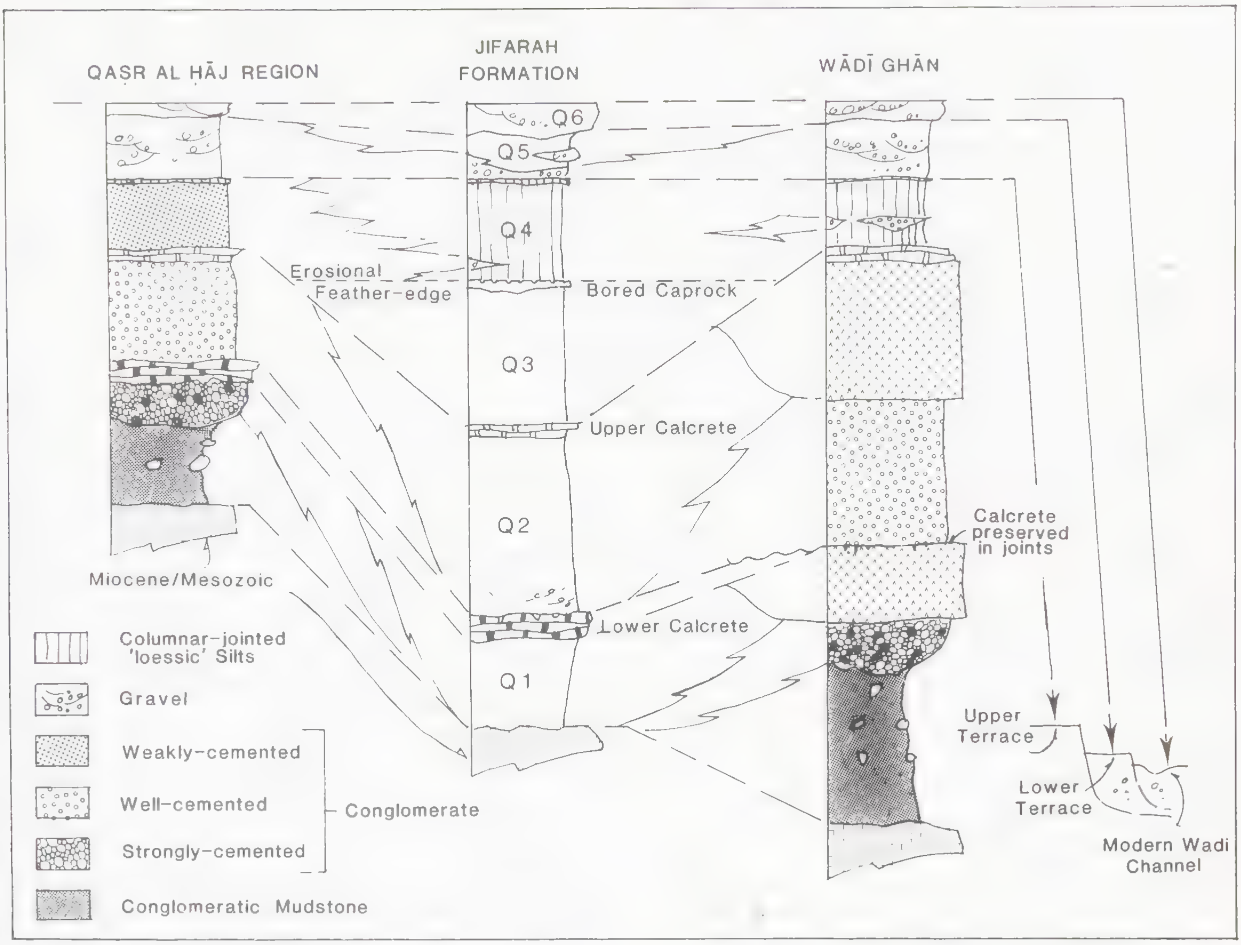
QAṢR AL ḤĀJ REGION
JIFARAH FORMATION
WĀDĪ GHĀN
Q6
Q5
Q4
Erosional
Feather-edge
Bored Caprock
Q3
Upper Calcrete
Q2
Calcrete preserved in joints
Lower Calcrete
Q1
Miocene/Mesozoic
Columnar-jointed 'loessic' Silts
Gravel
Weakly-cemented
Well-cemented
Strongly-cemented
Conglomerate
Conglomeratic Mudstone
Upper Terrace
Lower Terrace
Modern Wadi Channel

Fig. 3. Correlation of the major depositional units of the Jifarah Formation with the Qaṣr al Ḥāj Formation in the A. Qaṣr al Ḥāj and B. Wādī Ghān regions.

equivalent of unit Q1, defined by a strongly unconformable base and capped by the Villafranchian calcrete, comprises well cemented conglomerate overlying conglomeratic mudstone. The equivalent of Q2, comprised of less well cemented conglomerates, is in turn capped by the upper calcrete. This is overlain by weakly cemented gravels which pass northward and upward into the characteristic columnar-jointed silts of unit Q4 of the Jifarah Formation. The upper surface of this unit, which forms the Jifārah Plain and, where cut by wadis, the upper terrace, is locally capped by a thin calcrete.

Sediments of the lower terrace making up Unit Q5 and the modern wadi gravels of Unit Q6, display relationships to the older sediments similar to those seen to the north but are much coarser. They are easily identifiable throughout the Qaṣr al Ḥāj region although the lower terrace is commonly fragmentary.

At Wādī Ghān (Anketell and Ghellali, 1988) (Fig. 3) the succession comprises a conglomerate/gravel sequence containing two lava flows. The conglomerate sequence underlying the lower lava is similar to that underlying the Villafranchian calcrete at Qaṣr al Ḥāj while the gravels between the lavas are similar to those which succeed it. Correlation with the Qaṣr al Ḥāj and Jifarah sequence is, however, complicated in that here there is only one calcrete, resting on the upper of the two lava flows. However, the upper part of the lower lava flow displays laminar calcite-filled joints similar to those which invade the upper lava flow from the base of the calcrete. Furthermore, the younger gravels contain abundant pebbles of calcrete and locally, where the lavas converge, are composed entirely of these. There seems little doubt that the source of the pebbles was the Villafranchian calcrete, eroded so that only the veins remain. This erosional surface is the unconformity which defines the base of Q2 elsewhere (Anketell and Ghellali, 1988), in which case, the conglomerates below the lower lava are equivalent to Q1 while those sandwiched between the lavas are equivalent to Q2 (Fig. 3).

Columnar-jointed terrace silts and gravels in the Wādī Ghān area are clearly equivalent to Q4 and the silty upper part of these beds indicate a substantial southward incursion of the Jifarah Formation. The lower surface is strongly unconformable on underlying beds cutting down across the lavas, gravels and calcrete.

Equivalents of Units Q5 and Q6 in the Wādī Ghān area are easily identified and can be correlated along the lengths of the wadis, particularly in the eastern Jifārah region. Both deposits are very much coarser and thicker than their "downstream" Jifārah equivalents with which they grade and interdigitate.

El Hinnawy and Cheshitev (1975) recorded the type section of the upper member of the Qaṣr al Ḥāj Formation from the Wādī Ghān area. They do not quote a precise locality, however, it would appear from the accompanying plate (*ibid*, Pl. 11) that the section is in lower terrace deposits exposed in the walls of the modern wadi channel. The upper member as defined by El Hinnawy and Cheshitev (1975) thus corresponds to Q5 only.

Sediments equivalent to Member Q3 of the Jifarah Formation are absent from the Qaṣr al Ḥāj Formation both at Qaṣr al Ḥāj and Wādī Ghān and have not been recognized anywhere in the southern region. It can be demonstrated that they thin out to a feather edge in the eastern Jifārah (Anketell and Ghellali, 1983). In the area west of Bin Ghashīr they appear to have been removed by a combination of intraformational erosion and wedging out since, throughout this region, Unit Q3 is followed by Units Q4 and/or 5 and 6.

Jifarah and Gargaresh Formations

Subdivision of the Gargaresh Formation into six members corresponding to those of the Jifarah Formation is discussed by Anketell and Ghellali (1987). The major surfaces of erosion which define the lower surfaces of the Jifarah members are generally easily distinguished although their correlation demands care. The calcretes are less useful because they are either absent or thin and impersistently developed. Instead the deposits may show extensive veining and strong pervasive calcite cementation. This is generally accompanied by honeycomb weathering and solution pits, often associated with calcified and silicified rhizoids.

Figure 4 shows the relationships between the Jifarah and Gargaresh Formations in a number of cliff sections, only some of which are now accessible. Members of the Gargaresh Formation contemporaneous with Q1 and Q6 are designated GQ1 to GQ6. Aeolianites are identified by the suffix a, marine sands, gravels and coquinas by the suffix m. GQ1 deposits are seen in cliffs to the east at Abyār as Sabābīl (Fig. 1, Loc. 1; Fig. 4B) where Q1 silts, capped by Villafranchian calcrete pass northward across a marine platform into conglomerates and planar cross-bedded calcarenites (GQ1m). The conglomerates are succeeded by aeolian cross-bedded calcarenite in a small sea stack without a break, suggesting that they are pre-lower calcrete in age and equivalent to the indurated and calcreted silts of Q1 (Anketell and Ghellali, 1987). GQ2 deposits resting either on Miocene or on Villafranchian calcrete are seen at a number of localities, however, only one clearly displays GQ2a deposits. At Locality 2 (Figs 1, 4D), Q2 silts, capped by the upper calcrete, rest on Q1 deposits and pass northwards into and onto GQ2a dune cross-bedded calcarenites. The lower calcrete has been eroded at this locality so that both the Q2 red silts and the GQ2a deposits rest on an erosional surface within Q1 silts. These, which contain calcrete nodules and are strongly reddened, rest unconformably on Miocene limestones. The upper calcrete thins and all but disappears as the calcarenite is approached reducing to a patchily developed, laminated skin up to 5 mm in thickness with thin veins which invade the calcarenite along irregular joints. The surface of the calcarenites is deeply pitted by solution pipes which post-date the thin calcrete layer. No beach sands or gravels have been observed and GQ2a deposits rest directly on the erosional lower surface of the member.

Beach deposits occur at a number of localities typified by that illustrated in Fig. 1, Loc. 3, Fig. 4E (Anketell and Ghellali, 1987). Here Q2 silts, capped by upper calcrete and resting on an erosional surface cut in the lower calcrete and Miocene limestones, pass northward into beach sands and conglomerates. GQ2m conglomerates, succeeded by Q2 red silts with calcrete nodules and a well-developed upper calcrete, may also be seen at Loc. 4, Fig. 1, resting in a cliff notch cut in Miocene limestones and sandstones (Fig. 4F). The upper calcrete is overlain by aeolianites and beach gravels equivalent to Q3 (Anketell and Ghellali, 1987).

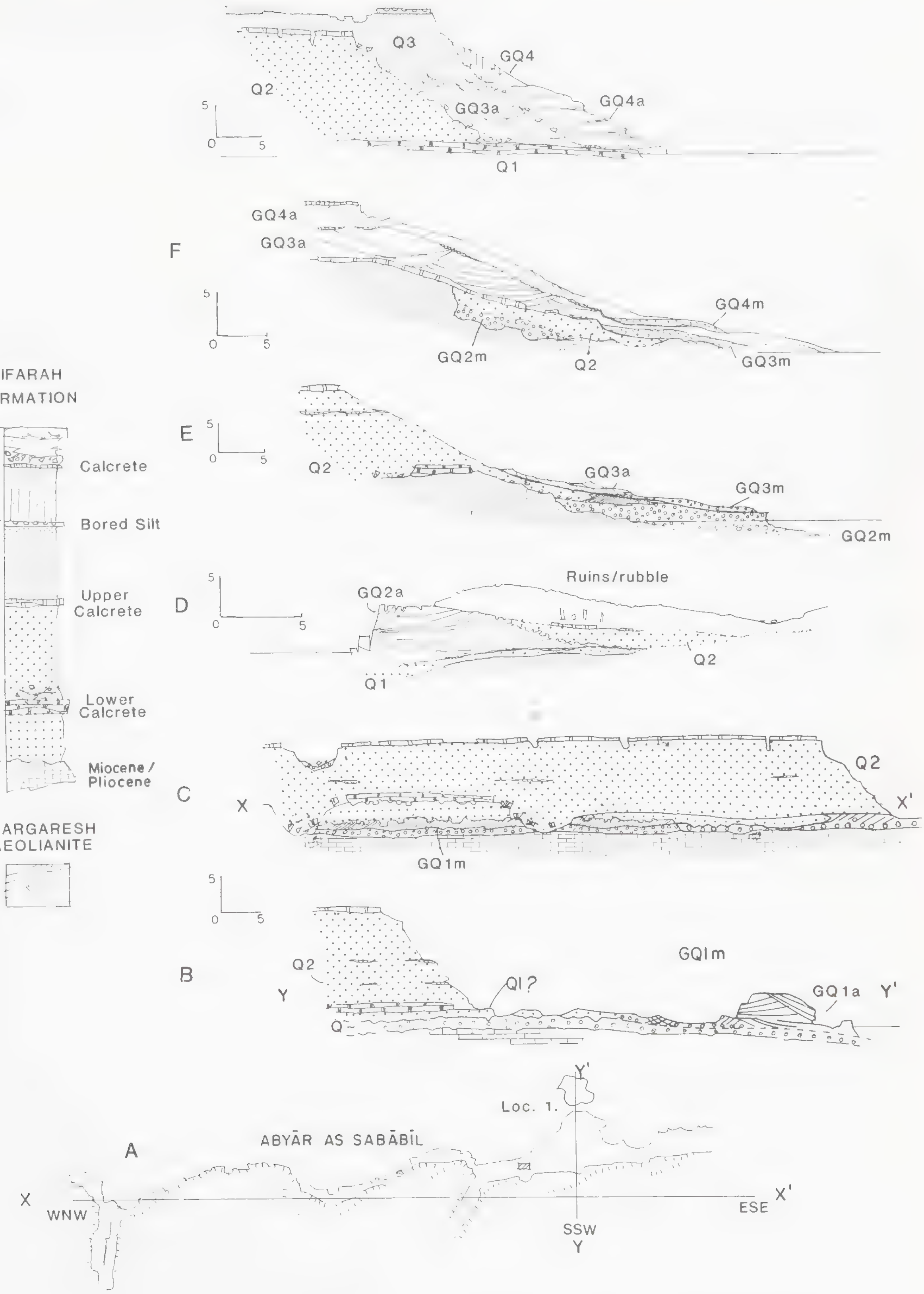
Q3
GQ4
Q2
GQ3a
GQ4a
5
0
5
Q1
GQ4a
GQ3a
F
5
0
5
GQ4m
GQ2m
Q2
GQ3m
JIFARAH
FORMATION
Q6
Q5
Calcrete
Q4
Bored Silt
Q3
Upper
Calcrete
Q2
Lower
Calcrete
Q1
Miocene /
Pliocene
GARGARESH
AEOLIANITE
E
5
0
5
Q2
GQ3a
GQ3m
GQ2m
D
5
0
5
GQ2a
Ruins/rubble
Q2
Q1
C
X
Q2
X'
GQ1m
5
0
5
B
Q2
Y
GQIm
QI?
GQ1a
Y'
Q
Y'
Loc. 1.
A
ABYĀR AS SABĀBĪL
X
WNW
SSW
Y
ESE
X'

Fig. 4. Correlation of the major depositional units of the Jifarah Formation with the Gargaresh Formation.

GQ3 deposits comprise the most spectacular developments of Gargaresh Formation in the region, commonly forming cliff-hugging dunes (Fig. 4G; Fig. 1, Loc. 5). These are banked against cliffs cut in Q2 red silts and rest either on a horizon cut low in Q2 or on the exhumed surface of the lower calcrete. Gargaresh deposits here and in immediately neighbouring localities appear to be aeolian, however, the cliff against which they are banked displays a well-developed basal notch and the surface on which they rest displays borings comparable to *Gastrochaenolites* attesting to a phase of marine erosion prior to their deposition. At some localities a thin layer of silt with fragments of calcrete is sandwiched between the platform and the aeolianites. This is interpreted as a continuation of the scree which is occasionally preserved on the fossil cliff face. The aeolianites pass up into white sands capped by a grey silt layer, the top surface of which is extensively bored by tube-dwelling bees (Anketell and Ghellali, 1984). Beach deposits of GQ3 age are common and may be seen, overlain by aeolianites, in the eastern Jifārah at Locs. 3 and 4 (Figs 1, 4E and F). Throughout this region the passage from the white sands and grey silt capping of member Q3 into Gargaresh aeolianites and coquinas is exposed in deflation hollows between modern dunes of member Q6.

Gargaresh aeolianites equivalent to member Q4 make up the bulk of the Gargaresh deposits in the Tripoli region, forming much of the consolidated dune belt which runs from Tājūrā' to Ṣabrātah and beyond. Spectacular outcrops also occur in the coastal zone between Wādī al Masīd and Ra's al Hallāb where they interfinger with buff columnar silts characteristic of Q4. These also occur at Marsā Zawāghah, resting with marked unconformity on the upper calcrete and Q2 member of the Jifarah Formation (Anketell and Ghellali, 1987). It has not been possible to identify GQ4m deposits with any certainty. Marine sands and gravels which follow GQ3a and GQ3m deposits at Locality 3, (Figs 1, 4E) may be of this age although they could be GQ5 or possibly a part of GQ3. Relationships between the two Formations in this region are as yet unresolved.

Calcarenite equivalents of the quartz-rich, orange-yellow sand dunes which make up the inter-wadi facies of member Q5 of the Jifarah Formation, occur patchily immediately to the east of Ra's al Hallāb and to the west of Tājūrā' where they are often indistinguishable from GQ4a. The aeolianites are well-cemented and rest on a sub-horizontal wave-cut platform, elevated 70 to 80 cm above sea level. The platform, cut in older Gargaresh deposits, continues offshore as a series of flat topped islets.

Gargaresh equivalents of member Q6 comprise beach sands and gravels reworked from older deposits from which they derive their calcareous composition. The modern aeolian sands are only very locally calcarenitic.

Summary

It is clear that the three formations are laterally equivalent one to the other and that this relationship has persisted from pre-"Villafranchian" times. The observation by both Desio *et al.* (1963) and Jones (1969) that the Jifarah Formation partially succeeds the Qaṣr al Ḥāj Formation is substantiated to a certain degree in that member Q4 of the Jifarah Formation extends well into the Jabal to rest on gravel deposits of the Qaṣr al Ḥāj Formation. In addition, there tends to be a general fining upwards in the gravel sequences, particularly in the lower terrace deposits making up member Q5.

The interpretation of the relationship between the Jifarah and Gargaresh Formations expressed by El Hinnawy and Cheshitev (1975) arises from stratigraphic relationships in the region which include the type localities they propose for both formations. At its type locality, the Jifarah Formation is succeeded by Gargaresh aeolianites. It can be shown, however, that the Jifarah deposits are equivalent to Q2 only and that the succeeding aeolianites, separated from the Jifarah silts by the upper calcrete, are GQ4 in age. While the interpretation of El Hinnawy and Cheshitev is valid in depicting the unconformable relationships which exist between members of the two formations, it masks the importance of facies relationships characteristic of sequences within the members and formations as a whole.

SEDIMENTARY HISTORY

Quaternary deposits of the Jifārah region have been subdivided into six members Q1 to Q6, bounded and separated from each other by surfaces of unconformity (Anketell and Ghellali, 1983). Deposition within members was more or less continuous with minor phases of soil formation. They display appreciable vertical and marked lateral variation in facies and, although significant differences exist between one member and another, patterns of facies variation are fundamentally the same. Each unit is deposited on a surface of erosion and is terminated by a period of non-deposition, generally leading to soil formation which is in turn terminated by the onset of the erosional episode preceding or concomitant with the next phase of sedimentation. This produces, between each depositional phase, a zone of unconformity which may display complex sediment relationships resulting from variable interplay between processes of soil formation, solution and erosion.

Depositional Facies

Gargaresh Formation

The Gargaresh Formation is characterized by two facies — dune-bedded calcarenites and shelly conglomerates with sands.

1. Dune bedded calcarenites.

Description. Buff to light grey, medium to coarse grainstones comprised predominantly of skeletal fragments of marine organisms. Locally the deposits contain high proportions of ooliths and quartz grains (Ghellali, 1977), generally well cemented by microsparite and occasionally by acicular aragonite. Porosity ranges up to 30% and is mainly intergranular. Moldic porosity, due to solution of land snails is minor. Horizons rich in root moulds (*dikaka*) are common. Fauna varies from marine microfauna to terrestrial gastropod macrofauna characterized mainly by *Helix* sp. The dominant feature of the deposits is large-scale dune cross-bedding. Dune shapes are preserved in young deposits.

Interpretation. The aeolian origin of the calcarenites is confirmed by the dune bedding and, in many instances the dune morphology. The significant feature is that they are composed of shell debris derived from marine organisms even though their macrofauna is typically terrestrial. Deposits of this type are widespread in the Mediterranean basin, occurring almost continuously along the North African and eastern Mediterranean coasts and locally around European shores and Mediterranean islands. They originated by reworking of "freshly exposed marine sediments during the regressions of world sea level that accompanied the advance of continental glaciers" (Butzer, 1972, p. 223). Butzer also points out (1972, p. 224) that while the deposits are "mainly lime sands, overwhelmingly derived from the rubble of marine organisms. In areas of bedrock other than limestone the importance of quartz and other minerals may jump ... to as much as 90%". Yaalon (1967, p. 1198), while agreeing that "major almost continuous ridges parallel to the beach, are no doubt indicative of early regressive phases during glacial advances", cautions against interpreting all aeolianites in this way. He notes that reworking of existing calcarenites results in dune formation unrelated to sea level fall and that it is dangerous to derive sweeping conclusions regarding either sea level change or palaeoclimates from aeolianites unless there is additional and independent evidence to hand.

2. Shelly conglomerates and sands

Description. Buff, pale brown to grey conglomerates comprised predominantly of limestone and rare sandstone pebbles derived from Miocene and Mesozoic formations. Calcrete pebbles are an important addition in younger developments. They are clast supported with a matrix of fine- to medium-grained calcarenite. Pebbles range up to 40 cm, are well rounded and commonly extensively bored by *Trypanites* ichnofacies. Often very shelly with whole to fragmented remains of a variety of bivalves and gastropods, the deposits are generally strongly cemented with fairly high intergranular porosity and locally, a high moldic porosity. Interbedded sands are closely similar to the aeolianites but display tabular cross-bedding and usually contain whole or fragmented, large marine shells. The conglomerates and sands always rest with sharp erosional unconformity on the underlying deposits.

Interpretation. The marine faunas, coarseness of the deposits and tabular cross-bedding closely comparable to that described by Elliot (1978) from beach environments, indicate that the deposits were laid down in near to onshore environments. At several localities the conglomerates are banked against cliffs which have a characteristic cliff notch and rest on platforms eroded in older deposits and bored by *Gastrochaenolites.* The association is closely comparable to wave-abraded marine platforms and cliff conglomerates described by Radwanski (1970, p. 372) as typical of cliff development in areas facing the open sea.

The Jifarah Formation

1. Pebbly sands

Description. Red and brown sands and coarse silts with limestone, calcrete and rare sandstone and basalt pebbles up to 5 cm in diameter, either widely scattered or concentrated in thin stringers. Sand and coarse silt grains are predominantly quartz with minor amounts of feldspar and are generally coated with a thin pellicle of goethite or limonite which gives the deposits their characteristic colour. The dominant sedimentary structure is shallow, trough cross-bedding and shallow, isolated channels.

Interpretation. These deposits compare closely with gravelly sand deposits seen in modern wadis and in the toe zone of alluvial fans in the Jifārah region. Occasional mud-clast horizons result from erosion of mud flakes formed by desiccation of ephemeral ponds in wadi courses and floodplain depressions.

2. Fine quartz sands

Description. These range from red to brilliant white in colour depending on the presence or absence of goethite grain coatings. Internal sedimentary structures are commonly difficult to distinguish, largely as a result of a high degree of sorting and their mineralogical maturity. Individual lamina are thin, seldom exceeding 2 mm, and range in attitude from horizontal to dips of 35° in cross-bedded units. Young deposits commonly display a dune-shaped top surface.

Interpretation. Much of the fine sand facies is aeolian in origin, particularly obvious where internal cross-bed structure can be married to dune geometry, which is the case with the modern sands and some of the younger deposits. Horizontally laminated beds are interpreted as fluvio-aeolian deposits, mainly dune material reworked by sheet-wash. Modern environments show that there is a complex interplay between aeolian and fluvial deposits with aeolian reworking of fluvial sands and *vice versa.*

3. Columnar jointed silts

Description. Tan to yellow, coarse, porous silts in units up to 1.5 m thick, characterized by columnar jointing which is often quite regular. The beds are commonly calcareous and the older deposits contain irregular calcrete concretions developed around fine root systems. Land snails are locally abundant. Grain size ranges from very fine sand to silt but as yet no clear field distinctions have been made.

Interpretation. This deposit displays many of the characteristics of loess, and was interpreted as such by Stella (1914) and Rathjens (1928). On the other hand, Penck (1909) points out that much of the Tripolitanian "loess" is in effect a fine sand, considered too coarse to be transported by aeolian suspension. Its structural similarity to loess was interpreted as largely due to cementation by calcium carbonate in combination with a small proportion of silt and clay.

The deposits are best referred to as "loessic" or loess-like. It is probable that they comprise a mixture of true loess and loess which has been reworked and mixed with contemporaneous, fine dune sands by alluvial processes such as sheet-wash (Butzer, 1972).

4. Calcareous grey quartz sands

Description. These deposits are present at one horizon only but comprise a very distinct facies. They consist of fine, light grey quartz sand and silt very similar to facies 2 of the Jifarah Formation but with a higher calcium carbonate content. They locally pass into white sandy limestone. The carbonate cement gives the deposits a higher resistance to erosion than surrounding sediments causing them to stand out as a distinctive "caprock". The deposits contain a rich fauna of freshwater gastropods. The surface of the grey sands is extensively invested with chambered borings similar to those made by masonry bees (Anketell and Ghellali, 1984).

Interpretation. The gastropod fauna contains species characteristic of still and slow moving water and indicates that the deposits accumulated in shallow freshwater ponds or lakes. The calcareous cement may be partly contemporaneous or early diagenetic. The possibility of some being due to soil formation is not discounted.

Qaṣr al Ḥāj Formation

1. Conglomeratic mudstones and siltstones

Description. Typically matrix supported and comprised of large pebbles up to 80 cm in diameter "floating" in a silty clay groundmass. The large fragments, which are generally quite well rounded, consist of Mesozoic limestones and sandstones together with Tertiary basalts.

Interpretation. The paraconglomeratic texture and gross morphology of the deposits suggest that they are debris flows.

2. Conglomerates and sandy conglomerates

Description. These contrast strongly with the conglomeratic mudstones in being clast supported and either matrix free or with a pervasive sand matrix. Older deposits tend to be matrix-rich and are progressively more strongly cemented resulting in a marked decrease in intergranular porosity with age. The clasts, which vary from subangular to well-rounded, range up to 2 m but more commonly they fall within the range 5 cm to 85 cm. Compositions cover the range of all the older deposits of Mesozoic and Tertiary age in Jabal Nafūsah and include pebbles derived from intra-Quaternary calcretes. Sedimentary structures tend to be masked by the scale of the clasts, however, trough cross-bedding is common in finer layers. These conglomerates are found in linear bodies along wadis and in fan cones along the Jabal front.

Interpretation. The coarse gravels are fluvial in origin. The sand matrix is largely due to infiltration from later fluvial and aeolian sands. Cementation is primarily a function of soil formation with development of calcrete.

Facies Associations

The various facies are distributed within members in the following manner:

Member Q1. With the exception of the Qaṣr al Ḥāj Formation, the beds making up this sequence are as yet known from only a few localities at and near the coast in the eastern Jifārah region. Debris flow deposits capped by alluvial fan gravels in the southern region pass northward into fluvial and colluvial silts and conglomeratic silts at the coast. In the coastal zone, a few exposures show pebbly silts resting unconformably on marine gravels and passing laterally into sands and shelly gravels which are succeeded by aeolianites. Inland, beds occupying a similar stratigraphic level to the coastal aeolianite, are typically "loessic" deposits interbedded with alluvial muddy silts. The unit is terminated by development of a thick calcrete which displays deep solution pits at a number of localities in the eastern Jifārah region.

Member Q2. The contact between Member Q2 and Q1 is always erosional, often with complete removal of the lower calcrete. From the southern zone, coarse fan and channel gravels grade northward into a thin sequence of red, fluvial pebbly siltstones and fine silty sands which pass upwards into a thick sequence of interbedded "loessic" deposits and fine alluvial silts. In the coastal zone, thin pebbly basal deposits lap over onto marine gravels displaying both unconformable and conformable relationships. The coarse lower beds contain horizons of red clay. At Al Jazīrah, the red silts prograde over a calcarenite dune and both deposits rest on a substrate of Q1 silts. The absence of the lower calcrete from beneath both deposits attests to very effective erosion at the base of the member prior or related to the marine retreat which preceded aeolianite formation. Erosion may have been marine, however, the absence of marine gravels militates against such a conclusion. It is, however, possible that only marine sands were produced and that these were subsequently incorporated in the aeolianite. Alternatively the area may have been above sea level and subjected to terrestrial erosional agencies only. Strong rubefaction of the underlying deposits suggests that this may have been the case.

Q2 deposits are terminated by the upper calcrete which is normally fairly flat with an overall gentle northward dip. Locally, however, it is hummocky and appears to have preserved dune topography. The most important topographic feature is seen in cliffs west of the mouth of Wādī al Masīd area where the calcrete preserves the shape of a gently dipping valley which subsequently formed a trap for a thick accumulation of Q3 deposits (Anketell and Ghellali, 1983).

Major features of the calcrete were noted above. The red soil which is present in many solution pits forms a thicker deposit in the fossil valley of Wādī al Masīd, probably due to reworking by slope wash.

Member Q3. This member is not developed in the southern region. It appears around parallel 32°40′ and thickens northward from a feather edge in the eastern Jifārah region but disappears west of Bin Ghashīr due to intraformational erosion. Throughout the area it comprises pure white quartz dune sands interbedded with buff to yellow "loessic" silts which increase in importance upward. The deposits are capped by the grey and white lacustrine silts and silty limestones which thicken in dune troughs and thin over dune crests. These beds are locally capped by a patchy calcrete crust up to 1.5 cm thick. Inland the member succeeds member Q2 with apparent conformity, however, the sands pass into cliff-hugging dunes all along the eastern Jifārah coast. If it were not for these and the spectacular fossil cliffs cut in Q2 which they bury, it would be difficult to prove that an important phase of erosion occurred prior to deposition of the sands. The relationship of Q3 sands to contemporaneous marine gravels differs from that displayed by the older members in that, throughout the area, GQ3m coquinas and gravels are always overlain by GQ3a aeolianite rather than by sands and silts.

Member Q4. "Loessic" deposits of member Q4 are found from the southern region to the coast. They rest with sharp unconformity on sediments of Q2 age in the south of the region where Q3 is absent and are also unconformable on Q3 in the medial and coastal zones. This is particularly apparent in the coastal region. In the south deposition commences with fluvial and colluvial gravels, stringers and lenses of which are found throughout the loess deposits in the Jabal. Rarely, in the vicinity of wadis the complete unit is comprised of gravel. In the medial Jifārah zone, gravels die out and the member comprises "loessic" deposits with local white sands reworked from member Q3. Brown soil horizons are common. At the coast the silts pass into Gargaresh aeolianite. The deposits are locally capped by a very thin calcrete and reddish soil.

Member Q5 and Member Q6. These display very similar characteristics with fluvial gravels fining northward in wadis which debouch from the main Jabal valleys and fangravels which grade out from the Jabal front. In the inter-wādī regions they are characterized by aeolian sands and fine silts which commonly lap over in the wadis where they are reworked by flood water.

The older dunes rest on the reddish soil noted above and pass into aeolianite in the coastal region. The modern dunes show only minor development of aeolianite derived from deflation and erosion of older deposits.

Zones of Unconformity

These zones are characterized by non-depositional phenomena such as erosion, solution, bioerosion and soil formation.

Erosional surfaces

Erosional surfaces mainly developed in response to marine and fluvial processes. Deflation by aeolian processes is less common or perhaps, less easy to recognize.

Large-scale fluvial erosion is seen in both ancient and modern wādī courses with removal of all or substantial parts of older units along well-defined linear trends. Terraces are well developed in the two youngest units.

Marine erosional surfaces capped by beach deposits are particularly important in the eastern Jifārah region where fossil cliffs with cliff notches and wave-cut platforms allow relative dating of units both within and between the Jifarah and Gargaresh Formations.

Deflation surfaces may be common but have only been observed with certainty in the western Jifārah where the surface of the upper terrace is sculpted into dune forms unrelated to the sub-horizontal bedding which typifies the internal structure of the deposits.

Soil formation

Soil profiles constitute excellent natural marker horizons especially useful in subdividing monotonous, non-fossiliferous sequences (Steel, 1974).

Calcrete. Calcrete displaying a wide range of morphologies indicative of varying stages of development, is one of the most striking features of the Jifarah Formation. Problems concerning the genesis and significance of such deposits are well documented by Gile *et al.* (1966), Goudie (1973), Steel (1974), Reeves (1976), and Birkeland (1984). Nodular calcretes (Stage II, Gile *et al.*, 1966) predominate, forming horizons which can be followed for tens of metres and can, with care, be used to correlate between closely adjacent outcrops. These horizons are particularly useful for recognition of erosional events within major units.

Two calcretes within the succession have developed a Stage IV profile (Gile *et al.*, 1966). The lowermost and thicker of these is the "Villafranchian" calcrete referred to above. Both display a well-laminated, highly indurated hardpan capping honeycombed and nodular lower levels (Netterburg, 1967). Tepee structure (Price, 1925; Reeves, 1976) is widely developed in the lower calcrete which locally also displays pisolitic structure and micro-lamination at its top and along joint surfaces (Kornicker, 1958; James, 1972). Both calcretes are developed in a variety of substrates ranging from silts to gravels with little significant change in character other than an increase in thickness in gravel deposits. The two units constitute the most significant marker horizons in the region and are important not only in correlation within the Jifarah Formation but, as is shown above, also in its correlation with the Gargaresh and Qaṣr al Ḥāj Formations. Since the same horizon may display different profiles from one area to the other depending on the nature of the substrate, correlation must be carried out with care.

Terra rossa. Soils of this type are much less common than calcrete and are only patchily preserved, commonly in solution pit infill. They are accompanied by a marked reddening of the associated sediments. Although volumetrically insignificant, they are valuable marker horizons and also play a significant role in environmental interpretation of the Quaternary sequence.

Surfaces of non-deposition such as wave-washed platforms and soil surfaces commonly display associated "minor" features which help in their recognition particularly where they separate two deposits of similar lithology.

Solution

Solution phenomena generated during surface or near-surface exposure are particularly well developed in association with the two main calcrete horizons and on Miocene limestone bedrock. Two types are common, (1) enlarged fissures and joints and (2) solution pipes which are independent of joint systems. Enlarged fissures and joints are common in the Miocene and Mesozoic limestones of the substrate and reach depths in excess of one metre, producing a complex network of fissures now filled with the succeeding sediment. The lower calcrete is locally invaded by fissures a few centimetres in depth. Solution pipes, generally cylindrical but occasionally ovate in cross section and ranging from 0.7 m in diameter to 2 m in depth, are one of the most striking features of the major calcrete horizons. Within the sequence they contain a fill comprised of the *terra rossa* soil with well-developed root systems. Association with *terra rossa* and root systems argues for their formation by leaching of the calcrete beneath and around tree root systems (Jennings, 1968; Perkins, 1977). In wadis and marine platforms, where the pipes are exposed to recent erosion, they are generally either empty or filled with recent deposits. It is possible that some of these may result from erosional potholing, however, their morphological similarity to, and close association with, soil-filled types argues for the majority having a similar origin.

Bioerosion

Surfaces developed under conditions of restricted or arrested sedimentation may be accentuated by boring and burrowing organisms. The upper surface of the lower calcrete displays a *Trypanites* ichnofauna dominated by *Gastrochaenolites* at several localities in the coastal region. The borings, filled with the succeeding sediment, indicate that the break in deposition recorded by the top surface of the calcrete has a complex history, ranging from soil formation through to marine bioerosion.

Although marine borings are the most widely documented (Warme and McHuron, 1978) borings, particularly those of insects, are common in a variety of terrestrial environments (Ratcliffe and Fagerstrom, 1980). Within the Jifarah Formation the surface of the grey silts capping Q3 is characterized by the borings of tube-dwelling bees (Anketell and Ghellali, 1984). Their absence would make it more difficult to establish that the surface records a substantial hiatus in sedimentation.

Association of non-deposition phenomena in unconformable zones

While each of the phenomena discussed above is individually of interest it is their association which is significant in unravelling the sedimentologic history of the Quaternary deposits. They occur in combinations of varying complexity but each with the same basic pattern. The most complex association occurs between units Q2 and Q3 (Fig. 5).

The Q2 depositional sequence is terminated by development of the upper calcrete (Anketell and Ghellali, 1983). Its relationship to the underlying strata suggests that the surface on which it was developed had an appreciable erosional topography in some areas and that channelled fluvial erosion of Q2 deposits occurred prior to its formation (Anketell and Ghellali, 1984).

The calcrete underwent solution with development of large solution pipes infilled by *terra rossa*. Since Stage IV calcrete developments represent only the K to Kml horizon of the soil profile, the upper part of the profile must have been removed prior to, or at the same time of *terra rossa* formation, probably by a combination of erosion and solution.

The *terra rossa* has, in turn, been eroded, reworked and locally incorporated in the overlying succeeding unit as red silty sands so that it is preserved only in the pipes and the white sands generally rest directly on the calcrete.

Erosional contacts between the succeeding depositional unit and the soil units is the dominant relationship within the Jifarah and the Qaṣr al Ḥāj Formations. Where the soil horizons are completely eroded and successive depositional sequences display similar lithologies, recognition of the erosional unconformity and in particular, distinguishing between those which are of regional rather than local importance, is difficult.

The proposed sequence of events leading to formation of the inter-member sediment packets is summarized in Fig. 6. Following deposition (A), a calcrete profile developed (B). A phase of erosion which removed the upper part or all of the calcrete (C) was followed by solution prior to, or contempo-

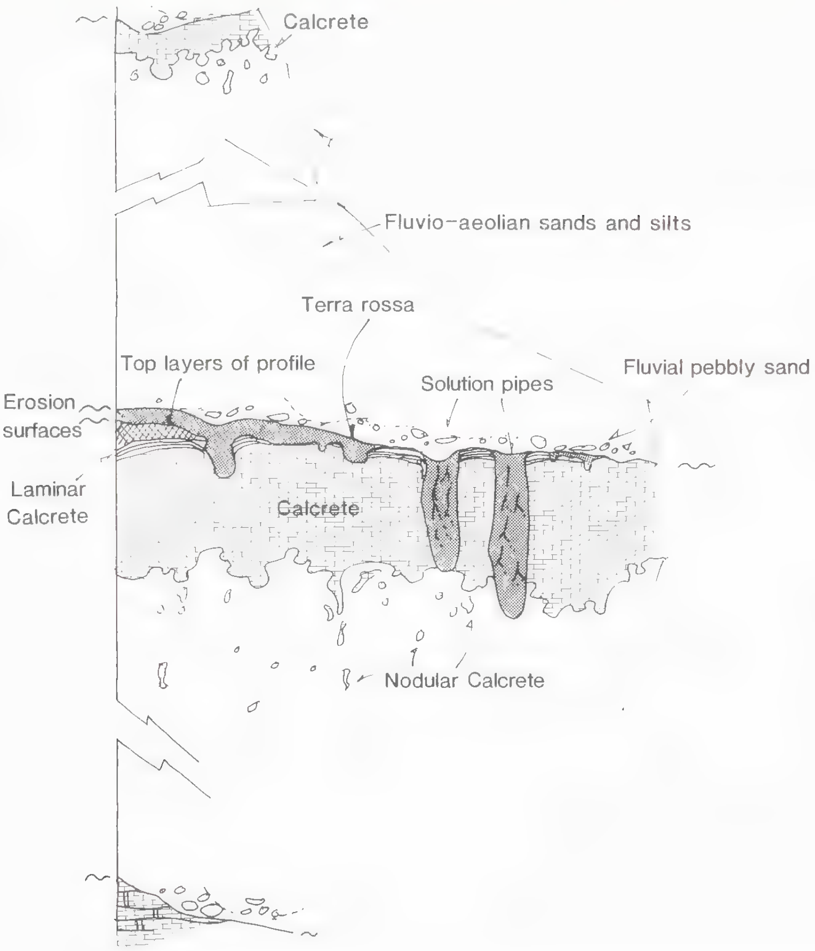

Fig. 5. Major features of soils and associated solution and erosion surfaces within zones of unconformity.

raneous with, development of *terra rossa* (D). This phase, in turn, was terminated by erosion and buried by the next depositional sequence (E). A similar sequence is developed between Q1 and Q2. Soils are less well developed on Q3 and even less so on Q4 and Q5.

The equivalent stratigraphic levels within the Gargaresh Formation display a more complex relationship. At several localities, notably where Q1 and Q2 interfinger with the Gargaresh Formation, basal marine gravels and sands of the Gargaresh members are overlain by red pebbly silts of the Jifarah Formation (Fig. 4A–C). The junction is commonly sharp and in some instances the surface of the gravels has suffered solution fissuring and fragmentation prior to deposition of the Jifarah sediments (Fig. 4C). It is proposed that solution occurred at the same time as pothole formation in the calcrete. Seaward, however, the passage is conformable and silts pass laterally into sands of marine Gargaresh type (Fig. 4B). The junction between the silts and the fissured solution surface is equivalent to, and records the same event as, the erosional surface which terminates the *terra rossa* level within the Jifarah sequences. Since the fissured gravels and associated marine cliff screes contain fragments of the immediately preceding calcrete, the erosional surface on which they rest is both post-calcrete and pre- the solution phase. It is proposed that this erosional event should be equated with that which modified the calcrete soil profile prior to potholing and *terra rossa* formation.

The development of solution fissures and pits on some of the marine gravels suggests that high sea level stand probably occurred prior to *terra rossa* formation. At the same time, the lateral passage from unconformable into conformable relation-

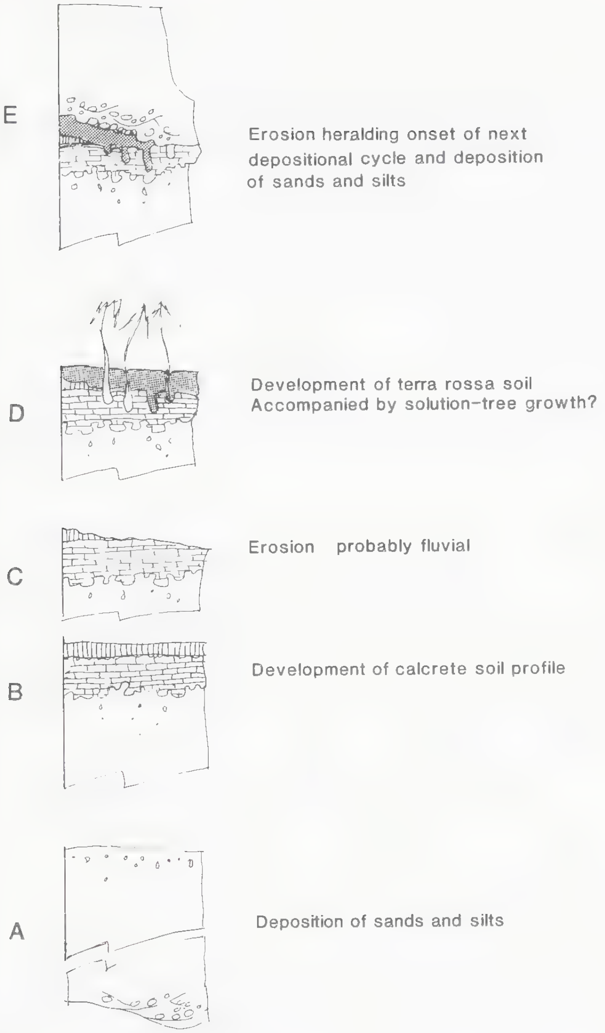
E
Erosion heralding onset of next depositional cycle and deposition of sands and silts
D
Development of terra rossa soil Accompanied by solution–tree growth?
C
Erosion probably fluvial
B
Development of calcrete soil profile
A
Deposition of sands and silts

Fig. 6. Sequence of events leading to development of unconformable zones.

ship between the marine deposits and the red silts, which are undoubtedly later than both solution surface and *terra rossa*, implies that some of the marine gravels may be contemporaneous with red soil formation.

The interplay between marine gravel, fluvial silts and red soil formation and their conformable and unconformable relationships is summarized in Fig. 7. During high sea level stand, gravels and sands situated between low and high tide levels are rapidly cemented to form beachrock. Fall in sea level would have left the beachrock stranded and open to attack by solution to produce fissures and pits. Time allowed for solution and fragmentation to develop suggests that advance of the terrestrial Jifarah silt and sand facies lagged behind sea level fall. As sea level continued to fall, however, unconsolidated marine deposits were exposed so that as the silts and sands prograded over the marine surface they came to rest first of all on the eroded surface of the beach rock and then on the unconsolidated sands and gravels with which they interfingered. Response to further sea level fall is discussed below in relation to the cycle of deposition of the terrestrial deposits.

INTERPRETATION

Quaternary deposits of the Jifārah region display a repeated pattern of sedimentation. Individual members of the Qaṣr al Ḥāj, Jifarah and Gargaresh Formations exhibit a fundamental interrelationship in which alluvial fan/wadi deposits pass northward into fluvio-aeolian sands and silts and finally into aeolian

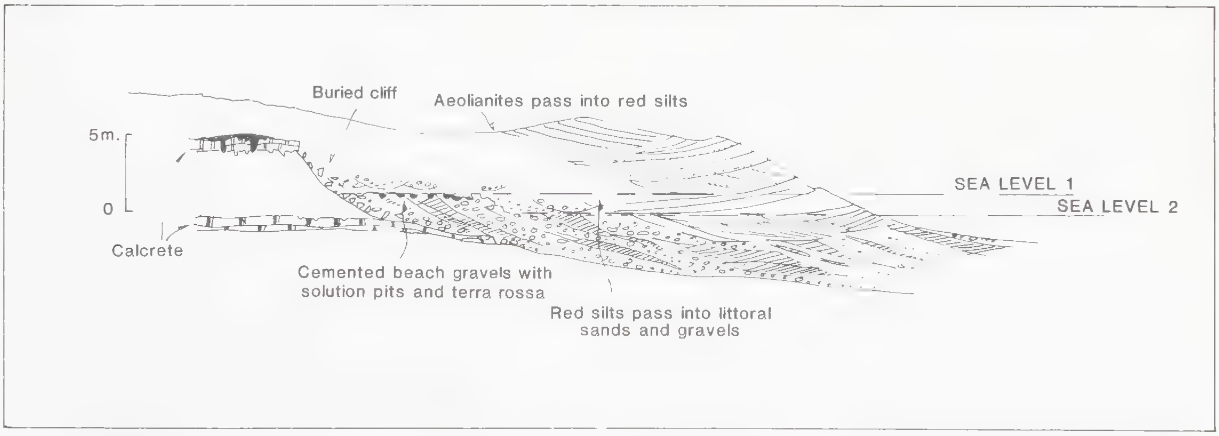
Buried cliff
Aeolianites pass into red silts
5m.
0
SEA LEVEL 1
SEA LEVEL 2
Calcrete
Cemented beach gravels with solution pits and terra rossa
Red silts pass into littoral sands and gravels

Fig. 7. Sketch to show relationship between erosion surfaces, marine deposits, solution pits, calcrete and *terra rossa*.

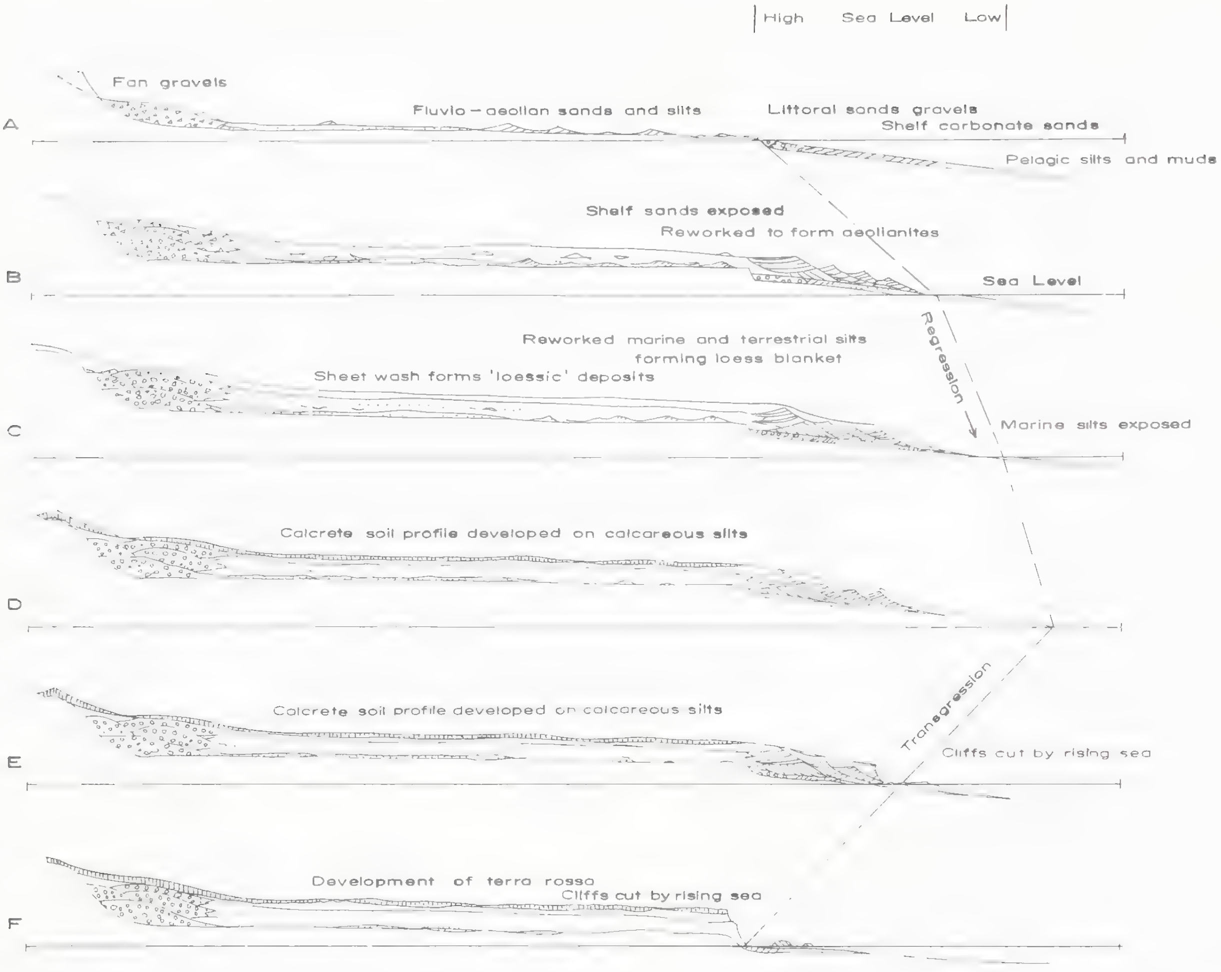
High Sea Level Low
Fan gravels
Fluvio – aeolian sands and silts
Littoral sands gravels
Shelf carbonate sands
Pelagic silts and muds
A
Shelf sands exposed
Reworked to form aeolianites
B
Sea Level
Regression
Reworked marine and terrestrial silts
forming loess blanket
Sheet wash forms 'loessic' deposits
Marine silts exposed
C
Calcrete soil profile developed on calcareous silts
D
Calcrete soil profile developed on calcareous silts
Transgression
Cliffs cut by rising sea
E
Development of terra rossa
Cliffs cut by rising sea
F

Fig. 8. Development of facies associations, horizons of soil formation and surfaces of erosion in relation to an interglacial–glacial–interglacial cycle.

calcerenitess with beach sands and gravels. There is also a trend, particularly clearly displayed by members Q1 to Q4 of the Jifarah Formation, for members to change rapidly upward from an erosional base with thin fluvial deposits to more aeolian "loessic" silts towards the top. Although Unit Q3 appears to have been dominated by aeolian processes throughout, it too rests on an erosion surface. The relationships would appear to indicate an abrupt change from wet to relatively drier conditions during the depositional history of each unit.

The termination of depositional episodes Q1–Q4 by a period of semi-arid soil formation which, on Q1 and Q2, changed with time to soils formed in wetter and/or warmer conditions, further confirms that climatic changes were important in controlling sedimentation.

It is clear, however, that other factors are equally important. The presence of aeolianites indicates that sea level fluctuation, either glacioeustatic or tectonic in origin, must have played a fundamental role in controlling facies distribution.

The evidence for change in climate accompanying the repetition of sedimentary facies relationships and palaeosol development, tends to argue for glacial rather than tectonic control.

Interpretation of the deposits in such terms can be expressed by an idealized cycle (Fig. 8) showing the proposed sequence of events leading to development of sedimentary facies and soils between two interglacial maxima. Similar but less pronounced changes would take place between interstadials. Terminology follows that of Trevisan (1949) and Fairbridge (1972a).

Figure 8A. Early anaglacial — Sea level began to fall. At the shore line, marine gravels of cliffed coasts became exposed, cemented and fissured. Lowering of base level resulted in erosion and downcutting which was followed and/or accompanied by major aggradation of mudflow-fangravel and finer fluvial deposits. Cliff profiles degraded to lower angles. Downcutting and subsequent spread of fangravels and silts lagged behind initial sea level fall. The fluvial nature of these early sediments indicates that plenty of water was available for sediment transport and erosion during the early anaglacial stage. Fairbridge (1972a, 1976) notes that during this stage sufficient rainfall would have resulted from evaporation of warm ocean waters still available in mid to high latitudes.

Figure 8B. With continued sea level fall, marine sands of the shallow shelf became exposed to the effects of weathering and erosion. Onshore winds built up dunes which lapped over onto cemented beach gravels and interfingered with prograding fluvio-aeolian silts and sands.

Figure 8C. Late anaglacial to early pleniglacial saw continuing sea level fall down to maximum with exposure of silts and clays of deeper offshore areas. These were probably blown landwards, blanketing earlier deposits and forming an important component of the loess in the northern part of the plain. To the south and in the Jabal, desert loess is probably more important. However, it is possible that development of loessic deposits above the fluvial basal layers may be related as much to source control as to increase in aridity and that they are a consequence of sea level fall exposing finer pelagic sediments to the effects of deflation.

Interpretation of the "loessic" deposits as loess reworked by sheet-wash, is a further indication that climate was not very arid during the early pleniglacial. Development of lacustrine deposits at the top of unit Q3 and the evidence for valley erosion before formation of the calcrete at the top of unit Q2, strongly suggest that in the later stages of glacial advance, when loess deposits were forming in western and central Europe (Fairbridge, 1972a), the climate in North Africa was, seasonally at least, very wet. In summary it would seem that during the late anaglacial to early pleniglacial, deflation and redeposition of pelagic and desert silts took place in a seasonal climate in which the sediments were extensively reworked by sheet-wash during wet periods with development of calcrete nodules during drier periods. It is also reasonable to assume that the climate grew steadily cooler during this time.

Figure 8D. Pleniglacial with maximum fall of sea level. Formation of thick calcrete, terminating the main phase of deposition, records a prolonged phase of landscape stability in a semi-arid climate. It has already been shown that this post-dates the depositional maximum and maximum progradation of facies. It also predates maximum rise in sea level inasmuch as pebbles of calcrete in the beach gravels of high sea level stand, attest to its having been well lithified before or during transgressive phase. This places the time of formation of the major calcretes as broadly coincident with the pleniglacial stage and maximum sea level retreat. At this time, most mobile sediment would have already been removed from the exposed sea floor and base level of erosion would have been re-established leading to a situation in which soil formation was paramount.

Figure 8E. Early post-glacial or kataglacial with rising sea level. During this phase, raising of base level suppressed sedimentation and rising sea level covered what remained of any marine sediment source. With advance of the sea, older sediments were eroded and locally, cliffs capped by resistant calcrete were formed. Fairbridge (1972a, b) notes that the kataglacial stage in the Mediterranean and North African regions was characterized by a wet climate. Erosion of the upper part of the calcrete soil profile prior to solution and formation of *terra rossa* may have resulted from fluvial erosion in this wet phase. Distinguishing this surface from those which occur at the base of the main depositional sequence developed in the early anaglacial stage is difficult.

Figure 8F. Interglacial stage with maximum rise in sea level. During this phase development of beach conglomerates and sands, wave-cut platforms and cliffs with cliff notches took place in a period of landscape stability. Development of solution features and *terra rossa* soils, particularly in the two oldest cycles implies that the climate was relatively warmer and wetter. Development of fissures and pits on some beach rock, stranded by sea level retreat in the initial stages of subsequent regression suggests that these climatic conditions persisted into the early phase of glacial advance. Butzer (1975) notes that *terra rossa* in the Majorcan sequence formed during minor regressive phases within transgressive complexes implying that they are the product of rather cooler phases within interglacial periods.

On the basis of the interpretation of facies relationships outlined above, it would appear that in the North African coastal region, major phases of deposition largely correspond to times of glacial advance while the pleniglacial stage through to and including the interglacial stage was mainly characterized by soil formation, solution and limited erosion. Less intense soil developments characteristic of members Q3 and Q4 record less extreme changes in climate and probably developed during interstadials.

GEOLOGIC AGE

While it is possible to interpret the depositional sequences and the unconformities which limit them in terms of response to glacial and interglacial processes, it is less easy to relate the sequences to specific glacial events. The reason for this is the paucity of reliable chronostratigraphic data. As yet the various faunal assemblages of the beach deposits remain to be studied in detail, however, it is already clear that it may be difficult to apply the assemblages chronostratigraphically partly because those from different levels contain similar faunas and, as Butzer (1975, p. 49) records from Majorca, "individual sites commonly include too few specimens or species, partly because faunal facies vary from site to site" and "it is difficult to hammer statistically significant samples out of cemented beach rock". Furthermore, Butzer's reappraisal of the Majorcan deposits (Fig. 9) records six terrestrial "hemicycles" F to A where A is modern. These are separated by five marine hemicycles V to Z where Z is the youngest. He notes that each marine hemicycle contains several oscillations with up to three superimposed beach levels and that assignment of any level to specific Tyrrhenian stages must be highly tentative and carried out with great care. This degree of complexity has not been recognized in Tripolitania and although the six depositional events with intervening beach deposits begs comparison with Q1 to Q6, it will be seen that attempts to compare the Libyan succession with that of Majorca and elsewhere in the Mediterranean, tend to raise more problems than they solve.

A chronostratigraphic framework for the Jifārah region will be discussed in relation to the stratigraphic schemes for western Italy (Ambrosetti *et al.*, 1972), Morocco (Stearns, 1978) and Majorca (Butzer, 1975) as displayed in Fig. 9. Tentative Alpine correlations are also shown.

In the Jifārah, one of the most important lines of chronostratigraphic evidence is a group of artifacts discovered in 1946 at a level 1.25 m, above the base of the Q4 upper terrace silt deposit at Wādī Ghān (Hey, 1962), and shown by McBirney and Hey (1955) to be characteristic of Aterian culture. Biberson (1966, p. 471) notes that the Aterian is "contemporary with the maximum of the Ouljian transgression" (Ouljian 2 of Morocco) and that this is widely accepted as equivalent to the Neotyrrhenian of Bonifay and Mars (Biberson, 1963). Stearns and Thurber (1965) have dated Neotyrrhenian deposits, also called Tyrrhenian III, from the Moroccan and Majorcan littorals at 60 000–95 000 B.P. This corresponds to beach level Y3 of the revised Majorcan sequence (Butzer, 1975). Description of the deposits of the succeeding continental hemicycle B as columnar-jointed and loessic in character support its correlation with Q4. The beach may also be equivalent to the 3rd strombus beach of western Italy, dated by Ambrosetti *et al.* (1972) at 90 000 B.P. It is proposed therefore that GQ4m beach deposits should be assigned to the Neotyrrhenian and the succeeding Q4 depositional cycle of Gargaresh aeolianites and "loessic" silts to the regression related to the late Wurm advance (Wurm II of Bonifay and Mars, 1959) (Fig. 9).

Dating of the later sequences can be partially established by comparison with the work of Sherif (1978) on Sabkhat Tāwarghā' in western Sirt. Here ponding of sea waters behind regressional dune barriers has led to the development of two sabkha deposits. The older is ponded by a dune development of a scale and appearance similar to the Q4a deposits of the Tripoli coast. The dunes provided dates in the range of 32 000 to 24 000 years B.P. and apparently record the post-Q4m regressive phase. The sabkha deposits record the subsequent transgression. The older sequence is followed by a second regressional dune phase dated at 3600 to 2000 years B.P. which has served to pond seawater following the last rise in sea level. The younger series of dunes is most probably related to the regression preceding development of the lower terrace Q5 deposits and may be assigned to Wurm IV (Fig. 9). Vita Finzi (1971) shows that the Q5 terrace deposits, which he named Lebda Alluvium, contain Roman and Greek artifacts which allow dating of the alluvial fill to 1300 to 1500 B.P. This face of desiccation, which includes a short period in Roman times when the climate was wetter (Fairbridge, 1972a) is recognized throughout the Mediterranean region (Vita Finzi, 1969).

While it is possible to arrive at a reasonable assignment of ages to deposits younger than Q3 it is

Western Italy, (Ambrosetti et al, 1972)	Morocco, (Stearns, 1978)	Majorca, (Butzer, 1975)	Northwest Libya,		Alpine and Deep sea record,
Stage, Continental, Marine,	Stage, Continental, Marine,	Hemicycle, Continental, Marine,	Units, Cont, Mar,	SA, Cont/Mar,	
		A,	Q5+Q6	Q5+Q6	
Versilian,	Mellahian,	Z,	GQ5m,	GQ5m,	
Pontinian,	Soltanien,	B,	Q4,	Q4,	4
58,000 B,P,					W
Strombus III	Ouljian II,	Y3,	GQ4m,	GQ4m,	U 5a
(Neotyrrhenian)					R
90,000 B,P,					M
Maspinian,	Soltanien,		Q3,	Q3,	5b
		Y2,	GQ3m,	GQ3m,	E 5c
110,000 B,P,					
			Q2,		E 5d
Strombus II	Ouljian I,	Y1,	GQ2m,		M 5e
(Eutyrrhenian)					
127,000 B,P,					
Maspinian,	Presoltanien,	C,		Q2,	R
Strombus I	Harounian,	XI-2,		GQ2m,	
200,000-230,000 B,P,					I
Rianan,	Tensiftien,	D			
Torrimpetran,	Anfatian II.	W4,			S
(Palaeotyrrhenian)					
368,000 B,P,					
Poriolian,					S
Tarquinian,	Anfatian I,	W1,			
700,000 B,P,					
					MINDEL
Galerian,	Amirian,	E.			
Portuensan,	Maarifian,	V,			
1,000,000 B,P,					
Upper Villafranchian,	Saletian,	F,?	Q1,?	Q1,?	GUNZ ?
Emilian,	Messaudian,		GQ1m,	GQ1m,	
Upper Villafranchian,	Moulouyan,				
Santernian,	Fouaratian,				

Fig. 9. Chart displaying possible ages of Quaternary deposits in northwest Libya.

less easy to decide on ages for the older deposits. Given that Q4 can be assigned to the Neotyrrhenian with reasonable confidence, the three older beach levels must represent some combination of the older Pleistocene stages. If the assignment of a Villafranchian age to the lower calcrete (El Hinnawy and Cheshitev, 1975) is correct then only GQ2m and GQ3m can be Tyrrhenian and GQ1m must be older than Portuensian (Fig. 9). Given their lithostratigraphic position in relation to GQ4m and its assignment to the Neotyrrhenian, it is obviously tempting to assign them to the Palaeo- and Eutyrrhenian respectively (Ghellali, 1977).

At the same time, it is clear from sketches and descriptions of the coastal region around Tripoli by Lipparini, such as Figure 5 (1940, p. 257) that the "red clayey sands with *Helicella*" and the succeeding "crostone" (calcrete), correspond to unit Q2 and the upper calcrete respectively. Lipparini indicates that these beds rest on a "panchina" containing the rich fauna with Senegalese affinities which he described from samples collected from Zuwārah (Lipparini, 1935). The presence of *Cerithium protractum, Tapes pullastra-saxatalis, Trochula dalat* and *Mytilus senegalensis* among others, led him to state that the beds are "equivalente degli strati a *Strombus bubonius*" (Lipparini, 1940, p. 260). Lipparini (*ibid*, p. 258) interpreted red silts with *Eremina desertorum* Forsk from below the "Tirreniano panchina" as continental steppe deposits of Riss age thus placing all the post-"panchina" sediments in the Wurm.

The chronostratigraphic scheme advanced by Lipparini and followed by Burollet (1960) and Banerjee (1980) means that the Q2m beach deposits should be assigned to the Eutyrrhenian (Tyrrhenian II) as defined by Bonifay (1964), and Lumley (1969–1971) who confine it to the Riss–Wurm interglacial (Fig. 9). If the age of the early Eem, equivalent to substage 5e of Shackleton (1969), is taken at 128 000 B.P. (Morner, 1972) then the deposits are equivalent to the 2nd strombus raised beach of western Italy (Ambrosetti *et al.*, *ibid*) (Fig. 9). Assignment of Q2m to the Eutyrrhenian/Riss–Wurm also makes it equivalent to Y1 of the revised Majorcan sequence, dated at 125 000–135 000 B.P. (Fig. 9). Since Butzer (1975) proposes that Y3 is equivalent to the Neotyrrhenian and hence, as noted above, to Q4m, Q3m is probably equivalent to Y2 in which case, the succeeding Q3 deposits would have formed during the period of sea level fall between maxima Y2 and Y3 (Fig. 9). The positioning of Q3 between Y2 and Y3 is supported by correlation of a well-developed *terra rossa* horizon which succeeds Y2 in the Majorcan sequence with that which precedes Q3 in the Jifārah region. Although there is no record of regressional deposits in Majorca equivalent to unit Q3, there is evidence from the Languedoc for a sharp fall in temperature between 97 000 and 92 000 B.P. (Duplessy *et al.*, 1970) which could have produced the aridity necessary for mobilization of the dune sands of unit Q3 in the Jifārah region. This cold period is recorded as substage 5b in deep sea cores marking the onset of the Wurm glaciation (Morner, 1972).

It is clear that, if Q2m deposits are assigned to the Eutyrrhenian as defined above, the major part of the Pleistocene succession in the Jifārah region is post-Riss in age and, if the lower calcrete is of Villafranchian age, then the erosional surface separating Q1 from Q2 in the Jifārah region must encompass a time gap equivalent to the Mindel and Riss glaciations (Fig. 9). It is also clear that the repetition of facies and erosional surfaces displayed by Q2 to Q6 must owe their origins to oscillation of the ice front on a stadial–interstadial rather than glacial–interglacial scale.

Assignment of the lower calcrete to the Villafranchian obviously has important implications as to the age of the older deposits i.e. Unit Q1. The main basis for the age assignment is correlation with a similar deposit in Tunisia (El Hinnawy and Cheshitev, 1975 p. 44) an opinion which received some support from the work of Grosse (1969). In a study of sediments of Pliocene to Recent age in the Cap Bon region he recorded a beach deposit with *Strombus bubonius* Lamarck, resting on a "croute calcaire" or calcrete. This in turn rests on an older beach deposit, a "plage a cardium et pectoncles" which in turn rests on Villafranchian calcrete. Grosse assigned the "Strombus beach" to the Eutyrrhenian and the lower deposit to the Palaeotyrrhenian. This is significant in that, since the calcrete is succeeded directly by Palaeotyrrhenian deposits, sediments equivalent to the Portuensian and Tarquinian of the Italian mainland, the Maarifian and Anfatian 1 of Morocco, are absent. The sequence is comparable to that of the Jifārah region where the equivalent of the Torrimpietran and Anfatian 2 is also missing (Fig. 9). Grosse also notes that the Cap Bon area suffered various episodes of Neogene tectonism and that Villafranchian and older deposits were tilted prior to the "Tyrrhenian". Arambourg and Arnould (1949) note that Villafranchian sediments at Lake Ichkeul in Algeria are tilted also and are succeeded with marked unconformity by sediments of "Tyrrhenian" age. In the Jifārah region, a similar episode of faulting and tilting of the lower calcrete recorded by Anketell and Ghellali (1983), lends further support to its correlation with the Tunisian horizon and thus its assignment to the Villafranchian.

The evidence for post-Villafranchian tilting suggests that the absence of Mindel–Riss deposits from the Jifārah region may have resulted from erosion following pre-Wurm tilting. This might also account for the fragmentary preservation of the lower calcrete. Remnant material would have been incorporated in the basal Q2 deposits.

Assignment of the lower calcrete to the Villafranchian also means that the Q1 depositional cycle may correspond to the Gunz, Donau or pre-Donau glacial events and that GQ1m deposits may range from Pliocene to Emilian in age (Fig. 9). Gignoux (1950, p. 619) states that no marine deposits of Calabrian or Sicilian age "have ever been discovered on the African coasts" and Desio (1971, p. 26) under-lines this in stating that no such deposits have been reported from northern Libya. On these grounds Ghellali (1977) argued for a Pliocene age for the deposits. While at the moment the age must remain in doubt, it should be noted that marine deposits equivalent to the "Calabrian and Sicilian", namely the Fouaratian, Messaudian and Maarifian, are known from Atlantic Morocco (Fig. 9). In addition, the interleaved continental sequences of the region, the Moulouyan and Saletian (Fig. 9), display lithologies comparable to Q1 (Biberson, 1963; Stearns, 1978). It is possible, therefore, that the Q1 sequence records either or both the Donau and Gunz glacial events. It is also possible that the calcrete represents a very long period of relative landscape stability which may have been equivalent to several fluctuations in the ice front in northern Europe. Absence of "typical" deposits may be due to the region having occupied a different geographic position relative to the ice front and hence undergone a different climatic response to glacial advance and retreat than occurred during later stages.

The chronostratigraphic scheme for the Jifarah deposits outlined above places the greater part of the sequence within the last glaciation and assigns Q2, the most extensive and thickest deposit, to a minor cold phase within the last interglacial. This arises from the acceptance of the "Tyrrhenian" shelly fauna described by Lipparini as Eutyrrhenian in age and from accepting the Eutyrrhenian as confined to the Riss–Wurm interglacial. There are, however, other possibilities (Fig. 9A). Marine hemicycle X of Majorca (originally T-IIb) dated by Stearns and Thurber at 190 000–200 000 B.P. and almost certainly equivalent to the 1st strombus level of western Italy dated at 177 000–200 000 B.P. (Ambrosetti *et al.*, *ibid*), contains the best developed strombus fauna of the Majorcan sequence. This horizon also appears to correspond to the Eutyrrhenian of the type area at 160 000–170 000 B.P. by Stearns and Thurber (1965, p. 302). If Q2m is equivalent to this horizon then Q2 would correspond to the late Riss (Riss II or Warthe). This possibility is supported by comparison of Q2 with continental hemicycle C which would be the equivalent continental deposit in the Majorcan sequence. This is comprised of aeolianites and reddened colluvial silts with calcrete and abundant *Helix* and *Helicella* and is obviously very similar in lithology to Q2 or the "red sands with *Helix*" of the Jifarah succession (Fig. 9).

Inasmuch as assignment of Unit Q2 to the Riss would better support the interpretation of the major facies changes it displays relative to younger deposits in terms of glacial versus interglacial events as opposed to minor fluctuations within the last interglacial, there is a tendency for the authors to favour this approach. It is clear, however, that a satisfactory chronostratigraphic scheme for the Quaternary deposits of the Jifarah is very necessary and that the answer as to which of several possible stratigraphic schemes is most feasible will not be reached until much more data is available. The problems which arise in attempting comparisons with successions described from elsewhere in the region also illustrate the need for an interdisciplinary approach towards establishing a firm chronostratigraphic framework for the Libyan Quaternary and for the North African region as a whole.

CONCLUSIONS

(1) Quaternary sediments of the Jifārah Plain display change in facies from alluvial fan through fluvio-aeolian silts and sands to aeolian calcarenites when followed north from Jabal Nafūsah to the coast. The three major facies comprise the Qaṣr al Ḥāj, Jifarah and Gargaresh Formations.

(2) Up to six separate episodes of deposition Q1–Q6 separated by zones of unconformity have been recognized in each formation. The members display the same pattern of lateral facies variation as the formations to a greater or less degree. The sediments also display increasing aeolian influence with time.

(3) The zones of unconformity commenced with a phase of soil formation characterized by the development of laminar calcrete in Q1–Q2. This was followed by a phase of erosion leading to solution in concert with formation of *terra rossa*. This phase was abruptly terminated by onset of erosion followed by, or concomitant with, the start of the next depositional event.

(4) The sequence is interpreted in terms of response to changing sea level and climate resulting from advance and retreat of glaciers in northern Europe.

(5) With the onset of glaciation, sea level fall was accompanied by erosion with progradation of fluvial gravels and sands and fluvio-aeolian sands and silts over marine gravels and sands. The terrestrial silts interfinger with calcarenites derived by aeolian action from marine sands newly exposed as sea level dropped. With time and further regression, fine silts and muds of deeper

waters were exposed and deflated to form a loess blanket which is extensively reworked by water to give loess-like deposits. These colluvial deposits display many of the characteristics of loess but are generally coarser. Loess was probably also derived from desert areas to the south. At maximum regression, the gradual establishment of a profile of equilibrium with some channelling of the floodplain silts and sands, and the onset of a period of relative landscape stability in a semi-arid climatic setting, lead to calcrete formation.

(6) With transgression, consequent on glacier retreat, climate gradually improved. There was probably some fluvial erosion adjusting old stream channels to the new erosional base level as the rising sea cut cliffs in older deposits. The period of maximum transgression appears to coincide with extensive solution and the development of *terra rossa*. However, fissures and pits developed on some cemented beach gravels imply that solution processes were active in the early stages of regression.

(7) Less intense soil development on the younger members Q3–Q5 implies less extreme climatic change and suggests that they were formed during interstadial rather than interglacial stages.

(8) Preliminary investigations of Quaternary deposits in northwest Libya suggest that it is possible to draw some parallels with studies of Quaternary sequences elsewhere in the North African–south Mediterranean region. However, the ages of the various deposits in the Jifārah area are as yet not firmly established.

ACKNOWLEDGEMENTS

We wish to thank the University of Manchester, England and Al-Fateh University, Tripoli, G.S.P.L.A.J., for financial and logistic aid during the course of this study. Thanks are also due to members of staff in the Geology Departments of both Institutions for their help in discussion.

REFERENCES

Ambrosetti, P., Azzaroli, A., Bonadonna, F.P. and Follieri, M. (1972). A Scheme of Pleistocene chronology for the Tyrrhenian side of central Italy. *Boll. Soc. Geol. Ital.*, **91**, 169–184.

Anketell, J.M. and Ghellali, S.M. (1983). Stratigraphic studies on Quaternary floodplain deposits of the eastern Jeffara Plain, S.P.L.A.J. *Libyan Studies*, **14**, 16–36.

Anketell, J.M. and Ghellali, S.M. (1984). Nests of a tube-dwelling bee in Quaternary sediments of the Jeffara Plain. *Libyan Studies*, **15**, 137–141.

Anketell, J.M. and Ghellali, S.M. (1987). Stratigraphic aspects of the Gargaresh Formation, Tripolitania, S.P.L.A.J. *Libyan Studies*, **17**.

Anketell, J.M. and Ghellali, S.M. (1988). Stratigraphic aspects of the Qasr Al Haj Formation, Tripolitania, S.P.L.A.J. *Libyan Studies*, **18**.

Arambourg, C. and Arnould, M. (1949). Notes sur les feuilles paléontologiques executées en 1947–1948 et 1949. *Bull. Soc. Sci. Nat.*, Tunis, **2**.

Balout, L. (1955). *Préhistorique de l'Afrique du Nord.* Arts et Métiers Graphiques, Paris, 554 p.

Banerjee, S. (1980). Stratigraphic Lexicon of Libya. *Ind. Res. Cent.*, Tripoli, Bull. **13**, 300 p.

Biberson, P. (1963). Human evolution in Morocco in the framework of the palaeoclimatic variations of the Atlantic Pleistocene. *In: African Ecology and Human Evolution* (*ed.* F.C. Howell and F. Bourliere). Aldine Publishing Co., Chicago, Ill.

Biberson, P. (1966). Some aspects of the lower Palaeolithic of Northwest Africa. *In: Background to Evolution in Africa* (*eds* W.W. Bishop and J.D. Clark). Viking Fund Publications in Anthropology. Chicago Univ. Press, Chicago, Ill.

Birkeland, P.W. (1984). *Soils and Geomorphology.* Oxford Univ. Press, Oxford, 372 p.

Bonifay, E. (1964). Pliocène et Pléistocène Méditerranéens. Vue d'ensemble et essai de corrélations avec la chronologie glaciaire. *Ann. Paleontol. Vertebr.*, **50**, 195–226.

Bonifay, E. and Mars, P. (1959). Le tyrrhennien dans le cadre de la chronologie Quaternaire Méditerranéenne. *Bull. Soc. Géol. Fr.*, **7**, 62–78.

Burollet, P.F. (1960). Lexique Stratigraphique International, 4, Afrique, Pt. 4a Libye. *Comm. Strat.*, *Cent. Nat. Rech. Sci.*, 62 p.

Butzer, K.W. (1972). *Environment and Archaeology, 2nd ed.* Methuen, London, 689 p.

Butzer, K.W. (1975). Pleistocene littoral sedimentary cycles of the Mediterranean Basin: A Mallorquin view. *In: After the Australopithecines* (*eds* K.W. Butzer and G.L. Isaac), 25–71. Mouton, The Hague.

Christie, A.M. (1966). Geology of the Gharian Area, Tripolitania, Libya. *Min. Ind. Geol. Sect.*, Tripoli, Bull. **5**.

Desio, A. (1940). Sulla Posizione Geologica e sull' Origine delle Falde Artisiane della Gefara Tripolina e del Misuratino. *La Ricerca Scientifica*, *Anno 11* Roma.

Desio, A. (1971). Outlines and problems in the geomorphological evolution of Libya, from the Tertiary to the present day. *In: Symp. Geol. Libya* (*ed.* C. Gray). Fac. Sci., Univ. Libya, Tripoli, 11–36.

Desio, A., Ronchetti, C.R., Pozzi, R., Clerici, F., Invernizzi, G., Pisoni, C. and Vigano, P.L. (1963). Stratigraphic studies in the Tripolitanian Jebel, Libya. *Riv. Ital. Paleontol. Stratigr.*, **9**, 1–126.

Duplessy, J.C., Labeyrie, J., Lalou, H. and Nguyen, H.V. (1970). Continental climatic variations between 130 000 and 90 000 B.P. *Nature*, **226**, 631–633.

El Hinnawy, M. and Cheshitev, G. (1975). Geological Map of Libya. Tarabulus (NI33-13). Explanatory Booklet. *Ind. Res. Cent.*, Tripoli.

Elliot, T. (1978). Clastic shorelines. *In: Sedimentary Environments and Facies* (*ed.* H.G. Reading). Blackwell, Oxford, 143–147.

Fairbridge, R.W. (1972a). Climatology of a glacial cycle. *Quat. Res.*, **2**, 283–302.

FAIRBRIDGE, R.W. (1972b). Quaternary sedimentation in the Mediterranean region controlled by tectonics, palaeoclimates and sea level. *In: The Mediterranean Sea (ed.* D.J. Stanley). Dowden, Hutchinson and Ross, Stroudsberg, Pa., 99–113.

FAIRBRIDGE, R.W. (1976). Effects of holocene climatic change on some tropical geomorphic processes. *Quat. Res.*, **6**, 529–556.

GHELLALI, S.M. (1977). *On the Geology of the Eastern Gefara Plain, North West Libya.* Ph.D. Thesis. Univ. Manchester, Manchester, 296 p.

GIGNOUX, M. (1950). *Stratigraphic Geology.* (English translation from 4th French Ed.). W.H. Freeman and Co., San Francisco, Calif., 682 p.

GILE, F.F., GILE, L.H., PETERSON, F.F. and GROSSMAN, R.B. (1966). Morphological and genetic sequences of carbonate accumulation in desert soils. *Soil Sci.*, **101**, 347–360.

GOUDIE, A.S. (1973). *Duricrusts in Tropical and Subtropical Landscapes.* Clarendon Press, Oxford, 174 p.

GROSSE, M. (1969). Recherches géomorphologiques dans le Péninsula du Cap Bon, Tunisie. *Inst. de Géogr. de Paris*, 358 p.

HECHT, F., FURST, M. and KLITZSCH, E. (1963). Zur Geologie von Libyen. *Geol. Rundsch.*, **53**, 413–470.

HEY, R.W. (1962). The Quaternary and Palaeolithic of northern Libya. *Quaternaria*, **VI**, 435–449.

JAMES, N. (1972). Holocene and Pleistocene calcareous crust (caliche) profiles; criteria for subaerial exposure. *J. Sediment. Petrology*, **42**, 817–836.

JENNINGS, J.N. (1968). Syngenetic karst in Australia. *In: Contributions to the Study of Karst (eds* P.W. Williams and J.N. Jennings). Res. School of Pacific Studies, Dept. Geogr. Publ. G/5/1968, Aust. Nat. Univ. Canberra, A.C.T.

JONES, J.R. (1969). Ground Water in Libya — A Summary. Hydrogeology of the Southern Mediterranean Littoral and the north central Sahara. *U.S. Geol. Surv. Open File Rep.*

KORNICKER, L.S. (1958). Bahamian limestone crusts. *Trans. Gulf Coast Assoc. Geol. Soc.*, **8**, 167–170.

LIPPARINI, T. (1935). Molluschi delle panchine Pleistoceniche di Zuara, Ras-el-Msid e Sidi Mesri in Tripolitania. *Boll. Soc. Geol. Ital.*, **54**, 93–108.

LIPPARINI, T. (1940). Tettonica e geomorfologia della Tripolitania. *Boll. Soc. Geol. Ital.*, **59**, 222–301.

LUMLEY, H. DE (1969–71). Le Palaeolithique inférieur et moyen du Midi méditerranéen dans son cadre géologique. *1–2, Gallia Prehist. Suppl.* **5**, 463 + 443 p.

MANN, K. (1975a). Geological Map of Libya, Al Khums, (NI33-14). Explanatory Booklet. *Ind. Res. Cent.*, Tripoli.

MCBIRNEY, C.B.M. and HEY, R.W. (1955). *Prehistory and Pleistocene Geology in Cyrenaican Libya.* Cambridge Univ. Press, Cambridge, 315 p.

MORNER, N.A. (1972). When will the present Interglacial end? *Quat. Res.*, **2**, 341–349.

NETTERBURG, F. (1967). Some roadmaking properties of South African calcretes. *Proc. 4th Regional Conf. Soil Mech. and Eng.* Cape Town.

PARONA, C.F., CREMA, C. and FRANCHI, S. (1913). La Tripolitania settentrionale: descrizione fisica e geologica della regione. *Min. Col. Comm. per lo Studio Agricolico della Tripolitania*, Roma, **1**, 3–42.

PENCK, A. (1909). Die Morphologie der Wüsten. *Geogr. Z.*, **15**, 545–558.

PERKINS, R.D. (1977). Depositional framework of Pleistocene rocks in south Florida. *Mem. Geol. Soc. Am.*, **147**, 131–198.

PICCOLI, G. (1969). Outlines of volcanism in northern Tripolitania. *In: Symp. Geol. Libya (ed.* C. Gray). Fac. Sci. Univ. Libya, Tripoli, 323–331.

PRICE, W.A. (1925). Caliche and pseudoanticlines. *Bull. Am. Assoc. Petrol. Geol.*, **9**, 1009–1017.

RADWANSKI, A. (1970). Dependence of rock borers and burrowers on the environmental conditions within the Tortonian of southern Poland. *In*: Trace Fossils (*ed.* T.P. Crimes and J.C. Harper). *Geol. J.*, Spec. Issue, **3**, 371–390.

RATCLIFFE, C.F. and FAGERSTROM, J.A. (1980). Invertebrate Lebensspuren of Holocene floodplains; Their morphology, origin and palaeoecological significance. *J. Paleontol.*, **5H**, 614–630.

RATHJENS, C. (1928). Löss in Tripolitanien. *Z. Ges. Erdk., Berlin*, 11–218.

REEVES, C.C. (1976). *Caliche.* Estacado Books, Lubbock, Texas.

REINECK, H.E. and SINGH, I.B. (1975). *Depositional Sedimentary Environments.* Springer-Verlag, New York, N.Y., 439 p.

SHACKLETON, N.J. (1969). The last interglacial in the marine and terrestrial records. *Proc. Royal Soc. London*, **B**, 135–154.

SHERIF, N. (1978). *Quaternary Sedimentation of the Western Coastal Plain of the Gulf of Sirt.* Ph.D. Thesis, Univ. London, London.

STEARNS, C.E. (1978). Plio-Pleistocene emergence of the Moroccan meseta. *Bull. Geol. Soc. Am.*, **89**, 1630–1644.

STEARNS, C.E. and THURBER, D.L. (1965). Th^{230}/U^{234} Dates of Late Pleistocene marine fossils from the Mediterranean and Moroccan littorals. *Quaternaria*, **7**, 29–42.

STEEL, R.J. (1974). Cornstone (fossil caliche) — Its origin and some features of its stratigraphic and sedimentological importance in the New Red Sandstone rocks of Western Scotland. *J. Geol.*, **82**, 351–359.

STELLA, A. (1914). Geologia. *In: La Missione Franchetti in Tripolitania*, **II** *Gebel*, Milano, 81–151.

TREVISAN, L. (1949). Genèse de terrasses fluviatiles en rélation avec les cycles climatiques. *C. R. Congr. Int. Geogr.*, Lisbon, **2**, 511–528.

VITA-FINZI, C. (1969). *The Mediterranean Valleys.* Cambridge Univ. Press, Cambridge, 131 p.

VITA-FINZI, C. (1971). Alluvial history of northern Libya since the last Interglacial. *In: Symp. Geol. Libya (ed.* C. Gray). Fac. Sci., Univ. Libya, Tripoli, 409–429.

WARME, J.E. and MCHURON, E.J. (1978). Marine borers; trace-fossils and their significance. *In: Trace Fossil Concepts (ed.* P.B. Basan). *SEPM Short Course*, **5**, 67–118.

YAALON, D.H. (1967). Factors affecting the lithification of eolianite and interpretation of its environmental significance. *J. Sediment. Petrology*, **37**, 1189–1199.

Part 11

Hydrogeology and Hydrology

Sedimentological Time Markers and Groundwater Dating: A Study of the Quaternary Evolution of Al Kufrah Area

R.E. BECKER[1] AND M. FÜRST[2]

العلاقات الزمنية الرسوبية وتأريخ المياه الجوفية ، مشاركة في دراسة تطور الحين الرابع بمنطقة الكفرة

ر. إ. بيكر وم. فورست

الخلاصــة

لقد تمّ التوصل إلى ترتيب تتابع الأحداث أثناء الحين الرابع بمنطقة واحة الكفرة ، وذلك بناء على التقسيم الطبقي للرسوبيات والتأريخ بواسطة أشعاع الكربون للمياه الجوفية والمواد العضوية (خشب وقشور بيض النعام) والتعرف على أدوات الإنسان القديم .

وهناك عدة تغيرات مناخية معروفة بمنطقة الدراسة تشير إليها مرحلتين من اللترتة تفصلها مرحلة من السيلكة التي حصلت عند مستوى سقف النجود الحالية .

وتتكشف أقدم رسوبيات الحين الرابع في الوسط بين النجود وأقل مستوى لسطح الأرض في الوقت الحالي. ويمثل هذه مصاطب الجرول التي ترجع إلى الحين الرابع الباكر والتي تبين لترتة عند القمة . وفي غياب البحيرات لا توجد عملية ترسيب على مستوى إقليمي .

وقد استعمل إشعاع الكربون في تأريخ المياه الجوفية والتي وجد أنها ذات طبقية زمنية تجاه العمق . وقد بلغ عمر العينات من أعمق الصفائح المائية المدروسة (حوالي 400 إلى 600م تحت مستوى الأرض) وذلك بواسطة تأريخ الأشعاع الكربوني حوالي 28,500 إلى 30,000 سنة مضت . وينقص عمر المياه الجوفية تجاه قمة المكمن المائي إلى حوالي 20,000 سنة .

وقد تبع هذه الفترة من المناخ الرطب مرحلة جافة قطعتها مرحلة رطبة من 11,000 إلى 9,000 سنة مضت .

وقد تكون رسوبيات المرحلة الرطبة عبارة عن تلك البقايا من المصاطب داخل منظومة المجاري المائية القديمة . ولم يتيسر اثبات وجود مياه جوفية حديثة إلى شبه حديثة حيث أن المناخ قد تبدل إلى ظروف جافة . وقد تخلل هذه المرحلة الأخيرة والتي ما زالت مستمرة حتى الآن على الأقل فترة واحدة هطلت خلالها الأمطار. وقد دل على ذلك رسوبيات الطين التي تعلو رمال الكثبان الرملية ويقتصر وجود هذه الرسوبيات الطينية على المنخفضات التي غالباً ما تحيط بها آثار لمواقد للنار قدر عمرها بحوالي 6000 إلى 2000 سنة وذلك بناء على الأشعاع الكربوني لقشور بيض النعام وأجزاء من الآنية الفخارية .

وقد تناقصت أماكن نمو الأعشاب حتى إقتصر وجودها في الوقت الحاضر على الواحات . وقد أثبتت ذلك بالتأريخ عن طريق الأشعاع الكربوني لقطع خشبية من روابي تامارسك . وقد بدأت أبعد هذه الروابي في التكون حوالي 2050 سنة مضت . . وانتهت حوالي 550 سنة مضت أما الروابي القريبة من الكفرة فقد انتهت حوالي 150 سنة مضت .

ويقودنا غياب رواسب البحيرات ووجود بقايا من الرواسب النهرية إلى الإستنتاج بأنه لم تكن هناك بحيرة كبيرة خلال زمن البليستوسين والهولوسين في منطقة الكفرة .

Abstract. A chronology of events during the Quaternary evolution of the area of Al Kufrah oasis is established on the basis of stratigraphic classification of sediments, radiocarbon dating of ground waters and organic material (wood and ostrich eggshells) and the determination of artefacts.

Several climatic changes are already known in the area of interest during the Tertiary. They are evident from two phases of "laterization" (iron-rich crusts) and a phase of silicification between them, which took place at the level of present-day cuesta plateaus.

---

[1] Hess. Landesamt für Bodenforschung, Leberberg 9, 6200 Wiesbaden, F.R.G.
[2] Universität Mainz, Institut für Geowissenschaften, Saarstraße 21, 6500 Mainz, F.R.G.

The oldest Quaternary sediments crop out midway between the plateaus and the lowest present-day ground level. They are represented by early Quaternary terrace gravels, which show an iron-rich crust at the top.

Ages of ground waters were determined using the radiocarbon method. The ground waters show a time stratification with depth. The lowest of the sampled ground water sheets (about 400–600 m below ground level) has a radiocarbon age of about 28 500 to 30 000 years B.P. Towards the top of the lower aquifer, the ages of the ground water decrease to about 20 000 years B.P.

This epoch of humid climate was followed by a dry period interrupted by a wet phase between 11 000 and 9000 years B.P. representing the higher aquifer.

Sediments of the wet phases could be the remains of terraces within the fossil drainage system. Ground water of recent to subrecent age could not be proved since the climate had changed to arid conditions. This last epoch, which has not yet ended, was interrupted at least once by a period of precipitation. This is documented by clayey sediments overlying dune sands. These pelitic sediments are restricted to local depressions which are often surrounded by Neolithic fireplaces dated to about 6000 to 5000 years B.P. according to the radiocarbon age of ostrich eggshells and fragments of pottery.

Vegetation retreated and is now limited to the oases. This process is proved by radiocarbon ages of wood chips from tamarisk mounds. The most distant mounds started to grow about 2050 years B.P., and died about 550 years B.P., those closer to Al Kufrah died about 150 years B.P.

The absence of limnic sediments and the presence of relics only of fluvial sediment leads to the conclusion that there was no large Pleistocene–Holocene lake within Al Kufrah area.

INTRODUCTION

The area of investigation is identical with the L.A.R. Fotomap 1 : 200 000, Al Kufrah (1977) (Fig. 1). It comprises an area of 14 000 km^2 and includes Al Kufrah oases with their largest town of Al Jawf.

Geologically, the region belongs to the Palaeozoic–Mesozoic Al Kufrah basin (Klitzsch, 1965; Bellini and Massa, 1980; Turner, 1980) with the "Nubian" formation as its youngest unit.

The Mesozoic rocks of the plateau are locally overlain unconformably by iron-rich and silica crusts with a thickness of several metres. The crusts were formed by the silicification of silt and sandstone and the cementation of sands, conglomerates and breccias by iron-rich fluids (crusts I and II). They occur as thin caps on the plateaus and inselbergs at an elevation of 480–500 m a.s.l. in the southwest and south, between 460 and 490 m a.s.l. in the southeast and east and around 450 m a.s.l. in the northeastern part. The existence of a former peneplain, gently dipping towards the northeast, can be inferred. The age is assumed to be Neogene, judging from the morphological position, the existing deep erosion and plant impressions (*Gramineae* sp. and *Equisetales* sp., pers. comm. with F. Schaarschmidt, 1977, Frankfurt, Germany). Figure 2 gives a summary of the morphology, the vegetation and the evidence of prehistory of the area of interest.

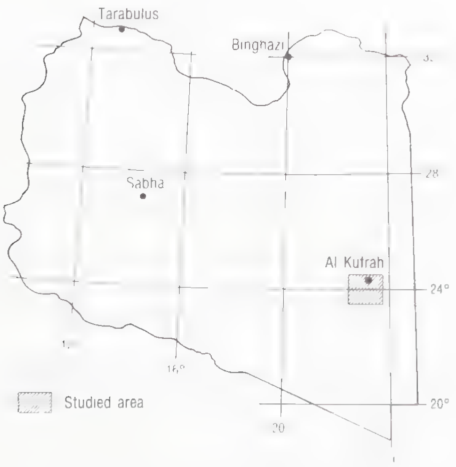

Fig. 1. Position of studied area.

The purpose of this study is to show the Quaternary development of the area by using sedimentological time markers and groundwater age determinations.

CHRONOLOGY OF QUATERNARY EVENTS

Early Quaternary Gravels

The oldest Quaternary sediments are coarse sandy gravels, up to 300 cm thick. They form a small height immediately south of Al Jawf, about 50 m below the level of the iron-rich crusts I and II. The grains are moderately sorted and rounded and consist mostly of quartz and quartzite, and in the upper part also of iron-rich crust material. The basal section is yellow, the upper part shows intense red to red-brown colours. The gravels are thought to be the oldest relics of Wādī Al Kufrah.

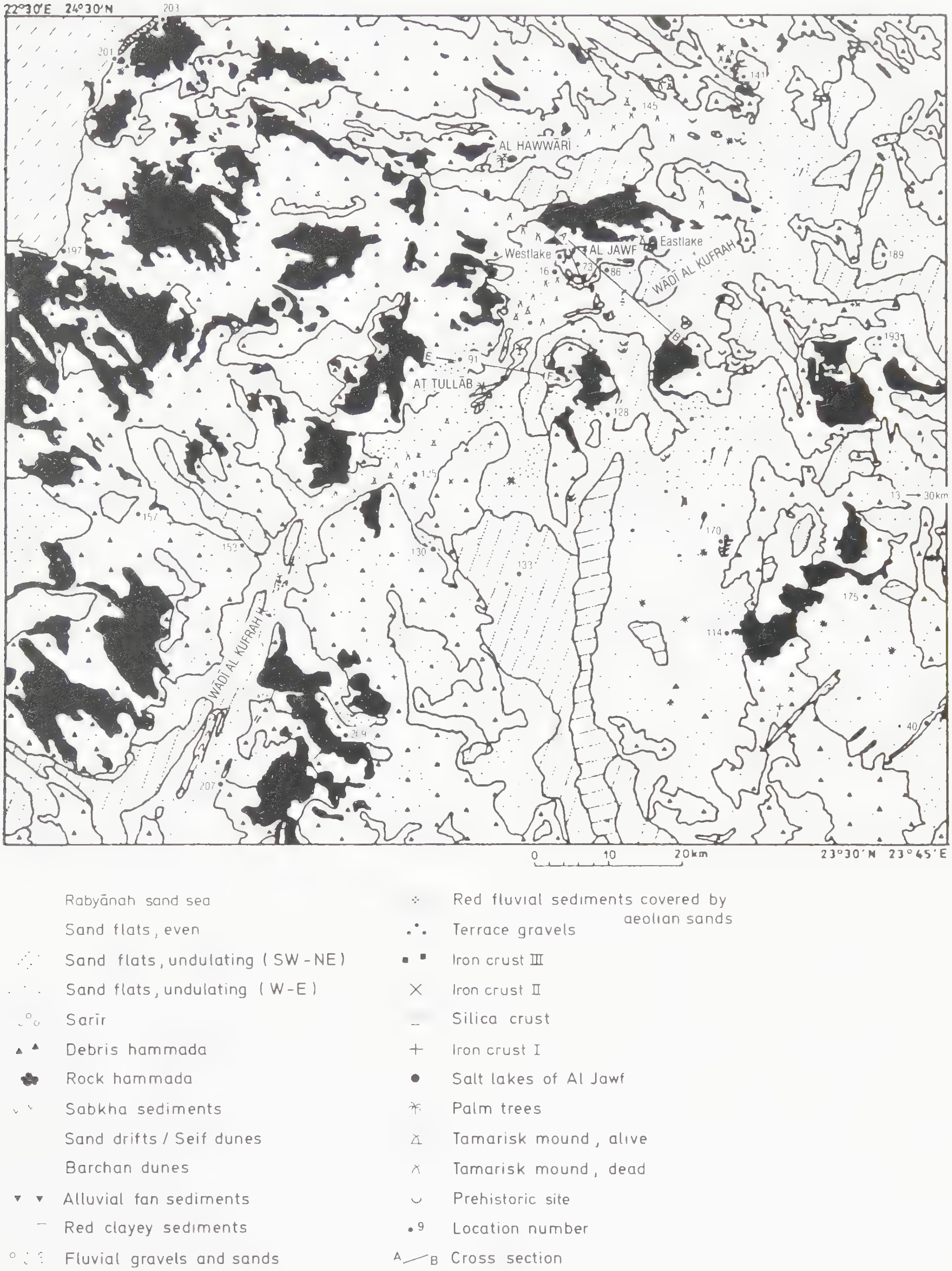
22°30'E 24°30'N
203
201
141
145
AL HAWWĀRĪ
Westlake
AL JAWF
Eastlake
WĀDĪ AL KUFRAH
197
189
A
16
73
86
B
193
E
91
F
AT TULLĀB
128
125
157
152
130
133
170
13 → 30km
175
114
WĀDĪ AL KUFRAH
209
207
40
0 10 20km
23°30'N 23°45'E
Rabyānah sand sea
Sand flats, even
Sand flats, undulating (SW-NE)
Sand flats, undulating (W-E)
Sarir
Debris hammada
Rock hammada
Sabkha sediments
Sand drifts / Seif dunes
Barchan dunes
Alluvial fan sediments
Red clayey sediments
Fluvial gravels and sands
Red fluvial sediments covered by aeolian sands
Terrace gravels
Iron crust III
Iron crust II
Silica crust
Iron crust I
Salt lakes of Al Jawf
Palm trees
Tamarisk mound, alive
Tamarisk mound, dead
Prehistoric site
9 Location number
A B Cross section

Fig. 2. Major morphogenetic units—positions of cross sections.

Iron-rich Crust III

The above-mentioned gravels were preserved by the cover of the overlying iron-rich crust III. This ferruginous layer represents a fanglomerate consisting of material of crusts I and II. The diameter of the components is 50 cm as a maximum, the cementing material being mainly ferric. The composition indicates that the transport was short; it is similar to alluvial fan sediments. The existence of iron crust III leads to the conclusion that there was a climatic change from humid to arid. The following wet phase caused almost complete erosion of this iron crust and further deepening of Wādī Al Kufrah. The maximum thickness of iron-rich crust III reaches 3 m.

Terrace Gravels

An alluvial terrace which is in part cemented by limonite occurs west of Aṭ Ṭullāb. Morphologically obvious, the terrace is several kilometres long, about 1 km wide and between 3 and 6 m thick. The subrounded to well-rounded components consist of mostly yellowish to reddish pebbles of quartz, quartzite and iron-rich crust. They are elongate, and have longest axes of a maximum of 15 cm. The terrace overlies conglomeratic sandstones of the "Nubian" Formation. Occurring 1–2 m below the level of the early Quaternary gravels and of iron-rich crust III, the terrace is considered to be younger than both units.

Younger Fluvial Sediments

Fluvial sediments of varying thicknesses are widespread in the fossil drainage system (Fig. 3). Sand and gravel layers predominate, while clay, silt, and fine sand are represented secondarily. The thickness and facial character is highly variable, so key horizons could not be distinguished.

In Wādī Al Kufrah especially, excavations have produced many outcrops of a thin Quaternary cover over solid rock. In a gravel pit south of Al Jawf (Location 8) a typical profile was exposed (Fig. 4). The top layer has a thickness of 1 m and consists of aeolian sand. This is underlain by fluvially redeposited dune sands and several horizons of bedded gravel with varying thicknesses and sorting, about 2.5 m thick in total. The components are mostly well-rounded but ill-sorted, especially in the coarse fractions. Grain sizes of 2–4 cm are abundant, the maximum diameters being up to 7 cm.

Thickness variations of the aeolian sand and relatively small differences in elevation prevented further classification into different terrace levels. Adjacent outcrops, only a few metres apart, show completely different profiles.

In most cases, the solid sandstone of the "Nubian" lies less than 5 m below the surface. In a few outcrops the sand cover is thicker, and the solid rock appears at a correspondingly deeper level.

Outside Wādī Al Kufrah the thickness of the fluvial sediments varies between several cm (Locations 28, 29, 109, 130) and about 2 m (Locations 131, 145, 174, 186).

Layers of Calcite Cementation

Up to 5 concretionary carbonate layers occur within the fluvial sediments, e.g. at Location 73, the top one at about 0.25 m and the basal one at 3.5 m below terrain surface. The bed rock appears at a depth of 4.10 m. The origin of the calcicrust is still unclear. Some authors assume capillary ascent and precipitation at or near the surface, others propose descending waters. Rohdenburg and Sabelberg (1969) showed them to have formed as concentrations below a decalcified surface horizon. Contrary to the crusts described by Rohdenburg and Sabelberg, those at the Al Kufrah oasis have a sharp lower boundary and a loose concretionary upper margin.

The spatial restriction of the carbonate crusts to regions of low elevation indicates that the crusts are confined to former stagnating groundwater elevations and are not primarily dependent on climate.

Location 7 (Fig. 4) shows 2 carbonate horizons in a gravel pit. The planar lower boundary of the crust can be seen very clearly.

No lime concentration was observed within the aeolian layers. This leads to the conclusion that the carbonization is older than the recent aeolian sands. The sediments below the carbonate crusts show greenish-grey and yellow colours throughout, whereas reddish colours predominate above the crusts.

To sum up, in the area of study the calcite layers formed during periods of stagnating ground water and are so-called "aclimatic crusts" (Geiger, 1970).

Fossil Ground Water

The existence of ground water in the Sahara desert has long been known and has been the subject of study by many authors (Pallas, 1980; Pachur, 1980;

24°30'N
AL JAWF
20 km
Fluvial drainage system
Main watershed
Morphological depression
23°45'E
23°30'N

Fig. 3. Fossil Pleistocene drainage system.

Klitzsch *et al.*, 1976), including many projects of radiocarbon-dating of organic material and ground waters and their interpretation (Geyh and Jäkel, 1974; Jäkel, 1978; Jäkel and Geyh, 1982; Rognon, 1976; Petit-Maire *et al.*, 1980; Giessner, 1981; Faure, 1966). In connection with a study concerning the groundwater resources of Al Kufrah region, several datings were carried out by the German Water Group (GWE) (1977) and in part interpreted (Dietrich, 1976; Becker, 1979; ElRamly, 1980). Now, an attempt is made to classify them according to the chronology of the Quaternary. Table 1 shows the radiocarbon ages and the sampling depth of the waters. At least three different stages can be distinguished (from top to bottom):

(1) 11 765–9745 years B.P. — younger humid phase. These ages correlate with the most shallow sampling depth.
(2) 24 550–19 000 years B.P. — intermediate humid phase. The waters were sampled at shallow and intermediate depths.
(3) 29 500–28 050 years B.P. — older humid phase. These samples were taken at the greatest and intermediate depths.

The correlation between sampling depths and age is clear and proves the existence of interstratified fossil ground water. GWE (1977) mentions the possi-

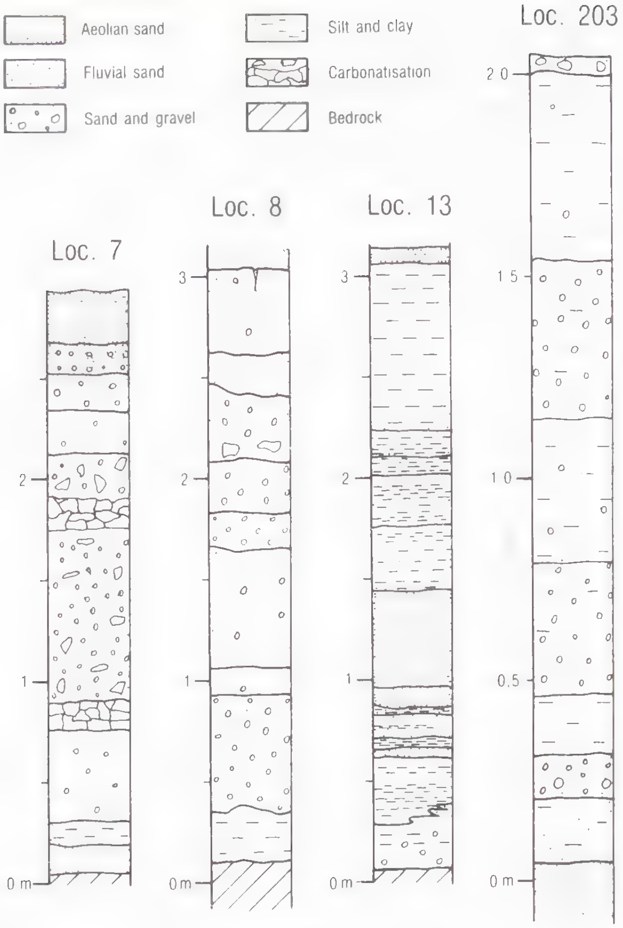

Fig. 4. Characteristic Quaternary profiles.

bility of the intermediate ages having been produced by mixed waters. This is contradicted by the age determinations of well No. C-78 and C-133-A from intermediate depths.

The terrace gravels of Aṭ Ṭullāb may have been deposited during the earliest humid phase, the younger fluvial sediments may represent relics of the two younger humid phases, depending on their elevation. The few sediments prove that the region of Al Kufrah oases can be considered as an erosion area of a fluvial system rather than of a Pleistocene sedimentation province.

This is inconsistent with suggestions by ElRamly (1980) that a Pleistocene Al Kufrah lake existed, about 100 km in length in a NE–SW direction and with a width of about 60 km. His argument is based on the fluvial sediments, the carbonate crusts and the interpretation of drill logs of former groundwater drill holes. The drilling revealed interlayered clayey silt, sand and marl at a depth of up to 35 m below terrain surface.

The authors encountered solid rock at a depth of a few metres in pits, drill holes, probings and penetration tests throughout Wādī Al Kufrah. Therefore, a misinterpretation of the upper drill section is most probable. The uppermost parts of the "Nubian" Formation are mostly friable, consequently the drilling samples can hardly be distinguished from those of loose sediments.

The gastropod *Melania tuberculata*, found by El-Ramly only at the margins of recent lakes, cannot prove a large Pleistocene Al Kufrah lake, since Pachur (1974) determined the radiocarbon ages of gastropod shells as between 8000 to 5000 years B.P. Besides, *Melania tuberculata* is still living in the Tībistī Mountains today (Jaeckel, 1969). Sections AB and EF (Fig. 5) show typical cross sections of Wādī Al Kufrah.

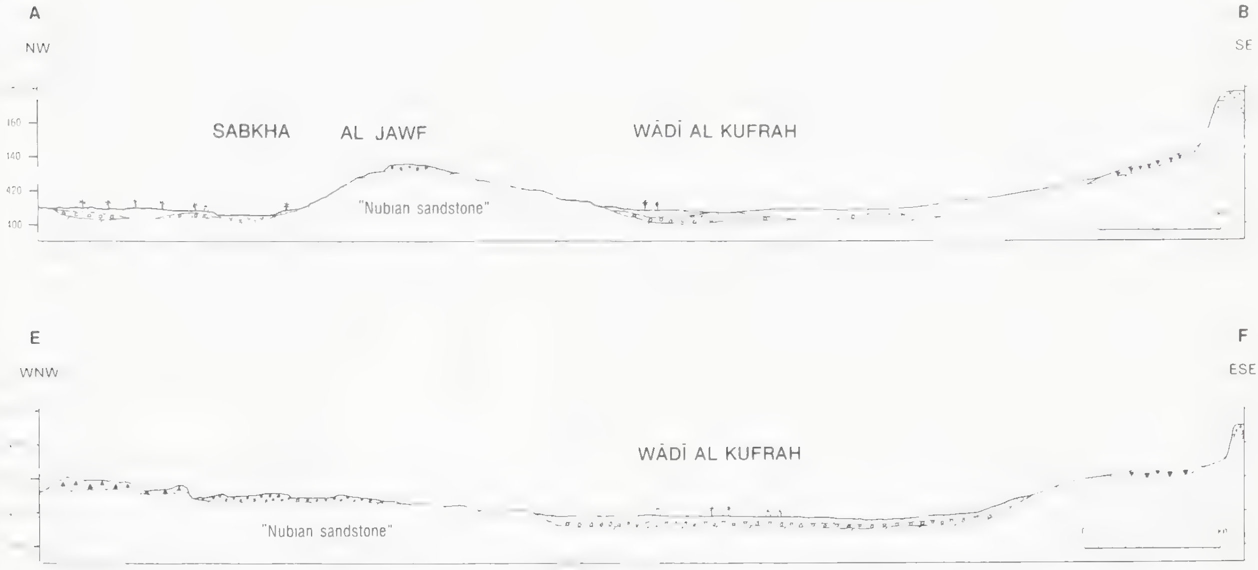

Fig. 5. Typical cross sections of Wādī Al Kufrah (position and legend in Fig. 2).

Red Alluvial Fan and Clay Deposits

Red silty to fine sandy clays and clayey silts were found at some locations in the study area with maximum thicknesses of more than 3.6 m (Location 141). These clays are always coloured red-brown and restricted to depressions near or at the base of cuestas. Adjacent to the clays poorly graded fanglomeratic sediments were found. These may be called alluvial fans, or, taking into consideration the arid climate, wadi fans after Glennie (1970). So the clays are considered to be the fine-grained end members of the wadi fans. The profile of Location 13 (Fig. 4) shows interlayered aquatic clay–silt/aeolian sand horizons. At exposure 201, located just east of the Rabyānah sand sea, large polygonal mud cracks, between 0.2 and 0.4 m wide and 0.7–1.0 m deep, were observed in fanglomerates of more than 2 m thickness. The mud cracks were filled with light-coloured aeolian sand. At Location 203, a little farther to the north, these sediments were exposed due to erosion. They occur as several overlapping fans which show a distinct layering, poor sorting and good rounding. Coloured intensely red-brown, they overlie yellow dune sands of 3–4 m thickness (Fig. 4). Episodic precipitation within a period of increasing aridity is again proved, but no recharge of ground water occurred according to Table 1.

Most of these clay-filled depressions were surrounded by remains of prehistoric camp sites. Ostrich eggshells, fragments of pottery, hand-mills, millstones, and artefacts were found and dated by B. Gabriel, pers. comm., 1976 (Geol. Inst. of Univ., Berlin). The ages of finds from Location 141 were determined as 6000–5500 years B.P., while radiocarbon dating of ostrich eggshells from the same location yielded an age of 5120 ± 115 years B.P. Gabriel dated some pieces of pottery from exposure 170 as 6820 ± 220 years B.P., comparing them with some of his own datings (Gabriel, 1977). Hence, a more humid climate can be inferred for this period of time which correlates with the climatic curve for the eastern Sahara proposed by Geyh and Jäkel (1974).

Aeolian Sediments

Aeolian sediments have been deposited from the beginning of the Holocene up to the present. Their great variety and genesis were described in detail by Becker (1979), so they are omitted from this paper.

Sabkha Sediments

Several sabkhas still exist today in Al Kufrah area, e.g., in the oases at Al Hawwārī, Aṭ Ṭullāb and Al Jawf. Covering an area of about 8 km^2, the sabkha of Al Jawf has an elongate form and is situated between the East Lake and the West Lake. Lateral inflow of fresh ground water into the sabkha and lakes can be

Table 1. Groundwater data related to depth (date of sampling November 1974)

Well No.	Depth of screens (m)	Water temperature during sampling (°C)	^{14}C-age (years before 1950)
SW drilling contractor's camp	?–54.0	26.9	9745 ± 420
SW 2 (east of production well No. 86)	60.1–84.9	27.2	11 765 ± 490
SW settlement camp	50.0–74.9	27.0	19 000 ± 1200
SW 1 (east of production well No. 27)	50.3–75.3	27.2	22 510 ± 1100
C-78	121 –241	28.2	22 250 ± 1600
C-133 A	130 –250	28.2	24 550 ± 1200
C-39	150 –275	30.0	28 050 ± 1000
1234	166 –455	29.8	28 500 ± 2800
WW 8 (Al Hawwārī)	486 –602	32.6	$29\,500\,^{+\,3100}_{-\,2200}$

proved by trenches. Photogeological interpretations also revealed ascending ground water along joint and fissure systems flowing into the sabkha.

To investigate the sediment filling of the sabkha, about 50 shallow drill holes were made and in 75% of the holes the "Nubian" bedrock was hit at a depth of less than 4.5 m. The results of drilling presented in Fig. 6 show that the filling of the sabkha consists of interlayered silty–clayey and sandy sediments. Pebbles are rare. The sands show white to grey or yellowish to brown colours and pH values between 7.5 and 9.0. The pelitic sediments are grey to black, or greenish to yellowish and contain a lot of plant remains. The pH values vary between 2.6 and 6.8.

In a few profiles thin carbonate-rich horizons were encountered at different depths. The upper 50 cm of sabkha sediments contained gastropods and ostracod shells at several places. E. Kuster-Wendenburg (Bremen, pers. comm. 1976) determined them as the gastropods *Hydrobia* sp., *Stenothyra* sp. and *Alvania* sp., and as the ostracods *Cypridopsis* sp. The maximum length of the gastropods measured was 5 mm, that of the ostracods 1.5 mm.

In the winter the sabkha is flooded, in the summer strong evaporation lowers the water table so that the surface is dry and presents a salt crust. This salt crust with a maximum thickness of 50 cm is built up of up to 39 alternating thin layers of salt, fine-grained sand, silt and silty clay. The grain size of the clastic sediments is controlled by the wind velocity.

Vegetation

Within the region of Al Kufrah oases, vegetation covers an area of about 500 km^2. It can be divided

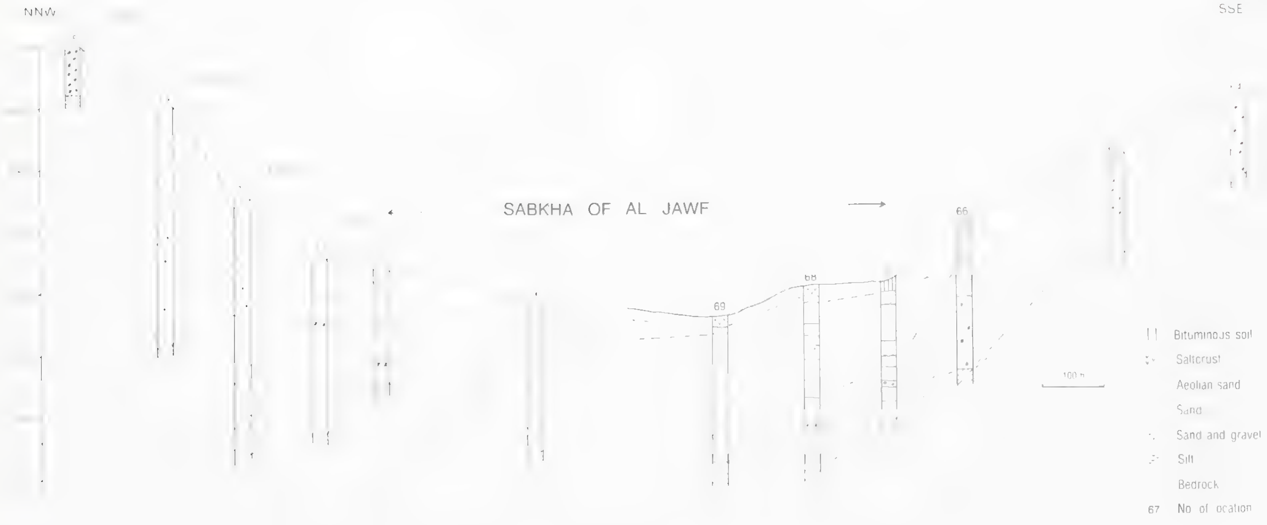

Fig. 6. Cross section of the present-day sabkha.

into three zones without sharp boundaries: (1) regions with tamarisk mounds, (2) a peripheral zone of low vegetation, and (3) inner zones of the oases with palm trees.

(1) Zone of tamarisk mounds

Tamarisk mounds occur in the present inner zones of the oases and in several areas outside the oases, e.g. at Locations 125, 128, 130. Many mounds no longer have living vegetation. The mounds are younger than the red clays of Location 141 and the sabkhas because they are found overlying both.

An attempt was made to determine the growth rates and ages of some of the dead mounds by radiocarbon dating. The highest ages were found at a mound at Location 128, which is 10.5 m high. Pieces of leaves were sampled 2.5 m above the base and were determined as 1790 ± 70 years B.P. At Location 43 in the inner zone of the Aṭ Ṭullāb oasis samples were taken from the top of a dead mound which was 3.5 m high and from 1 and 2 m below. Radiocarbon dating showed that the first sample from the surface was formed in the year 1960/1961, the two lower samples originated within the period between 1535 and 1765 A.D. A growth rate of 0.9 cm/year and a total age of 400 years can be concluded for the mound. From the Tībistī area Pachur (1974) mentions an age of 2300 ± 145 years B.P. for the base and 1625 ± 145 B.P. for the top of a mound with a height of about 7 m which corresponds to a growth rate of about 1 cm/year. A sample from a clay area near Location 141 was taken from 3 m below the top of a mound and dated as 705 ± 50 B.P. Another sample, taken from a dead mound near the eastern salt lake, also about 3 m below the top, yielded an age of 670 ± 60 years B.P. Therefore, the following relations become obvious: The mounds near Location 128 outside Wādī Al Kufrah died first, followed by mounds near Location 141 and near the eastern salt lake. Mounds within the inner zones of the oasis Aṭ Ṭullāb have died only recently.

(2) Peripheral zone of low vegetation

In Wādī Al Kufrah and in some depressions outside the wadi and around the palm zone of the oases, wide areas exist with many sand mounds up to 1 m high, called "Kupsten" (Meckelein, 1959). Small thorn bushes grow in their centre, being responsible for the sand accumulation. In this area, palm trees do not grow at present; in some places, however, relics of dead palm trees are found. These "kupsten" mark the outer boundary of the zone where vegetation is still possible.

(3) Inner zones of the oases with palm trees

The oasis of Al Jawf forms the largest continuous palm tree zone; the villages Al Hawwārī to the north, and Aṭ Ṭullāb to the south of Al Jawf are smaller zones. The palm tree zones often have sharp boundaries due to the availability of near surface ground water within morphological depressions. A very few acacias grow there in addition to the palm trees and other useful plants.

The modern relics of vegetation within Al Kufrah area lead to the following conclusions: Regions with tamarisk mounds represent the oldest evidence of a formerly larger extension of the oases.

Tamarisks are still growing there when palm trees and thorn bushes are already dead. The older the tamarisk mounds are, the greater the distance is to the inner zones of the oases. The peripheral belts of vegetation surround the modern inner zones of the oases. They replace the dead palm trees and indicate that the inner zones of the oases have grown successively smaller. Today the inner zones with a high groundwater level form the areas of active vegetation.

CONCLUSIONS

Using sedimentological time markers and age determinations, the following chronological table of dry and humid phases has been developed:

Iron-rich crust I	Tertiary
Surface silica crust	
Iron-rich crust II	
Main erosional phase and development of the fluvial drainage system	Quaternary–Pleistocene
Gravel and sand	
Coarse debris (fanglomerate)	
Iron-rich crust III	
Erosional phases within the fluvial drainage system	
Terrace accumulations (gravel)	ca. 30 000 years B.P. (?)
Younger fluvial sediments (sand and gravel)	ca. 24 000–9000 years B.P. (?)
Oldest sabkha sediments (sand, silt, clay)	Quaternary–Holocene
Calcretes	
Aeolian sands	
Wadi fans with red clayey sediments	7000–4000 years B.P. Neolithic sites

Aeolian sands	
Younger sabkha sediments (sand, silt, clay)	
Retreat of vegetation:	
– from areas of tamarisk growth	ca. 2000 years B.P.
– to peripheral zones of bush vegetation	ca. 400 years B.P.
– to oases with palm trees	

The chronological relations discussed above lead to the conclusion that a large Pleistocene lake did not exist within Al Kufrah area. The area of investigation is, rather, considered to have been an erosive system during this time draining towards the NE and showing relics only of non-limnic deposits.

REFERENCES

Becker, R.E. (1979). Die tertiäre und quartäre Entwicklung im Bereich der Kufrah-Oasen (Zentrale Sahara) unter besonderer Berücksichtigung aktualistischer Vorgänge. *Geol. Rundsch.*, **68**(2), 584–621.

Becker, R.E. (1984). Äolische Sande aus Südhessen und der libyschen Sahara im korngrößenanalytischen und rasterelektronenmikroskopischen Vergleich. *Geol. Jahrb. Hessen*, **112**, 139–164.

Bellini, E. and Massa, D. (1980). A stratigraphic contribution to the Palaeozoic of the southern basins of Libya. *In: The Geology of Libya* (*eds* M.J. Salem and M.T. Busrewil). Academic Press, London, **I**, 3–56.

Dietrich, G. (1976). Die Al-Kufrah-Projekte als Beispiel für die Nutzung fossilen Grundwassers. bbr, **27**(2), 45–48.

Elramly, I.M. (1980). Al Kufrah Pleistocene lake — Its evolution and role in present-day land reclamation. *In: The Geology of Libya* (*eds* M.J. Salem and M.T. Busrewil). Academic Press, London, **II**, 659–670.

Faure, H. (1966). Evolution des grand lacs sahariens à l'Holocène. *Quaternaria* VIII, **15**, 167–175.

Gabriel, B. (1977). Zum ökologischen Wandel im Neolithikum der östlichen Zentral-Sahara. *Berl. Geogr. Abh.*, **27**, 111 p.

Geiger, F. (1970). Die Aridität in Südostspanien — Ursachen und Auswirkungen im Landschaftsbild. *Stuttg. Geogr. Studien*, **77**.

Giessner, K. (1981). Die jungquartäre Klimageschichte der Sahara. *In: Würzb. Geogr. Arb.*, **53**, 111–127.

Geyh, M.A. and Jäkel, D. (1974). Spätpleistozäne und holozäne Klimageschichte der Sahara aufgrund zugänglicher ^{14}C-Daten. *Z. Geomorph.*, N.F., **18**, 82–98.

Glennie, K.W. (1970). Desert sedimentary environments. *Developments in Sedimentology*, **14**. Elsevier, Amsterdam, 222 p.

GWE German Water Group, Executing Company: German Water Engineering GmbH (1977). Hydrogeological Study of Groundwater Resources in the Kufrah Area, Final Report. Vol. 2, Parts I–IV, Hydrogeology (unpublished).

Jaeckel, S.H. (1969). *Molusken aus dem Tibesti-Gebirge und dem Gebiet des ehemaligen Tschad-Sees.* Freie Universität, Berlin (unpublished).

Jäkel, D. (1978). Eine Klimakurve für die Zentralsahara. *In:* Sahara — 10.000 Jahre zwischen Weide und Wüste. *Handb. Ausstellung, Mus. Köln*, 382–396.

Jäkel, D. and Geyh, M.A. (1982). ^{14}C-Daten aus dem Gebiet der Sahara, hervorgegangen aus Arbeiten der Forschungsstation Bardai und des Niedersächsischen Landesamtes für Bodenforschung in Hannover. *Berl. Geogr. Abh.*, **32**, 143–165.

Klitzsch, E. (1965). Zur regional geologischen Position des Tibesti-Massivs. *Max Richter Festschrift Clausthal-Zellerfeld*, 111–125.

Klitzsch, E., Sonntag, C., Weistroffer, K. and Elshazly, E.M. (1976). Grundwasser der Zentralsahara: Fossile Vorräte. *Geol. Rundsch.*, **65**(1), 264–287.

L.A.R. Fotomap 1 : 200 000, Al Kufrah (1977). Edition 1, produced on behalf of the Council of Agricultural Development, Tripoli; prepared by Hansa Luftbild, Münster, F.R.G.

Meckelein, W. (1959). *Forschungen in der Zentralen Sahara.* Erweiterte Habilitationsschrift, Westermann, 181 p.

Pachur, H.-J. (1974). Geomorphologische Untersuchungen im Raum der Serir Tibesti (Zentralsahara). *Berl. Geogr. Abh.*, **17**, 58 p.

Pachur, H.-J. (1980). Climatic history in the later Quaternary in southern Libya and the Western Libyan Desert. *In: The Geology of Libya* (*eds* M.J. Salem and M.T. Busrewil). Academic Press, London, **III**, 781–788.

Pallas, P. (1980). Water Resources of the Socialist People's Libyan Arab Jamahiriya. *In: The Geology of Libya* (*eds* M.J. Salem and M.T. Busrewil). Academic Press, London, **II**, 539–594.

Petit-Maire, N., Casta, L., Delibrias, G. and Gaven, Ch. with an appendix by Testud, A.-M. (1980). Preliminary data on Quaternary palaeolacustrine deposits in the Wadi Ash Shati area, Libya. *In: The Geology of Libya* (*eds* M.J. Salem and M.T. Busrewil). Academic Press, London, **III**, 797–805.

Rognon, P. (1976). Les oscillations du climat saharien depuis 40 millénaires. Introduction à un vieux débat. *Rev. Géogr. Phys. Géol. Dyn.*, **XVIII**(2–3), 147–156.

Rohdenburg, H. and Sabelberg, U. (1969). "Kalkkrusten" und ihr klimatischer Aussagewert — Neue Beobachtungen aus Spanien und Nord-Afrika. *Gött. Bodenkundl. Berichte*, **7**, 3–26.

Turner, B.R. (1980). Palaeozoic sedimentology of the southeastern part of Al Kufrah basin, Libya: A model for oil exploration. *In: The Geology of Libya* (*eds* M.J. Salem and M.T. Busrewil). Academic Press, London, **II**, 351–374.

Lakes in the Awbārī Sand Sea of Fazzān, Libya

DAVID J. BURDON[1] AND ROBERTO GONFIANTINI[2]

بحيرات ببحر أوباري الرملي ، فزان ، ليبيا

د. بيردون ور. جونفيانتيني

الخلاصـــة

يتناول هذا البحث جيولوجية وجيولوجيا المياه وكمية المياه وكيمياء النظائر الموجودة بإحدى عشر بحيرة بمنطقة الرملة عند جانب الدواده من بحر رمال أوباري بفزان بليبيا. وقد تم وصف أصلها وطريقة تكوّنها ومحاولة تفسير إستمراريتها ، مع التركيز على بحيرة المندرة وهي أكبرها.

وبصورة عامة يمكن القول بأن البحيرات قديمة في تواجدها ، بالرغم من أن بعضها قد اختفى وتكونت أخرى جديدة أو عادت بعض تلك التي اختفت لتظهر من جديد من تحت الكثبان الرملية العالية المتحركة. وتحت الظروف المناخية الحالية لا بد وأن هذه البحيرات تتغذى بنسبة كبيرة أو كلياً من المياه الجوفية الأرتوازية من طبقات مائية عميقة.

وقد وجد بأن مياه البحيرات والآبار والبرك المجاورة ترجع إلى مصدرين وعمرين. فالمصدر الرئيسي عبارة عن طبقة مائية تحتوي على مياه جوفية مالحة ، وترجع في عمرها إلى الحين الكربوني. وتؤكد التحاليل الكيميائية للمياه طبيعة تدفق المياه المالحة ، كما تشير النظائر إلى أنها مياه قديمة. ولهذه الطبقات المائية التي ترجع إلى الحين الكربوني تكشفات مطمورة تحت تكوين مرزق من الحين الرابع تغطية كثبان بحر أوباري الرملي. كما وجد بأن هناك مياه حديثة وجيدة ببعض البرك والآبار الضحلة. وهذا واضح من الإستعمال المحلي للمياه في السقي والري أحياناً إلى جانب تأكيد ذلك بالتحاليل الكيميائية. كما أن دراسات النظائر تربطها بأمطار وقتنا الحاضر بمنطقة فزان (1977 – 1979) وباقي المناطق بجزء إفريقيا الجاف. وتنفذ هذه المياه الحديثة من خلال الكثبان الرملية وذلك عقب فترة أمطار غزيرة ونَادرة.

ويعزى بقاء هذه البحيرات ومحتواها من القشريات الصالحة للأكل إلى تعميق منخفضاتها عن طريق ظاهرة الكارست ، حيث تذيب المياه الجوفية طبقات الجير المائية ومن ثم تتكون فجوات تحت البحيرة ، ثم يهوى سقفها فيما بعد. ولولا هذه الظاهرة لكانت هذه البحيرات قد ملأتها الرمال والرسوبيات البخرية منذ زمن بعيد.

Abstract. This study describes the geology, hydrogeology, hydrochemistry and isotope chemistry of 11 lakes occurring in the Ramlat ad Dawādah portion of the Awbārī sand sea in Fazzān, Libya. Their origin and mode of formation are described, and their persistence explained, with emphasis on Lake Mandara, the largest of them.

These lakes are ancient, though some may have disappeared and others appeared or re-appeared under the shifting high sand dunes. Under present climatic conditions, these lakes must be fed in great part, by artesian discharge of ground waters from deep aquifers; some small current recharge is probable.

It is found that the waters of the lakes and surrounding wells and pools are of two origins and ages. The main source of water supply is from aquifers containing saline ground water of Lower Carboniferous age. The hydrochemistry confirms the saline nature of the discharges. The isotopic composition shows that they are old ground waters. These Lower Carboniferous aquifers have a sub-outcrop under the Murzuq Quaternary formation, covered by the dunes of the Awbārī sand sea. Some young, good-quality water is also present, found in shallow wells and pools. This is clear from the use of the water for domestic supplies, for crops and even limited irrigation. It is supported by the chemical analyses. In addition, the isotopic work shows its relation to present-day rains in Fazzān (1977–1979) and elsewhere in arid Africa. This young ground water infiltrates through the sand dunes following rare but short and heavy rains.

It is thought that the persistence of the lakes, as evidenced by their limited edible crustacean fauna, is due to deepening and sinking of the lake depressions into underground openings of a karstic nature. The limestone aquifers are dissolved by the ground water and collapses occur. Otherwise, the wind-blown sands and the evaporite deposits would long ago have filled up the lakes.

---

[1] Recently deceased — correspondence to second author.

[2] International Atomic Energy Agency, P.O. Box 100, A-1400 Vienna, Austria.

INTRODUCTION

This work is based on fieldwork carried out in Fazzān, Libya in 1976 and 1979. Reports were then made to the Secretariat of Dams and Water Resources of the Socialist People's Libyan Arab Jamahiriya. These remained unpublished, and it seems opportune to revise them in the light of later experience and to present the findings to the "Third Symposium on the Geology of Libya".

Background

The existence of some 11 lakes and lakelets in the middle of the Sahara must awaken surprise and interest. But they do exist, in the Ramlat ad Dawādah of the Awbārī sand sea between Wādī ash Shāṭi' in the north and Wādī al Ḥayāh (Wādī al Ajāl) in the south. The first European report on their existence was from the explorer Edward Vogel, spending the winter of 1852/53 at Murzuq, the capital of Fazzān. The lakes are certainly that old, but probably existed in prehistoric times, in the pluvials; they may have been known to the Romans after desiccation of the region was well advanced. In the course of time, some may have been buried, and new ones formed, due mainly to the movement of the shifting sand dunes by which they are surrounded.

In all cases examined, they are surrounded by date palms, which are highly tolerant of saline water. But in some cases, there are real oases around the saline lake, with water of reasonably good quality for domestic purposes, for stock and even for limited irrigation. A grove of well-grown eucalyptus trees was seen near Lake Mandara.

This paper presents the results of investigations into these 11 lakes and lakelets. Following studies of climate, geology, hydrogeology, hydrochemistry and isotopic chemistry, some details are given on the formation and persistence of Lake Mandara. From the analyses made of the data, ten conclusions have been drawn.

Location

The regional location of the lakes and lakelets which occur in the Awbārī sand sea of Fazzān, Libya is shown in Fig. 1; this figure also shows the high annual potential evaporation over much of North Africa. While the whole region under study here lies within Awbārī sand sea, the subarea within which the lakes occur is known as the Ramlat ad Dawādah.

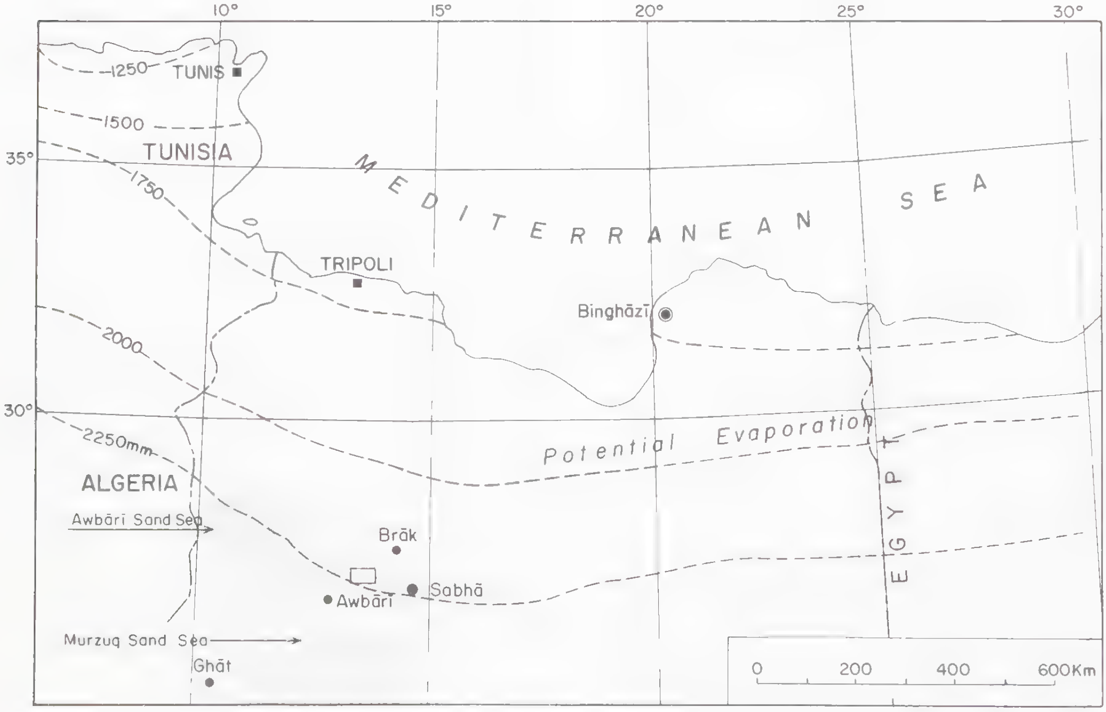

Fig. 1. Regional annual potential evaporation map, showing location of the lakes occurring in the Awbārī sand sea Fazzān, Libya.

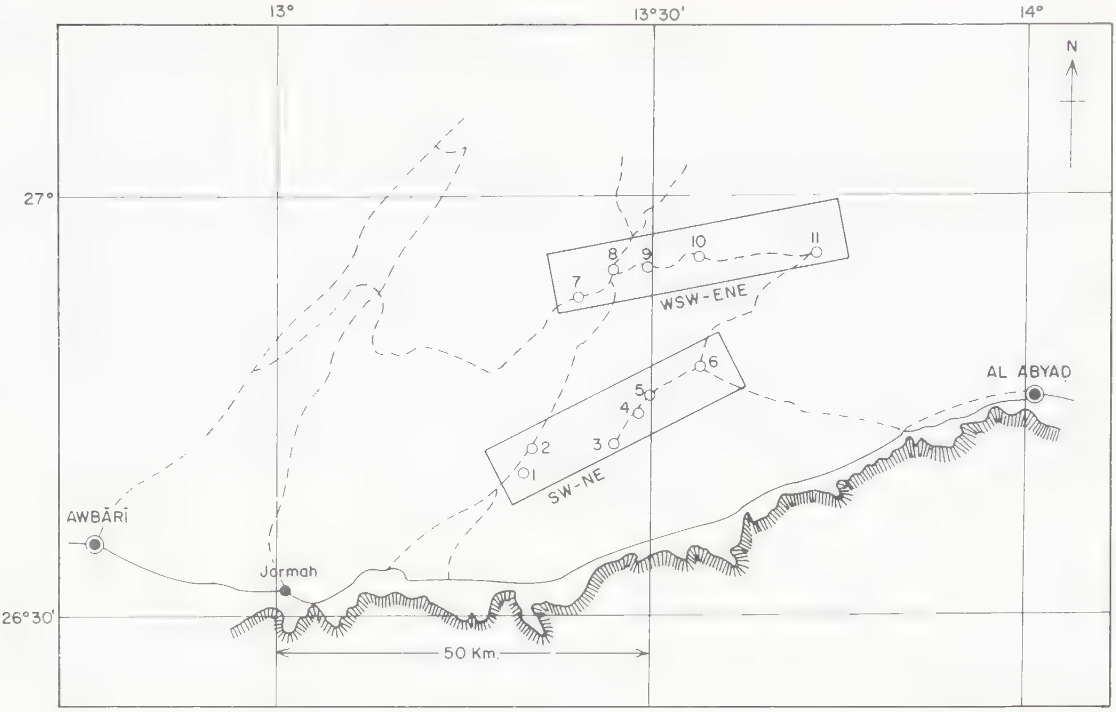

Fig. 2. Detailed location of 11 small lakes and lakelets in Ramlat ad Dawādah portion of the Awbārī sand sea of Fazzān.

The Awbārī sand sea itself occupies almost all the area between Wādī ash Shāṭi' in the north and Wādī al Ḥayāh in the south; it is widest in the west, and narrows towards the east, but is still of considerable width to the north of Sabhā.

Figure 2 summarizes existing data as to the number and location of 11 lakes occurring in the Awbārī sand sea. Table 1 gives their names, as well as latitude and longitude. The information thus presented was obtained mainly from a photocopy of a French or Italian map. It carried reference No. N.G.-33.NO and might well be a French map made in the 1944–1952 period.

Table 1. Names and locations of 11 lakes occurring within the Awbārī sand sea, Fazzān

Ref. No.	Name	Location		Notes
		North	East	
1	Mandara	26°10′	13°19′	Permanent; main lake
2	Umm al Miah	26°12′	13°20′	Permanent
3	Maḥrūqah	26°12′	13°27′	Temporary
4	Bacat	26°15′	13°29′	Permanent
5	Taxurounas	26°16′	13°30′	Permanent
6	Gabr ‘Oun	26°18′	13°33′	Major permanent lake; 100 ha
7	Oumelress	26°22′	13°24′	Temporary
8	Freduha	26°26′	13°27′	Temporary
9	Trouna	26°25′	13°29′	Major permanent lake
10	Oumhassa	26°26′	13°33′	Permanent
11	Tademka	26°26′	13°43′	Permanent

Number and Names

The names are rather uncertain; but it would seem that the names of the lakes change. Also, they are likely to be different in the different languages and dialects used in that isolated part of Fazzān.

On the Landsat satellite imagery the larger lakes can be identified, but they are too few to produce any pattern. When viewed from the air, the location of the lakes can be seen as influenced or controlled by the dunes. Here there are two patterns for the dunes. One set is elongated from southwest to northeast, and is dominant in volume. But there are also thinner, sharper ridges which run southeast to northeast. The two form a network mesh within whose general pattern the lakes are fitted. Clearly, there cannot be a lake where there is a mountain of sand; but do lakes appear where the sand is blown away or otherwise removed?

Figure 2 also indicates how the 11 lakes fall into two sets. Nos. 1–6 (Mandara to Gabr ‘Oun) form a

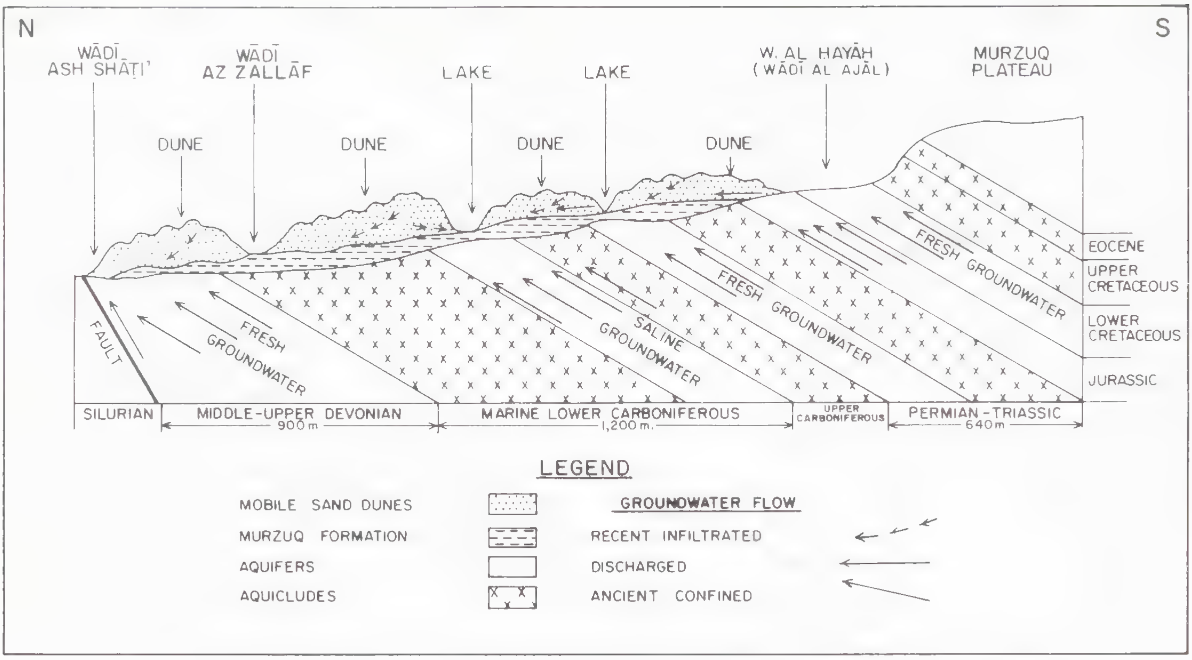
N
S
WĀDĪ ASH SHĀṬI'
WĀDĪ AZ ZALLĀF
LAKE
LAKE
W. AL HAYĀH (WĀDĪ AL AJĀL)
MURZUQ PLATEAU
DUNE
DUNE
DUNE
DUNE
FAULT
FRESH GROUNDWATER
SALINE GROUNDWATER
FRESH GROUNDWATER
FRESH GROUNDWATER
EOCENE
UPPER CRETACEOUS
LOWER CRETACEOUS
JURASSIC
SILURIAN
MIDDLE-UPPER DEVONIAN
900 m
MARINE LOWER CARBONIFEROUS
1,200 m.
UPPER CARBONIFEROUS
PERMIAN-TRIASSIC
640 m
LEGEND
MOBILE SAND DUNES
MURZUQ FORMATION
AQUIFERS
AQUICLUDES
GROUNDWATER FLOW
RECENT INFILTRATED
DISCHARGED
ANCIENT CONFINED

Fig. 3. Geological and hydrogeological section through the Awbārī sand sea from Wādī ash Shāṭi' in the north to Wādī al Ḥayāh in the south.

line running from the southwest to northeast, which is very marked and regular. Nos. 7–11 (with Trouna in the middle) also form a line, but running almost west to east, and less linear than the southern line. Linear features such as these might be related to subsand (and sub-Murzuq Formation) outcrops of confined aquifers of Triassic (or Permian age); such is indicated on the hydrogeological section (Fig. 3). Faults which allow ground water to rise might also result in such linear alignment of the lakes.

Age of the Lakes

The age of the lakes is not certain. Generally, one thinks of Fazzān as undergoing desiccation, with less water now than in the past as in Pachur (1980). Hence, one might think that in the past the lakes were more numerous and larger. No evidence is available as to this point. However, the presence of water crustacea (said to be edible) in the lakes points to a long period of existence. We have evidence that they were in existence in the winter of 1852/53. The explorer Edward Vogel spent that winter at Murzuq, as in Pesce (1969). From there he went to see a lake in the Ramlat ad Dawādah, which was reported to be bottomless. He measured its depth as some 7 metres. It is of interest that he went to see this lake, some distance from Murzuq, and does not mention anything of lakes in the Murzuq sand sea, much nearer to where he was spending the winter.

Most of the lakes shown on Fig. 2 are noted as “permanent”; the exact meaning of this term is not clear. Presumably they are “permanent” in that they contain water or evaporite minerals at all times; water may dry up at times, and there are reports from Mandara that there is an appreciable (say 2 m) annual change in water level. This could be due to increased evaporation in summer or, if fed by infiltration to decreased infiltration over certain periods, or if fed by underground water to decreased upwelling at periods.

Climate

The climate of the Awbārī sand sea is extremely hot and arid. Precipitation averages less than 20 mm, but there can be very rare rainstorms, producing some runoff in the wadis. Such may occur one year in ten. Temperatures are high, ranging from 42–46°C in July/August to 1–4°C in December/January. As a result, evapotranspiration is extremely high; the Atlas of World Water Balance shows annual potential evaporation as between 2 250 mm and 2 500 mm, the highest in the world (Fig. 1).

This high potential evaporation is of importance in assessing whether or not there may be some infiltration of precipitation (including dew) into the sand dunes of the Awbārī sand sea. Such infiltration was demonstrated by Dincer *et al.* (1974) for sand dunes in central Saudi Arabia and could occur in the sands of Fazzān of Libya. Such sands are usually in the size range 0.20–0.45 mm diameter (Allen, 1969) and Dincer found for the Dahna sand dunes that precipitation of 50 mm per annum gave an annual recharge of 20 mm, or 40% of the limited precipitation. How much would infiltrate for average annual precipitation of 20 mm is uncertain; it is unlikely to be 8 mm. However, under a rainstorm once in ten years, there could be appreciable present-day recharge to the Awbārī sand sea.

Geological Setting

Table 2 summarizes the regional stratigraphy, lithology, geology and hydrogeology and is based on Collomb (1962), Dubay (1980) and Zaluski and Sadek (1980). These formations, from the Devonian to the Eocene occur on the northern flank of the great Murzuq basin, and dip very gently to the south. Towards the north they are uparched to form Jabal Fazzān (Goudarzi, 1980); there are large E–W faults along Wādī ash Shāṭi’, on the northern limit of the Awbārī sand sea. In the Quaternary there was a large lake or series of lakes in the region from Wādī ash Shāṭi’ south to Wādī al Ḥayāh. At times and in areas, the lakes were fresh; but they were mainly saline (Petit-Maire, 1980), with a well-studied fauna of *Cardium glaucum* (Gaillard, 1980). In these lakes there was considerable sedimentation from water-borne and wind-blown material plus precipitate salts from the saline waters. They are known as the Murzuq Formation, and are up to 60 m thick. A drainage network must have eroded in the Murzuq Formation in pluvial times. During the present desiccation period and the current aridity, high sand dunes accumulated over the Murzuq Formation

Table 2. Summary of the regional geology and hydrogeology, from the Lower Carboniferous to the Quaternary and Recent

Age	Formation or lithology	Thickness (m)	Aquifer or aquiclude	Hydrochemistry TDS (ppm)
Recent	Mobile sand dunes	to 120	?	
Quaternary	*Murzuq Formation*	60	Aquiclude	
Eocene–Palaeocene	Limestones, with subordinate shales	140	Aquiclude	
Upper Cretaceous	Shales, with subordinate limestones and little dolomite	270	Aquiclude	
Lower Cretaceous	Sandstones	300	Aquifer	170
Jurassic	*Touratine Formation*	30	Aquiclude	
(250 m)	Sand and sandstone	30	Aquifer	76
	Clay and claystones	30	Aquiclude	
	Fine/medium sand and sandstones	40	Aquifer	75–120
	Claystones	70	Aquiclude	
	Medium/coarse yellow and grey sand	50	Aquifer	96–165
Triassic	Alternating strata of clay, claystone, mudstone with sandy clay at base	360	Aquiclude	
to Permian	Coarse/medium sandstones and sand; yellow-brown	280	Aquifer	175–185
Upper Carboniferous (continental)	Shale, clay and siltstone. Saline water in thin lower sandstone beds	330	Aquiclude	Saline water in lower beds
Lower Carboniferous (marine)	*Dembaba.* Limestone, dolomite and gypsiferous clay.	110	Aquifer	Saline water
	Assedjefar. Alternating shale/limestone with fine-grained sandstone.	190	Aquifer	Saline water
	Collenic Zone. Limestone and clay.	50	Aquifer	Saline water
	Mrar. Alternating shales, siltstones and fine-grained sandstones.	850	Aquiclude	

and surrounding areas, extending from Wādī ash Shāṭi' south to Wādī al Ḥayāh. The dunes can be over 120 m high.

Hydrogeology

The hydrogeology of the lakes in the Awbārī sand sea is that of the Upper Aquifer of Pallas (1980), which lies above the thick (850 m) aquicludes of the Mrar Formation of the marine Lower Carboniferous, and the 330 m aquiclude of the continental Upper Carboniferous. However, as shown in Table 2, there are some 350 m of uncertain aquifers (Collenic Zone, Assedjefar and Dembaba of Collomb, 1962) at the top of the marine Carboniferous, while in the lowermost portion of the continental Upper Carboniferous there are some sandy beds which may be aquifers. One fact is certain — these ground waters of the marine and continental Carboniferous are all highly saline. They have been cut by a number of oil and water-seeking boreholes, the latter to test and develop the good quality ground water in the Devonian to Cambrian age sandstones — the Lower Aquifer of Pallas.

The Upper Aquifer consists of terrestrial formations from Permian to Lower Cretaceous, in which all the aquifers are sands and sandstones (Table 2). The total thickness of these formations is some 1200 m, of which 700 m are aquifers. Much of their ground waters are confined, and flowing boreholes are common; there is probably some artesian seepage where these aquifers outcrop. They outcrop in Wādī al Ḥayāh where they have been studied by Zaluski and Sadek (1980). As Fig. 3 shows, they are considered to be the aquifers supplying the ground water developed in and to the south of Wādī al Ḥayāh.

The saline Carboniferous ground waters are accordingly considered as outcropping further north, under the Murzuq Formation and the mobile dunes of the Awbārī sand sea. They are confined ground waters, with potential artesian discharge. The upward movement of the saline ground water will be along the aquifers, but may in places occur upwards along possible faults, of which one is shown in Fig. 3. The saline ground water may outflow directly from the aquifers and faults where the Murzuq Formation is absent, or possibly through more permeable portions of the Murzuq Formation. Beneath the dunes they may then flow in the old drainage channels eroded in the Murzuq Formation in pluvial and earlier times.

The fresh ground waters of the Permian–Triassic–Jurassic aquifers may outflow not only in Wādī al Ḥayāh, but some distance to the north, under the southern edge of the Awbārī sand sea. Such artesian outflowing could give rise to some fresh waters flowing in the Murzuq Formation, protected from evaporation by the overlying sand dunes.

The possibility of some infiltration of the rare precipitation into the sand dunes has already been noted, based in part on Dincer's work on sand dunes in central Saudi Arabia. Such infiltrated water or water vapour would be of excellent chemical composition, since the dunes are pure quartz grains, and the amount of soluble minerals very low. The isotopic work summarized in Tables 4 and 5 confirm that there is infiltration of present-day rainfall.

There is extremely sparse vegetation growing up through the dunes, where the topography is favourable. This vegetation has not been studied, either in composition or extent. In some places old roots were seen and some vegetation may have been removed for fuel, while more was swamped by the moving dunes. However, it is fair to deduce that the presence of some sparse vegetation on the dunes indicates that in places, at least, there is some water present in or at the base of the sand dunes.

CHEMICAL AND ISOTOPIC RESULTS

Hydrochemistry

On a regional scale, Table 2 summarizes the hydrochemistry of the ground waters from the aquifers of Permian to Lower Cretaceous age. They increase slightly from TDS of 75 ppm at the top of the Jurassic to some 175–185 ppm in the Lower Triassic or Permian (Zaluski and Sadek, 1980). In the Lower Cretaceous, ground water averages TDS of around 170 ppm. All these ancient ground waters flow in sandstone aquifers, in which there are few or no soluble minerals; hence they are all waters with very low total soluble salts. Their detailed chemical composition need not be reported here.

On a regional scale also, the chemical composition of the saline ground waters of the Carboniferous aquifers is of interest.

Turning to the results of sampling around the lakes in 1976 and 1977, the main results are presented in Table 3. They have also been plotted on the Schoeller diagram of Fig. 4.

The Schoeller diagram is very suitable for the comparison of a limited number of water analyses,

Table 3. Chemical analyses made by IAEA of five water samples from and around Lakes Mandara and Umm al Miah, collected on 8 November, 1976. Results are in milligrams per litre, with underneath in brackets the same as milli-equivalents per litre. LIB-T-9. Dug Well No. 2, SW of Lake Mandara; see Fig. 6. LIB-T-10. Dug Well No. 3, NW of Lake Mandara; see Fig. 6

	LIB-T-9	LIB-T-10	LIB-T-11	LIB-T-12	LIB-T-13
Ca	59.1 (2.95)	31.4 (1.57)	166 (8.28)	264 (13.2)	108 (5.39)
Mg	18.7 (51.3)	10.1 (1.54)	349 (0.83)	865 (28.7)	624 (71.2)
Na	106 (4.61)	102 (4.44)	11 600 (505)	24 600 (1070)	117 000 (5089)
K	26.6 (0.68)	31.2 (0.80)	2800 (71.6)	4920 (126)	21 600 (552)
HCO_3^-	117 (1.92)	82.4 (1.35)	1065 (17.5)	650 (10.7)	602 (9.87)
Cl^-	172 (4.85)	162 (4.57)	19 400 (547)	39 400 (1111)	167 000 (4711)
SO_4^{2-}	106 (2.21)	63.4 (1.32)	2690 (56.0)	7960 (166)	41 200 (858)
TDS	605 (18.8)	482 (14.9)	38 070 (1234)	78 660 (2568)	348 000 (11 280)

such as the five considered here. In this case, however, the concentrations in the two samples from Lake Umm al Miah (LIB-T-11 and LIB-T-12) have had to be reduced ten times, while that from Lake Mandara (LIB-T-13) has had to be reduced 100 times, so as to fit on the diagram. Ratios have not been changed and comparison of ratios is much facilitated by the use of the Schoeller diagram.

The two waters from the wells are normal ground waters typical of the artesian aquifers of Fazzān but with a three or fourfold increase compared with the ground waters of Table 2. The Na : K ratios are about 7 : 1 and 5 : 1 which suggest a slightly higher amount of K than usual, but not enough to call for explanation. Chloride is the dominant anion, which is expected in ground waters, but unlikely in recently infiltrated precipitation which as yet has not taken salts into solution. It is possible that these waters are a mixture of infiltrated precipitation, plus some water from an artesian aquifer.

In the three lake waters Mg has increased strongly relative to Ca; this may be due to precipitation of Ca. The Na : K ratio has changed a little, and if Na has precipitated as trona or other sodium carbonates, some K has also precipitated; so, there could be K salts in the evaporite suite of minerals. As usual, Cl has increased, and the water of Lake Mandara must be precipitating. Thus, comparisons of the Lake Mandara water chemistry with the waters of the two wells is much complicated by the amount of mineral precipitation which has taken place. This also applies to the waters of Lake Umm al Miah, where, as observed in the field and confirmed by analyses, precipitation of gypsum–anhydrite is taking place.

With regard to possible future hydrochemical work, attention is drawn to the value of trace element determination, and in particular ratios of trace elements (not precipitated) to major elements undergoing precipitation. Thus the ratios of boron to chloride can be of value in determining the genesis of waters. A B : Cl ratio of 0.0002 indicates oceanic and surface water types; a B : Cl ratio of 0.02 indicates oil-field brines; while a B : Cl ratio of 0.1 is common in hot springs of volcanic origin. Lithium is another trace element which could have diagnostic value in this study.

Isotopic Hydrogeochemistry

The isotopic results of Fazzān lakes are reported in Table 4, (section a), together with those of selected water samples from the same area. These additional results given for the sake of comparison refer to: (b) ground water from shallow wells located in the proximity of the lakes, which in principle should have the same isotopic composition as the water feeding the lakes; (c) water from pools occasionally replenished by rain; (d) ground water from wells believed to be recharged at least in part by modern rains (the tritium content is frequently high); (e) the mean isotopic composition of deep ground water in three Fazzān areas, which are the Wādī al Ḥayāh valley, the Wādī ash Shāṭi' valley, and the zone from Jabal Qarqaf to Al Jufrah. These latter data, taken from Salem *et al.* (1980), refer to "old" ground water, with a very low ^{14}C content and no tritium.

Table 5 gives the isotopic composition of 10 individual rainfalls in various Fazzān locations from late 1977 to early 1979, collected by field staff of the consulting firms Idrotecneco and Aquater. Mean values of the isotopic composition of rains in other arid or semi-arid locations in North Africa are reported in Table 6 for comparison. These latter data derive from the IAEA–WMO network of stations for determining the isotopic composition of precipitation on a global scale.

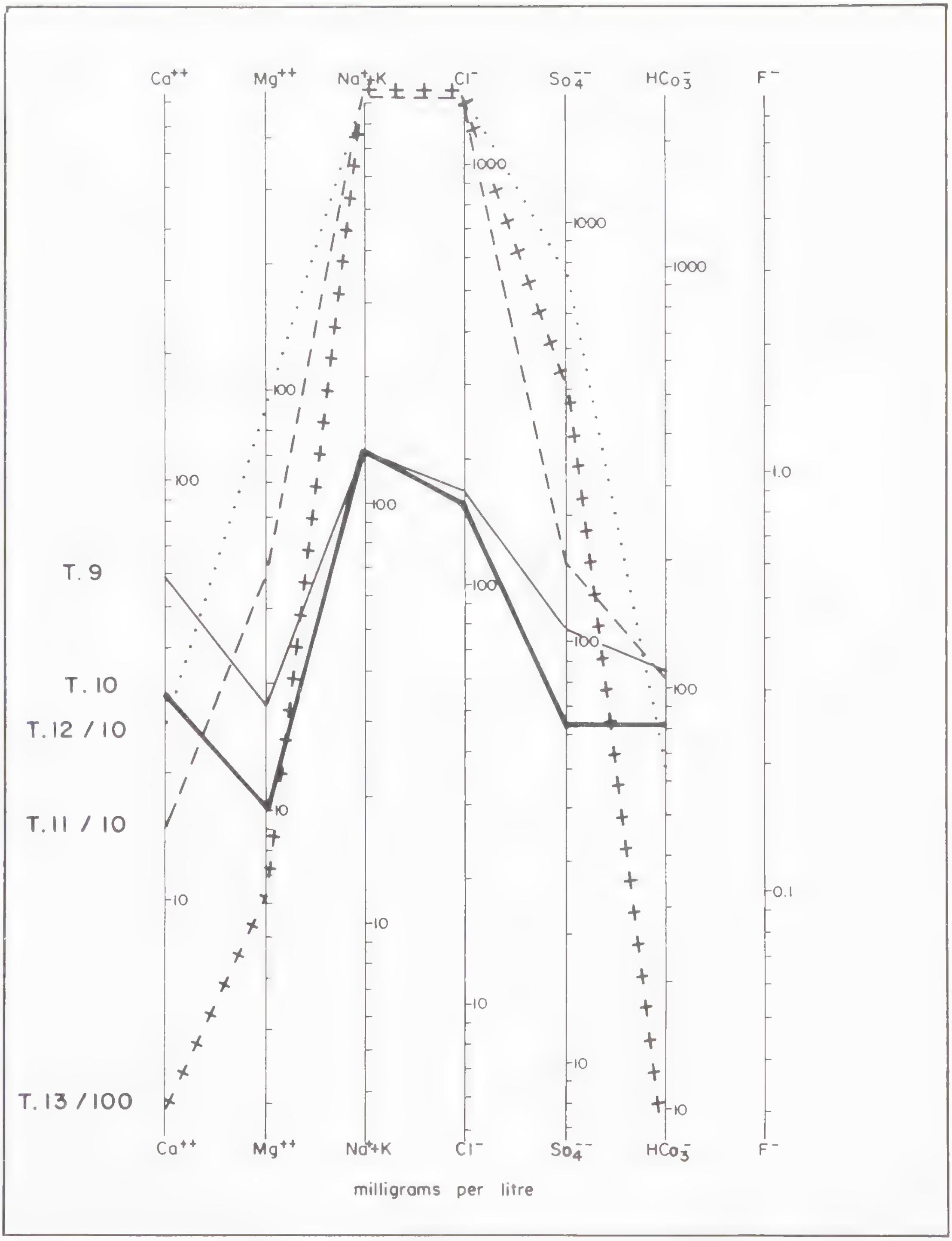

Fig. 4. Five chemical analyses of waters from and around Lakes Mandara and Umm al Miah, in the Awbārī sand sea, plotted on the Schoeller diagram.
LIB-T-11. S edge of Lake Umm al Miah (26°12′N, 13°19′E).
LIB-T-12. N edge of Lake Umm al Miah.
LIB-T-13. NE corner of Lake Mandara (26°10′N, 13°19′E); see Fig. 6.

Table 4. Isotope composition and chloride content of water samples from Fazzān (sampled in 1976–1979)

No.	Location	δD (‰)	δ^{18}O (‰)	TU	Cl$^-$ (mg/l)
(a) *Lakes*					
1	Lake Mandara, NE edge	−26.7	+1.92		167 000
2	Lake Umm al Miah SW edge	−43.6	−1.85		19 400
3	Lake Umm al Miah NE edge	−20.8	+1.86		39 400
4	Lake Magfur	+18.8	+15.14	17.0 ± 3.8	76 600
5	Lake Mawo	−8.7	+4.97	12.4 ± 1.0	45 900
6	Lake Gabr 'Oun	−13.3	+4.01	13.0 ± 2.2	51 800
(b) *Ground water in the lake area*					
7	Mandara, well No. 2, SW of lake	−74.1	−9.50	0.1 ± 0.2	1 180
8	Mandara, well No. 3, NW of lake	−77.4	−10.06	0.5 ± 0.3	840
9	Gabr 'Oun, well 400 m N of lake	−77.5	−10.19	0.8 ± 0.3	
10	Gabr 'Oun, well in the village	−74.3	−9.88	0.1 ± 1.2	
	Average	−75.8	−9.91		
(c) *Pools*					
11	Wādī Tizuenat	−2.1	+2.53	29.9 ± 1.0	0.5
12	Wādī Tizuenat	−4.1	+0.59	32.5 ± 1.0	0.5
13	Bi'r Guerbaja	+20.4	+12.45		
14	Idrī Area	+0.8	+1.02		
(d) *Ground water recharged by modern rains* (at least in part: generally high tritium)					
15	Shaguayga (25 km NW of Mizda)	−37.7	−5.84	25.6 ± 0.7	
16	Wādī Tanezzuft (40 km N of Ghāt)	−10.4	−1.41	248 ± 7 (!)	519
17	Alrar	−35.8	−5.49	57.4 ± 1.6	330
18	Jabal as Sawdā', shallow well	−42.0	−6.46	1.9 ± 0.4	222
19	Bi'r al Washkah, Jabal as Sawdā'	−44.3	−6.43	1.8 ± 0.4	539
20	Tashnah	−44.9	−5.26	8.3 ± 0.4	533
21	Al Ḥamādah al Ḥamrā'	−49.7	−6.0	6.0 ± 0.2	
	Average (excluding sample 16)	−42.4	−5.91		
(e) *Deep old ground water* (mean values; no tritium; ^{14}C always less than 10% of modern (generally corresponding to an age of more than 15000 years)					
22	Wādī al Ḥayāh, Mesozoic Aquifer	−80.1	−10.81		
23	Wādī ash Shāṭi', Palaeozoic Aquifer	−79.7	−10.96		
24	Jabal al Qarqaf–Al Jufrah, Palaeozoic and Mesozoic Aquifer	−75.8	−10.24		
	Average	−78.5	−10.67		

Table 5. Isotopic composition of rains in Fazzān

No.	Location	Date	Amount (mm)	δD (‰)	δ^{18}O (‰)	TU
25	Al Farjān	late 1977		−4.9	−2.37	26.1 ± 3.0
26	Al Jufrah	13/11/77	1.5	−0.8	−2.23	21.6 ± 3.8
27	Al Jufrah	14/2/78	3.0	−43.4	−5.19	43.4 ± 3.4
28	Al Farjān	13–14/4/78	2.6	+3.4	−5.80	
29	Jabal as Sawdā'	28/4/78	4.1	−23.3	−2.23	32.8 ± 3.3
30	Al Farjān	16/10/78	3.3	−2.2	−1.90	30.0 ± 4.4
31	Jabal al Qarqaf	23–28/10/78	3.4	+9.3	+3.30	18.6 ± 5.8
32	Brāk	1/11/78	18.2	−2.9	−2.04	22.8 ± 5.3
33	Brāk	18/3/79	2.8	+1.0	+0.22	
34	Jabal al Qarqaf	19/3/79	0.8	−2.2	+0.88	18.2 ± 3.6
	Weighted average		(39.7)	−6.2	−1.86	

Table 6. Isotopic composition of rains in arid and semi-arid stations in North Africa (data from IAEA/WMO network)

No.	Station name and rainy season	Mean annual precipitation (mm)	Total precipitation averaged (mm) and number of monthly samples averaged (n)	δD (‰)	δ^{18}O (‰)
35	Sidi Barrani, Egypt — winter		607 (25)	−19.9	−4.48
36	Alexandria, Egypt — winter	190	3856 (122)	−10.1	−2.69
37	Ouargla, Algeria — mainly winter		86 (5)	−35.5	−5.03
38	Faya Largeau, Chad — summer	16	38 (3)	−4.9	−1.96
39	Geneina, Sudan — summer	549	2900 (36)	−8.5	−1.81
40	Khartoum, Sudan — summer	164	1336 (37)	−11.9	−1.96

The stable isotope results are expressed as usual in δ‰, that is in terms of normalized parts per mil difference from the isotopic ratio of the V-SMOW reference sample (V-SMOW = Vienna Standard Mean Ocean Water). The definition of δ‰ is:

$$\delta‰ = \left(\frac{R_{\text{sample}}}{R_{\text{V-SMOW}}} - 1\right) \times 1000$$

where $R = {}^{18}\text{O}/{}^{16}\text{O}$ or D/H (D = ^{2}H, deuterium).

The reproducibility (1σ) is usually ±1‰ for the δD determinations and 0.1‰ for the δ^{18}O determinations. The stable isotope results of Tables 4 and 5 are plotted in Fig. 5.

The concentration of tritium, the radioactive isotope of hydrogen with mass 3 (T = ^{3}H, tritium; half life 12.43 years), is expressed in TU, Tritium Units: 1 TU corresponds to a concentration of 1 atom of tritium in 10^{18} atoms of hydrogen. The error associated with the measurement is quoted in Tables 4 and 5.

As is well known (see, for instance, Gonfiantini, 1986, for a comprehensive discussion of isotopic effects in evaporation and in lakes), the heavy isotope content of a water evaporating in the free atmosphere increases following a linear trend in a (δ^{18}O, δD) plot, towards δD and δ^{18}O maximum values which depend on various parameters: the relative humidity of the atmosphere, the isotopic composition of the feeding water and of the atmospheric vapour, the ratio between evaporation and inflow, the degree of mixing, etc. High salt concentration — say, above 50 g/l — may also affect considerably the isotopic composition of the evaporating water, by reducing its thermodynamic activity and therefore also its evaporation rate, and through the isotopic fractionations occurring between the water "bound" in the hydration sphere of ions and the "free" water. Also, precipitation of hydrated salts may introduce isotopic effects: however, these are most probably negligible for the Fazzān lakes, because the major salt precipitated is sodium chloride which does not contain water of crystallization.

The fact that the δD and δ^{18}O values of the Fazzān lakes are linearly correlated (Fig. 5) is a confirmation that the environmental conditions governing the evaporation are very similar for all lakes, as well as the isotopic composition of the feeding water. Excluding Lake Mandara, where sodium chloride is deposited, and Lake Magfur (chloride content 76.6 g/l), which because of their high salt concentration may deviate from the linear correlation, the relationship between δ^{18}O and δD exhibited by the other four lake samples is:

$$\delta\text{D} = (5.12 \pm 0.44)\,\delta^{18}\text{O} - (33.1 \pm 1.0) \qquad (1)$$

with r (correlation coefficient) = 0.993. The four pools also show a linear correlation between δD and δ^{18}O, which however obeys a different equation:

$$\delta\text{D} = (2.02 \pm 0.32)\,\delta^{18}\text{O} - (4.6 \pm 1.3) \qquad (2)$$

with $r = 0.976$.

The ground water and precipitation samples are now considered. There is definitely a marked difference between the isotopic composition of the deep old ground water and that of ground water recently recharged: the latter, although showing a considerable scatter of values definitely has a higher heavy isotope content. This difference between recent and old ground water in the Sahara desert is attributed to climatological differences between past (humid) and present (arid) conditions and as has been reported several times (Sonntag *et al.*, 1978; Edmunds and Wright, 1979; Srdoc *et al.*, 1980; Dray *et al.*, 1983). It is also worth noting that the shallow ground water in the lake area has an isotopic composition close to that of old ground water, thus showing that the latter is by far the major source of the first.

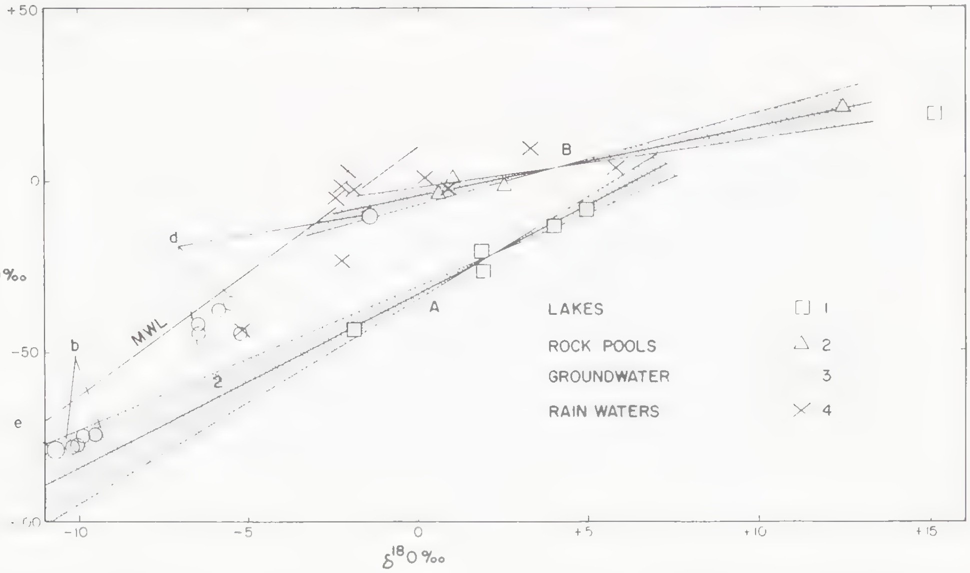

Fig. 5. $\delta^{18}O/\delta D$ plot of Fazzān waters. *1* = lakes; *2* = rock pools; *3* = ground water (*b* = shallow ground water in lake areas; *d* = recently recharged ground water (generally high tritium); *e* = mean value of deep ground water (low ^{14}C)); *4* = rain waters. Line *A*: correlation for lakes (equation 1); line *B*: correlation for rock pools (equation 2).

The Fazzān precipitation samples show values which, although scattered, are generally more enriched than recent ground water. Moreover, some of them show an enrichment in heavy isotopes, probably due to evaporation while the raindrops were falling, and this matches the $\delta D/\delta^{18}O$ trends of the pools (Fig. 5). Also the isotopic composition of precipitation of other stations in North Africa (Table 6) is similar to that of the Fazzān rains, indicating that these, although few and collected over a short period of time, may however be isotopically representative.

Old and recent ground waters together have δD and $\delta^{18}O$ values which parallel the so-called world meteoric water line, but with a somewhat lower intercept.

If now one prolongs the line of equation (1) for Fazzān lakes towards the meteoric water line, one can see that this passes close to the values of the deep ground water and of the shallow ground water from wells close to the lakes: this confirms once more that the Fazzān lakes are recharged by deep ground water which probably reaches the surface through faults. On the contrary, the equation (2) line for rock pools confirms that these are recharged by modern rains.

FORMATION AND PERSISTENCE OF LAKE MANDARA

Lake Mandara is the lake in the Awbārī sand sea which has been most studied in the preparation of this paper. It was visited on 11 July and 8 November, 1976. Figure 6 is a map of the Mandara lake and oasis, indicating the location from which samples LIB-T-9, LIB-T-10 and LIB-T-13 were taken. Figure 7 is a hydrogeological section, indicating one theory as to how the lake could have persisted for a long time.

Map and Formation of Lake Mandara

Lake Mandara was approached from the west and southwest. On the east it is protected by very high sand dunes, forming a hill or mountain. There are shelters for animals on the slopes towards the oasis. The lake is roughly square, with an area of the order of 5 hectares. On the NE and SW there are low cliffs (2–5 m high) almost down to the water. On the SE and NW there are flats which have been invaded by date palms forming dense groves. The whole of the lake is surrounded by date palms which decrease in number as the thickness of sand cover increases. The village is situated on the higher ground NE of the lake, but there are scattered habitations all around the lake. The main area of cultivation lies around

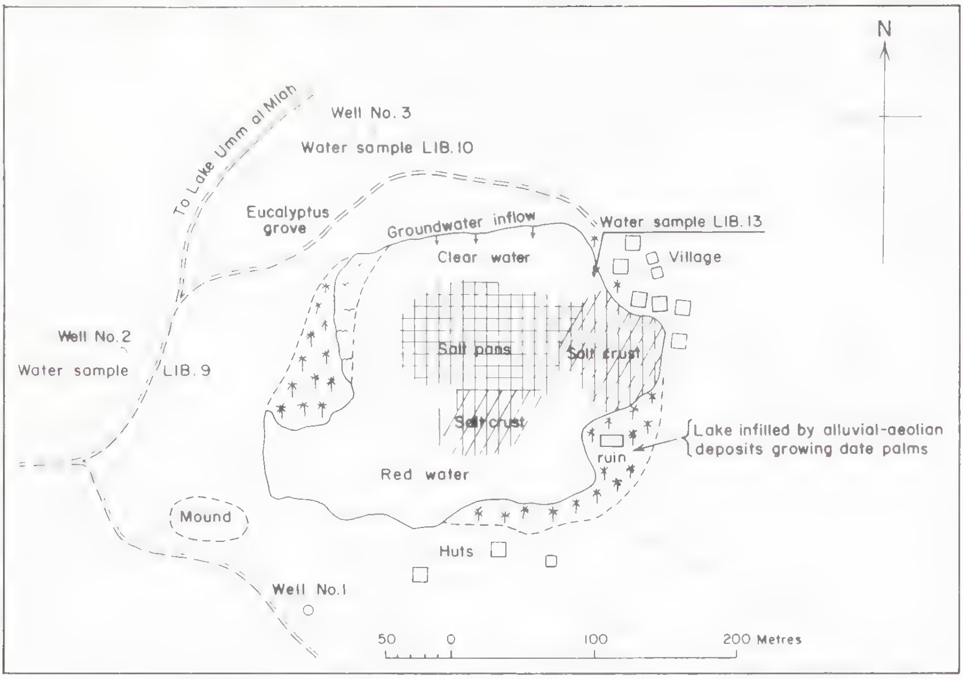
N
To Lake Umm al Miah
Well No. 3
Water sample LIB.10
Eucalyptus grove
Groundwater inflow
Water sample LIB.13
Clear water
Village
Well No. 2
Water sample
LIB. 9
Salt pans
Salt crust
Salt crust
Lake infilled by alluvial-aeolian deposits growing date palms
ruin
Red water
Mound
Huts
Well No.1
50
0
100
200 Metres

Fig. 6. Map of Mandara Lake, with an area of some 5 ha, in the Awbārī sand sea.

the village, but small irrigated plots occur around the lake. Water of good chemical composition is obtained from open wells.

The lake is composed partly of water and partly of evaporite deposits. Much of the lake is solid precipitate, and there are tracks where people walk across the salt pans. It would seem that the lake is solid in places throughout the year. The salts were not studied; it may be taken that they are halite, trona and related sodium carbonates, plus possibly gypsum–anhydrite. The chemical analyses made of the lake water (LIB-T-13) do not add much on this point.

The inflow of water of good chemical composition to the lake from the surrounding area is well attested. It can be seen on the shores of the lake. It is tapped by wells, and so permits of permanent habitation around the lake and the creation of the oasis. It is used by the date palms and extracted for limited irrigation. There are also eucalyptus trees on the NW shore of the lake. Samples LIB-T-9 and LIB-T-10 were taken from open wells supplying irrigation water to the west and north of the lake.

Persistence of Lake Mandara

Figure 7 presents a section indicating the way in which Lake Mandara could have been formed, could be maintained as a lake, and could be supplied with rising ground water under artesian pressure. It attempts to provide answers to many pertinent questions which have been raised regarding Lake Mandara (and therefore the other lakes).

Why has Lake Mandara not been infilled with blown sand? The sand moves with the wind, but is trapped when it falls into water. Hence, in time, a lake such as Mandara should have been filled with blowing sand. It is considered that the lake does not fill because it is continuously being deepened (or its depth maintained) by solution of the underlying rock.

This hypothesis has a number of implications, but it also solves a number of problems in addition to the non-filling of the lake. It implies a type of karst origin for the lake, by the solution of a carbonate (or gypsum) aquifer. Thus, in Fig. 7, a limestone aquifer (or semi-aquifer) is shown overlying a sandstone aquifer, both bounded by impermeable shales. The water rising in the limestone aquifer is of poor chemical quality and is saturated in bicarbonates, while the sandstone waters could be undersaturated (and so aggressive) with regard to calcite. When the water, rising under artesian pressure, reaches the atmosphere, there is solution of fresh carbon dioxide from the atmosphere, and the limestone aquifer comes under solu-

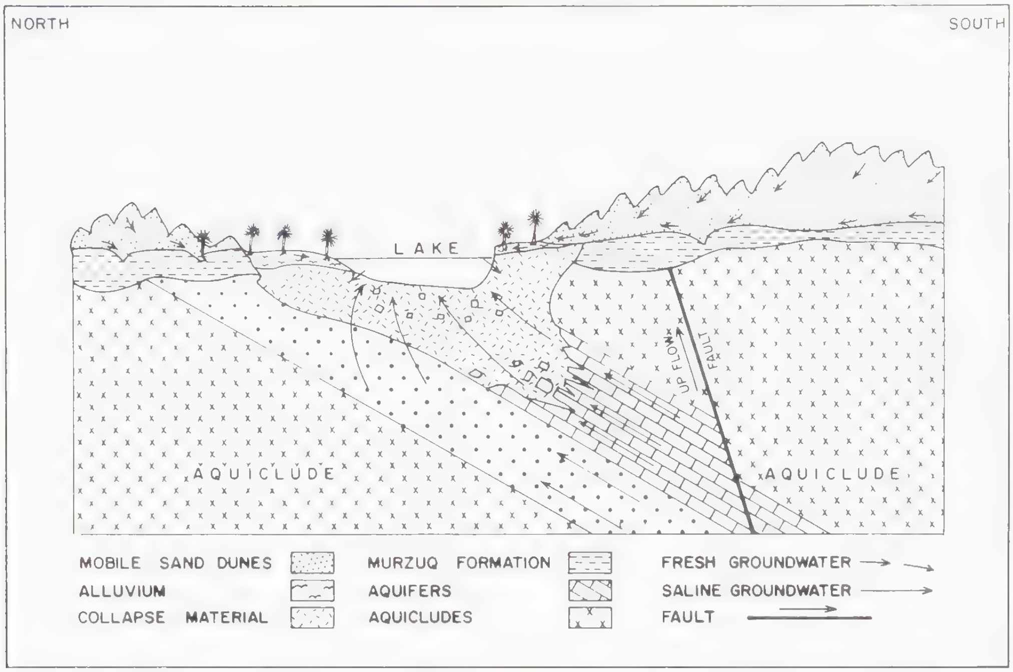

Fig. 7. Hydrogeological section, indicating a possible way in which Lake Mandara has persisted.

tion. Karstic openings and collapse occur, and a lake is formed under conditions which enable it to deepen itself and make room for infalling aeolian sand grains.

Concentration by evaporation then commences to affect the rising ground waters, and precipitation takes place. The present water in the lake has TDS of 348 000 ppm, a brine ten times as salty as the ocean! The removal of the precipitate presents problems under natural conditions. It, as much as sand grains, could fill the depression and replace the water by a solid evaporite deposit. In the past salts have been extracted from the lakes and used; this would represent but a small amount of the total deposition over the ages.

Below and around the present lake there would thus seem to be a volume of material of mixed origin — precipitates, remnants of the original rock aquifers, bits of Murzuq lacustrine marl, infallen sand grains and rotting vegetative roots. Where permeable, the mixture will be saturated, and through it the artesian water upwells and finds its way directly and by lateral flow to the open lake. The surface of this open lake is kept depressed by high evaporation, so that there is a steady flow from the surrounding area into the lake.

It is admitted that this hypothesis as to the origin and persistence of Lake Mandara has some weaknesses. It needs factual checking. Some of this may come from hydrological and hydrochemical studies, but a little drilling would be most welcome. A borehole sunk to provide the small community with good water would also reveal much of the geology and hydrogeology; it could make a major contribution to an understanding of the true nature of these strange lakes in the middle of the Awbārī sand sea.

CONCLUSIONS

The data presented and analyzed here indicate that some firm conclusions can be drawn regarding the 11 lakes and lakelets known to exist in the Awbārī sand sea.

(1) Lakes can occur under the hot aridity of the Fazzān of Libya only by discharges of ground water; small supplementary supplies of surface runoff can infiltrate and supplement the ground water discharge under special circumstances.

(2) The main water supply to the 11 lakes in the Awbārī sand sea is from saline ground water discharging from the Carboniferous aquifers; this is confirmed by the isotopic studies.

(3) This saline ground water is under artesian pressure, and discharges at the outcrops of the

aquifers or ascends along faults; all discharges are buried under the mobile dunes of the Awbārī sand sea.

(4) A secondary water supply is provided by infiltration of rainfall and possibly dew into the highly permeable sand dunes of the Awbārī sand sea. This isotopic work indicates that the amount of this recent ground water is small.

(5) This small amount of infiltrating water is of excellent chemical composition, and remains so while in the dune sands; it picks up salts when flowing over the Murzuq Formation and when mixed with saline Carboniferous ground water.

(6) A possible tertiary water supply is from artesian discharge of ground water in the Permo-Triassic aquifers outcropping to the south of Wādī al Ḥayāh.

(7) This tertiary ground water is of very good chemical composition.

(8) All three waters discharging under the sand dunes can flow and mingle in complex ways in the drainage network eroded in the lacustrine Murzuq Formation by runoff during Pluvial times.

(9) The lakes are liable to infilling with wind-blown sand, with advancing dunes and by precipitation of salts; there could be many such ancient lake sites buried under the dunes.

(10) The known persistence of some of the lakes is due to collapses of the limestone and evaporite aquifers due to solution by aggressive ground waters; such collapses provide space for precipitates and wind-blown sands.

ACKNOWLEDGEMENTS

The list of references acknowledges briefly the debt of the authors to the many co-workers in fields related to these lakes in the Awbārī sand sea. The work was done while Dr. Burdon was FAO consulting hydrogeologist under Trust Fund 9184 in the Secretariat of Dams and Water Resources. He was much engaged on the water resources of Fazzān, and the fieldwork for this study was done in cooperation with Mr. Ali M'Sattar, Dr. Abdul Kader El Houdari, Dr. Mohamed El Chair, Mr. F.I. Peters and Mr. Matti Taka. For the isotope work, there were visits by Dr. Roberto Gonfiantini and his colleagues, who completed the isotopic study at IAEA HQ in Vienna.

REFERENCES

ALLEN, J.R.L. (1969). *Physical Processes of Sedimentation.* Earth Sciences Series 1. Elsevier, New York, N.Y.

BURDON, D.J. (1980). Infiltration conditions of a major sandstone aquifer around Ghat, Libya. *In: The Geology of Libya* (*eds* M.J. Salem and M.T. Busrewil). Academic Press, London, **II**, 595–610.

COLLOMB, G.R.O. (1962). Etude Géologique du Jebal Fazzān et de sa Bordure Palaeozoïque. *Notes Mém. Comp. Fr. Pétrole*, **1**.

DINCER, T., AL-MUGRIN, A. and ZIMMERMANN, U. (1974). Study of the infiltration and recharge through the sand dunes in arid zones, with special reference to the stable isotopes and thermonuclear tritium. *J. Hydrol.*, **23**, 79–109.

DRAY, M., GONFIANTINI, R. and ZUPPI, G.M. (1983). Isotopic composition of groundwater in the Southern Sahara. *In*: Palaeoclimates and Palaeowaters: a Collection of Environmental Isotope Studies. IAEA, Vienna, 187–199.

DUBAY, L. (1980). Ground water in Wādī ash Shāṭi', Fazzān — a case study of resource development. *In: The Geology of Libya* (*eds* M.J. Salem and M.T. Busrewil). Academic Press, London, **II**, 611–628.

EDMUNDS, W.M. and WRIGHT, E.P. (1979). Groundwater recharge and palaeo-climate in the Sirte and Kufra Basins, Libya. *J. Hydrol.*, **40**, 215–241.

FREULON, J.M., LEFRANC, J.P. and LELUBRE, M. (1955). Carte Géologique de Reconnaissance du Sahara Libyan — (feuille N.G. 33 N-), Sabhā; scale 1 : 500 000, Publ. I.R.S., Alger.

GAILLARD, J.M. and TESTUD, A.M. (1980). Comparative study of Quaternary and present-day lagoon populations of *Cardium glaucum*, Mollusca, Bivalvia. *In: The Geology of Libya* (*eds* M.J. Salem and M.T. Busrewil). Academic Press, London, **III**, 809–814.

GONFIANTINI, R. (1986). Environmental isotopes in lake studies. *In*: Handbook of Environmental Isotope Geochemistry, **2**, *The Terrestrial Environment*, B. Elsevier, Amsterdam, 113–168.

GOUDARZI, G.H. (1970). Geology and mineral resources of Libya — a reconnaissance. *U.S. Geol. Surv. Prof. Pap.*, **660**, 104 p.

GOUDARZI, G.H. (1980). Structure — Libya. *In: The Geology of Libya* (*eds* M.J. Salem and M.T. Busrewil). Academic Press, London, **III**, 879–892.

JONES, J.R. (1971). Ground Water Provinces of Libyan Arab Republic. *In: Symp. Geol. Libya* (*ed.* C. Gray). Fac. Sci., Univ. Libya, Tripoli, 449–458.

MULLER-FEUGA, R. (1954). Contribution à l'Etude de la Géologie, de la Pétrographie, et des Ressources Hydrauliques et Minérales du Fazzān. *Ann. Mines Géol., Tunis.*

PACHUR, H.J. (1980). Climatic history in the late Quaternary in southern Libya and the western Libya Desert. *In: The Geology of Libya* (*eds* M.J. Salem and M.T. Busrewil). Academic Press, London, **III**, 781–788.

PALLAS, P. (1980). Water resources of the Socialist People's Libyan Arab Jamahiriya. *In: The Geology of Libya* (*eds* M.J. Salem and M.T. Busrewil). Academic Press, London, **II**, 539–594.

PESCE, E. (1969). Exploration in the Fazzān. *In*: Geology, Archaeology and Prehistory of Southwestern Fazzan, Libya. *Petrol. Explor. Soc. Libya*, 53–66.

PETIT-MAIRE, N., CASTA, L., DELIBRIAS, G. and GAVEN, C. (1980). Preliminary data on Quaternary palaeolacustrine deposits in the Wādī ash Shāṭi' area, Libya. *In: The Geology of Libya* (*eds* M.J. Salem and M.T. Busrewil). Academic Press, London, **III**, 797–808.

Salem, O., Visser, J.H., Dray, M. and Gonfiantini, R. (1980). Groundwater flow patterns in the western Libyan Jamahiriya evaluated from isotopic data. *In: Arid Zone Hydrology: Investigations with Isotope Techniques.* IAEA, Vienna, 165–179.

Sonntag, C., Klitzsch, E., Lohnert, E.P., El Shazly, E.M., Munnich, K.O., Junghans, Ch., Thorvehe, V., Weistroffer, K. and Swailem, F.M. (1978). Palaeoclimatic information from deuterium and oxygen-18 in carbon-14 dated north Saharian groundwaters: Groundwater formation in the past. *In: Isotope Hydrology*. IAEA, Vienna, 569–581.

Srdoc, D., Sliepcevic, A., Obelic, B., Horvaticic, N., Moser, H. and Stichler, W. (1980). Isotope investigations as tool for regional hydrogeological studies in the Libyan Arab Jamahiriya. *In: Arid Zone Hydrology: Investigations with Isotope Techniques.* IAEA, Vienna, 153–164.

Unesco (1977). Atlas of the World Water Balance (originating at Gidrometeoizdat, Leningrad). *UNESCO.*

Zaluski, M. and Sadek, K.E. (1980). Hydrogeology of Mesozoic aquifers in the western part of Wādī al Ajāl. *In: The Geology of Libya* (*eds* M.J. Salem and M.T. Busrewil). Academic Press, London, II, 635–642.

Isotope Hydrological Investigations in the Tāwarghā' Area, Libya

M. WOLF[1], H. MOSER[1] AND H. ZEINO[2]

إستعمال النظائر في دراسة جيولوجيا المياه بمنطقة تاورغاء

م. وولف وه. موسر وه. زينو

الخلاصة

لقد تمّ قياس تركيز النظائر المشعة : كربون (ك^{14}) وهيدروجين (يد^{3}) والنظائر الثابتة (هيدروجين يد$_{2}$) وكربون (ك^{13}) وأكسجين (أ^{18})، في المياه الجوفية ومياه العيون والمياه السطحية بمنطقة تاورغاء، لدراسة عمر وأصل هذه المياه. وقد وجد أن تركيز الهيدروجين (يد^{3}) أقل من 0,1 إلى 12 (Tu)، ووجد أنه لا يوجد تغذية حالية للخزانات الجيرية والحجر الرملي العميقة.

وأعطى تركيز الكربون (ك^{14}) الذي يتراوح بين 0,6 إلى 118٪ لمياه الآبار العميقة ذات نموذج (كربون^{14})، أعمار أكثر من 30000 سنة.

وقد استعملت كيمياء المياه (مع حسابات النموذج جيوكيمياء المياه والتحليلات المعدنية وحسابات الكربون-^{13} لعينات من أحجار الخزانات الجوفية المختلفة) لتفسير تركيز الكربون^{14} في المياه الجوفية. وقد وجد أن قيم الكربون^{13} تتراوح بين − 3.6٪ و− 11.6٪ كما أنه تظهر انحرافات مهمة مقارنة بالمياه ذات الأصل العادي. ويمكن أن يعزي هذا إلى تبادل النظائر من ترابط الأحجار عن طريق الهيدروجين^{2} − 19.4 و73.6٪) والأكسجين-^{18} (− 9,6 إلى − 3٪) يمكن التمييز بين المياه ذات الأصل المختلف. وستناقش نتائج النظائر في سياق الحديث عن جيولوجيا المياه للموضوع.

Abstract. Radioactive isotope (^{3}H, ^{14}C) and stable isotope (^{2}H, ^{13}C, ^{18}O) concentrations were measured on ground water, springs and surface water in the Tāwarghā' area to study the age and origin of these waters. ^{3}H concentrations are between <0.1 and 12 TU. Lowest concentrations occur in the deep carbonate and sandstone aquifers and indicate no recent recharge. The ^{14}C concentrations are between <0.6 and 118% modern and give model ages of generally more than about 30 000 years for the deep well waters. The chemistry of the water (together with hydrogeochemical model calculations), mineralogical analyses and ^{13}C determinations on rock samples from different aquifers are also used to interpret the ^{14}C concentrations of the ground waters. The δ^{13}C values of the waters are between -11.6 to -3.6‰. The higher values might be attributed to isotope exchange with the rock matrix by recrystallization and/or dissolution/precipitation processes. From the δ^{2}H (-73.5 to -19.4‰) and δ^{18}O values (-9.6 to -3.0‰) it is possible to distinguish between waters of different origin. The isotope results are discussed in relation to the hydrogeological situation.

INTRODUCTION

As part of a hydrogeological research programme in the Tāwarghā' Project area in Libya, ^{2}H, ^{3}H, ^{13}C, ^{14}C and ^{18}O isotope analyses of water samples were performed to get an insight into the origin and age structure of the ground water. The project area is in the northwest of Libya, east of Tripoli. There are several springs and a relatively large number of wells in the area (Fig. 1). In most cases the wells lead to bodies of water under pressure at a relatively large depth. Hydrogeologically, these bodies of water are presumed to come from the south or southwest and flow to the north or northeast (Pallas, 1980). The rock matrix of the upper aquifers consists primarily of limestone and dolomite; the rock matrix of the lower aquifers consists of sandstone.

---

[1] GSF-Institut für Hydrologie, D-8042 Neuherberg, F.R.G.
[2] WAKUTI-Karl Erich Gall KG, D-5900 Siegen, F.R.G.

REGIONAL GEOLOGY AND HYDROGEOLOGY

The Zlīṭan–Miṣrātah–Tāwarghā' area is located on the intersection of several geological structures and includes the boundary of two large basins, Al Ḥamrā' and Sirt.

The mainly continental and shallow marine sediments of the Lower Mesozoic have a decreasing thickness from north to south. They are characterized by a series of sandstones and clays, but an abrupt change of facies to dolomite can be observed north of the latitude of Tāwarghā'. On the rim of the basins, platform limestones, evaporites (mainly dolomite and gypsum), and sandstones prevail and rock fracturing is widespread. For this reason the rim represents a more favourable environment for aquifers than the basin centres.

NW–SE rift faulting during the Eocene led to the subsidence of troughs with thick and rapid sedimentation compared to the adjacent areas. One prominent structure of this type is the Hūn graben with a thick Cretaceous and Tertiary sequence. It is the natural division between Al Ḥamādah al Ḥamrā' and Sirt basins. The vertical throw is about 900 m, but in the Tāwarghā' area the graben wedges out.

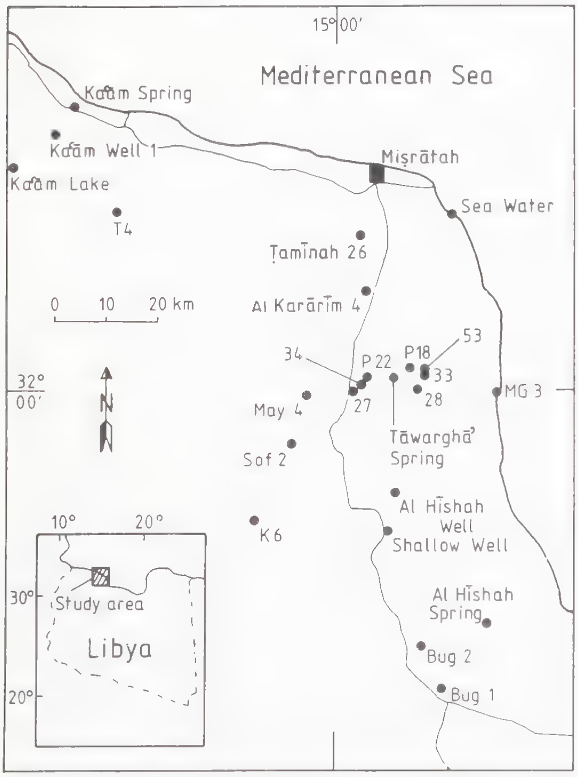

Fig. 1. Location of the sample sites in the study area.

Several long faults parallel to the Hūn graben can be observed in Al Ḥamādah al Ḥamrā' as well as in the Sirt basin.

Two main reservoirs can be distinguished: an upper aquifer in Quaternary, Pliocene and Miocene sediments and a lower aquifer including early Tertiary, Mesozoic and Palaeozoic series. The latter can be subdivided into an upper carbonaceous and a lower sandstone reservoir.

The sandstone reservoir is of very great extent, covering the entire area. It consists of a succession of different water-bearing formations in hydraulic continuity which are essentially of Cambro-Ordovician, Upper Silurian, Lower Devonian and Lower Cretaceous age.

In the NE part of the study area the water migrates into Upper Cretaceous limestones and dolomites through faults or through direct contact with the sandstone aquifers due to the disappearance of impervious layers. The reason for this transfer to a new water-bearing formation seems to be the change of facies in the Lower Cretaceous from predominantly sandy south of Tāwarghā' to predominantly dolomitic and less permeable in the north. In this area the Upper Cretaceous aquifers also receive some water from the west. Most of the water discharges through two important springs, the Tāwarghā' spring and the Wādī Kaʿām spring.

In the north-central and NW part of the basin the main ground water flow in the lower Mesozoic sandstones and Triassic dolomites is S–N.

The water in the sandstones shows TDS (total dissolved solids) values ranging from 1 to 1.8 g/l. To the northwest the quality of the water flowing towards Al Qarāhbūllī improves slightly through the addition of local recharge along the foot of the jabal, while, in contrast, the water flowing towards Miṣrātah shows an important increase in salinity, up to 4 g/l in the Lower Cretaceous and 5 g/l after transition into the Upper Cretaceous aquifers. To the east, the water quality deteriorates rapidly and becomes saline east of Wādī Jārif.

The carbonate reservoir includes two main aquifers, the Upper Cenomanian Nālūt and the Turonian–Senonian Mizdah–Taghrinnah aquifer, separated by impervious layers. The piezometric surface in these aquifers is obviously lower than in the Palaeozoic Kiklah in spite of more direct recharge from rainfall and runoff.

The Nālūt aquifer usually does not provide a good water supply because of its poor hydraulic properties and poor water quality. However, in the outcrop area SE of Al Khums (Wādī Ka'ām area) and in the Tāwarghā'–Abuqrīn area the characteristics are much better, with a transmissivity of more than 10^{-2} m^3/s m and a salinity below 2 g/l. Karstic conditions are observed along the northern coast, but the mineralization is high.

Like the Nālūt, the Mizdah–Taghrinnah aquifer is mostly of very limited interest, but shows transmissivities exceeding $5 \cdot 10^2$ m^3/s m in the Zlīṭan–Miṣrātah–Tāwarghā' area. The salinity is mostly more than 3 g/l except in the Tāwarghā'–Al Karārīm area with 1.5–2 g/l, probably in connection with important inflow from the Nālūt aquifer.

In Al Ḥamādah al Ḥamrā' basin the Upper Cretaceous aquifers are considered to be in a perched position in relation to the main groundwater body.

The Palaeocene–Eocene aquifers consist of several aquiferous levels. The lower aquifer is found in the Palaeocene limestones west of the Hūn graben, the middle aquifer exists in several individual limestone lenses in a mostly gypsiferous and clayey sequence, the upper aquifer is only developed in and east of the Hūn graben in a carbonaceous series of the Eocene.

Most of the aquifers are, in one way or another, in hydraulic connection. These connections are not continuous but occur on a regional basis only, which means that aquifers which are generally separated may be locally in contact.

Unconformities provide contact between aquifers such as transgressive sands or rim facies dolomites overlying partly truncated aquifer sections. This contact occurs especially between the widely distributed Cambro-Ordovician sandstone and the overlying formations in Al Ḥamrā' basin.

Groundwater transmission is also possible where two different aquifer horizons come into contact across a fault. Fracture zones and faults can also connect aquifers with fracture permeability, penetrating impermeable or semi-permeable rocks. Basin rims are very susceptible to fracturing as well as volcanic zones, and continuous fracture zones are not restricted to faults.

SAMPLING AND MEASURING METHODS

Samples were taken from a total of 24 wells, springs and surface water over a period of 6 weeks (24 August–5 October, 1981). Depending on the carbon content, the inorganic carbon in the water samples was precipitated from 60 to 240 litres of water with $BaCl_2 \cdot 2H_2O$ and NaOH as $BaCO_3$ for the ^{14}C analysis. For the purpose of the ^2H, ^3H, ^{13}C, ^{18}O and chemical analyses, 50 ml and 2 × 0.5 litre or 2 litres respectively of water were filled into glass or polyethylene bottles. Temperature, conductivity, pH, redox and O_2 measurements were also carried out in the field. The acid constant AC 4.3 and base constant BC 8.2 were also determined (Table 1).

^{14}C contents were determined in the laboratory, applying liquid scintillation radiometry of bencene (Eichinger *et al.*, 1980); results are expressed as percent modern carbon (% modern or pmc) where 100% modern corresponds to 95% of the NBS oxalic acid standard. ^3H concentrations were determined radiometrically in a proportional counter tube (Wolf *et al.*, 1981) after electrolytical enrichment of ^3H (Eichinger *et al.*, 1981); results are expressed as TU (tritium unit) where 1 TU corresponds to a $^3H/H$ ratio of 10^{-18}. ^2H, ^{13}C and ^{18}O analyses were performed by mass spectrometry. ^2H and ^{18}O results are expressed as ‰ deviations (δ values) versus SMOW (Standard Mean Ocean Water) standard with a twofold standard deviation (2σ) of 1‰ and 0.15‰ respectively. The ^{13}C results are expressed as ‰ deviations versus PDB (Pee Dee Belemnite) standard with a twofold standard deviation of 0.4‰. The results of the hydrochemical analyses (Table 2) were kindly made available by the Department of Soil and Water, SARLD (Tripoli).

RESULTS AND DISCUSSION

^{14}C and ^{13}C Results

The ^{14}C content in the water samples examined (Table 3) ranges from <0.6 to 118% modern and can be subdivided in formal terms into three groups. Samples with ^{14}C concentrations above 100% modern (sea water, shallow well, Ka'ām lake and Ka'ām well 1) contain bomb ^{14}C and therefore classify as recent water (age or residence time <35 years). This is also confirmed by the relatively large ^3H content of these samples (see section on ^3H results), which also shows the influence of bomb ^3H. Samples with a ^{14}C content from 2.1 to 34.2% modern give ^{14}C model ages of <2000–33 000 years, depending on the model concept applied (Table 4) and possibly contain a certain amount of palaeowater. It cannot be excluded that in the springs and relatively shallow wells the ^{14}C content in the ground water has in-

Table 1. Results of the field analyses on water samples (measurements at the given water temperature)

Sample	Sampling date 1981	Depth of aquifer (m)	Temperature (°C)	pH-value	Eh-value (mV)	Specific conductivity (mS/cm at 25°C)	O_2 (mg/l)	CO_2 (mmol/l)	HCO_3^- (mmol/l)
Sea water	1.9		27	8.45	–	>10	6.7 ± 0.6	<0.1	2.65
Al Hīshah spring	13.9		28	7.2	252	8.55	8.1 ± 0.6	0.4	2.6
Tāwarghā' spring	15.9		30.5	7.05	53–233	4.45	4.6 ± 0.6	0.75	4.6
Shallow well	21.9	50	22.5	7.75	239	9.40	5.9 ± 0.6	0.55	8.45
33	19.9	50	30	6.9	53	3.85	2.2 ± 0.6	1.3	4.85
34	7.9	50	24	7.1	–	4.55	–	0.45	2.75
May 4	30.8	200	37	7.1	–	3.35	0.2 ± 0.1	1.2	4.4
Sof 2	30.8	400–600	38	7.2	158	4.60	0.2 ± 0.1	0.7	3.2
Al Hīshah well	21.9	400–600	43.5	6.9	−37	2.95	<0.1	1.0	3.95
P22	31.8	400–600	31	7.5	−37	2.30	<0.1	0.7	5.05
53	29.8	400–600	36.5	7.2	68	2.78	<0.1	1.1	5.55
P18	7.9	400–600	37	7.1	153	2.72	<0.2	1.15	5.6
28	29.8	400–600	39	7.1	−53	2.90	<0.1	1.3	5.5
Al Karārīm 4	10.9	400–600	36	6.9	49	2.80	<0.1	1.4	5.5
Ṭamīnah 26	8.9	400–600	37	6.75	–	5.45	–	2.05	7.0
K6	9.9	950–1500	49.5	7.1	−31	3.35	<0.4	0.55	2.4
27	6.9	950–1500	48	7.5	–	2.95	–	0.4	2.75
Bug 1	16.9	950–1500	57	7.0	−57	4.30	<0.1	1.15	4.95
Bug 2	16.9	950–1500	56.5	7.0	−67	3.50	<0.2	1.15	4.4
MG 3	1.9	950–1500	48	6.9	–	4.76	<0.1	1.8	6.65
Ka‘ām spring	24.9		27	7.5	206–286	3.75	5.6 ± 0.6	0.35	4.65
Ka‘ām lake	27.9		26	7.8	286	0.30	7.3 ± 0.6	<0.1	2.55
T4	28.9	135–530	29	6.95	184	4.33	<0.1	0.75	4.15
Ka‘ām well 1	29.9	50	26.5	7.95	246	0.51	4.8 ± 0.6	<0.1	2.65

Table 2. Chemical composition of the water samples. The analyses were performed by the Department of Soil & Water, SARLD (Tripoli)

Sample	Sampling date, 1981	Composition (mg/l)								Mineralization [180°C]
		Ca^{2+}	Mg^{2+}	Na^+	K^+	NH_4^+	Cl^-	SO_4^{2-}	HCO_3^-	
Sea water	1.9	460	1 593	12 000	435	4.00	22 340	2 630	134	39 800
Al Hīshah spring	13.9	452	272	1 308	34	1.00	2 401	1 508	183	6 190
Tāwarghā' spring	15.9	308	143	536	30	0.28	957	940	268	3 162
Shallow well	21.9	516	347	1 720	52	0.22	2 635	1 720	512	7 442
33	19.9	474	117	225	58	3.00	348	1 680	256	3 140
34	7.9	278	147	636	34	2.40	1 099	988	183	3 390
May 4	30.8	216	91	282	37	2.40	422	710	287	2 025
Sof 2	30.8	234	141	380	18	4.80	660	1 120	195	2 770
Al Hīshah well	21.9	210	96	175	36	0.08	206	805	232	1 686
P22	31.8	190	67	182	35	0.40	227	620	268	1 550
53	29.8	168	94	222	43	1.20	346	565	305	1 700
P18	7.9	160	85	215	44	0.80	330	510	329	1 620
28	29.8	168	86	215	46	2.20	346	510	329	1 650
Al Karārīm 4	10.9	156	94	225	46	1.60	372	491	348	1 660
Ṭamīnah 26	8.9	246	120	600	64	2.20	1 117	570	397	3 024
K6	9.9	304	83	127	31	1.60	291	848	153	1 850
27	6.9	156	80	192	30	2.00	355	500	183	1 500
Bug 1	16.9	66	77	447	38	0.04	613	346	305	1 780
Bug 2	16.9	104	61	283	35	0.04	358	405	268	1 414
MG 3	1.9	138	110	490	68	2.30	968	545	348	2 626
Ka‘ām spring	24.9	254	137	430	18	0.12	700	884	275	2 646
Ka‘ām lake	27.9	28	24	13	4	0	20	33	165	220
T4	28.9	282	191	500	17	0.12	975	960	244	3 114
Ka‘ām well 1	29.9	42	21	30	4	0.004	46	58	165	300

Table 3. Measured results of the isotope analyses on water samples (the indicated errors correspond to the twofold standard deviation)

Sample	Sampling date, 1981	^{14}C (% modern)	$\delta^{13}C$ (‰)	^{3}H (TU)	$\delta^{2}H$ (‰)	$\delta^{18}O$ (‰)
Sea water	1.9	107.5 ± 7.3	+2.7	5.0 ± 0.5	+6.6	+1.36
Al Hīshah spring	13.9	3.8 ± 0.6	−7.9	<0.1	−59.3	−7.34
Tāwarghā' spring	15.9	3.5 ± 0.7	−6.3	0.3 ± 0.1	−58.8	−7.67
Shallow well	21.9	117.8 ± 7.4	−7.7	7.7 ± 0.7	−28.5	−3.63
33	19.9	34.2 ± 2.4	−8.1	<0.1	−69.8	−9.13
34	7.9	10.4 ± 1.0	−3.8	<0.1	−61.6	−7.89
May 4	30.8	2.1 ± 0.5	−7.6	<0.2	−67.0	−8.78
Sof 2	30.8	<1.9	−5.9	<0.2	−62.8	−8.30
Al Hīshah well	21.9	<0.7	−7.8	<0.2	−68.9	−8.87
P22	31.8	<1.0	−8.2	<0.2	−66.8	−8.85
53	29.8	<0.9	−4.7	<0.1	−68.9	−8.94
P18	7.9	<0.6	−4.4	<0.1	−73.5	−9.33
28	29.8	<1.0	−3.6	<0.2	−70.0	−9.60
Al Karārīm 4	10.9	<0.6	−4.2	<0.1	−71.1	−9.19
Ṭamīnah 26	8.9	<0.6	−5.9	<0.2	−68.3	−9.12
K6	9.9	<2.0	−8.8	<0.2	−66.6	−8.58
27	6.9	<2.3	−11.6	<0.2	−70.0	−8.53
Bug 1	16.9	<0.6	−10.2	<0.1	−68.4	−8.96
Bug 2	16.9	<0.9	−9.8	<0.2	−67.9	−8.85
MG 3	1.9	<1.1	−6.8	<0.2	−70.2	−9.47
Ka‘ām spring	24.9	24.1 ± 1.7	−8.2	0.5 ± 0.1	−58.0	−7.57
Ka‘ām lake	27.9	101.9 ± 6.4	−8.7	12.0 ± 1.0	−19.4	−2.97
T4	28.9	<1.2	−5.4	<0.1	−53.7	−7.07
Ka‘ām well 1	29.9	106.8 ± 6.7	−9.5	12.1 ± 1.0	−20.4	−3.17

creased due to ^{14}C exchange processes with the CO_2 in soil gas and/or the atmosphere, even if it was not possible to detect any ^{3}H concentrations in the samples.

At Ka‘ām spring natural conditions may have been impaired due to the large amount of water extracted by a pumping station. The ^{14}C concentrations measured in all other samples are below detection limit and indicate only the upper limit as far as the ^{14}C content is concerned (<0.6 to $<2.3\%$ modern). With these water samples being classified as palaeowater, a bottom limit can be provided only for the ^{14}C model age, ranging from >22 000 to >41 000 years, depending on the model applied. Not considered were the addition of volcanic CO_2 or oxidation of organic material in the aquifer. Klitzsch *et al.* (1976), Salem *et al.* (1980) and Srdoc *et al.* (1980), among others, also determined low ^{14}C contents and high ^{14}C model ages in deep waters from Libya.

Isotope exchange requires, however, some consideration. The $\delta^{13}C$ results obtained in the water samples range from −11.6‰ to −3.6‰, thus partly indicating a substantial deviation from water with a normal geochemical evolution. This might be attributable to isotopic exchange processes with the rock matrix of the aquifer as a result of recrystallizations and/or precipitation and dissolution processes. Such exchange processes are particularly likely in the upper aquifers (where the rock matrix consists primarily of limestone and dolomite), whereas they probably play only a minor role in the lower strata (where the rock matrix consists mainly of sandstone). This interpretation is supported by the generally low $\delta^{13}C$ values obtained in water samples from deep aquifers.

^{13}C, ^{18}O and mineralogical analyses on two sand dune samples (sampled near well MG3) and five core samples from different depths of the wells May 4 (depth 132 m), Bug 1 (depths 252, 551 and 936 m) and K 6 (depth 1000 m) show that the carbonate minerals of the rock samples are on the whole of marine origin ($\delta^{13}C = -2.1$ to 3.9 ‰; $\delta^{18}O = -11.1$ to -1.3‰) and consist mainly of calcite, dolomite and, in minor amounts, aragonite.

To calculate the uncorrected ^{14}C model ages (Table 4) we applied an initial ^{14}C content C_0 of 85% modern (Vogel, 1970) and a ^{14}C half life of 5730 years and calculated age A according to the equation $A = 8267 \times \ln(C_0/C)$; C being the ^{14}C content of the sample.

Table 4. Measured ^{14}C contents and calculated or estimated ^{14}C initial contents and ^{14}C model ages of the investigated water samples (on the basis of a ^{14}C half-life of 5730 years and the twofold standard deviation)

Sample	^{14}C (% modern) $\pm 2\sigma$	Uncorrected ^{14}C model age[a] (years)	Chemically corrected ^{14}C model age[b] (years)	Calculated ^{14}C initial content C_0[b] (% modern)	^{13}C corrected ^{14}C model age[c] (years)	Estimated ^{14}C initial content C_0[c] (% modern)
Al Hīshah spring	3.8 ± 0.6	26 000 ± 2 000	22 000 ± 2 000	54	19 000 ± 2 000	38
Tāwarghā' spring	3.5 ± 0.7	26 000 ± 2 000	23 000 ± 2 000	56	18 000 ± 2 000	30
Shallow well	117.8 ± 7.4	<35	<35	50	<35	37
33	34.2 ± 2.4	8 000 ± 1 000	4 000 ± 1 000	58	<2 000	39
34	10.4 ± 1.0	17 000 ± 1 000	14 000 ± 1 000	56	5 000 ± 1 000	18
May 4	2.1 ± 0.5	31 000 ± 2 000	27 000 ± 2 000	55	24 000 ± 2 000	36
Sof 2	<1.9	>31 000	>28 000	54	>22 000	28
Al Hīshah well	<0.7	>40 000	>37 000	58	>33 000	37
P22	<1.0	>37 000	>33 000	52	>30 000	39
53	<0.9	>38 000	>34 000	54	>26 000	22
P18	<0.6	>41 000	>38 000	56	>29 000	21
28	<1.0	>37 000	>33 000	55	>23 000	17
Al Karārīm 4	<0.6	>41 000	>38 000	58	>29 000	20
Ṭamīnah 26	<0.6	>41 000	>38 000	61	>32 000	28
K6	<2.0	>29 000	>27 000	55	>25 000	42
27	<2.3	>29 000	>25 000	52	>25 000	55
Bug 1	<0.6	>41 000	>38 000	57	>36 000	49
Bug 2	<0.9	>38 000	>34 000	57	>33 000	47
MG 3	<1.1	>36 000	>33 000	58	>28 000	32
Ka'ām spring	24.1 ± 1.7	10 000 ± 1 000	6 000 ± 1 000	52	4 000 ± 1 000	39
Ka'ām lake	101.9 ± 6.4	<35	<35	50	<35	41
T4	<1.2	>35 000	>32 000	58	>25 000	26
Ka'ām well 1	106.8 ± 6.7	<35	<35	51	<35	45

[a] Calculated with a ^{14}C initial content $C_0 = 85\%$ modern (Vogel, 1970).

[b] Calculated from the C-species distribution derived with the computer program PHREEQE.

[c] Estimated according to Ingerson and Pearson (1964) by assuming δ^{13} values of $-21‰$ for the soil gas and $0‰$ for the rock.

In calculating the chemically corrected ^{14}C model age (Table 4) we assumed that the initial ^{14}C content C_0 could be determined from the chemical composition of the water sample examined (Tamers, 1967, 1975), with allowance also being made for the C-species to be found as association complexes. The distribution of C-species concentration required for determining the initial ^{14}C content was calculated by means of the PHREEQE computer program developed by Parkhurst *et al.* (1980). In so doing we proceeded from the water sample temperatures, pH and Eh values determined *in situ* (Table 1) and the results of the chemical analyses conducted in the laboratory (Table 2).

The ^{14}C model age corrected for ^{13}C was estimated following Ingerson and Pearson (1964). In this context δ^{13}C values of $-21‰$ and $0‰$ were assumed for the soil gas and rock, respectively, the assumed ^{14}C content being 100% and 0% modern, respectively. While the ^{13}C-corrected ^{14}C model age of water samples from the deep aquifers consisting mainly of sandstone (e.g.: Kiklah sandstone with samples Bug 1 and Bug 2, Table 4) deviate from the chemically corrected ^{14}C model age by only 1000–2000 years, the deviation with samples from the upper aquifers consisting mainly of limestone and dolomite was up to 10 000 years (the largest deviation being found with sample 28). ^{14}C model age calculations conducted for comparative purposes with the ISOTOP computer program developed by Reardon and Fritz (1978) provided results ranging from >23 000 to >34 000 years in the case of sample 28, depending on the original pH, original CO_2 partial pressure and chemical model applied (and with a comparable range of fluctuation of ^{14}C model age).

^{3}H Results

The ^{3}H concentrations (Table 3) measured in the water samples examined range from <0.1 to 12 TU and thus remain at a relatively low level. As already mentioned with reference to the ^{14}C results, four

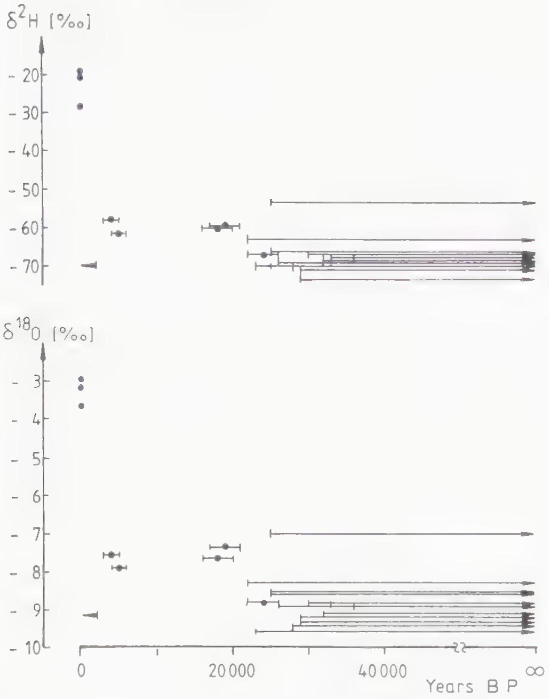

Fig. 2. δ^2H and δ^{18}O values of the water samples (without sea water) as a function of their ^{14}C model age (^{13}C corrected).

samples (sea water, shallow well, Ka'ām lake and Ka'ām well 1) contain bomb ^{3}H and, accordingly, at least a certain amount of water from the last 35 years. This is possibly rainwater that has accumulated or infiltrated in recent years, which may have such a relatively low ^{3}H content. As an example, rainwater measured in Tunis and Alexandria in the period 1976–1978 had a ^{3}H content of 46–28 TU and 51–39 TU respectively (IAEA, 1981, p. 84 and 96), with the trend pointing downwards. It is also conceivable that the water from Ka'ām well 1 is replenished at short intervals by water from Ka'ām lake, as their isotope contents are virtually the same. With the exception of the recent samples mentioned above, small concentrations of tritium were detected only in the Tāwarghā' spring (0.3 TU) and Ka'ām spring (0.5 TU) samples. However, both these springs may possibly be contaminated by tritium from air humidity. Another possibility for explaining this low ^{3}H content is the admixture of small amounts of recent water containing ^{3}H.

^{2}*H and* ^{18}*O Results*

With the exception of the seawater sample, the δ^2H and δ^{18}O values measured show two groups, which may be classified as recent water and palaeowater. The recent water has δ^2H and δ^{18}O values comparable to rainwater in Tunis and Alexandria (IAEA, 1981, p. 84–85 and p. 96–97), although these values vary substantially. Plotting the δ^2H and δ^{18}O values versus the ^{14}C model age (Fig. 2), we do not find — in contrast to the examination of palaeowater from Europe (Moser and Stichler, 1981) and Libya (Srdoc *et al.*, 1980) — any clear increase in δ^2H and δ^{18}O values in the last 20000 years compared to ground water older than 22000 years. Rather, all one finds is a substantial increase in the δ^2H and δ^{18}O values of recent water. Assuming that all of the water found is mainly palaeowater (with the exception, of course, of recent water), one might explain the relatively large ^{14}C content of the samples with a ^{14}C model age of less than approximately 20000 years by mixing of ground water (age < 20000 years) with much older ground water and/or ^{14}C exchange processes with CO_2 from soil gas and/or from the atmosphere.

Plotting the δ^2H values versus the δ^{18}O values (Fig. 3), we obtain (without considering the seawater sample) a straight line running parallel to the global

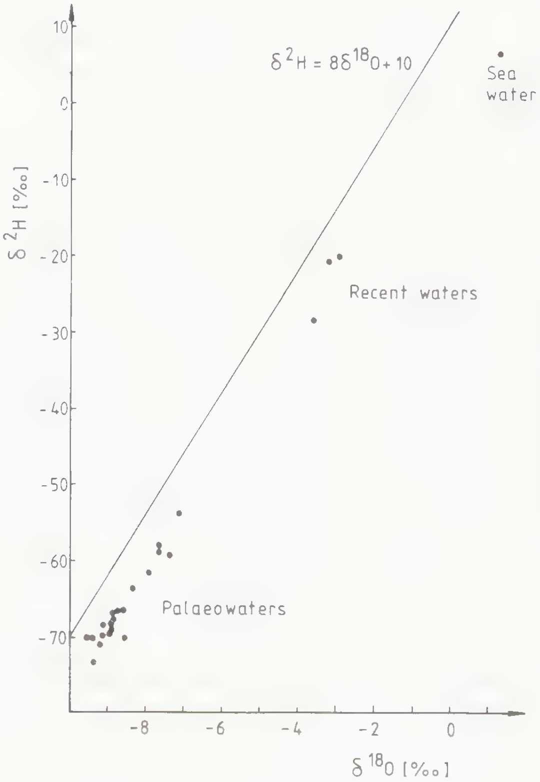

Fig. 3. δ^2H–δ^{18}O relations of water samples.

meteoric water line $\delta^2H = 8\delta^{18}O + 10$ (Craig, 1961) and with a deuterium excess of 3, around which all samples are grouped. The very low δ^2H and $\delta^{18}O$ values compared with recent water may be attributed to the fact, among other things (e.g.: continental effect), that precipitation in earlier times was formed at lower temperatures than nowadays (palaeoclimatic effect) and/or that the ground waters in far higher catchment areas (compared with the area examined) have recharged (altitude effect).

HYDROGEOLOGICAL CONCLUSIONS

The ^{14}C concentrations in the deep carbonate and sandstone aquifers (depth below 200 m) of the Tāwarghā' area correspond to ^{14}C model ages of generally more than about 30 000 years. They do not contain a modern input as documented by tritium data. From the δ^2H and $\delta^{18}O$ values it is possible to distinguish between ground waters of different origin. The ground waters from the sandstone aquifer have the lowest δ^2H and $\delta^{18}O$ values. They flow mainly SSW–NNE and partly recharge the carbonate aquifer. Some higher δ^2H and $\delta^{18}O$ values of ground waters from the upper carbonate aquifer indicate, as a whole, water of different origin or they may be the result of admixture of deep ground water to waters of other origin coming possibly from the west/southwest.

ACKNOWLEDGEMENTS

The authors thank W. Rauert and W. Stichler for isotope measurements and helpful discussions. For useful comments on an earlier version of this paper we thank Profs. P. Fritz, H. Polach and an anonymous reviewer. We also thank Prof. R. Herold for performing mineral analyses, Dr. Phillips for core samples and S. Hengst for assistance during preparation of the manuscript. The Tāwarghā' Project investigations were carried out in collaboration with the Secretariat of Agricultural Reclamation and Land Development (SARLD), Tripoli.

REFERENCES

CRAIG, H. (1961). Isotopic variations in meteoric waters. *Science*, **133**, 1702–1703.

EICHINGER, L., RAUERT, W., SALVAMOSER, J. and WOLF, M. (1980). Large-volume liquid scintillation counting of carbon-14. *Radiocarbon*, **22**, 417–427.

EICHINGER, L., FORSTER, M., RAST, H., RAUERT, W. and WOLF, M. (1981). Experience gathered in low-level measurement of tritium in water. Low-level Tritium Measurement. IAEA, Vienna, TECDOC-**246**, 43–64.

IAEA (1981). Statistical Treatment of Environmental Isotope Data. IAEA, Vienna, *Tech. Rep. Ser.*, **206**.

INGERSON, E. and PEARSON, JR. F.J. (1964). Estimation of age and rate of motion of ground-water by the ^{14}C method. *In: Recent Researches in the Fields of Hydrosphere, Atmosphere and Nuclear Chemistry*. Maruzen, Tokyo, 263–283.

KLITZSCH, E., SONNTAG, C., WEISTROFFER, K. and EL-SHAZLY, E.M. (1976). Grundwasser der Zentralsahara: Fossile Vorräte. *Geol. Rundsch.*, **65**, 264–287.

MOSER, H. and STICHLER, W. (1981). Isotope als Temperaturindikatoren im Grundwasser (Zusammenfassendes Literaturreferat). *Z. Dtsch. Geol. Ges.*, **132**, 659–670.

PALLAS, P. (1980). Water resources of the Socialist People's Libyan Arab Jamahiriya. *In: The Geology of Libya* (*eds* M.J. Salem and M.T. Busrewil). Academic Press, London, **II**, 539–594.

PARKHURST, D.L., THORSTENSON, D.C. and PLUMMER, L.N. (1980). PHREEQE-A computer program for geochemical calculations. *U.S. Geol. Surv. Wat. Resour. Invest.*, 80–96.

REARDON, E.J. and FRITZ, P. (1978). Computer modelling of groundwater ^{13}C and ^{14}C isotope compositions. *J. Hydrol.*, **36**, 201–224.

SALEM, O., VISSER, J.H., DRAY, M. and GONFIANTINI, R. (1980). Groundwater flow patterns in the western Libyan Arab Jamahiriya evaluated from isotopic data. *In: Arid-Zone Hydrology: Investigations with Isotope Techniques*. IAEA, Vienna, AG-158/12, 165–179.

SRDOC, D., SLIEPCEVIC, A., OBELIC, B., HORVATINCIC, N., MOSER, H. and STICHLER, W. (1980). Isotope investigations as a tool for regional hydrogeological studies in the Libyan Arab Jamahiriya. *Arid-Zone Hydrology: Investigations with Isotope Techniques*. IAEA, Vienna, AG–158/11, 153–164.

TAMERS, M.A. (1967). Surface-water infiltration and groundwater movement in arid zones of Venezuela. *Isotopes in Hydrology*. IAEA, Vienna, SM-83/23, 339–353.

TAMERS, M.A. (1975). Validity of radiocarbon dates on groundwater. *Geophys. Surveys*, **2**, 217–239.

VOGEL, J.C. (1970). Carbon-14 dating of groundwater. Isotope Hydrology 1970. IAEA, Vienna, SN-129/15, 225–239.

WOLF, M., RAUERT, W. and WEIGEL, F. (1981). Low-level measurement of tritium by hydrogenation of propadiene and gas counting of propane. *Int. J. Appl. Radiat. Isot.*, **32**, 919–928.

A Review of Arid Zone Hydrogeological Mechanisms in Regional Sedimentary Basins

J.W. LLOYD [1]

مراجعة لميكانيكيات جيولوجية مياه المناطق القاحلة بالأحواض الرسوبية الإقليمية

ج. و. لويد

الخلاصـــة

تعد دراسات المياه الجوفية المقتصرة على السطح غير كافية لوضع التقديرات الصحيحة لتغذية المياه الجوفية في الأحواض الجافة أو شديدة الجفاف. وتوضح نماذج دراسات المياه الباطنية أن ممالات سطح المياه تبقى ثابتة مدة طويلة تحت تأثير التفريغ المائي مع كمية ضئيلة جداً من التغذية غير المباشرة. وتصبح دلائل التغذية في حدود أخطاء التوازن المائي. أما كميات الصرف فتبدو ضئيلة كذلك.

ونظراً للمسافات الكبيرة التي يقطعها الجريان فإن آبار تنمية المياه البعيدة عن مناطق التغذية قد لا تتأثر بالمعدلات الصغيرة للتغذية. ومن الضروري أن تكون هناك مراقبة مستمرة للمواقع القريبة من مناطق التغذية لتفهم عمليات التغذية على أكمل وجه.

Abstract. Surface hydrological studies are seen as inadequate to provide reliable estimates of recharge, in hyperarid and arid regional basins. Groundwater models show that gradients are sustained by long-term dewatering and very small amounts of modern indirect recharge. Recharge indications are well within the error of a hydrological balance. Discharges appear equally small.

Because of considerable flow distances groundwater developments well away from potential recharge areas are probably unaffected by the very low recharge inputs. In the vicinity of recharge areas continual monitoring and assessment of the groundwater conditions are essential to understand recharge.

INTRODUCTION

In any understanding of hydrogeology in arid areas the science of the subject tends to be tempered by the practicalities of water resources demands and in consequence, while many of the processes are qualitatively appreciated, quantitative understanding is often poor. Such a situation is understandable in that many of the truly arid areas exist in developing countries desperate for water, logistics are frequently difficult and the collection of scientific data is very expensive.

In the development of groundwater resources the basic concept concerns the understanding and manipulation of the input to the groundwater system (recharge), the flow through the system (throughput) and the output from the system (discharge). In the non-arid areas data on all of these three main flow facts are normally available, but unfortunately this is not the situation in the arid areas because of the extreme nature of the climate, irrespective of access, cost of data collection, *etc*.

In the following discussion the hydrological and hydrogeological processes pertinent to groundwater in arid areas are considered and an indication of the quantities involved in recharge and discharge from groundwater systems is examined. Climatic terms such as "arid" are really nebulous in the hydrogeological context; however, for the purpose of this discussion only, the following broad classification is assumed but avoided where possible:

---

[1] Professor of Hydrogeology, Department of Geological Sciences, University of Birmingham, P.O. Box 363, Birmingham B15 2TT, U.K.

	Annual average precipitation (mm)
Hyperarid	0– 50
Arid	50–200
Semi-arid	200–500(?)

CLIMATIC CONTROLS

Aridity is an expression of the qualitative or quantitative dryness of an area and has been defined in a variety of ways to classify deserts (Thornthwaite, 1948; Meigs, 1957). Strict definitions describing such multiparameter features pose problems and it is sufficient to say that they are areas of low and very erratic precipitation. They can occur in any latitude but are most extensive along the two Tropics which are characterized by semipermanent high pressure cells and by hot, dry subsiding air. This controlling feature of aridity is a function of the global atmospheric circulation and unrelated to land and sea distribution.

A number of secondary controls influence aridity. In a large landmass distance from the ocean results in decreasing precipitation as maritime air sheds much of its moisture vapour while being forced over cooler denser continental air in coastal areas. This continental aspect of aridity is often combined with coastal mountain rain-shadow effects which accentuate the decrease in aridity landwards. Further features of aridity are the stability of the high pressure cells over the oceans, and the presence of cold oceanic currents.

Because of the influences of the high pressure cells, areas bordering deserts can be subjected to periodic weather changes related to cell stability and southern oscillation such that prolonged droughts develop extending desertic conditions into normally less arid areas.

HYDROLOGICAL BALANCE AND RECHARGE CONCEPTS

In terms of groundwater, providing suitable aquifer conditions exist, the perplexing aspect of deserts is a quantitative appraisal of the hydrological balance. The balance input of precipitation, with its extreme variation in time and space, is very difficult to quantify by traditional hydrological methods or with remote sensing techniques. The real lack of quantitative hydrological data in most desert areas also makes stochastic analysis ineffective.

For groundwater resources determination, the output from the hydrological balance is obviously recharge which is dominated in arid areas by indirect recharge. This is in contrast to temperate areas where direct recharge from precipitation through the soil profile normally dominates on a regional aquifer scale. The mechanisms by which recharge can occur in desert areas are reasonably well documented although quantification of the various elements in the process is extremely poor. The reason for the difficulties can be seen in the conceptual balance given in Fig. 1.

In Fig. 1 four possible means of recharge in deserts are given:

(1) direct recharge from precipitation through the soil profile;
(2) indirect recharge from runoff through joints;
(3) indirect recharge through runoff ponding; and
(4) indirect recharge through transmission losses during river runoff and floodout (i.e., total disappearance of flows in a river bed).

In considering the processes it is of course important to take account of the extreme variability in rainface amount and frequency in arid and hyperarid areas. Conditions are such that direct recharge is likely to be a rare event. Direct recharge through sand dunes in deserts, however, has been subject to much speculation and measurement as dunes are extensive in some areas and provide an easy sampling medium. Dincer *et al.* (1974) have postulated direct recharge through dunes in the arid eastern desert of Saudi Arabia for extremely high rainfall events using tritium moisture profiles in the unsaturated zone. The tritium evidence is indisputable although whether such infiltration actually reaches the water table as recharge is another matter (Sonntag *et al.*, 1980). Indeed as can be witnessed in semi-arid areas such as the Kalahari and central Australia, moisture movement within many dunes is ultimately controlled by lithological laminations and the limited infiltration is rejected along dune leading faces to support meagre vegetation.

If direct recharge is not of major importance in desert areas the various indirect mechanisms become paramount and indeed in terms of groundwater resources the separation between semi-arid and arid may be taken as the condition where direct recharge ceases to be significant. Even in the semi-arid en-

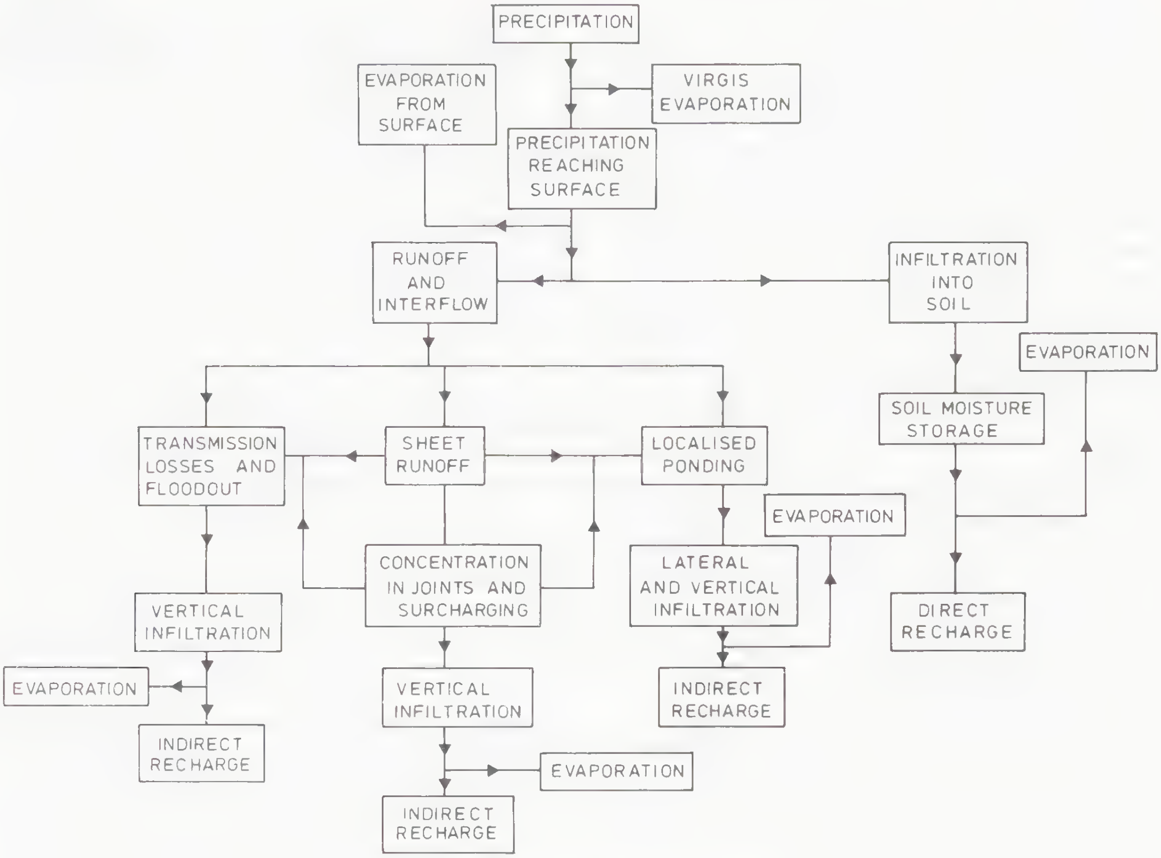
PRECIPITATION
EVAPORATION FROM SURFACE
VIRGIS EVAPORATION
PRECIPITATION REACHING SURFACE
RUNOFF AND INTERFLOW
INFILTRATION INTO SOIL
EVAPORATION
SOIL MOISTURE STORAGE
TRANSMISSION LOSSES AND FLOODOUT
SHEET RUNOFF
LOCALISED PONDING
EVAPORATION
CONCENTRATION IN JOINTS AND SURCHARGING
LATERAL AND VERTICAL INFILTRATION
DIRECT RECHARGE
VERTICAL INFILTRATION
EVAPORATION
INDIRECT RECHARGE
VERTICAL INFILTRATION
INDIRECT RECHARGE
EVAPORATION
INDIRECT RECHARGE

Fig. 1. Elements in recharge in an arid area.

vironment high threshold precipitation is required to initiate recharge and overcome soil moisture deficits.

There is no question that recharge occurs in even the most arid areas. In many cases, as in the Atacama, Gobi and adjacent to the Nile in the Sudan and Egypt, such recharge is imported by river flows from outside of the desert area. With the exception of this type of recharge, the evidence of modern recharge occurring from precipitation over aquifers in arid areas is fairly extensive. In the Sahara, Conrad *et al.* (1975) report the presence of tritiated groundwaters in southern Algeria and similar evidence is given for central Saudi Arabia (Bakiewicz *et al.*, 1982). Along the Arabian Gulf modern groundwater mounds are present in Bahrein, Qatar and at Damman.

To quantify the indirect recharge on the basis of the elements shown in Fig. 1 is probably impossible. For resources assessments therefore the hydrologist is denied any real knowledge of the major flow input to the aquifer system.

The problem for the hydrogeologist in any resources assessment is to obtain a reliable flow element that can be simulated and used as a control for modelling purposes. In arid areas natural discharges are very rare controls so that considerable emphasis is often placed upon total recharge balances despite the measurement difficulties. Many examples of balance calculations exist but few are convincing. Lloyd (1969) reports trial catchment studies which had no surface flows of the total three-year study period. Watson *et al.* (1976) in a major study of the Nevada desert in the United States, a fairly wet desert by many standards, were unable to determine any reliable statistical measurement of recharge, basically because of the multiple unknowns. In many studies the enormity of the recharge calculations task is such that often a percentage of precipitation is simply accepted as recharge despite hydrological examination and calculation (Maxey and Eakin, 1949; Groundwater Development Consultants, 1979).

Unfortunately it must be concluded that hydrological balance methods so extensively used outside of arid areas have not proved reliable in these latter areas. In hydrogeological terms at present there appears to be limited value in hydrological studies other than qualifying the climatic conditions or in understanding constraints on any subsequent groundwater use.

GROUNDWATER FLOW MECHANISMS

Fossil Gradients

In many arid areas the paucity of precipitation and runoff has led some hydrogeologists to question whether recharge in fact occurs in any meaningful amounts at present despite the existence of well-established groundwater gradients.

Burdon (1977) proposed the existence of fossil gradients and postulated a number of contributory mechanisms through the example of a simple single aquifer unit. In 1978, Lloyd and Farag used a resistance model to examine the maintenance of a fossil gradient in an Egyptian aquifer over a period of 10 000 years, based on storage release in the unconfined area. Subsequently, the possibilities of fossil gradients existing in single aquifer units has been investigated using digital models by Wright *et al.* (1982), for a Libyan aquifer, and Bakiewicz *et al.* (1982), for a Saudi Arabian aquifer.

Lloyd and Farag (1978) showed that a fossil gradient could be maintained using realistic aquifer coefficients but with a significant head decline in the recharge area. Bakiewicz *et al.* (1982) also found that their model could not maintain recharge zone heads at field values unless they allowed inflow from a lower aquifer and modern recharge of the order of 15% of rainfall or about 1000 million m^3 per annum in central Saudi Arabia. Wright *et al.* (1982) obtained their best gradient simulation by allowing one millimetre of distributed recharge, over what is essentially an unconfined aquifer, combined with fossil gradient decay over 6000 years. Because of the difficulty of determining possible recharge mechanisms many consultants' reports make the conservative assumption that no recharge occurs.

Although there is evidence that more modern recharge does occur groundwater gradients suggest that the volume of water flowing is significantly greater than the recharge, so more than one mechanism would appear to be operative. This certainly would appear to be the case in North Africa and Arabia.

Hydrogeological Information

Before considering the flow mechanisms, it is useful to list the conflicting hydrogeological information relating to recharge.

Evidence supporting modern recharge:

(1) intermittent flooding;
(2) high tritium values in confined area groundwaters; and
(3) difficulty of maintaining realistic heads in the unconfined area when modelling fossil gradient decline.

Evidence supporting mechanisms other than modern recharge:

(1) extremely low precipitation combined with high potential evaporation and soil moisture deficits;
(2) uneven distribution of tritiated groundwaters and old waters in recharge areas;
(3) presence of old waters in the confined zone immediately adjacent to the unconfined zone; and
(4) little evidence of recent groundwater head fluctuation on a regional scale.

In understanding the environment the following factors need to be appreciated:

(1) The basins are vast with groundwater flow line lengths of several hundreds of kilometres.
(2) Groundwater gradients universally occur but are small, of the order of 1 in 1000.
(3) Any recharge is likely to be intermittent.
(4) Discharge is via sabkhas or oases or is submarine.
(5) The basins contain multilayered aquifer systems that are possibly controlled by a common discharge mechanism so that flow across aquifer boundaries occurs.

Recharge Amounts and Throughput

Because of the problems of obtaining comprehensive data bases attempts to quantify present-day recharge amounts contributing to groundwater throughput in the required basins have been concentrated upon sensitivity analyses using stylized models (Lloyd and Miles, 1986).

In Fig. 2 some of the results are shown for a basin section of 400 km length, an outcrop area of

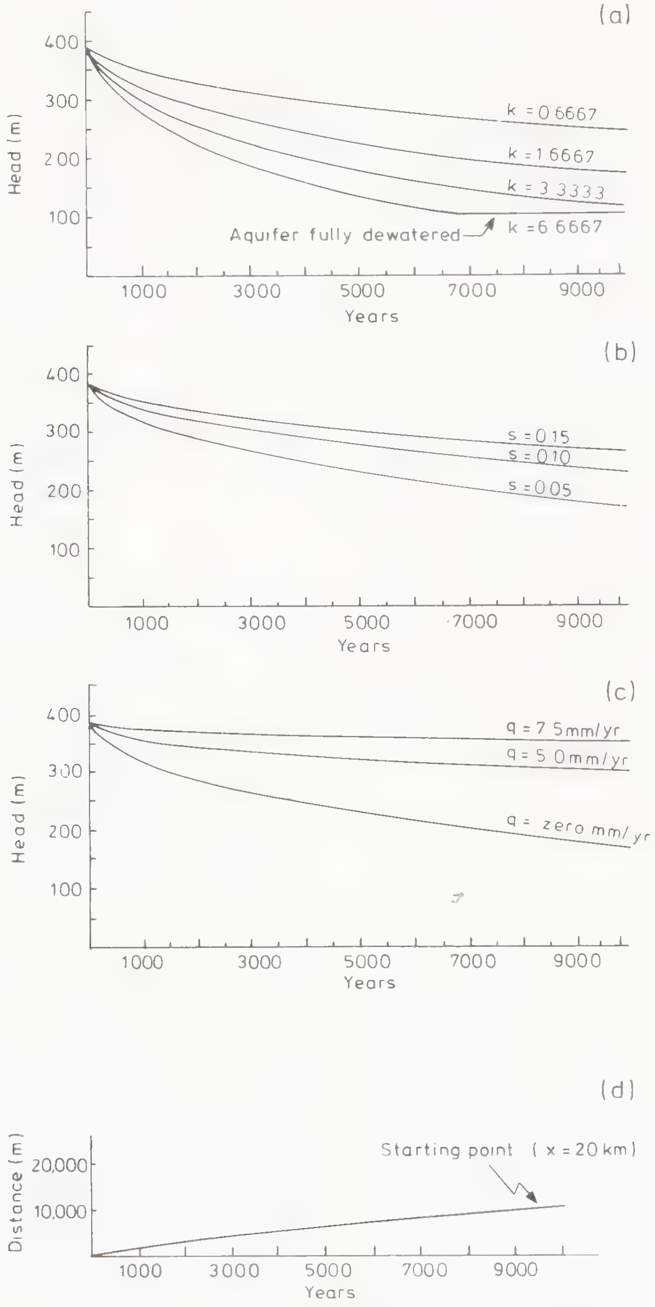

Fig. 2. Examination of groundwater gradient control: head decay at outcrop with no recharge: (a) k = permeability (m/day), s = specific yield = 0.05; (b) k = 1.67 m/day. (c) With recharge, s = 0.05, k = 1.67 m/day. (d) Distance of groundwater movement, no recharge s = 0.05, k = 1.67 m/day, x = distance from edge of aquifer down the hydraulic gradient (after Lloyd and Miles, 1986).

20 km and an aquifer thickness of 300 m. Figures 2a and b show the type of decay expected at outcrop with zero recharge but Fig. 2c shows that for the postulated aquifer conditions heads can be maintained with recharge as low as 5–7.5 mm/yr.

In Fig. 2d the age of groundwater computed from Darcy velocities indicates that the waters would not have moved far over a period of 10 000 years, of the order of 10 km, so that it is not surprising that old waters are found beneath and adjacent to out-

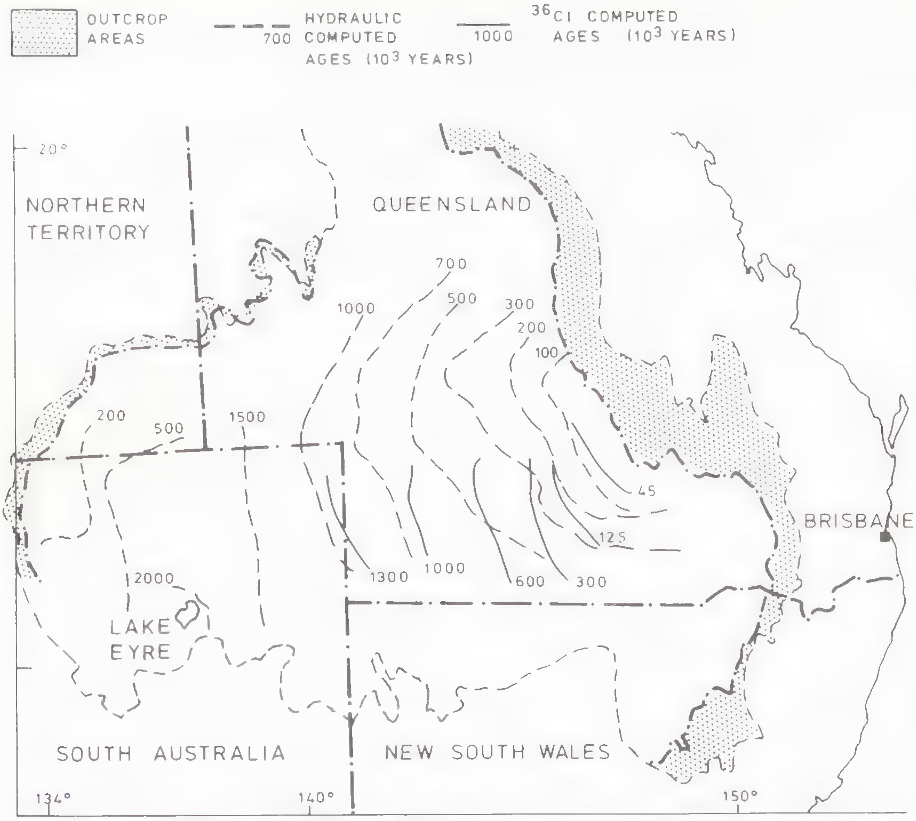

Fig. 3. Hydraulic and ^{36}Cl age distributions for the great artesian basin of Australia showing groundwater ages of up to 2 million years (after Airey *et al.*, 1983).

crop areas particularly as the spatial distribution of modern recharge is uneven. In a regional example depicting age Airey *et al.* (1983) have used ^{36}Cl to date groundwaters in the great artesian basin of Australia. Although the results are preliminary and subject to some criticism the flow periods for the basin are considerable and most instructive, as shown in Fig. 3.

Lloyd and Miles (*op. cit.*) have also examined the effects of head controls in the discharge zone upon head declines in the recharge areas and the effects of multi-aquifer conditions upon heads in a basin. The indications are that head responses in the recharge area do not differ significantly whether a basin discharges at distance to the sea or to an oasis through upward leakage. This is not surprising in view of the distances involved. Multi-aquifer conditions are always difficult to determine in terms of non-aquifer leakage. Again, however, it would appear that heads cannot be maintained regionally by upward leakage because the recharge area heads will decline accordingly. Again this is not surprising; however, by examining the various head controls with allowance for dewatering in the recharge area and commensurate head decline it can be shown that throughput in the regional units varies with distance and time under a steady dewatering regime (Fig. 4).

These various studies indicate mixed controls as would be expected from the available evidence, namely that the past pluvial conditions have had influences on current gradients and that dewatering is important, although some modern recharge must occur to help maintain gradients. The interesting point is that the amount of recharge required would appear to be very small and in many areas certainly within the error of any conventional hydrological balance. Despite the very small amounts, however, in terms of percentages of precipitation the amounts indicated above are significant and it would appear that under real conditions assumed recharge averages of the order of only about 1 mm are more likely as indicated for the Sirt basin by Wright *et al.* (1982).

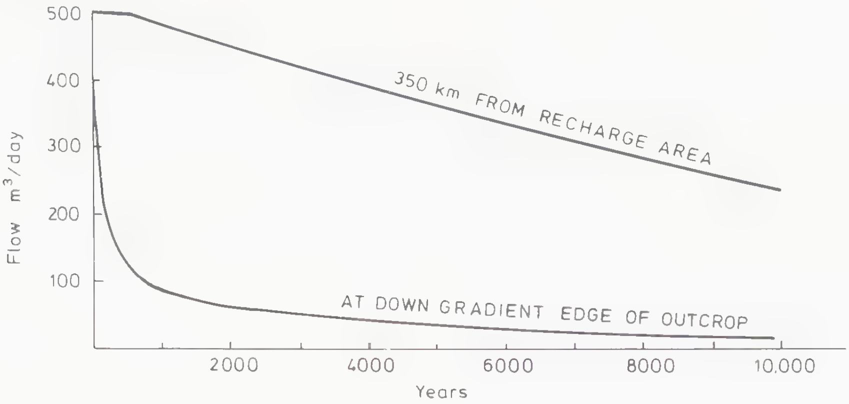

Fig. 4. Spatial and time-variant flows in basin dewatering (after Lloyd and Miles, 1986).

Discharge

Discharge may be comparable to recharge (see above), so should be similarly small in the arid areas. In many areas discharge occurs to coastal sabkhas complicated by sea effects or to the sea itself so that assessment is very difficult although it has been attempted in Saudi Arabia. In the Middle East discharge occurs in certain areas from elevated sabkhas which provide reasonable conditions for assessment. Pike (1970), using energy balance methods, has shown that evaporative losses (equivalent to discharge) are of the order of 70 mm/yr and similar results have been obtained by Idrotecneco (1979) in northern Libya. Such losses are substantially below potential evaporation rates.

In Australia a lot of attention has been paid to "playa" evaporation. Allison and Barnes (1985) provide an estimate of 120 mm/yr from a salt lake surface in South Australia based upon stable isotope and chloride profiles while Ullman (1985) reports evaporation rates of 90–280 mm/yr for Lake Eyre based upon chloride and bromide profiles. Studies in central Australia by Chen Xiang Yang (pers. comm. 1985) indicate similar evaporation rates from small lysimeters set in Lake Amadeus. A summary of the evaporative losses from discharge zones is given in Table 1.

Unfortunately most of the discharges have not been evaluated in terms of recharge but in the Amadeus case the weighted evaporation loss when distributed over the groundwater catchment provides a recharge estimate of 2–5 mm/yr in an area of approximately 200 mm annual precipitation (Jacobson, 1988). The large difference between rainfall and estimated recharge is interesting. Central Australia has existed under predominantly arid conditions since the Middle Eocene and consequently an extremely efficient arid zone vegetation has evolved which has not been disrupted by pastoral practice as for example in the Middle East. The desert is very heavily vegetated by normal desert standards where precipitation, interception, and stem flow are important factors in concentrating precipitation for plant use and in limiting the availability of moisture for recharge.

In the Sahara Fontes *et al.* (1986) have used the stable isotope techniques applied elsewhere to playas (Table 1) to determine evaporation losses from shallow-water tables. Interestingly the losses calculated are about 2 mm/yr, in keeping with the very small recharge–discharge values cited above.

Table 1. Rates of evaporative losses from playa surfaces as groundwater discharge

Country	Method	Amount (mm/yr)
Saudi Arabia	Energy balance	700
Libya	Energy balance	500
Australia	Stable isotope + Cl^-	170
Australia	Br^- + Cl^-	200
Australia	Lysimeter	120

CONCLUSIONS

Experience shows that hydrological balances frequently do not provide adequate assessments of recharge in arid areas. As surface discharges are also normally absent, groundwater resources assessments depend exclusively upon ground investigations and interpretations, which normally leave a lot to be desired. All the indications are that recharge and discharge in the hyperarid and arid areas are of the order of millimetres per annum so it is not surprising that reliable values cannot be determined by conventional balances.

Examination of groundwater gradients and head decline with time to indicate that present gradients in the regional basins may be maintained by a combination of gradual dewatering beneath the outcrop areas and the very low recharge postulated.

Because of the very considerable flow distances involved the recharge conditions are probably of limited importance for groundwater developments that are some distance from a recharge area. Developments in or close to recharge areas, however, require a sensitive examination of the mechanisms involved based upon comprehensive monitoring.

REFERENCES

AIREY, P.L., BENTLEY, H., CALF, G.E., DAVIES, S.N., ELMORE, D., HABERMEHL, M.A., PHILLIPS, F., SMITH, J. and TORGERSEN, T. (1983). Isotope hydrology of the Great-Artesian Basin, Australia. Int. Conf. on Groundwater and Man, Sydney. *Aust. Wat. Resour. Council Conf.*, **8**(1), 1–11.

ALLISON, G.B., and BARNES, C.J. (1985). Estimation of evaporation from the normally dry Lake Frome in South Australia. *J. Hydrol.*, **76**, 229–242.

BAKIEWICZ, Q., MILNE, D.M. and NOORI, M. (1982). Hydrogeology of the Umm Er Rhaduma aquifer, Saudi Arabia, with reference to fossil gradients. *Q. J. Eng. Geol. London,* **15**, 105–126.

BURDON, D.J. (1977). Flow of fossil groundwater. *Q. J. Eng. Geol. London*, **10**, 97–124.

CONRAD, G., MARCE, A. and PHILLIPPE, O. (1975). Mise en evidence par le tritium, de la recharge actuelle des nappes libres de la zone aride Saharienne (Algerie). *J. Hydrol.*, **27**, 207–224.

DINCER, T., AL-MUGRIN, A. and ZIMMERMANN, U. (1974). Study of the infiltration and recharge through sand dunes in arid zones with special reference to the stable isotopes and thermonuclear tritium. *J. Hydrol.*, **23**, 79–87.

FONTES, J.C., YOUSFI, M. and ALLISON, G.B. (1986). Estimation of long-term, diffuse groundwater discharge in the northern Sahara using stable isotope profiles in soil water. *J. Hydrol.*, **18**, 36–43.

GROUNDWATER DEVELOPMENT CONSULTANTS. (1979). Umm Er Rhaduma Study. Hydrology Rept. Min. Agric. and Water, Saudi Arabia, 78p.

HABERMEHL, M.A. (1980). The Great Artesian Basin, Australia. *Bur. Min. Res. J. Aust. Geol. Geophys.*, **5**, 9–38.

IDROTECNECO (1979). Quantity of water evaporated from sabkha. Rept. to Dept. Soil and Water Resources, Libya, 26 p.

JACOBSON, G. (1988). Hydrology of Lake Amadeus, a groundwater-discharge playa in central Australia. *Bur. Min. Res. J. Aust. Geol. Geophys.* **10**, 301–308.

LLOYD, J.W. (1969). The hydrogeology of the southern desert of Jordan. *Food and Agriculture Rept., AGL: SF/Jor 9, Tech. Rept.* **1**, 207 p.

LLOYD, J.W. and FARAG, M.H. (1978). Fossil groundwater gradients in arid regional sedimentary basins. *Groundwater*, **16**, 388–393.

LLOYD, J.W. and MILES, J.C. (1986). Examinations of the mechanism controlling groundwater gradients in arid regional sedimentary basins. *Wat. Resour. Bull.*, **22**(3), 1–8.

MAXEY, G.B. and EAKIN, T.E. (1949). Groundwater in White River Valley, White Pine, Nye and Lincoln countries. *Nevada State Eng. Wat. Resour. Bull.* **8**, 59 p.

MEIGS, P. (1957). Arid and semi-arid climatic types of the world. *Proc. Int. Geophys. Un., 17th Congr. Washington*, 135–138.

PIKE, J.G. (1970). Evaporation of groundwater from coastal playas (Sabkhah) in the Arabian Gulf. *J. Hydrol.*, **1**, 79–88.

SONNTAG, C., THOMAS, G., MUNNICH, K.O., DINCER, T. and KLITZSCH, E. (1980). Environmental isotopes in North African groundwaters; and the Dahna sand-dune study, Saudi Arabia. *Arid-zone Hydrology: Investigations with Isotope Techniques.* IAEA, Vienna, AC-158/6, 77–84.

THORNTHWAITE, C.W. (1948). An approach toward a rational classification of climate. *Geogr. Rev.*, **38**, 55–94.

ULLMAN, W.J. (1985). Evaporation rate from a salt pan: estimates from chemical profiles in near surface groundwaters. *J. Hydrol.*, **79**, 365–373.

WATSON, P., SINCLAIR, P. and WAGGONER, R. (1976). Quantitative evaluation of a method for estimating recharge to the desert basins of Nevada. *J. Hydrol.*, **31**, 334–357.

WRIGHT, E.P., BENFIELD, A.C., EDMUNDS, W.M. and KITCHEN, R. (1982). Hydrogeology of the Kufra and Sirte basins, eastern Libya. *Q. J. Eng. Geol. London*, **15**, 83–103.

A Stochastic Rainfall Model for the Wādī Zārat Watershed, Northwestern Libya

SANOUSI SALEM SANOUSI[1]

نموذج عشوائي لسقوط الأمطار بحوض صرف وادي زارت شمال غرب ليبيا

س . س . السنوسي

الخلاصة

لقد تم تطوير نموذج عشوائي لسقوط الأمطار لمحاكاة سلسلة من أحداث سقوط المطر على المدى الطويل لحوض صرف وادي زارت. فقد تم تعريف الحادثة بأي يوم من أيام السنة تزيد فيه كمية سقوط الأمطار عن 0,25 ملليمتر. ولقد تم إستعمال متغيرين عشوائيين اثنين لوصف عملية سقوط الأمطار. أحدهما زمن الوصول بين هذه العمليات، والآخر كمية الأمطار في كل مرة. ولقد تطلب تطوير النموذج تجميع لأشهر غير مختلفة احصائياً بناءً على المتغيرين العشوائيين والتوزيع الإحتمالي للأمطار الملائم لهذه المجموعات، بأشعة جاما وهندسياً. ولقد تم إستعمال كميات سقوط الأمطار اليومية لمدة 26 سنة لحساب المعايير الإحصائية لتطوير النموذج. والنموذج هذا يحاكي 100 سنة لسقوط الأمطار اليومي. وقد أظهرت المقارنة بين عملية سقوط الأمطار الفعلية والمحاكاة تأدية ممتازة للنموذج. ويستطيع هذا النموذج، من خلال محاكاة أحداث تأدية ذات مدى طويل، تحسين فهم عملية سقوط الأمطار، إضافة إلى عمليات أخرى يعتمد عليها، مثل الإنسياب السطحي ونقل الرواسب بحوض صرف وادي زارت.

وبالإمكان تعميم نتائج هذا الأسلوب، مع إدخال تعديلات طفيفة لكل منطقة شمال غرب ليبيا.

Abstract. An event-based stochastic rainfall model was developed to simulate long-time series of rainfall events for the Wādī Zārat watershed. An event was defined as any day of the year having a rainfall amount in excess of 0.25 mm. Two random variables were used to describe the rainfall process: the interarrival time between events, and the amount of rainfall per event. Development of the model required the grouping of statistically non-different months based on the two random variables, and the fitting of theoretical probability distributions, gamma and geometric, to these groups. A record of 26 years of daily rainfall was used to calculate the statistical parameters needed to develop the model. The model simulates 100 years of daily rainfall. Comparison of the actual and simulated rainfall process showed excellent performance by the model. The model, through simulation of long-time events, can improve the understanding of the rainfall process and other dependent processes such as runoff and sediment transport in the Wādī Zārat watershed. Results of the model can be generalized, with minor modifications, for the whole region of northwestern Libya.

INTRODUCTION

The purpose of this paper is to present a model that simulates long series of daily rainfall using stochastic modelling techniques. The model was developed for the Wādī Zārat watershed of northwestern Libya.

The stochastic modelling of rainfall utilizes the inherited random nature of the rainfall process and considers it, like other hydrologic variables, as a random process in time. Hence, the stochastic analysis of hydrological events assumes these events to be part of a stationary process that conserves the same statistical characteristics over time.

The model developed utilizes the statistical properties of the historical data of rainfall to stochastically simulate long-time series of rainfall events. The

---

[1] Department of Earth Sciences, University of Sabhā, Sabhā, Libya, G.S.P.L.A.J.

simulated series will reflect the statistical properties of the original data.

The model is an event-based stochastic model in which the rainfall event is considered as an intermittent stochastic process. A single event is defined as any day of the year having rainfall in excess of a minimum depth. Duckstein *et al.* (1972) developed an event-based stochastic model to simulate summer rainfall, based on their previous work (Fogel *et al.*, 1971). In their model they used two random variables to model the rainfall process; the rainfall per event and the number of events per season.

Duckstein *et al.* (1975) developed an event-based stochastic model to stimulate mountainous winter storms where they added more random variables to describe the rainfall process. Successful use of the event-based stochastic modelling was to follow by Heckman (1977), Duckstein *et al.* (1978), Fogel *et al.* (1980), Jones (1981), Almestad (1983) and Sanousi (1985).

In the present model an event is defined as any day of the year having rainfall in excess of 0.25 mm. Two random variables are used to describe the rainfall process. These are the interarrival time between events and the amount of rainfall per event. The development of the model involved the following stages: (1) initial data analysis and grouping of statistically non-different months based on the two random variables, (2) fitting of theoretical probability distributions to the grouped months, and (3) simulation of the rainfall process using the fitted distributions and the Monte Carlo simulation procedure. The different stages of the rainfall simulation model were performed on a computer using programs written in FORTRAN IV and are available on request from the author.

The model simulates 100 years of daily rainfall. Comparison of the simulated and recorded rainfall showed excellent performance by the model. Data records for 26 years were used to develop and test the model. The model developed can be used to simulate long rainfall records for the Wādī Zārat watershed and can be adopted for rainfall simulation in other parts of Libya where the rainfall pattern is similar to the study area.

DESCRIPTION OF WATERSHED

The Wādī Zārat watershed is located in the central part of Jabal Nafūsah, northwestern Libya. The watershed is about 120 km southwest of Tripoli and about 30 km west of Gharyān (Fig. 1). The watershed extends in a N–S direction, has an area of about 213 km^2 and has elevations ranging between 300 and 800 m. Climate is typical Mediterranean, dry steppe with cold and rainy winter and hot and dry summer. The rainy season begins in October and ends in March with trace amounts during the rest of the year. The average annual rainfall amount is about 270 mm, and temperature ranges from 0°C to as high as 45°C. Rainfall records for 26 years were available from the Kiklah station on the western edge of the watershed.

MODEL DEVELOPMENT

Grouping of Months

The daily rainfall record over 26 years was used to obtain statistical parameters needed to decide on the grouping of statistically non-different months. Two random variables, the interarrival time between events and the rainfall amount per event, were used for the analysis of each month's data.

A rainfall event was defined as any single day of the year with rainfall amount of more than 0.25 mm. The 0.25 mm limit was chosen as the minimum rainfall needed to produce any runoff on the present watershed.

The interarrival time between events is in full days. Thus, four consecutive rainy days are four events with a 1-day interarrival time between each two events. Two rainfall events with one day separating them were considered to have a 2-day interarrival time. The two random variables used to describe the rainfall process are shown in Fig. 2.

The data for each month of the year are analyzed to help in the identifying and grouping of months that are statistically non-different. The grouped months are then fitted to theoretical probability distributions. The grouping of months was done to minimize the number of theoretical probability distributions needed, otherwise, to fit each month of the year.

The grouping of months was based on the fact that for any two months having their underlying probability distributions coming from the same population, their means must also come from that same population. Consequently, a test hypothesis can be formulated for the means of the two months. In the present model a two-tailed Student-*t* test was performed to find the statistically non-different months. The test uses the null hypothesis of $u_1 - u_2 = 0$, and the alternative hypothesis of $u_1 - u_2 \neq 0$. The u_1 and

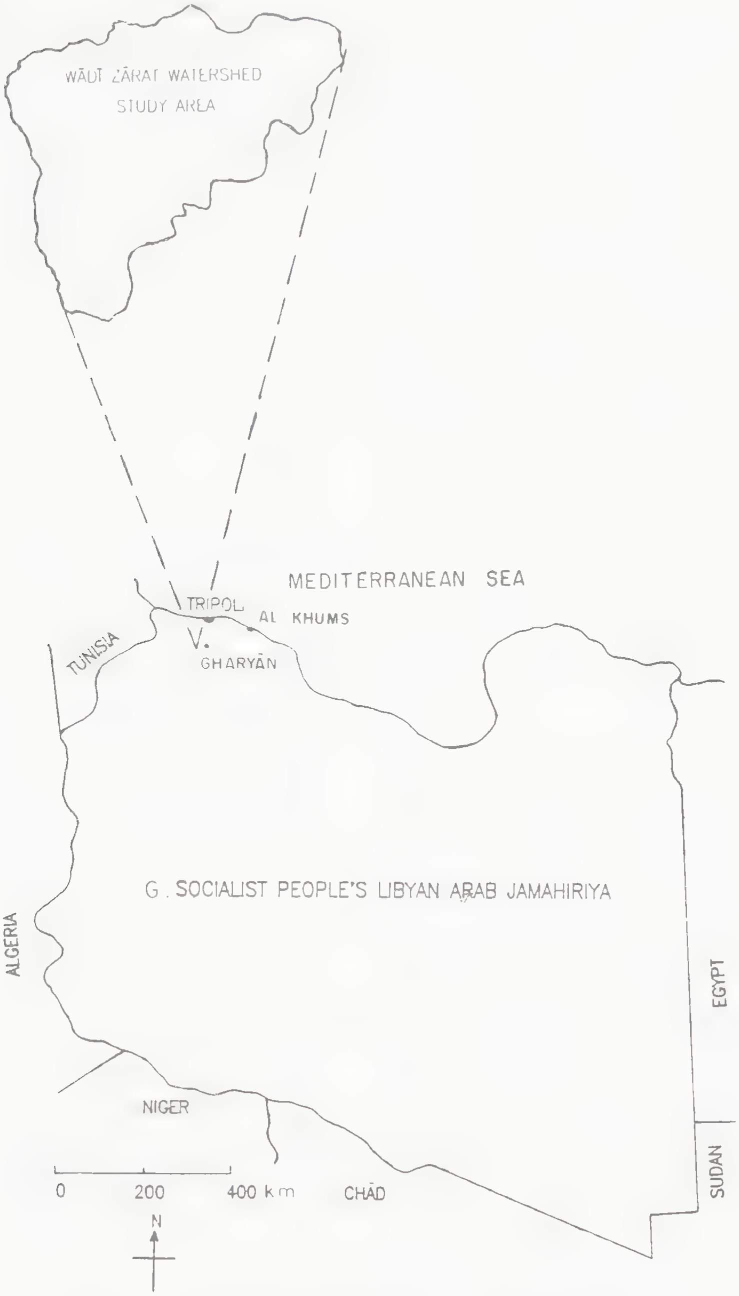
WĀDĪ ZĀRAT WATERSHED
STUDY AREA
MEDITERRANEAN SEA
TRIPOLI
AL KHUMS
GHARYĀN
TUNISIA
G. SOCIALIST PEOPLE'S LIBYAN ARAB JAMAHIRIYA
ALGERIA
EGYPT
NIGER
SUDAN
CHĀD
0
200
400 km
N

Fig. 1. Location map of the Wādī Zārat watershed study area.

u_2 are the population means for the first and second months respectively. The test was performed assuming that the population variances are not known and cannot be assumed to be equal.

The test for non-different months involved the following: the determination of statistic-*t* and the corresponding degrees of freedom for the data, the finding of the tabulated *t*-value for the degrees of freedom obtained and a 5% significance level, and the comparison of the tabulated and calculated *t*-values.

The null hypothesis was rejected if the absolute value of the calculated *t*-value is larger than the tabulated one. Rejection of the null hypothesis means that the two months do not belong to the same population, therefore they are statistically different and

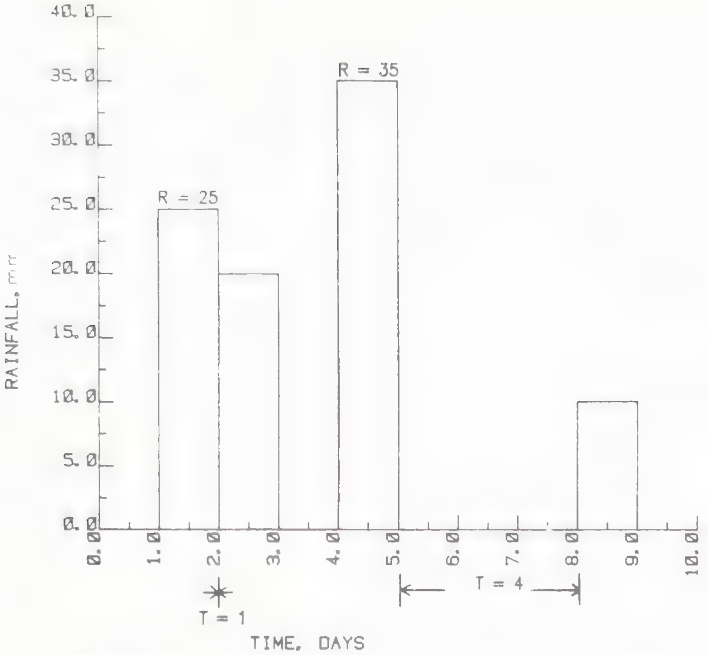

Fig. 2. Components of the rainfall process represented by interarrival time (T) and rainfall per event (R).

cannot be included in the same group. The testing of non-different months was done for both the interarrival time and the rainfall per event random variables for a total of 66 combinations. The method of moments was used to calculate the statistical parameters, mean and variance, needed for the grouping procedure.

The grouping of months required having the following rules: (1) all months in a single group should be statistically non-different, for both the interarrival time and the rainfall per event groups, (2) the interarrival time groups should contain only consecutive months, this allows for the possible extension of interarrival time over the boundary between adjacent months.

During the initial analysis of data the rainfall events were examined in intervals of 4 mm and a maximum of 172 mm, which is the highest recorded amount in the area. The interarrival time period considered is a one-day unit.

The initial data analysis revealed the following preliminary groups for interarrival time: (1) January–February–March, (2) April, (3) May–June–July–August, and (4) September–October–November–December. The rainfall per event groups were: (1) September–October–November–December–January–February–March–April, (2) July, and (3) May–June–August. The fact that some of these groups were too large created a difficulty in finding theoretical distributions that would fit such groups. It was necessary to break the large groups into smaller ones that could be modelled with theoretical probability distributions.

Fitting of theoretical distributions

Theoretical distributions were examined to find the ones that best fit the distributions reflected by the actual data. Among the theoretical distributions used in the modelling of hydrological events are: the binomial, the Poisson, the exponential, the geometric, and the gamma. The fitting of theoretical distributions to the actual data enables us to understand the underlying properties of the rainfall process. Consequently, the fitted distributions were used to generate random values of the rainfall event, and values outside the range of available data can be simulated (Law and Kelton, 1982).

The fitting of a theoretical distribution to any of the grouped months is based on testing the hypothesis of whether or not the group belongs to a specific probability distribution. If this hypothesis, "the null hypothesis", could not be rejected the group was modelled by the tested distribution.

The Kolmogorov–Smirnov (K-S) test was used to decide on how to fit the distributions to the grouped months. The K-S test involves the following steps:

(1) the data cumulative density funcion ($P_x(x)$) is obtained for the number of observations;
(2) the theoretical CDF ($F_x(x)$) is calculated using the theoretical distribution chosen and the parameters obtained from the data;
(3) a test statistic D is obtained by the equation:

$$D = \max_{i=1}^{n} |F_x(x_i) - P_x(x_i)|$$

where n is the number of observations;
(4) using a level of significance of 5% and special tables (Benjamin and Cornell, 1970) the critical value of the K-S test is obtained and compared to the calculated value of D. The null hypothesis cannot be accepted at the 5% level of significance if the calculated value of D is greater than the critical value of the test. The null hypothesis is that the examined theoretical distribution can fit the group in question.

Some of the large groups had to be modified to smaller ones for it was impossible to find distributions that would fit such large groups. During the fitting process, two probability distributions, the geometric and the gamma, were used. The CDF for the geometric distribution has the following form:

$$F_x(x) = 1 - (1 - P)^x$$

where $P = 1/\bar{x}$ and the gamma distrubution PDF is:

$$f_x(x) = \frac{\lambda^k x^{k-1} \mathrm{e}^{-\lambda x}}{(k-1)!} = \frac{\lambda^k x^{k-1} \mathrm{e}^{-\lambda x}}{\Gamma(k)}$$

where $\Gamma(k)$ is the gamma function of k, and λ and k are given by:

$$\lambda = \bar{x}/s^2; \quad k = \bar{x}^2/s^2$$

The variable x can be either the random variable interarrival time in days or the rainfall per event in millimetres. The statistics $\bar{x}$ and s are the mean and variance obtained from the data record. The parameters λ and k are known as the scale and shape parameters for the gamma distribution.

The CDF for the gamma distribution has no simple closed form to directly calculate the gamma CDF, therefore, an algorithm described by Law and Kelton (1982) was used to evaluate the CDF of the gamma distribution.

All groups could be fitted to either geometric or gamma distributions except for the interarrival time group of the month of June. The actual data distribution for June was divided into two parts, each modelled separately. The 30 days interarrival time was assigned a fixed probability obtained from the data and the rest of the month was fitted to a shifted geometric distribution. The months of July and August were modelled by a fixed probability of one for zero rainfall and an interarrival time of 31 days. This fixed probability of one was based on the data record which covers records over a 26-year period and which showed no rainfall in July and an 86% chance that August would receive no rainfall.

Rainfall Simulation

The fitted distributions were used to simulate the interarrival time and amount of rainfall for each group using the Monte Carlo method of simulation. This simulation involves the use of random numbers to generate random variables from probability distributions.

The simulation process utilizes the fact that the cumulative probability function for a given random variable is uniformly distributed over the interval 0 to 1 (Haan, 1982). Hence, the rainfall random variables, interarrival time and rainfall per event were generated from the fitted theoretical distributions by the method of the inverse transform of the probability distribution. This method involves the following steps: (1) generation of a uniformly distributed random variable over the interval 0 to 1; (2) setting these random numbers equal to the CDF of the theoretical distribution; (3) solving the CDF equation for the random variable, where the random variable can be either the interarrival time or the rainfall per event.

The model for the rainfall simulation for the Wādī Zārat watershed was finalized by the fitting of theoretical distributions to the groups of months developed during the early stages of model construction. The fitting required the use of six interarrival time groups and four rainfall per event groups. The months of July and August were treated as a single group having a fixed interarrival time of 62 days and zero rainfall for the period of simulation. This was based on the historical record of no rainfall for July and only two events for August.

The simulation procedure treated the grouped months as separate units of time within a single year. Consequently, the interarrival time and the rainfall per event were evaluated for each group and for 100 years of simulation.

The simulation algorithm observed the following chronological steps: (1) the day of the year is set to zero; (2) the current group corresponding to the calendar day is determined; (3) the interarrival time random variable is determined in days using the relevant distribution of the current group and the calendar day is updated accordingly; (4) the group is updated using the current calendar day; and (5) the rainfall amount is generated for the current group. The above simulation procedure was performed for each year and for the 100 years of simulation.

RESULTS AND DISCUSSION

Development of the present rainfall simulation model required the analysis of each month for the variables of interarrival time and rainfall per event for 26 years of records.

The months were grouped into statistically non-different groups to facilitate the fitting of a few theoretical distributions to these groups. Analysis of the grouped months gave the actual CDF for the two random variables describing the rainfall process and the statistical parameters ($\bar{x}$, s^2, λ, k) needed for the simulation process.

The first stage of monthly groupings resulted in long groups. The fitting of distributions to these groups was very difficult and in some cases impossible. Consequently, while obeserving the rules for monthly grouping some of the groups were deformed to include fewer months. The final grouping (Table 1) consisted of six interarrival time and four rainfall per event groups. For convenience, the months of July and August were considered as one group having no rainfall and an interarrival time of 62 days for the period of the simulated years.

Table 1. Actual distributions and their fitted theoretical distributions used to model the rainfall process

Rainfall parameter and month	Theoretical distribution
Interarrival time	
Jan–Feb–Mar	Gamma
Apr	Gamma
May	Geometric
Jun	Shifted Geometric
Jul	Fixed
Aug	Fixed
Sep–Oct	Gamma
Nov–Dec	Gamma
Rainfall per event	
Nov–Dec–Jan–Feb–Mar	Gamma
Apr	Gamma
May–Jun	Gamma
Jul–Aug	Fixed
Sep–Oct	Gamma

Table 2. Theoretical probability distributions and their parameters used to simulate the rainfall process

Rainfall parameter and month of the year	Theoretical distribution	Distribution parameter value
Interarrival time		
Jan–Feb–Mar	Gamma	$\lambda = 0.0386$ $k = 0.3269$ $\Gamma(k) = 2.7347$
Apr	Gamma	$\lambda = 0.0547$ $k = 0.5332$ $\Gamma(k) = 1.6651$
May	Geometric	$P = 0.0583$
Jun	30 day (fixed) <30 day (shifted geometric)	PB* = 0.5429 $P = 0.0762$
Jul	31 day (fixed)	PB = 1.0000
Aug	31 day (fixed)	PB = 1.0000
Sep–Oct	Gamma	$\lambda = 0.0321$ $k = 0.4262$ $\Gamma(k) = 2.0795$
Nov-Dec	Gamma	$\lambda = 0.0409$ $k = 0.4442$ $\Gamma(k) = 1.9943$
Rainfall per event		
Nov–Dec–Jan–Feb–Mar	Gamma	$\lambda = 0.0495$ $k = 0.5863$ $\Gamma(k) = 1.5216$
Apr	Gamma	$\lambda = 0.0625$ $k = 0.8191$ $\Gamma(k) = 1.1434$
May–Jun	Gamma	$\lambda = 0.0424$ $k = 0.3936$ $\Gamma(k) = 2.2556$
Jul–Aug	0.00 Rainfall (fixed)	PB = 1.0000
Sep–Oct	Gamma	$\lambda = 0.0409$ $k = 0.5883$ $\Gamma(k) = 1.5167$

λ = Scale parameter for Gamma Distribution.
$\lambda = \bar{x}/s^2$ (sample mean divided by sample variance).
k = Shape parameter for Gamma Distribution.
$k = \bar{x}/s^2$.
$\Gamma(k)$ = Gamma Function of k.
PB* = Fixed probability

The fitting of theoretical distributions to the grouped months involved the use of the K-S test using the actual CDF from the data and the theoretical CDF from the tested distributions with a 5% level of significance. The CDF for each theoretical distribution was calculated using the distribution formula and the parameters obtained from the data analysis.

The gamma distribution was found to best fit the groups based on the rainfall per event reflecting the natural behaviour of the rainfall process where larger events have lower probabilities than smaller events. The fitting of interarrival time groups was comparatively difficult and more than a single distribution was needed to fit these groups. Both the gamma and the geometric distributions were used to fit the interarrival time groups, and a shifted form of the geometric distribution was also used.

Due to the dry climate of the study area, long interarrival times were more probable than shorter ones. In the extreme case of the month of June, long interarrival times of 30 days were the rule in the 26 years of records. In such a case the use of the regular form of the geometric distribution was impossible and the shifted form of this distribution was used. The shifting process involved the assigning of a fixed probability to the 30 days interarrival time and fitting the rest of the month to a regular geometric distribution. The 30-day fixed probability was calculated from the data record.

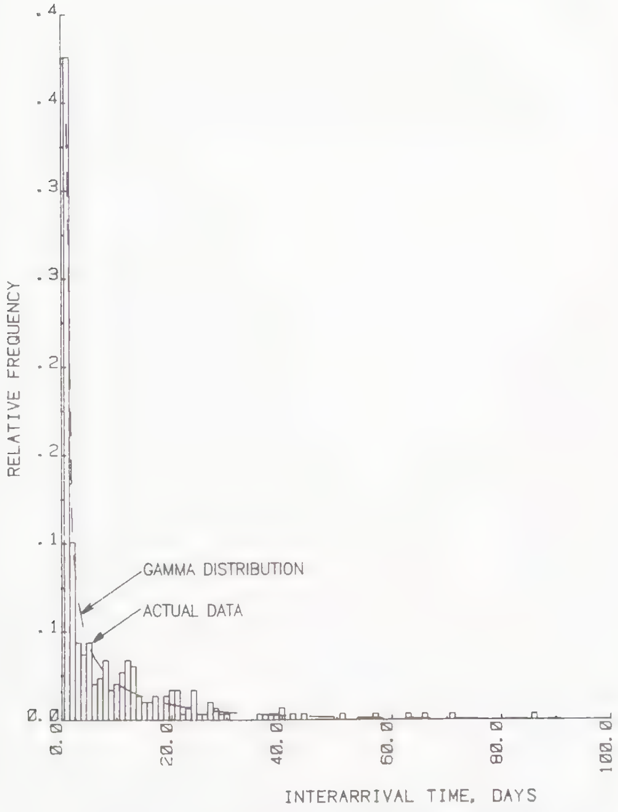

Fig. 3. Comparison of actual data and fitted theoretical distributions for the interarrival time variable (January–February–March).

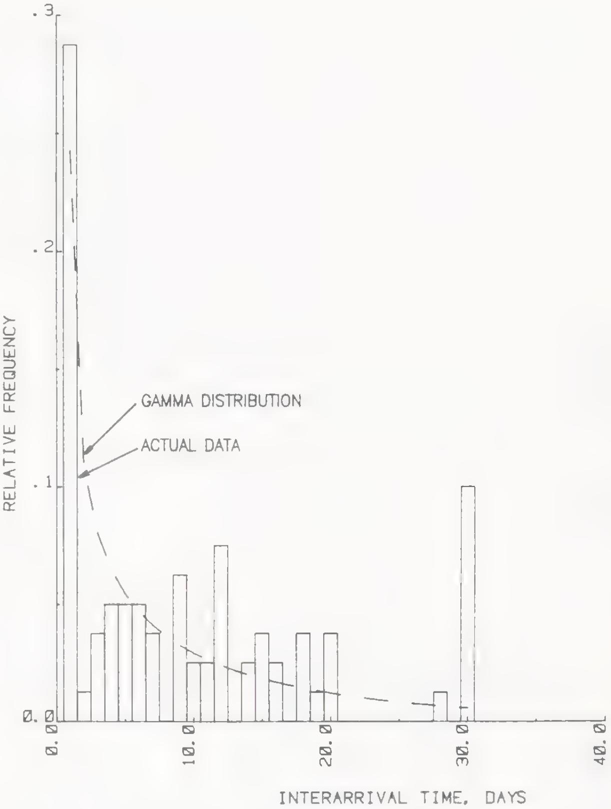

Fig. 4. Comparison of actual data and fitted theoretical distributions for the interarrival time variable (April).

The fitted distributions for the groups of interarrival time and the rainfall per event are all given in Table 2; also included are the parameters for each distribution as calculated by the method of moments. Figures 3 through 12 compare the actual and fitted distributions for the interarrival time and the rainfall per event random variables for the different groups.

The Monte Carlo simulation methods were used to simulate the rainfall process. The simulation utilizes the randomness of the variables describing the rainfall process and uses the fitted theoretical probability distributions. The simulation computer program used in the present model simulates 100 years

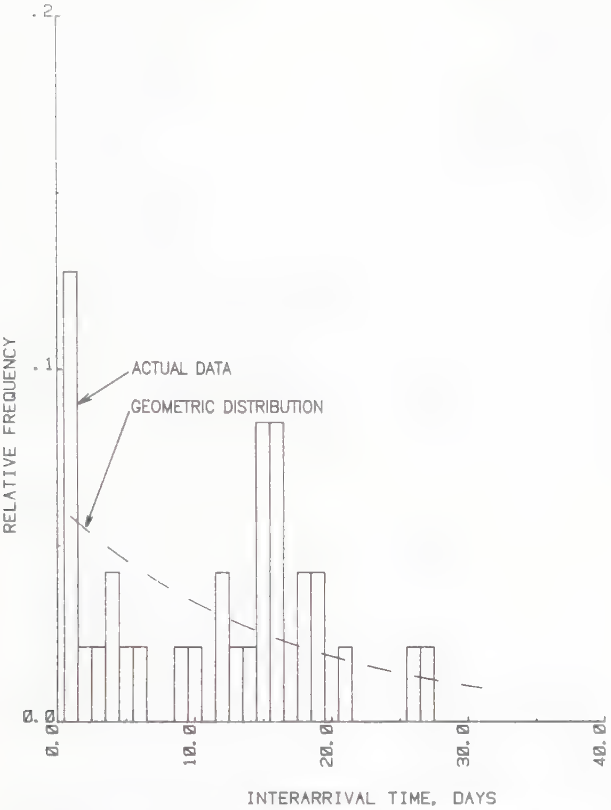

Fig. 5. Comparison of actual data and fitted theoretical distributions for the interarrival time variable (May).

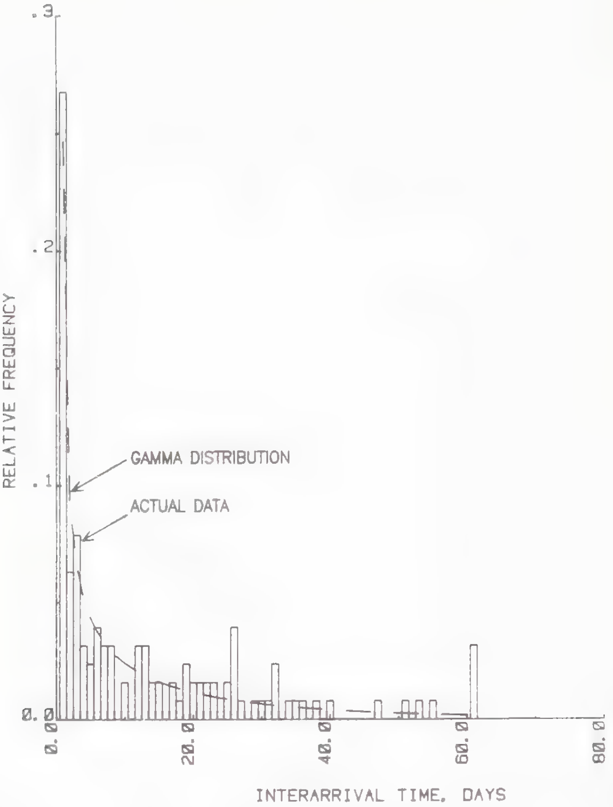

Fig. 7. Comparison of actual data and fitted theoretical distributions for the interarrival time variable (September–October).

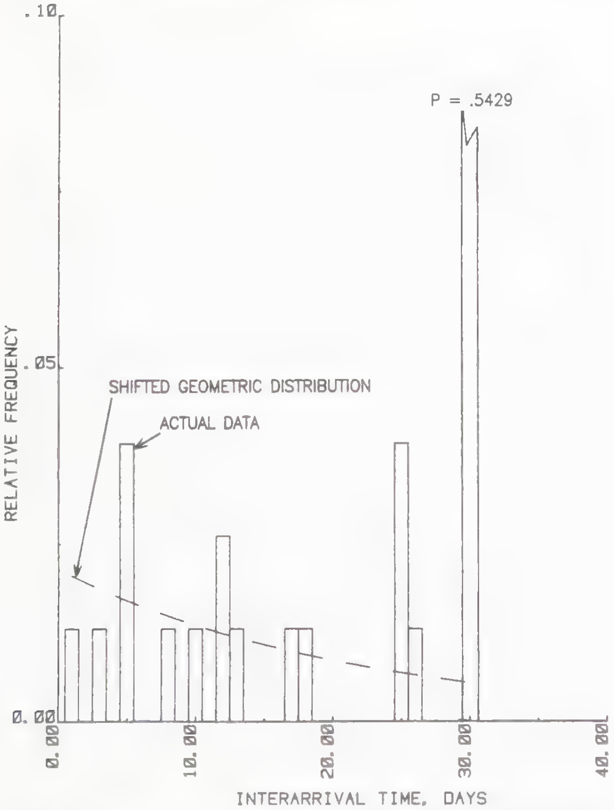

Fig. 6. Comparison of actual data and fitted theoretical distributions for the interarrival time variable (June). *P* is the fixed probability of the shifted 30-day interarrival time.

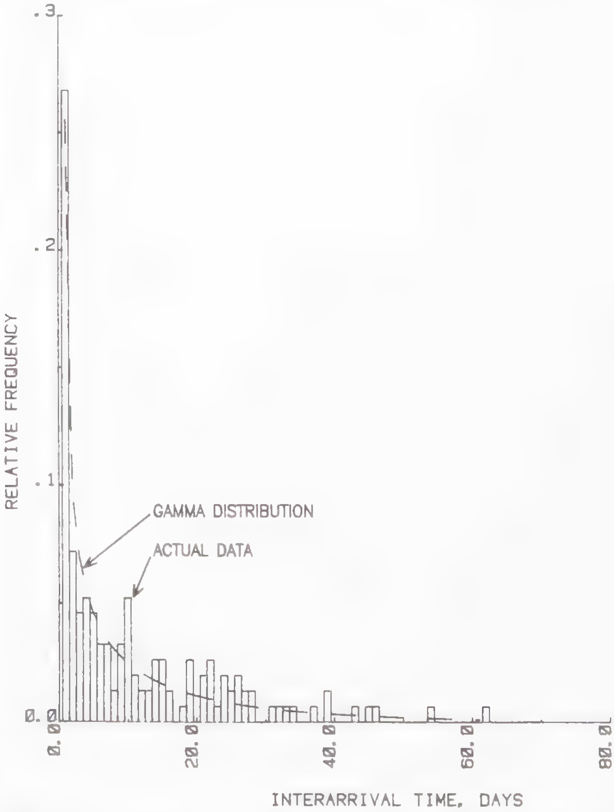

Fig. 8. Comparison of actual data and fitted theoretical distributions for the interarrival time variable (November–December).

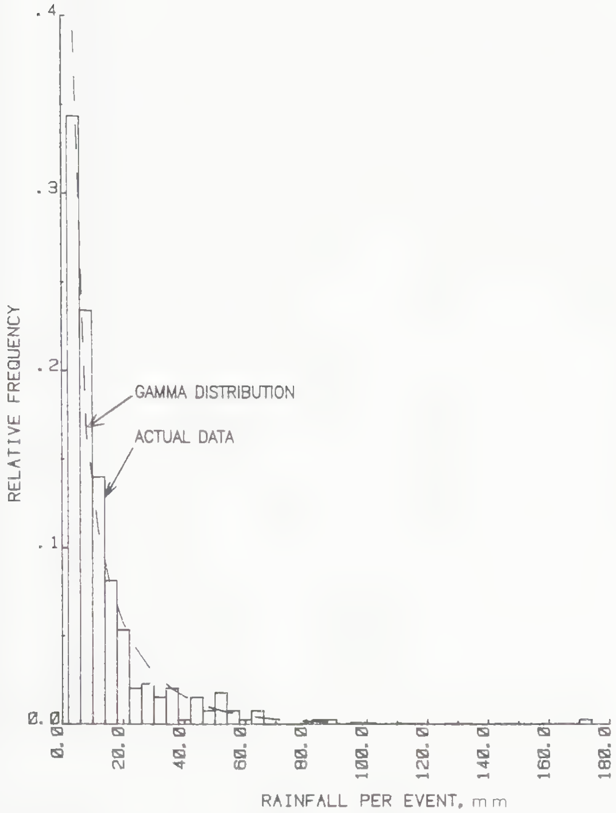

Fig. 9. Comparison of actual data and fitted theoretical distributions for the rainfall per event variable (November–December–January–February–March).

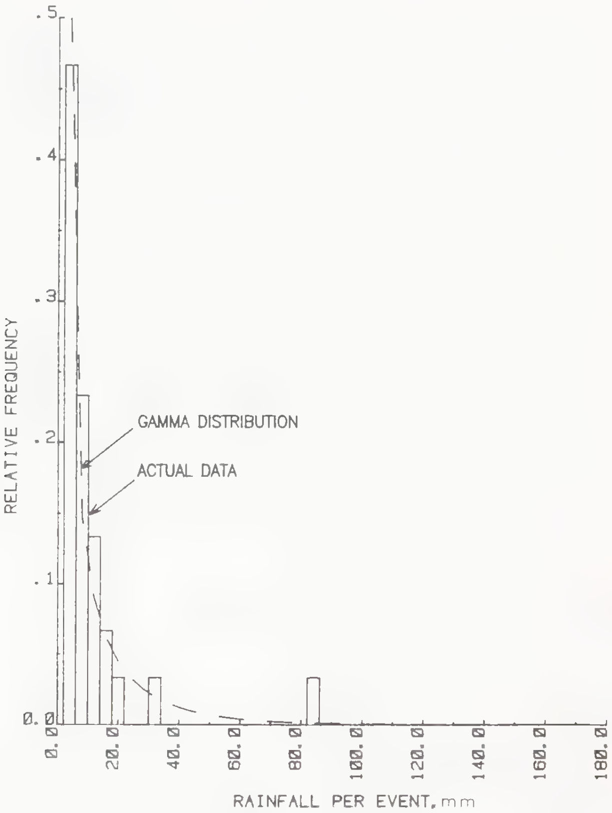

Fig. 11. Comparison of actual data and fitted theoretical distributions for the rainfall per event variable (May–June).

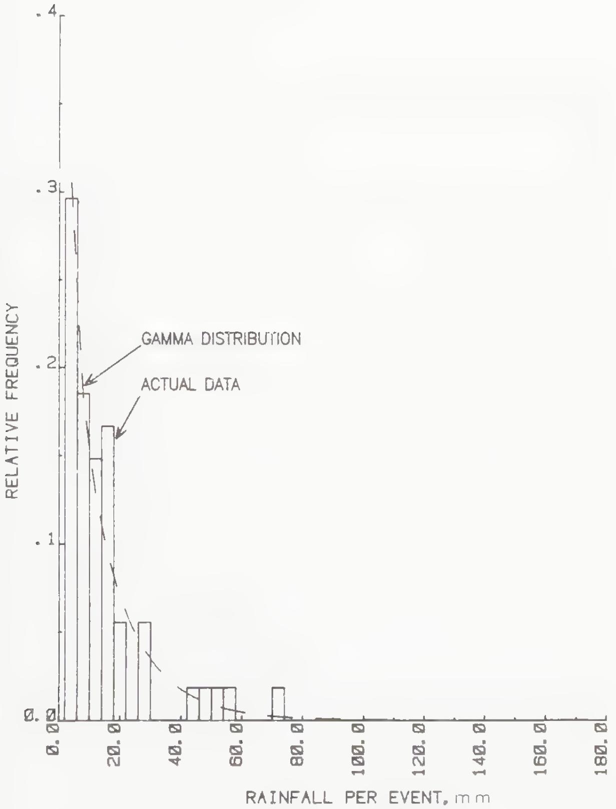

Fig. 10. Comparison of actual data and fitted theoretical probability distributions for the rainfall per event variable (April).

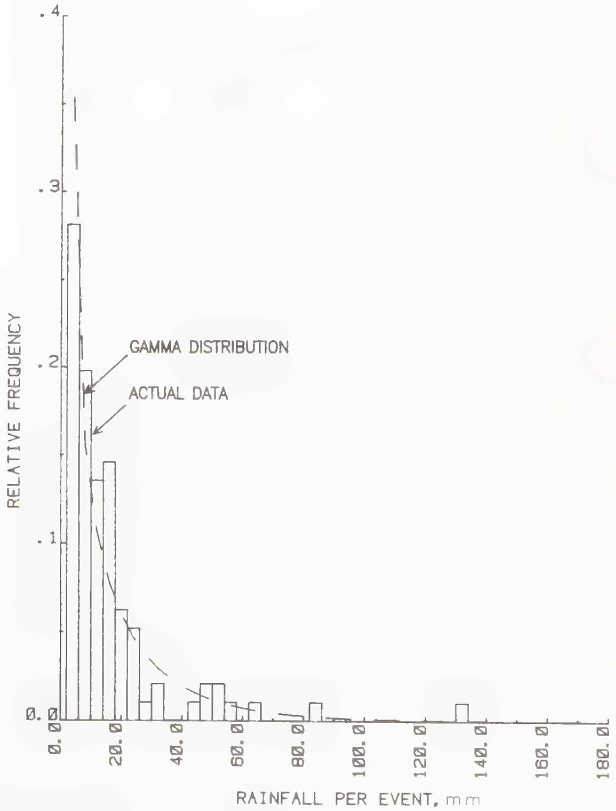

Fig. 12. Comparison of actual data and fitted theoretical distributions for the rainfall per event variable (September–October).

Table 3. Comparison of actual rainfall parameters for 26 years of records and simulated rainfall parameters for 100 years of simulation

Rainfall parameter	Mean			Variance		
	Observed	Simulated	% Difference	Observed	Simulated	% Difference
Interarrival time (days)						
Jan–Feb–Mar	8.46	9.44	+10.38	218.90	200.43	−8.63
Apr	9.75	10.09	+3.37	178.28	149.89	−15.92
May	17.15	16.60	−3.21	427.41	251.53	−41.15
Jun	22.29	22.38	+0.40	601.18	123.48	−79.46
Jul–Aug	62.00	62.00	0.00	0.00	0.00	0.00
Sep–Oct	13.28	14.98	+11.35	413.52	434.43	+4.81
Nov–Dec	10.86	11.41	+4.82	265.34	220.38	−16.94
Rainfall per event (mm)						
Nov–Dec–Jan–Feb–Mar	11.85	12.02	+1.41	239.68	197.21	−17.72
Apr	13.10	11.52	−12.06	209.57	140.50	−32.96
May–Jun	9.28	11.51	+19.37	218.96	216.23	−1.25
Jul–Aug	0.00	0.00	0.00	0.00	0.00	0.00
Sep–Oct	14.37	15.44	+6.93	350.89	413.76	+15.20

of daily rainfall and longer periods of simulation can be performed.

Examination of how well the simulation model represents the actual rainfall process in the study area involved a comparison test between the simulated and actual daily rainfall. The test of model performance included comparing the mean annual rainfall amount for the 26 years of records and the simulated 100 years. The test further involved comparison of the mean and variance of the actual and simulated rainfall for the interarrival time and rainfall per event groups. Percentage differences between these means and variances were also calculated.

The mean annual rainfall for the simulated years is 271.1 mm compared to a mean of 270.9 mm for the 26 years of recorded data, a difference of only 0.07 percent. Table 3 presents the rest of the comparison results which all show satisfactory results from the simulation model.

CONCLUSIONS

The results of the simulation model indicate a satisfactory performance and representation of the actual rainfall process for the Wādī Zārat watershed area. The results also show that the two-parameter model used (rainfall per event and interarrival time) was sufficient and that the addition of more parameters to describe the rainfall process proved to be unnecessary.

The rainfall simulation model presented in this paper was being used for the first time for the study area and for Libya in general. The potential of the present model is immense as is shown by the simulation results. The model can be modified for application in other parts of the country.

The model is intended for simulating long records of rainfall events where it can be used as part of many hydrological models where little or no rainfall data exist.

REFERENCES

Almestad, C.H. (1983). *A Methodology to Assess Stock Pond Performance using a Coupled Stochastic and Deterministic Computer Model.* M.S. Thesis, Univ. of Arizona, Tucson, Ariz., 207 p.

Benjamin, J.R. and Cornell, C.A. (1970). *Probability, Statistics, and Decision for Civil Engineers.* McGraw-Hill, New York, N.Y., 684 p.

Duckstein, L., Bogardi, I. and Fogel, M. (1978). An event-based stochastic model of phosphorus loading into a lake. *Adv. Wat. Resour.*, **1**, 321–329.

Duckstein, L., Fogel, M.M. and Kisiel, C.C. (1972). A stochastic model of runoff-producing rainfall for summer type storms. *Wat. Resour. Res.*, **8**(2), 410–421.

Duckstein, L., Fogel, M. and Davis, D. (1975). Mountainous winter precipitation: A stochastic event-based approach. *In*: *Nat. Symp. Precipitation Analysis for Hydrologic Modeling*, Davis, California, Am. Geophys. Union, 172–188.

Fogel, M.M., Duckstein, L. and Kisiel, C.C. (1971). Space time validation of a thunderstorm rainfall model. *Wat. Resour. Bull.*, **7**(2), 309–316.

Fogel, M.M., Heckman, Jr. L.H., and Duckstein, L. (1980). Predicting sediment yield from strip-mined land. *In*: *Symp. Watershed Management*, Boise, Idaho. ASCE, **1**, 176–187.

Haan, C.T. (1982). *Statistical Methods in Hydrology*. Iowa State Univ. Press, Ames, Iowa, 378 p.

HECKMAN, L.H., JR. (1977). *Simulation and Evaluation of Water Yield Response to Vegetation and Management on a Forested Watershed in Arizona*. Ph.D. Thesis, Univ. of Arizona, Tucson, Ariz., 202 p.

JONES, A.D. (1981). *A Methodology of Rainfall Data Analysis and Stochastic Rainfall/Runoff Synthesis*. M.S. Thesis, Univ. of Arizona, Tucson, Ariz., 199 p.

LAW, A.M. and KELTON, W.D. (1982). *Simulation Modeling and Analysis*. McGraw-Hill, New York, N.Y., 400 p.

SANOUSI, S.S. (1985). *A Method for Assessing the Use of Small Water Impoundments for Sediment Detention and Local Water Supplies on the Wādī Zārat Watershed, Northwestern Libya*. Ph.D. Thesis, Univ. of Arizona, Tucson, Ariz., 233 p.

Moser, H. and Rauert, W. (1980). *Isotopenmethoden in der Hydrogeologie. Lehrbuch der Hydrogeologie.* Gebr. Borntraeger, Berlin, **8**, 400 p.

Pallas, P. (1980). Water resources of the Socialist People's Libyan Arab Jamahiriya. *In: The Geology of Libya (eds* M.J. Salem and M.T. Busrewil). Academic Press, London, **II**, 539–594.

Regwa, (1973/74). *Detailed hydrogeological studies on Wadi Ajal, Wadi El Shatti and Traghen, for Agricultural Development Contract.* Unpublished Rep., Agric. Dev. Council, Tripoli, 194 p.

Richards, L.A. (1954). Diagnosis and improvement of saline and alkali soils. *U.S. Dept. Agric.*, **60**, 160 p.

Richter, W. and Lillich, W. (1975). *Abriss der Hydrogeologie.* Nägel und Obermiller, Stuttgart, 281 p.

Roether, W. (1970). Tritium and Kohlenstoff-14 im Wasserkreislauf. *Z. Dt. Geol. Ges.*, 183–192.

Sadykov, L. (1978). *Situation of Piezometric network in Marzuq Basin as of 1st October 1987 and suggestions for its improvement.* Unpublished Rep., Secretariat Dams Wat. Resour., Tripoli, 24 p.

Salem, O., Visser, J.H., Dray, M. and Gonfiantini, R. (1980). Groundwater flow patterns in the western Libyan Arab Jamahiriya, Evaluated from isotopic data. *IAEA-Symp., Vienna*, **158**/12, 165–179.

Seiler, K.P. (1969). Kluft- und Porenwasser im Mittleren Buntsandstein des südlichen Saarlandes. *Geol. Mitt.*, **9**, 75–96.

Sonntag, C., Klitzsch, E., El-Shazly, E.M., Kalinke, Ch. and Münnich, K.O. (1978). Paläoklimatische Informationen im Isotopengehalt ^{14}C-datierter Saharawasser. Kontinentaleffekt in D und ^{18}O. *Geol. Rundsch.*, **67** (2), 414–423.

Sonntag, C., Klitzsch, E., Löhnert, E.P., Münnich, K.O., Thorweihe, U., Weistroffer, U. and Swailem, F.M. (1978). Paleoclimatic information from deuterium and oxygen-18 in C-14 dated north Saharian groundwater. Groundwater formation in the past. *Isotope Hydrology 1987, IAEA, Vienna*, **III**, 569–581.

Sonntag, E., Thorweihe, U., Rudolph, J., Löhnert, E.P., Hunghans, Ch., Münnich, K.O., Klitzsch, E., El-Shazly, E.M. and Swailem, F.M. (1979). Isotopic identification of Saharian groundwaters. Groundwater formation in the past. *Arbeitstagung "Isotope in der Natur", Leipzig, 5–9 Nov. 1979.*

Theis, C.V. (1935). The relation between the lowering of the piezometric surface and the rate and duration of discharge of a well using groundwater storage. *Trans. Am. Geophys. Un.*, **16**, 519–524.

Todd, D.K. (1959). *Groundwater Hydrology*. John Wiley & Sons, New York, 336 p.

— **علي الريس ، أحمد (1978) :**

تقرير عن آبار المراقبة بين الفترة 1973 إلى 1977 — أمانة السدود والموارد المائية/فرع سبها.

— **كلش ، عدنان. أبو المعاطي ، أحمد. بشير حسن ، محمد (1981) :**

نوعية مياه الري في فزان — التقرير الدوري الأول ، المركز الفرعي للبحوث الزراعية بمنطقة فزان/سبها.

— **عبد الله ، خميس (1982) :**

نتائج التحاليل الكيميائية لمياه السواني بسبها (٣٠ عينة) — المختبر المركزي للمياه ببلدية سبها.

— **الشاعر، محمد (1984) :**

الخواص الهيدروجيولوجية والهيدروكيميائية والتركيب الأيزوتوبي (النظائري) للمياه الجوفية لمنطقة حوض مرزق. الجزء الثاني : المياه الجوفية بالأحجار الرملية بدهر الحياة الوسطى بمنطقة سبها بالطرف الشمالي لحوض مرزق (بحث الحصول على درجة الدكتوراه من جامعة توبنجن بالمانيا الغربية).

REFERENCES

Asquith, G. and Gibson, C. (1982). Basic Well Log Analysis for Geologists. *Am. Assoc. Petrol. Geol.*, Tulsa, Oklahoma, 216 p.

Burdon, D.J. (1977). *Evaluation of Water Consuming Projects in Remaining Districts of Fazzan*. Unpublished Rep., Secretariat Dams Wat. Resour., Tripoli, 7 p.

Burdon, D.J. (1977). *Annotated Bibliography on Water in Fazzan*. Unpublished Rep., Secretariat Dams Wat. Resour., Tripoli, 31 p.

Chanduvi, F., Rasheed, M.A. and Fayed, O. (1978). *Soil and Water Salinity Appraisal of the Fazzan Region*. Agricultural Res. Cent., Sebha, 64 p.

Chow, V.T. (1952). On the determination of transmissivity and storage coefficient from pumping test data. *Trans. Am. Geophys. Un.*, **33**, 397–404.

Cooper, H.H. and Jacob, C.E. (1946). A generalized graphical method for evaluating formation constants and summarizing well field history. *Trans. Am. Geophys. Un.*, **27**, 526–534.

Dubay, L. (1980). Groundwater in Wadi ash Shati, Fazzan: A case history of resource development. *In: The Geology of Libya* (*eds* M.J. Salem and M.T. Busrewil). Academic Press, London, **II**, 611–627.

Dürbaum, H.J. (1961). Porostität und Durchlässigkeit von Gesteinen. *In: Lehrbuch der Angewandten Geologie* (*ed.* A. Bentz). Enke-Verlag, Stuttgart, **I**, 934–949.

El-Chair, M., Taka, M., Peters, F.I. and Rayes, A. (1977). *About Hydrogeology of General Southern Libya*. Unpublished Rep., Secretariat Dams Wat. Resour., Sabha/Tripoli, 23 p.

Ettalji, A.J., Krokovic, D. and Banerjee, S. (1978). *Bibliography of the Geology of Libya*. Ind. Res. Cent., Tripoli, Bull. **11**, 135 p.

Geyh, N.A. (1971). Die Anwendung von ^{14}C-Methode. Die Entnahme, Auswahl und Behandlung von ^{14}C-Proben, sowie die Auswerung und Verwendung von ^{14}C-Ergebnissen. *Clausthaler tektonische Hefte*, **11**, 118 p.

Gonfiantini, R. (1977). *Progress Report on the Application of Isotope Techniques to Hydrology*. Unpublished Rep. Secretariat Dams Wat. Resour., and IAEA-Vienna.

Hem, J.D. (1970). Study and Interpretation of the Chemical Characteristics of Natural Water (2nd Ed.). *U.S. Geol. Surv. Wat. Supply Pap.*, **1473**, 363 p.

Hölting, B. (1980). *Hydrogeologie, Einführung in die allgemeine und angewandte Hydrogeologie*. Enke-Verlag, Stuttgart, 340 p.

Keys, W.S. and MaCary, L.M. (1971). Application of borehole geophysics to water resource investigations. Techniques of water resources investigations. **2**, E1, *U.S. Geol. Surv.*, 126p.

Klitzsch, T. (1970). Die Strukturgeschichte der Zentralsahara, neue Erkenntnisse zum und zur Paläogeographie eines Festlands. *Geol. Rundsch.*, **59** (2), 459–527.

Klitzsch, E., Sonntag, C., Weistroffer, K. and El-Shazly, E.M. (1976). Grundwasser der Zentralsahara: Fossile Vorrate. *Geol. Rundsch.*, **65** (1), 264–287.

Kruseman, G.P. and De Ridder, N.A. (1973). *Untersuchung und Anwendung von Pumpversuchsdaten*. M. Verlagesgesellschaft Rudolf Muller, Koln, Braunsfeld, 181 p.

Langguth, H.R. and Voigt, R. (1980). *Hydrogeologische Methoden*. Springer-Verlag, Berlin, 486 p.

Matthess, G. (1973). *Die Beschaffenheit des Grundwassers. Lehrbuch der Hydrogeologie*. Gebr. Borntraeger, Berlin, **2**, 324 p.

بعض الآراء الأخرى التي تعتبر أن هذه الخزانات بطبقات دهر الحياة الوسطى جميعها بحوض مرزق عموماً تمثل وحدة هيدرولوكية واحدة كما يعتقد PALLAS (1980م) . لا تتفق مع الواقع ولا توجد لها حسب المعطيات والدلائل الحالية أي مبرر.

كذلك ترقيمها من أعلى إلى أسفل بأرقام (1، 2، 3، . . . إلخ . . . على سبيل المثال بوادي الحياة ZALUSKI and SADEK (1980م) دون وضع الدراسات الأخرى كالتي أجريت من قبل شركة ريجوا (74/73) في عين الإعتبار يكون غير موضوعي . حيث أن بهذه المنطقة بالذات تعتبر وضعية الخزانات الجوفية المائية واضحة ومشابهة لمنطقة سبها .

إنّ كميات المياه الضخمة (606 مليون م^3/السنة) المستغلة حالياً بمنطقة سبها ومعدلات الهبوط السنوية . شكل (11) التي تعتبر عالية تدعو إلى العناية التامة باستغلال المياه بالمنطقة خاصة أن وضعنا في عين الإعتبار بأن هذه المياه قديمة دفينة غير متجددة . هذا بالإضافة إلى أن موقع منطقة سبها في الطرف الشمالي لحوض مرزق تترتب عليه محدودية إمكانيات هذه الخزانات المائية فسمكها يعتبر في طرف الحوض الشمالي ضئيل جداً وذلك بالمقارنة بالمناطق الأخرى لحوض مرزق خاصة الوسطى وأن امتدادها واتساع رقعتها لا يتعدى الأطراف الشمالية المتاخمة لمنطقة سبها حيث ينتؤ جزء منها على السطح .

حركة المياه الجوفية من الجنوب إلى الشمال قد تعوض جزء بسيط جداً من المياه المستغلة . إلاّ أن هذا التعويض يقل بعشرات المرات عن كميات المياه المسحوبة كما أن إستغلال المياه الجوفية في المناطق الأخرى بحوض مرزق جنوب وشرق منطقة سبها يحد من كميات وحركة المياه اتجاه الشمال . وفي حالة استمرار استغلال المياه بالمعدلات الحالية من الخزانات بطبقات الحياة الوسطى فإن ذلك يهددها بالجفاف في فترة لا تتعدى 150 سنة (المجموعة الأولى) ، 200 سنة (المجموعة الثانية) . هذا إن لم تزد كمية المياه المستغلة عن ما هو عليه الآن وإلاّ أنها ستنفد في فترة زمنية أقصر .

أما المياه الجوفية بالخزان الكمبرو- أردوفيشي فلم يتم إستغلالها بمنطقة سبها إلاّ عن طريق البئر س – 1 – 74 بمشروع سبها الزراعي . ولا تتعدى كمية المياه المستغلة من هذا البئر 10 مليون م^3/ السنة مع العلم بأنه من المتوقع أن يكون جزء من هذه المياه صادر من مجموعة الخزانات السفلية بدهر الحياة الوسطى نظراً لإحتمال اختلاط مياهها بمياه الخزان الكمبرو- أردوفيشي وذلك عن طريق تصميم البئر كما أشير إليه سابقاً .

قد يصبح الخزان الكمبرو- أردوفيشي في المستقبل هو المصدر الأساسي لإستغلال المياه بمنطقة سبها خاصة إذا وضعنا في عين الإعتبار جفاف الخزانات الجوفية بدهر الحياة الوسطى بعد الفترة الزمنية المتوقعة . إلاّ أن الآبار التي ستنفذ لاستغلال هذا الخزان الجوفي العميق ستكون مكلفة حيث أن أعماقها سوف لن تقل في المتوسط عن 1000متر هذا بالإضافة إلى أن درجة حرارة مياهها المرتفعة تتطلب وضع احتياطات وترتيبات خاصة من أجل امكانية استغلالها في الأغراض المختلفة .

شكر وتقدير

من أجل انجاز هذه الدراسة كان بعض الأخوة سند لي في الحصول على بعض المعلومات وفي إجراء بعض الأعمال الميدانية كتجارب الضخ وأخذ قراءات آبار المراقبة ، لهذا أود أن أتقدم بجزيل شكري إلى كل من :

الأخ/علي العجيلي أحميد النجار (رئيس فرع مصلحة المياه والتربة بسبها) . والأخ/الجيولوجي أحمد حسن الريس والأخ الجيولوجي نادر لويس طنيوس الذين كانوا زملاء لي أثناء عملي معهم بالهيئة العامة للمياه ثم أمانة السدود والموارد المائية (مصلحة المياه والتربة حالياً) .

كما أشكر الجيولوجي المبروك يوسف بأمانة الزراعة والإستصلاح الزراعي بسبها للمساعدة في الحصول على احصائية عدد الآبار التي نفذت بمنطقة سبها وكذلك الأستاذ عبد الرحمن المهدي الحضيري الذي تكرم بكتابة التوضيحات على الأشكال الواردة في هذا البحث وإلى كل من ساعد بطريقة أو أخرى في إنجاز هذه الدراسة .

تقارير ودراسات غير منشورة

مصلحة المياه والتربة/سبها :
— ملف حفر بئر سبها العميق رقم س/74/1 بمشروع سبها الزراعي .
— ملف حفر بئر سبها العميق رقم س/س 76/0074/15 بجي القرضة بسبها .

— **الريس ، أحمد** (1977) :

نسبة الأملاح في مياه الشرب للبلديات : سبها ، أوباري ، مرزق ، الشاطئ – أمانة السدود والموارد المائية/فرع سبها .

التغيرات التي طرأت على مستوى المخزون المائي الجوفي :

نتج عن الاستهلاك الكبير للمياه الجوفية التي تعتبر كما أشير إليه مسبقا قديمة دفينة غير متجددة في جميع أنحاء منطقة سبها هبوط ملحوظ في مستوى سطح الماء وبالتالي في كمية المياه المخزونة. وقد تم تتبع التغيرات التي طرأت على مستوى سطح الماء عن طريق خمسة آبار مراقبة أربعة بالخزانات الجوفية العلوية وواحد بالخزانات السفلية. هذا بالإضافة إلى ما تمت ملاحظته عن طريق العديد من الآبار الإنتاجية المستغلة في الأغراض المختلفة المشار إليها أعلاه.

ويوضح شكل (11) متوسط المعدلات السنوية لهبوط مستوى سطح الماء بالخزانات العلوية. هذا ويبلغ بوسط منطقة سبها حوالي 0,36 م/السنة وبأطراف المنطقة الشمالية بتمنهنت حوالي 0,26 م/السنة وحوالي 0,125 م/السنة بالمنطقة على بعد 40كم جنوبي غربي سبها على طريق سبها أوباري شكل (11). وعن طريق بئر مراقبة واحدة فقط بمشروع الأبقار بسبها وبعض من الآبار الإنتاجية وغير المستغلة لوحظ أن معدل الهبوط السنوي بمياه الخزانات الجوفية السفلية بوسط سبها يبلغ في المتوسط 0,54 م/السنة بأطراف المنطقة تعذر مراقبة الخزانات حيث لم يتم إلاّ أخيراً مع نهاية سنة 1986م حفر بئر مراقبة على بعد 50كم جنوب مدينة سبها على طريق سبها غدوه شكل (11).

من خلال المعدلات السنوية لهبوط مستوى سطح الماء يتوقع أن تصبح الخزانات العلوية بعد 100 سنة غير قابلة للإستغلال إلاّ تحت ظروف ومعطيات معينة وبعد 150 سنة وستكون جافة ومستنزفة بالكامل أما الخزانات الجوفية السفلية فسيتعذر إستغلالها بعد 150 سنة وستكون ناضبة ومستنزفة بالكامل بعد 200 سنة تقريباً.

هذه الإحتمالات تكون قريبة إلى الواقع في حالة ثبات كميات المياه المستغلة بالمقادير والمعدلات الواردة أعلاه في حالة إزدياد الإستهلاك السنوي عن ما هو عليه الآن فان عمر الخزانات الجوفية المائية سيكون أقصر من المتوقع بكثير.

الخزان الكمبرو- أردوفيشي قد يكون في المستقبل هو المصدر الأساسي لإستغلال المياه بمنطقة سبها خاصة وان وضعنا في عين الإعتبار جفاف الخزانات الجوفية بدهر الحياة المتوسطة بعد الفترة الزمنية المتوقعة المشار إليها أعلاه. إلاّ أن الآبار التي ستنفذ لإستغلال هذا الخزان الجوفي العميق ستكون مكلفة حيث أن أعماقها سوف لن تقل في المتوسط عن 1000 متراً تقريباً هذا بالإضافة إلى أن درجة حرارة مياهها المرتفعة تتطلب وضع إحتياطات وترتيبات خاصة من أجل إمكانية الإستفادة منها في الأغراض المختلفة.

الإستنتاج

المياه الجوفية تمثل المورد الأساسي الذي تعتمد عليه منطقة سبها، من أجل تغطية الإحتياجات المائية في شتى مجالات الحياة. نتج عن مناخ المنطقة الحار الجاف نسبة تبخر عالية محتملة «تتراوح بين 3,44 إلى 4,82 م/السنة تفوق بعشرات المرات كمياه الأمطار النادرة الضئيلة التي رصدت بمنطقة سبها.

من خلال الدراسة تم التوصل إلى أن المياه الجوفية الصالحة للإستغلال تتواجد أساساً في عدة طبقات لأحجار رملية تتخللها أحجار طينية بطبقات دهر الحياة الوسطى. هذه الأحجار الرملية التي تمثل خزانات جوفية مائية أمكن تقسيمها إلى مجموعتين أساسيتين هما :

خزانات المجموعة الأولى (العلوية). وخزانات المجموعة الثانية (السفلية). يتكون الفاصل بينها من طبقات الأحجار الطينية. هذا التصور مبني على الإختلافات في نتائج الدراسات الجيوفيزيائية. شكل (4، 5) والتحاليل الكيميائية والنظيرية للمياه الجوفية الجداول (1 إلى 4) والأشكال (6، 7، 8، 10) وبعض الفوارق البسيطة الأخرى في الخصائص الصخرية والهيدرونيكية بين مجموعة الخزانات الجوفية العلوية القريبة من السطح حتى عمق يبلغ في المتوسط 40 متراً ومجموعة الخزانات السفلية حتى عمق 200 متر تقريباً.

هذا التقسيم للطبقات الحاملة للمياه بدهر الحياة المتوسطة بمنطقة سبها يتناسب عموماً في مضمونه مع ما تم التوصل إليه عن طريق الدراسة التي أعدتها شركة ريجوا (1974/1973) عن حوض مرزق. حيث تم تقسيم الطبقات الحاملة للمياه بدهر الحياة المتوسطة القابلة للإستغلال إلى الخزانات أ، ب، ج، د (A. B. C. D.). إلاّ أنه يتضح من خلال هذه الدراسة بأنه لا توجد فوارق تذكر في الخصائص المشار إليها أعلاه بين الخزان أ (A) والخزان ب (B) هذا بالإضافة إلى أن كلاً منها يتكون من أكثر من خزان وليس بالإمكان تحديد مكان فصلها عن بعضها البعض وذلك لإنعدام وجود طبقات طينية أو غيرها ذات سمك أو أي دلائل أخرى هيدروجيولوجية لهذا أقترح أن يتم دمجها كمجموعة لخزانات جوفية مائية لوحدة هيدرولوكية واحدة.

الخزان الجوفي ج (C) حسب ريجوا (74/73) إتضح أنه يتكون أساساً من طبقات سميكة (متوسط 35 متراً) لأحجار طينية، شكل (4) ويعتبر فاصل أو عازل بين مجموعة الخزانات التي تعلوه وليس بالإمكان إستغلال مياهه. لهذا أرى أن توصف هذه الطبقات الطينية بأنها فاصلة بدلاً من خزان جوفي مائي غير قابل للإستغلال.

مجموعة الخزانات السفلية تتفق مع ما تم التوصل إليه عن طريق دراسة ريجوا حيث وصفت بالخزان د (D). من المستحسن أن نعتبرها مجموعة الخزانات السفلية بدلاً من الخزان د حيث أنها تتكون من أكثر من طبقة حاملة للمياه (مجموعة الخزانات).

من هنا يتضح أنه من الأفضل تقسيم الخزانات الجوفية المائية بطبقات دهر الحياة الوسطى لمنطقة سبها إلى مجموعتين رئيسيتين. المجموعة الأولى (العلوية) والمجموعة الثانية (السفلية) وإعتبار الطبقات الطينية (الخزان ج) فاصل بينهما هذا التصور الجديد سيكون أقرب إلى الواقع والوضعية المائية بالمنطقة وبالإمكان تطبيقه على هذه الخزانات بجميع أنحاء حوض مرزق.

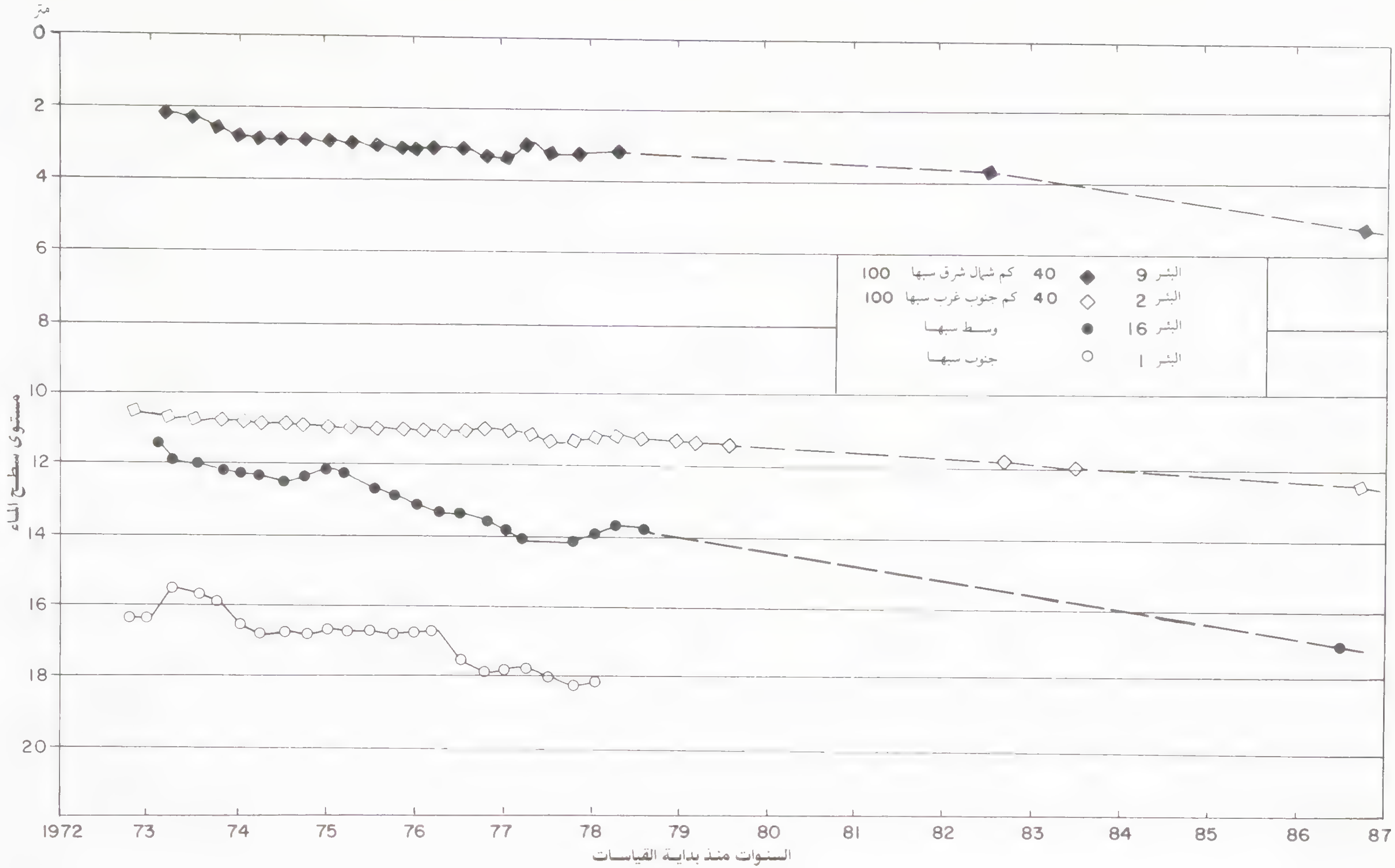

شكل (11) : التغيرات التي طرأت على مستوى سطح الماء بالخزانات الجوفية العلوية.

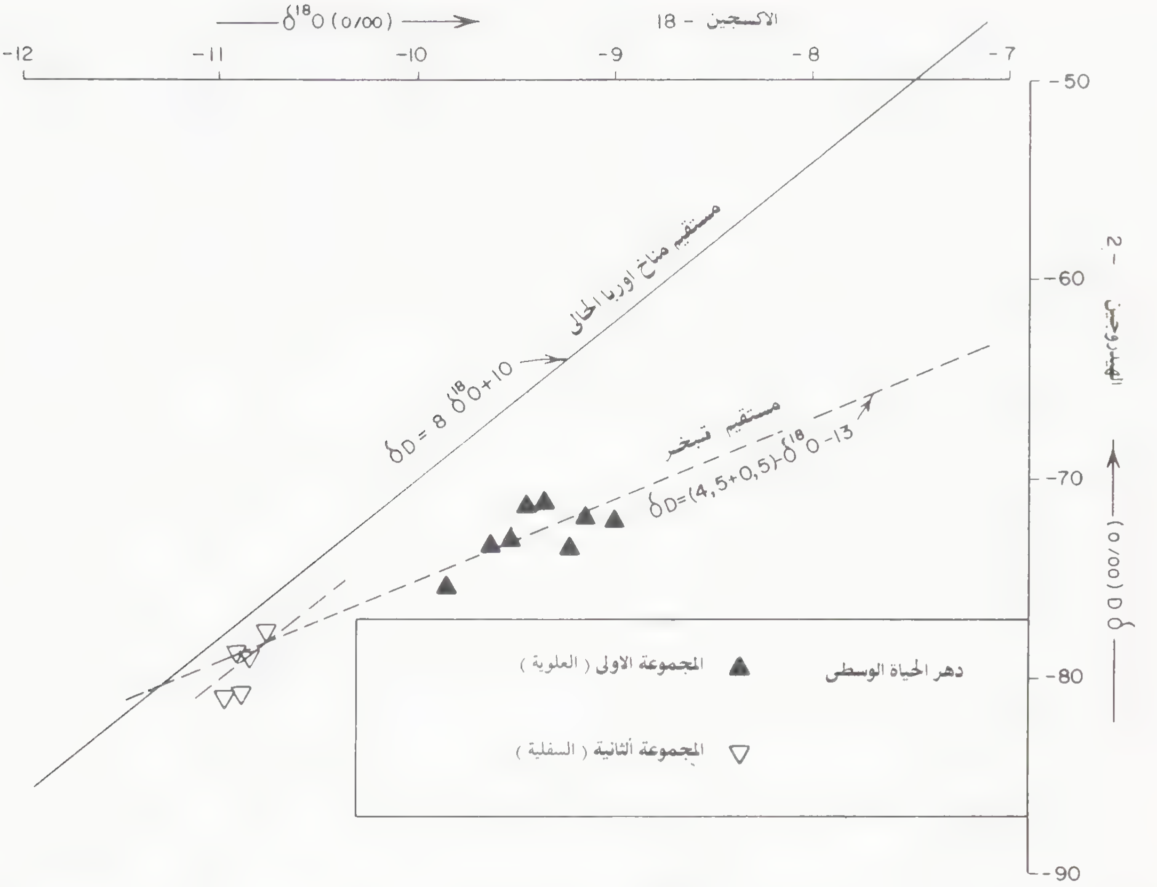

شكل (10) : العلاقة بين نسب تواجد الأكسجين – 18 والهيدروجين – 2 بمياه الخزانات الجوفية بطبقات دهر الحياة الأوسط ، سبها .

وتقدر المياه المستغلة من هذه الخزانات للأغراض العامة عن طريق 95 بئراً بحوالي 36 مليون م^3/السنة منها 21,5 مليون م^3/السنة لأغراض الشرب (35 بئراً) و1 مليون م^3/السنة لأغراض الصناعة (10 آبار) و13,5 مليون م^3/السنة لأغراض الزراعة العامة (50 بئراً) بالإضافة إلى كمية المياه المستغلة من هذه الخزانات لأغراض الزراعة الخاصة عن طريق 500 بئر تقريباً . والتي تقدر بحوالي 160 مليون م^3/السنة .

وبالتالي ستكون كمية المياه المستغلة بمنطقة سبها من الخزانات الجوفية بطبقات دهر الحياة المتوسطة حالياً حوالي 606 مليون م^3 السنة منها 410 مليون م^3 السنة من الخزانات الجوفية العلوية و196 مليون م^3/السنة من الخزانات الجوفية السفلية .

من الملاحظ أن كمية المياه المستغلة من الخزانات الجوفية السفلية تساوي على ما يقرب نصف كمية المياه المستغلة من الخزانات الجوفية العلوية . وهذا راجع إلى تركيز الزراعة الخاصة التي تستهلك الجزء الأكبر من المياه المستغلة بمنطقة سبها (570 مليون م^3/السنة) على مياه الخزانات العلوية . هذه الوضعية بدأت تتغير في السنوات الأخيرة . فمنذ عشر سنوات كانت الزراعة الخاصة تعتمد أساساً على الآبار السطحية والتي حفر جزء منها بطريقة يدوية بالخزانات الجوفية العلوية ولكن نظراً لتنوع المزروعات من نباتات وأشجار في السنوات الأخيرة والتي تتطلب مياهاً عذبة بالإضافة إلى إزدياد الملوحة عموماً بهذه الخزانات وادخال التقنية الحديثة في تنفيذ وحفر وإستغلال الآبار إتجه جزء كبير من المزارعين إلى تعميق آبارهم أو حفر آبار تستغل مياه الخزانات السفلية على حدة .

وإذا إستمرت هذه الحالة تكون مياه الخزانات الجوفية السفلية في السنوات القادمة هي المصدر الأساسي للمياه المستغلة بمنطقة سبها .

المياه الجوفية بالخزان الكمبرو- أردوفيشي لم يتم إستغلالها بمنطقة سبها إلاّ عن طريق البئر العميق س – 1 – 74 بمشروع سبها الزراعي . وتقدر كمية المياه المسحوبة من هذا البئر بحوالي 10 مليون م^3/السنة ، مع العلم بأنه من المتوقع أن يكون جزء من هذه المياه صادرة من مجموعة الخزانات السفلية بدهر الحياة المتوسطة نظراً لاختلاط مياهها بمياه الخزان الكمبرو- أردوفيشي وذلك عن طريق تصميم البئر كما أشير إليه سابقاً .

عمر الكربون – 14 وبالتالي عمر المياه يبلغ حوالي 7810 سنة. معدل تواجده بالعينتين الأخريين بلغ 11,65 ± 0,7٪ مدرن، 9,8 ± 0,8٪ مدرن وفي هذه الحالة سيكون عمر الكربون – 14 وبالتالي عمر المياه الجوفية حوالي 15965 و17350 ألف سنة على التوالي، أما بالعينة الأخيرة وكانت نسبته حوالي 5,4 ± 0,79٪ مدرن هذا يعني أن عمر الكربون – 14 الذي يعكس عمر المياه يبلغ حوالي 21500 سنة.

توضح النتائج المتمثلة في الأعداد الواردة أعلاه اختلافاً في أعمار الكربون – 14 بالمياه الجوفية بالمنطقة مما يدل على أنها لم تتكون في فترة زمنية واحدة ولا توجد علاقات هيدروليكية بين الخزانات المشار إليها أعلاه.

يدل التقارب في أعمار العينتين اللتين تم أخذهما من الآبار بالمياه الجوفية بالمجموعة السفلية على أن هذه المياه تكونت في فترة زمنية متقاربة ولها علاقة هيدرولوكية مع بعضها البعض.

يبدو أن المياه بالخزانات الجوفية العلوية حديثة العهد حيث أن عمر الكربون – 14 بها يبلغ حوالي 710 سنة. وهذا راجع إلى تلوث واختلاط المياه الجوفية بهذه الخزانات بمياه السبخ والمستنقعات التي تحتوي على نسبة عالية من الكربون – 14 وذلك نتيجة لتعرضها للهواء الجوي أو لهطول أمطار حديثة.

جدول (5): معدلات تواجد الأكسجين – 18 والهيدروجين – 2 والكربون – 14 بالمياه الجوفية بمنطقة سبها.

	الديوتريوم		الأكسجين – 18		الكربون – 14
	من	إلى ^{2}H	من	إلى ^{18}O	^{14}C
أ	– 71,2 ،	– 75,2	– 9,37 ،	– 9,85	77 + مدرن
ب	– 77,94 ،	– 81,57	– 10,72 ،	– 10,92	11,65 ± 0,7 و9,8 ± 0,8
جـ	– 81,18		– 10,96		5,4 ± 0,79 مدرن

أ — المياه الجوفية لمجموعة الخزانات العلوية بسبها.

ب — المياه الجوفية بمجموعة الخزانات السفلية بسبها.

جـ — المياه الجوفية بالخزان الكمبرو – أردوفيشي.

الديوتريوم (^{2}H) والأكسجين – 18 (^{18}O):

بالإضافة إلى النظائر المشعة الواردة أعلاه تم في السنوات الماضية الأخيرة التركيز على النظائر الثابتة كالهيدروجين – 2 (الديوتريوم) والأكسجين – 18 وذلك من أجل دراسة الخواص الهيدروجيولوجية والمناخية للمياه السطحية والجوفية. هذه النظائر التي تكون جزءا بسيطا من الماء على هيئة مركب أساسي يعرف بالماء الثقيل تتواجد بالمياه الجوفية بالمنطقة بالمعدلات المبينة في جدول (5) وشكل (10).

تدل هذه النتائج على وجود فروق في معدلات النظائر الثابتة بالمياه حيث أن نسبها على هيئة ماء ثقيل بالخزانات الجوفية العلوية أكبر منها بالخزانات الجوفية السفلية لدهر الحياة الأوسط. لو قورنت هذه العينات المختلفة بالمستقيم الذي تقع عليه مياه مناخ أوربا الحالي الذي يطابق مستقيم الماء الجوي (Meteoric water line) كما هو مبين بالشكل (10) نلاحظ أن مياه الخزانات السفلية تقع تقريباً على خط موازي لمستقيم مناخ أوربا الحالي وبأسفله. في حين أن مياه الخزانات العلوية تقع على مستقيم يشكل زاوية حادة معه. عندما تقع عينات مائية على مستقيم يبعد عن خط الماء الجوي بزاوية معينة نتيجة لارتفاع نسبة الماء الثقيل (خاصة الأكسجين) بها يوصف هذا بأنه (خط) مستقيم تبخر (Evaporation line) كما ورد في MOSER and RAUERT (1980)، وهذا يعني أن المياه المكونة لهذا المستقيم في هذه الحالة مياه الخزانات العلوية قد تعرضت للتبخر أثناء تكوينها أو أنها إختلطت في فترة زمنية لاحقة بمياه تعرضت للتبخر في ظروف مناخية من دافئة إلى حارة.

وتدل العينات من الخزانات السفلية والعينة المائية من الخزان – الكمبرو – أردوفيشي على أنها تكونت في فترة زمنية مشابهة لمناخ أوربا الحالي وأقل منه برودة وذلك كما ثبت أيضاً عن طريق العديد من العينات الأخرى التي أخذت من هذه الخزانات بمختلف مناطق حوض مرزق SONNTAG *et al.* (1978)، من هنا نلاحظ أن نتائج التحاليل النظيرية لمياه الخزانات الجوفية لدهر الحياة الوسطى تقسم إلى مجموعتين رئيستين، فالاختلاف في نسب الكربون – 14 وبالتالي في أعمارها المتوقعة خير دليل على هذا. كذلك نسب الأكسجين – 18 والهيدروجين – 3 بها تدل على أن مياهها تكونت تحت ظروف مناخية مختلفة، حيث كانت على ما يبدو حارة من رطبة إلى جافة (مياه المجموعة العلوية) وباردة رطبة (مياه المجموعة السفلية). إن نسبة التريتيوم (الهيدروجين – 3) الذي يعتبر شبه معدوم تؤكد على نفي أية احتمالات متوقعة لتجديد وتغذية هذه المياه الجوفية بمياه حديثة كالأمطار وغيرها. من خلال جل هذه النتائج (النظيرية) نلاحظ أن المياه الجوفية بالمنطقة تكونت في أوضاع مناخية تختلف عما هو عليه الآن وأنها تعتبر قديمة ودفينة غير متجددة، (شكل 10).

كمية المياه الجوفية المستغلة في المنطقة:

في العشرين سنة الأخيرة تم بمنطقة سبها حفر قرابة 3000 بئرٍ وذلك من أجل إستغلال المياه الجوفية بطبقات دهر الحياة المتوسطة. منها حوالي 2800 بئرٍ حفرت لأغراض الزراعة الخاصة وتستغل عن طريقها في أغلب الحالات مياه الخزانات الجوفية العلوية، (2300) بئرٍ بمعدل سنوي حالي يقدر بحوالي 410 مليون م^{3}/السنة.

المياه الجوفية بالخزانات السفلية تستغل عموماً لأغراض الزراعةالعامة (المشاريع الزراعية والحيوانية) والشرب والصناعة. ولكن في السنوات الأخيرة تم تعميق عشرات الآبار لأغراض الزراعة الخاصة حتى أنها أصبحت تستغل جزءاً من مياه الخزانات السفلية أو تعتمد عليها بالكامل.

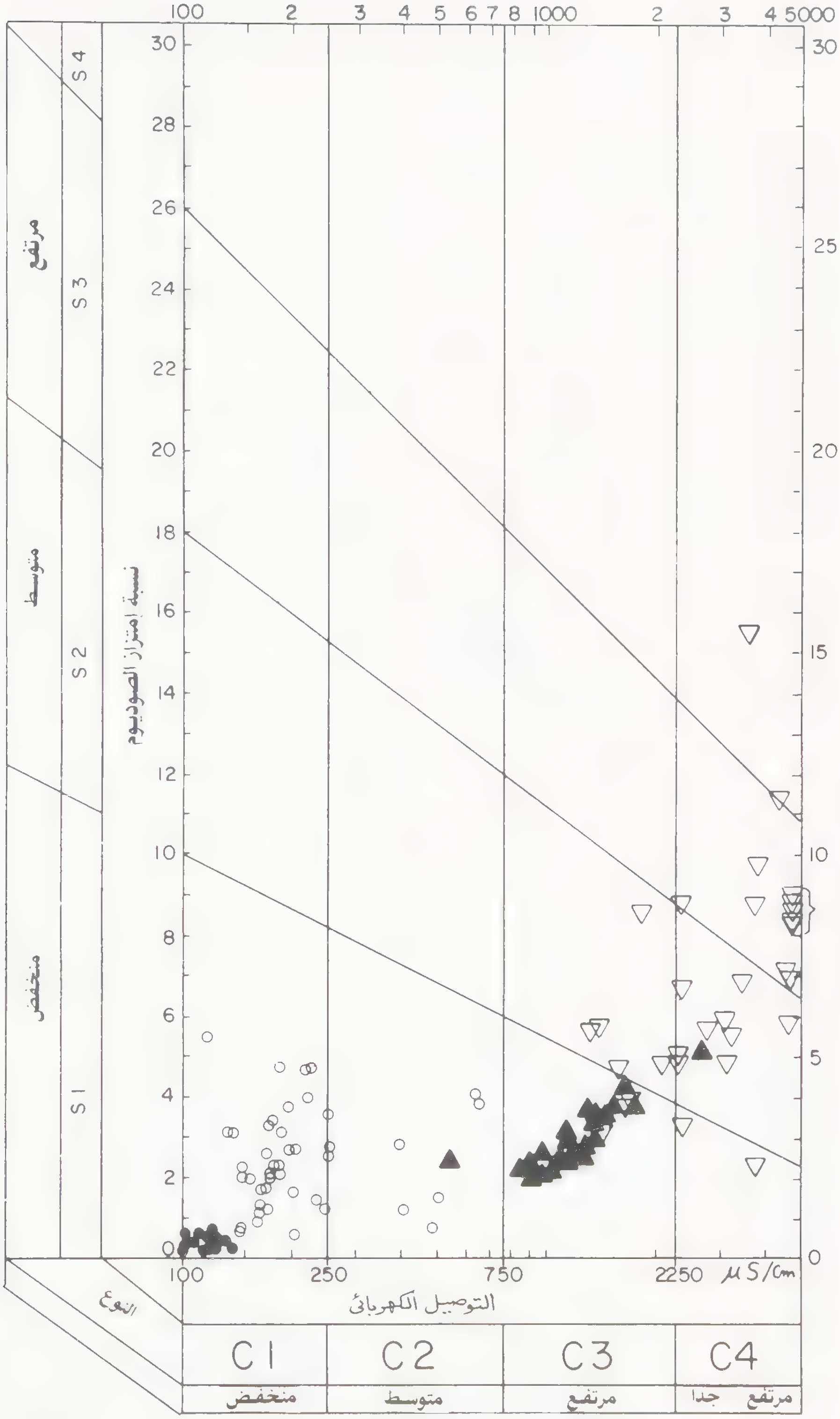

شكل (9) : صلاحية المياه الجوفية بمنطقة سبها لأغراض الزراعة حسب طريقة RICHARDS (1954). دليل الرموز موضح بشكل (8).

هذه المياه لأغراض الزراعة موضح بالشكل 9] والذي تم فيه توضيح العلاقة بينها حسب طريقة RICHARDS (1954).

المياه الجوفية لخزانات المجموعة الثانية تعتبر بدون إستثناء صالحة لأغراض الزراعة حيث أن معدل إمتزاز الصوديوم بالتربة منخفض وكذلك توصيلها الكهربائي وذلك كما يمكن إستنتاجه من الشكل (9) المشار إليه أعلاه.

أثبتت نتائج التحاليل عموماً بأنه لا توجد أية عناصر أو أيونات تزيد نسبها عن المعايير المسموح بها والتي لها تأثير سلبي على النبات والحيوان.

تأثير المياه على المعدات والأجهزة المستعملة في الأغراض الواردة أعلاه :

تدل نتائج التحاليل الكيميائية على أن المياه الجوفية بمنطقة سبها لها تأثير على المعدات والأجهزة المستعملة في أغراض الشرب والصناعة والزراعة.

فالمياه بالخزانات الجوفية العلوية تؤدي نظراً لإرتفاع نسبة الأملاح المذابة بها إلى تكوين طبقات ملحية (INCRUSTATION) بداخل الأنابيب والمواسير المستعملة خاصة بشبكات المياه لأغراض الشرب والزراعة مما يؤدي إلى سدها وعدم تمريرها للمياه، هذا بالإضافة إلى أن ثاني أكسيدالكربون الطليق النشط (العدواني) (AGGRESSIVE CO_2) يؤدي إلى تآكل الأنابيب وغيرها من المعدات الأخرى حيث أن نسبته بهذه المياه تتراوح بين 10 إلى 15 ملجم/لتر.

لقد لوحظ في العديد من الحالات بمنطقة سبها بأن أنابيب شبكات مياه الري وتعليق المضخات بالآبار تتعرض بعد فترة من الإستعمال تتراوح بين 5 إلى 10 سنوات إلى التلف. هذا راجع بالإضافة إلى عوامل أخرى كحرارة الجو والأكسجين المتواجد بالهواء إلى ما أشير إليه أعلاه.

المياه بالخزانات الجوفية للمجموعة الثانية (السفلية) عموماً تعتبر ملوحتها منخفضة جداً وبالتالي سيكون تكوين طبقات ملحية بالكيفية المشار إليها أعلاه أقل وطأةً. إلاّ أن نسبة ثاني أكسيد الكربون الطليق النشط (العدواني) التي تتراوح بين 15 إلى 30 ملجم/لتر تؤدي إلى تآكل المعدات والأجهزة حيث أن المعايير المسموح بها من أجل تفادي التآكل لا تتعدى بضع ملجم/لتر أو يكون منعدماً تماماً شكل (9).

يتراوح الأس الهيدروجيني بين 6,7 إلى 6,9 ودليل لانجلير (Langelier-Index) الناتج عن الفارق في مقدار الأس الهيدروجيني من القياس المباشر وبين الذي يمكن الوصول إليه رياضيا حسب طريقة لانجلير Langelier (1936) كما أوردها ماتيس MATHESS (1973م) بلغ في المتوسط — 1,66 إلى — 1,99. هذه النتائج تعتبر دليلاً آخر على أن هذه المياه بها خاصية التآكل وتؤدي مع الزمن إلى اتلاف المعدات والأجهزة. في العديد من الحالات لوحظ هنا أيضاً بمنطقة سبها التآكل والتلف الذي طرأ على الأنابيب خاصة المستعملة في الأغراض الزراعية بعد فترة من الإستغلال تبلغ في المتوسط 7 سنوات.

الخصائص النظيرية للمياه :

مع بداية السبعينات تم أخذ العديد من العينات من مختلف مناطق حوض مرزق لغرض دراسة الخصائص النظيرية للمياه الجوفية وقد تم نشر نتائج الدراسات في البحوث التي أعدت على وجه الخصوص من قبل KLITZSCH *et. al* (1979)، SONNTAG *et.al*. (1978).

في فترة زمنية لاحقة سنة 1981م تم أخذ مجموعة أخرى من العينات المائية وكانت منطقة سبها أحد الأماكن التي تم التركيز عليها بصفة مميزة وذلك من أجل معرفة الخواص النظيرية لمياهها الجوفية حيث أن الدراسات المشار إليها أعلاه لم تتناولها بصفة خاصة ومركزة. في جميع التحاليل النظيرية اللازمة أجريت بمعهد فيزيائية البيئة المحيطة بجامعة هيدلبرج (INSTITUTE FÜR UMWELTPHYSIK DER UNIVERSITÄT HEIDELBERG). وقد تضمنت على وجه الخصوص نسب تواجد كل من التريتيوم (^{3}H) والكربون — 14 (^{14}C) كنظائر مشعة والديوتريوم (^{2}H) والأكسجين — 18 (^{18}O) كنظائر ثابتة للمياه.

وقد أسفرت التحاليل عن الآتي :

التريتيوم (^{3}H) :

أجريت التحاليل اللازمة على أربع عشرة عينة من أجل معرفة نسبة التريتيوم بها وقد كانت موزعة بحيث أخذت (7) عينات من الخزانات العلوية و(6) عينات من الخزانات الجوفية السفلية وعينة واحدة فقط من المياه الجوفية بطبقات دهر الحياة القديمة.

أوضحت جل هذه العينات بأن نسبة التريتيوم لا تتعدى في المتوسط (0,5 وحدة من التريتيوم) وهذا المعدل يعتبر ضئيلاً جداً ومن المتبع أن لا يعتد به في حساب عمر المياه خاصة وأن نسباً كهذه ربما قد تسربت إلى المياه من الهواء الجوي أثناء تعبئة العينة أو أثناء فترة النقل والتحليل.

الكربون — 14 (^{14}C) :

من أجل تحديد نسبة الكربون — 14 بالمياه أخذت أربعة عينات فقط بحيث كانت واحدة من أحد الآبار بالخزانات العلوية واثنتان من بئرين بالخزانات السفلية بدهر الحياة المتوسطة وواحدة من بئر بالخزانات بدهر الحياة القديمة. أثبتت نتائج التحاليل وجود اختلاف نسب كربون — 14 بالمياه الجوفية بالمنطقة حيث كانت العينة الأولى المشار إليها أعلاه 77 + 0,7 ٪ مدرن (Modern). ويشير ذلك إلى أن

800 ملجم/لتر) وبالإمكان إستعمالها إن دعت الضرورة كمياه شرب. أما مياه خزانات المجموعة الثانية (السفلية) تعتبر صالحة للشرب حيث أن نسبة الأملاح المذابة بها منخفضة جداً (جدول 4). ولا توجد أيونات أو مركبات كيميائية تتعدى نسبتها المعايير المسموح بها.

صلاحيتها للصناعة:

نظراً لأن شروط ومتطلبات إستعمال المياه لأغراض الصناعة تختلف من حالة إلى أخرى وذلك حسب نوعية الصناعة والغرض منها فإن المياه الجوفية بمنطقة سبها تعتبر عموما صالحة لأغراض الصناعة.

صلاحيتها للزراعة:

مياه خزانات المجموعة الأولى توصف عموماً بأنها غير صالحة للإستعمال في الأغراض الزراعية إلاّ تحت ظروف ومعطيات محدودة جداً. وذلك نظراً لإرتفاع نسبة الأملاح المذابة بها وتوصيلها الكهربائي (جدول 1) هذا بالإضافة إلى إرتفاع نسبة الصوديوم التي تبلغ بالمناطق الشمالية والشمالية الغربية في المتوسط 524,0 ملجم/لتر وفي المناطق الجنوبية 124,0 ملجم/لتر.

التوصيل الكهربائي [وبالتالي نسبة الأملاح المذابة ومعدل إمتزاز الصوديوم بالتربة (Sodium Absorption Ratio) ومدى صلاحية

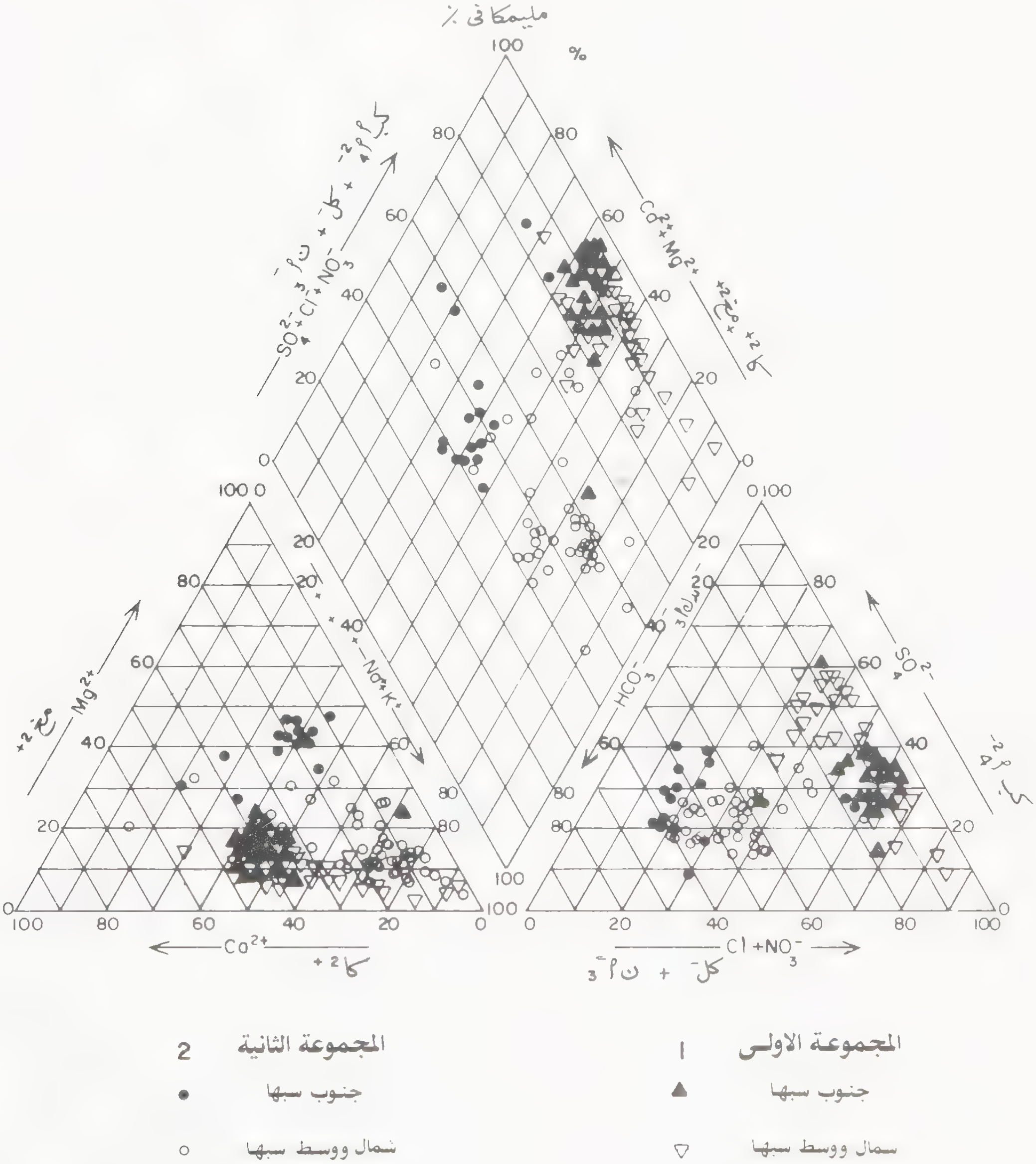

شكل (8): توزيع النسب المكافئة للكاتيونات والأنيونات بالمياه الجوفية بخزانات دهر الحياة الأوسط، حسب طريقة PIPER (1944).

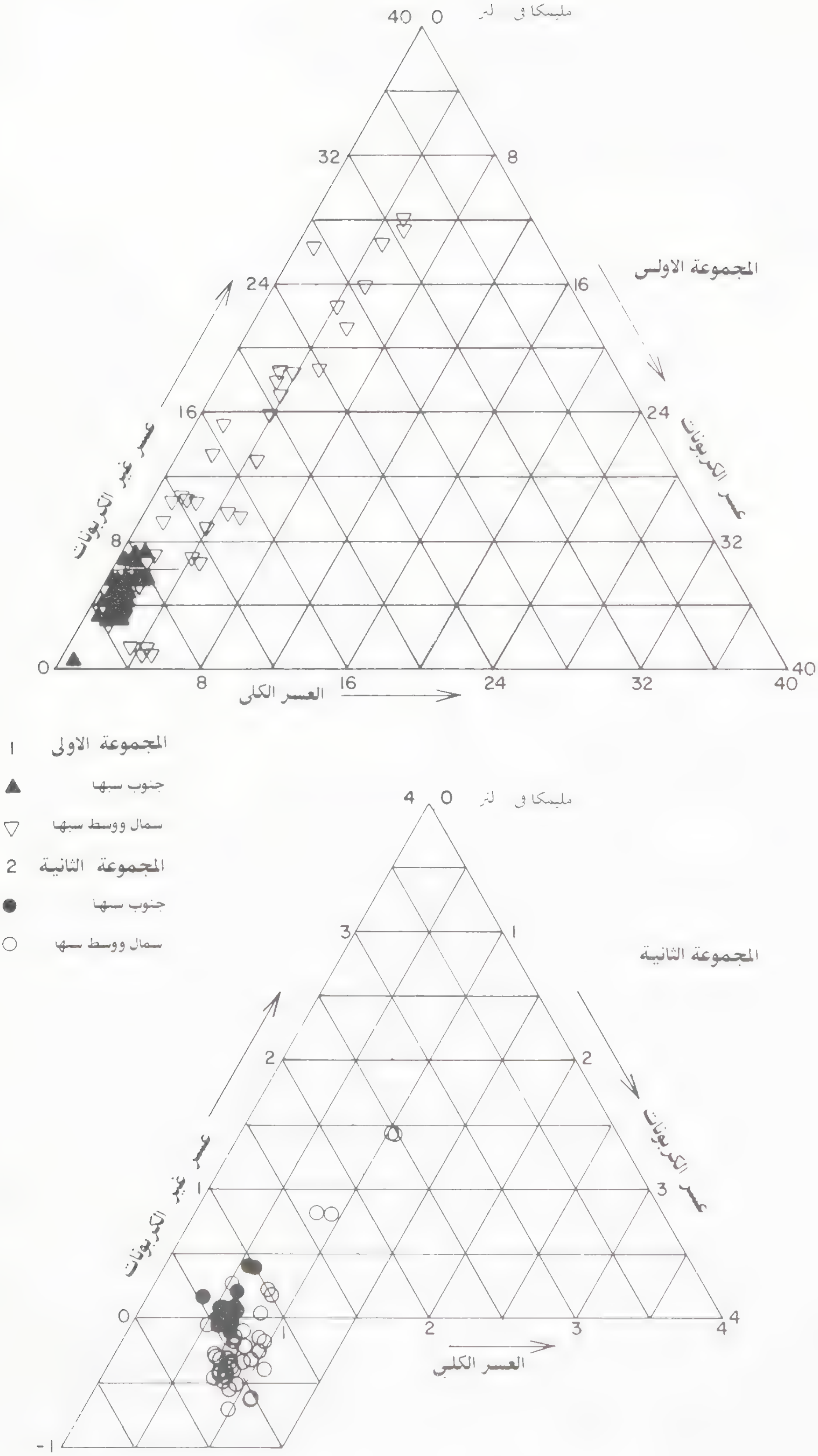

شكل (7) : الإختلافات في عسر المياه الجوفية بطبقات دهر الحياة الأوسط حسب طريقة SCHWILLE (1957).

بناء على نتائج التحاليل ، توصف هذه المياه عموما بأنها عسرة إلى عسرة جداً . من خلال جدول (2) وشكل (6) و(8) يتضح أن مياه هذه الخزانات تتميز عموماً في جميع أجزاء منطقة سبها بايونات الصوديوم والكالسيوم (الكاتيونات) وأيونات الكلوريد والسلفات (بالأنيونات) . هذا يدل على أن مصادر ارتفاع وازدياد الأملاح بها تعتبر متشابهة إن لم تكن واحدة .

جدول (2) : متوسط مقادير الأيونات المذابة ونسبها المئوية بمياه الخزانات الجوفية العلوية (المجموعة الأولى) .

	الأنيونات				الكاتيونات				
	كب أ$_4^{2-}$	بدك أ$_3$	ن أ$_3^-$	كل$^-$	مغ$^{2+}$	كا$^{2+}$	بو$^+$	ص$^+$	
أ	197	67	31,0	243,0	20,7	96,2	14,5	124,1	ملجم/لتر
	4,1	1,1	0,5	6,6	1,7	4,8	0,4	5,4	ملمكافيء/لتر
	3,3	9,0	4,0	54,0	14,0	39,0	3,0	44,0	ملمكافيء ٪
ب	778	384	12,4	716,3	47,4	256,0	105,5	524,0	ملجم/لتر
	16,2	6,3	0,2	20,2	3,9	12,8	2,7	22,8	ملمكافيء/لتر
	38,0	15,0	0,5	47,0	9,0	31,0	6,0	54,0	ملمكافيء ٪
	SO_4^{-2}	HCO_3^-	NO_3^-	Cl^-	Mg^{+2}	Ca^{+2}	K^+	Na^+	

أ — الأجزاء الجنوبية لمنطقة سبها .

ب — الأجزاء الشمالية والوسطى لمنطقة سبها .

مياه الخزانات الجوفية السفلية . (المجموعة الثانية) :

أخذت غالبية العينات المائية التي أجريت عليها تحاليل كيميائية وتمت دراستها (70 عينية) من الآبار المستغلة لمياه هذه الخزانات . وأسفرت نتائج التحاليل عموماً بأنها مياه عذبة . وهذا يتناسب مع ما قدتم إستنتاجه من دراسة الجسات الجيوفيزيائية ومن خلال التجربة . متوسط المجموع الكلي للأملاح المذابة بهذه المياه وبعد الخصائص الأخرى الهامة مبينة بالجدول (3) ، وشكل (6) .

جدول (3) : متوسط المجموع الكلي للأملاح المذابة وبعض الخصائص الأخرى الهامة للمياه الجوفية لمجموعة الخزانات السفلية .

	المجموع الكلي للأملاح ملجم/لتر	التوصيل الكهربائي ميكروسيمنس/سم	العسر الكلي CaCo$_3$1 – ملجم/لتر كا ك أ^3	الأس الهيدروجيني
أ	82	115	34	6,8
ب	180	250	32	6,9

أ — المياه بالأجزاء الجنوبية لمنطقة سبها .

ب — المياه بالأجزاء الشمالية والوسطى لمنطقة سبها .

في هذه المياه نلاحظ أيضاً إزدياد في التوصيل الكهربائي وفي الأملاح المذابة في اتجاه الغرب التي تصل في المنطقة جنوب سبها إلى 130 ملجم/لتر وبالمناطق الشمالية الغربية إلى 500 ملجم/لتر . العسر الكلي لهذه المياه يعتبر منخفض جداً وتوصف بأنها لينة جداً . من خلال العديد من العينات إتضح أن العسر الناتج عن الكربونات (عسر الكربونات) يضاهي بل يتعدى في حالات عديدة العسر الكلي وبالتالي يصبح عسر غير الكربونات سالباً كما هو مبين بالشكل (7) .

إلى جانب الخصائص المشار إليها أعلاه فإن الأيونات المميزة لهذه المياه تتمثل في المغنيسيوم – والكالسيوم بالكاتيونات والبيكربونات والسلفات بالأنيونات بالأجزاء الجنوبية لمدينة سبها . أما المناطق الشمالية والوسطى لمدينة سبها فتكون الأولوية لأيونات الصوديوم بالكاتيونات والبيكربونات والكلوريد والكبريتات بالأنيونات جدول (4) شكل (6) و(8) .

جدول (4) : متوسط مقادير الأيونات المذابة ونسبها المئوية بمياه الخزانات الجوفية السفلية (المجموعة الثانية) .

	الأنيونات				الكاتيونات				
	كب أ$_4^{2-}$	بدك أ$_3^-$	ن أ$_3^-$	كل$^-$	مغ$^{2+}$	كا$^{2+}$	بو$^+$	ص$^+$	
أ	15,4	35,4	4,3	7,4	5,4	7,4	3,4	4,4	ملجم/لتر
	0,32	0,58	0,07	0,31	0,44	0,37	0,09	0,2	ملمكافيء/لتر
	27,0	49,0	6,0	18,0	40,0	34,0	8,0	18,0	ملمكافيء ٪
ب	24,0	52,4	2,5	49,0	4,0	7,4	11,5	26,8	ملجم/لتر
	0,5	0,85	0,04	0,80	0,32	0,37	2,3	1,2	ملمكافيء/لتر
	32,0	40,0	1,8	36,0	15,0	17,0	14,0	55,0	ملمكافيء ٪
	SO_4^{-2}	HCO_3^-	NO_3^-	Cl^-	Mg^{+2}	Ca^{+2}	K^+	Na^+	

أ — الأجزاء الجنوبية لمنطقة سبها .

ب — الأجزاء الشمالية والوسطى لمنطقة سبها .

صلاحية المياه لاستعمالها في الأغراض العامة :

من خلال نتائج التحاليل الكيميائية يتضح أن المياه الجوفية بمنطقة سبها يمكن إعتبارها مقبولة إلى صالحة للإستعمال في الأغراض العامة كالشرب والصناعة والزراعة .

صلاحيتها للشرب :

مياه خزانات المجموعة الأولى (العلوية) : خاصة بالمناطق الشمالية والشمالية الغربية تعتبر غير صالحة للشرب نظراً لإرتفاع نسبة الأملاح المذابة بها (في المتوسط 2800 ملجم/لتر) وفي بعض الحالات التي تصل فيها الملوحة إلى أكثر من 5000 ملجم/لتر تعتبر غير مستصاغة تماماً وليس بالإمكان تناولها كمياه شرب . هذا بالإضافة إلى أن نسبة الكلوريد (716,0 ملجم/لتر) والكبريتات (778,0 ملجم/لتر) بها تتعدى المعايير العالمية المقترحة من منظمة الصحة العالمية سنة 1971 م . WORLD HEALTH ORGANIZATION (1971) في RICHTER AND LILLICH (1975) .

بالمناطق الجنوبية تعتبر مياه هذه الخزانات أقل ملوحة (في المتوسط

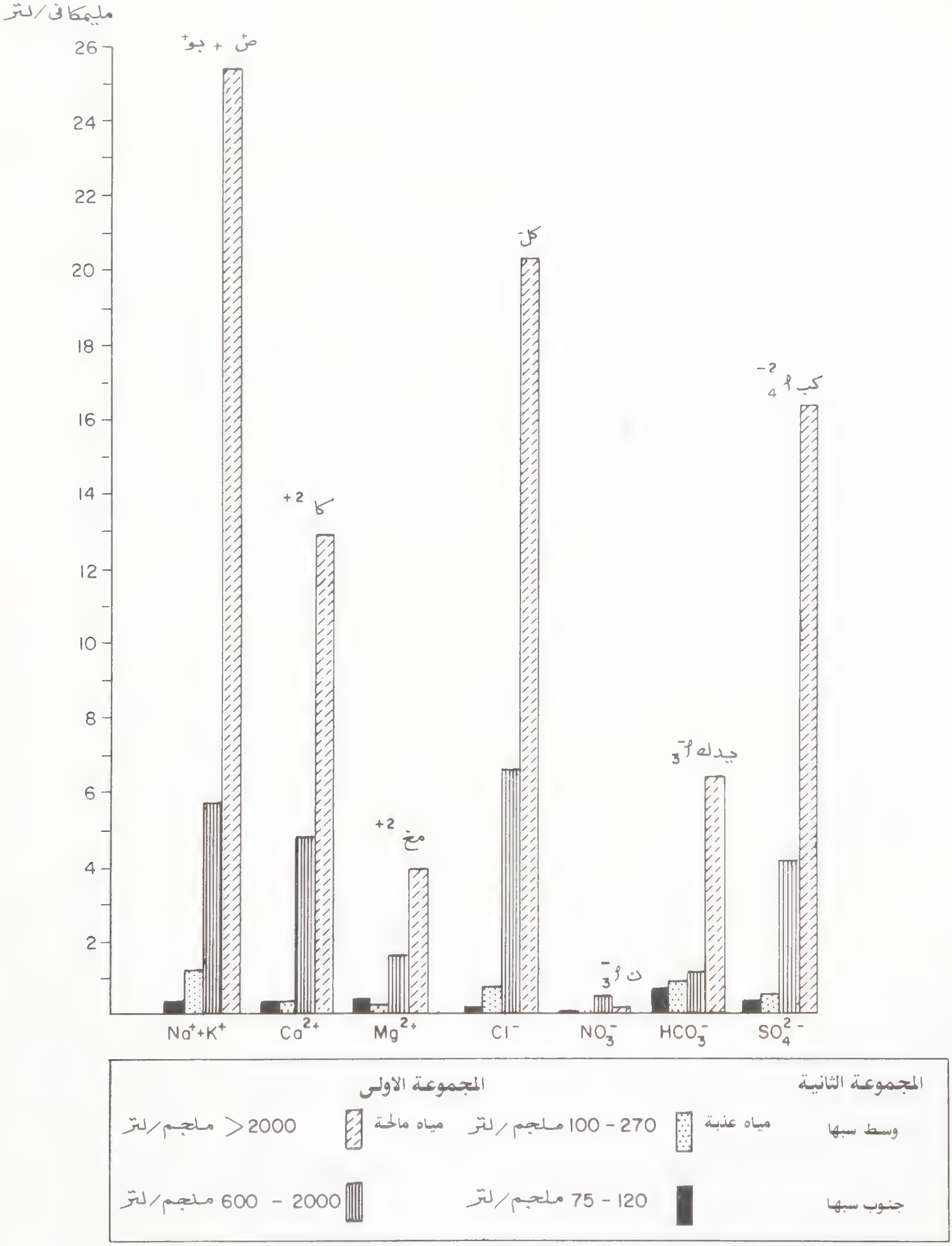

شكل (6) : مقادير الكاتيونات والأنيونات بالمياه الجوفية بطبقات دهر الحياة الأوسط.

رقم س/س 80/246/101 يتبعها عل بعد 50 مترابئر المراقبة رقم س/س/81/444/271 بمشروع الأبقار بالجزء الشمالي الشرقي لمدينة سبها. وتعتبر هذه أول تجربة ضخ متكاملة لمياه الخزانات السفلية بالمنطقة. أمكن عن طريقها دراسة معامل الانتقالية ومعامل التخزين في آن واحد.

أمكن دراسة معامل الإنتقالية علىوجه العموم عن طريق الآبار العديدة الأخرى التي صممت بالخزانات المشار إليهاأعلاه في وسط وأطراف مدينة سبها المختلفة في الفترة منذ 1976م وحتى هذا التاريخ.

نتائج تجربة الضخ بالبئر الإنتاجي رقم س/س 80/246/101 وبئر المراقبة رقم س/س 81/444/271 حسب الطرق المشار إليها فيما سبق أثبتت في المتوسط الآتي:

معامل الإنتقالية: $0{,}63 \times 10^{2}$ م^2/ثانية
معامل التخزين: $4.2 \cdot 10^{4}$

معامل الإنتقالية من نتائج بعض الآبار (22 بئراً) الأخرى المتواجدة في وسط وأطراف مدينة سبها الشمالية بلغ في المتوسط $0{,}72 \times 10^{-2}$ م^2/الثانية.

وبلغ متوسط معامل الانتقالية بالأطراف الجنوبية حسب النتائج التي تمت دراستها (20 بئراً) $1{,}7 \times 10^{-2}$/الثانية. أما معامل التخزين فلم يكن بالإمكان إستنتاجه بطريقة سليمة وذلك لعدم وجود تجربة مكتملة شملت بئراً إنتاجية ضخت مياهها وبئر مراقبة أجريت عليه القياسات. حسب ما ورد في LOHMANN (1972) و LANGGUTH and VOIGT (1980م) والذي أشار إلى امكانية الوصول إلى عدد تقريبي لمعامل الإنتقالية في حالات كهذه وذلك بضرب متوسط سمك الطبقات الحاملة للمياه المستغلة بالعدد $3{,}3 \times 10^{6}$ إستناداً على هذا يمكن تقدير معامل التخزين لمجموعة الخزانات السفلية التي يبلغ سمكها بالأجزاء الجنوبية لمدينة سبها في المتوسط 35 متراً بما يقارب على $8{,}2 \times 10^{-4}$.

هذا العدد التقريبي لا يختلف كثيراً عن معامل التخزين الذي تم الوصول اليه عن طريق تجربة الضخ التي أجريت على الخزانات المشار اليها أعلاه بالجزء الشمالي الشرقي لمدينة سبها خاصة حسب طريقة CHOW (1952م). حيث كان مقداره $5{,}6 \times 10^{-4}$.

من خلال متوسط مجمل الأعداد الواردة أعلاه نلاحظ أن معامل الإنتقالية لمجموعة الخزانات الجوفية المائية السفلية بمنطقة سبها يبلغ في المتوسط $1{,}016 \times 10^{2}$ م^2/ثانية. ومعامل التخزين يمكن تقديره بحوالي $4{,}2 \times 10^{4}$.

تدل نتائج تجارب الضخ التي أجريت على جميع الخزانات الجوفية (المجموعة العلوية والمجموعة السفلية) على أنه لا توجد فوارق تذكر بينها في الخصائص الهيدروليكية.

لقد سبق وان إتضح أيضاً من خلال دراسة المسامية الكلية بأنها تكاد تكون متشابهة في الحالتين.

التحاليل الكيميائية للمياه:

من أجل التعرف على نوعية المياه ودراسة مدى صلاحيتها للشرب والصناعة والزراعة أخذت عينات من جميع الآبار التي نفذت للأغراض العامة والعديد من آبار الأغراض الزراعية الخاصة. هذه العينات تم تحليلها في الغالب بالمختبر المركزي للمياه ببلدية سبها. من أجل المقارنة ودراسة إحتمال حدوث تغييرات في نوعية المياه وذلك بعد فترة من إستغلال بعض الآبار، تم في سنة 1981م أخذ مجموعة أخرى من العينات (30 عينة) أجريت عليها التحاليل اللازمة بمعهد الجيولوجيا بجامعة توبنجن وأسفرت نتائج التحاليل الكيميائية عموماً عن الآتي:

مياه الخزانات الجوفية العلوية (المجموعة الأولى):

لقد إتضح من خلال التجربة والدراسات الجيوفيزيائية التي أجريت على هذه الخزانات بأن مياهها مالحة أو زائدة الملوحة. هذه النتيجة المبدئية عززتها التحاليل المعملية.

متوسط بعض نتائج التحاليل موضحة في الجدول (1) وشكل (6).

جدول (1): متوسط المجموع الكلي للأملاح المذابة وبعض الخصائص الأخرى لمياه الجوفية لمجموعة الخزانات العلوية.

	الأملاح المذابة ملجم/لتر	التوصيل الكهربائي ميكروسيمنس سم$^{-1}$	العسر الكلي CaCO3/1 ملجم لتر كاك أ$_3$	الأس الهيدروجيني
أ	800	1250	303,0	6,7
ب	2800	5500	790,0	7,5

أ المياه بالأجزاء الجنوبية لمنطقة سبها

ب المياه بالأجزاء الشمالية والوسطى لمنطقة سبها.

ومن الملاحظ أن المجموع الكلي للأملاح المذابة والتوصيل الكهربائي لهذه المياه يتزايدان على وجه الخصوص بمنطقة سبها بالإتجاه إلى الغرب والشمال والشمال الغربي حتى أنها يصلان إلى الضعف أو أكثر. فالأملاح المذابة بهذه المياه على سبيل المثال بمشروع حمزة غربي مشروع سبها الزراعي شكل (3) و(4) تصل الى أكثر من 2000 ملجم/لتر وبالطرف الشمالي الغربي للمدينة قد تبلغ 5000 ملجم/لتر أو أكثر كما نلاحظ أيضاً إختلافاً بسيطاً في الأس الهيدروجيني. يرتفع العسر الكلي كذلك في المناطق الشمالية والشمالية الغربية عنه في المناطق الجنوبية ويتكون في الأساس من عسر غير الكربونات (NCH) الذي يبلغ في المتوسط 80٪ في حين عسر الكربونات يساوي 20٪ فقط من العسر الكلي. شكل (7).

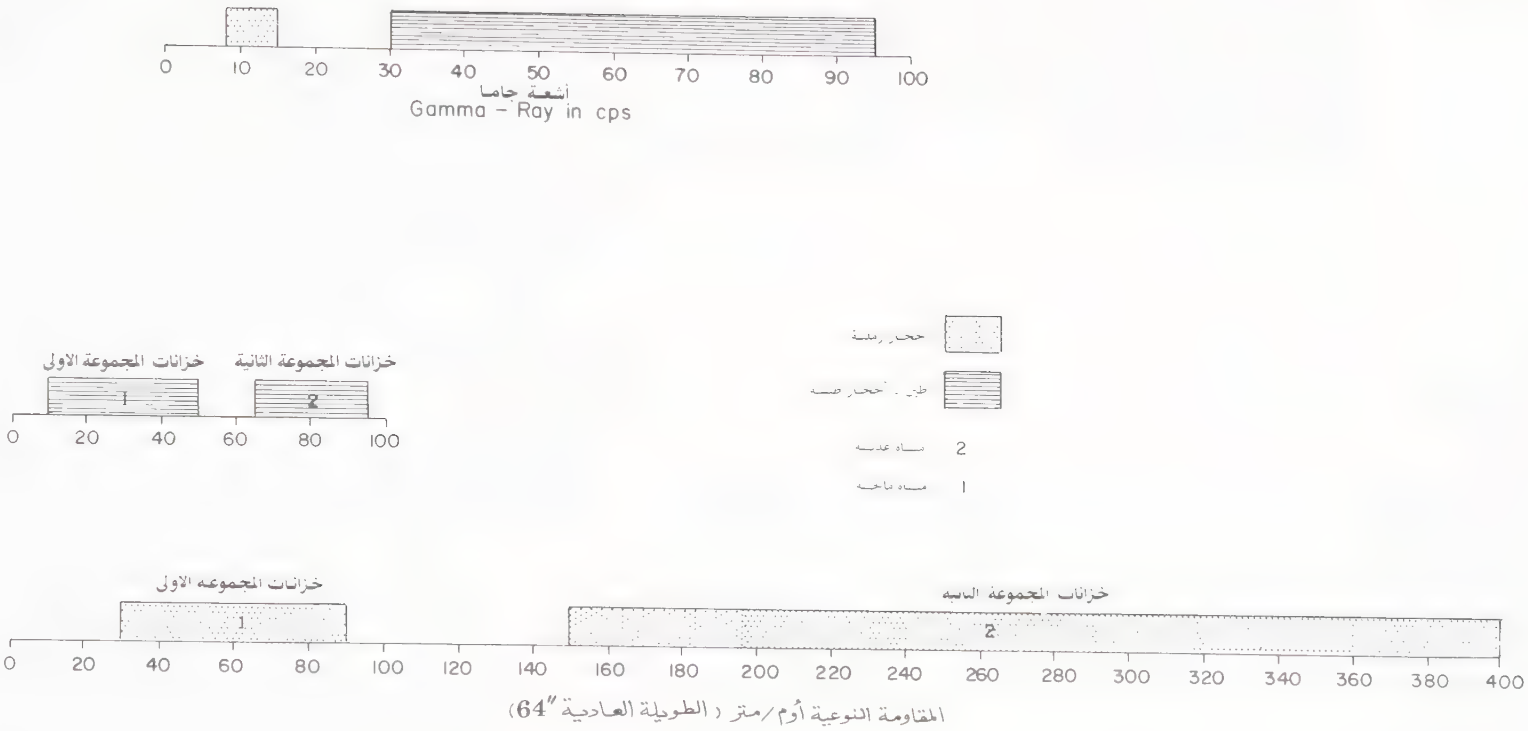

شكل (5) : الإختلاف في مقادير اشعة جاما والمقاومة النوعية ("64) بالخزانات الجوفية العلوية (مياه مالحة) والخزانات الجوفية السفلية (مياه عذبة) بدهر الحياة الأوسط .

الرملية التي تقع على عمق بين 117 إلى 118م بالطبقات السفلية تبلغ مساميتها الكلية 30٪ تقريباً والتي تقع على عمق 65 إلى 66 متراً بالطبقات العلوية تبلغ مساميتها 33٪ تقريباً.

رغم أن هذه الأعداد للمسامية تعتبر ناتجة عن قياسات محدودة جداً حيث أن سمك العينة الواحدة التي أجريت عليها الدراسة لا يتعدى 10سم. إلاّ أنها ربما تساعد على الوصول إلى نتائج أفضل للمسامية الكلية حيث أن القياسات أجريت مباشرة على عينات صخرية. بالمقارنة بين النتائج التي تم الحصول عليها عن طريق المعمل وتلك التي عن طريق المقاومة النوعية يتضح وجود فروق بسيطة في الحالتين بين الأحجار الرملية العلوية والسفلية.

ولم تتاح الفرصة لاستنتاج المسامية الفعلية التي بالإمكان إستخلاص مياهها في حالة إستغلال الخزان الجوفي المائي معملياً بدقة. حيث أن العينتين اللتين أجريت عليها التجارب المسامية الكلية لم تكونا في حالة جيدة تسمح بإجراء دراسات دقيقة للمسامية الفعلية. وحسب ما تم التوصل إليه وبالمقارنة بأحجار رملية ذات خواص ومميزات مشابهة للحين الترياسي بألمانيا الغربية (RAMBOW, 1969م MATHESS AND DÜRBAUM في HOLING 1980م)، فمن المتوقع أن تكون مقادير المسامية الفعلية للأحجار الرملية بمنطقة سبها تتراوح بين 8٪ إلى 10٪. من خلال عينات ناتج الحفر والجسات الجيوفيزيائية التي تمت دراستها في الفقرات أعلاه يتضح أنه بالإمكان وضع تصور مبدئي لوضعية الخزانات الجوفية المائية بدهر الحياة الأوسط. هذا التصور يتلخص أولاً في أن المياه الجوفية الصالحة للإستغلال تتواجد في طبقات عديدة لأحجار رملية تصل إلى خمسة عشر طبقة تقريباً في بئر عمقه 200 متر. هذه تتخللها تكوينات طينية غرينية يزداد سمكها عادة بوضوح عند عمق 40 إلى 70 متراً حيث يكون في المتوسط 35 متراً، هذه الطبقات تكون فاصل يؤدي إلى تقسيم رسوبيات الأحيان الوسطى حتى أعماق الآبار المشار اليها فيما سبق إلى مجموعتين: مجموعة سفلية ومجموعة علوية.

هاتان المجموعتان يتكون كل منها من العديد من طبقات لأحجار رملية وطينية وغرينية. كما يتضح أن المجموعة السفلية لهذه الطبقات تحتوي على مياه عذبة والمجموعة العلوية على مياه ذات ملوحة عالية. هذا بالإضافة إلى وجود فروق بسيطة في صلادة وتماسك ومسامية الأحجار الرملية.

هذه الأحجار الرملية التي تمثل خزانات جوفية مائية يمكن تقسيمها إستناداً على ما أشير إليه أعلاه إلى مجموعتين أساسيتين هما: مجموعة الخزانات الجوفية المائية الأولى (العلوية) ومجموعة الخزانات الجوفية المائية الثانية (السفلية). أنظر شكل (2، 4، 5).

تجارب الضخ:

الآبار التي تم تنفيذها وأجريت عليها تجارب ضخ بمنطقة سبها كانت تلك التي حفرتها شركة ريجوا (REGWA) وذلك ضمن برنامج دراسة للمياه والتربة لحوض مرزق سنة 1972م إلى 1974م. ومنذ هذا التاريخ فصاعداً تم إجراء تجارب ضخ على جميع الآبار التي نفذت بمنطقة سبها وذلك لغرض إستغلال مياهها للمصلحة العامة. هذه الآبار كانت حتى سنة 1976م لا تتعدى أعماقها بمدينة سبها 100 متر تقريباً. جل تجارب الضخ التي أجريت على الآبار التي نفّذت في الفترة من 1972م إلى 1976م والتي درست في هذا البحث استهدفت المياه الجوفية بالخزانات العلوية لطبقات الأحيان الوسطى.

ومع نهاية 1976م تم التركيز على حفر آبار أعمق لأغراض إستغلال مياهها للمصلحة العامة هذه الآبار التي اخترقت الطبقات السفلية للأحيان الوسطى حتى عمق 200 متر تقريباً كانت ذات نتائج إيجابية حيث أنها أسفرت عن مياه عذبة بكميات وفيرة.

بما أن أغلب الآبار التي حفرت لأغراض المصلحة العامة تم تنفيذها منذ سنة 1976م وحتى هذا التاريخ تعتمد على إستغلال مياه مجموعة الخزانات السفلية فإن أغلب تجارب الضخ التي درست في هذا البحث أجريت على هذه الخزانات.

المعاملات الهيدروليكية لخزانات المجموعة العلوية (الأولى):

عن طريق تجارب الضخّ أمكن أساساً دراسة معامل الانتقالية (Transmissivity) ومعامل التخزين، (Storage Coefficient).

من أجل المقارنة والوصول إلى نتائج تم حسابها بطريق كل من COOPER AND JACOB (1946م) وCHOW (1952م) وTHEIS (1935م).

نفذت أهم التجارب المتكاملة التي تناولها هذا البحث بمشروع سبها الزراعي (جنوب سبها) وبمشروع الأغنام شمال شرقي سبها وذلك في سنة 1972م. حيث تم بالموقعين عن طريق شركة ريجوا تنفيذ حفر بئر اختباري إنتاجي بكل موقع ضخت مياهه يتبعه على بعد 42 متر بئر للمراقبة. من خلال دراسة نتائج القياسات التي أجريت على هذه الآبار إضافة إلى نتائج التجارب التي أجريت على أكثر من عشرين بئراً أخرى إتضح تقارب مقادير الخصائص الهيدروليكية لهذه الخزانات وذلك بالمواقع المختلفة وحسب الطرق المختلفة المشار إليها أعلاه. حيث كان متوسط هذه المعاملات بمنطقة سبها على النحو التالي:

معامل الإنتقالية: $1,2 \times 10^{2}$ متر^{2}/الثانية.
معامل التخزين: 2.0×10^{4}

المعاملات الهيدروليكية لخزانات المجموعة السفلية (الثانية):

حيث أن أغلب الآبار التي نفذت من أجل سد إحتياجات المنطقة من الماء صممت على أساس إستغلال مياه الخزانات الجوفية السفلية فقد أتيحت الفرصة لدراستها وذلك عن طريق نتائج تجارب الضخ العديدة التي أجريت على هذه الآبار.

وأهم هذه التجارب أجريت سنة 1981م بعد تنفيذ البئر الانتاجية

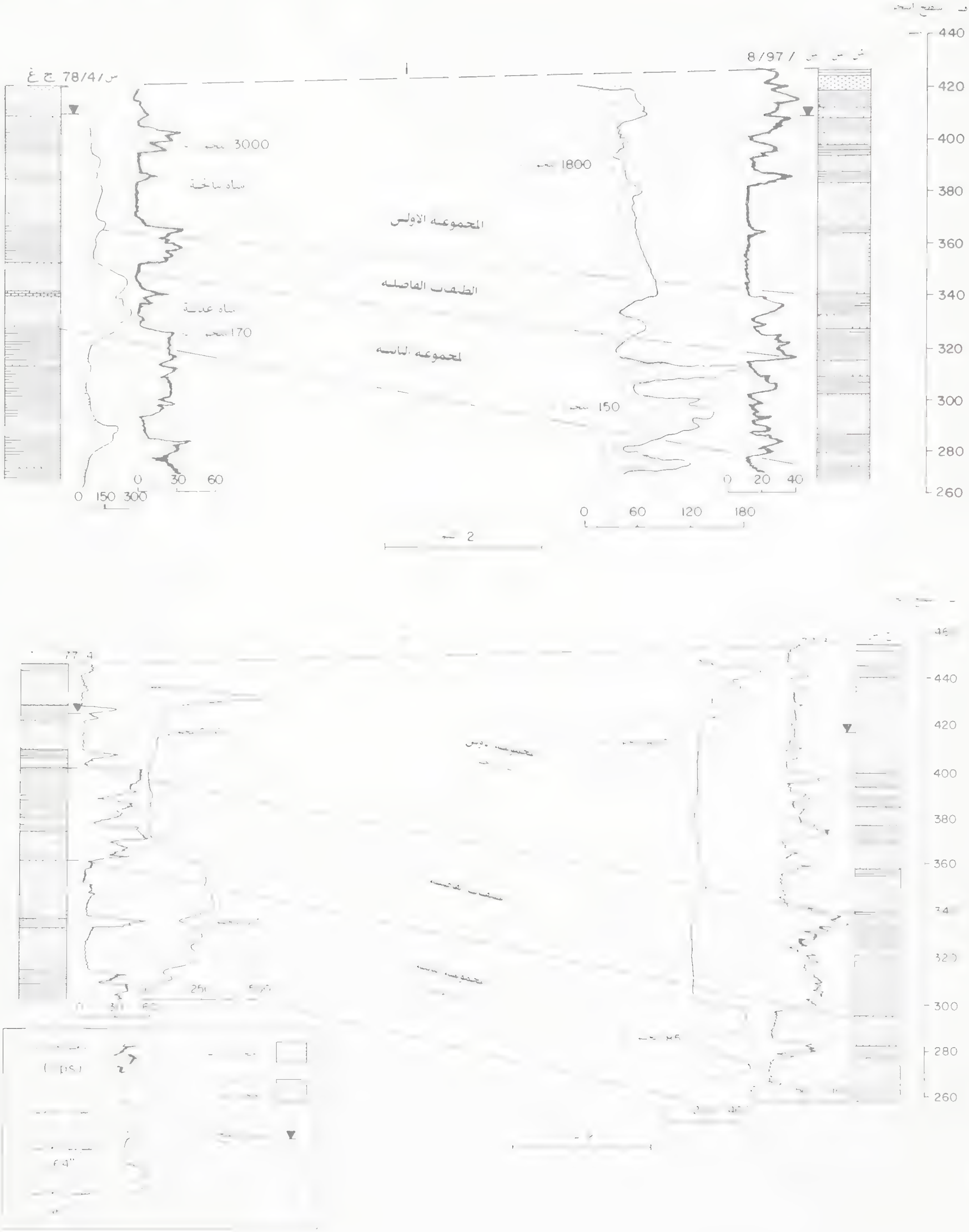

شكل (4) : العلاقة بين الطبقات والخزانات الجوفية المائية المتشابهة بدهر الحياة الأوسط بمنطقة سبها وذلك حسب نتائج الدراسات الجيوفيزيائية من حيث سمكها وعمقها وارتفاع نسبة الأملاح المذابة بالخزانات الجوفية العلوية عنها بالخزانات السفلية.

حتى حطية رامي) وبالمنطقة ما بين حجارة وبلدة تمنهنت بالطرف الشمالي لمدينة سبها. هذه الأشجار التي إستغلت المياه الجوفية مباشرة أصبحت الآن إن لم يتم ريها عرضة للجفاف.

نظراً للتطور الزراعي والعمراني الذي عم المنطقة في السنين الأخيرة أصبح من الضروري حفر آبار عميقة تتناسب ومستوى سطح الماء المنخفض باستمرار وتتمشى مع إحتياجات المنطقة المائية. لهذا السبب تم مؤخراً حفر مئات الآبار الحديثة بمدينة سبها والمناطق المحيطة بها وذلك كما هو عليه الحال في جميع أنحاء حوض مرزق. جل هذه الآبار تستغل مياه الخزانات الجوفية المائية لطبقات دهر الحياة الوسطى (شكل 3).

وتعتمد هذه الدراسة أساساً على نتائج حفر قرابة المئة بئر التي تنفذ لغرض المصلحة العامة كالتي حفرت بالمشاريع الزراعية والحيوانية ولأغراض الشرب والصناعة حيث أنها الوحيدة التي يمكن الإعتماد على نتائج حفرها وذلك لأنها نفذت بطريقة حديثة سليمة. شكل (3).

أما الآبار التي حفرت لأغراض الزراعة الخاصة والتي يزيد عددها على 2800 بئر والتي تمثل الجزء الأكبر فلا توجد عنها أيةَ معلومات يمكن الإستفادة منها في هذه الدراسة إلاّ في حالات نادرة جداً. حيث أنها لم يراعي في تنفيذها العديد من الجوانب والمتطلبات العامة أثناء عمليات تنفيذ حفرها وتصاميمها هذا بالإضافة إلى أنها لم توثق عنها بيانات تذكر.

وفيما يلي سيتم التطرق إلى نتائج الحفر التي تم إستخلاصها من الآبار التي نفذت للأغراض العامة كما أشير إليه أعلاه وما تم التوصل إليه من خلال هذه الدراسة وذلك من أجل تفهم وضعية المياه الجوفية بسبها بصورة واضحة.

النتائج والمعلومات التي درست تتمثل في عينات ناتج الحفر والجسات الجيوفيزيائية وتجارب الضخ، هذا بالإضافة إلى التحاليل الكيميائية المائية وبعض التحاليل الخاصة لعدد من العينات من آبار مختلفة وذلك من أجل التعرف على التركيب النظائري isotopic للمياه.

عينات ناتج الحفر والتصوير الجيوفيزيائي:

لقد ساعدت عينات ناتج الحفر التي أخذت أثناء تنفيذ عمليات الحفر كل متر أو مترين على وضع تصور واضح للتتابعات الطبقية للأحيان الوسطى وذلك حتى عمق يتراوح عادة بين 100م بالطرف الشمالي – و150م في الطرف الجنوبي للمدينة وذلك حتى العمق النهائي للطبقات الحاملة لمياه صالحة للإستغلال.

شملت الجسات الجيوفيزيائية التي أجريت على جميع الآبار المعتمد عليها في هذا البحث المقاومة النوعية (64" و16") (16" و RES 64") وأشعة جاما (GR) والجهد الذاتي (SP) والنيترون (NL) بالإضافة إلى درجة الحرارة وقياس إتساع ثقب الحفر (caliper).

تعتبر هذه القياسات ذات أهمية كبيرة حيث أنها ساعدت على دراسة جزء من الخواص الصخرية والهيدروليكية والهيدروكيميائية للتتابعات الطبقية للأحيان الوسطى والمياه المتواجدة بها.

من خلال عينات ناتج الحفر أمكن التعرف على أن التكوينات الجيولوجية لدهر الحياة الأوسط بمدينة سبها تتكون في مجملها من تبادلات طبقية لأحجار رملية وطينية وغرينية ذات ألوان مختلفة كالفاتح والبني والبنفسجي والرمادي الفاتح.

الأحجار الرملية تكون عادة هشّة إلاّ في حالات نادرة توجد مستويات تكون فيها الأحجار الرملية صلدة جداً.

الأحجار الطينية والغرينية ليست لها مميزات هامة تذكر إلاّ أنها تكون عادة لينة مما يتطلب العناية بسائل الحفر لكي لا يحدث تجوف أو إنهيار في ثقب الحفر كما كان عليه الحال في عدد من الآبار.

ويتضح من خلال جسات المقاومة النوعية (64" و16") أن طبقات الأحجار الرملية التي تقع على أعماق بين 70 إلى 200 متر تقل إتجاه الشمال وتزداد إتجاه الجنوب والشرق، ذات مقاومة تتراوح بين 150 إلى 400 أوم/متر شكل (4، 5).

تزداد الأحجار الرملية التي تتواجد على عمق من 10 إلى 70 متراً تقريباً، سمكاً أيضاً بعض الشيء إتجاه الجنوب والشرق وتقرب من السطح إتجاه الشمال والغرب. تتراوح مقاومتها النوعية بين 30 إلى 90 أوم/متر شكل (4، 5). يرجع الإختلاف في المقاومة النوعية إلى احتواء الأحجار الرملية السفلية (عمق 70 إلى 200 متر) على مياه عذبة وإلى إحتواء الأحجار الرملية العلوية (10 إلى 70 متر) على مياه مالحة أو زائدة الملوحة هذا بالإضافة إلى أنها تعتبر أقل تماسكاً وصلادة من الأحجار الرملية التي في أسفلها.

وتتراوح المقاومة بالطبقات السفلية التي تحتوي على مياه عذبة بالأحجار الطينية الغرينية بين 65 إلى 90 أوم/متر أما الطبقات العلوية التي تحتوي على مياه مالحة فقد اتضح أن مقاومتها تقع بين 10 إلى 45 أوم/متر. شكل (4، 5).

وقد أمكن عن طريق أشعة جاما بالإضافة إلى عينات ناتج الحفر تمييز الطبقات الطينية والغرينية من الأحجار الرملية. حيث أن تردداتها تتراوح عادة بالأحجار الرملية بين 8 إلى 15 تردداً/ثانية (cps) وبالأحجار الغرينية والطينية بين 30 إلى 95تردداً/ثانية، شكل (5).

كما إتضح أيضاً بأنه توجد طبقات طينية وغرينية بسمك من 20 إلى 50 متر فاصلة بين طبقات الأحجار الرملية العلوية والسفلية المشار إليها أعلاه شكل (4). تم حساب مقادير تقريبية للمسامية الكلية للأحجار الرملية عن طريق جسات المقاومة النوعية. من خلال نتائج خمسة وستين بئراً اتضح أنها بالأحجار الرملية السفلية تبلغ في المتوسط 24٪ وبطبقات الأحجار الرملية العلوية تبلغ في المتوسط 31٪.

أمكن استنتاج المسامية الكلية أيضاً عن طريق التجارب المعملية التي أجريت على عينتين اسطوانيتين لأحجار رملية من البئر رقم س/س 81/0444/273 (مشروع الأبقار بسبها). فقد إتضح بأن الأحجار

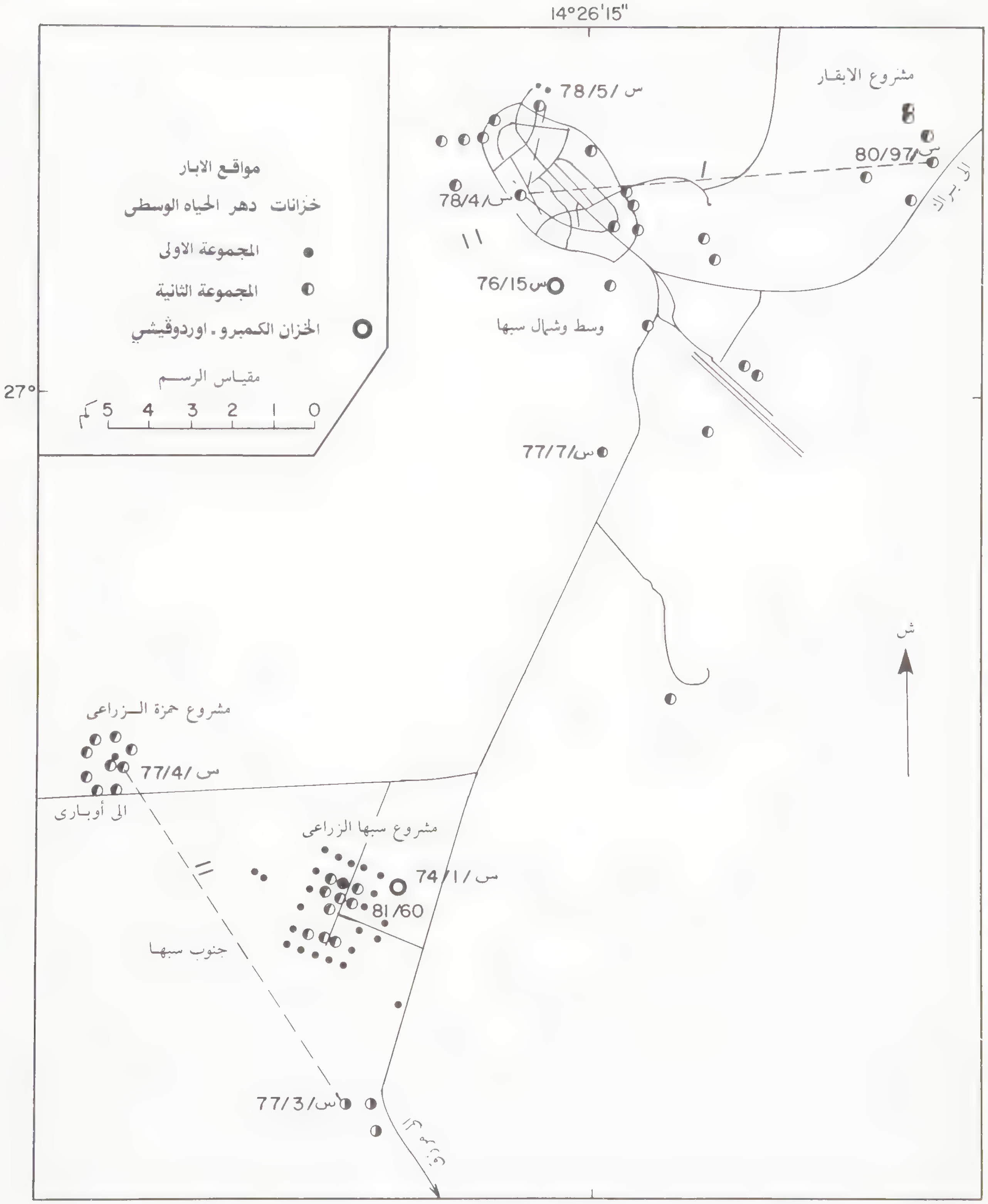
14°26'15"
27°
مواقع الابار
خزانات دهر الحياه الوسطى
● المجموعة الاولى
◐ المجموعة الثانية
○ الخزان الكمبرو . اوردوفيشي
مقياس الرسم
0 1 2 3 4 5 كم
س/ 78/5
مشروع الابقار
س/ 80/97
I
س/ 78/4
II
س/ 76/15
وسط وشمال سبها
س/ 77/7
ش
مشروع حمزة الزراعى
س/ 77/4
الى أوبارى
مشروع سبها الزراعى
س/ 74/1
81/60
II
جنوب سبها
س/ 77/3

شكل (3) : خريطة موضح عليها مواقع أهم الآبار المستغل عن طريقها الخزانات الجوفية المائية المحيطة بالمنطقة واتجاهات القطاعات الهيدروجيولوجية (شكل 4).

التي تتكون من أحجار الجرانيت وذلك كما أشير إليه أعلاه في الجزء الخاص بالوصف الجيولوجي.

الخزانات الجوفية المائية وخصائصها الهيدروليكية :

يتم تخزين المياه الجوفية الصالحة للإستغلال عادة في الطبقات المتكونة منّ أحجار رملية صلبة متماسكة. يرجع حفظ وتخزين المياه بها، بالدرجة الأولى، إلى الشقوق والفوالق المتواجدة بها وذلك كما أمكن ملاحظته ببعض العينات الإسطوانية وأثناء عمليات الحفر خاصة بالبئر رقم س/س - 76/74/15 ومن بعض الآبار الأخرى التي تخترق هذه الطبقات بطرف الحوض الجنوبي الغربي بوادي تان الزّفت (أسين - غات - تهاله) وخاصة بطرف الحوض الشمالي كما ورد في العديد من الدراسات والتقارير التي لم تنشر عن وادي الأريل وكما أشار إليه DUBAY (1980) عن وادي الشاطي.

أثبتت نتائج تجارب ضخ المياه الجوفية التي تتواجد في حالة تخزين مضغوطة حيث أنها تصعد من مصدر تخزينها على سبيل المثال بئر سبها رقم س/س - 76/74/15 حوالي 800 مترٍ حتى تكاد تتدفق على السطح، أن معامل الانتقالية يبلغ في المتوسط $2,4 \times 10^{-2}$ م^2/ثانية ولم يكن بالإمكان حساب معامل التخزين وذلك لعدم وجود بئر مراقبة (بيزومتر) بجانب أحد البئرين المشار إليها أعلاه.

وقد أثبتت نتائج تجارب الضخ لخزانات المياه الجوفية بالحينين الكمبري والأردوفيشي كالتي أجريت بالمناطق الأخرى الواردة أعلاه ما يلي :

(متوسط) معامل الانتقالية	(متوسط) معامل التخزين
وادي تان الزّفت : $2,6 \times 10^{-2}$ م^2/ثانية	$5,5 \times 10^{-4}$
وادي الشاطي والأريل : $2,5 \times 10^{-2}$ م^2/ثانية	$6,2 \times 10^{-4}$

بالمقارنة نلاحظ تقارب معامل الإنتقالية بالمناطق الثلاثة (سبها - طرف الحوض الجنوبي الغربي - طرف الحوض الشمالي) وأيضاً معامل التخزين بطرفي الحوض الذي يمكننا من خلالها توقع مقداره بمنطقة سبها حيث لا يوجد إختلاف متوقع يذكر في الخصائص الهيدروليكية لهذه الخزانات الجوفية خصوصاً بمنطقتي وادي الشاطئ وسبها.

التركيب الكيميائي للمياه :

نظراً لقلة عدد الآبار التي حفرت بالمنطقة بهذه الخزانات لم يكن بالإمكان دراسة الخواص الكيميائية لمياهها بدقة. أثبتت نتائج التحليل الكيميائي لثلاثة عينات مائية فقط من البئرين المشار إليها فيما سبق بأنها صالحة للإستغلال لأغراض الزراعة والشرب والصناعة. حيث أن المجموع الكلي للأملاح المذابة ببئر سبها العميق رقم س - 74/1 يبلغ حوالي 110 ملجم/لتر بدرجة حرارة قدرها 27 درجة مئوية وإتضح أن مجموع الأملاح المذابة بالبئر رقم س/س - 76/74/15 يبلغ حوالي 470 ملجم/لتر وتبلغ درجة حرارة المياه حوالي 55 درجة مئوية.

تُوضح نسبة العناصر الأساسية المذابة بمياه البئرين تقارب نوعية المياه حيث أنها في كل منها تغلب أيونات الصوديوم والكالسيوم على التوالي بالكاتيونات وأيونات البيكربونات والسلفات والكلوريد على التوالي بالأنيونات.

يبدو أنّ الإختلاف الملاحظ في مقدار الأملاح المذابة ودرجة الحرارة راجع إلى تصميم الآبار وذلك لأن البئر الأولي رقم (1) لم تخترق جميع الطبقات الحاملة للماء بالحينين الكمبري والأردوفيشي حيث أن مياهها ناتجة من الجزء العلوي فقط لهذا الخزان الجوفي والى عيوب متوقعة في التصميم أدت إلى تسرب مياه طبقات علوية أخرى مما أدى إلى إختلاط المياه حيث أن مياه جوفية يقع مصدرها على عمق أكثر من 1000م بمنطقة حوض مرزق عموماً بالطرف الشمالي خاصة. ويجب أن تكون درجة حرارتها أكثر من 27 درجة مئوية ويجب أن تزيد الأملاح المذابة بها عن العدد الوارد أعلاه أيضاً.

الخزانات الجوفية بطبقات دهر الحياة الأوسط :

الأحجار الرملية التي تكون جزءاً كبيراً من طبقات دهر الحياة الأوسط من الحين الترياسي وحتى الحين الكرتياسي الأسفل تشكل بحوض مرزق عموماً وبمنطقة سبها على وجه الخصوص خزانات جوفية مائية هامة حيث أن مياهها تكون المصدر المائي الوحيدالذي يتم إستغلاله لأغراض الزراعة والشرب والصناعة.

وحتى نهاية الخمسينات كان إستغلال المياه بمدينة سبها يعتمد أساساً على الآبار السطحية اليدوية التي لا تتعدى أعماقها عادة العشرة أمتار. ويتراوح مستوى سطح الماء بهذه الآبار بين أقل من متر وخمسة أمتار. كانت هذه الآبار تستغل عن طريقها المياه الجوفية بالطبقة السطحية الأولى للحين الجوراسي الأعلى أو الكريتاسي الأسفل. وأدى إنخفاض مستوى سطح الأرض بالطرف الغربي لمدينة سبها إلى إنسياب المياه في الماضي من هذه الخزانات على هيئة طبيعية مما أدى إلى تكوين أماكن سبخية ومستنقعات أو بحيرات كبحيرة عين الظلام غربي حي الجديد وبحيرة عين كرى بحطية رامي غرب حبل بن عريف.

وأدى إنخفاض مستوى سطح الماء إلى إندثار هذه التجمعات المائية بالكامل وذلك في الفترة ما بين أواسط الستينات (بحيرة عين الظلام) وحتى أواسط السبعينات (بحيرة عين كرى). وساعد قرب مستوى سطح الماء خلال مئات السنين الماضية على غرس آلاف الأعداد من أشجار النخيل البعلية بالطرف الغربي لمدينة سبها (حطية أم الغزلان

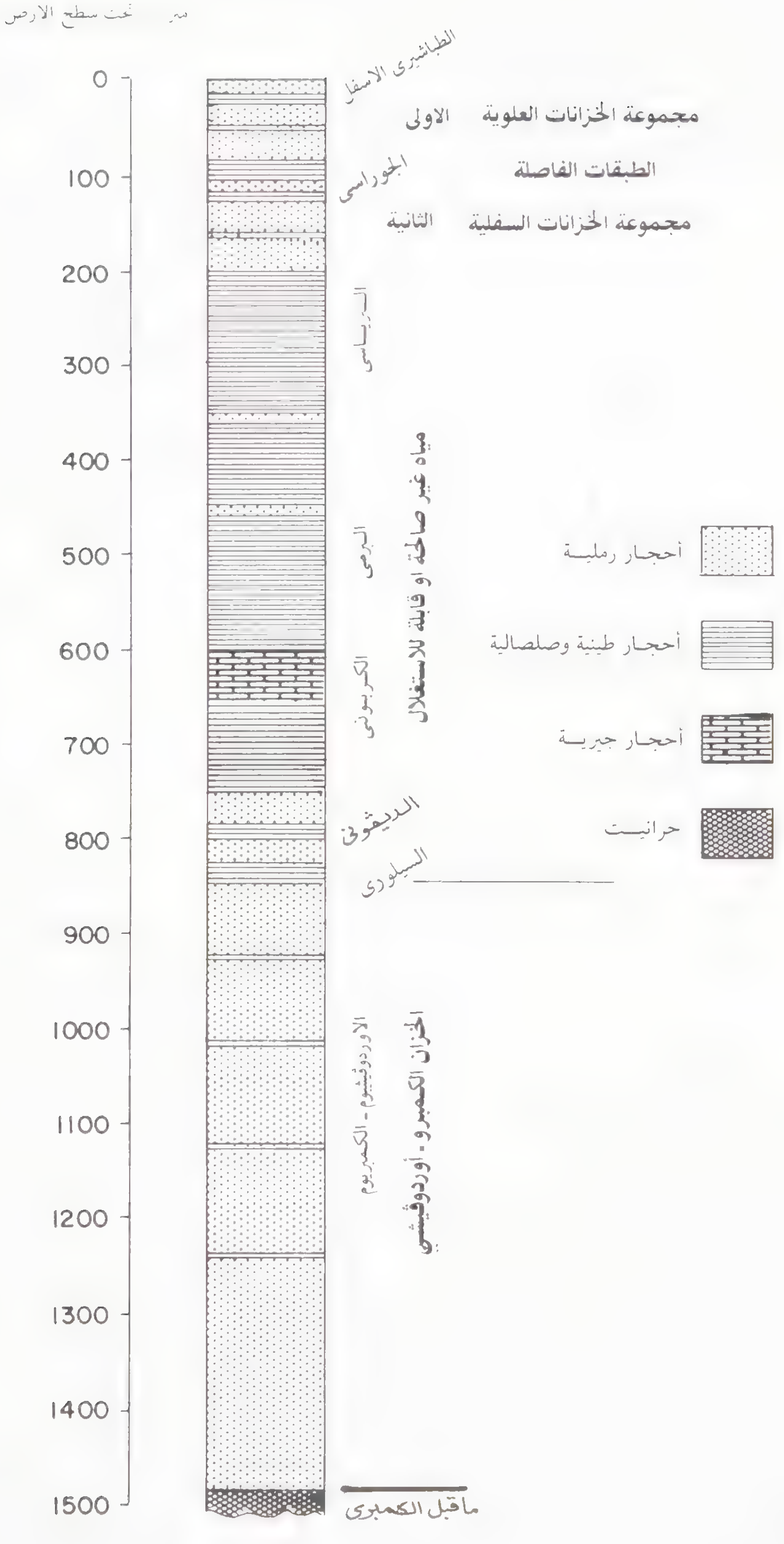
متر تحت سطح الارض
0
100
200
300
400
500
600
700
800
900
1000
1100
1200
1300
1400
1500
الطباشيرى الاسفل
مجموعة الخزانات العلوية الاولى
الجوراسى
الطبقات الفاصلة
مجموعة الخزانات السفلية الثانية
الترياسى
البرمى
الكربونى
مياه غير صالحة او قابلة للاستغلال
الديفونى
السيلورى
الاوردوفيشوم - الكمبريوم
الخزان الكمبرو - أوردوفيشي
ماقبل الكمبرى
أحجار رمليـة
أحجار طينية وصلصالية
أحجار جيريـة
جرانيـت

شكل (2) : عمود هيدروجيولوجي عام للتتابعات الجيولوجية والخزانات الجوفية بمنطقة سبها.

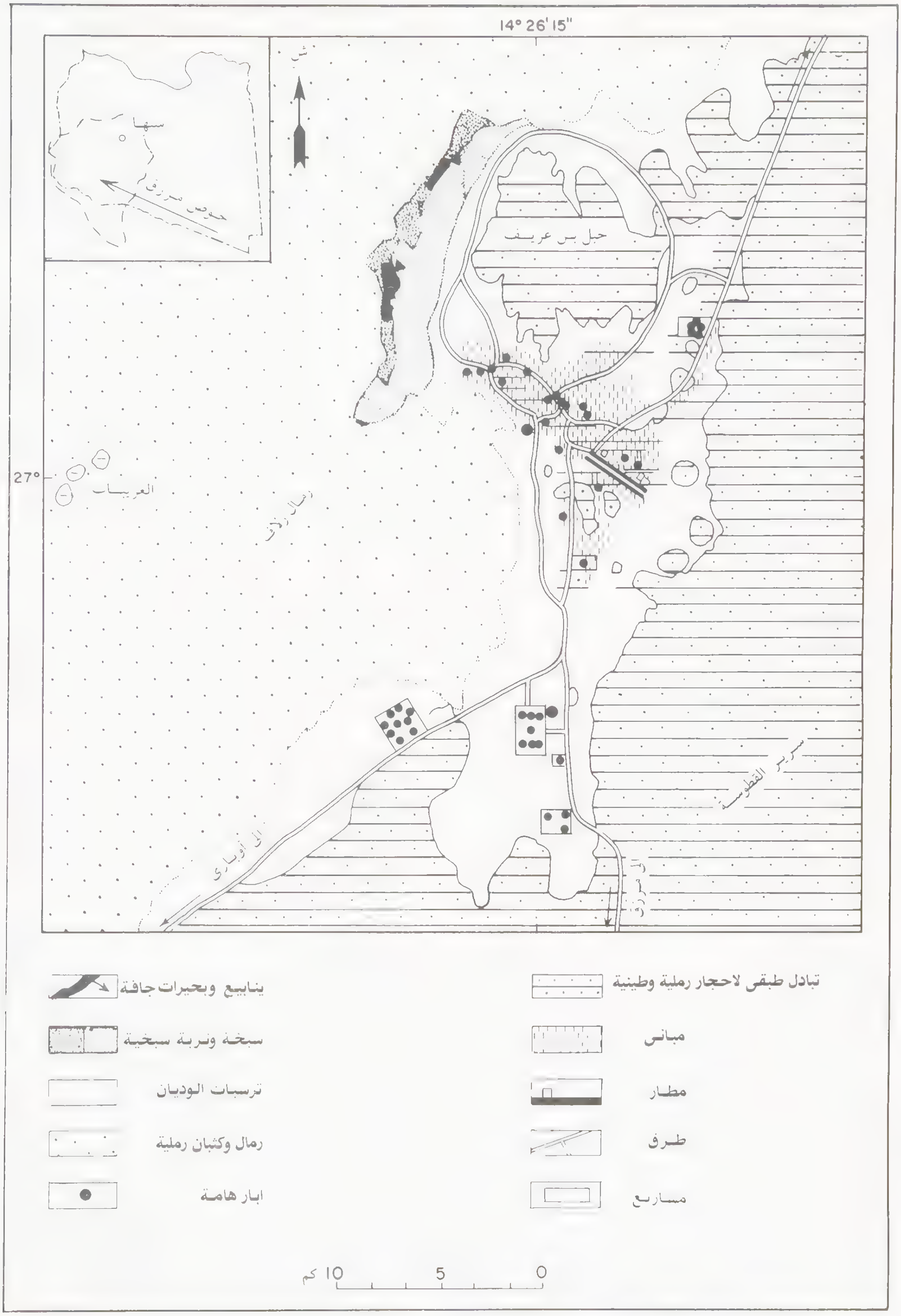
14° 26' 15"
27°
ش
سبها
حوض مرزق
جبل بن عريف
العريبات
رمال زلاف
سرير القطوسة
الى أوباري
الى مرزق
ينابيع وبحيرات جافة
سبخة وتربة سبخية
ترسبات الوديان
رمال وكثبان رملية
ابار هامة
تبادل طبقي لاحجار رملية وطينية
مباني
مطار
طرق
مشاريع
0
5
10 كم

شكل (1) : خريطة جيولوجية مبسطة لمنطقة سبها.

دهر الحياة القديمة :

صخر الجرانيت تليه صخور رسوبية تتكون في غالبها من أحجار رملية متماسكة من صلدة إلى عالية الصلادة ومن متوسطة إلى دقيقة الحبيبات الكوارتيزية ذات ألوان فاتحة تتخللها بعض الطبقات الصلصالية الغرينية التي لا يتعدى سمكها في أغلب الحالات بضع سنتمترات. هذه التكوينات التي يرجع عمرها إلى الحين الكمبري والحين الأردوڤيشي تتواجد على عمق 870 إلى 1484,5 متراً.

الصخور الرسوبية المشار إليها أعلاه تعلوها بسمك 100 متر تقريبا أحجار رملية مشابهة صلدة قاتمة إلى بنية اللون تتواجد بها تداخلات طينية غرينية وصلصالية يغلب عليها اللون الغامق والأسود قد يصل سمكها إلى عدة أمتار هذه يرجع عمرها من المتوقع إلى الحين السيلوري أو الديڤوني.

تلي التكوينات الواردة أعلاه على عمق يقع في المتوسط عند 770 متراً تقريباً طبقاتٌ تتكون في غالبها من الأحجار الغرينية والصلصالية التي يغلب عليها اللون الرمادي الغامقِ والبنّي مع تداخلات لأحجار رملية. تحل محلها على عمق 650 متراً أحجار جيرية ودلوميتية صلده يرجع عمرها إلى الحين الكربوني. الأحجار الكلسية تعلوها بمنطقة سبها تكوينات تشير إلى أنها ترسبت في بيئة قارية.

هذه تتكون من أحجار طينية وغرينية يغلب عليها اللون البني والبنّي المحمر تتخللها تكوينات بسيطة لأحجار رملية بنية إلى فاتحة اللون هذه التكوينات من المتوقع أن يرجع عمرها إلى الحين البرمي.

دهر الحياة المتوسطة :

استمرت بالأحيان الترياسي – الجوراسي – الكريتاسي حالة الترسيب القاري التي وضع أساسها في الحين البرمي كما أشير إليه أعلاه على ما يبدو بدون انقطاع طيلة الفترة حتى الكريتاسي الأسفل.

تشير بعض الدراسات إلى هذه الوضعية خاصة التي أعدت من قبل KLITZSCH (1970م) بمنطقة سبها كما هو عليه الحال في أجزاء الحوض الأخرى تتكون هذه التتابعات القارية في الجزء الأسفل منها من أحجار طينية بنية إلى محمرة كما سبق التنويه تتغير سحناتها إلى أحجار طينية ورملية وغرينية مع إزدياد في عدد وسمك تداخلات الأحجار الرملية بالإتجاه إلى أعلى. وفي مراحل الترسيب الأخيرة القريبة من السطح تزيد نسبة الأحجار الرملية بوضوح وتصبح الأحجار الطينية على هيئة تداخلات محدودة السمك. يرجع عمر الأجزاء السفلية لهذه التكوينات القارية إلى الحين البرمي كما أشير إليه أعلاه. والجزء الأوسط إلى الترياسي والتكوينات العلوية منها إلى الحينين – الجوراسي والكرتياسي الأسفل حيث يتواجد جزء منها بمنطقة سبها على السطح مشكلا مرتفعات جبلية بسيطة متصلة أو معزولة على هيئة شواهد وجزر صحراوية.

دهر الحياة الحديثة :

تنعدم صخور الحين الثالث بمنطقة سبها حيث لا توجد أية ترسبات تشير إلى أنها لها هذا العمر. في الجزء الغربي لمنطقة سبها تتواجد تكوينات قارية ربما يرجع عمر جزء منها إلى الحين الحديث وذلك حسب ما ورد في خريطة جيولوجية ليبيا – لوحة سبها، مركز البحوث الصناعية (1984م).

وتمثل الحين الرابع، على وجه الخصوص، التربة الناتجة عن عوامل التجوية التي تم ترسيبها في المنخفضات المتواجدة عند أقدام المرتفعات الجبلية خاصة في المناطق الجنوبية لمنطقة سبها وبالأطراف الشمالية والغربية تتواجد بقايا لترسبات بحيرية وسبخية التي كانت إلى فترة قريبة جداً مغمورة جزئياً بالماء. أما الجزء الأكبر لترسبات هذه المرحلة الزمنية فيتكون من الكثبان الرملية التي تحيط بمدينة سبها من الناحية الشمالية والغربية (كثبان رمال زلاف وأوباري) شكل (1).

الخزانات الجوفية المائية

(هيدروجيولوجية منطقة سبها) :

ساعدت الميزات الرسوبية والحركية للتراكيب والتكوينات الجيولوجية التي أشير إليها تحت فقرة جيولوجية المنطقة، على تجميع وحفظ كميات كبيرة من المياه.

هذه الطبقات التي تكون على هيئة خزانات جوفية مائية يتكون جزء منها من الأحجار الرملية لتكوينات الأحيان (الكمبري والأردوڤيشي والديڤوني) والجزء الآخر الذي تكونه الأحجار الرملية للأحيان الترياسي – والجوراسي – والكرتياسي الأسفل، شكل (2).

فيما يلي سيتم التعرض إلى النتائج التي تم التوصل إليها حول المعاملات الهيدروليكية والخصائص الكيميائية النظيرية لمياه الخزانات الجوفية المشار إليها أعلاه شكل (2).

الخزانات الجوفية المائية بطبقات دهر الحياة القديمة :

طبقات دهر الحياة القديمة الحاملة لمياه صالحة للإستغلال أمكن دراستها مبدئيا بمنطقة سبها عن طريق البئرين العميقين: بئر سبها العميق س – 1 – 1974 بعمق 1330م الذي يقع جنوبي المدينة بمشروع سبها الزراعي والبئر رقم س/س – 76/74/15 بعمق 1519,5 متراً بحي القرضة بسبها. شكل (3).

في البئر الأول لم يتم الوصول إلى صخور دهر ما قبل الكمبري وبالتالي لم تتح الفرصة لدراسة الخزانات الجوفية المائية بها بالكامل أما البئر الثاني تخلل الحفر به جميع الطبقات الحاملة لمياه صالحة للإستغلال وذلك حتى عمقها النهائي بطبقات دهر ما قبل الكمبري

من خلال دراسة نتائج الآبار التي تم حفرها بالمنطقة اتضح أن الأحجار الرملية التي يرجع تكوينها إلى دهر الحياة القديمة خاصة الأحيان الكمبري والأردوفيشي والديفوني التي تقع على عمق يتراوح بين 800 إلى 1484,5 متراً تمثل خزانات جوفية مائية جيدة حيث تتوفر بها مياه عذبة. كما أثبتت الدراسة أن الأحجار الرملية لدهر الحياة الوسطى (الأحيان الترياسي – حتى الكريتاسي الأسفل) هي أيضاً عبارة عن خزانات مائية جيدة حيث مساميتها العالية ساعدت على تخزين كميات ضخمة من المياه. مياه هذه الطبقات تكوّن الآن المورد المائي الرئيسي الذي يتم الإعتماد عليه في شتى مجالات الحياة بمدينة سبها.

ولقد أثبتت الدراسة أن الخزانات الجوفية المائية لطبقات الحياة الوسطى يمكن تقسيمها إلى مجموعتين رئيستين حيث، بالإضافة إلى دلائل أخرى، إنّ المجموع الكلي للأملاح المذابة بمياه الطبقات العلوية من السطح وحتى عمق 40 متراً في المتوسط (خزانات المجموعة الأولى) يتراوح بين 600 ملجم/لتر– إلى أكثر من 2500 ملجم/لتر. أما الأملاح المذابة بمياه الخزانات الجوفية السفلية (المجموعة الثانية) على عمق بين 100 إلى 200 مترٍ تقريباً تبلغ حوالي 80 إلى 200 ملجم/لتر. الخزانات المائية للمجموعة الأولى (العلوية) والخزانات المائية للمجموعة الثانية (السفلية) تفصلها طبقات أغلبيتها طينية بسمك يتراوح بين 20 إلى 50 متراً. كما أمكن التعرف على أن الطبقات الرسوبية التي تقع على عمق من 200 إلى 800 مترٍ تقريباً التي تتكون في الأساس من الأحجار الطينية والطينية رملية والصلصالة والكلسية والتي تتخللها بعض الأحجار الرملية الضئيلة السمك لا تحتوي على مياه صالحة للإستغلال وإن هذه التتابعات الطبقية تمثل فاصلاً سميكاً بين المياه الجوفية للأحجار الرملية لدهر الحياة القديمة التي من أسفلها وبين المياه الجوفية للأحجار الرملية لدهر الحياة الوسطى التي في أعلاها (المجموعتان الأولى والثانية).

كما أمكن الاستنتاج من خلال هذا البحث وبحوث أخرى عن طريق دراسة الخواص النظائرية الإشعاعية للمياه الجوفية المتواجدة بمدينة سبها وضواحيها بأنها في مجملها عبارة عن مياه قديمة دفينة تم تخزينها نتيجة لهطول أمطار غزيرة في فترات زمنية مختلفة وذلك في الخمسين ألف سنة الأخيرة وربما أكثر وذلك كما هو عليه حال المياه الجوفية في حوض مرزق والصحراء الكبرى بالشمال الأفريقي.

مقدمة

تقع مدينة سبها في الجزء الشمالي لحوض مرزق عند خط عرض ′27:00 شمال وخط طول ′14:30 ° شرق. متوسط إرتفاع المنطقة عن سطح البحر يبلغ حوالي 420 متراً.

في السنوات الأخيرة خاصة ما بين 1976م حتى 1986م. تم حفر المئات من الآبار بالمدينة وضواحيها – العشرات من هذه الآبار أعدت لها مواصفات حديثة تتمشى مع ما توصلت اليه التقنية في هذا المجال. وقد تم إعداد المواصفات الخاصة بتصميمها والإشراف على تنفيذها عن طريق الهيئة العامة للمياه ثم أمانة السدود والموارد المائية سابقاً ومصلحة المياه والتربة حالياً. ومن خلال متابعة الأعمال التي أجريت على عدد كبير منها بطريقة مباشرة أو غير مباشرة في الفترة الزمنية المشار إليها أعلاه ومن خلال دراسة النتائج التي استخلصت منها تم محاولة وضع تصور علمي لوضعية المياه الجوفية بمنطقة سبها. هذا التصور تم عرضه كجزء من إطروحة الدكتوراه التي أعدت بجامعة توبنجن بألمانيا الغربية والتي تم إعتمادها في شهر يناير 1984م.

يرتكز هذا البحث في مجمله على ما تم التوصل إليه وعرضه في الإطروحة المشار إليها أعلاه بالإضافة إلى بعض النتائج المستحدثة عن المنطقة في السنوات من 1984م إلى 1986م. فمن خلال دراسة نتائج عينات الحفر والتصوير الجيوفيزيائي والتجارب التي أُجريَتْ على العينات الإسطوانية وحساب نتائج تجارب الضخ والتحاليل المائية الكيميائية والتحاليل المائية النظيرية وما أسفرت عنه أمكن وضع تصور ربما يساعد على تفهم وضعية المياه الجوفية بالمنطقة بكيفية مجدية وعلمية، الذي قد يكون منطلقاً لإجراء دراسات أخرى موضوعية مماثلة للمياه الجوفية بمنطقة حوض مرزق.

التراكيب الجيولوجية بمنطقة سبها

عينات ناتج الحفر وعينات لب الآبار التي أخذت من البئرين العميقين بسبها خاصة رقم س/س –76/0074/15 وناتج حفر العديد من الآبار التي تخللت الطبقات العلوية فقط للتكوينات الجيولوجية بالمنطقة حتى أعماق لا تتعدى المئتي متر بالإضافة إلى الإنطباعات الخاصة عن التكوينات الجيولوجية المتواجدة على السطح وغيرها من الدراسات التي أجريت عن حوض مرزق عموماً كالتي من قِبَل KLITZSCH (1970م) ومركز البحوث الصناعية: خريطة ليبيا الجيولوجية (لوحة سبها ش ز –33 –2، لوحة الفقهاء ش ز –33 3 لوحة تمنهنت ش ز 33– 6 – 1984م). هذه جميعها تساعد على تفهم التراكيب الجيولوجية بمنطقة سبها. فيما يلي سيتم التعرض لوصف التتابعات الجيولوجية بالمنطقة بصورة موجزة.

دهر ما قبل الكمبري:

تتواجد صخور القاعدة ببئر سبها العميقة (س/س 76/74/15) على عمق 1484,5 متر وتتكون من صخر الجرانيت وذلك كما إتضح من عينات ناتج الحفر ومن العينة الإسطوانية التي أخذت عند العمق النهائي للبئر (1518,5 – 1519,5 متر).

Ground Water of Sabhā Area

Mehimed M. El-Chair[1]

Abstract. The ground water in the Sabhā area and throughout the Murzuq basin constitutes the only water resource which can be widely exploited for agriculture, industry and normal domestic use.

This ground water is found in sedimentary layers of different geological ages. These sedimentary rocks overlie granitic basement rocks at a depth of about 1500 m. They consist of mostly sandstone, claystone and shale; with some limestone beds at a depth of 650 m.

It appears from the results of the well studies in this area that the sandstones of Palaeozoic age, situated at a depth of 800–1500 m represent a good groundwater reservoir where large amounts of fresh water are available.

The study also shows that the sandstones of Mesozoic age form a very good groundwater reservoir. The high porosity of this reservoir helps to store a large quantity of water, which constitutes the most important and reliable multi-purpose water resource. It was also confirmed that the ground water in the Mesozoic sandstones can be clearly divided into two aquifer groups. The upper groundwater reservoirs (aquifer group 1) occurring at depths of 40 and 70 m contain mainly brackish water, whereas the lower groundwater reservoirs (aquifer group 2), occurring under 20–50 m-thick layers of clay and claystone and reaching a depth of between 100 and 200 m, contain only fresh water.

Chemical water analysis further supports such a subdivision of the aquifers. The TDS content of the ground water in the upper aquifer system ranges from 600 to more than 2500 mg/l, while the TDS content of the aquifer group 2 is usually below 200 mg/l.

This study, and other research into the isotopic characteristics of the Sabhā ground water, has shown that it is of a type which originated as a result of heavy falls of rain during the last 50 000 or more years. This is in keeping with the general groundwater conditions in the Murzuq basin and the Sahara of North Africa.

المياه الجوفية بمنطقة سبها

د . محمد محمد الشاعر
قسم علوم الأرض . كلية العلوم
جامعة سبها ج . ع . ل . ش . إ . ع .

الخلاصـــة

تكون المياه الجوفية بمدينة سبها المصدر المائي الذي يتم إستغلاله على نطاق واسع لأغراض الزراعة والشرب والصناعة حيث لا توجد موارد مائية أخرى بالمنطقة وذلك كما هو عليه الحال في جميع أنحاء حوض مرزق .

هذه المياه الجوفية متواجدة في طبقات لدهور جيولوجية مختلفة . فالتركيب الجيولوجي بمدينة سبها يتمثل في صخور القاعدة التي تقع على عمق 1484 متراً والتي تتكون من صخور جرانيتية . وهذه تعلوها حتى السطح طبقات رسوبية تتكون غالباً من أحجار رملية وصلصالية وطينية وغرينية تتخللها على عمق 650 متراً تقريباً أحجار كلسية .

UNIV[redacted] CALIFORNIA, DAVIS
3 1175 01793 4541